Patrons de sédimentation et caractéristiques de la ripisylve dans les casiers Girardon du Rhône : approche comparative pour une analyse des facteurs de contrôle et une évaluation des potentialités écologiques

Bianca Räpple

Numéro National de Thèse : 2018LYSEN006

THESE de DOCTORAT DE L'UNIVERSITE DE LYON

opérée par

l'Ecole Normale Supérieure de Lyon

Ecole Doctorale N° 483

Sciences sociales (Histoire, Géographie, Aménagement, Urbanisme, Architecture, Archéologie, Science Politique, Sociologie, Anthropologie)

Spécialité de doctorat : Géomorphologie fluviale / biogéomorphologie

Discipline : Géographie

Soutenue publiquement le 08/06/2018, par :

Bianca RÄPPLE

Sedimentation patterns and riparian vegetation characteristics in novel ecosystems on the Rhône River, France

A comparative approach to identify drivers and evaluate ecological potentials

Patrons de sédimentation et caractéristiques de la ripisylve dans les casiers Girardon du Rhône

Approche comparative pour une analyse des facteurs de contrôle et une évaluation des potentialités écologiques

---

Devant le jury composé de :

CHIN, Anne	Professeure, University of Colorado Denver	Examinatrice
EVETTE, André	Docteur, IRSTEA	Examinateur
FRANQUET, Evelyne	Professeure, Aix Marseille Université, CNRS	Co-encadrante
GAUTIER, Emmanuèle	Professeure, Université Paris 1	Rapporteure
PIEGAY, Hervé	Directeur de Recherche, CNRS	Directeur
PONT, Bernard	Conservateur, Réserve Naturelle île de la Platière	Examinateur
STEIGER, Johannes	Professeur, Université Clermont Auvergne	Rapporteur
STELLA, John C.	Professeur assoc., State University of New York	Co-encadrant

Numéro National de Thèse : 2018LYSEN006

THESE de DOCTORAT DE L'UNIVERSITE DE LYON
opérée par
l'Ecole Normale Supérieure de Lyon

Ecole Doctorale N° 483
Sciences sociales (Histoire, Géographie, Aménagement, Urbanisme, Architecture, Archéologie, Science Politique, Sociologie, Anthropologie)

Spécialité de doctorat : Géomorphologie fluviale / biogéomorphologie
Discipline : Géographie

Soutenue publiquement le 08/06/2018, par :
Bianca RÄPPLE

Sedimentation patterns and riparian vegetation characteristics in novel ecosystems on the Rhône River, France

A comparative approach to identify drivers and evaluate ecological potentials

Patrons de sédimentation et caractéristiques de la ripisylve dans les casiers Girardon du Rhône

Approche comparative pour une analyse des facteurs de contrôle et une évaluation des potentialités écologiques

---

Devant le jury composé de :

CHIN, Anne	Professeure, University of Colorado Denver	Examinatrice
EVETTE, André	Docteur, IRSTEA	Examinateur
FRANQUET, Evelyne	Professeure, Aix Marseille Université, CNRS	Co-encadrante
GAUTIER, Emmanuèle	Professeure, Université Paris 1	Rapporteure
PIEGAY, Hervé	Directeur de Recherche, CNRS	Directeur
PONT, Bernard	Conservateur, Réserve Naturelle île de la Platière	Examinateur
STEIGER, Johannes	Professeur, Université Clermont Auvergne	Rapporteur
STELLA, John C.	Professeur assoc., State University of New York	Co-encadrant

Ce travail a bénéficié d'une aide de l'Etat gérée par l'Agence Nationale de la Recherche au titre du Labex DRIIHM, programme « Investissements d'avenir » portant la référence ANR-11-LABX-0010, ainsi que de l'Observatoire Hommes-Milieu Vallée du Rhône.

RESUME

A l'image du Rhône au sud-est de la France, les fleuves font l'objet de multiples usages, entrainant des modifications profondes de leurs dynamiques fluviales. Par conséquent, les fonctionnements hydro-sédimentaire et écologique de leurs chenaux ainsi que de leurs plaines alluviales sont altérés. Des programmes intégrés de restauration s'attellent à définir les potentiels et les risques liés à de tels 'écosystèmes anthropo-construits' et de comprendre les interactions entre divers facteurs de contrôle ayant influencé leur formation. La présente étude s'est focalisée sur 293 casiers Girardon – des unités rectangulaires délimitées par des digues submersibles longitudinales et latérales construites dans le lit mineur au 19ème siècle afin d'améliorer la navigabilité du Rhône. Ceux-ci sont distribués sur quatre secteurs court-circuités au 20ième siècle pour la production hydro-électrique. Nous avons analysé les patrons spatio-temporels de la sédimentation, ainsi que la structure et la composition des boisements grâce à des données issues de la télédétection et de terrain. Nous proposons également un modèle conceptuel des facteurs de contrôle et des processus potentiels en lien avec les patrons observés. Quatre-vingts pourcents des casiers ont évolué du stade aquatique à un stade terrestre et boisé, suivant des trajectoires historiques variées à la fois inter- et intra-secteurs. Les boisements diffèrent en caractéristiques structurelles de boisements de référence plus naturels. Leur composition est plus proche de celle des systèmes matures que pionniers. Nous observons également une forte présence d'espèces allochtones, comme par exemple l'Érable negundo (*Acer negundo*), invasive, en particulier dans les stades de régénération. Notre approche comparative constitue une première étape pour démêler les effets cumulatifs des facteurs de contrôle et hiérarchiser leurs rôles individuels. Nous avons constaté que des facteurs locaux jouent un rôle majeur, en particulier la connectivité au chenal principal court-circuité. L'évolution des facteurs environnementaux eux-mêmes a contribué à la complexité des patrons. Ce travail ouvre la voie à des futures études sur des écosystèmes anthropo-construits sur cours d'eau, et donne une nouvelle perspective aux gestionnaires du Rhône relativement à son échelle spatiale innovante.

Mots clés : patrons de sédimentation ; végétation ligneuse ; Anthropocène ; facteurs de contrôle ; Rhône ; chenalisation ; dérivation ; réhabilitation

ABSTRACT

The multiple uses made of large rivers, such as the Rhône in south-eastern France, have provoked profound modifications of their fluvial dynamics. As a consequence, the hydro-sedimentary and ecological functioning of their channels and floodplains are highly altered. Integrated restoration programmes struggle in defining potentials and risks related to such 'novel ecosystems' and to understand the various interacting drivers which influence their formation. This study comparatively focused on 293 dike fields—rectangular units delimited by longitudinal and lateral submersible dikes constructed in the channel in the late 19th century to promote the navigability of the Rhône. They are distributed over four reaches by-passed in the 20th century for hydro-electric energy production. We investigated the spatio-temporal patterns of sediment deposition and the structure and composition of the forest stands using remote sensing and field data. We also propose a conceptual model of potential drivers and processes behind the observed patterns. Eighty percent of the dike fields have evolved from the aquatic to a terrestrial and forested stage, following variable historical trajectories both between and within reaches. The forest stands presented structural characteristics which differed from more natural reference stands and compositional characteristics closer to mature than to pioneer systems. They featured a high presence of non-native species, such as the invasive Box elder (*Acer negundo*). Our comparative approach constituted a first step to disentangle the cumulative effects of the drivers and define their individual roles: we discovered a prominent role of local factors, especially the connectivity to the main by-passed channel. The evolution of the environmental factors themselves added to the complexity of the patterns. This work provides a basis for future studies of novel ecosystems on rivers, and a new perspective to river managers on the Rhône due to its innovative spatial-scale.

Keywords: sedimentation patterns; woody riparian vegetation; Anthropocene; control factors; Rhône River; river training; river regulation; river rehabilitation

REMERCIEMENTS / ACKNOWLEDGEMENTS / DANKSAGUNG

Tout d'abords, je souhaite remercier mes directeurs et mon co-encadrant de thèse, Hervé Piégay, Evelyne Franquet et John C. Stella. Hervé, je te remercie particulièrement pour ta patience, pour ta sérénité et ta confiance, ainsi que pour m'avoir confié deux projets de recherche complexes mais très passionnants sur la Drôme (projet de Master) et le Rhône. Grace à toi j'ai eu l'occasion de travailler pendant ces dernières années dans un domaine qui me tient particulièrement à cœur et dans un environnement très chaleureux. Mme Franquet, je tiens à vous remercier pour votre disponibilité et vos encouragements. Merci également de m'avoir montré (ensemble avec Maxine Thorel, merci à toi aussi) les casiers d'Arles qui se différencient des casiers de mes secteurs d'étude, ainsi que les casiers de Péage d'un autre angle. John, je te remercie très chaleureusement pour ton implication, le temps consacré aux détails méthodologiques et techniques, les relectures pertinentes. J'ai beaucoup apprécié le travail avec toi dans ces différents projets, au cours desquels j'ai pu beaucoup apprendre.

Je tiens à remercier Anne Chin, André Evette, Emmanuèle Gautier, Bernard Pont et Johannes Steiger d'avoir accepté de participer à mon jury de thèse, en particulier les deux rapporteurs pour le temps consacré à évaluer ce manuscrit.

Cette thèse a profité d'un financement par le Labex DRIIHM et l'Observatoire Homme-Milieu (OHM) Vallée du Rhône. Je leur adresse en outre mes remerciements pour les rencontres avec les autres doctorants et post-doctorants de l'OHM, ainsi qu'avec la « communauté OHM » en général (Michal Tal, Pierre Marmonier, Georges Carrel, Nicolas Lamouroux, Carole Barthélémy, …). J'ai également apprécié l'occasion qui m'a été offerte de pouvoir participer à l'organisation d'une table ronde alternative au sein du séminaire annuel du Labex. Je pense également aux membres de la ZABR et leur énergie positive : Anne Clémens et Dad Roux-Michollet. Je remercie l'ENS de Lyon pour m'avoir accueillie dans des conditions superbes et l'Ecole Doctorale 483 qui a cofinancé des conférences.

Un grand grand merci à tous mes « stagiaires » (Patrick Modrak, Jakub Ondruch, Robin Gruel, Gabrielle Seignemartin, Oriane Villet, Axel Candy). J'ai énormément apprécié votre motivation et votre investissement à la fois en termes de réflexion et en termes de muscles sur le terrain (vive la tarière !!). Sans vos efforts, cette base de données serait loin de ce qu'elle est aujourd'hui.

Pour leurs efforts sur le terrain, je remercie Robin (qui vaut son pesant d'or au niveau de l'identification des espèces, ainsi que de volume de sédiment excavé (on n'en parle pas plus ici)), Gabrielle (j'ai peur qu'on va encore parler de ce terrain quand on arrivera à la retraite…), Oriane, Dad, Christine, John, Véro, Regis, Ludo, Patrick, Jakub, Axel, Lucie et Jordane.

Concernant la mise à disposition de données, je remercie Simon Dufour pour les données sur la Drôme, Maya Hayden pour des données sur l'Ain, Bernard Pont pour des données de ainsi que pour l'accès à la Réserve de l'Ile de la Platière, la CNR pour des données de débit, la BDOH pour des données de matière en suspension, Jérémie Riquier & Alvaro Tena-Pagan pour de nombreuses données, comme Gabrielle Seignemartin, Katka pour ses modèles, Elsa Parrot pour les données de thalweg et les cartes anciennes fournies par Guillaume Raccasi, Guillaume Fantino & Nicolas Talaska (GeoPeka) pour des données de tarière. Pour la mise à disposition de son mémoire, je remercie Pierre-Gil Salvador ainsi que Jean-Paul Bravard. Merci à Chloé de Bescond pour son aide concernant mon compte sur la BDOH. Merci à Gwenaëlle Roux and Thierry Winiarski pour les références en termes de taux de sedimentation. Je remercie Silvain Reynaud et Christophe Moiroud de la CNR, ainsi que leurs collègues, pour des échanges autour des casiers. L'ONEMA et, en particulier, Vincent Gaertner pour les analyses granulométriques et l'accueil au laboratoire.

Je tiens à remercier Anne Honegger pour son soutien à plusieurs reprises, Séverine Morin, Monique Noharet, Sandy Artero et Patrick Gilbert pour leur engagement du côté administratif, souvent en situation d'urgence. Sans oublier l'équipe souriante et attentionnée du RU, l'équipe de la repro et le service courriel, ainsi que Mme Monni.

Il y a de nombreuses raisons pour moi de remercier Jérémie, tant pour les échanges riches sur les bras morts et les casiers que pour tes conseils scientifiques/méthodologiques, ton aide sous Illustrator/R/ArcGIS, ta disponibilité, des données, ton écoute ou ton soutien et encouragement pendant des heures difficiles. Pour leur conseil et aide technique je remercie également Thomasito (Illustrator et plein d'autres choses), Lise (R, les stats), Guillaume (ArcGIS, ta connaissance en lien avec les casiers), Mathieu (R, pdfXchange viewer), Kristell (avec tout et n'importe quoi, elle m'a aussi accueillie au labo le tout premier jour, quand je ne comprenais qu'un mot sur trois), Christine (Access), Fanny, Elsa and many more, un grand merci à vous tous.

Je remercie Pierre, Jérémie, Mélanie, Emeline, Elisabeth et Gerard pour les relectures du manuscrit.

Je pense bien sûr à tous mes co-bureaux qui ont témoigné (et en partie causé) ma transition de l'allemande travailleuse calme (au moins au public) à la semi-râleuse franco-allemande : Elsa, Fanny, Robin, Stepha, Thomasito, Mathieu, Dandan, Remy, Jérèm, Anna, Ludivine (enfin, il y en a beaucoup que je dois exclure de la liste des râleurs, mais vous savez de qui je parle).

Une pensée à tous ceux dont j'ai eu la chance de rencontrer au labo: Véro, Mélanie, et Pierre, Karen (thanks for the English touch to the lab when I arrived, the many convivial lunch-times, all the supportive and fun moments, also with Steph and little Sammy), Valeria (te ringrazio per delle ore ed ore di grandi risate), Fanny (merci pour les moments de convivialité, les conversations autour des voyages/des activités de bien-être/de recettes et bien plus), Thomasito (merci pour les promenades à la boulangerie, d'avoir partagé cette passion pour les ptits goûters et les discussions toujours très 'profondes' en allemand), Alvaro (merci pour ta bonne humeur chaque jour et l'atmosphère espagnole au labo, ainsi que pour ton encouragement continu, des gros bisous à Clara et les enfants), Séb & Nina (merci pour les milles et une nuit d'aventures et votre chaleur), Aurélie (merci de m'avoir inspirée à découvrir de nouvelles choses autour du bien-être), Gabi (tu es toujours à l'écoute, as toujours des nouveaux résultats motivants à partager ou une bonne blague à raconter. De plus : tous ces gâteaux et cette glace !!! Merci à toi, et un ptit coucou aussi à Robert), Emeline (merci pour ta nature ouverte et directe, ta coolness et ton immense serviabilité), Yves (merci pour les échanges au RU et dans la cfète), Marylise (je pense toujours à toi en préparant ce super gâteau aux marrons), Somi & Saleh (thank you both for your cheerfulness), Katka (thanks for your kindness, your funny nature and all your energy), Marie (je te remercie pour les très bons échanges tant personnels qu'autour de la thèse), Silvia (la rigolote, merci pour les moments fun en R 2.38, Grüezi à Valentin), Lise (tu nous as gâtés avec ton savoir-faire en cuisine et avec le ptit Bertrand. De plus, quel inspiration en termes de bijouterie/vêtements/etc. faits maison !), Vincent Dr Wow (quel film classique français/allemand next ?), Hélène (la souriante, qui nous rend le jour plus joyeux (et notre « Heinzelmännchen » !)), Ludo (« Saluuut Luudoooo », je suis tjs impressionnée par ton sens du rangement, même des coquilles de moules), Kristell (j'espère qu'on passera toutes les deux bientôt moins de soirées/week-ends au labo, même si c'était chouette d'avoir de la compagnie), Mathieu (dsl pour la choucroute, c'était surtout

symbolique), Bertrand (la cuisine lyonnaise n'est pas pour les végétariens, mais heureusement que je suis fléxitarienne), Barbie (merci pour les premières sorties qui m'ont aidé à tout de suite être fan de ce labo et merci aussi pour le partage autour de tes expériences avec la thèse), Guillaume (merci pour ton aide technique, les heures de travail bien conviviales aux archives ou à Paris), Robin Jenkinson (thanks for your openess and kindness), Zhang & Dandan (thanks for your company at ENS late at night and at the week-ends), Volodia (tu penses qu'on y arrivera encore un jour à se voir à Strasbourg ?), Pierre C (plein de blagues et de bonne humeur), Clément R (j'ai pas mal pensé à toi et Margaux pendant la rédaction, autour de la vie que vous avez choisie il y a quelques années). Une pensée aussi à Brice, Samuel, Jean-Benoît, Hossein, Peter & Sabrina, John & Beth, Anna & Matt, Kéo, Hervé Pa., Stepha, Clément D, Martin, Ines, Elise, David, Jérôme, Paul Arnaud, Marie-Laure, Marie-Christine, Anne-Lise, Valentin, Lallandi, Hind, Christophe, Baptiste, et tout ceux qui sont arrivées pendant que j'avais la tête dans mon manuscrit.....

Un grand merci à l'équipe de l'IRSTEA pour l'inoubliable trip sur l'Amazone, surtout à Benoît, Jérôme et Guillaume.

Ich denke auch an den Lehrstuhl Gewässerschutz in Cottbus zurück, vor allem an Herrn Mutz, der mit seinen Vorlesungen meine Leidenschaft für Fließgewässer und ihre Gehölze (tot oder lebendig) geweckt hat und mir mit seinem Engagement die wissenschaftliche Arbeit schmackhaft gemacht hat. Clara Mendoza Lera, thanks for your support, motivation, and inspiration, especially in Lyon.

Ich danke all meinen Freunden und meiner Familie für die unterstützenden und lieben sms / I thank all my friends for their support via numerous text messages / Je remercie tous mes amis, les collègues de qi gong et de yoga, qui m'ont soutenue et motivée pendant les phases les plus difficiles par des textos, du qi, et leur amitié.

Ein großes Dankeschön à la famille Lemaire, qui m'a accueillie à plusieurs reprises pour la rédaction au calme de Metz et des Pyrénées, acceptant chaque fois que je m'enferme et prenant toujours soin de moi. Merci également pour votre contribution à la relecture des parties en français du manuscrit même tard le soir.

Pour trois personnes j'ai des remerciements spéciaux, pour m'avoir intégrée et pour leur soutien tout au long de ces années au labo/à Lyon/en France : Mél, tu m'as déjà sauvée pendant des moments de crise et cette super période que j'ai pu passer au labo est aussi largement grace à toi. Vivement le prochain concert, la prochaine rando

ou juste le prochain coup de fil ! Véro, meine liebe Freundin, je te remercie chaleureusement pour ton amitié, tes conseils, tes nombreux coups de fils, tes critiques constructifs. Tu m'as aidée avec autant de choses, toujours avec plein de motivation, d'énergie et ton talent d'organisatrice. Même quand il s'agissait de trucs pénibles (liste de références…) – tu as largement tenu les promesses de ton manuscrit. Pierre, der mit mir durch dick und dünn gegangen ist! Je te remercie pour les trois tonnes de chocolat qui m'ont aidé à (presque) finir le manuscrit (et quasiment sans dépression majeure), les relectures critiques et pertinentes, ton aide précieux avec la biblio, ton engagement, le fait d'avoir partagé tes expériences de thèse avec moi, ton amitié, le voyage en Bretagne qui m'a laissée respirer pour un moment.

Und schließlich meine gesamte liebe Familie (und sie ist nicht klein diese Familie), die mich jahrelang angefeuert haben, mich ertragen haben, mitgefiebert haben, mich haben wieder einmal fortgehen lassen. Ich danke ganz herzlichst jedem einzelnen von euch!

TABLE DES MATIERES / CONTENTS

LISTE DES FIGURES / LIST OF FIGURES

CHAPTER I

CHAPTER II

CHAPTER III

CHAPTER IV

CHAPTER V

CHAPTER VI

CHAPTER VII

APPENDICES

LISTE DES TABLES / LIST OF TABLES

CHAPTER II

CHAPTER III

CHAPTER IV

CHAPTER V

CHAPTER VI

APPENDICES

PREAMBULE / PREAMBLE

Cette thèse a été menée dans le cadre de l'Observatoire Homme-Milieu Vallée du Rhône (OHM-VR), un dispositif de recherche qui regroupe des scientifiques de disciplines diverses autour d'un même site d'étude, le corridor rhodanien. L'observatoire a été créé par le CNRS en 2011. Son but est de mieux connecter différents projets de recherche, d'établir des échanges interdisciplinaires ainsi que de créer de nouveau projets de recherche à partir d'un socle commun de connaissances. Un des axes prioritaires de cet observatoire en 2012 était focalisé sur les marges alluviales anthropoconstruites qui sont le centre d'intérêt du présent travail. Après seulement quelques études pilotes dans des sites isolés (par exemple Clozel-Leloup et al., 2013), ces milieux étaient encore peu appréhendés, surtout à une échelle plus large. Ce travail de thèse vise donc à établir une première caractérisation de ces espaces.

La première partie du manuscrit (chapitres I à III) présente le contexte scientifique (chapitre I) autour à la fois des processus et des fonctionnements naturels des plaines alluviales des rivières ainsi que les contraintes des rivières fortement anthropisées. Dans le cadre géographique (chapitre II), les spécificités du fleuve Rhône sont introduites, incluant notamment les aménagements hydrauliques à courant libre qui ont créé les unités étudiées dans cette thèse : les casiers Girardon. A la fin du 19ème siècle, afin de faciliter la navigation, un réseau extensif de digues longitudinales et latérales construites dans le lit mineur a corseté son tracé. Les digues forment des sortes de rectangles, les casiers, appelés selon la région caissons ou encore carrés, qui ont provoqué le comblement de ces milieux initialement aquatiques. Cela a donc fortement modifié le caractère du fleuve, limitant notamment sa dynamique latérale. Une deuxième phase d'aménagement au début du 20ème siècle a vu naître une série de dérivations à des fins de production hydroélectrique. Cette phase a fortement influencé le régime hydraulique des secteurs court-circuités. Depuis les années 1980, un changement de paradigme a eu lieu partant de cette notion de dompter le fleuve vers une approche plus écologique. Aujourd'hui, c'est notamment le concept d'espace de liberté qui dirige des interventions d'aménagement. C'est ainsi le cas de la reconnexion des « lônes », anciens bras du Rhône qui avaient été coupés du fleuve ou encore le démantèlement d'ouvrages hydrauliques. Ceci se fait dans les parties court-circuitées du fleuve, où la navigation est devenue obsolète, fournissant ainsi des

espaces potentiels pour des mesures de réhabilitation ou de mitigation. Mais le démantèlement des ouvrages soulève aussi des questions sur les milieux des casiers encore peu étudiés et leur devenir. Par exemple, dans le cadre d'un fleuve aussi fortement aménagé que le Rhône, il s'agit de savoir si des milieux anthropoconstruits pouvaient avoir des fonctions écologiques. Certains travaux les ont qualifiés comme des annexes fluviales qui contribuent à la diversification des conditions dans un espace tellement homogénéisé. La notion de '*novel ecosystems*' (nouveaux écosystèmes, *sensu* Hobbs et al., 2009 ; Morse et al., 2014) met en avant que certains milieux anthropoconstruits pourraient contribuer aux valeurs d'un écosystème et donc mériter d'être conservés. Cela est surtout considéré comme une option quand une réhabilitation du système est empêchée par des seuils infranchissables ou des coûts trop élevés. Y a-t-il des enjeux en termes de services écosystémiques, comme des stockages importants de carbone dans les boisements ? A une échelle plus large, pourraient-ils constituer des traits d'union entre des écosystèmes éloignés comme ils sont présents quasiment tout au long du fleuve ? Dans le cas des casiers, il y a également la question des usages par les riverains, comme lieu de pêche par exemple. Toutefois, comme les casiers constituent des endroits de stockage de sédiments fins, les polluants potentiellement associés sont un aspect à prendre en compte. Surtout, en cas de démantèlement, y aurait-il des risques pour des écosystèmes en aval ? Et y aurait-il donc des casiers plus ou moins pollués, ce qui pourrait jouer un rôle dans la sélection des sites du démantèlement ?

Dans le cadre de cette thèse, l'objectif était de caractériser ces unités en termes de patrons spatio-temporels de la sédimentation ainsi que d'évaluer leur potentiel écologique pour la ripisylve. Nous cherchions également à expliquer ces patrons en analysant des facteurs potentiels de contrôle. Pour ce faire, nous avons choisi une approche comparative fondée sur quelques centaines de casiers situés dans quatre secteurs court-circuités (chapitre III). Ces derniers ont été construits à différents périodes : en 1952 sur le secteur de Donzère-Mondragon (DZM), en 1957 sur Montélimar (MON), en 1966 sur Pierre-Bénite (PBN) et en 1977 sur Péage-de-Roussillon. Ils sont également repartis dans des zones climatiques différentes : continentale en amont avec PBN et PDR d'une part, et d'autre part méditerranéenne vers l'aval avec MON et DZM. De plus, entre ces deux ensembles (PBN et PDR, MON et DZM), le Rhône conflue avec l'Isère, un de ses principaux affluents en termes de sédiments en suspension. Ainsi, l'approche comparative nous a permis également

d'analyser de potentiels facteurs de contrôle. Des analyses multivariées nous ont servi pour détecter des patrons à un niveau plus complexe. Au niveau des outils, nous avons utilisé un système d'information géographique (SIG) ArcGIS pour analyser des données issues de la télédétection (images aériennes, orthophotographies, modèles numériques de terrain (MNT)), mais aussi des cartes anciennes. Nous avons complété ces analyses par des campagnes de terrain où nous avons à la fois mesuré les épaisseurs de sédiments fins et inventorié la végétation ligneuse. Une recherche bibliographique sur des unités qui ressemblent, au sens large, dans leur fonctionnement aux casiers (champs d'épis ou bras abandonnés) nous a servi pour établir un modèle conceptuel autour des facteurs contrôlant l'atterrissement. Nous avons intégré des facteurs à l'échelle du secteur, comme les flux de sédiments en suspension entrant par les barrages. A l'échelle locale, nous considérons surtout la connexion des casiers au chenal principal court-circuité comme facteur clé. Elle est à la fois influencée par le niveau d'eau qui dépend du régime hydrologique et des opérations liées l'exploitation des barrages ainsi que de la géométrie du chenal et des caractéristiques des digues. A l'intérieur du casier, ce sont ensuite les conditions hydrauliques qui déterminent potentiellement également les patrons spatiaux de la sédimentation. Cela peut inclure la rugosité exercée par la végétation ou encore les caractéristiques des écoulements.

La deuxième partie du manuscrit présente des résultats plus spécifiques par rapport aux analyses menées. Ainsi, le chapitre IV est focalisé sur les conditions spatio-temporelles contemporaines de l'atterrissement dans les casiers à l'échelle inter- et intra-secteur. Nous discutons également quelques premières variables explicatives. L'objectif était de connaître la gamme et l'organisation spatiale des conditions contemporaines afin d'évaluer l'hétérogénéité, ou inversement l'homogénéité, des habitats actuels. Des analyses comparatives et multivariées ont été menées dans ce but. Pour faciliter les interprétations des patrons observés, nous commentons ensuite dans le chapitre V des éléments concernant les trajectoires évolutives des dépôts pour répondre également aux caractères non-stationnels de ces milieux. Cela nous a permis d'interpréter les patrons en termes de processus sous-jacents. Nous nous sommes appuyés à la fois sur des analyses comparatives à l'échelle du secteur ainsi que sur des analyses longitudinales plus fines des patrons de sédimentation et des facteurs de contrôle. Le chapitre VI concerne les caractéristiques actuelles de la ripisylve. Nous nous sommes intéressés en détail à la structure et à la composition des boisements,

ce qui nous permettait d'évaluer la durabilité de ces milieux dans le futur. L'analyse des boisements s'appuyait sur la campagne de terrain de 2014. Pour mieux pouvoir comprendre les conditions qui prédominent dans les casiers, nous l'avons comparé à deux sites de référence, situés aux deux extrémités d'un gradient de succession et de connectivité : une base de données sur la rivière Drôme représente les conditions d'îlots pionniers, tandis que des relevés issus de la Réserve Naturelle de l'Ile de la Platière fournissent des références de boisements d'un stade mature.

La dernière partie de la thèse soulève des réflexions plus globales. Dans le chapitre VII, nous synthétisons et discutons des interprétations concernant les résultats principaux des chapitres IV à VI en s'appuyant sur la bibliographie. Nous revenons ici aux principales questions de recherche visant à caractériser les conditions d'habitat des casiers. Pour conclure, dans le chapitre VIII, nous souhaitons résumer les différents aspects étudiés dans les chapitres précédents afin de donner une vue sur l'ensemble des caractéristiques des casiers mais aussi réfléchir aux travaux de réhabilitation à plus large échelle, en ne se limitant pas uniquement au domaine des casiers. Nous abordons la question d'une potentielle contribution des casiers, à l'état actuel ou modifié, à une diversification des habitats sur le Rhône au sein même des secteurs individuels (entre les casiers et vis-à-vis d'autres unités, comme le chenal du Rhône total, le Rhône court-circuité, les lônes) et entre les secteurs. Outre cet éventuel potentiel écologique, sont aussi pris en compte ici les risques potentiellement liés aux polluants ou aux espèces exogènes. Ces éléments serviront de base pour un processus de décision plus éclairé.

CHAPTER I INTRODUCTION

Résumé du chapitre I : introduction

La première partie du chapitre I dessine d'abord le contexte naturel et anthropique des cours d'eau, leur plaines alluviales et leur ripisylve, afin de fournir un référentiel en termes de processus, de fonctionnement et d'habitat pour l'étude des casiers Girardon. Parmi les multiples pressions exercées sur les grands fleuves, nous présentons en détail les principaux aménagements hydrauliques et leurs impacts. Nous rappelons également les effets cumulatifs des facteurs de contrôle. Ensuite, nous abordons les changements de paradigme qui ont eu lieu en termes de gestion des rivières. Nous sommes en effet passé d'une notion de domptage de la rivière vers des approches écologiques et plus durables, intégrant le bassin versant dans sa globalité. Nous finissons cette partie en présentant quelques exemples d'approches intégratives de gestion sur d'autres fleuves Européens, qui souvent visent à intégrer simultanément des aspects de navigation, de risque d'inondation, de production hydroéléctrique et d'écologie. La deuxième partie du chapitre fournit des éléments conceptuels du manuscrit, incluant les objectifs de recherche et la structure de la thèse.

In this chapter, we shall first define river-floodplain systems in the Anthropocene context. We present natural processes, functions and habitats of undisturbed floodplains. Based on this, we then describe some of the major engineering works applied on large rivers and their impacts. Subsequently, we refer to the paradigm shifts in river management in light of the highly modified systems and the implications for the evolving conservation and restoration practice. We investigate several approaches to large river restoration. In the final section of this chapter we introduce the objectives and research hypotheses of this work, and guide through the structure of the manuscript.

1 Context: River-floodplain systems in the Anthropocene

The long history of human uses of rivers and their floodplains has created complex systems, often with partly natural, partly 'novel' ecosystem characteristics, sometimes

even 'designed' (*sensu* Hobbs et al., 2009; Morse et al., 2014). Scientists have proposed to consider a new geological era, which is based on a 'dominant' or 'overwhelming' impact on environmental processes by human activity, compared to natural processes (Crutzen, 2002; Rhoads et al., 2016; Waters et al., 2016; Brown et al., 2017). Flow regulation and training are among the human activities which have most profoundly changed the natural riverine processes and functioning worldwide (Brookes, 1992; Dynesius & Nilsson, 1994; Nilsson et al., 2005). Particularly channel-floodplain interactions are extremely threatened, although they are amongst the most productive and ecologically diverse systems on earth (Tockner & Stanford, 2002; Opperman et al., 2009; Brown et al., 2017). Yet, it remains difficult to disentangle the effects of human activities and natural environmental change, as well as to define exactly when a system is human 'dominated' and when it is not. Abundant research over the last centuries has provided a better understanding of the processes in natural fluvial systems, but there is still a knowledge gap when it comes to highly modified large river systems. Generally, such rivers are subject to a multitude of different uses, whose individual roles have changed through time, and which sometimes have contrasting objectives. Restoration programmes struggle to define sustainable objectives which integrate human uses and ecological functioning—what should the rivers of tomorrow look like?

1.1 Natural floodplains

According to Leopold et al. (1995, p. 317), a floodplain is "a strip of relatively smooth land bordering a stream and overflowed at time of high water". Lewin (1978, p. 408) adds the notion of floodplains as "sediment sinks or stores," to this hydrological definition, "in which eroded and sorted sediments accumulate, are reworked, or indeed undergo biogenic or pedogenic processing for extended timespans." The term 'reworking' points out that floodplains are formed and reformed by both, deposition and erosion processes. Nanson & Croke (1992, p. 460) more specifically distinguished the genetic floodplain, to introduce the notion of geomorphic history, which they defined as "the largely horizontally-bedded alluvial landform adjacent to a channel, separated from the channel by banks, and built of sediment transported by the present flow-regime." Terraces, formed under prior flow regimes, are distinguished from floodplains by a much lower frequency of their overflow (Wolman & Leopold, 1957). They can be created by tectonic or climate change events, which force the river to incise

its bed below the ancient floodplain. Hence only when changes in the structural, climatic, or physiographic conditions occur, which control the natural regime. However, such a spatial distinction of ancient and contemporary alluvia is in reality often more complex (Nanson & Croke, 1992).

1.1.1 Processes of floodplain formation and evolution

Goudie et al. (1999, p. 446) define fluvial sediment as "particles derived from rock or biological material that are, or have been, transported by water". This may involve the "contemporary transport" but also the "deposits associated with contemporary and past fluvial activity" and thus the alluvia floodplains and terraces consist of. It is helpful to consider the differences between fine (colloidal particles, clay, silt, i.e. ≤ 63 µm) and coarse sediments (sand, gravel, cobble, boulder, i.e. > 63 µm), which play different roles in the river system and behave differently (e.g. Kondolf et al., 2014). Coarse sediment is generally moved as so-called 'bed load' by sliding, rolling, or saltation on or very close to the river bed. Fine-grained sediment is transported in suspension in the water column due to turbulence. Depending on the conditions of flow, as well as the material properties, a particle that has been moved as bed load at one instant may be moved as suspended load at another instant and vice versa. Generally speaking, the grain size threshold between bed load and suspended load lies between 0.2 mm and 0.7 mm, sometimes up to 1 mm or higher (Maniak, 2010; Owens, 2005). Due to their cohesiveness, fine particles frequently form aggregates or flocs and are primarily transported as such (Slattery & Burt, 1997; Droppo & Ongley, 1994).

Floodplain sedimentation occurs during overbank flows, when sediments (and momentum) are transferred out of the channel. While inbank flow has three-dimensional characteristics, it is the one-dimensional flow in downstream direction which is generally considered to predominate. At the channel-floodplain interface, as well as on the floodplain itself, conditions are generally more complex, and all three dimensions need to be considered. Consequently, sediment transfer may involve different mechanisms, namely convection and turbulent diffusion processes, bedload transport of coarser material, advective suspended sediment transport and secondary flow paths (James, 1985; Pizzuto, 1987; Marriott, 1992), or combinations of them. Sediment is deposited where flow velocities decrease below the transporting capacity. Deposition patterns thus depend on flow velocity and current characteristics, suspended sediment concentrations and grain size distributions, floodplain micro-

topography, as well as inundation time. Typical patterns include, for instance but not necessarily: an exponential decrease in deposition as well as grain size of the deposited material with distance from the channel (Pizzuto, 1987; Walling & He, 1998) or an increased deposition in depressions (Marriott, 1992; Asselman & Middelkoop, 1995). The latter is an effect of a) high water depth more likely to contain a high total mass of sediment, b) long inundation time as flood water is ponded after the flood retreat and sediment settles out, and c) local variations in flow velocities and directions.

The described overbank vertical accretion processes are however not the only processes of floodplain formation. They further include processes such as lateral point bar accretion, braid-channel accretion, oblique accretion, counterpoint accretion, or abandoned-channel accretion. Depending on the river channel pattern and physiographic constraints within the valley, these processes can highly vary in their respective importance. First floodplain classifications were primarily based on channel planform types (e.g. Lewin, 1978). Different planforms have been related to typical sedimentary features on the floodplain, such as oxbow lakes (abandoned meanders) or point bars on meandering rivers or abandoned braid channels, longitudinal and transverse bars in multi-channel rivers. In reality, the various planform types and related processes occur along a continuum or in combination and are thus not necessarily discreet in space or time (Brierley & Hickin 1992; Brown, 1996). It became evident that both sedimentological and fluvial geomorphological aspects should be considered in the analysis of floodplain deposition processes. This culminated in the architectural element approach (e.g. Miall, 1985; Brierley & Hickin 1992). Nanson & Croke (1992) finally proposed a classification system where they integrated fluvial processes, sediment characteristics, and stream power. They distinguished three classes, namely high-energy non-cohesive, medium-energy non-cohesive, and low-energy cohesive; and thirteen orders and sub-orders.

1.1.2 Diversity of forms, conditions and habitats

The complex processes on natural floodplains of dynamic migrating rivers and the resulting array of landforms described in the previous subsection provide diverse habitats and ecotones (Figure I–1; Amoros et al., 1982; Amoros et al., 1987). These show gradients of connectivity to the channel and of successional stages, ranging from

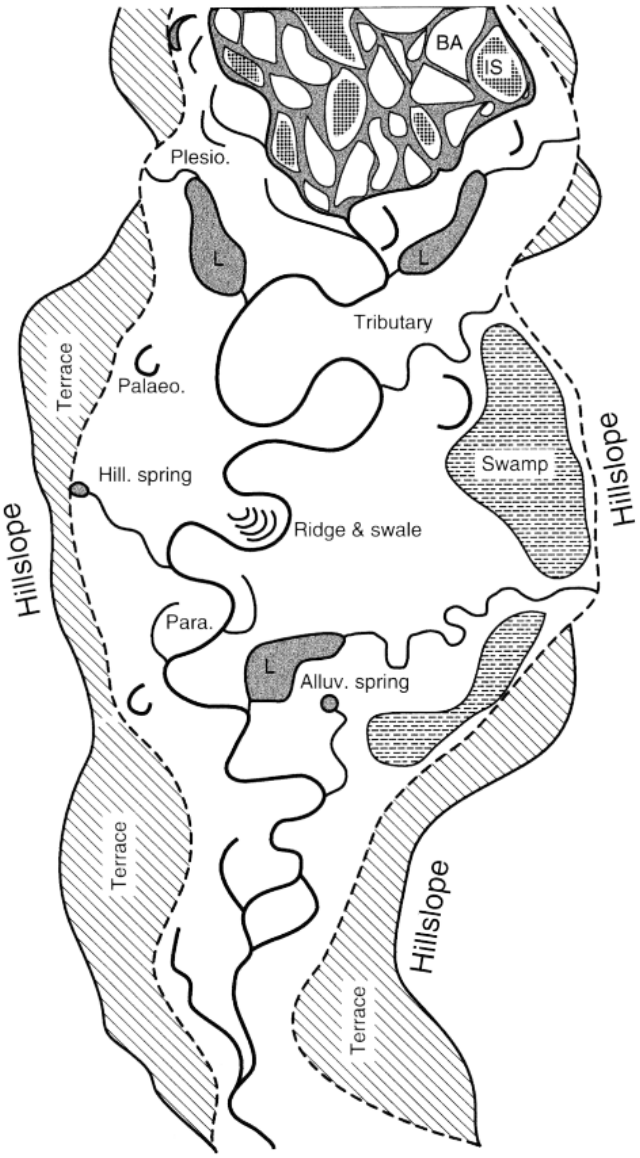

Figure I–1: Schematic example of geomorphic landforms of river-floodplain systems along a gradient of connectivity and successional stage (Ward et al., 2002, based on the classification from Amoros et al., 1982 and Amoros et al., 1987): lotic main and side channels (= eupotamon), tributary streams and alluvial springbrooks, semi-lentic cut-off channels connected to the main channel system at the downstream end (= parapotamon; e.g. abandoned braid channels close to the active channel), permanent or temporary lentic water bodies without permanent or direct connection to the main channel system but highly influenced by river discharge (= plesiopotamon), and permanent or temporary lentic water bodies without permanent or direct connection to the main channel system and only mildly influenced by river discharge (= paleopotamon; e.g. abandoned meander loops), terrestrial bars or levees.

aquatic and semi-aquatic (both lotic and lentic) to terrestrial. Terrestrialisation denotes the evolution of a water body from an aquatic to a terrestrial state, by processes of sedimentation (both autogenic and allogenic) and / or dewatering due to the disconnection from the channel or groundwater (e.g. Hohensinner et al., 2011). This dewatering can be gradual or abrupt depending on the mechanisms controlling the

disconnection. Along with the succession of the habitats goes an ecological succession, both being spatially as well as temporally diverse. Many species in these biocoenoses are adapted either to the conditions of a specific biotope or change between biotopes of different connectivity in the course of their life cycle (Jungwirth et al., 2003). In the following we shall look in more detail at the colonisation and succession patterns of woody riparian vegetation.

1.1.3 Co-evolution with riparian forests

In alluvial rivers, the formation and reformation of floodplains is also closely inter-linked with vegetation colonisation and the evolution of riparian forests (Florsheim et al., 2008; Corenblit et al., 2007; Corenblit et al., 2011). Where new landforms are created, or older ones reworked, bare and moist substrate becomes available for colonisation by pioneer species (Scott et al., 1996; Mahoney & Rood, 1998). In turn, the physical presence of the plants themselves will have an impact on hydraulic conditions and will thus influence sedimentation and erosion patterns (Gurnell et al., 2001; Corenblit et al., 2007; Corenblit et al. 2011). Pioneer species, such as the *Salicaceae* family, have developed specific traits to adapt to the dynamic and disturbance prone fluvial environment (Braatne et al., 1996; Karrenberg, 2002; Corenblit et al., 2014). Their colonisation pathways are manifold, and the individual contribution of each varies between river systems, according to prevailing physical processes (e.g. Cooper et al., 2003; Dykaar & Wigington, 2000; Räpple et al., 2017). The respective physical template leaves an imprint in the characteristics of the riparian vegetation patches, especially their spatio-temporal distribution patterns (e.g. Ortmann-Ajkai, 2014). Common pathways and related vegetation patterns include:

- lateral point bar formation with the development of even-aged bands of vegetation (Everitt, 1968; Bradley & Smith, 1986);
- evolution of other bar forms, such as central bars and side bars, which show varying spatial patterns in vegetation stands, but often even-aged patches (Dykaar & Wigington, 2000; Cooper et al., 2003);
- vertical accretion of intermittent or abandoned channels, resulting in more irregular spatio-temporal vegetation patterns (Friedman et al., 1996; Dykaar & Wigington, 2000; Cooper et al., 2003; Polzin & Rood, 2006; Stella et al., 2011);

- low-elevation parts of the channel bed exposed during prolonged periods, i.e. when flows remain below those with channel reworking capacities (Scott et al., 1996). Spatio-temporal vegetation patterns are variable;
- wood deposits and related island landforms (Gurnell et al., 2005).

Recruitment success and establishment rates differ between these pathways (Stella et al., 2011). In general, the recruitment of pioneer species depends on a complex set of interacting abiotic and biotic factors. Räpple et al. (2017) have summarised the successive establishment phases based on a literature review. This starts with available seed sources or other propagules (Salicaceae can reproduce abiotically), the timing of dispersal with respect to hydrological events, transport mechanisms (wind and water), and entrapment on a suitable, i.e. bare and moist surface (Rood et al., 1994; Chambers, 1995; Scott et al., 1996; Gage & Cooper, 2005; Gurnell et al., 2004; Stella et al., 2006; Francis et al., 2005). Once in place, many factors influence germination and seedling establishment, or the establishment from vegetative propagules, respectively (Cooper et al., 1999; Guilloy-Froget et al., 2002; Francis et al., 2005; Corenblit et al., 2014). The mortality rate of young seedlings is high, mainly related to erosion, burial or desiccation (Johnson, 1994). Mahoney & Rood (1998) proposed the so-called 'recruitment box model' where they present conditions for successful recruitment, including the recurrence interval of the flood event, flow recession rates, and elevation. Further research suggests that recruitment can also successfully sustain the species pool under less favourable conditions by shifting to 'safe sites', i.e. (Bertoldi et al., 2011; Stella et al., 2011; Dufour et al., 2015).

Reach scale vegetation dynamics and the resulting mosaic of vegetation patches are highly dependent on the floodplain turnover dynamics. Turnover rates vary greatly with channel pattern, with usually high rates in braided channels and much lower rates in straight channels (Beechie et al., 2006). Straight channels are hence generally dominated by older surface patches, braided channels by younger surface patches, and island-braided and meandering channels show a combination of both young and old (Ward et al., 2001; Beechie et al., 2006; Surian et al., 2015). This has implications for the age distribution in vegetation and thus their succession, which consequently will influence biodiversity. Four successional stages are generally described (Oliver & Larson, 1996, cited by Naiman et al., 2005), which will involve different species (Figure I–2). In the establishment phase, plants colonise bare surfaces. This is followed by the

stem exclusion phase, during which the available space is first completely occupied and then competition becomes a primary factor of survival. Some fast-growing pioneers change from a multi-stemmed to a single-stemmed habit. Mortality in the overstorey then allows new understory development, often with more shade-tolerant species. In this so-called understorey re-initiation phase, a multi-layered canopy evolves. Finally, in the mature stage, mortality of individuals opens up space for extensive regeneration and a multi-aged stand of diverse structure develops. Such stands show all, a diverse understorey, living old trees, dead standing trees, and fallen logs. A major flood disturbance event can partly or fully remove vegetation stands at any stage and re-initiate a successional pathway in this site. In a river reach, patches of different stand ages and successional stages co-exist.

1.2 Nature and functioning of river engineering works

The first hydraulic works have been applied to rivers by the very first civilisations in China, Mesopotamia, and Egypt for flood control and to improve the conditions for agriculture and navigation (Bethemont, 2000; Downs & Gregory, 2014). The culmination point was reached in the late twentieth century, when massive installations of engineering structures left behind highly modified rivers. River engineering works can be divided according to Downs & Gregory (2014) into a) river channel modifications (which include so-called 'channelization' measures as used in

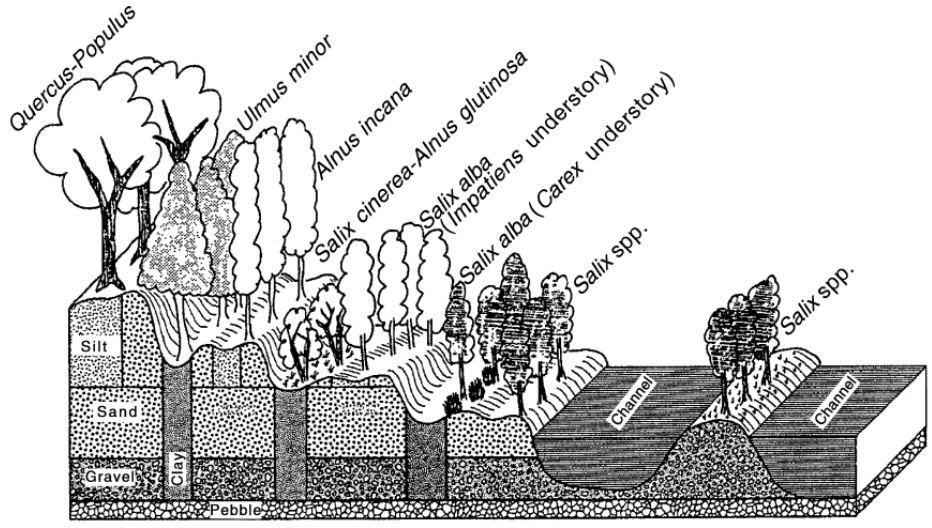

Figure I–2: Zonation of dominant species in woody riparian vegetation assemblages along a lateral transect on a braided reach of the Upper Rhône River (Ward et al., 2002, modified after Pautou, 1984).

American terminology (e.g. Brookes, 1992; or Wasson et al., 1995, who adapted Brookes' work for the French territory) but goes also beyond) and b) river discharge regulation (e.g. Petts, 1999). Measures of channel modification aim at controlling the channel morphology, while regulation measures are used to modify the river discharge regime and control water levels. We shall present some of the measures that are common to many large rivers in- and outside of Europe.

1.2.1 River channel modification measures

Several measures are used in channel modification, sometimes individually, but often in combination, including (Downs & Gregory, 2014; American terminology in brackets based on Brookes, 1992):

- Maintenance, clearing and snagging (AE: Clearing and snagging)
- Dredging (AE: Clearing and snagging)
- Channel training
- Re-sectioning (AE: widening/deepening)
- Embankments (AE: levee construction)
- Realignment (AE: straightening)
- Canalization
- Bank protection (AE: bank stabilization)
- Bed protection
- Flood walls and lined channels
- Floodplain modifications

The first river channel modification/training works date back to the 16th century and were carried out on the Yellow River in China using embankments (Przedwojski et al., 1995). In Europe, the largest part of the channel modification actions took place in the 18th and 19th century. We shall present in more detail some of the measures which are relevant to this research, including mainly river training and bank protection structures. Przedwojski et al. (1995) name

- **longitudinal dikes**
- **groynes** (also 'groins' or 'spurs/spur dikes/spur dykes' or transverse dikes)

- **cross dikes** tying in longitudinal structures to the bank to divide the closed-off channel spaces
- **closures** to cut off secondary channels
- **sills** to stabilise the bottom of the river according to a corresponding longitudinal slope
- **revetments** for bank protection
- **bed load traps.**

They can constitute permanent or impermanent structures according to construction materials (Downs & Gregory, 2014).

Longitudinal dikes and cross dikes

Longitudinal dikes, like embankments, can be applied for flood risk management. They protect the floodplain from flooding by confining all flow up to the so-called design discharge. The design discharge determines their crest height. Confining the flow to a narrower cross-section leads to increased water depths and higher flow velocities, increasing scouring. Longitudinal dikes are therefore also used within the active channel to improve the navigability. Their aim is then to direct the current along a designed alignment to induce scour and obtain a channel of controlled dimensions. The resulting channel will provide greater water depths and boundaries with smooth curvatures and without shoals, providing a gentler current line. To facilitate the silting up of the areas behind the dike (in direction of the former banks), and to prevent undercutting, cross dikes are built to tie the longitudinal dikes to the river banks.

Groynes

Groynes are transverse structures whose purpose is to deflect the flow, prevent bank erosion, and modify and maintain a certain channel form (Przedwojski et al., 1995). They are traditionally used in river training and bank protection. They consist of small dams that are generally attached to the river bank or another training structure at their so-called 'root' end. The end facing the river is called the groyne head. The design of groynes depends on the actions on stream flow that are sought. The following parameters play a major role (e.g. Beckstead & Samide, 1975; Yossef, 2005; Weitbrecht, 2004):

- **permeability**, depending on the construction materials (stone, gravel, rock, earth, pile, bamboo, timber) and their arrangement;

- **crest height and slope**, either submerged or non-submerged, completely or partially;
- **shape in plan**, including straight with round/T-shaped/L-shaped head, wing or tail, hockey/inverted hockey, among others;
- **crest width and side slopes;**
- **spacing** between successive groynes (= width);
- **projection into the river** (= length);
- **width to length ratio;**
- **orientation to the flow**, resulting in either attracting, deflecting, or repelling groynes;
- **groyne roots;**
- **location within the river reach.**

Initially, groyne design was based on practical experiences. On the River Elbe, the first groynes were constructed in the 1500s (Weitbrecht, 2004). The long and wide-spread tradition of groyne use resulted in a multitude of different design schemes.

Sills

Sills, or low-flow weirs, are submersible structures which are installed perpendicular to the flow, extending across the entire width of the channel (Przedwojski et al., 1995; Brookes, 1992). Downs & Gregory (2014) name as objectives the control of the local bed slope, of bed and water surface elevation, as well as the prevention of bed degradation and upstream head-cutting. They cause only a minimal backwater effect due to their low crest height (0.20 to several meters according to Przedwojski et al. (1995) and lead to the formation of a scour pool directly downstream. The eroded material is deposited a little further downstream where it may form riffles. Both the crest height and spacing (when built in series) of the sills are important design parameters. To prevent lateral erosion, banks around them generally require protection and the sills need to be tightly fixed to them.

1.2.2 River regulation works

For the control of river flows and water levels principally dams and weirs are applied:

Dams

Bligh (1915, p. 2) defines a dam as ‘an impervious wall of masonry, concrete, earth or loose rock which upholds a mass of water at its rear, while its face or lower side is free from the pressure of water to any appreciable extent’. The objective of dams is to capture the water and control the magnitude and timing of the flow released

downstream according to the respective human demands (Poff & Hart, 2002). These demands include irrigation, hydropower production, water supply, flood control, recreation, or fish passaging, either in single- or multi-purpose approaches (World Commission on Dams, 2000). Large dams are defined by the International Commission on Large Dams (2011) as a) dams with a height ≥ 15 m, or b) a dam of a height between 5 and 15 m with a reservoir volume > 3 million m^3. Are distinguished reservoir storage dams, which impound water (seasonally, annually, or inter-annually) and regulate the flow, and run-of-river dams (World Commission on Dams, 2000). The latter have no, or very small reservoirs and their functioning is based on the creation of a hydraulic head, using diversion dams which direct the flow to a canal or power station. In both categories of dams, their design (scale, construction material), operation and consequently impacts are highly diverse.

The earliest known large-scale dam, the Sadd el-Kafara gravity dam, had been constructed on the Nile River in approximately 2600 to 2700 BC but burst relatively soon under the force of the water (Murray, 1955; Garbrecht, 2016). Although an ancient technique, technological innovations from the period following the industrial revolution have greatly increased the size and use of dams for various purposes (Downs & Gregory, 2014). In the early 2000s, more than 45,000 large dams were counted worldwide and an estimated 1,700 were under construction (World Commission on Dams, 2000). The number of small dams was estimated to amount to several millions. In Western Europe and North America a peak in dam construction was reached in the 1970s and most of the potentials are today exploited. Several thousand new projects are currently being planned or under construction in developing countries and emerging economies, especially in Southeast Asia, South America, Africa or the Balkans (Zarfl et al., 2015).

Weirs

A weir is essentially a dam, whose crest is overflown by the water and whose tail water forms below the structure (Bligh, 1915). This implies different conditions of stress on a weir, compared to a dam. Weirs absorb the energy of the flow and thus reduce the sediment transport capacity. They fix the river bed, raising bed and water levels upstream and potentially inducing erosion downstream (Downs & Gregory, 2014).

1.3 Impacts from river engineering works

Nilsson et al. (2005) demonstrated that more than half of the world's large river systems are impacted by dams. Most large rivers, but also many smaller ones, have undergone channel modifications (e.g. Brookes et al., 1983). Due to the various technologies and designs of both river regulation and channel modification measures, impacts can vary significantly from one project to another. Also, the individual history and river basin characteristics of each river system will influence responses to engineering. The consideration of change in fluvial systems must take into account varying temporal scales (Przedwojski et al., 1995): compared to geological time scales, hydraulic conditions may change rapidly, while the consequent adaptation of the morphological parameters can take place over much longer time scales. Consequently, in many fluvial systems, several transient processes might be occurring at any one time, whose origins may date back to different periods. On the spatial scale, three dimensions need to be considered additionally to the temporal dimension following the fluvial system concept after Schumm (1977) and the fluvial hydro-system concept after Amoros & Petts (1993): the longitudinal, lateral, and vertical dimensions. In the following we shall summarize exemplarily some hydro-geomorphological and ecological impacts of river engineering works.

1.3.1 Hydro-geomorphological impacts

River channel modifications

River training works using lateral and longitudinal dikes fix the channel planform by directing the flow toward the thalweg and away from the banks. They also reduce the width of the channel cross-section. The concentration of the flow increases stream power and induces a degradation or incision of the channel, as well as changes in bed slope (Wyżga, 1991). While scour implies a temporary and localised erosion of the channel bed, degradation is a more extensive longer-term process over longer distances (Galay, 1983). As a consequence of degradation, the water carrying capacity of the channel increases and overbank flows thus become less frequent. This reduces the sediment storage capacity of the floodplain, while suspended sediment transport in the channel itself is increased (Wyżga, 2001a). The increased depth of the water column also has an effect on the grain size of the sediment deposited on floodplains, as the concentration of coarser suspended sediment decreases in the water column

toward the top (Vanoni, 1946, cited by Wyżga, 2001b). On many rivers, in-channel gravel or sand mining activities locally exacerbated the degradation trend (e.g. Bravard, 1994; Landon & Piégay, 1994).

When bed scour creates a knickpoint, this can lead to an upstream progression and an adjustment of the channel slope beyond the trained river reach (Kondolf, 1997). Conversely, as floods propagate more rapidly downstream in a trained river, this generally also leads to adjustments of channel sections in these parts of the river. On the one hand, this leads to channel enlargement and/or deepening due to bank erosion and/or degradation. On the other hand, sediments eroded in the trained reach may also lead to aggradation by deposition downstream. Eventually, also tributaries will adjust to bed level changes in the main channel.

Toward the banks, where the engineering structures are implanted, the situation is different, as shall be exemplified through the case of groyne fields. Groynes are most commonly built in sequence and the area between two groynes is commonly denoted as groyne field. Under conditions where the groynes are not submerged, so-called dead water zones establish in the groyne fields, with complex recirculating flows. Flow separation at the groyne head leads to secondary flows: according to the geometric characteristics of the groyne fields (width-to-length ratio, shape), one or several gyres, i.e. a vortex with a vertical rotation axis, form (Uijttewaal, 1999; Sukhodolov et al., 2002). The recirculating flows produce distinct and diverse patterns of sediment deposition and erosion, for which Sukhodolov et al. (2002) published a first morphological typology based on the work from Hannappel & Piepho (1996) and Hinkel (1999) (Figure I–3). Yossef & de Vriend (2010) showed different suspended sediment input processes under emerged and submerged conditions of the groynes: under emerged conditions, advection follows the direction of the primary gyre, while under submerged conditions, residual advective transport prevails. Erosion in groyne fields on the River Waal was highly influenced by navigation (Ten Brinke et al., 2004). Groyne fields influence the momentum and mass transport in the river and thus for instance also the transport and fate of contaminants. They function as temporary sinks for sediment and related contaminants (Weitbrecht, 2004; Weitbrecht et al., 2008; Schwartz & Kozerski, 2003). Due to the complex nature of the hydraulic conditions in groyne fields, their extensive use and highly variable designs and applications,

Class	Definition	Pattern
1	weak deposition	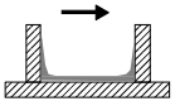
2	downstream triangle-shaped deposition	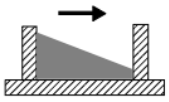
3	upstream triangle-shaped deposition	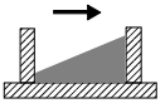
4	downstream wave-shaped deposition	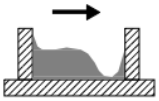
5	upstream wave-shaped deposition	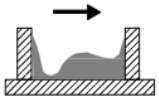
6	uniform partial deposition	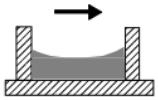
7	uniform complete deposition	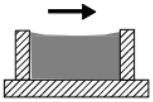

Figure I–3: Morphological classification of groyne field sediment deposits (Sukhodolov et al., 2002; based on works from Hannappel & Piepho, 1996 and Hinkel, 1999).

research continues to be accomplished in this field (Wirtz, 2004; Tritthart et al., 2009; Zsugyel et al., 2012).

River flow regulation

Dams directly modify the water and sediment regimes of a river and thus the driving variables (Thorne et al., 1997) of its inherent morphological processes. Dam characteristics, purposes, and operation are highly variable and consequently their impacts are highly complex. In general, the timing of characteristic water flows is modified, as well as the flood hydrographs in all its dimensions: reduced magnitude of peak flows, frequency, duration, volume (Kellerhals, 1982). Sediments are commonly trapped by the dam, leading to an excess of sediment upstream of the dam and deficits in downstream sections. A short overview of some of the potential local-, reach-, and river basin-scale impacts of reservoir dams shall be given in the following. More specific

information on run-of-river dams is given in chapter II exemplified by the Rhône River diversion schemes.

In the reservoir of dams, often most of the bed load and part or most of the suspended sediment load are deposited under the conditions of quiet water (Guertault et al., 2014). Backwater effects may extend further upstream and likewise lead to deposits there (Kondolf, 1997), and even in tributaries (Wang et al., 2007). Most research has focused on the conditions downstream of dams, which are likewise spatially and temporally complex (e.g. Kellerhals, 1982; Brandt, 2000; Surian & Rinaldi, 2003; Petts & Gurnell, 2005; Schmidt & Wilcock, 2008; Rollet et al., 2014). Following the relationships established by Lane (1955), the modified water and sediment regimes entail an adjustment of either cross-sectional geometry, gradient, planform, or sediment texture (Petts 1984; cited by Church, 2015). For instance, the general reduction in water flows reduces the sediment transport capacity below the dam, implying that bed materials of certain calibres may not be moved anymore. At tributary confluences, this entails the risk of aggradation, as the sediment supplied to the main stem is no longer moved. Where flood flows are reduced, the channel is not reworked over its entire width anymore, which leads to channel narrowing. Channel bars are less frequently or no longer submerged. Both narrowing and bar emersion favour vegetation colonisation (e.g. Johnson, 1994), which eventually reinforces fine sediment accumulation and further channel narrowing. Eventually, this reduces the channel capacity with implications for flood risk management.

The sediment deprived clear water reaching the downstream section below dams with high sediment trapping may in certain cases lead to extensive bed degradation (‘hungry water effect’; Kondolf, 1997). This is generally the case when the flow released is still competent enough to transport the respective bed grain size, often when the river bed is made up of fine-substrate or dam operation allows flood waters to pass. This may also lead to channel bed ‘armouring’, where a selective transport has removed fine bed material, leaving only the coarse sediment in place (Kondolf, 1997). Channel narrowing and degradation may eventually induce changes in channel pattern of the main stem (Surian & Rinaldi, 2003). Lowered water levels or base levels in the main channel might moreover imply morphological adjustments in the tributaries (Brandt, 2000).

It is commonly agreed today that most large river systems experience a deficit in sediment at their outlet, largely as an effect of dams and reservoirs (Walling & Fang, 2003; Vörösmarty et al., 2003; Syvitski et al., 2005). Even where increased erosion and denudation activity related to land use changes are observed in the river basin, the sediment yield to the sea may have declined due to dams which trap the sediments (Syvitski et al., 2005). This leads to severe coastal erosion (Owens, 2007).

International Sediment Initiative (2011) summarise some of the operational aspects related to sediment issues around dams: when dams trap large quantities of sediment in their reservoir without any counter-measures, their storage capacity can greatly reduce over little time. The high social, economic, and environmental costs of reservoir dams however require an optimised use by extending their life time. Both water intakes and outlets for hydropower production may be clogged and abrasion of the machinery can lead to significant maintenance costs. Downstream of the dams, sediment deficits can imply damages to engineering structures related to channel degradation and erosion around the structures (Kondolf, 1997). This leads to security risks, for instance when bridges show cracks or collapse.

1.3.2 Ecological impacts

The physical modifications of human engineering works on rivers entail significant impacts on their ecosystems, some of which we present in the following. Impacts from river channel modifications have not been as well documented as for instance river flow regulation impacts (Ward, 1998; Van Looy et al., 2003; Dufour et al., 2007).

River channel modifications

River channel modifications primarily concern the lateral dimension of the fluvial hydrosystem by disrupting the hydrological connectivity between the channel and its floodplain, as well as lateral channel migration. Resulting channel degradation induces a decline in the water table, also the associated groundwater table lowers with consequences for related ecosystems (Stromberg et al., 1996; Stella et al., 2013). In riparian vegetation stands, this may include the die-back of phreatophytic species and eventually changes in species composition and structural characteristics (Décamps, 1988; Schnitzler, 1994; Trémolière et al., 1998; Dufour et al., 2007). Reduced disturbance frequencies limit the creation of suitable habitat for pioneer riparian species (Egger et al., 2007). Floodplain waterbodies which provided—often seasonally

changing—feeding, spawning and nursery grounds, may either no longer be reached by laterally migrating animal species or undergo accelerated succession (Ward, 1998; Hohensinner et al., 2011). As a consequence, habitat diversity generally declines, even if this trend is not always exactly unidirectional (Hohensinner et al., 2011). Riparian vegetation species diversity sometimes decreases (VanLooy et al., 2003) and sometimes increases (Trémolière et al., 1998), however always at the expense of alluvial species and with alterations of structural characteristics.

River flow regulation

The most obvious and direct effect of dams on ecosystems it the obstruction of migratory pathways and also the inundation of huge areas of land, including both formerly terrestrial and riparian zones, in the case of large reservoir dams (Nilsson & Berggren, 2000). Reservoirs generally destroy the former ecosystems and the decomposing organic matter poses a risk of greenhouse gas emissions, nutrient and other chemical substances releases, and conditions of anoxia (Baxter, 1977). This in turn may lead to excessive growth of plants and potentially eutrophication. Conditions in large reservoirs often rather resemble lake ecosystems—being it with regards to flow velocities, substrate, turbidity, or thermal stratification—to which rheophile species are not adapted (Jungwirth et al., 2003). An excess of sediment in the reservoir sections or downstream caused by operational measures such as flushing (see section 1.6.2) can likewise cause significant environmental impacts. This includes clogging, i.e. the deposition of fine sediment within the interstices of coarse sediment constituting the channel bottom, with impacts on hydraulic conductivity, fish spawning sites and macroinvertebrate habitat, and the self-purification potential of the river (e.g. Wood & Armitage, 1997). Turbidity, can likewise be an important factor for species survival or loss, impacting organisms directly or indirectly via changed primary production, and thus food webs, nutrient cycling and biochemical processes. New shore-line ecosystems may develop along the reservoir edge, which are however controlled by regulated water level fluctuations and develop under specific soil conditions and sedimentation and erosion processes. Downstream of the dam, altered hydrological and sediment regimes, including lowered groundwater levels, modify the species composition of riparian vegetation (Décamps et al., 1988; Nilsson & Berggren, 2002). Pioneer species are adapted to the specific disturbance regime of the river (Johnson, 1994), which is eliminated by the effects of the dam, impeding regeneration and

leading to the die back of existing individuals (Stromberg et al., 1996). In contrast, other species may find favourable conditions, often including non-native species. The modified timing of floods disrupts the specific cycles of riparian vegetation, but also of mammals or birds (Nilsson & Deynesius, 1994; Dudgeon et al., 2000). Dams can thus have far reaching impacts, which superimpose each other where chains of dams exist along rivers. Downstream ecosystems which rely on a sediment and associated nutrient delivery for their functioning, such as wetlands, floodplains, estuaries or coastal zones may degrade far away from the dam itself. Overall, dams are counted among the most important threats for riverine biodiversity (Nilsson & Deynesius, 1994; Dudgeon et al., 2006).

1.4 Other pressures

Generally, it is the combined effects and interactions between all the pressures acting on river-floodplain systems which exacerbate the effects on their functioning (see section 1.5). We shall thus give some background information on other major pressures, too. As mentioned earlier, human uses of rivers are multifaceted, vary spatially, and the importance of individual uses has changed through time, although the principal interests remained (resource use, transportation, risk reduction; Jungwirth et al., 2003; Netzband, 2007). Indirectly, land use changes in the river basin (agriculture, urbanisation) modify the hydrological and sediment regimes. They are among the most ancient human pressures on rivers. Direct influences, next to the engineering works already mentioned, include settlements and agricultural uses on floodplains, in-channel sediment mining, drinking water supply. On a very simple scale, Lewin (2013) distinguished four major phases of floodplain transformation (Figure I–4), admitting that considerable spatial variations exist. He noted the reduction in industrial pollution in rivers of the developed countries due to point source control measures, however Dudgeon et al. (2006) stressed the fact that overall, pollution is still increasing in rivers today, particularly as a result of diffuse sources (nutrients and other chemical substances, including endocrine disruptors). Furthermore, even though water pollution has decreased, the historical pollution of sediments persists and has become an important issue in relation to sediment storage environments, such as floodplains.

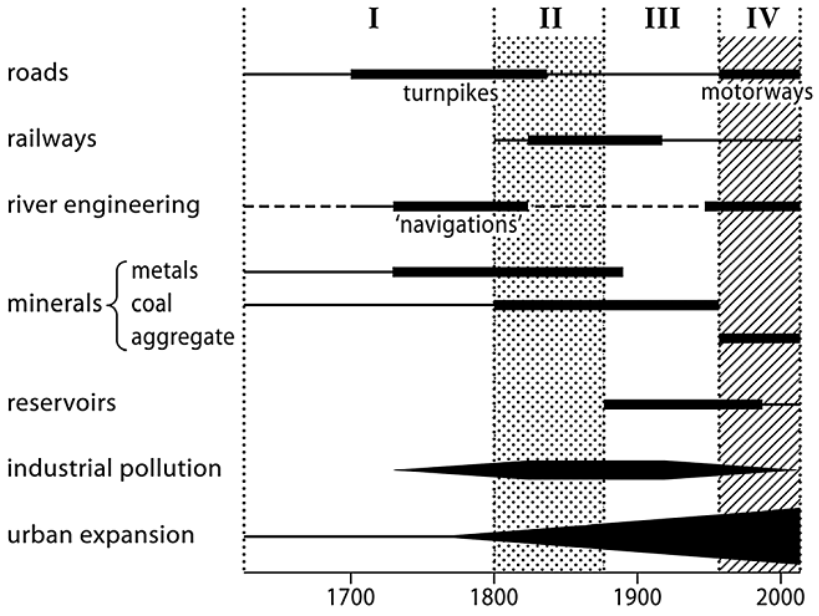

Figure I–4: Simplified overview of historical and present pressures on floodplains (Lewin, 2013). Phase I: an early morphological period, following a historical floodplain modification period. Phase II: A contamination window. Phase III: River regulation and suburban expansion. Phase IV: Engineering control period, but also conservation and recreation values increased.

Some more sediment related issues, both quantitative and qualitative, shall be further discussed. Increases in sediment yields were reported in relation to changed land use and related human activities in river basins, including land clearing for agricultural use, but also logging, mining and construction activities (Walling, 1999; Walling & Fang, 2003; Owens et al., 2005; Walling, 2008). Declines of sediment yields have been attributed to extensive soil and water conservation and sediment control programmes. Climatic changes, both natural and human-induced, can result in increased (wetter climate) or decreased (drier climate) yields. The results depend also on the quality of the change in rainfall characteristics, being it in magnitude, intensity, frequency or form (Glymph, 1954). It is generally not evident to disentangle the effects and interactions of the various factors (Walling & Fang, 2003). Aggregate mining constitutes until today an important cause for local sediment deficits in rivers (Wyżga, 1991; Bravard, 1994; Landon & Piégay, 1994; Kondolf, 1997; Rinaldi et al., 2005). Consequences are channel bed degradation, and as a result of the morphological adjustment often bank erosion and thus a deepening and widening of the channel. Through knickpoint erosion this phenomenon can travel upstream and impact over longer distances.

The major sediment quality issues currently deal with the interactions between sediments and chemical contaminants. The latter are primarily associated to the fine fraction (< 63 µm) of the sediment load in a river. Especially clay (< 2 µm) is chemically (re)active due to its particularly high specific surface area and ion exchange capacity. Widespread contaminants include heavy and trace metals, nutrients (mainly phosphorus), radionuclides, organic micro-pollutants (pesticides, persistent organic pollutants (POPs; including e.g. Polychlorinated biphenyls ('PCBs'), polyaromatic hydrocarbons (PAHs), Dichlorodiphenyltrichloroethane (DDT), dioxins, etc.), pharmaceuticals, endocrine disruptors) or pathogens. They originate from diverse point sources (identifiable and stable sources, such as municipal or industrial wastewater effluents, tailings) and diffuse sources (widespread and dynamic sources, including surface runoff, groundwater runoff, atmospheric deposition, inputs by erosion e.g. from agricultural land) (European Sediment Research Network, 2004) and enter river systems via multiple pathways (see e.g. Owens, 2005). Recent efforts in the reduction of pollution in Europe have much reduced the contribution of point sources, leading to an increase in the relative importance of diffuse sources.

The contaminants are adsorbed to and may then be transported or deposited with the fine sediment. The potential risks from such contaminated sediments depend much on the sediment and contaminant characteristics, as well as on the environmental conditions (Xiaoqing, 2003). If they are adsorbed to sediment particles under certain environmental conditions (certain pH, temperature, ion exchange capacity, redox potential, sediment grain size and sediment concentration ranges) and these conditions remain stable, they may not be remobilised over a long time period. They would thus present a low actual risk, at least from a human perspective. Nonetheless, the future risk of such contaminant sinks would remain unclear—Owens et al. (2005, p. 699) speak of a 'chemical time bomb'. Re-erosion might transform such sinks into secondary pollution sources. Irreversibly bound contaminants and processes of degradation may decrease their bioavailability. Contrarily to being permanently adsorbed, the contaminants can also remain at the interface between water and sediment, posing a risk to water quality.

The numerous contaminants commonly encountered in river systems have diverse impacts (European Sediment Research Network, 2004; Owens et al., 2005): high phosphorus levels are often a cause for eutrophication, as this element is usually a

limiting factor in the environment. Many toxic contaminants reduce the abundances of organisms or even lead to their complete disappearance. This can entail impacts on biodiversity as well as on entire food-webs and ecosystems. Bioaccumulation and biomagnification, i.e. the accumulation of contaminants in organisms and through the food chain, entails toxicity effects for the organisms and eventually human health effects. Health risks can likewise arise in relation to toxic chemicals in the water body itself. Sediment quality is also linked to sediment quantity issues. As such, a reduction in sediment loads may for instance involve nutrient depletion in ecosystems which depend on the delivery by the river, such as wetlands, floodplains or coastal zones. When this occurs in agriculturally used floodplains, this may furthermore require the utilisation of fertilisers where there was no need under natural conditions. Additional adverse effects on the entire system are the consequence.

Another more recent issue of sediment quality is related to plastic contamination. While initially mainly marine environments have been studied, some first publications on river systems indicate the necessity to focus on this aspect in future scientific works (Williams & Simmons, 1996; Morritt et al., 2014). Lechner et al. (2014) found that plastic particles outnumbered fish larvae in the Danube basin. And not only surface waters are concerned but also sediment deposits, as the example of the St. Lawrence River showed: plastic densities there were comparable to the most polluted marine sediments (Castañeda et al., 2014). The entanglement of organisms which frequently leads to their death, ingestion and ingestion-related leaching of potentially harmful chemicals are some of the environmental issues of plastic waste. Since plastic is not biodegradable, it keeps accumulating in the environment. Perhaps one may ask whether plastic beads will one day become an essential component of riverine sediments if no actions are taken?

1.5 Cumulative impacts from multiple pressures

The relationships between individual drivers and response variables show complex effects, which can furthermore differ under changing environmental contexts (Tockner et al., 2010). Cumulative impacts of several drivers can cause antagonistic, synergistic or additive responses. Impacts and responses are also scale-dependent: some factors will mainly influence the river locally, such as gravel mining, while others entail regional changes including land use changes in the river basin or dam and reservoir projects. Lag effects and resulting transient processes (Schumm, 1969; Przedwojski et al.,

1995), already mentioned in section 1.3, add considerably to the complexity. Floodplains 'store' impacts of the diverse pressures of the entire river basin and reflect this history in a sort of landscape memory (Brierley, 2010). Studying their evolution may therefore help us further our understanding of cumulative pressures.

With the combined effect of multiple uses and the resulting pressures exerted on river-floodplain systems, future management faces great challenges (Habersack et al., 2014; Grizzetti et al., 2017). Not to speak of the interaction between human and natural drivers, especially climatic effects (Newson & Lewin, 1991). In the following section, we provide an overview of the recent changes in river management practice induced by such challenges, as well as some examples of integrated approaches to river conservation and restoration.

1.6 From river regulation to sustainable river management: changing paradigms and contemporary river management practice

Based on an improved understanding of river adjustment in the late twentieth century, river management evolved from hard engineering to ecologically-based approaches (Downs & Gregory, 2014). It is now commonly agreed that initiatives need to be adapted in accordance to the state of a river system, as well as of its historical context (e.g. Downs & Gregory, 2014). On a gradient of river status between natural or semi-natural and degraded conditions Boon (1992) defined relevant measures from preservation, to limitation, mitigation, restoration, to dereliction (Figure I–5). Preservation of pristine or near-natural rivers or river section, as well as mitigation

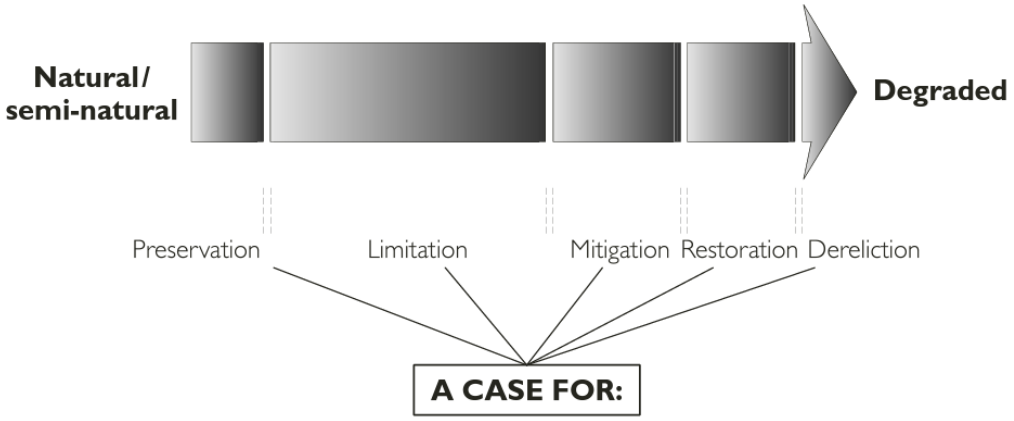

Figure I–5: River management options in response to the environmental state of the river (Downs & Gregory, 2014, modified after Boon, 1992).

measures shall be treated in more detail in the following sub-sections. Where river reaches show only light degradation, management should focus on the limitation of further damage. This means that river basin development should be limited (Boon, 1992). Restoration applies to systems situated toward the more degraded end of the gradient involving measures to change this state to a more natural one. Different terms and concepts can be regrouped under this management option (rehabilitation, revitalisation, renaturalisation, reconversion, restructuring, enhancement, etc.). Definitions vary between authors and have evolved over time (Muhar et al., 1995; Dufour & Piégay, 2009). Often restoration is now used as an umbrella term. When improvement is impossible or costs outweigh benefits, the last option is dereliction—"giving up and accepting the status quo" (Boon, 2012, p. 11). Resources should then be directed into other, more promising restoration projects.

The initial management attempts in the 1970s and 1980s concerned mainly local measures within the channel, followed principally single goals and were restricted to the restoration or conservation of static forms (Muhar et al. 1995; Dufour & Piégay, 2009). Some of these approaches failed, when for instance the focus was on the symptoms and not the causes of degradation or when the forms which were recreated were not compatible with the actual system processes (Kondolf et al., 2001). This led to discussions about the adequateness of form-based approaches (Simon et al., 2007; Rosgen, 2008; Lave, 2009). In the 1980s and 1990s, the notions of a pre-disturbance reference state came up, the German '*Leitbild*', which was later criticised (Dufour & Piégay, 2009). Noticeably, as it was then recognised that an appropriate pre-disturbance state was difficult to define and unachievable under contemporary conditions. In regions where reference sites are rare, the risk was also to create monotonous stretches of rivers restored according to the same reference (Muhar et al., 1995). Type-specific measures were thus called for, moving later to a more dynamics-oriented, process-based restoration. This was based on studies of natural processes in remaining near-natural systems (e.g. the Tagliamento in Italy, Ward et al., 1999). Giving space to the rivers (the French idea of '*espace de liberté*' is now a concept applied to large rivers (Opperman et al., 2009). This consists in re-connecting floodplains and former side arms, as well as re-initiating bank erosion processes by removing engineering infrastructure. The latter provide a sediment source to restore bed load transport and to create in-channel and riparian habitats (Florsheim et al., 2008). With the upcoming notion of sustainability, longer-term and multi-goal solutions

were sought for, based on an integrated and inter-disciplinary view of river systems in their entire basin (Thorel et al., 2018). Such a management requires the implementation of all the measures proposed by Boon (1992) based on a strategic planning (Muhar et al., 1995; Rohde et al., 2006). The EU WFD constitutes an international holistic policy framework which requires the enhancement, protection, and restoration of water bodies (Article 4 EU WFD). By 2009, a large-scale assessment of the status of European rivers (river basins ≥ 10 km^2) was carried out, based on consistent and comprehensive datasets. Only 43% of the water bodies attained a good ecological status or potential (European Commission, 2012). Many were classified as heavily modified or as artificial.

1.6.1 Preservation / conservation / protection

Remaining near-natural river-floodplain systems or reaches have become extremely rare in the developed world and are facing accelerated deteriorating in the developing world despite their strategic importance (Ward et al., 1999; Stein et al., 2002; Tockner & Stanford, 2002). Hein et al. (2016) point out the value of intact floodplains for both flood risk management and ecological functioning, as an example. Tockner & Stanford (2002) emphasise the multiple services and resources provided by them. Preventing them from degradation should be a management priority (Tockner & Stanford, 2002; Jones et al., 2010). For Boon (1992) the preservation of rivers involves certain management initiatives but could in some pristine cases also consist of a simple 'leave-alone' approach. The author emphasises that the term 'preservation' should, in the case of river systems, be understood as to integrate the natural dynamics. However, he admits that drawing the line between natural and anthropogenic changes remains a challenge to the conservationist. The adoption of the Ramsar Convention on Wetlands in 1975 was a first step to promote the conservation and wise use of wetlands at an early stage (Convention on Wetlands of International Importance especially as Waterfowl Habitat, 1971). In the EU, the first environmental piece of legislation was the Birds Directive (Directive 79/409/EEC in 1979, amended in 2009: Directive 2009/147/EC), which established a network of Special Protection Areas (SPA). Their aim was to protect habitats for endangered and migratory birds, among which many wetlands. With the adoption of the Habitats Directive (Council Directive 92/43/EEC), the SPAs were included into the Natura 2000 network. Annex I of the Habitats Directive lists several natural running water habitats which require the

designation of special areas of conservation. Annexes II and IV list animal and plant species which occur in river-floodplain systems, among other, with the same obligations or need strict protection. The Natura 2000 network also forms the backbone of the EU green infrastructure strategy, including for example the blue band. Eventually, in 200, the EU WFD was adopted (Directive 2000/60/EC of the European Parliament and of the Council establishing a framework for the Community action in the field of water policy). It states in Article 4 as one of its highest objectives the non-deterioration of surface water bodies and explicitly mentions prevention next to enhancement and restoration. The management of natural and semi-natural sites must thus aim for the reduction of risks and damaging actions down to a minimum (Bloesch, 2003; in Hein et al., 2016). Between the various directives many synergistic but also some conflicting objectives exist, which sometimes necessitate careful planning and coordination (Janauer et al., 2015). Under the EU WFD, for instance, historical reference conditions may be used as a restoration objective. This may result in a conflict with the objectives of the Habitats Directive, which is concerned with the preservation of present conditions. An example would be the case of an artificially cut-off side arm or meander where the objective under the EU WFD would be to re-install hydrological connectivity. Where these habitats host flora and/or fauna of very high conservation value a conflict arises. Some recommendations and experiences are compiled by European Commission DG Env (2011) and Janauer et al. (2015).

While first conservation attempts focused on some rare and endangered species, over time, rare and endangered habitats were included (Muhar et al., 2011). This constrained consideration of isolated, often small units in highly fragmented landscapes was more recently expanded. Inter-linkages between units as well as spatial processes were integrated to address issues of ecosystem functioning and biodiversity (Verhoeven et al., 2008): e.g. dispersal processes or gene flows but also the four-dimensional connectivity of hydrosystems and related processes (discharge- and morphodynamics). Evidence of this development is given by the evolution of European legislation (Natura 2000, green infrastructure), as presented above. Some authors early underpinned the necessity to define what values are to be preserved (Boon, 1992; Dunn, 2004). Generally, the ecological value of rivers is related to their naturalness, representativeness, diversity or richness, rarity, special features (Dunn, 2004). These values are translated into criteria and indicator sets to render them operational, however legal and planning frameworks for conservation strategies are

still lacking (Muhar et al., 2011). To improve the coordination of the diverse ecological, societal, and economic interests related to river systems, several authors have developed prioritisation approaches, to guide the selection of sites for preservation actions at the national level (Rohde et al., 2006; Scheikl et al., 2016). Coherent, spatially comprehensive and comparable databases are essential for such tasks. In Europe, the comprehensive assessment of river reaches carried out in the framework of the EU WFD provides a sound basis. Particularly the compatibility of the conservation of valuable river reaches and the further development of hydropower is in the focus of many such approaches (Muhar et al., 2011; Scheikl et al., 2016; Adaptive Management of Barriers in European Rivers (Amber) research project: https://amber.international/).

The substantial extent to which natural floodplains have already been permanently lost under current uses raises the question of the potential role of novel ecosystems to sustain certain physical and ecological functions. This idea is not new, already in the 1980s, researchers saw certain potentials in the diversification of physical conditions by certain engineering structures in monotonous engineered rivers (e.g. Burch et al., 1984). A very careful assessment of the risks and benefits of conserving the current ecosystem in its novel functioning are needed (Hobbs et al., 2009). This option is especially considered where the costs of restoration toward a historical state are high and success unsure due to high thresholds.

1.6.2 Mitigation

The concept of mitigation is mainly related to rivers of lower quality, where uses such as water regulation and abstraction are essential for the population and therefore accepted (Ferrar, 1988; Boon, 1992). Ferrar (1988) lists mainly indirect measures for this management option, including measures at the river basin scale, land use planning, legislation, as well as monitoring. The EU Water Framework Directive (EU WFD) requires member states to apply mitigation measures to their heavily modified and artificial water bodies with the aim to reach a good ecological potential by 2019. In the framework of the legislation, heavily modified water bodies refer in this case to “a body of surface water which as a result of physical alterations by human activity is substantially changed in character”. These should opt for the best ecosystem conditions possible within the anthropogenic context. Examples of mitigation measures regarding trained and regulated rivers are provided in the following.

Adaptating river training structures

Since several decades, also the beneficial aspects of river training structures with respect to ecological restoration goals have been pointed out and adapted design guidelines have been compiled (Burch et al., 1984; Brookes, 1992; Thompson, 2002; Seidel, 2008). Ongoing research also aims to install new or re-design existing training structures in light of integrated restoration programmes, where multiple aspects of river use need to be considered (e.g. on the Rhine: Simons et al., 2001; on the Danube: Klasz et al., 2009).

Adapting dam and reservoir management

In their review, Kondolf et al. (2014) compiled available options in dam and reservoir management and described several experiences. According to them, many options exist to make operations more sustainable with regard to sediment issues but are often not applied even where it would be possible. The authors reckon that there might be a lack of knowledge or of the demonstration of successful applications. They distinguish three broad categories of measures (p. 259, based on Morris & Fan (1998) and Kantoush & Sumi (2010)):

- "methods to route sediment through or around the reservoir,
- methods to remove sediments accumulated in the reservoir to regain capacity, and
- approaches to minimize the amount of sediment arriving to reservoirs from upstream." They furthermore discuss a fourth category which includes
- methods to add sediments to the downstream part.

While the first two categories address both upstream and downstream issues related to sediment around dams, the third and fourth options each address only one of the two issues. Measures to route sediment and thus anticipate extensive sedimentation in reservoirs include sediment by-passing, off-channel reservoir storage sluicing, and turbidity current venting. The idea of sediment by-passing is to divert highly sediment-laden waters, principally flood flows, away from the reservoir. In one approach, a weir is used upstream of the reservoir, which diverts the water during times of high sediment discharges. It redirects the sediment-laden flow into a channel or tunnel to then reinject them to the river channel further downstream of the dam. Another approach operates with an off-channel reservoir storage, which is filled during clear water periods using a weir. During flood flows when suspended sediment concentrations are high, the water remains in the original river channel. Sediment sluicing, also called drawdown routing,

has the objective to reduce sediment trapping during high flows to a minimum and involves letting rapidly pass the flow through the reservoir and the dam. For this purpose, the reservoir pool is lowered prior to high sediment discharge flood events. The venting of turbidity, or density currents is based on the phenomenon of turbidity currents which form in many reservoirs. The high density of sediment-laden inflows to the reservoir makes them flow close to the bottom, underneath the lower density clearer water in a distinct layer. These currents can be passed through the reservoir and eventually the dam via bottom outlets, while the storage water remains in the reservoir. Further options to minimise the settlings of fines within the reservoir include the turbining of suspended sediment and the exploitation of turbidity currents by structures such as screens, water jets, or bubble curtains (see Schleiss & Oehy, 2002; International Sediment Initiative, 2011).

When reservoirs already feature high sediment deposits, the following approaches are common to increase or recover the reservoir volume: flushing involves the scouring or re-suspension of the sediments and further transporting downstream by opening the bottom outlets. The accelerated flows thus created remove the sediments by hydraulic force. In drawdown flushing, the reservoir is emptied, removing sediment from a vast zone within the reservoir. In contrast, during pressure flushing, only a small cone-shaped area near the outlet, as the reservoir is not drawn down. It therefore is not very effective in restoring reservoir capacity, but rather serves to prevent abrasion of machinery by reducing sediment concentrations in the intake. Hydraulic dredging employs pumps on barges to suck in accumulated sediments. In addition, cutter heads may be required for cohesive sediments. Instead, hydrosuction can be used when there is sufficient head between upstream and downstream of the dam. In this case the head creates the suction. When reservoirs are completely drawn down, mechanical removal of deposits with scarpers or dump trucks can be used.

Sediment augmentation refers to the addition of sediment (usually sand and gravel from quarries, less frequently from the reservoir or sediment traps upstream of the reservoir) downstream of the dam. This measure counteracts sediment deficits in the downstream section. Kondolf et al. (2014) provide information on operational benefits and drawbacks of various techniques and highlights experiences from applications around the world.

A costly and only short-term measure to increase the storage capacity of a reservoir is to heighten the dam à posteriori (International Sediment Initiative, 2011). Generally, also the intake and bottom outlets are raised at this point. As an alternative, some projects now include dead storage capacities for sediment or they oversize the reservoir already in the planning phase, when excess sediment issues are expected to play a major role (International Sediment Initiative, 2011).

Over the last two decades, awareness of the importance of a natural flow regime for ecological integrity has led to restoration actions implementing so-called environmental flows (Poff et al., 2007). In its simplest form, this would mean to raise the minimum flow passed into the by-passed channel, while more sophisticated approaches integrate other characteristics of the natural flow regime, besides magnitude. This includes the timing of certain flows, their duration, frequency, and the rate of change. The definition of appropriate flows in the restoration practice is complicated and many different methods are applied (Acreman & Dunbar, 2004) However there is still a lack of evaluations concerning actual ecological responses to environmental flows (Webb et al., 2015).

Since the late 20th century, the decommissioning and removal of dams has started, with many such projects in the United States (O'Conner et al., 2015; Duda et al., 2016; Bellmore et al., 2017). Often this would involve dams which are no longer in use as they have filled up with sediments, do no longer serve their original purpose, pose a safety hazard or have become inefficient (Graf, 2001; Doyle et al, 2008; American Rivers, 2017). Indeed, most engineering projects, including dams, are planned to sustain over a period of 50–100 years (Downs & Gregory, 2014), and many of them have silted up even faster than anticipated. Different methods of decommissioning and related impacts for the river system are being studied (Wilcox et al., 2014; Magillian et al., 2016). Several databases are organised with follow ups on projects around the United States (Wieferich et al., 2016; American Rivers, 2017).

Until today, even new dam projects are often still planned on an individual basis, without taking into account the impacts from other dams on the same network. Innovative research projects try to emphasise the need for a strategic planning in concert with other uses and management objectives (Schmitt et al., 2018; Amber project, see section 1.6.1).

1.7 What future for heavily modified floodplain environments? Management examples from other large European rivers

Large-scale integrated mitigation and rehabilitation programmes have been launched on many large rivers, with the aim to integrate human uses and ecological requirements. Most often, such approaches will consist in mitigating effects from river channel modifications and river regulation. The reconnection of floodplains is one of the major aspects (Buijse et al., 2002; Opperman et al., 2009). But also the implementation of environmental flows (Erskine et al., 1999), and measures to enhance the sediment regime (river widening, addition of aggregates (Sarriquet et al., 2007; Arnaud et al., 2017). Sometimes floodplains are excavated to facilitate their reconnection (Geerling et al., 2008).

On the Danube River, for instance, the objective of the Integrated River Engineering Project ('*Flussbauliches Gesamtkonzept*') is to bring together navigation and nature conservation requirements (Reckendorfer et al., 2005; Klasz, et al., 2009). Principal actions include the removal of riprap, the re-design of existing groynes and the building of new ones, reconnection of side arms, as well as a granulometric bed improvement. The measures target the improvement and conservation of riparian habitat in the Lobau National Park, while allowing safe navigation and reducing channel degradation.

On the Rhine River, Simons et al. (2001) presented a project where a longitudinal dike was built near a sequence of groyne fields to create an artificial secondary channel to diversify habitats while allowing continued navigation. The groynes were likewise adapted and shortened to interconnect the various embayments. Further upstream on the Rhine, the Integrated Rhine Project ('Integriertes Rheinprogramm') combined objectives of flood risk management and floodplain rehabilitation (Pfarr et al., 1996).

For both Rivers, the Danube and the Rhine, international commissions have been established to coordinate river basin wide transboundary measures (International Commission for the Protection of the Rhine (ICPR), International Commission for the Protection of the Danube River (ICPDR)). On the Rhône, only several bilateral contracts regulate a close inter-action between Swiss and French water authorities (Bréthaut & Pflieger, 2015; Bréthaut, 2015).

2 Conceptual framework

2.1 Research aims and objectives

On the Rhône River, the active floodplain is made up in part by artificial dike fields. These units were built in the late nineteenth, early twentieth century to improve the navigability of the river (for a more detailed definition of the dike fields refer to chapter II, section 2.3.2). In the framework of the River Basin Management Plan of the EU Water Framework Directive, large scale rehabilitation works are scheduled to re-activate channel dynamics. The aim is to induce bank erosion in pilot by-passed channels which had significantly narrowed under the heavy engineering works of the last two centuries. The dike fields are amidst the units which shall be deconstructed in suitable sections and works have started in 2009. However, little is known about the evolution and characteristics of these dike fields. And consequently, there is little knowledge concerning any inherent ecological potentials or any risks related to their dismantling. Aquatic dike field habitats have been studied in the 1990s and 2000s on the Total Rhône near Arles regarding Chironomid assemblages and environmental conditions (Franquet et al., 1995; Franquet, 1999), as well as hydro-sedimentary conditions and fish assemblages (Nicolas & Pont, 1995; Nicolas & Pont, 1997). They are also currently studied in the by-passed reach of Péage de Roussillon (PDR) and the Total Rhône near Arles in a project of the OHM VR ('*Fonctionnement écologique des casiers Girardon: Le cas des casiers aquatiques*' coordinated by Franquet & Marmonier). Studies of terrestrial habitats are still rare, especially of dike fields in by-passed sections (Piégay et al., 1997; Gaydou, 2013).

The overall objective of this thesis is therefore to understand sedimentation and forest patterns in Rhône River dike fields at several spatio-temporal scales. This will provide a first overview of the range of conditions in these units to derive potentials and risks of future management measures. In summary, the aims are to:

1. Characterise the present-day spatial patterns of overbank fine sediment deposits in the dike fields and examine the variability within and between the study reaches;
2. Identify the evolutionary trajectories of the deposits;

3 Explore potential drivers of these patterns, as well as their individual roles and interactions;

4 Determine the present-day structural and compositional characteristics of dike field forest stands and compare them to more natural reference systems;

5 Speculate on the future ecological potential of the dike fields as a sustainable habitat given the present-day characteristics and potential management options.

2.2 Thesis structure

This thesis is organised into three main parts (Figure I–6). Chapters I, II, and III provide the general and site-specific contexts to this research, as well as the general methodological framework that was adopted. Chapters IV, V, and VI present data, observations, and some interpretations concerning our specific aims and hypotheses. Chapters VII and VIII synthesise and discuss these results in light of the overall objective to provide a characterisation of dike fields to better inform future management measures. Here we also establish the links between the results of the various part two chapters.

CHAPTER II provides the geographical context of the Rhône River and presents the major engineering phases related with the creation of the dike fields and their evolution. It furthermore introduces the four study reaches in which we conducted our analyses.

CHAPTER III gives an overview of the methodological framework and the datasets which concern all the following three chapters. This includes analyses carried out in a Geographical Information System (GIS), as well as the integrated sampling scheme for the field campaign. Further methods and data relevant to each subject of the following chapters are provided at the beginning of each them.

In **CHAPTER IV** we focused on present-day characteristics of the overbank fine sediment deposits derived from orthophotographs and digital elevation models. Comparative analysis and multivariate statistical analysis were used to reveal spatial patterns and to determine potential drivers and possible interactions. We could thus point out variability in patterns both between and within by-passed reaches.

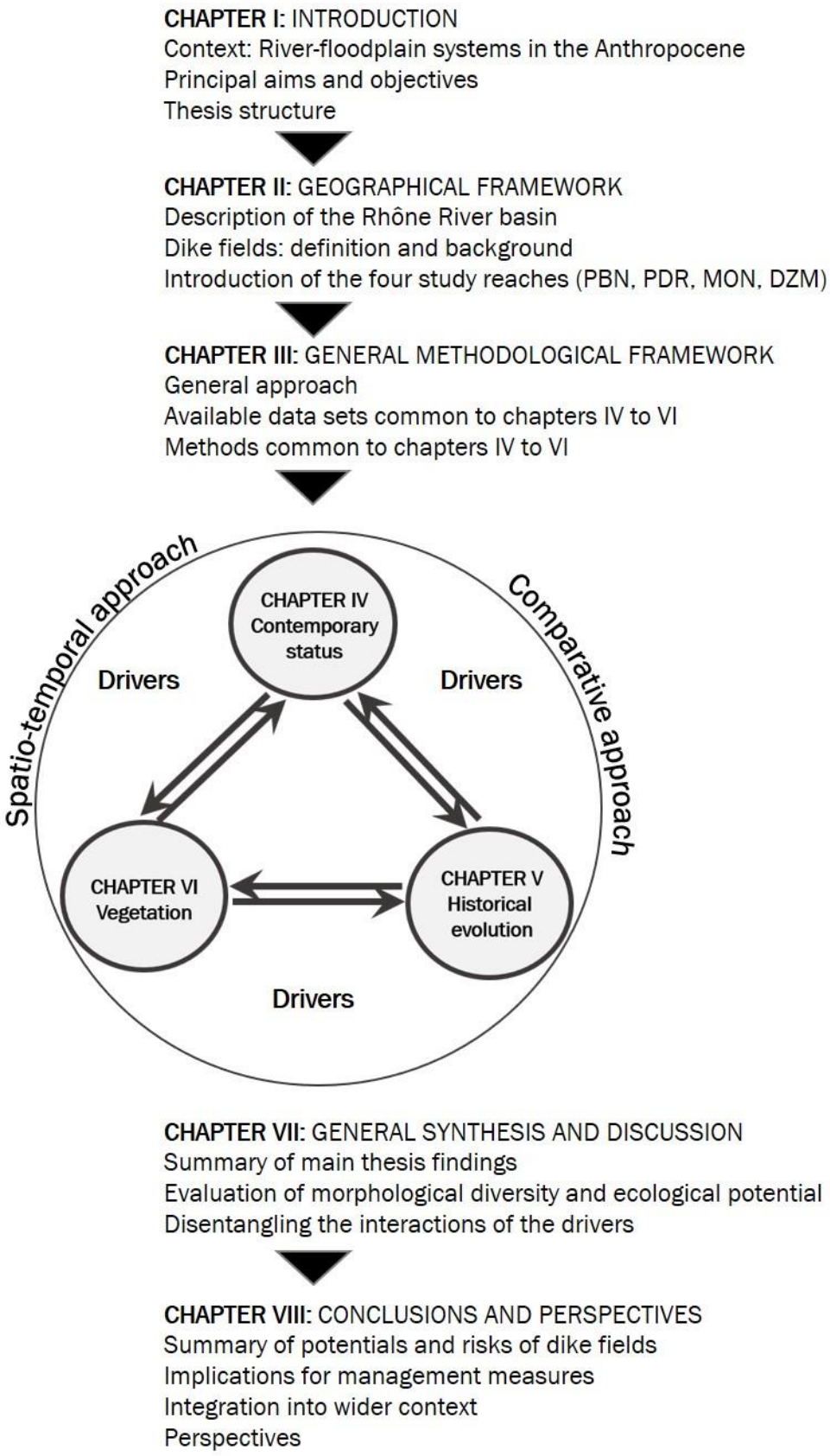

Figure I–6: Schematic diagramme of the thesis structure.

CHAPTER V documents spatio-temporal trajectories of the dike fields both planimetrically and vertically to improve our understanding on the patterns observed in chapter IV. This was based on a retrospective analysis of aerial images and overbank fine sediment depths measured during the field campaign. The comparative analyses were extended by an analysis of the longitudinal patterns of all descriptive and control variables which gave additional insight into the functioning of the by-passed reaches and their dike fields.

CHAPTER VI characterises stands of woody riparian vegetation in the dike fields in terms of structure and composition. At the centre of the analyses are comparisons between by-passed reaches, between surfaces which had terrestrialised prior to and following the dams, as well as between dike fields and reference sites. The references were chosen to constitute semi-natural sites which correspond to the two ends of a gradient of hydrological connectivity and maturity, namely pioneer islands and mature floodplain units. We also analysed potential drivers behind the observed patterns.

CHAPTER VII synthesises the main findings of chapters IV to VI and establishes the links between them. This facilitated the evaluation and extension of the conceptual model. The chapter further discusses implications for future management measures. In particular we focused on the ecological potentials and risks related to the dike fields in light of management plans to rehabilitate channel dynamics in the by-passed reaches.

CHAPTER VIII provides general conclusions which can be drawn from this large-scale study of Rhône River dike fields. It relates our findings to ongoing and planned studies on the dike fields and provides perspectives to study and manage novel ecosystems.

CHAPTER II GEOGRAPHICAL FRAMEWORK

Résumé du chapitre II : cadre géographique

Nous introduisons dans la partie suivante du manuscrit le Rhône avec ses spécificités hydrogéographiques et biogéographiques, avant de nous focaliser sur les principales phases d'aménagements historiques qui ont fait naître les casiers Girardon. Celles-ci ont profondément altéré la nature du fleuve, qui montrait jusqu'en 1855 environ un cours qui basculait entre des styles en tresses et méandriforme. On distingue généralement quatre phases d'aménagement principales. La première phase commençait avec l'installation de digues hautes visant à protéger des terres agricoles et des zones urbaines. Toutefois, ces stratégies, très locales, pouvaient avoir un impact négatif sur les conditions de navigation. Avec l'invention des machines à vapeur, les avancées de la navigation ont entraîné la construction d'un réseau dense de digues dans les lits moyen et mineur. Tout d'abord il s'agissait de digues longitudinales de type non-submersibles, puis le design ainsi que les arrangements ont été adaptés au fur et à mesure en fonction de leur réussite. Les digues évoluaient vers des digues submersibles, puis des digues basses auxquelles on ajoutait des digues latérales, des épis et des seuils de fond pour concentrer les eaux d'étiage et fixer le thalweg. Les digues longitudinales et latérales, qui existent toujours, délimitent des champs rectangulaires, dénommés casiers Girardon selon l'ingénieur en chef qui a optimisé le système. A partir du 20ème siècle, des dérivations à visée hydroélectrique ont été installées le long du Rhône. Les secteurs court-circuités ont été soumis, pendant la plus grande partie de l'année, à un débit réservé très faible par rapport au débit naturel. Ensemble, les deux types d'aménagement ont bouleversé le fonctionnement naturel du fleuve en fixant à la fois son tracé en plan et en régulant fortement ses écoulements. Les marges alluviales, incluant les casiers, ainsi que les bras secondaires découpés du chenal principal, ont vu une forte tendance à l'atterrissement, tandis que le chenal s'est souvent incisé. La dynamique fluviale ainsi fortement réduite fait aujourd'hui l'objet de projets de réhabilitation dans des endroits où la navigation n'est plus exercée. A la fin du chapitre, nous présentons les quatre secteurs court-circuités étudiés dans ce manuscrit, et qui sont destinés entre autres à être restaurés. Il s'agit de deux secteurs en aval de Lyon, Pierre-Bénite (PBN) et Péage de Roussillon (PDR), ainsi que deux secteurs plus vers l'aval, Montélimar (MON) et

Donzère-Mondragon (DZM). Ils ont tous subis la dérivation à différentes périodes et présentent des conditions hydro-climatiques différents entre amont et aval.

1 Introduction

The Rhône River is the largest river in France in terms of discharge and of great economic, social, and ecological importance. This chapter first provides a general introduction to the river's geography and geology, its hydrology, and biogeographical setting. As a multi-use river, the Rhône has been assuming diverse roles, whose relative importance has changed through time with technological developments and the evolution of society. We shall describe the two major historical river engineering phases which a) were at the basis of the implementation of the Girardon dike fields and b) marked their historical evolution. We will then put into perspective the present-day context, which provided the motivation for this research. The final section will present the four by-passed reaches of Pierre-Bénite, Péage de Roussillon, Montélimar, and Donzère-Mondragon, where we conducted our research.

2 The Rhône River

To understand the river's current state, we need to investigate its natural settings, as well as its past development, including natural phenomena and human interventions. Extensive information has been collected and published by Bravard & Clémens (2008) and Bethemont & Bravard (2016), which were used as references for the following summaries.

2.1 Hydrogeography and geology

The Rhône originates from the Rhône glacier located at 1,753 m a.s.l. in the Saint-Gotthard Massif in the canton of Valais, Swizzerland, from where it initially flows in south-easterly direction and into France (Figure II–1; Haond, 2008). Downstream of Lyon, its course is directed southwards until it reaches the Mediterranean Sea, where it forms a delta after 812 km. With a mean annual discharge of 1,700 m^3/s at its mouth, the 9th order river is the most water-rich in France (baseflow = 575 m^3/s; Q_{100} = 11,300 m^3/s). Its drainage basin covers an area of 98,500 km^2, with diverse geologic and topographic landscapes, as well as climatic regions. Indeed, the river drains mainly

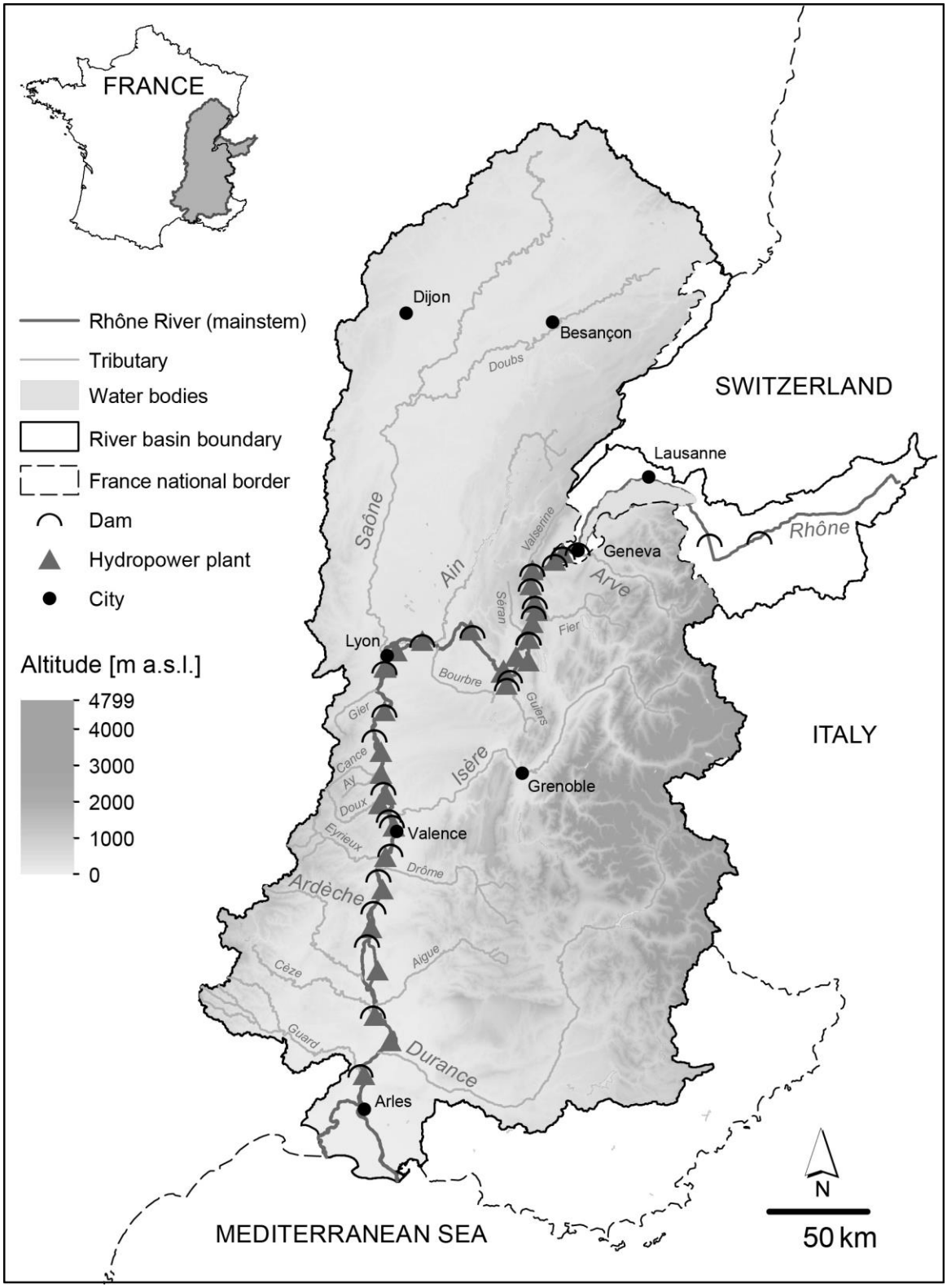

Figure II–1: Rhône River basin. Data source: BD Alti®. IGN©.

various alkaline rocks (Jurassic and Cretaceous sediments, Tertiary and Quaternary deposits), but also some acidic metamorphic rocks (Olivier et al., 2009). It flows

through three major ecoregions, namely the Alps, the Western Highlands, and the Mediterranean part of the Western Plains (Olivier et al., 2009). In a common geographical zonation of the Rhône we distinguish, according to Bravard & Clémens (2008):

- From its source to Lake Geneva, the **Alpine Rhône** is a high-slope mountain torrent (average slope 0.9%; Haond, 2008), with a transitional nival to nivo-pluvial hydrological regime since the installation of hydropower schemes (Reynard et al., 2009). At its entry to the lake, the Alpine Rhône forms a delta. It contributes ¾ of the water input to the lake (Grandjean, 1990; Loizeau, 1991), which in turn influences its discharge together with the Seujet dam at Geneva. The lake furthermore traps the vast majority of the Rhône's sediments so far transported.
- Downstream of its outlet from Lake Geneva the **Upper Rhône** passes through the Jura and Prealp mountains with an average slope of 0.1% (Haond, 2008) and through at times tight gorges and at times wide plains. It is joined along its sinuous course by two of its major tributaries in terms of suspended matter contribution: the Arve and the Saône (Launay, 2014). The Arve is an alpine torrent joining the Rhône on its left bank downstream of Geneva. The Saône, originating from the Vosges mountains, drains the vast and flat Bresse and Dombes plains. Its confluence with the Rhône is located in Lyon on the right bank of the river. Another principal tributary, the Ain River, likewise joins the Upper Rhône on its right bank coming from the Jura Mountains. The Ain marks the limit of the upstream part of the Rhône which experienced the Würm ice sheet and its downstream part which was under fluvio-glacial influence (Mandier, 1984). Tributaries of secondary importance include: The Valserine, Usses, Séran on the right bank originating from the Jura mountains; the Fier, Guiers, and Bourbre on the left bank, draining the Prealps.
- According to the reference system used by the National Rhône Company (Compagnie Nationale du Rhône, abbreviated 'CNR'), which we refer to in this work, Lyon marks river kilometre 0. The **Middle Rhône** flows southward of the city between the Saône and Isère confluences. It is constrained to its right by the Massif Central, to its left by the Prealp mountains. Its average slope in this section amounts to 0.05% (Haond, 2008). The Isère is a major tributary both in

terms of water discharge and suspended matter, which has its confluence on the left bank north of Valence. Smaller tributaries include the left bank tributaries originating from the Massif Central, generally short and steep, such as the Gier. Except during floods, they do not contribute substantially to the flow or sediment delivery to the Rhône. The Middle Rhône valley is characterised by alternating plains and more constrained sections (Bravard, 1987).

- The **Lower Rhône** is situated between the Isère confluence and the Rhône delta at Arles and features an average slope of 0.06% (Haond, 2008). The Rhône here enters the Mediterranean climate region and features some of its widest plains, which can take widths of up to 2,000 m and 5,000 m (Bethemont, 1972). The Durance is the principal tributary to this reach, draining the Prealps and joining the Rhône on its left bank, as do the secondary tributaries Drôme, Aigues, and Ouvèze. Violent floods are often related to the Cévenol secondary tributaries Eyrieux, Ardèche, Cèze, and Gard.
- At Arles, the Rhône divides into two distributaries, the 'Petit Rhône' and the 'Grand Rhône' and forms a **delta** before it reaches the Mediterranean Sea. Both distributaries have a very low slope of on average 0.004% (Haond, 2008). The Camargue plain, which they enclose, is classified as Ramsar site and thus as a wetland of international importance. It also hosts a UNESCO biosphere reserve and a regional nature park.

This zonation is not necessarily fix in its delimitation. The urban perimeter of Lyon has evolved over time and so does the limit of the Mediterranean climate region, which is hardly definable. It often varies between authors and can thus be questioned as to its usefulness (see Comby, 2015). In this work, it rather serves to underline the variability of the physical conditions along the river continuum (Vannote et al., 1980) or in this case discontinuum (Bruns et al., 1984). Regarding the studied reaches, we shall later refer to upstream and downstream reaches, which distinguish the sections upstream and downstream of the Isère River, as well as continental/oceanic and Mediterranean influences (see section 3). However, to come back to the discontinuum: one characteristic which distinguishes the Rhône from comparable rivers, such as the Rhine or Danube, is that it keeps its mountain torrent characteristics all along its course (Bravard, 1987). Indeed, it receives large quantities of coarse sediments from its alpine and Massif Central tributaries even in the lower sections. Its slope remains

high even where it almost approaches the sea, so that the sediments are further transported. Therefore, it does not produce a typical wide lowland floodplain section but rather continues to show an alternation of plains and narrow valleys or gorges. All these phenomena explain the many braided sections the river had prior to major human interventions and the great difficulties that were faced by navigation.

Several climatic zones are covered by the drainage basin, ranging from oceanic (moderate precipitation throughout the seasons) to continental in the eastern part (summer storms and cold winters) and Mediterranean influences in the southern part (hot and dry summers, rainfall in spring and autumn) (Olivier et al., 2009). Bethemont (1972) gives a more detailed overview of the complexity and variability of the air masses and resulting phenomena. Here we shall put the focus on a short description of the different flood regimes, which are related to these climatic characteristics:

- **Oceanic floods** occur mostly between October and March as a consequence of rainfalls coming in with western winds. They concern the Alpine and the Upper Rhône, as well as the Saône, whose contribution downstream of Lyon generally prolongs these floods.
- **'Cévenole' floods** are related to intense rainfalls with currents from the South to south-east. The floods are characterised by rapid increases, and later decreases, of the water stage and their power, which are due to the high slopes and impermeable of the Cevennes catchments.
- **Extensive Mediterranean floods**, generally in late autumn, early winter, are similar to Cévenol floods, although their extension can be vast.
- **General floods** are floods which englobe the entire Rhône catchment due to the succession or combination of the different floods mentioned above.

Some of the most catastrophic recent flood events on the Rhône occurred in the years (Pardé, 1925; Barthélémy & Souchon, 2009; Bravard, 2010; GRAIE, 2016):

- 1840 (13,000 m^3/s (> Q_{100}) at Beaucaire);
- 1856 (12,500 m^3/s (> Q_{100}) at Beaucaire);
- 1993 (9,800 m^3/s at Beaucaire);
- 1994 (11,000 m^3/s at Beaucaire);
- 2002/2003 (11,500 m^3/s (> Q_{100}) at Beaucaire).

Extreme low flows on the Lower Rhône at Beaucaire occurred in (Pardé, 1925):

- 1884;
- 1894;
- 1906;
- 1908; and particularly in
- 1921 (360 m^3/s at Beaucaire), which was also the year with the most extreme low flows on the Upper and Middle Rhône.

2.2 Biogeography

The Rhône drainage basin covers three of the biogeographic regions of Europe, namely the Alpine, continental, and Mediterranean regions (European Environment Agency, 2010). Phytogeographic regions according to Julve (1998) include a central-European plain unit, a mountain and hill unit, and a Mediterranean unit. Wasson (1996) and Wasson et al. (2004, 2007) proposed a European-wide geographical framework for the typology of rivers in the framework of the EU Water Framework Directive (EU WFD). It constitutes a regional approach, based on large-scale geophysical (relief, geology) and climatic structures. The Rhône basin falls into 11 of the first-level so-called hydro-ecoregions (HER–1), namely Alsace, Vosges, Jura-Northern Prealps, Eastern Calcerous Hills, Saône plain, Northern Massif Central, Southern Massif Central, Cevennes, Inner Alpes, Southern Prealps, Mediterranean.

2.3 Anthropogenic influences: major engineering works and their impacts

The Rhône River, just like any other large river, was and is subject to multiple uses (Bravard et al., 2008a; Bethemont & Bravard, 2016): Human activities in the drainage basin have had an impact on the water and sediment inputs early on by changing the land cover. The floodplains, likewise, have been used since the earliest civilisations for agriculture and were modified by drainage or irrigation measures. Long before any systematic channelization of the river, fords, (cable) ferries, and bridges enabled its crossing. It also provided numerous resources, such as biomass (timber), fish, clay, hydropower (water mills) or salt in the Camargue. Gravel and sand mining was extensively performed on the Rhône, as well as its tributaries. Initially in the channel

itself, this activity has today shifted into the floodplain. In 1873, the first hydraulic energy exploitation (not yet electric but based on telecontrol) began at the confluence of one of the Rhône's tributaries (Valserine) near Bellegarde (Bravard, 1987). Today, the main stem of the Rhône itself hosts a dense series of hydroelectric power schemes (see section 2.3.3). The river water is furthermore used for cooling in both thermal and nuclear power plants (Fruget, 2003). Waste water treatment plants discharge into the river making use of its self-purification potential. Railway lines, a motorway (A7), and two national highways (N7 and N86) follow the river course in close proximity, occupying ancient tow paths in some locations (Bravard et al., 2010). And the Rhône is also a place for recreation activities, such as bathing and tourism. The economic and social development of the neighbouring regions have always been in close inter-dependence with the river and its resources.

Two extensive recent river engineering phases have profoundly changed the course of the Rhône, as well as its hydro-sedimentary and ecological functioning: one to favour navigation and the second to favour the hydro-electric development but also to further improve navigation and irrigation for agriculture. These two phases shall be presented in some detail, as they describe the 'birth' of the Girardon dike fields and the changing environmental settings under which they evolved. The Rhône was considered 'natural' prior to these two phases—indeed the term refers to its pristine state but later also to a semi-natural state under the first human influences. As multiple other uses have impacted the river locally, they shall be shortly described in the last of the following sub-sections. For more detailed information on the evolution of the entire Rhône, see for instance Bethemont (1972), Bravard et al. (2008b), Bravard (2010), and for the Upper Rhône Bravard (1987).

2.3.1 The so-called 'natural' Rhône (< ~1840)

The floodplain of the Rhône is a complex system which has evolved not only vertically under the influence of flood deposits. It was also influenced by changing tectonic and climatic conditions (Bravard et al., 2008b; Bravard, 2010). The Upper Rhône was influenced by glaciation processes until the period of the Little Ice Age. The Middle and Lower Rhône experienced the last glaciation in the Pleistocene. Drastic sea level changes of the Mediterranean during the Messinian salinity crisis re-modelled the longitudinal profile of the river several times (Bravard, 2010).

The processes of the Holocene much shaped the current characteristics of the Rhône. During this epoch, the river faced several fluvial metamorphoses (Bravard et al., 2008b; Bravard, 2010), where generally its channel shifted between a braided and meandering planform pattern. The Little Ice Age, period of modest cooling and glacier expansion in the Northern Hemisphere between the mid-16th and mid-19th century (Goudie et al., 1999; Mann, 2002), initiated a period of particularly intense braiding. High sediment inputs from the glaciers propagated through river networks. They reached the main stem of the Rhône with certain delays, depending on the delivering tributaries. Sediment input quantities were probably exacerbated by the overpopulation in mountainous regions at the time and related agricultural practices (Bravard & Peiry, 1993): silvo-pastoral practices involved extensive deforestation in the Alpine regions, which additionally increased erosion and hence sediment delivery. Meander scars on the Rhône, which dated from previous periods (Middle Ages/Roman period), have probably been filled or re-worked during this period. This leaves relatively little direct evidence of the meandering patterns; however, some scars have yet been identified and dated along the river course (Salvador et al., 2002 and 2004, cited in Bravard, 2010). Detailed information on the establishment and evolution of the braided pattern on the Rhône are still rare. Toward the end of the Little Ice Age in the 19th century, just prior to the major engineering works, a discontinuous braided pattern of varying intensity was observed on the Rhône (Bravard, 2010, Figure II–2a). Around this period, massive torrent control programmes were initiated, which entailed active and natural reforestation, as well as channel engineering structures in the headwaters (Liébault & Piégay, 2002). At the same time, the glaciers started their retreat. The resulting naturally and human-induced reduction in the sediment delivery is believed to have potentially accelerated the effects of the river training works of the late 19th century (see sections 2.3.2 and 2.3.3). The transformation of the braided channels into single channels in particular. Both meandering and braided planform patterns of the Holocene epoch are at the origin of the secondary channels which persist or are still detectable today on the Rhône. Meander scars to a lesser extent than the braids for the reasons described in this paragraph. These secondary channels are currently the object of restoration measures, as shall be described in section 2.3.5.

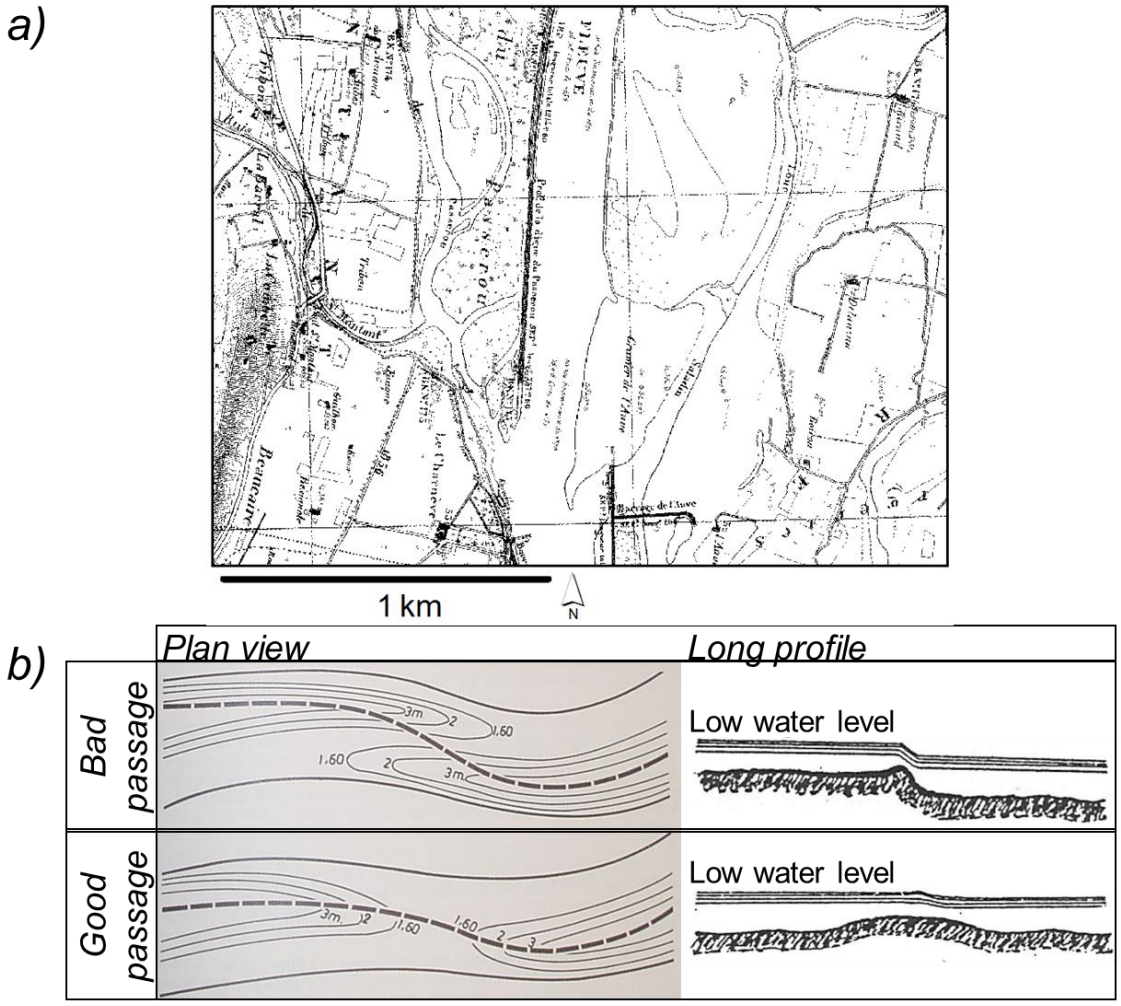

Figure II–2: Conditions on the Rhône prior to the major engineering works. a) Excerpt of the 1860 map showing the conditions corresponding to the natural Rhône and b) illustration of 'good' and 'bad' passages for navigation (modified after Bethemont, 1972; Poinsart, 1992). A 'good' passage is characterised by riffles which naturally occurred with sufficient minimum depths for navigation, a smooth passage of the thalweg from one river bank to the next and by a long profile without major abrubt changes. In contrast, a 'bad' passage describes riffle sections where water depth is low, the thalweg changes sharply and the long profile is marked by a notable break in slope which induces high current velocities.

2.3.2 Girardon and his predecessors (~1840–1920): river training or the birth of the dike fields

The natural conditions on the Rhône evoked several difficulties for transportation (Escudié et al., 1991; Bethemont & Bravard, 2016):

- tow paths were discontinuous due to side arms and tributaries;
- in 1876, only during 165 days of the year a minimum water depth of 1.6 m was attained and only during these days the river was thus shippable;

- in the 1850's, numerous accidents occurred in relation to difficulties, some of which entailed the loss of entire ships.

Yet, for a long time, engineering works with a major impact on the river course have been impeded. Several reasons can be mentioned, such as the high energy of the river, related primarily to its high slopes, but also social, political, legislative, technical, and financial constraints (see for instance Tricart & Bravard, 1991). Even when river training works on other rivers had already advanced, works on the Rhône were still in their infancy. Only with the ongoing technological development and a systematic large-scale approach could the river eventually be 'tamed'. The resulting extensive dike system evolved progressively. Poinsart & Salvador (1993) distinguish four phases in line with the continuous adaptation of the design of the training structures:

- 1st phase until ~1855: The first longitudinal training structures on the Rhône consisted in local **levees and non-submersible dikes** constructed by private individuals or trade unions with the aim to protect agricultural land and settlings (15th century). In the Donzère plain, the dike crests lay between 5 and 8 m above the conventional low water discharge. Additionally, bank revetments and spur dikes hindered bank erosion. These construction works were not yet organised on a larger scale and thus would sometimes have adverse effects on other parts of the river. Indeed, on the Rhône, no extensive network of flood protection measures is found, as is the case on many other large rivers (Tricart & Bravard, 1991). Such protections were only present at Chautagne and around the major cities, as well as toward the delta. Downstream of Beaucaire they date from the 12th century and were more elaborated, consisting of approximately 6 m high earth structures (Tricart & Bravard, 1991).

- It was with the formation of the '*Service Spécial du Rhône*' within the '*Ponts et Chaussées*' administration, following the destructive inundations from 1840 and 1856 that the large-scale systematic channelization of the river started. Their principal aim, alongside the protection from floods, was to improve the conditions for navigation. Technological progress now allowed the shipping of large steam-driven vessels and thus rendered the waterway an important means of transport. However, to increase the number of days per year during which navigation was possible on the Rhône, local low water zones during low flows had to be deepened: the minimum channel depth should not fall below

1.60 m with reference to the conventional baseflow. The dikes constructed so far on the Rhône did generally not create favourable conditions for navigation; indeed, sometimes they even created obstacles (Girardon, 1894). Under the direction of the engineers Kleitz, and later Tavernier, a slightly sinuous river with smooth bends and a unique channel was envisaged in which the ships could navigate more securely. For this purpose, they installed a network of discontinuous non-submersible dikes, especially in the concave bends of the river. They were supposed to induce the incision of the riffle sections to regulate the longitudinal slope of the channel. However, even with these systematic works the coverage of the dikes remained low and first experiences showed that the system had several drawbacks; mainly high maintenance costs due to the erosive power of the high waters which were trapped between and along the dikes. As a consequence, the dikes were undercut, or their crests eroded. As such, in 1856, only 103 km of protective dikes were inventoried between Lyon and Arles (Bethemont, 1972) and this first system was abandoned.

- 2nd phase 1855–1876: The chef engineer O'Brien had already recommended a new system in 1840, with the objective to narrow the channel and concentrate the mean water discharge in a single channel. At least in the reaches of Pierre-Bénite and Donzère-Mondragon it would however not be realised before 1855 (Poinsart & Salvador, 1993). Practically, two means were employed: all side arms were disconnected using **closure dikes and additional lateral dikes** (French: '*barrages*' and '*traverses*'); the banks were fixed using **submersible longitudinal dikes** (crests of both dike types were 2–3.5 m above conventional baseflow). These submersible dikes were designed to let pass higher flows to counter the drawbacks of the first phase. They were generally discontinuous, either parallel or alternating between the banks. First, they had been installed in the concave sections of the river. Later in the process, they were elongated into the convex sections to best guide the flow and thus fix the location of riffle and pool sections; and consequently the longitudinal slope of the channel. It was essential that the resulting flow followed the created channel forms and would not become misaligned. While locally, this system produced some positive results, the induced incision was in fact in many locations excessive and led to counteractive results instead. For instance, riffle sections were

excessively scoured, not only affecting the water levels of the upstream pools but leading also to the deposition of the eroded material further downstream.

- 3rd phase 1876–1884: Chef engineer Jacquet envisaged a system of **low longitudinal dikes** (French: '*digues basses*'), which were attached to the existing structures or the river bank employing lateral **cross dikes** (French: '*tenons*'). The low dikes concentrated only the low flows and let pass mean flows to prevent excessive incision of the main channel. The cross dikes were conceived such as to prevent erosion behind the dikes. The addition of this new set of training structures reduced the low flow channel to an average 150-m-width on the Middle and Lower Rhône (Poinsart & Salvador, 1993). From 1880 onwards, and under the advice of engineer Kozlowski who guided the regularisation works on the Elbe River, Germany, two types of **groynes** (French: '*épis'*) were employed in addition to the low dikes: 'spill over' groynes (French: '*épis noyés*') were built in pool sections, perpendicular to their orientation, to favour sediment deposition without modifying the channel. 'Diving' groynes (French: '*épis plongeants*') were placed in the convexities to stabilise the accretion zones and thus again the channel. In 1878, the so-called 'plan Freycinet' and the law of 13 Mai 1878 came into action, which would greatly accelerate the construction works due to an increased financial support (Escudié et al., 1991). The efficiency of the new technique applied now extensively along the river was proven in 1882: 20% of the riffle sections from 1878 which had shown a water depth inferior of 1.60 m at conventional baseflow had disappeared. According to Escudié et al. (1991), Jacquet's technique was only applied on the Middle Rhône between Lyon and the Isère confluence.
- 4th phase > 1884: The chef engineer Girardon, who the Rhône dike fields were named after, 'revolutionised' the channelization approach (Poinsart & Salvador, 1993). Although applying the same types of structures as those used by his predecessors and even on other rivers beforehand, he largely considered and made use of the natural local conditions, which he studied in depth (Girardon, 1894). Each single structure would be adapted in its height, distance to the next structure, orientation, or length to the local hydraulic necessities (Allix, 1930). This resulted in a high structural variability, but the various entities complemented each other. Indeed, it was the ensemble of neighbouring structures in one section which was designed to collectively fulfil the overall

goal. Girardon still aimed at obtaining a slightly sinuous channel with a continuous minimum depth of 1.60 m above the conventional baseflow and a constant width of approximately 150 m. Based on his observations, he defined so-called 'good' and 'bad' passages for navigation, according to the orientation and distance between two adjacent riffles (Figure II–2b, see legend for explanations). To transform 'bad' into 'good' passages, practically he planned (Girardon, 1894):

- to concentrate the flow in a single-bed channel by damming secondary channels during low flows (the height of the closure dikes was calculated as to locally let pass mean to high flows). Additionally, lateral dikes were implanted at regular distances over the entire width of the secondary channel to gradually reduce the slope of the water line and thus the energy each of the structures had to withstand. We refer to the resulting, more or less rectangular compartments, as '**dike fields in secondary channels**' (refer to the next paragraph for further explanations on dike field terminology).
- to fix the position of the pools and subsequently also the riffles, respecting the natural conditions. For this, Girardon still implanted low dikes in the concave sections but he carefully adapted their course with regard to the envisaged thalweg and the curvature of the channel. Also the height of these dikes was adapted from their upstream to downstream end: he designed them to decrease toward the inflexion points between the concave and convex sections. In any case, he considered that the maximum height of the dikes should not exceed 1 m above the lowest water levels. During construction and in the first period in which the dike acted on the channel, the actual dike height was often higher and was then adapted later in the process. Scour damages to the longitudinal dikes and the formation of secondary flows behind the dike during higher discharges, and thus the creation of a new channel, had to be prevented. Hence, the dikes were attached to the river bank or existing structures by lateral cross dikes (French: '*traverses' / 'tenons' / 'rattachements'*). These were oriented in upstream direction, while their slope would decrease toward the longitudinal dike. Where the two structures met, the cross dike reached

the same height as the longitudinal dike at that specific point. Again, the dimensions of each one of the cross dikes were adapted according to its longitudinal position in the channel. The resulting rectangular compartments enclosed by the dikes were later known as the '*casiers*', '*carrés*', or '*caissons*' Girardon, which we refer to as '**dike fields in the main channel**' (Figure II–3). This terminology has already been used in previous publications (Franquet et al., 1995; Nicolas & Pont, 1995; Poizat & Pont, 1996; Nicolas & Pont, 1997, Franquet, 1999). It follows the principle of the often-used terms 'groyne field' or 'groin field', which defines the area between two groynes (e.g. Uijttewaal, 1999; Sukhodolov et al., 2002; Yossef & de Vriend, 2010), and 'dike field', which defines the area between dikes (e.g. Burch et al., 1984). In some less complex sections on the Rhône, with a weak slope and curvature, this system could be reduced to the lateral structures, leaving out the longitudinal dike. Girardon further emphasised that the convex bank should never present a longitudinal dike due to the risk of another pool forming on this side. Instead, he suggested creating a beach of minor slope, as is found under natural conditions, using 'diving' groynes where the beach is inexistent or does not show enough resistance to the flow. Creation of a relief by the structures was avoided to maintain a smooth deposit. Their orientation and slope were chosen as to incite the current to principally follow the thalweg of the channel. Again, the slope of neighbouring groynes would be adapted according to their position in the curvature or toward the inflexion point.

– to regulate the orientation of the riffle sections. Girardon observed that although the regularisation of the channel would relatively well produce pools and riffles at the intended locations, the form and orientation of the riffles would often greatly vary according to the channel slope and the bed material. Further measures were thus envisaged in such cases: spill-over groynes were constructed at some depth in the channel, thus preventing disturbances to shipping traffic or surface perturbations. Their heads were oriented in upstream direction and their crests sloped toward the river to direct the current to their lowest point. The height and

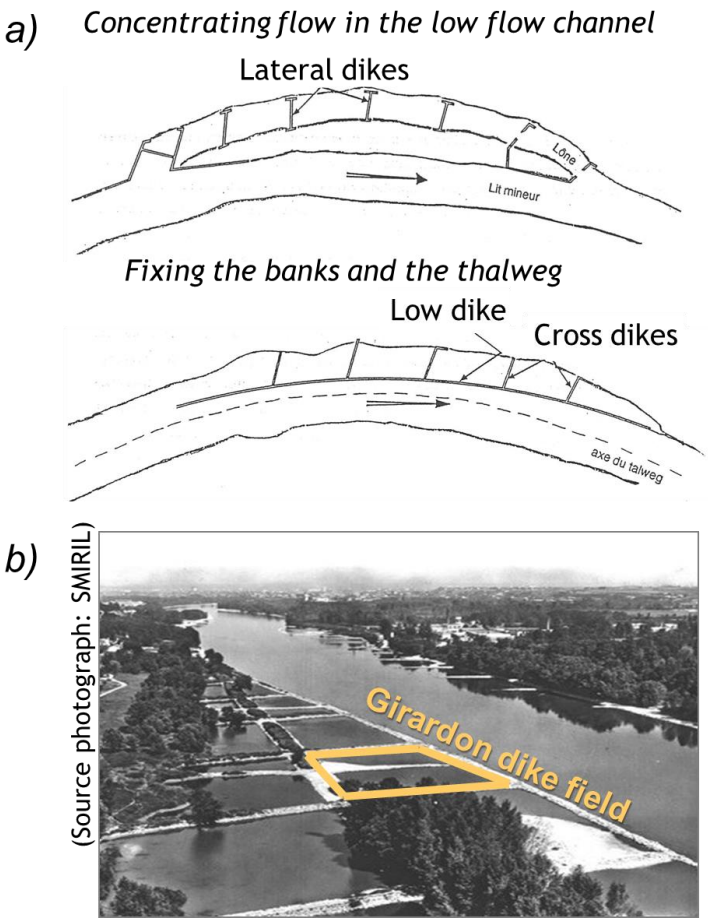

Figure II–3: What is a dike field? a) Idealised schemes of the arrangement of dikes in secondary channels (top) and in the main channel (bottom) (modified from Poinsart (1992) and b) the resulting dike fields.

slope of each individual groyne again depended on its position in the curvature and were determined in gradual continuity of the neighbouring groynes. Where the channel bed was easily scoured, a solution was to extend the groynes over the entire width of the channel (then becoming a **ground sill or weir**, French: '*seuil de fond*'), thus fixing the bed. The tip of these v-shaped weirs was oriented in upstream direction.

The different systems were successively added to the existing infrastructures, which were left in their actual state. For instance, Salvador (1983) points out that when the Girardon system was finally employed at the reach of PBN, the longitudinal dikes already existed along practically the entire reach. It was thus mainly lateral dikes which were added as a complement in this period. As a consequence of this long process, we find a high density of training structures in many cross-sections of the river and

complex assemblages which finally could also diverge from the schemes in Figure II–3 (Figure II–4; Poinsart, 1992).

Although the success or not of the third phase was difficult to evaluate since little time had passed, the application of the 'Girardon system' finally led to considerable improvements for navigation (Poinsart & Salvador, 1993). It is probable that the efficiency of the training structures was amplified by the natural reduction on the sediment delivery following the period of the Little Ice Age. In any case, the fast evolution of shipping technologies soon left even the Girardon measures insufficient

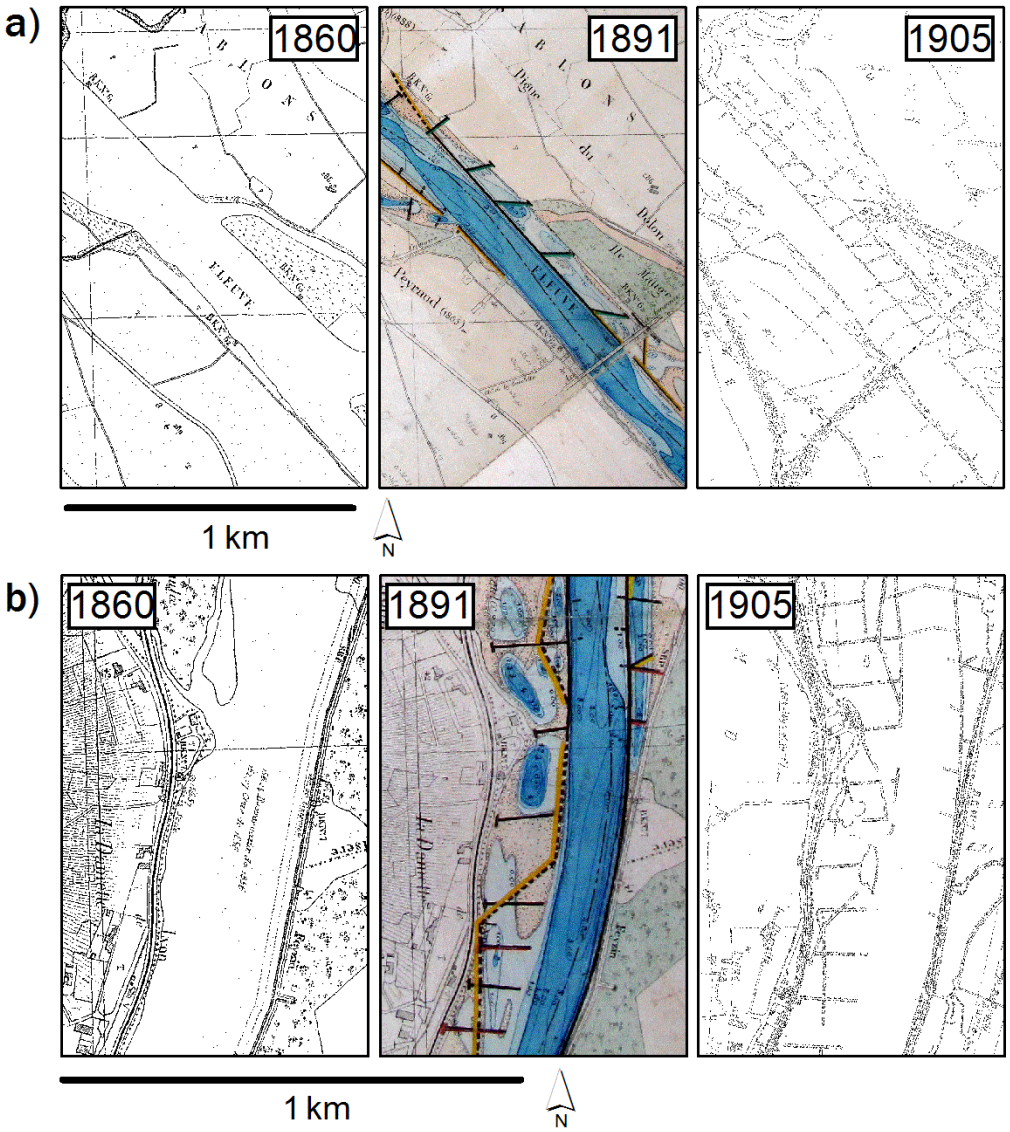

Figure II–4: Illustration of the successive evolution of the dike system. (a) section of PDR reach, (b) section of PBN reach.

regarding increasing requirements. Only the regularisation schemes which were realised in the second major river engineering phase would finally resolve the obstacles of navigation. Before passing on to this second phase, Table II–1 summarises again the characteristics and objectives of the main river training structures.

2.3.3 Hydroelectric power schemes (1899–1986)

In 1899, following the invention of the water turbine, the first power plant started exploiting the hydroelectric potential of the main stem Rhône River. It was the power plant of Cusset, upstream of Lyon (Figure II–1), which is today exploited by 'Electricité de France' (EDF). In Swizzerland, upstream of Lake Geneva, Chippis-Rhône (1911; the years in parentheses refer to the year the plant was put into operation or inaugurated) is operated by 'Forces Motrices Valaisannes' (FMV; http://www.fmv.ch) and the run-of-river power plant Lavey (1950) by the 'Service de l'électricité' of Lausanne (SEL; Müller et al., 2010). Downstream of Lake Geneva, the Seujet dam and run-of-river power plant control the water level of the lake (Grandjean, 1990). They replaced the Coulouvrenière power plant and pont de la Machine dam in 1995 (Grandjean, 1990) and are exploited by the 'Services industriels de Genève' (SIG). SIG likewise holds the concession for the run-of-river power plant Verbois (1944). Situated on the border between Switzerland and France, the run-of-river power plant Chancy-Pougny (1924) is operated by the 'Société des Forces Motrices de Chancy-Pougny' (SFMCP), whose stakeholders are the Swiss SIG and the French 'Compagnie Nationale du Rhône' (CNR). The CNR was founded in 1933 and is the company which obtained the concessions of the Public Fluvial Domain along the Rhône corridor from the French state (Savey, 1992). It started building power schemes in 1939 and today exploits nineteen of the power plants on the French part of the river. Their aim is threefold: energy production, further development of navigation, and agricultural irrigation (Fruget, 2003). By 1995, a total of twenty-four dams and hydroelectric power plants were thus present along the Rhône River, of which sixteen feature a diversion scheme (162 km out of 522 km of the natural channel are by-passed in France alone, Lamouroux et al., 2015).

Table II–1: Summary of the river training structures employed on the Rhône River during the four phases.

Dike type	Dike orientation	Crest height	Objectives/functioning
		1st phase (< 1855)—flood risk management and navigation oriented	
Levees / non-submersible dikes	Longitudinal	5–8 m above conventional baseflow	Placed in concave bends for the creation of a single channel with smooth curvatures
		2nd phase (1855–1876)—principally navigation oriented	
Submersible dikes	Longitudinal	2–3.5 m above conventional baseflow	placed in concave bends and prolonged into convexities to concentrated mean flows and create a smooth-curvature channel, submerged at higher flows
Closure dikes (and additional lateral dikes)	Lateral (with respect to the secondary channel)		Disconnection of secondary channels during low and mean flows by closure dikes at the upstream and downstream ends of the channel, additional lateral dikes reinforce closure dikes and further reduce the flow energy throughout the secondary channel
		3rd phase (1876–1884)—principally navigation oriented	
Low dikes and cross dikes	Longitudinal and lateral	1–1.5 m above conventional baseflow	Low longitudinal dikes concentrate low flows, submerged at mean and high flows. Lateral cross dikes reinforce them, link them to the original river bank or older structures, and prevent erosion behind them
'Spill over groynes'	Lateral		Built in pool sections to favour sediment deposition and control the location of the thalweg
'Diving groynes'	Lateral		Maintain/reinforce accretion zones in the convexities
		4th phase (1884–abandonment)—principally navigation oriented	
Closure dikes (and additional lateral dikes)	Lateral (with respect to the secondary channel)		Disconnection of secondary channels by closure dikes at the upstream and downstream ends of the channel to concentrate the flow during low discharge conditions. Additional lateral dikes reinforce closure dikes and further dissipate the flow energy throughout the secondary channel
Low dikes and cross dikes	Longitudinal and lateral	≤ 1 m above conventional baseflow	To fix the location of the pools, low dikes were built in concave bends and reinforced by cross dikes, which were oriented upstream against the flow. Sometimes cross dikes only were considered sufficient.
'Diving groynes'	Lateral		To fix the location of the riffles, groynes were implemented in the convex bends
'Spill over groynes' or sills	Lateral		Regulate the orientation of the riffles

An illustration of a typical CNR power scheme is given in Figure II–5: A diversion dam (a), also called retention dam, directs the water into the diversion canal (b) on which the power plant (c) is located for energy production, as well as a lock (d) which facilitates shipping traffic. Most of the dams of the Middle and Lower Rhône are so-called 'open dams' or 'barrages' (after Bligh, 1915), equipped with gates which close the spans when required, but let pass flood waters for instance. The dam is generally situated upstream of the power plant, although the configuration varies in some reaches, as is the case at Pierre-Bénite (PBN), presented in section 3.1. Upstream of the dam a shallow reservoir (e) is created, which is confined laterally by dikes. The residence time for water in the reservoirs is generally of a few hours only (Savey, 1992). The counter canals (f) or side canals represent drainage canals used to regulate alluvial groundwater levels on both sides of the river. The head-race canal is built up higher than the floodplain, while the tail-race canal is built into the floodplain (Bravard & Gaydou, 2015). The former, natural river course (g); referred to as the Old Rhône or by-passed Rhône (French: '*Vieux Rhône*' or '*Rhône court-circuité (RCC)*') receives a discharge which depends on the operation of the power plant (Savey, 1992): over much of the year, it receives a minimum (or compensation) discharge, which in some reaches varies seasonally, but generally makes up only a small percentage of the natural discharge (10–60 m^3/s prior to recent restoration, i.e. on average 5% of the natural discharge (Bravard & Gaydou, 2015)). It also serves as floodway: it receives approximately the difference between the upstream discharge and the maximum discharge exploitable by the turbine without causing any damage to it. The by-passed channel itself was left in its state from prior to diversion, i.e. with all river training structures. The parts of the Rhône which are not by-passed are referred to as the Total Rhône (g), French: '*Rhône total*'). Three Rhône hydropower schemes differ considerably from this typical CNR scheme: The Génissiat power scheme is the only one with a large impoundment dam (total crest height: 104 m), which furthermore directly hosts the power plant. Its functioning is based on a large storage reservoir. Indeed, all other dams are of the type run-of-river, with low reservoir capacities. Seyssel and Vaugris have the particularity that their power plants are directly appended to their dam. In total, the hydroelectric schemes on the French section of the Rhône contribute 25% of the hydroelectricity in France (Lamouroux et al., 2015).

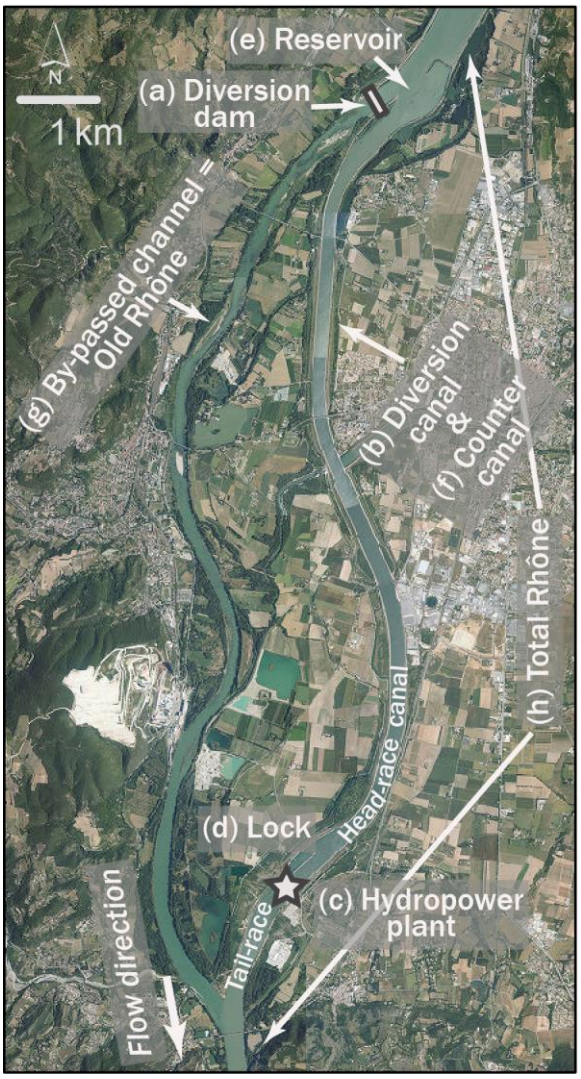

Figure II–5: Typical arrangement of a diversion scheme on the Rhône. Example of the by-passed reach of Péage de Roussillon.

2.3.4 Cumulative impacts from the two major river engineering phases

The river training works on the Rhône have successfully increased the number of shippable days to 318 in 1900 (Escudié et al., 1991), yet they entailed profound modifications of the channel and the floodplain (Salvador, 1983; Fruget & Michelot, 1997; Fruget, 2003; Parrot, 2015): The banks of the main channel being fixed, any lateral evolution in the planform was impeded. Disconnected secondary channels entered a process of terrestrialisation (Depret et al., 2017): today some originally connected channels are semi-lotic to lentic, while others are terrestrial. Although originating mainly from braided patterns, terrestrialisation rates are similar to those observed after natural meander neck cutoffs: the closure dikes inhibited the bedload

infilling phase thus reducing the terrestrialisation rate. However, their terrestrialisation still advanced and the loss in fluvial dynamics inhibited the creation of new aquatic floodplain habitats. Eventually, this led to an overall homogenisation and impoverishment of the system. The main by-passed channel on average incised vertically (Piégay et al., 1997; Gaydou, 2013; Parrot, 2015), entailing a drop in the water level, while the dike fields and the active floodplain accreted due to fine sediment deposits. They would become permanent stocks due to a lack of erosion processes. As a result, water surfaces in the dike fields diminished, while forests expanded and matured, replacing dynamic pioneer vegetation islands. In turn, most of the in-channel islands, became attached to the river banks and open gravel banks disappeared due to erosion. Nicolas & Pont (1995), Poizat & Pont (1996), and Nicolas & Pont (1997) studied dike fields located in the main channel of the Total Rhône near Arles and found relatively natural sedimentation and erosion processes. This was explained by the relatively unimpacted hydrological and sediment transport regimes in this reach. Roditis & Pont (1993) remarked the high proportions of fine and medium sand in these dike fields and their diverse granulometric conditions. This contrasted with the other fluvial forms along the river margins that they had sampled.

With regards to fishes, these dike fields represented valuable nursery and thus recruitment sites, which were considered to replace lost natural floodplain habitats. With respect to macroinvertebrates these dike fields are likewise considered to increase the habitat heterogeneity of the channel (Franquet et al., 1995; Franquet, 1999; Gandouin et al., 2006). Contrary to these Lower Rhône dike fields, the dike fields studied in the context of the present research are located in by-passed sections. Hence, they were additionally exposed to the phase of river regulation on the Rhône, which further altered conditions.

With the realisation of the hydroelectric energy schemes, the hydrology was highly modified at the reach scale. Particularly for discharges below the maximum turbine capacity, the difference between original and altered flows in the by-passed channel is considerable (Klingeman et al., 1998). Yet all other discharge levels may show alterations, too (Figure II–6a). The minimum flows generally provided to the by-passed channel go along with a drastic dewatering of surfaces over most of the year. As this came as an addition to the continued gradual incision of the channel (e.g. Klingeman et al., 1994; Parrot, 2015), the drop in the groundwater level was significant in many

sites. As a result, it became unavailable to the riparian vegetation (Fruget & Michelot, 1997). Indeed, the entire disturbance regime in the riparian zone was altered, as the flood hydrograph was modified in all its characteristics: being it magnitudes, durations, volumes, frequencies, or hydrograph shape. Peak flows were reduced, and the hydrographs narrowed. The downstream sections of the by-passed channels on the Rhône are usually affected by the backwater from the next hydropower scheme situated downstream. Although the dams are operated to let pass the solid discharge, bed load deposits require regular dredging to avoid the increase of water levels during floods (Savey, 1992). Flow velocities in the diversion schemes on the Rhône are generally high enough to impede the decantation of suspended matter. This is not the case for the few reservoir dams, which accumulate fine sediments and therefore require regular flushing (Guertault et al., 2014). However, the sediment transport regime within the by-passed reaches is altered, as the transport capacity of the flow is greatly diminished over much of the year. Many of the reaches consequently show armouring (Parrot, 2015), where a selective transport has removed fine bed material, leaving the course sediment in place (Kondolf, 1997). In the backwater-impacted reaches, too, the change in slope has reduced the transport capacity (Cortier & Couvert, 2001). The homogenisation in the planform pattern of the reaches was further exacerbated by the diversions, as the morphology gradually adapted to the changing inputs of water and sediment (Figure II–6b). Finally, the dams interrupt the longitudinal continuity for migratory species, as was shown for instance for fish of the genus Alosa (Rameye et al., 1976; Fruget, 2003). Below the dams, we find reduced flow velocities and water depths, as well as abrupt changes in these parameters when the maximum capacity of the turbines is exceeded. Also grain size conditions are modified. These alterations in habitat conditions have had varying effects on benthic macroinvertebrate and fish communities (Klingeman et al., 1998; Fruget, 2003). For instance, the by-passed reaches are adapted for reproduction and nursery of fish, increasing abundances in juveniles. However, depending on the presence or absence and the connectivity of refugia, large and long floods can greatly reduce their numbers by carrying them downstream out of the reach.

Beyond these direct impacts, the hydroelectric schemes have allowed further economic development of the entire region, with profound changes in the landscape (urbanisation, industrialisation, intensive agriculture down to the lower floodplains).

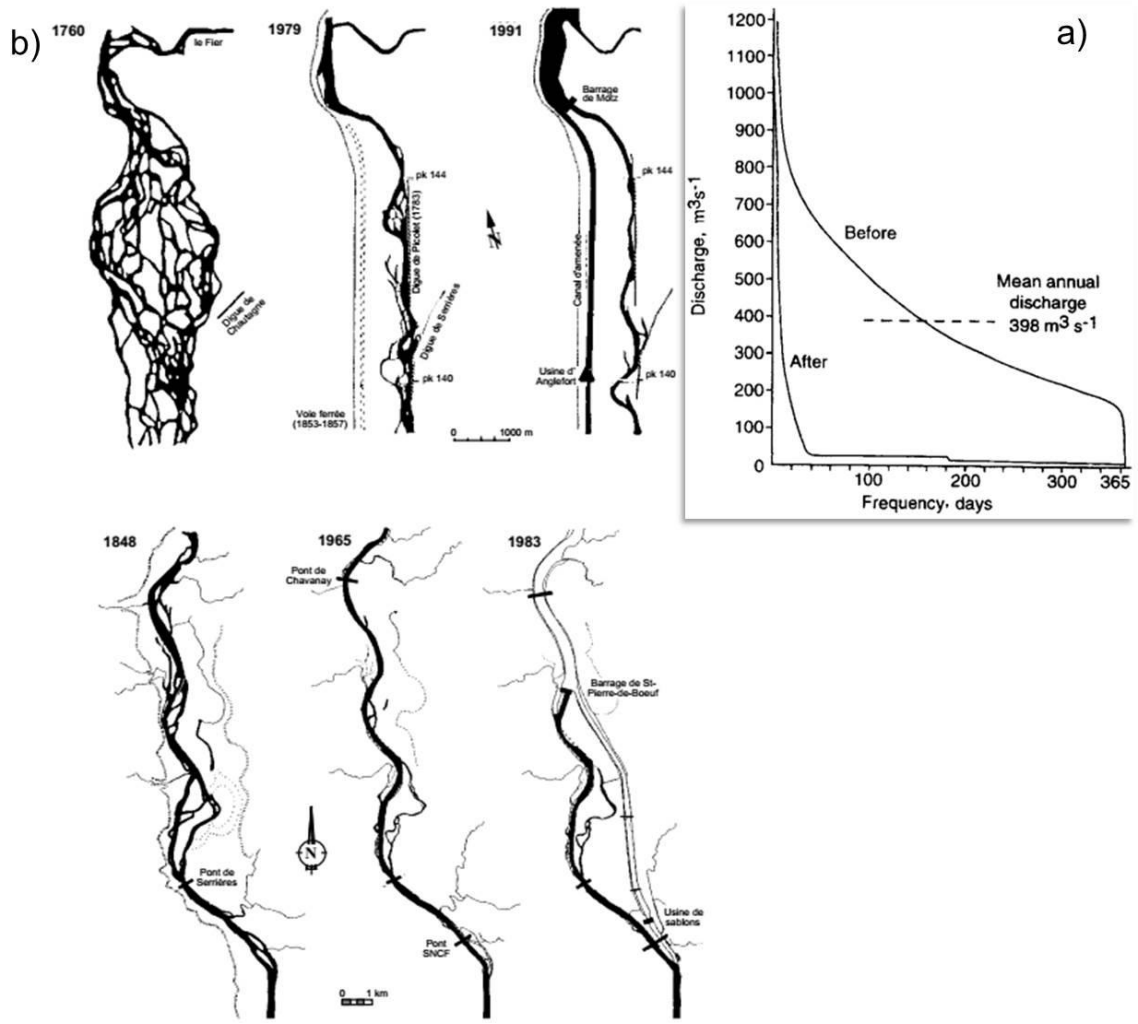

Figure II–6: Cumulative impacts of the two river engineering phases on the Rhône River: a) Flow duration curves of Chautagne prior to and following diversion (Klingeman et al., 1998; modified after Klingeman et al., 1994). b) Planform evolution of the Rhône at Chautagne, on the Upper Rhône, and at Péage de Roussillon on the Middle Rhône.

Other human interventions and natural changes accelerated certain trends. This is the case for the reduced sediment transit through the river compared to conditions during the Little Ice Age, which is the result of reforestation measures in the catchment, sediment trapping in the reservoirs of hydroelectric schemes, both of the tributaries and the Rhône itself, but also of gravel and sand extraction (Bravard & Gaydou, 2015). Extraction of bed material likewise exacerbated the incision of the bed level.

2.3.5 Present and future development: '*Le schéma directeur du Rhône*' (> 1992)

Indeed, the two phases of river engineering were efficient and for some time served their purpose. Yet the simultaneous detrimental effects, further technological development, shifts in the major uses of the river and changing paradigms over time

led to new concepts in river management. A sustainable approach to reconcile both current and future societal and ecosystemic needs is sought for. The by-passed sections on the Rhône are no longer used for navigation, potentially making the river trainining structures obsolete. The societal demand and later National as well as European legislation brought forward new objectives in river management (Stroffek et al., 1996). They were based on scientific advances, such as under the '*PIREN*' programme ('*Programme interdisciplinaire de recherche sur l'environnement*'). A law in 1992 (loi sur l'eau no. 92–3 du 3 janvier 1992) provided the legal framework for an integrated management of the Rhône River at the scale of the basin '*Rhône-Méditerranée-Corse*'. In 1996, a first management plan, the '*Schéma Directeur d'Aménagement et de Gestion des Eaux*' (SDAGE) was elaborated. In 2009, it would be adapted to conform to the requirements of the EU Water Framework Directive (EU WFD, 'Directive 2000/60/EC of the European Parliament and of the Council establishing a framework for the Community action in the field of water policy') and would thus become the so-called 'River Basin Management Plan (RBMP)'. A restoration programme was put into operation in the framework of the first SDAGE in 1998 (initially named '*Programme Décennal de Restauration Hydraulique et Ecologique du Rhône*'). It was based on hydraulic and ecological objectives. Three measures were undertaken to improve the physical habitat conditions:

- Increase of the minimum flow in the by-passed reaches of 8 priority sites (including the reaches studied in this work)
- Restoration of disconnected secondary channels ('*lônes'*) by excavation and reconnection
- Restoration of fish migration axes

These measures included a scientific monitoring from the beginning onwards: the programme '*RhônEco*' (2000–2018). Its aim was to develop a methodological framework to measure the effects from restoration on biodiversity. The researchers are organised in the scientific network of the '*Zone Atelier Bassin du Rhône*' (ZABR) labelled by the National Centre of Scientific Research ('*Centre National de la Recherche Scientifique*' (CNRS)) in 2001.

The violent floods of 2002 and 2003 on the Rhône put forward the questions of flood risk management and of giving back space to the river. As a reaction to the floods, the so-called '*Plan Rhône*' was developed between 2002 and 2006. It constitutes a

management strategy based on an integrated and sustainable development of the entire Rhône River basin, including numerous actors and several thematic fields (heritage and culture, flood risk prevention, water quality and biodiversity, transport, energy, tourism). In 2007, the first contract (CPIER ('*Contrat de Plan Interrégional Etat-Régions*')) was signed for the period 2007–2013. The partial dismantling of the constructed river margins, i.e. of the river training structures including the dike fields, is added as an important objective. This point envisages the restoration of the fluvial dynamics of the river, with the aim to remobilise the sediment trapped by the river training structures. The restoration programme was integrated in the '*Plan Rhône*' in 2007 in the thematic of 'water quality, resource, biodiversity'. The second part of the '*Plan Rhône*' was signed for the period 2015–2020 and reaffirmed the principal objectives. In this context, the research observatories in line with the river are to be mentioned: the Rhône Sediments Observatory ('*Observatoire des Sédiments du Rhône*' (OSR)), created in 2009, and the Human-Environment Rhône Valley Observatory ('*Observatoire Homme-Milieu*' (OHM)), dating from 2010 and created by INEE ('*Institut Ecologie Et Environnement*' of the CNRS). Both aim to produce scientific knowledge and extensive databases in pluridisciplinary networks. For the OSR, the dynamics of the sediment fluxes and stocks, as well as related pollutants are in the focus. The OHM is centred around creating bridges between the various projects concerning the contemporary evolution of the river and the riparian communities, including all disciplines. It also develops new projects in less studied fields within its scope.

3 Study sites

Four by-passed sections along the Middle and Lower Rhône have been chosen as study sites (the order in which the reaches are presented throughout this study follows their location along the river course, from upstream to downstream; Figure II–7): Pierre-Bénite (PBN) and Péage de Roussillon (PDR) in the upstream part of the river, and Montélimar (MON) and Donzère-Mondragon (DZM) in the downstream part. Their diversion schemes were implemented at different dates (Table II–2), which allowed us a) to evaluate the factor of time since diversion in our comparative analyses. Furthermore, the upstream reaches present a rather continental/oceanic climate, while the downstream reaches are in the Mediterranean climate zone. This would facilitate the evaluation of b) a latitudinal effect, e.g. on species composition. And

finally, the Isère River, one of the major tributaries in terms of suspended sediment concentration, has its confluence with the Rhône just upstream of the MON reach. We can thus study c) the influence of a major suspended sediment supply, comparing upstream and downstream reaches.

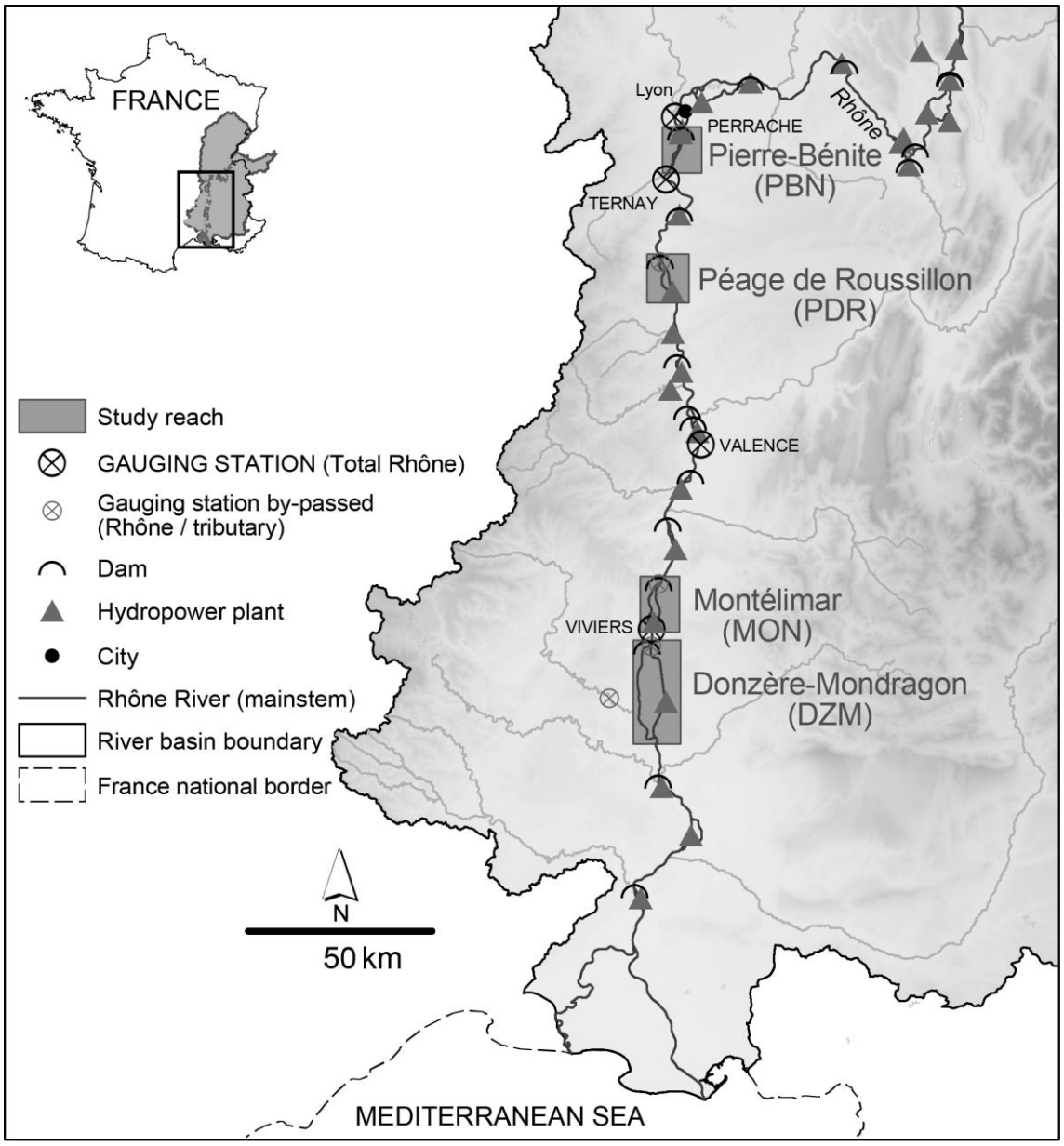

Figure II–7: Location of the four study reaches (background data source: BD Alti®, IGN©).

Table II–2: Characteristics of the four study reaches (Olivier et al., 2009; Gaydou, 2013).

	Upstream reaches		Downstream reaches	
	PBN	PDR	MON	DZM
Longitudinal position (distance from Lyon [km])	~4	~50	~	~170
Length of the reach [km]	13	12	13	29
Mean channel slope [%]	0.05	0.06	0.08	0.07
Inauguration of the diversion scheme	1966	1977	1957	1952
Minimum discharge prior to restoration [m^3/s]	April–Aug: 10, other months: 20	April–Sept: 10, other months: 20	15–60	60
Minimum discharge since restoration [m^3/s]	Since 1999: 100	Since 2014: 100		
Discharge measurement station	Perrache	Ternay	Viviers	Viviers, Ardèche

3.1 Pierre-Bénite (PBN)

The reach of PBN is situated a few kilometres downstream of the city of Lyon and of the confluence of the Rhône and Saône rivers. It is characterised by a rather narrow valley, compared to the other sites, and by an urban and industrial imprint, due to its proximity to Lyon: the harbour Edouard Herriot is close, the national highway A7 passes above the site, and railway lines follow its course (Bétin & Cottet-Dumoulins, 1999), whose earth wall added to the constriction of the floodplain on the right bank (Gaydou & Bravard, 2013). Beyond this, the heavy industry is abundant in the area, especially the chemical industry, giving it its name 'the chemical corridor' (Bétin & Cottet-Dumoulins, 1999). A wastewater treatment plant is located next to the dam since 1972, which treats sewage from the agglomeration and whose outputs are directed into the canal (Bravard, 2001). Piégay et al. (1997), underline the agricultural history of the reach itself.

The active channel of PBN ranged from only 600 m to 700 m in 1860. It had been reduced from initially 1800 m to 2000 m under the effect of first dikes at the beginning of the 19th century (Gaydou, 2013). DIREN (2007) furthermore hypothesise that the sediment delivery from the Ain is rapidly depleted in the downstream direction and that the input to the reach was thus already low as well. The active channel is accompanied by a low terrace which was inundated during the 1856 flood. The gradual installation

of the river training structures has been traced back by Salvador (1983) and Poinsart & Salvador (1993). Salvador (1983) gives detailed information on each of the longitudinal dikes, their length and sometimes width and height, and the context of their construction. We will therefore not describe this part in depth, however it should be mentioned that at PBN, all longitudinal dikes were established by 1882, with the exception of the Ternay dike, which would be constructed in 1896. During the period when engineer Girardon had optimised the system, at PBN lateral dikes were finally only added to the existing infrastructure. Piégay et al. (1997) and Parrot (2015) highlighted the strong trend of incision of the channel in this reach since the 19th century, following channelization.

The diversion dam of PBN was constructed between 1962 and 1966 (Salvador, 1983). Contrary to the typical CNR diversion scheme, the power plant is located upstream of the diversion dam, which is due to the local conditions in relation to the dense urban and industrial zone. It was one of the first on the Rhône to be equipped with a bulb turbine (Cazenave, 1997). It was also a pilot site on which the minimum discharge was raised from 10/20 m^3/s to 100 m^3/s in 1999. Subsequently, a small hydropower plant was installed on the diversion dam itself in the year 2000 to compensate for the losses. A morphological, amphibian, and phyto-ecological study in the light of rehabilitation measures had been carried out by Piégay et al. (1997). They noted profound modifications in the characteristics of the riparian forest, which was at a rather mature state and presented non-native and nitrophilous species. For flood risk management reasons, the CNR intervenes on the prairies at lower elevations of the reach to avoid the installation of shrubs and forest stands.

3.2 Péage de Roussillon (PDR)

PDR is situated approximately 50 km south of Lyon. Despite all river engineering measures, this reach features sites of high ecological value, such as the 'île des Graviers' island, which led to the establishment of several nature protection areas in this site (Figure II–8): the national nature reserve '*Réserve Naturelle de l'île de la Platière*' established in 1986 and an '*Espace Naturel Sensible*' (1992). They were later included in a Natura 2000 site, first based on the Habitats Directive (Council Directive 92/43/EEC). Then in 2006 a Special Protection Area (SPA, French: '*Zone de Protection*

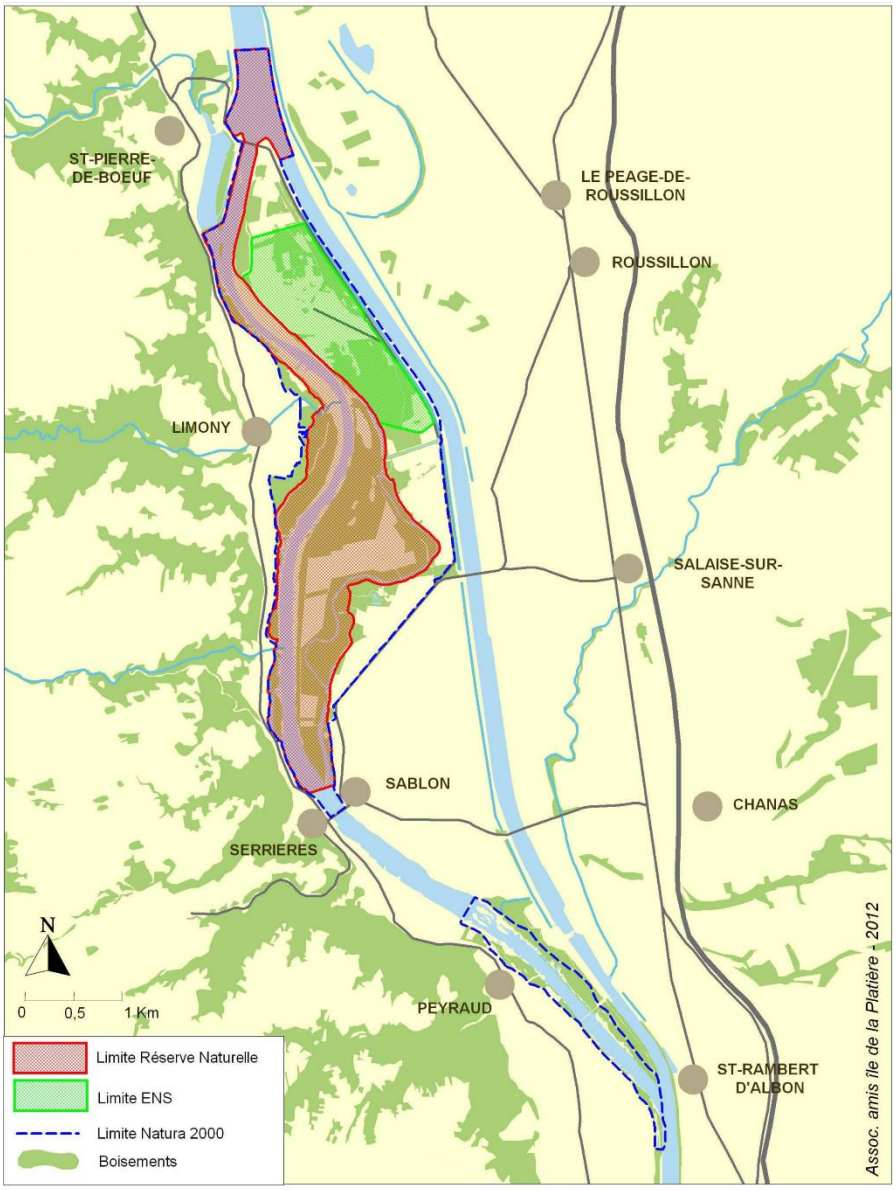

Figure II–8: Nature protection areas within the by-passed reach of PDR, including a nature reserve (transparent red), the Espace naturel sensible (transparent green), Natura 2000 (blue). Forested areas are marked in darker green. Source: Association des amis de l'île de la Platière.

Spéciale' (ZPS)) was established under the Birds Directive (Directive 2009/147/EC since an amendment in 2009). However, the site is also under the influence of pumping activities for industrial, drinking water, and agricultural purposes (in the order of their importance) in close proximity. This led to a gradual but important decline in the groundwater table, which in 1991 required first remedial measures (Stroffek et al., 1996). The PDR reach counts several small tributaries which however feed the by-passed Rhône only marginally. Indeed, the principal tributary to the by-passed Rhône

is the Limony stream, which is almost permanently aquatic, unlike the other tributaries, also coming from the Pilat mountains, which only episodically carry water.

Maps from 1781 ('*Grandvoinet'*) and from 1860 ('*Ponts et Chaussées*'), prior to the two major river engineering phases, depicted numerous islands in the reach, which had slightly diminished in this phase (des Chatelliers, 1995). This braided pattern pursued a meandering phase (Bravard et al., 2008b). The river training works at the end of the 19th century froze the fluvial dynamics. Michelot (1983) describes some of the modifications they imposed on the reach. The hydropower scheme, with the Saint-Pierre-de-Boeuf dam, was implemented between 1973 and 1977, it is thus the most recent of the four schemes studied. It constitutes the only by-passed reach in which the dam was not built in the natural by-passed channel (the Old Rhône) but in an artificially dredged one. The natural channel constitutes today a lake (des Chatelliers, 1995). In 1979, the Peyraud weir was constructed at PK 60.5, with the aim to raise the ground water levels and thus preserve the Peyraud and Sablons plains, as well as the Serrières and Sablons river margins (Michelot, 1983; des Chateliers, 1995). Its height was dimensioned just below the water level at mean discharge prior to damming. The backwater effect affects the upstream part up to PK 53.5. Downstream of the weir, the backwater effect of the next hydro-power scheme downstream is felt (Saint Vallier, PK 75.7) (CNR, 2012). Since 1994, the Nature Reserve regularly carries out forest inventories on permanent plots, applying since 2013 the forest reserves' dendrometric monitoring protocol ('*Protocol de suivi dendrométrique des réserves forestières, module alluvial*', PSDRF-MA) of the National Forestry Office ('*Office National des Forêts*', ONF). In 1987, one campaign had been carried out on non-permanent plots (Pont, 2017). A few of these plots are located in dike fields. One dike field within the Nature Reserve has been subject to intense studying, including a historical analysis of the evolution of the deposits, and samples had been taken in a systematic approach to analyse sedimentological, granulometric, and chemical (PCBs, metals) characteristics (Clozel-Leloup et al., 2013). In 2013, a pilot study had been carried out in twelve dike fields of the reach by Modrak (2013) in the framework of this research.

3.3 Montélimar (MON)

The reach of MON is located few kilometres downstream of Valence. Its plains have long been used for agricultural purposes but exhibit today increasing urbanisation (CNR, 2000; DIREN, 2007; Gaydou, 2013). Principal tributaries to the reach include the Le Meyrol, Roubion/Jabron and La Riaille on the left bank, the Le Lavézon, Le Frayol, and Escoutaye on the right bank. The Roubion, which today discharges into the diversion canal, left a huge dejection cone on the floodplain, which was high enough not to be inundated during the 1856 flood. In 1860, the braided pattern was well developed in the reach. Gaydou (2013) describes the approximate timing of the construction of the river training structures of the reach, of which several already existed in 1860. The construction of the diversion scheme started in 1953. It was put into operation in 1957.

3.4 Donzère-Mondragon (DZM)

Just downstream of MON, we encounter the DZM reach. Its plains—among which Donzère-Mondragon, Pierrelatte, and Lapalud, which are relatively wide compared to other plain sections on the river—have since long been subject to agricultural uses. For this reason, the reach has seen numerous human interventions from fairly early onwards: dredging and dikes in the smaller tributaries, drainage networks and also some minor irrigation measures (e.g. canal de Pierrelatte, which had already been planned in 1611 and was however only fully operational two centuries later, and never gained any importance) (Bethemont, 1972; Allix, 1930). In the upstream part, the channel features some bedrock outcrops which limit its incision. Principal left-bank tributary to the reach is the Ardèche River. The Tricastin nuclear power plant is situated in the reach.

In 1860, the active channel of the reach ranged from 765 m to 4165 m. Yet, the active braid channel had a width of only 140 m and 929 m due to numerous dikes and levees that had already been built (Gaydou, 2013). Poinsart (1992) and Poinsart & Salvador (1993) illustrate the evolution of the dike system in this reach, which had its beginnings early on, to protect or gain new agricultural land. The reach presents the oldest hydropower scheme of the four study reaches and of the Rhône south of Lyon in general (construction works started in 1948 and it was put into operation in 1952). It also features the longest diversion canal (Table II–2).

CHAPTER III METHDOLOGICAL FRAMEWORK

Résumé du chapitre III : cadre méthodologique

Le troisième chapitre présente d'abord les hypothèses structurant notre étude ainsi que l'approche choisie pour y répondre. Il s'agit d'une approche comparative à plusieurs échelles, spatiale et temporelle, qui s'appuie à la fois sur des analyses à partir d'un système d'information géographique (SIG) ainsi que d'une campagne de terrain. Les trois axes principaux de notre recherche sont les suivants : l'état contemporain des casiers ; leur évolution historique ; les caractéristiques de la ripisylve ligneuse. Ils se servent en grande partie des mêmes jeux de données, nous illustrons donc ici les éléments communs. Les méthodes spécifiques à chaque sujet sont ensuite détaillées dans chacun des chapitres IV à VI. Les données communes incluent trois jeux de cartes historiques qui dessinent le chenal et les ouvrages de la période de 1860 jusqu'à 1910. Nous disposons également d'images aériennes (à partir des années 1930) ainsi que d'orthophotographies récentes. Un modèle numérique de terrain (MNT) construit à partir de données de LiDAR (*Light Detection And Ranging*) obtenu lors des années 2007 à 2010 complète ces données en plan par des données tridimensionnelles. En outre, nous avons obtenu des données issues de traitements réalisés lors d'autres études : un MNT relatif, des modèles de submersion et des données de l'évolution du thalweg ainsi que de la ligne d'eau. Des données hydrologiques ont été acquises auprès de la Compagnie Nationale du Rhône (CNR) pour la période 1920 à 2010. Dans un premier temps, nous avons délimité les casiers à partir des données historiques. Ensuite, en préparation de la campagne de terrain, nous avons défini sous SIG des surfaces émergées avant et après la dérivation pour appliquer une approche stratifiée aléatoire d'échantillonnage. Pour 83 placettes, réparties en environ 10 placettes par secteur et période d'aménagement, nous avons mesuré au centre les épaisseurs de sédiments fins à l'aide d'une tige métallique en 2014. Dans deux cercles emboités d'un rayon de 10 m et 20 m, nous avons inventorié la végétation ligneuse d'un diamètre respectivement de 7,5 cm à 30 cm et de plus de 30 cm. Dans trois sous-placettes de 1,5 m nous avons également inventorié des stades de régénération. Pour les analyses comparatives, nous avons appliqué des statistiques inférentielles et produit des illustrations en forme de boîtes-à-moustache,

des régressions linéaires et des coefficients de corrélation pour les relations entre les variables, ainsi que des statistiques multivariées.

1 Introduction

We start this chapter by providing information on the general comparative approach of this study. Since the three principal axes of our research (contemporary status of the dike fields, their historical evolution and vegetation characteristics) were based in large part on the same datasets and sampling schemes, we shall then illustrate the available data and the measures and statistics common to all of them. More specific methodologies are presented at the beginning of each of the chapters IV to VI.

2 General approach

First case studies of the sedimentation in dike fields on the Rhône River have revealed the complex nature of the deposits and their evolution (Clozel-Leloup et al., 2013). Beyond this, field observations indicate that the dike fields have not all evolved in the same way. Indeed, we find today a whole gradient of conditions from aquatic over semi-terrestrial to terrestrial. To describe the range in dike field characteristics and overcome potential peculiarities of individual dike fields, we aimed at analysing as many dike fields as possible. For that purpose, we chose a comparative approach where we combined similarity analyses and connectivity analyses (Figure III–1). Comparative approaches are used in fluvial geomorphology and ecology to allow for generalisations and to build conceptual models.

“Similarity analysis,” as defined by Piégay (2016, p. 86), “focuses on a set of landforms at a single spatial scale level for which the comparison of the attributes allows groups to be identified and ordered”. This may be tackled in a synchronous perspective, where measurements are conducted simultaneously at several sites. Likewise, a retrospective (or diachronous) perspective is possible, in which a component is analysed with respect to its change over time. In this framework, space-for-time substitution is applied to study stages of landscape evolution, or chronosequences (Picket, 1987; Fryirs et al., 2012; Piégay, 2016). This method has been used for two centuries under various denominations, such as location for time substitution (Paine, 1985) or ergodic reasoning (Fryirs et al., 2012). It is based on river adjustment trajectories, as well as process-form interactions and involves studying sites of

different age to ultimately infer temporal patterns. In a wider context, this can aid the interpretation of underlying controls and better understand the organisation of cumulative drivers (Fryirs et al., 2012; Depret et al., 2017). A prerequisite for the application of space-for-time substitution is that initial conditions at the various sites are similar. All sites must further underlie the same processes in a comparable physical context or geological setting. These conditions also show the shortcomings of this analysis, in that sites can be similar but never identical so that interpretations may still require further support (Picket, 1987). It is however well adapted to aid the formulation of hypotheses around a conceptual model. Our similarity analysis focused on four by-passed study reaches, each of which presents a set of dike fields. Each study reach has been by-passed at a different point in time, introducing also a space-for-time substitution approach to this comparison.

Connectivity analysis is based on the relationships between system components of different scales and the fact that adjustments in any one will have a cascading effect on the others. As an example, Piégay (2016) named the link between a reach and its former channels, which can be extrapolated to our case of by-passed reaches and their dike fields.

We compared the characteristics of the dike fields at several spatial scales to aid the interpretation of patterns in terms of potential drivers: (a) between upstream and downstream reaches, (b) between individual by-passed reaches, (c) within by-passed reaches (i.e. between pre- and post-dam sites and between individual dike fields). Both present-day characteristics and several dates in the past were treated this way.

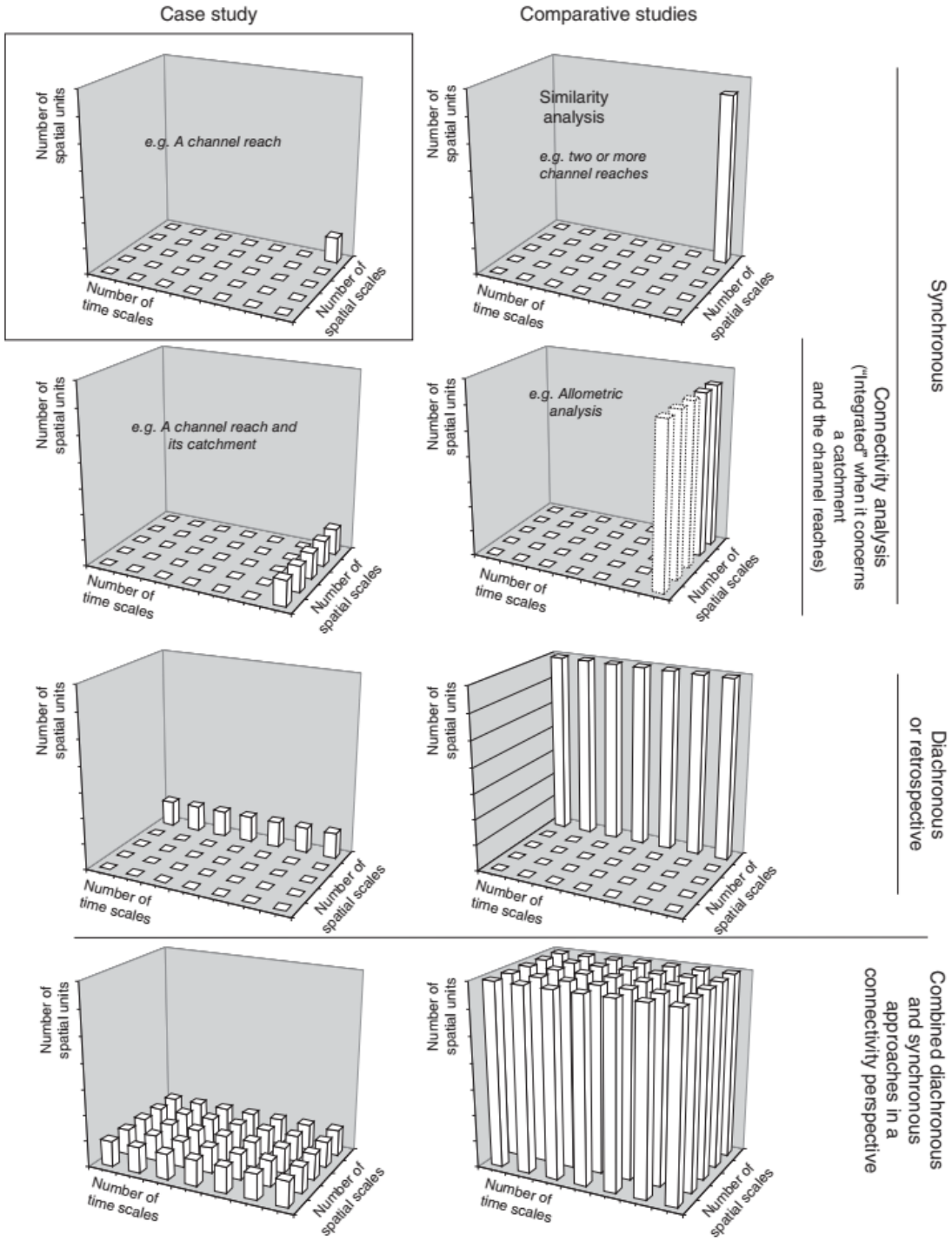

Figure III–1: Schematic 3-D models of fluvial system study approaches based on different spatio-temporal scales, as well as the number of spatial units/components considered (Piégay, 2016, source: Piégay & Schumm, 2003).

3 Data sources

3.1 Historical maps

Three sets of historical maps were available for the identification and delimitation of the dike fields: a scan of a) the topographical map of the course of the Rhône River dating from 1857-1876 (referred to as '1860 Atlas'), of b) a bathymetric map from the Compagnie Nationale du Rhône (CNR, 1897–1908), and of c) the so called Branciard cartographic map from approximately 1910 (Figure III–2, Table III–1). The 1860 Atlas was drawn by the public administration Ponts et Chaussées ('Bridges and Roads'). It provided a reference of the fluvial geomorphologic and land use conditions prior to the principal river management measures, showing, however, early engineering structures, their type and date of construction. It also depicts the limits of the 100-year flood from 1856 (Bravard et al., 2010). The series of bathymetric maps show many of the major river engineering structures, however a lot of dike fields do not yet appear in their final state, as especially some of the lateral dikes had not been constructed yet. The bathymetric survey data are provided with reference to the water levels of extreme low flow conditions of 1897 (were marked -0.60 m at Givors, +0.05 m at Valence, -0.35 m at Avignon, and -0.70 m at Arles). The Branciard map gave a relatively complete picture of the final phase of the engineering structures.

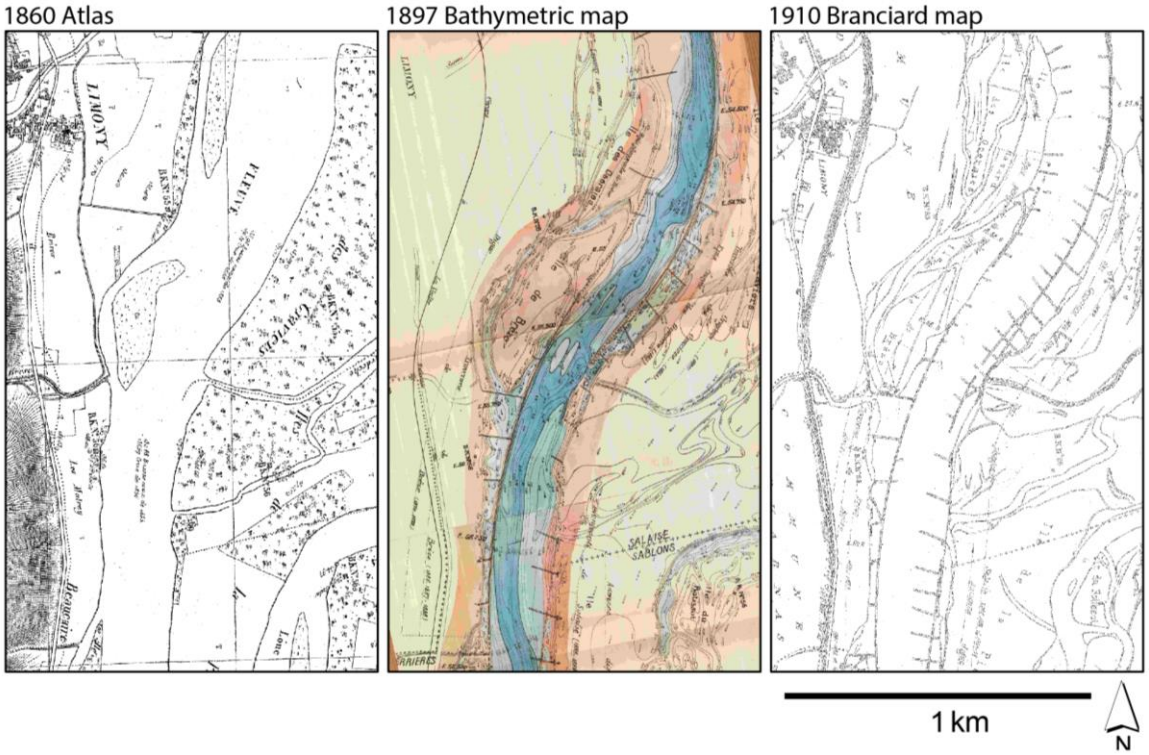

Figure III–2: Available maps, zoom to PDR by-passed reach.

Table III–1: Overview of cartographic material.

Denomination	Year	Origin / Author	Source	Scale	Number of sheets used	Colour, format	Legend	Discharge	Georeferencing	References
Carte topographique du Cours du Rhône ('1860 Atlas')	1857–1866 and 1870–1876	Service spécial du Rhône, Administration des Ponts et Chaussées	Archives of the Compagnie Nationale du Rhône (CNR)	1:10,000	PBN: 2 PDR: 2 MON: 3 DZM: 5	B + W, jpeg	Yes	Baseflow	P. Gaydou (UMR- CNRS 5600)	Gaydou, 2013
Carte bathymétrique ('Bathymetric map')	1897 (PBN, PDR, MON, DZM), 1902 (DZM), 1908	?	Direction Régionale de la CNR Avignon, obtained from G. Raccasi (CEREGE)		PBN: 3 PDR: 3 MON: 6 DZM: 9	Colour, jpeg	?	Low flow/ Baseflow conditions of 1897	J. Ambert; L. Mathieu; E. Parrot (UMR-CNRS 5600)	G. Raccasi, Ambert, 2013; Mathieu, 2013; Parrot, 2015
Plan cartographique Branciard ('Branciard map')	~1910	CNR?	Archives of the CNR, obtained from G. Raccasi, (CEREGE)	1:5,000	PBN: 4 PDR: 3 MON: 1(*) DZM: 5(*)	B + W, tif	?		P. Gaydou (UMR- CNRS 5600)	

(*) The available sheets do not cover the entire by-passed reach

3.2 Aerial images and orthophotographs

The available planimetric (2-dimensional or 2-D) data sets were comprised of aerial images and orthophotographs derived from the French National Institute of Geographic and Forestry Information (Institut National de l'Information Géographique et Forestière, IGN) (Figure III–3, Table III–2). The aerial images were obtained georeferenced by J. Riquier and A. Tena-Pagan (UMR-CNRS 5600 EVS). For our analyses, we selected one aerial image series per reach to represent pre-dam conditions at a set interval since dike construction (in the 1940s, approximately 60 years since intensive dike construction). Then we selected a set of recent orthophotographs (from the 2000s, approximately 120 years since intensive dike construction) to represent contemporary conditions for each of the four reaches.

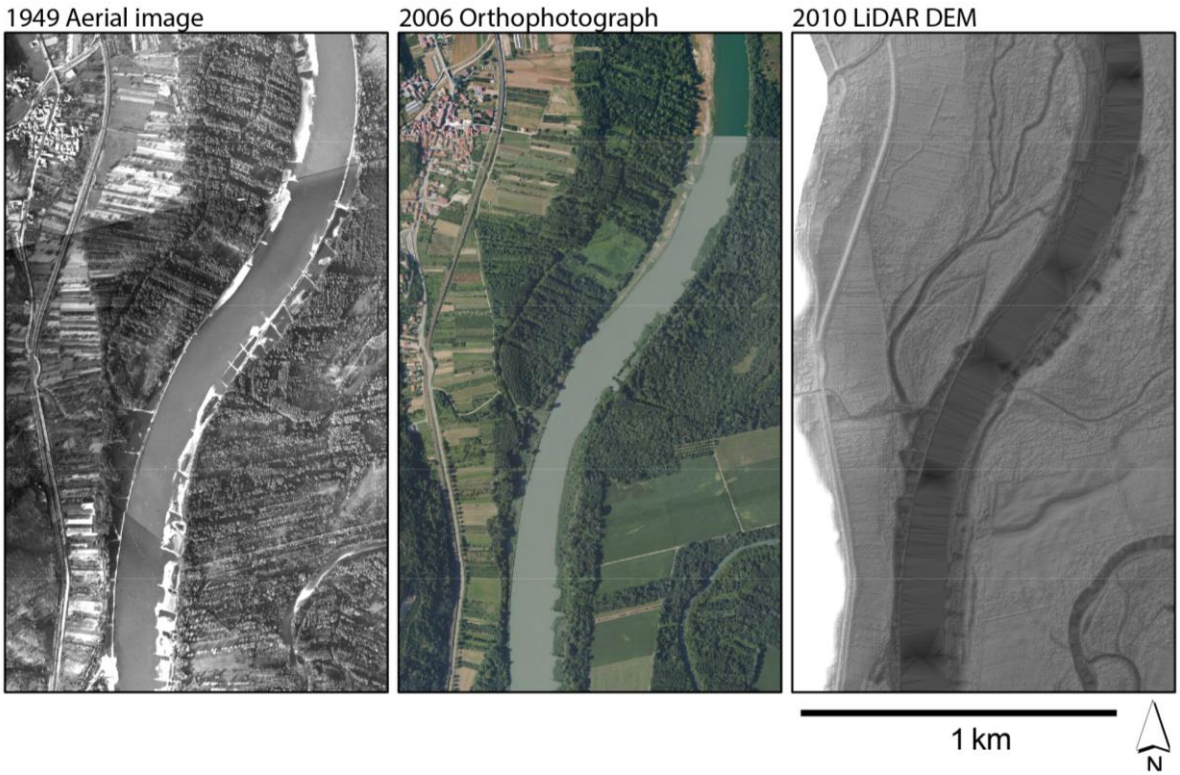

Figure III–3: Available aerial images, orthophotographs, and LiDAR data-derived DEM. Zoom to the same site in the PDR by-passed channel. Source: IGN©.

Table III–2: Characteristics of aerial image and orthophotograph sets from IGN.

Reach	Year	Purpose	Acquisition date (day/month)	Type	Scale	Colour depth	Mean daily discharge [m^3/s] – station(*)
PBN	1945	Pre-dam, comparable date	30/09	Aerial image	1:25,000	Grey-scale	451 – Perrache, 596 – Ternay
	2008	Contemporary post-dam, comparable date	---	Orthophoto		Colour	---
PDR	1948 and 1949	Pre-dam, comparable date	31/05 and 01/10	Aerial image	1:25,000 and 1:16,500	Grey-scale	810 – Ternay, 342 – Ternay
	1958	Directly prior to dam construction	16/06	Aerial image	1:25,000	Grey-scale	860 – Ternay
	1986	Directly after dam construction	---	Aerial image	---	Grey-scale	---
	2006/07/09	Contemporary post-dam, comparable date	---	Orthophoto		Colour	---
MON	1949	Pre-dam, comparable date	01/10	Aerial image	1:16,500	Grey-scale	520 – Viviers
	2006/07	Contemporary post-dam, comparable date	---	Orthophoto		Colour	---
DZM	1947	Pre-dam, comparable date and directly prior to dam construction	03/09 and 07/11	Aerial image	1:25,000 and 1:15,000	Grey-scale	760 – Viviers, 462 – Viviers
	1954 and 1955	Directly after dam construction	13/05 and 15/03	Aerial image	1:25,000 and 1:25,000	Grey-scale	1090 – Viviers, 1110 – Viviers
	1976	Intermediary date after dam construction	19/06	Aerial image	---	Grey-scale	---
	2006/07/09	Contemporary post-dam, comparable date	---	Orthophoto		Colour	---

(*) see Figure II–7 for location of the various stations

For PDR and DZM, a more detailed analysis was carried out to capture conditions directly prior to and directly after dam construction, as well as several decades after dam construction. For PDR, we selected one more image series as close as possible prior to dam construction (1958, with dam construction in 1977). For DZM the 1947 images covered this purpose (dam construction in 1952). Beyond this, we chose one series as shortly after dam construction as possible, as a reference for the direct impacts of the dam (1986 for PDR, 1954/55 for DZM). At DZM, we furthermore selected an image series from 1976, representing an intermediary state, which was represented by the years 2000 orthophotographs for PDR.

All aerial image series were chosen as to cover a maximum of the extent of each of the four reaches. We tried to avoid images taken at high flows. In any case, we obtained the date of image acquisition and determined the associated discharge conditions. We were thus able to study the extent of bars, the geomorphic units which are the most affected by water level or discharge changes.

Covering several administrative units, the orthophotographs consisted of mosaics of several photographs of which we were unable to obtain all the corresponding dates of acquisition from the IGN at the time the analyses were carried out. In visually comparing the water levels with other images we assumed that generally low flow conditions (legal residual flow) prevailed.

3.3 LiDAR data

The planimetric data sets were complemented by 3-dimensional remote sensing data: airborne LiDAR (Light Detection And Ranging) data based digital elevation models (DEMs) from the IGN, were available for the four by-passed reaches (Figure III–3). The surveys had been carried out in the framework of the Rhône topographic database (Base de Données Topographiques du Rhône, BDT) in 2007–2008 at DZM, and in 2009–July 2010 at PDR, PBN, and MON. Prevailing discharge conditions corresponded to the legal residual flow in each reach (Džubáková et al., 2015). The models covered the entire floodplain of the by-passed reaches with a resolution of 2 m and a vertical accuracy of 0.2 m.

Following a first evaluation by Džubáková et al. (2015), we carried out a differential global positioning system (DGPS) survey to determine the accuracy of the LiDAR data along the narrow dike units (Figure III–4). Using an R8-Trimble global navigation

satellite system receiver, we surveyed ground points along selected longitudinal dikes at PDR, MON, and DZM, which featured varying vegetation cover. We distinguished between bare rock / sediment, shrub, and tree cover. The survey was carried out in March 2014, when leaves had not yet developed, and the vegetation canopy cover was thus at a minimal extent. We surveyed a total of 460 points, at the locations of which we extracted the corresponding LiDAR DEM elevation values. Then we calculated the elevation difference between ground-surveyed and simulated values:

$$Accuracy = z_{DGPS} - z_{LiDAR}, \qquad (Equ. III-2)$$

with z [m] = elevation.

As expected, accuracy was highest for bare dikes, followed by shrub and finally tree cover (Table III–3).

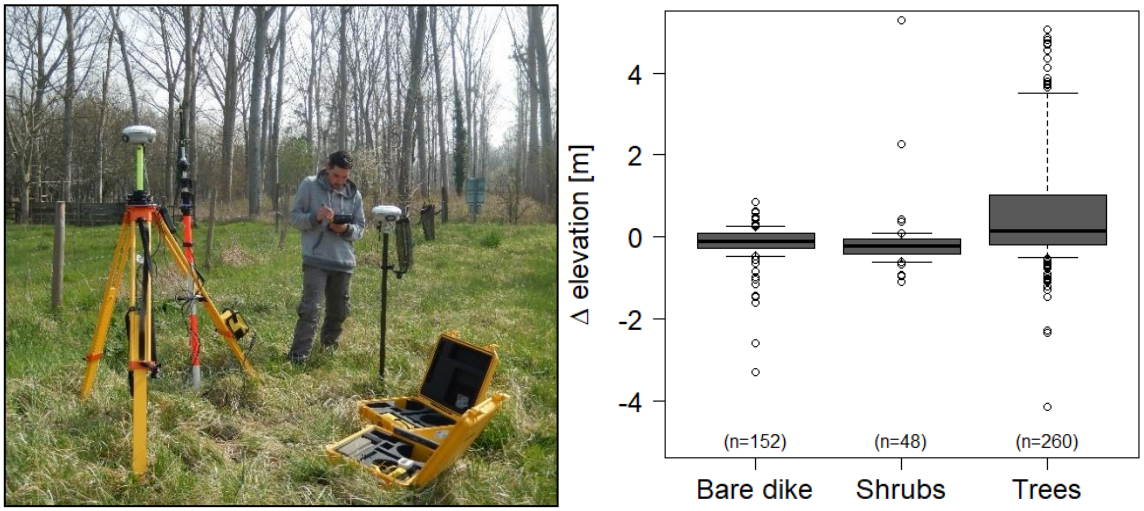

Figure III–4: Preparation of the DGPS in the field, with the fixed station in yellow to the left-hand and the mobile station in black to the right-hand side of the operator (left). LiDAR accuracy under varying vegetation cover (note that the y-axis was cut) (right).

Table III–3:

	Sample size	Mean [m]	RMSE [m]
Bare dike / sediment	152	0.16	0.51
Shrubs	48	–0.10	0.92
Trees	260	0.82	3.05

3.4 Data provided from previous treatments on the data sets presented

Džubáková et al. (2015) computed relative elevations, as well as submersion duration, frequency, and discharge based on the LiDAR DEM, rating curves, flow time series, and field reconnaissance (Table III–4). The resulting data sets were used in the present work to explore both the longitudinal dike characteristics, as well as contemporary topographical conditions within the dike fields. We assumed that the dikes had undergone only minor changes (albeit some sedimentation, some passages whose origins were uncertain, or vegetation installation) as many of them were still visible during field campaigns or even on orthophotographs. Water surfaces had been assigned as zero values by Džubáková et al. (2015).

Parrot (2015) had extracted points of the thalweg, i.e. the lowest points in each lateral profile across the channel, every 500 m along the by-passed channels of the four study reaches from a) the bathymetric map from 1897 / 1907–1908 (see section 3.1) and b) from lateral profiles stemming from the Topographic Database (BDT, 2007–2010). The BDT data from the IGN had been provided to her by the Compagnie National du

Table III–4: Overview of available sumbersion models, bed and water level data.

Data provided	Units	Date or period represented	Initial data source	Reference
Relative elevations	m a.w.l. (at a discharge of 100 m^3/s)	2007–2010	LiDAR DEM (Topographical Database of the Rhône (Base de Données Topographiques du Rhône, BDT)	Džubáková et al. (2015)
Submersion duration	d/yr	2007–2010		
Submersion frequency	events/yr	2007–2010		
Submersion discharge	m^3/s	2007–2010		
Early bed level change	m	1897 / 1907–1908 to pre-dam year	Bathymetric map and bathymetric numerical data	Parrot (2015)
Recent bed level change	m	Pre-dam year to 2007–2010	BDT	
Early water level	m a.s.l.	1902–1903	Official report (Ponts et Chaussées, 2010)	Bravard (2010)
Recent water level	m a.s.l.	~2010	BDT	IGN

Rhône (CNR). The long profiles Parrot (2015) created based on these data constitute a reference of a) the conditions of the channel bed during the adjustment phase in response of the first dikes and b) contemporary conditions. Numerical bathymetric data provided to Parrot (2015) by the CNR, was used to compile profiles which c) corresponded to channel bed conditions just prior to the construction of each dam. Parrot (2015) calculated elevation changes between the three profiles to determine the impacts of the two major management phases: 'Early bed level change' was calculated as the difference in bed level between the construction phase of the dikes and the construction of the dam. 'Recent bed level change' constituted the difference in bed level between the construction of the dam and today. Based on these data, we additionally calculated 'net bed level change', as the sum of 'early bed level change' and 'recent bed level change'.

For the four study reaches, we obtained a set of water level data from J.-P. Bravard (UMR-CNRS 5600 EVS) representing the low flow conditions of 1902–1903. The data had been derived in kilometre steps from an official report (Ponts et Chaussées, 2010) by Bravard (2010). The proclaimed vertical precision was of 1 cm, although Bravard (2010) questioned this value, while he estimated that averages over several kilometres could be considered reliable for the calculation of slopes.

The Topographical Database of the Rhône (Base de Données Topographiques du Rhône, BDT) constituted a second set of available water level data. The surveys date from at DZM and from July 2010 at PBN, PDR, and MON. It was carried out by the IGN under mean discharge conditions.

3.5 Hydrological data

We obtained mean daily discharge series of the total Rhône from the Compagnie Nationale du Rhône (CNR): from 1920 to 2010 for PDR, MON, and DZM, and from 1920 to 2009 for PBN. For the period after dam construction, discharge values had been modelled and provided by Lamouroux et al. (2015).

4 General methods

4.1 Study objects

4.1.1 Identification and delimitation of the dike fields

We used historical maps and aerial photographs, together with more recent remote sensing data (see section 3) to identify a maximum of longitudinal and lateral dikes which make up dike fields along the four study reaches. The Girardon dike system evolved over a time span of several decades, involving extensive correction works—addition, removal, displacement, and adjustment of dikes. Detailed information on these works are only partially available in archived maps and reports. The final digitisation of the dike fields therefore focused, where possible, on their present location and extent, including a maximum of information from the historical data.

We concentrated on sedimentation and vegetation patterns within the area comprised between a few meters distance of the dike crests to avoid analysing potential phenomena related to the dikes themselves. Therefore, we adapted the digitisation of the dike field units accordingly (Figure III–5). The lateral boundary of the dike fields in inland direction was defined as the river bank prior to the two major management

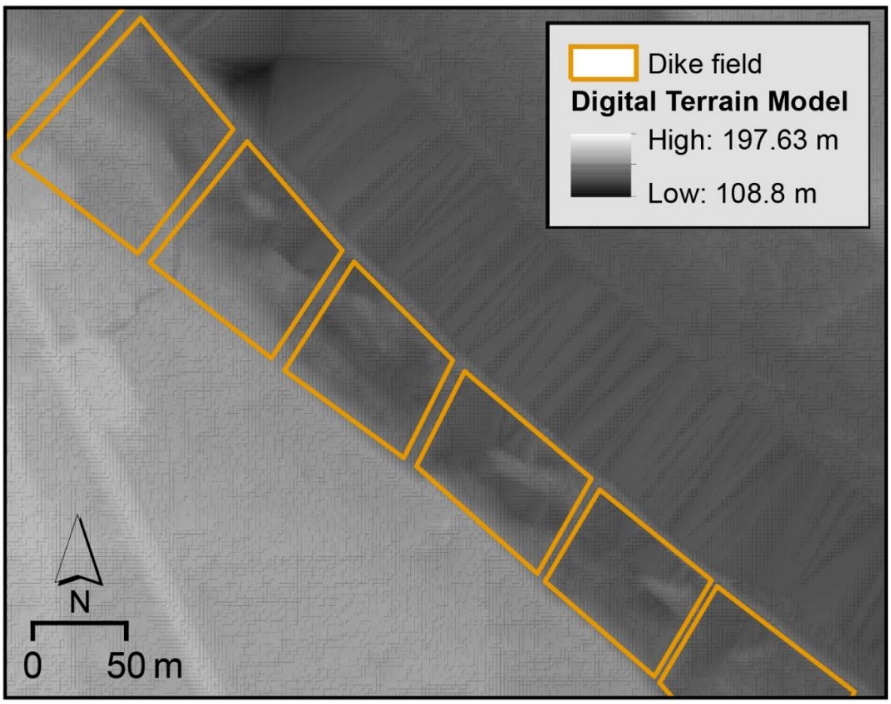

Figure III–5: Dike field delimitation and digitisation (orange). Zoom to PDR by-passed reach.

phases and approximated based on the 1860 Atlas. In locations where the channel bed had undergone major changes between 1860 and the installation of the dikes, the boundaries were approximated using the Digital Terrain Models (DTMs). Sharp breakpoints in the slope were often identifiable.

At the reach of MON, which was included in the study at a later point in time than the other three reaches, a different operator carried out the identification and digitisation of the dike fields (Villet, 2014). We minimised the error related to a change in operators by close collaboration and a clearly defined procedure.

4.1.2 Selection criteria

Out of 524 dike fields thus delineated (PBN: 157; PDR: 120, MON: 93, DZM: 154) we selected 360 (PBN: 113; PDR: 73; MON: 65; DZM: 109) for general analyses. At this step, dike fields were excluded when sedimentation and/or vegetation patterns were potentially influenced (Table III–5). For certain further analyses, only sub-sets of the entire set of dike fields were used (Figure III–6), for varying reasons. For instance, only a small subset of dike fields could be sampled during the field campaign due to the necessary limitation in time and effort. Furthermore, not all variables could

Table III–5: Criteria of exclusion of dike fields from further analyses.

Exclusion criterion	Details	% of excluded dike fields
Significant amount of infrastructure / human activities within the dike field (except agriculture → see below)	Buildings, roads, weirs, barrages, canals, mining activities, landfills, leisure activities infrastructure, ports, etc.	22.0
Subject to rehabilitation measures / land use modification in the past	Re-modelling of the initial landscape for various reasons, e.g. excavation of artificial channels or ponds following initial sediment deposition	20.1
Particularly complex shape of the dike field		16.5
Existence today doubtful or localisation impossible		11.0
Subject to near future restoration measures	E.g. complete or partial removal of dikes planned during the period of the study (based on CNR report (CNR, 2012)	9.8
Major agricultural use		7.3
Direct influence by a tributary	Hydrosedimentary / geomorphic influence (erosion/sediment deposition)	2.4
Position isolated from other dike fields		1.2

always be recorded for each individual dike field (e.g. when a part of reach was not covered by the LiDAR data or an aerial image series). Yet some R packages for multivariate analyses, for instance, require input data tables made up entirely of complete cases (i.e. individuals/rows containing no single NA value).

4.2 A combined geomorphologic and ecological sampling campaign

The aim of the field campaign was to integrate both the geomorphologic and ecological aspects of the study. This had implications on the final sampling scheme and the plot set-up, as described in the following. It also meant that the focus of the field effort was on forested surfaces of the dike fields.

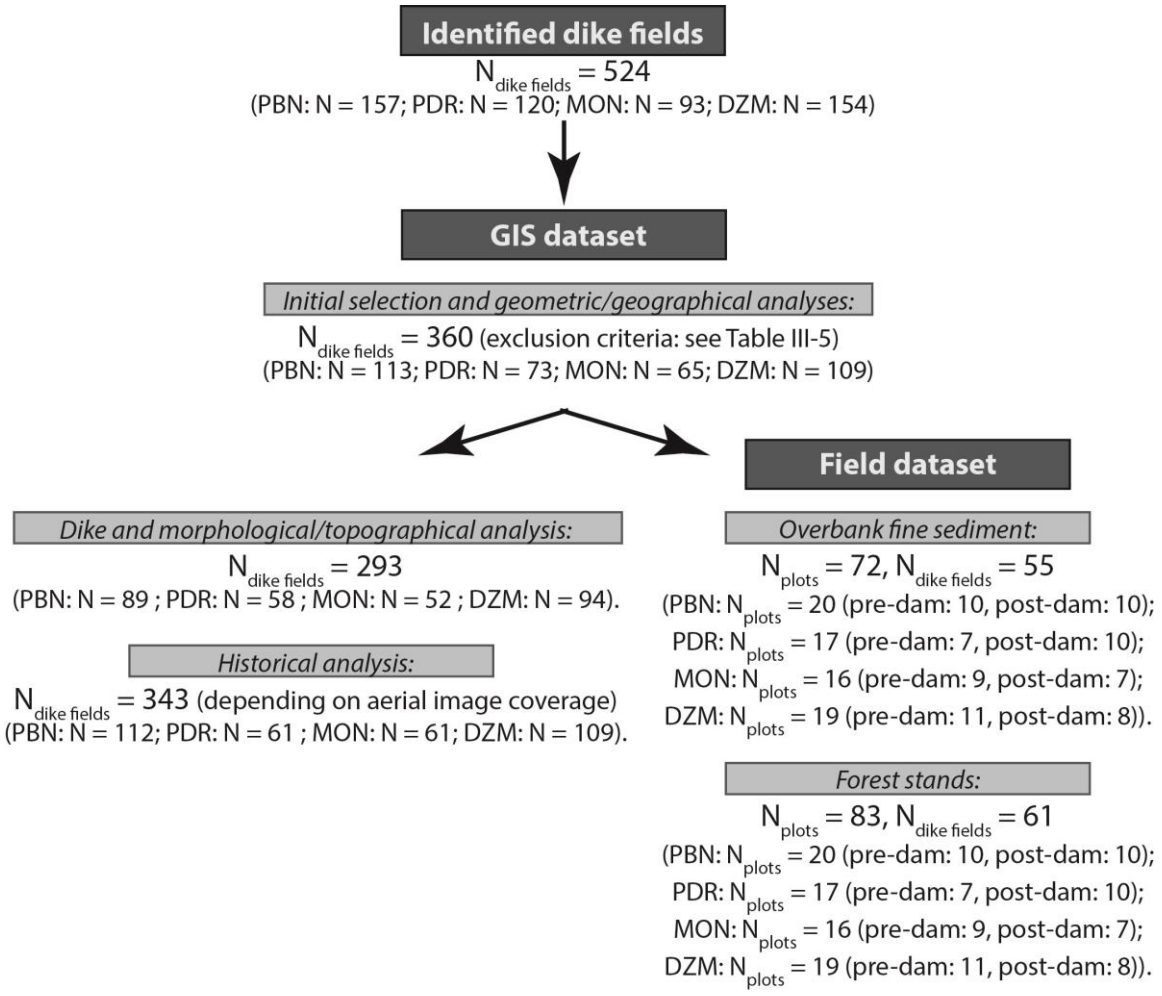

Figure III–6: Schematic overview of sample sizes available for the different analyses carried out in the framework of this PhD work.

4.2.1 General sampling scheme

We chose a stratified random approach for the distribution of our sampling plots. This allowed us to focus on differences in sedimentation and vegetation patterns between pre- and post-dam surfaces within the four study reaches (Table III–6). With these terms, we refer to surfaces which have become emerged over an extended period of the year either prior to dam construction (pre-dam surfaces) or following dam construction (post-dam surfaces). This thus represents a spatial approach to study the chronosequence of two management phases and the respective geomorphologic and ecological impacts.

In each reach, we therefore mapped the river bank and other emerged surfaces in the 1860s, and pre- and post-diversion surfaces within the dike fields (Gruel, 2014). For this we used the editing tool in ArcGIS software on the historical maps and aerial images. We then superposed the resulting polygons of the various years and, using the ArcGIS *intersect* tool, created a 'surface age' or rather a 'management phase' map (Figure III–7). The availability of images has been limited at the time when the Geographical Information System (GIS) work was carried out. At PDR, therefore, the images of the year 1958 were used to represent the break between pre- and post-dam surfaces (diversion having taken place in 1977), while at PBN the only image series available was from 1945 (diversion in 1966) (Table III–6). Eventually, we also digitised

Table III–6: Pre- and post-dam periods in each study reach.

Reach	Pre-dam period	Post-dam period	Historical map used to digitise emerged surfaces prior to dike construction	Image series used to digitise pre-dam surfaces	Years of image series used to represent post-dam surfaces
PBN	1860-1966	1966-2009	Atlas 1860	Aerial image 1945	Orthophoto 2008
PDR	1860-1977	1977-2009	Atlas 1860	Aerial image 1958	Orthophoto 2009
MON	1860-1956	1956-2009	Atlas 1860	Aerial image 1949	Orthophoto 2007
DZM	1860-1952	1952-2009	Atlas 1860	Aerial image 1947	Orthophotos 2007 and 2009

the current forest cover within the dike fields from the orthophotos of the years 2000 and intersected this information with the surface age map. The resulting surfaces were furthermore cut by the polygons of the dike fields, to avoid sampling the dikes.

The *Create Random Points* tool from the *Sampling* toolbox in the *Data Management* Tools in ArcGIS version 11.0 allowed us to randomly distribute our sampling plots (Seignemartin, 2014). A minimum of 10 plots were located on forested pre-diversion surfaces of each reach and a minimum of 10 plots on forested post-diversion surfaces of each reach. Additional plot locations served as back-up in case of unexpected conditions in the field. Around each plot centre a buffer (minimum allowed distance) of 20 m was used to avoid overlapping plots. Another buffer of 6 m buffer centred on the boundary between the two management period's surfaces was applied to account for digitisation or georeferencing errors.

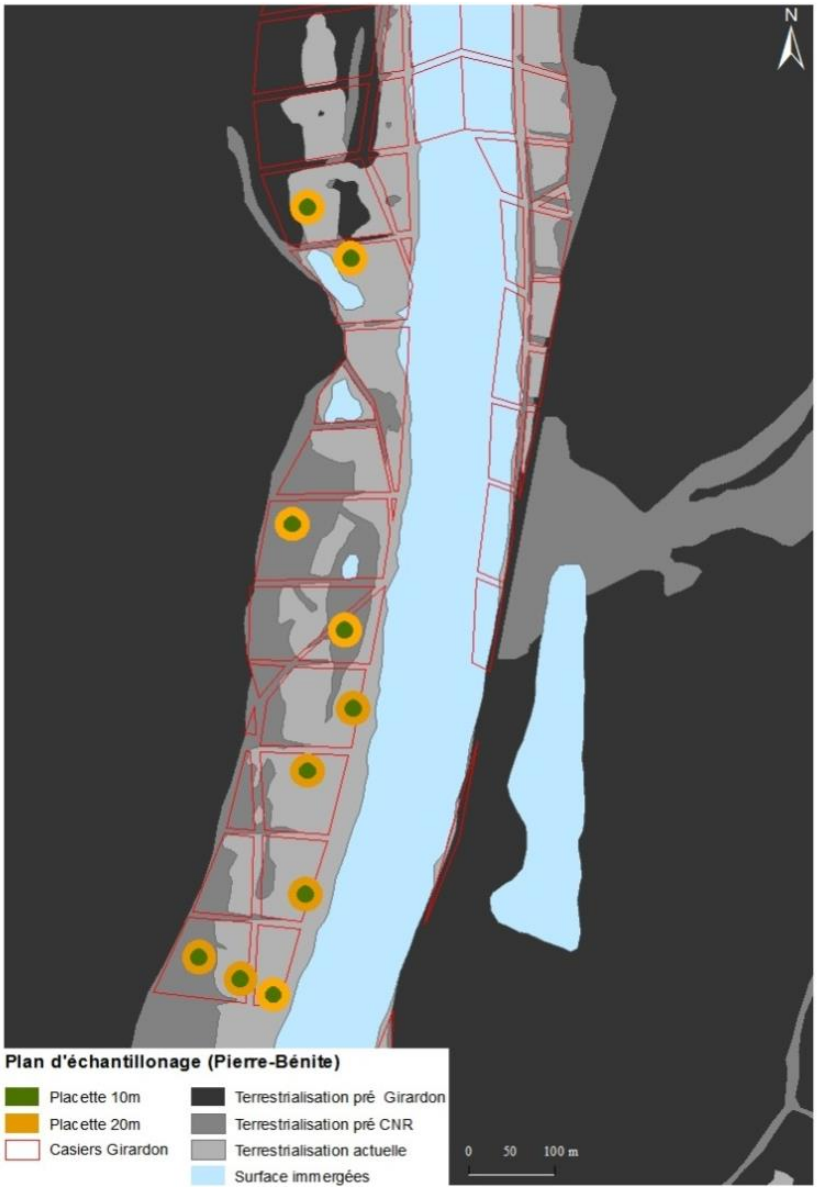

Figure III–7: Surface age map and examples of plot distribution at the by-passed reach of PBN (Gruel, 2014).

4.2.2 General field plot set-up

Field work took place between March and Mai 2014. We worked in nested circular plots of 1,257 m^2 following the alluvial protocol of the French National Forest Office (Office National des Forêts, ONF; Figure III–8). On site, we located the pre-determined centre of each plot using a portable Trimble GeoXH Global Positioning System (GPS) (Figure III–9). Plot centres were moved parallel to the by-passed channel (generally 10 m) when all or part of the 10-m radius plot or 1.5-m radius sub-plots fell in a disturbed

or managed zone (e.g. cleared zones around river kilometres marks), which had not been detected on the aerial images.

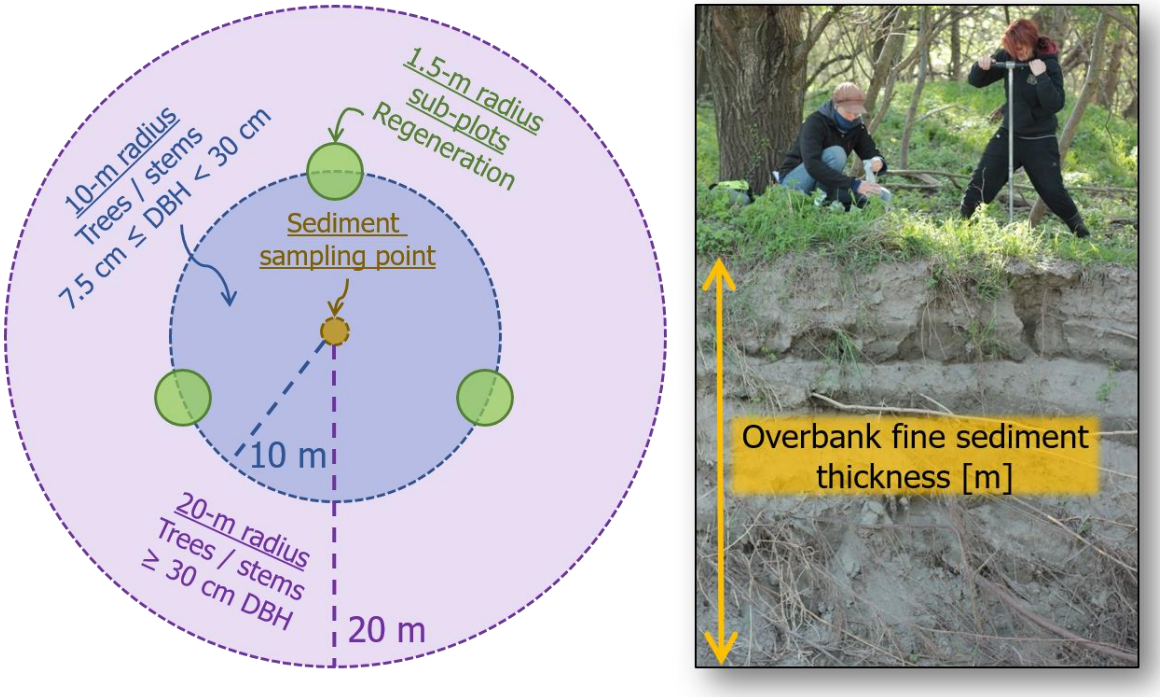

Figure III–8: Sample plot set up (left) and overbank fine sediment measurement and sampling using a soil auger (right; photo taken by Gruel in 2014).

Figure III–9: Use of the GeoXH GPS.

The plot centre served as sampling point for overbank fine sediment (sand and finer; ⌀ ≤ 2 mm; Figure III–10). We assumed that this fine grain-dominated material was deposited on coarse-grained material which a) made up the former river channel or b) had accumulated in the initial phase following dike construction, when the dike field was still frequently hydraulically connected. Using an iron rod, we followed the procedure described by Constantin et al. (2010) to determine the fine sediment layer thickness. We therefore penetrated the rod into the ground until a dull sound was heard, and an increased resistance was felt. This was assumed to reflect the boundary to the gravel-dominated layer. We then measured the distance from the ground level to the gravel layer. Sediment samples were likewise extracted in 20-cm intervals down to the gravel layer using a soil auger. The analyses and results of these data are only partially described in the framework of this study but were further exploited in the PhD project of G. Seignemartin (in prep.). Oftentimes, fine sediment thickness was determined with the soil auger when taking the samples, as a comparison of the results of the rod and the auger revealed good correspondence. When the plot centre (i.e. the sediment sampling point) was inaccessible due to a thick vegetation cover, woody debris or roots in the vertical profile (which prevented completion of the sediment sampling down to the gravel layer) we moved the sampling point 1 m to the north.

The forest inventory was based on a nested approach to optimally account for differences in stem diameter and related density, while minimising the field effort. Within a 20-m radius (1,257 m^2 plot) we inventoried all live and dead standing trees ≥ 30 cm diameter at breast height (DBH). Within a 10-m radius (314 m^2 plot), we

Figure III–10: Use of the iron rod to determine overbank fine sediment thickness (left). Overbank fine sediment sample extracted using the soil auger (right).

inventoried all live and dead standing trees in the range of 7.5 cm ≤ DBH < 30 cm. On the 10-m radius circle we located the centres of three sub-plots of 1.5-m radius each (7 m^2)—one was positioned at 0 degrees (true North), one at 133 degrees, and one at 267 degrees. In these sub-plots, we inventoried regeneration stems < 7.5 cm DBH, distinguishing furthermore saplings (< 7.5 cm DBH and ≥ 0.5 m height (H)) and seedlings (H < 0.5 m). For more details on the various inventory parameters, refer to chapter VI.

4.3 Conceptual model of control factors

Based on a literature research on potential drivers of overbank fine sedimentation patterns we formulated an initial conceptual model. We focused on reach-scale as well as local-scale drivers, based on studies of similar entities, such as former side arms, groyne fields, and lateral cavities. But also natural channel-floodplain interactions were considered. The resulting model guided our hypotheses and their testing. We shall therefore briefly present it in the following.

One of the key processes regarding riverine floodplains is their hydrological connectivity to the channel, as we saw in chapter I section 1.1 (Junk et al., 1989; Heiler et al., 1995; Amoros & Bornette, 2002; Tockner & Stanford, 2002; Opperman et al., 2010). The water transfer between the channel and the floodplain during overbank flows provides and exchanges energy, matter (sediment, nutrients), and organisms. The complex pathways of water transfer (both surface and subsurface) lead to vast gradients of connectivity and consequently a large range of different water bodies (Amoros et al., 1987; Ward et al., 2002). The connectivity determines the supply of suspended sediment (Citterio & Piégay, 2009). This led us to our first hypothesis at the local scale:

H1: Sedimentation and terrestrialisation rates reached a maximum at an intermediate level of connectivity between dike fields and the main by-passed channel. The connectivity is itself dependent on the height of the longitudinal dike, the channel geometry, local flow level controls, and the hydrological regime or dam operation.

In H1 we assumed that at high frequency and magnitude of connection, scour processes predominate over sedimentation, while at very low frequencies of connection the amount of sediment provided to the dike fields decreased.

At the local-scale, we furthermore expected hydraulic conditions at the interior of the dike fields to influence the quantity of the sediment that was eventually deposited.

Several authors highlighted the influence of local flow patterns (CHAPTER I, section 1.1.1; Pizzuto, 1987; Marriott, 1992; Asselman & Middelkoop, 1995; Walling & He, 1998).

H2: Within the dike fields, hydraulic conditions determined sediment trapping, with low flow velocities and shear stresses favouring deposition.

We approximated hydraulic conditions based on parameters affecting flow velocity (Equation III–1):

a) Roughness related to land cover (in the dike fields mainly forest vs. pasture). For a given level of connectivity, we expected accelerated sedimentation and terrestrialisation in forest-dominated dike fields compared to pasture-dominated dike fields.
b) Topographic or slope conditions.

$$V = \frac{1}{n} \times R^{\frac{2}{3}} \times i^{\frac{1}{2}}, \qquad (Equ.\,III-1)$$

where:

V is the average flow velocity of the cross-section [m/s]
n is the Gauckler-Manning coefficient
R is the hydraulic radius [m]
i is the slope of the hydraulic grade line or linear hydraulic head loss, which equals the channel bed slope under conditions of constant water depth.

At the reach scale, we presumed that the suspended sediment supply to the by-passed channel controled the rate of evolution of the deposits. This supply will depend on the land use patterns in the river basin, as well as on supplies from tributaries. Depret et al. (2017) found significantly higher evolution rates of former channels downstream than upstream of the Isère River, one of the major tributaries in terms of suspended sediment supply. This pattern was expected in dike fields, too. Walling & He (1998, p. 217f) stated that "[…] the amount of sediment deposited per unit area will be proportional to the total mass of sediment in the overlying water column […]".

Our third hypothesis therefore addressed this question:

H3: For a given level of connectivity, sedimentation and terrestrialisation rates were higher in the reaches downstream of the Isère confluence (MON, DZM) than in those upstream of the confluence (PBN, PDR).

Furthermore, we had to account for the changing nature of some of these factors with time. The connectivity, for instance, may change with the installation of a dam and related water level changes (Nilsson & Berggren, 2002) or according to the morphological evolution of the channel, such as aggradation or incision (e.g. Wyżga, 2001; Citterio & Piégay, 2009). We hypothesised that hydrological connectivity changes through time would induce changes in the trajectory of sedimentation and terrestrialisation.

- **H4a: The by-passing of the old Rhône reaches implied a decrease in the water level, which favoured the process of terrestrialisation by rapid dewatering. In contrast, overbank fine sediment deposition decreased due to the reduced frequency of connection between the dike fields and the by-passed channel.**
- **H4b: Degradation of the main by-passed channel led to dewatering and decreased overbank fine sediment deposition. Inversely, channel aggradation first conserved aquatic surfaces but also led to higher sediment inputs to the dike fields.**

Eventually, we anticipated that also the time span since diversion might have an impact on the terrestrialisation status of the dike fields. Our last hypothesis therefore was:

H5: The longer the time span since diversion, the more advanced the terrestrialisation state.

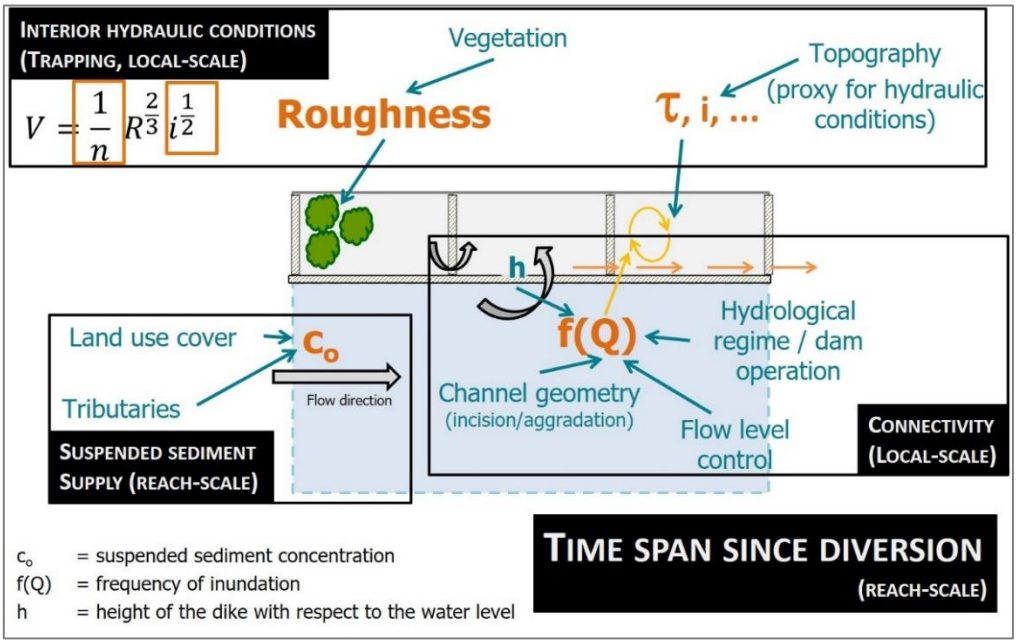

Figure III–11: Working version of a conceptual model of drivers of dike field sedimentation / terrestrialisation.

Based on these hypotheses and the literature research, we composed an initial scheme of control factors (working version, Figure III–11). Over the course of this manuscript, we shall further develop the individual roles of each factor and their interactions.

4.4 Data analysis methods

We used R software (R Core Team, 2016) and Excel (Microsoft, 2010) for all statistical computations. In terms of descriptive statistics, we mainly employed boxplot representations to describe the distributions of variables and compare them between reaches, reaches and periods, or between reaches and reference sites. In this thesis, the boxplots represent the median, the 10^{th}, 25^{th}, 75^{th}, and 90^{th} percentiles, and extreme values (outliers) (Figure III–12).

In terms of inferential statistics, we applied one-way analysis of variance (ANOVA) to test for significant differences between normally distributed variables (determined using shapiro test). For non-normally distributed variables we used Kruskal–Wallis followed by pairwise Mann–Whitney U tests. To explore relationships between two variables, linear regression analyses were carried out and correlation coefficients calculated—Pearson correlation for normally distributed variables and Spearman rank tests for non-normally distributed variables (Hollander & Wolfe, 1973). Reported R^2 refer to adjusted R^2. We used logistic regression to predict the probability of a binary categorical data in response to a predictor variable.

Finally, multivariate analyses served to explore patterns which might not be evident from simple bivariate analysis of the same variables. The principal components analysis (PCA) structures and simplifies a data set (which we centred and scaled) by transformation. The data can thus be visually represented in a space of reduced dimensionality (1-D, 2-D, 3-D). Where the objective was to classify the individuals (dike fields) according to their similarity/dissimilarity regarding the input variables, we used the results from the PCA in hierarchical cluster analysis. The results from clustering were represented in a dendrogram. For the compositional characteristics of the dike field forests, we carried out a detrended correspondence analysis. Compared to classical correspondence analysis or other ordination methods, DCA overcomes arch and edge effects related to gradient data (Hill & Gauch, 1980).

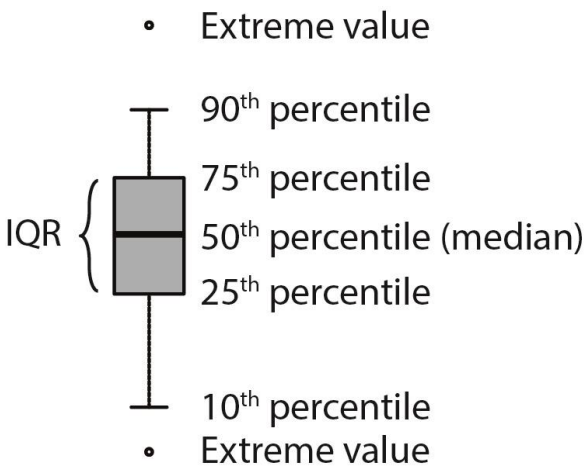

Figure III–12: Values represented by the boxplots presented in the framework of this thesis.

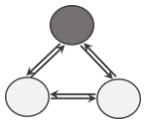

CHAPTER IV CONTEMPORARY STATUS OF DIKE FIELD DEPOSITS

Résumé du chapitre IV : état contemporain des casiers

L'intérêt du chapitre IV consistait tout d'abord en une caractérisation des conditions actuelles dans les casiers, afin d'évaluer les patrons spatiaux de la sédimentation ainsi que la diversité ou l'homogénéité des habitats associés. Nous avons commencé avec une analyse du système des digues dans les quatre secteurs d'étude : la chronologie de la construction, ainsi que la géométrie des casiers qui en résulte. Ensuite, nous avons caractérisé les dépôts sédimentaires ainsi que les unités paysagères à partir d'une vectorisation du matériel cartographique et des images sous SIG. Pour ajouter des informations topographiques, nous avons extrait du modèle numérique de terrain (MNT) les hauteurs relatives moyennes des surfaces émergées dans les casiers, ainsi que l'écart-type des hauteurs absolues pour estimer la variabilité topographique. Pour établir une typologie morphologique et topographique des conditions actuelles des dépôts de sédiments, une analyse en composantes principales (ACP) centrée normée, suivie par une classification ascendante hiérarchique ont été effectuées. Pour investiguer les facteurs de contrôle potentiels, nous avons à la fois appliqué l'approche comparative, et ajouté les variables au plan factoriel issus de l'ACP.

Nous avons notamment pu constater une possible différence de datation entre les digues longitudinales dans les différents secteurs. Ainsi, leurs caractéristiques sont potentiellement variables. La géométrie des casiers en découlant varie également. La plupart des casiers sont aujourd'hui quasiment totalement terrestres, alors qu'il existe encore quelques différences inter-secteurs, avec plus de zones aquatiques à PDR et à DZM qu'à PBN ou MON. Sept types de casiers ont été distingués à partir de l'ACP, dont la distribution spatiale semble fortement liée à des facteurs locaux. De fait, en rajoutant les facteurs de contrôle à cette analyse, nous avons constaté que le taux d'atterrissement ainsi que la hauteur relative des surfaces sont liés aux variables de connectivité du casier au chenal principal (fréquence et durée de submersion de la digue longitudinale, hauteur de la digue). La géométrie du casier semble contrôler la variabilité topographique. Ceci a été confirmé par les analyses comparatives.

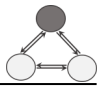

1 Introduction

The starting point of our investigations was the characterisation of the contemporary conditions in the dike fields. This allowed us to get a first impression of inherent spatial patterns of sedimentation and to evaluate the potential diversity or inversely homogeneity of patterns and habitats. It also provided an assessment of the land cover units in their present-day extent to prepare the field work necessary for the other chapters. In this chapter we also introduced the first potential control factors to interpret these patterns.

2 Methods

2.1 Characterising dikes and dike fields

Larger scale studies on dike fields are still rare. One of the aims of this thesis was thus to give an overview of the characteristics of the dikes and the resulting dike fields and related environments encountered in the four study reaches.

2.1.1 Construction periods of longitudinal and lateral dikes

Due to the complex evolutionary history of the Rhône dike system, it was not feasible to define an age for individual dike fields, which would have marked the beginning of a modified sedimentation pattern. As we saw in chapter II, the dike system evolved over several decades, with individual dikes being added gradually. For instance, Salvador (1983) remarked that the majority of dikes at Pierre-Bénite (PBN) had been built in the period between 1838 and 1910. Following construction, correction and maintenance works were carried out. Furthermore, the available data sets did not always cover the entire four reaches from upstream to downstream, and not all individual dikes were named or dated. For some dikes visible on early aerial images, we found no trace on the historical maps. The lack of legends on additional maps rendered it difficult to know which dikes were planned (and perhaps never built) and which ones were already in place. We also saw that some of the first dikes did not necessarily induce the sedimentation process but significant scour. Eventually, differences in dike field age would have been masked by imprecisions related to limited data availability, both in space and time. To overcome these constraints, we compared construction periods at the reach level, rather than at the level of individual dike fields.

For this, we used the information on historical maps, aerial images, as well as bibliographic references (Salvador, 1983; Poinsart, 1992) to determine the age of individual longitudinal and entire groups of lateral dikes.

2.1.2 Geometric characterisation of dike fields

As we saw in chapter I, studies of harbours, groyne fields, and abandoned channel entrances revealed that the number of gyres, or re-flow structures, developed between dikes is related to their shape, mainly the aspect ratio or width to length ratio (Langendoen, 1992; Uijttewaal et al., 1999; Uijttewaal et al., 2001; Sukhodolov et al., 2002; Le Coz et al., 2010; Mignot et al., 2013). We determined the size and perimeter of dike fields, using the *calculator* tool in ArcGIS. As a proxy of dike field shape, we related these two variables to each other performing a linear regression on the log-log-transformed values. Moreover, we applied the *Minimum Boundary Geometry* tool of the *Features* toolset in the *Data Management* toolbox. This tool drew a rectangle of minimum width around each dike field polygon and calculated the minimum width of the rectangle, as well as the resulting length (the long side of the rectangle) (Figure IV–1). This automatic procedure did not take into account the position of the dike fields with regards to the by-passed channel, and thus at some occasions inversed width and length. We manually corrected these cases.

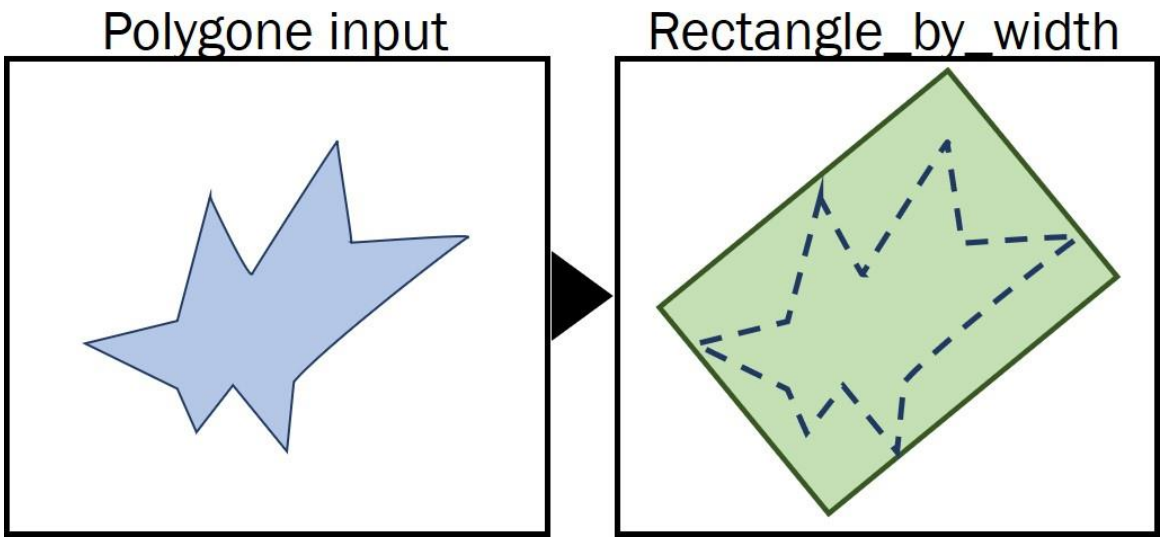

Figure IV–1: Principle functioning of the ArcGIS tool "Minimum Bounding Geometry", with the option "Rectangle by width".

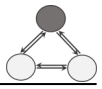

Eventually, we analysed the width of a small sub-sample of dike fields with regards to the width of the former river channel in 1860 using the equation

$$\frac{W_{Right\ river\ bank\ dike\ fields} + W_{Left\ river\ bank\ dike\ fields}}{W_{1860\ channel}}, \qquad (Equ.\ IV-1)$$

with W = width, and $W_{1860\ channel}$ corresponding to the width of the initial channel arm in which the dike fields were constructed.

We then verified if the former channel width would have determined dike field width.

2.2 Identifying contemporary terrestrialisation patterns in dike fields

2.2.1 Planimetric (2-D) extent of sediment deposits and land cover units

For each dike field, we mapped land cover units to describe the contemporary state of terrestrialisation. We used orthophotographs (PBN: 2008; PDR: 2009; MON: 2006/7; DZM: 2006/7/9) from the French National Geographic and Forestry Information Institute (Institut National de l'Information Géographique et Forestière, IGN) (Table III–2). The mapping consisted in an aerial photograph interpretation using a zoom corresponding to a scale of 1:2,000 in ESRI ArcGIS 10.1. We distinguished aquatic (water surfaces) and terrestrial units (bare sediment and herbaceous layer, forest stands, agricultural fields, and infrastructure elements) (Figure IV–2, Appendix I: Figure A–I–1). We then calculated the percentage of terrestrial surfaces per dike field (terrestrialisaton status), as well as the percent surface cover of each individual land cover unit.

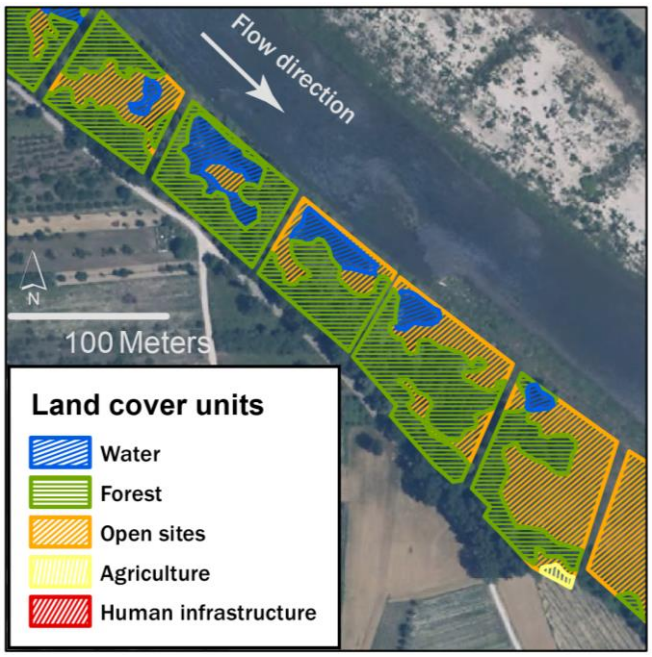

Figure IV–2: Mapping of land cover units in ESRI ArcGIS (source orthophotograph: IGN©).

2.2.2 Topographic characteristics of sediment deposits

Using the *Zonal Statistics as Table* tool (*Zonal* tool set in the *Spatial Analyst Tools* toolbox in ArcGIS), we extracted summary statistics from the DEM and detrended DEM to describe the topography of the dike field deposits. From the DTM, we extracted the standard deviation (SD) of the absolute altitude for each dike field as a proxy for the topographic variability of the sediment deposit. The tool uses the following formula to calculate standard deviation:

$$\boldsymbol{SD} = \sqrt{\frac{\mathbf{1}}{\boldsymbol{N}}\sum_{\boldsymbol{i=1}}^{\boldsymbol{N}}(\boldsymbol{x_i} - \overline{\boldsymbol{x}})^{\mathbf{2}}}, \qquad (\boldsymbol{Equ.IV-2})$$

We chose the standard deviation over the range to avoid a strong influence of extreme values (e.g. due to errors in the delimitation of dike fields toward the former river bank). Yet, linear regression revealed a strong relationship between the two parameters (R^2 = 0.72, Figure IV–3).

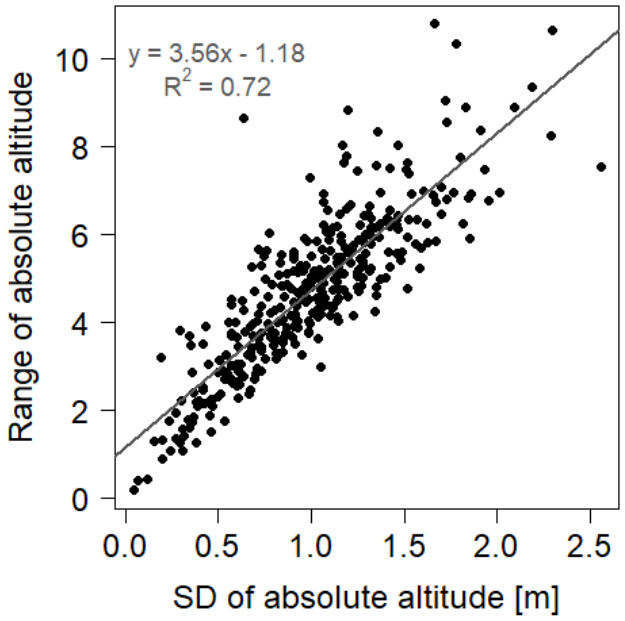

Figure IV–3: Relationship between the standard deviation and the range of absolute elevations of surfaces in dike fields.

From the detrended DEM, we used the extracted mean value of relative elevation above the water level at a discharge of 100 m^3/s. This served as a proxy to compare the surface elevation of the deposits, and thus the thickness of the deposits.

2.2.3 Describing patterns using multivariate analysis

Using a principal components analysis, followed by hierarchical clustering on the resulting principal components, we analysed potential gradients in dike field terrestrialisation patterns. Active input variables comprised the terrestrialisation state (% terrestrial surface), topographic variability (SD of absolute altitude), and the mean relative elevation of emerged surfaces above the water level at a discharge of 100 m^3/s. The analyses were carried out in R using the '*ade4*' package.

2.3 Assessment of potential factors controlling sedimentation

We chose a comparative approach to identify potential control factors and analyse their individual roles on sedimentation processes. For this we worked at different scales (inter- and intra-reach as well as inter- and intra-dike field comparisons). Furthermore, using FactoMineR in R (Lê et al., 2008), we projected the variables as supplementary variables to the PCA factor map to visualise correlations with sedimentation /

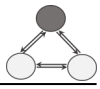

terrestrialisation patterns. Moreover, we plotted the distribution of the variables against the typology which resulted from the hierarchical cluster analysis in form of boxplots to demonstrate potential gradients. The analysis of the control factors is structured around our hypotheses (CHAPTER III section 2).

2.3.1 Hydrological connectivity: hypothesis H1

Following recent findings regarding the evolution of abandoned channels, we assumed that the connectivity of the dike fields to the main by-passed channel to be a major control on sedimentation. It is assumed to depend on longitudinal and lateral dike characteristics, primarily height. The water level in the by-passed channel likewise plays a role. It depends itself on the discharge regime or any modifications undertaken to its regard (dam management, weirs), as well as on the topographic evolution of the by-passed channel (e.g., incision, narrowing) (see Chapter V).

In a GIS approach, we identified the mean relative height of the longitudinal dikes relative to the water level at a discharge of 100 m^3/s. We thus included in this analysis dike fields which are separated from the by-passed channels by a longitudinal dike. Dike fields without longitudinal dikes, such as those situated in side arms, were excluded from the analysis. First, the longitudinal dike crests were digitised in ESRI ArcMap based on orthophotographs and DTMs. Where the dikes were buried with sediment we approximated the location of the crest based on the old maps and aerial photographs available. We used a buffer of 2 m width at both sides of the digitised polylines to capture the whole dike and to reduce errors concerning inaccurate crest digitisation.

Second, using the detrended DEM, we extracted minimum and mean relative heights of each dike crest above the water level at a discharge of 100 m^3/s. From the submersion models provided by Džubáková et al. (2015), we extracted maximum dike submersion duration and maximum dike submersion frequency. Submersion duration is defined as the number of days during which the dike is submerged per year. Frequency represents the number of events during which the dike is submerged per year.

We further extracted the minimum threshold discharge of submersion from the respective model from Džubáková et al. (2015). To be able to compare threshold discharges between reaches, we calculated the respective return periods. First, we

applied the Gumbel statistical method to define a linear equation, then we used the following equation to calculate T:

$$T = \frac{1}{1 - e^{-e^{-u}}}, \qquad (Equ.\,IV-3)$$

where u corresponds to the Gumbel variate.

The relationship between submersion threshold discharge and return period is displayed in Figure IV–4.

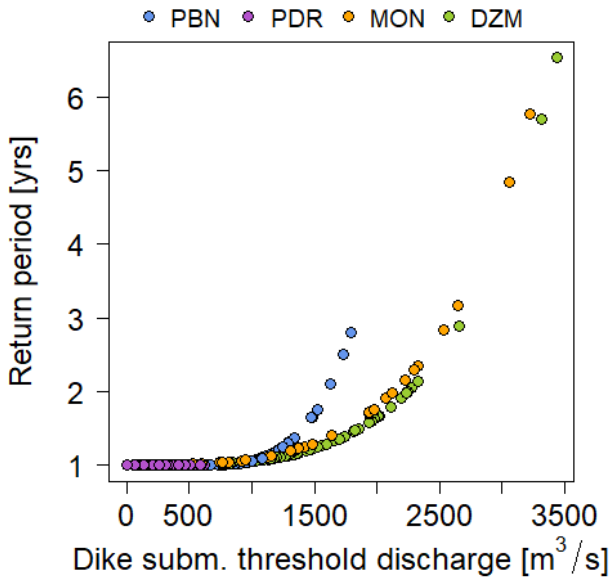

Figure IV–4: Relationship between dike submersion threshold discharge and return period of dike submersion threshold discharge for each reach.

2.3.2 Suspended sediment supply: hypothesis H3

We hypothesised that the transit of suspended sediment into the dike field depended on its level of connectivity, i.e. the higher the connectivity, the more frequent the potential input of suspended sediment from the by-passed channel. We would therefore expect that for a given level of connectivity, sedimentation patterns in dike fields would vary depending on the concentration of suspended sediment supplied to the reach. Our assumption was that the Isère River, one of the major tributaries of the Rhône in terms of sediment supply, would significantly increase the concentration of suspended sediments. We therefore compared sedimentation patterns between

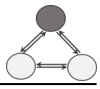

upstream and downstream reaches: PBN and PDR are located upstream of the Isère, while MON and DZM, are located directly downstream of the confluence of the Isère and the Rhône.

2.3.3 Hydraulic conditions at the interior of the dike fields: hypothesis H2

In hypothesis 2, we assumed that at the interior of the dike fields, roughness elements, such as vegetation, as well as microtopographic conditions influence the trapping of sediments delivered to the dike field. Woody vegetation is supposed to enhance trapping compared to bare sediment surfaces or herbaceous layers. We compared sedimentation patterns between woody vegetation dominated and bare sediment/herbaceous layer dominated dike fields of similar connectivity conditions using boxplots and Mann-Whitney U tests. Following the findings from the literature of geometry effects on hydraulic conditions and thus sedimentation and erosion patterns we explored the size of the dike fields and their width to length ratios. We included

3 Results

3.1 General dike field characteristics

3.1.1 Localisation of dikes and dates of construction

Girardon finalised an extensive system of dikes over hundreds of kilometres along the Rhône River. In the four study reaches we identified 524 dike fields (PBN: 157; PDR: 120, MON: 93, DZM: 154), covering an area of 498.3 ha (PBN: 78.5 ha, PDR: 68.4 ha, MON: 89.3 ha, DZM: 262.2 ha) (Figure IV–5). Three hundred and thirty-three dike fields were situated along the banks of the former main channel (PBN: 90, PDR: 83, MON: 81, DZM: 79), 191 dam former side arms (PBN: 67, PDR: 37, MON: 12, DZM: 75). In general, they occurred in sequences of several dike fields, seldom as isolated units.

Additional, more detailed information on many of the dikes, such as their detailed chronologic evolution and characteristics, the conditions in the channel which provoked their installation, or the global context, are given by Salvador (1983) for the reach of PBN and by Poinsart (1992) for DZM. Gaydou (2013) described the objectives of each individual dike unit and the evolution of deposits and land cover at a coarser temporal time scale for all four reaches.

The earliest longitudinal dikes (non-submersible) were constructed in the downstream reaches, and mainly at DZM (Figure IV–6). In this reach, most longitudinal dikes were built in the first two periods of construction (see chapter II for details) and thus consist mainly of non-submersible and submersible dikes. At PBN and MON we find principally submersible and low dikes, whereas at PDR the largest number of dikes, with some exceptions, were constructed comparatively late. They essentially consist of low dikes

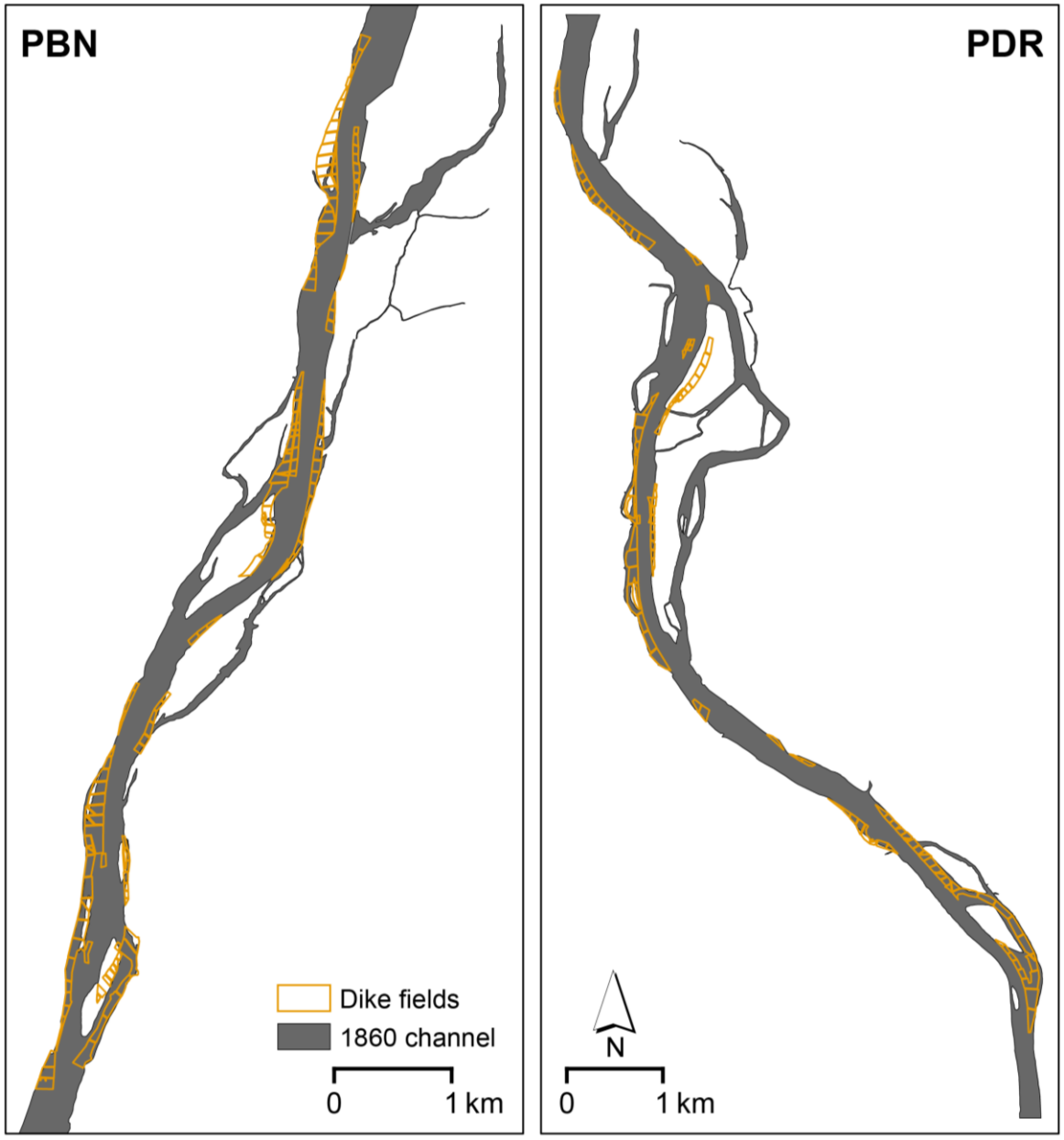

Figure IV–5: Localisation of dike fields in the four reaches. The channel in the background represents conditions from 1860 (digitisation: Gruel, 2014; based on the 1860 Atlas—note that some areas show an offset due to low quality georeferencing).

Figure IV–5 continued.

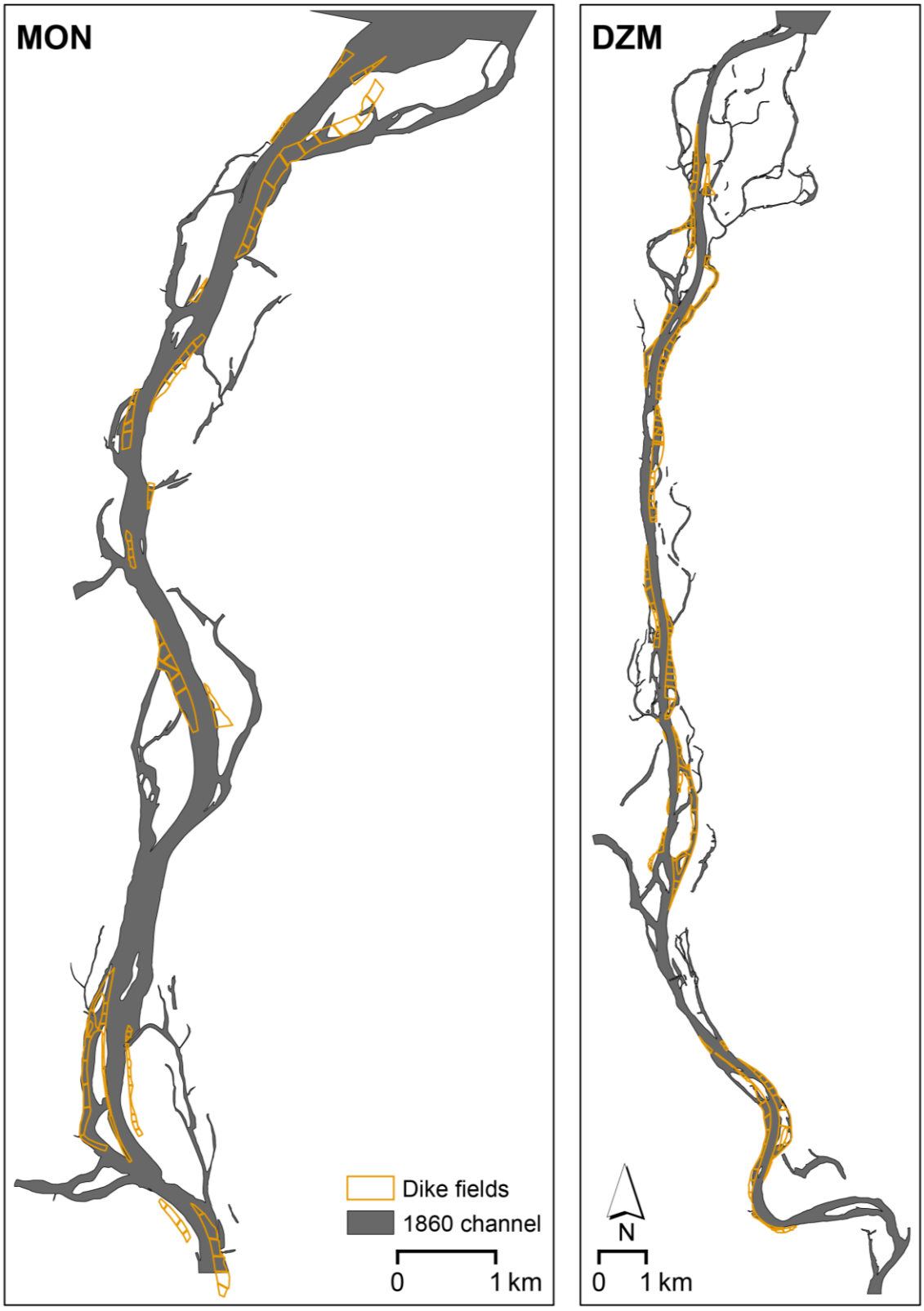

and Girardon dikes. In summary, we state that the majority of the longitudinal dikes were constructed before Girardon and that their implantation did not follow the same

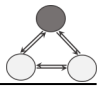

temporal patterns in the four study reaches. According to the prevailing period in which the dikes were built we expected differences in their characteristics, i.e. in their design (notably crest elevation; Poinsart & Salvador, 1993) but potentially also other characteristics, such as crest width or construction materials, as observed in the field.

Among the lateral dikes in the study reaches, few were constructed in the second and third periods of construction (Figure IV–7). Instead, it was under Girardon's guidance that the majority of cross dikes ('*tenons*', '*traverses*', and '*épis*') were added to the longitudinal dikes. At MON the large majority of dike fields seemed to be finalised by 1900. At PBN, PDR, and DZM, often one decade or two passed between the construction of the first and the addition of the final lateral dikes in a sequence. The final configuration of several dike fields would therefore only be reached in the early 1900s. Indeed, Salvador (1983) notes that the main period of dike construction took place between 1838 and 1910. Following this period, individual lateral dikes were still added in order to accelerate the process of sedimentation, but their numbers remained low.

The spatial distribution of dike fields resulting from the installation of the mentioned engineering structures varies between reaches (Figure IV–5). At MON for instance, the dike field network was less dense compared to the other reaches, with several kilometres of the river banks showing no engineering structures. We found no parallel dike field sequences on the same river bank in this reach and only few at DZM, too. This is more common in the upstream reaches of PBN and PDR.

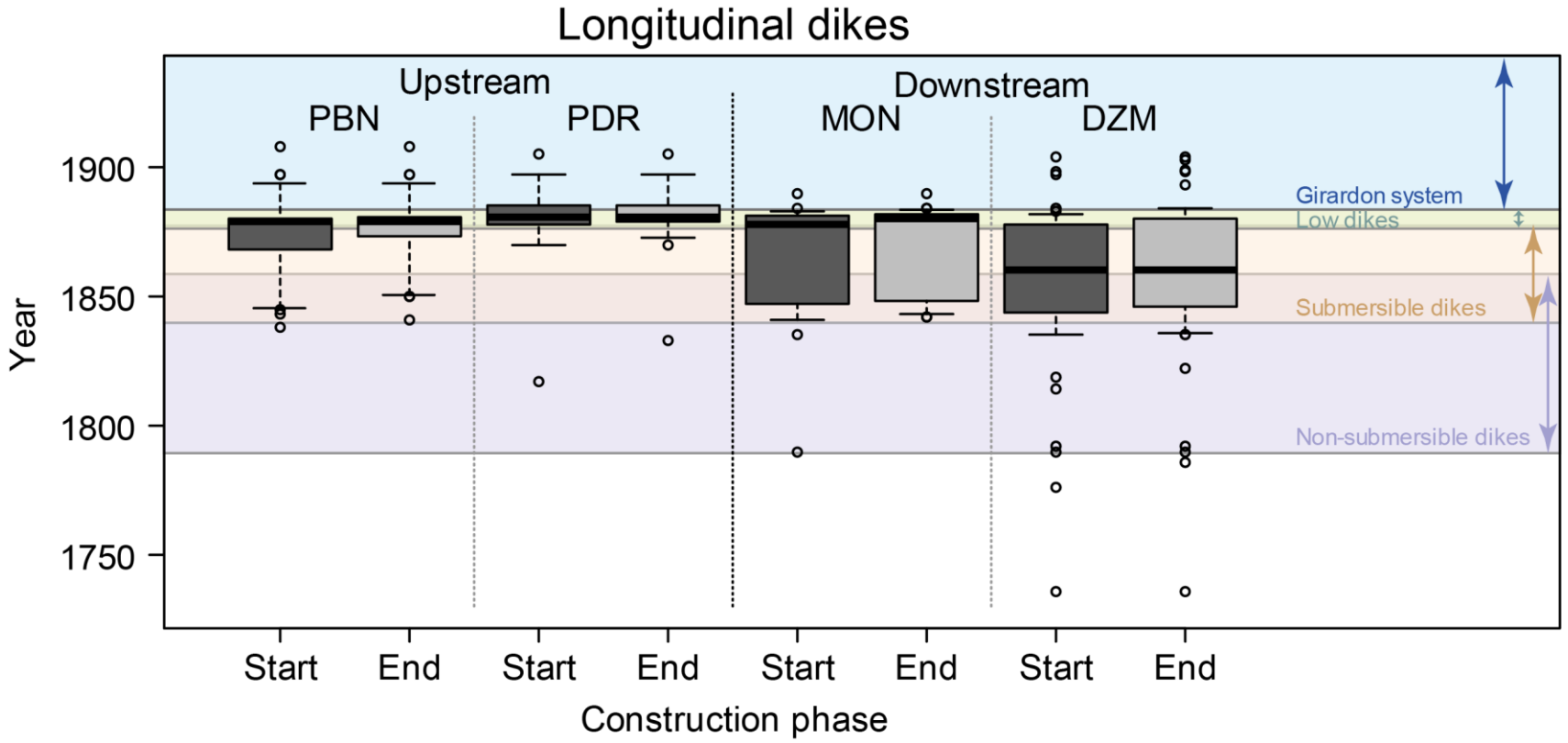

Figure IV–6: Spatio-temporal representation of the evolution of the longitudinal dike system (extent of the four periods based on Poinsart & Salvador, 1993).

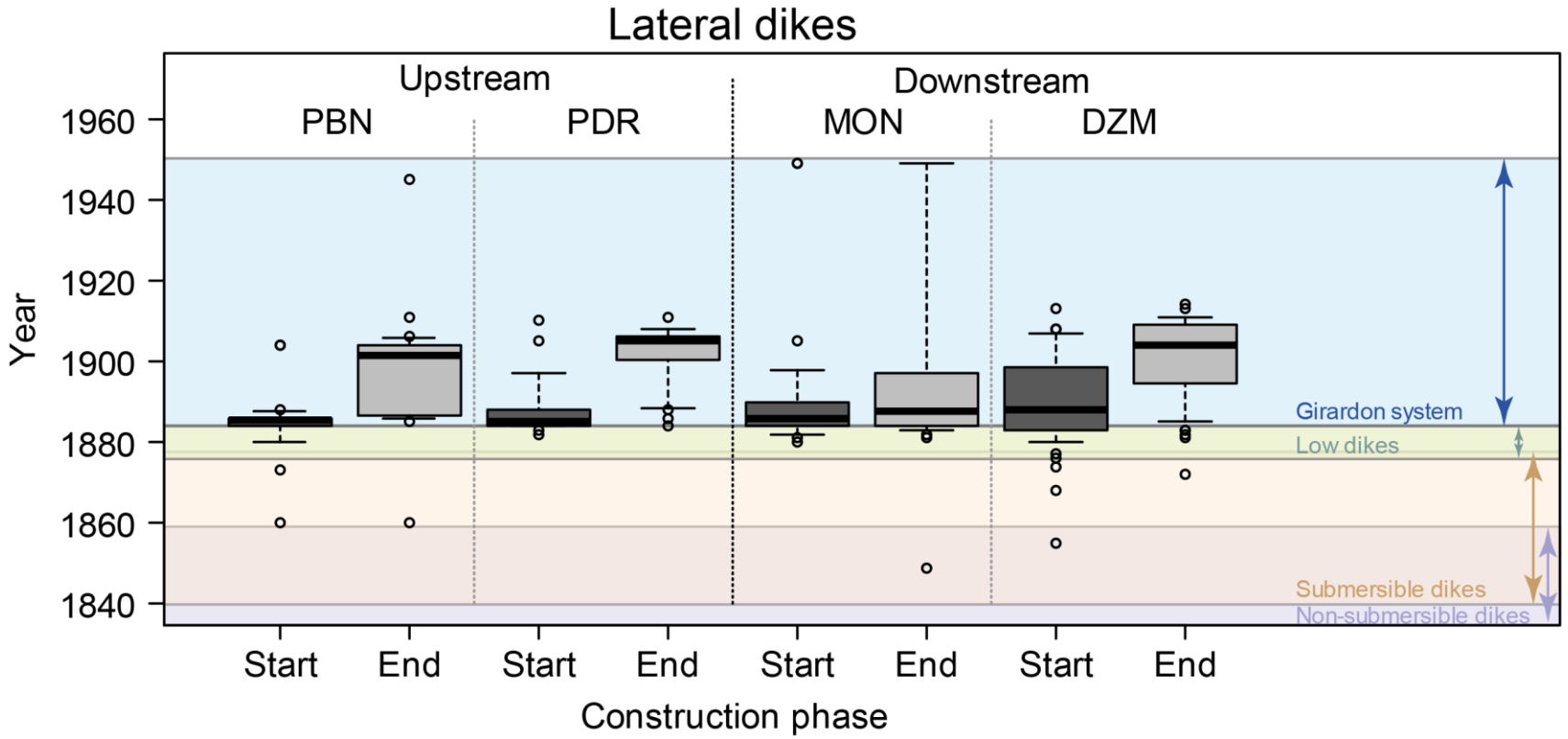

Figure IV–7: Spatio-temporal representation of the evolution of the lateral dike system (extent of the four periods based on Poinsart & Salvador, 1993).

3.1.2 Dike specifics

During field visits we identified several types of connections between the dike fields and their surroundings—the by-passed channel and/or other dike fields (Figure IV–8). Generally, the longitudinal or lateral dike becomes submerged at a certain discharge (threshold submersion discharge). In some dike fields, we observed discontinuous dikes or passages, i.e. the dikes were locally lowered. Discontinuous dikes were often constructed in this way, as could be confirmed based on historical maps. Scour, and perhaps fishermen, are potentially responsible for localised lowering, i.e. passages. For the concerned dike fields, a connection is established at the threshold discharge related to the crest height at this passage. Permeable dike construction materials finally facilitate the connection of the dike field to the main by-passed channel or neighbouring dike fields via seepage, even when the dikes are not submerged. Various construction materials and techniques seemed to have been applied which most likely do not have the same porosity characteristics (Appendix I: Figure A–I–2).

Figure IV–8: Dike fields are connected to the main by-passed channel by various mechanisms: a) submersion, b) passages, c) 'seepage'. Aerial image source: IGN©.

3.1.3 Dike field geometry

In the Girardon system, the characteristics of the individual Rhône dikes were adapted to local conditions, especially in later periods of construction. The resulting dike fields thus varied considerably in their geometric characteristics, especially size and geometry. They ranged in size from 0.01 ha to 9.79 ha (mean = 0.90 ha, SD (standard deviation) = ±1.17 ha). Dike fields in the two downstream reaches were significantly larger than in the two upstream reaches (Mann-Whitney U test, W=24686, p < .001; Figure IV–9). Dike fields at DZM were by far the largest. Mean dike field size was 0.45 ha (SD = ±0.38 ha) at PBN, 0.42 ha (SD = ±0.35 ha) at PDR, 0.79 ha (SD = ±0.77 ha) at MON, and 1.75 ha (SD = ±1.69 ha) at DZM.

Most of the Rhône dike fields are of rectangular or squared shape, while some are triangular or of irregular shape. Especially dike fields located in former side arms, which are constructed around islands showed strongly irregular shapes. The approximated width to length ratio of the dike fields ranged between 0.06 and 4.68 (Figure IV–10a, mean = 0.64, SD = ±0.59). They varied significantly between upstream and downstream reaches (Mann-Whitney U test, W = 11,010, p < .0001). In the

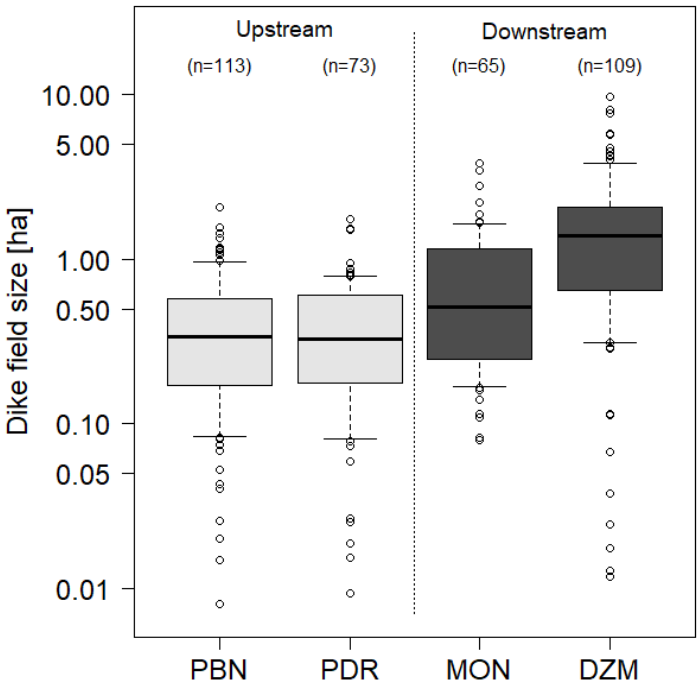

Figure IV–9: Comparison of dike field size distributions between study reaches.

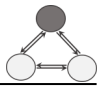

downstream reaches, the larger part of the dike fields had width to length ratios below 0.5, while the distributions in the upstream reaches showed more diverse patterns. Mean values amount to 0.83 (SD = ±0.68) for PBN, 0.74 (SD = ±0.75) for PDR, 0.41 (SD = ±0.22) for MON, and 0.51 (SD = ±0.43) for DZM. Research on marine ports and groyne fields has shown that width to length ratios < 0.5 and > 2.0 produce two-gyre hydraulic systems, compared to one-gyre systems in squared systems (Langendoen, 1992; Uijttewaal et al., 1999; Uijttewaal et al., 2001; Sukhodolov et al., 2002; Le Coz, 2010).

Linear regression of the log-transformed perimeter as a function of log-transformed dike field size (Figure IV–10b, $F_{1,358}$= 3,290, p < .001) yielded an *adjusted* R^2 of 0.90 and the relationship

$$Perimeter = 0.46 \times dike\ field\ size + 6.16, \qquad (Equ.IV-4)$$

Generally speaking, the larger the area of a rectangle for a given perimeter, the closer the geometry is to a rectangle.

To gain an insight on possible reasons for the significant size differences in dike fields between reaches, we tested on a small sub-sample whether this was related to original channel width. The ratio of dike field width to original channel width amounted to, on average, 0.35 (SD= ±0.15) and varied between reaches (Figure IV–11). DZM dike fields seem indeed to be disproportionately larger with respect to the original channel size than dike fields of the other reaches.

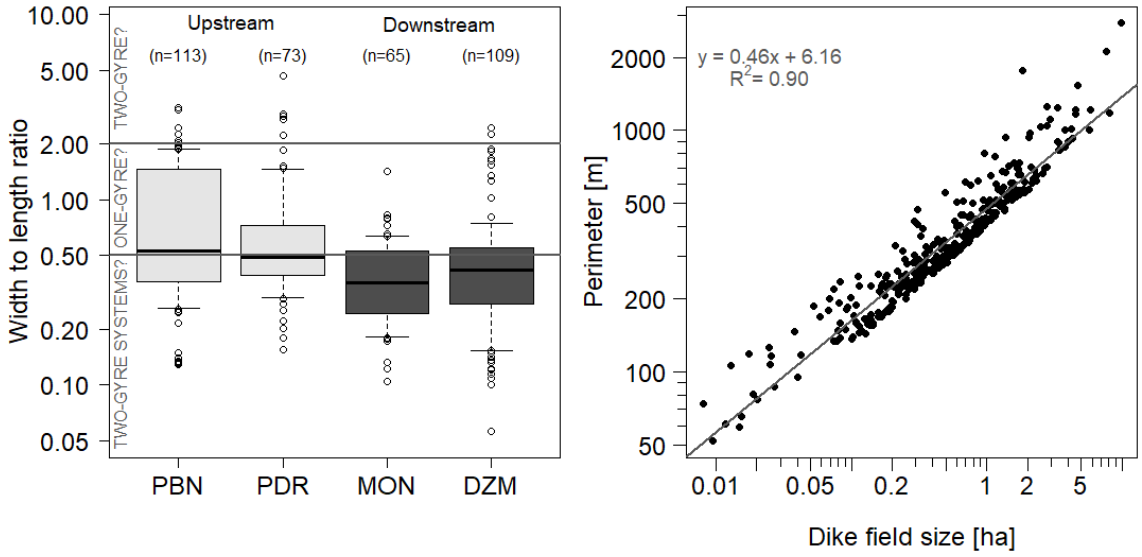

Figure IV–10: Dike field geometry: comparison of the distribution of width to length ratios between reaches (left; the horizontal grey line indicates a potential threshold for varying hydraulic conditions found in the literature for marine harbours and groyne fields). Relationship between log-log-transformed dike field size and perimeter (right).

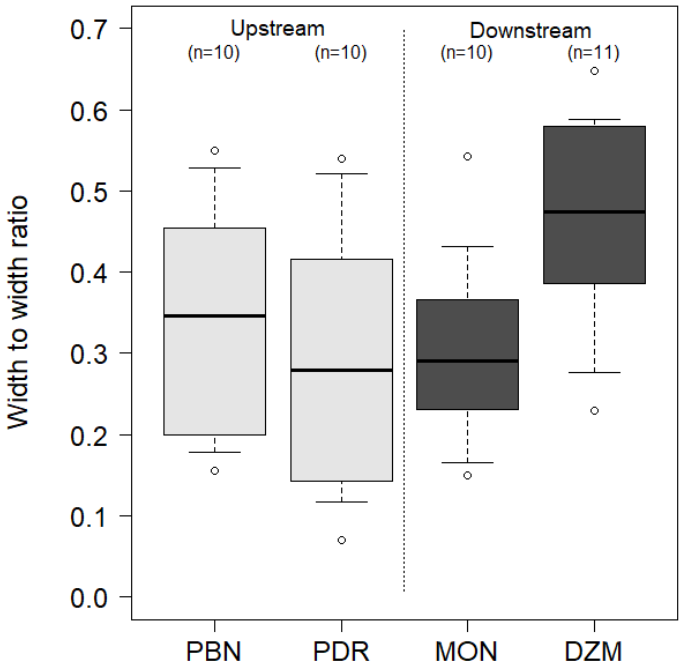

Figure IV–11: Comparison of the distributions of dike field width to original channel width ratios between reaches (note that this analysis was carried out on a small sub-set of dike fields located in the main by-passed channel).

3.2 Contemporary characteristics of dike field sediment deposits

3.2.1 Terrestrialisation state (planimetric)

The interpretation of the contemporary orthophotographs revealed that the Rhône dike fields were in an advanced terrestrialisation state in the 2000s. The whole range of terrestrialisation degrees were observed at legal residual discharge conditions (0% to 100%). However, 79.6% of the 285 dike fields studied in detail were terrestrial over more than 90% of their surface area (mean degree of terrestrialisation = 90.8%, SD = ±20.3%). Only 1.1% of the studied dike fields were still aquatic (terrestrial over less than 10% of their surface area) and only 6.0% featured aquatic zones over up to 50% of their surface area. We observed significant differences in the terrestrialisation state between study reaches (Kruskal-Wallis test, chi-squared = 66.80, df = 3, $p < .001$), although not between upstream and downstream reaches (Mann-Whitney U test, W = 10239, p = 0.87). Instead, there are significant differences between PBN and PDR, between PBN and DZM, PDR and MON, PDR and DZM, and between MON and DZM (Figure IV–12, Annexe Table). At PBN, 97.4% of the total studied surface area was

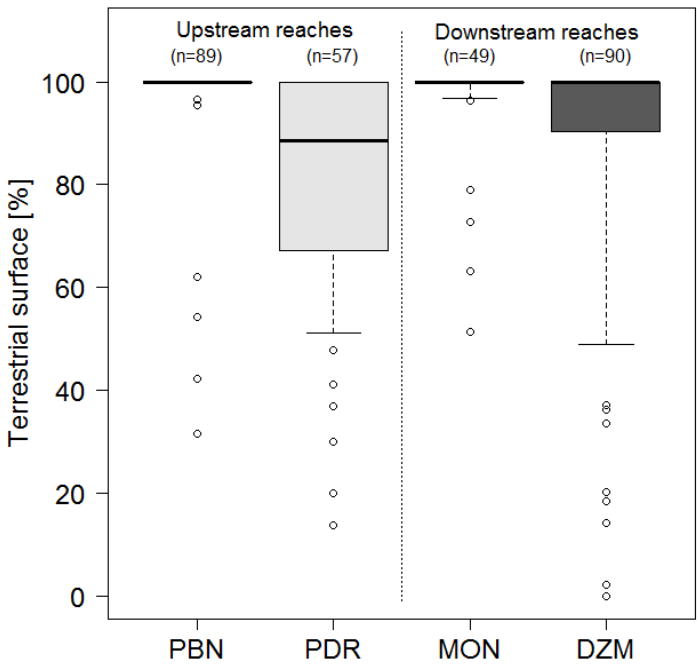

Figure IV–12: Comparison of dike field terrestrialisation status in the four study reaches.

terrestrial. Its dike fields showed the highest terrestrialisation degrees of the four reaches (mean = 97.6%; SD = ±11.2%). At MON, 95.9% of the total studied surface area was terrestrial (mean = 97.1%; SD = ±9.7%). At DZM we observed a higher percentage of remaining water surfaces—90.3% of the total surface area is terrestrial—and the highest variability (mean = 87.2%; SD = ±25.9%). Dike fields at PDR were in the least advanced terrestrialisation state (78.9%, mean = 80.8%; SD = ±22.7%).

3.2.2 Topographic characteristics

The mean relative elevation of emerged surfaces within dike fields, derived from the LiDAR data based DEMs, ranged between 0.48 m and 7.57 m above the water level at a discharge of 100 m^3/s (mean = 3.58 m, SD = ±1.44 m). We stated significant differences between the four reaches (Figure IV–13a, one-way ANOVA, df = 3, F-value = 53.08, $p < .001$): not only between upstream and downstream reaches (Welsh two-sample t-test, t = 8.40, df = 312.82, $p < .001$) but between each pairwise combination (Annexe). Although this variable only considers emerged surfaces, we found some moderate positive linear relationships with terrestrialisation degree. Predominantly aquatic dike fields generally had lower elevation surfaces than predominantly terrestrial dike fields (Figure IV–13b). The slope of this relationship differed between reaches (PBN: slope = 0.05, $R^2 = 0.28$; PDR: slope = 0.01, $R^2 = 0.02$; MON: slope = 0.02, $R^2 = 0.03$, DZM: slope = 0.03, $R^2 = 0.39$).

We approximated topographic variation of dike field surfaces using the standard deviation of the absolute altitude derived from the LiDAR data-based DEM. It ranged from 0.04 m to 2.55 m (mean = 0.99 m, SD = ±0.42 m) and varied significantly between upstream and downstream reaches (t-test, t = –2.30, df = 357.63, $p < .05$; Figure IV–14).

3.2.3 Multivariate analysis

Binary relationships between the three variables, which describe the sediment deposits within the dike fields showed no straight forward relationships (Figure IV–15).

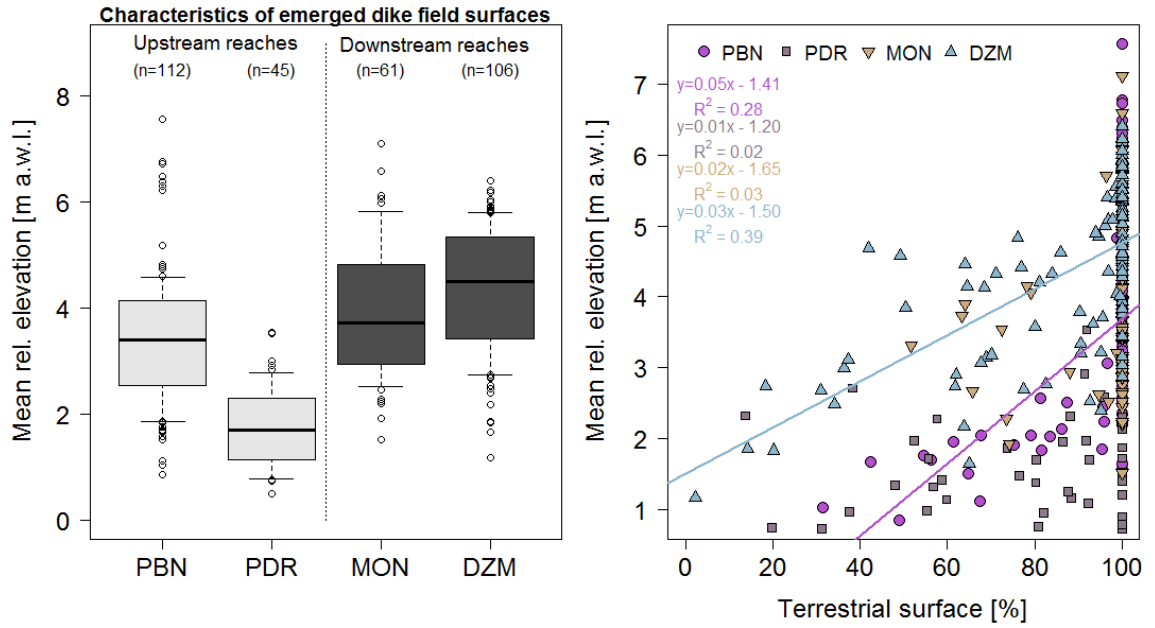

Figure IV–13: Comparison of average elevation of emerged dike field surfaces between reaches (left). Relationships between planimetric and vertical sediment deposit extent (right).

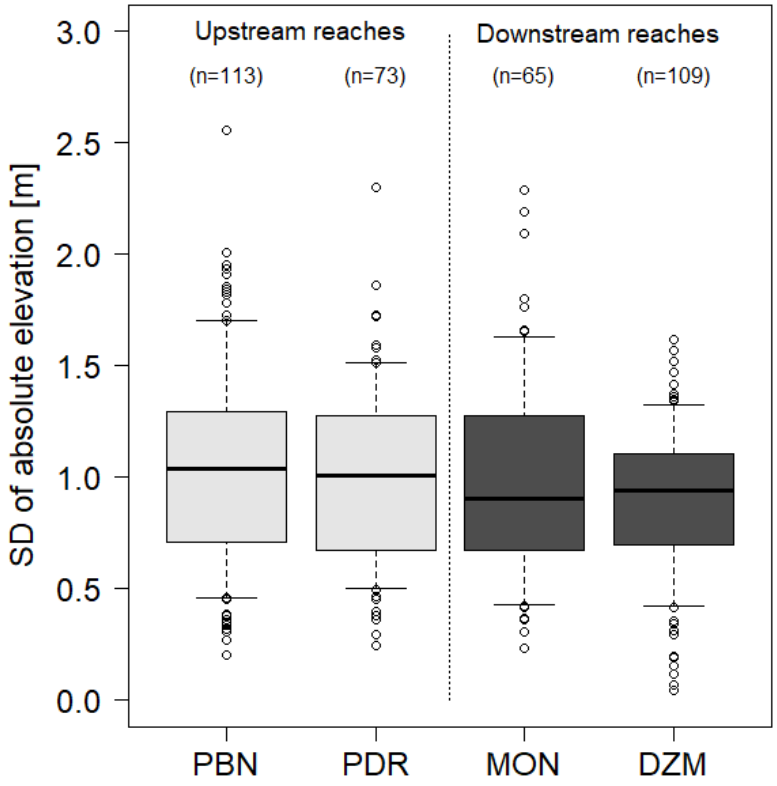

Figure IV–14: Inter-reach comparison of the topographic variability of dike field deposits.

We used them as active variables in the Principal Components Analysis (PCA), which revealed two gradients across our dike field sample set (Figure IV–16): factorial axis F1 was influenced by the mean relative elevation of the emerged dike field surfaces ($r = 0.85$, $p < .001$) and the state of terrestrialisation ($r = 0.80$, $p < .001$). The topographic variability (SD of absolute elevation) contributed to factorial axis F2 ($r = 0.93$, $p < .001$). Axes 1, 2, and 3 represented 49.5%, 32.6%, and 17.9%, respectively, of the total inertia.

We distinguished 7 types of dike fields from hierarchical clustering, which was based on the results of the PCA (Figure IV–17, top). Cluster 1 dike fields (N = 27) showed water surfaces which covered 0% to 45.4% of their surface area (Figure IV–17, centre). They showed a high topographic variability and a relatively low mean relative elevation, implying a relatively high connectivity to the by-passed channel. Cluster 2 (N = 25) represented dike fields which were still mainly aquatic (35.1% to 97.7%), with an average topographic variability and a low mean surface elevation. Cluster 3 dike fields

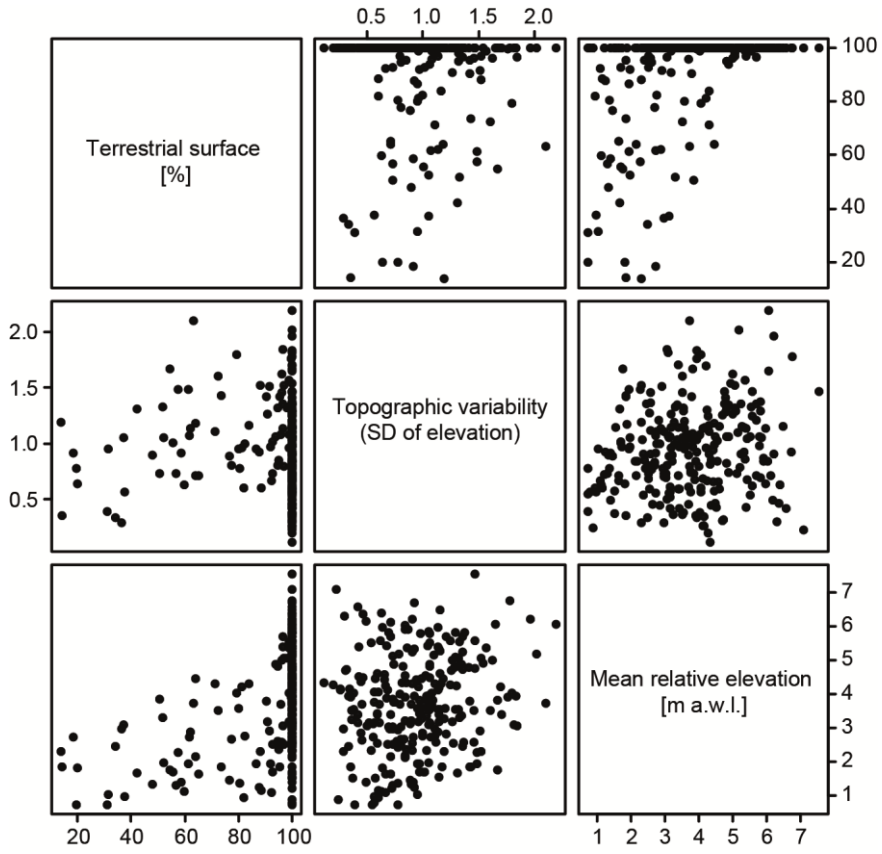

Figure IV–15: Binary relationships between PCA input variables.

(N = 46) had similar topography and elevation as cluster 2 but were between 76.5% and 100% terrestrial. Clusters 4 (N = 45), 5 (N = 53), 6 (N = 41), and 7 (N = 26) consisted of completely terrestrial dike fields. They varied in terms of topographic variability, with clusters 5 and 7 showing the most homogeneous surfaces of all dike fields, while clusters 6 and 4 proved highly variable in their topography. Clusters 6 and 7 furthermore had a very high mean elevation with respect to the water level, while cluster 4 was average. We visualised the distribution of the clusters on the factor map (Figure IV–17, bottom). The highest topographic variability was generally related to important slopes along former river banks (especially when combined with high relative elevations), abandoned channel features, or prevailing erosional processes which create fluvial features, such as high flow channels or circular depressions. Even though water surfaces are represented by flat surfaces in the models used to describe the elevation data, and thus underestimate bathymetric variability we still find considerable variation.

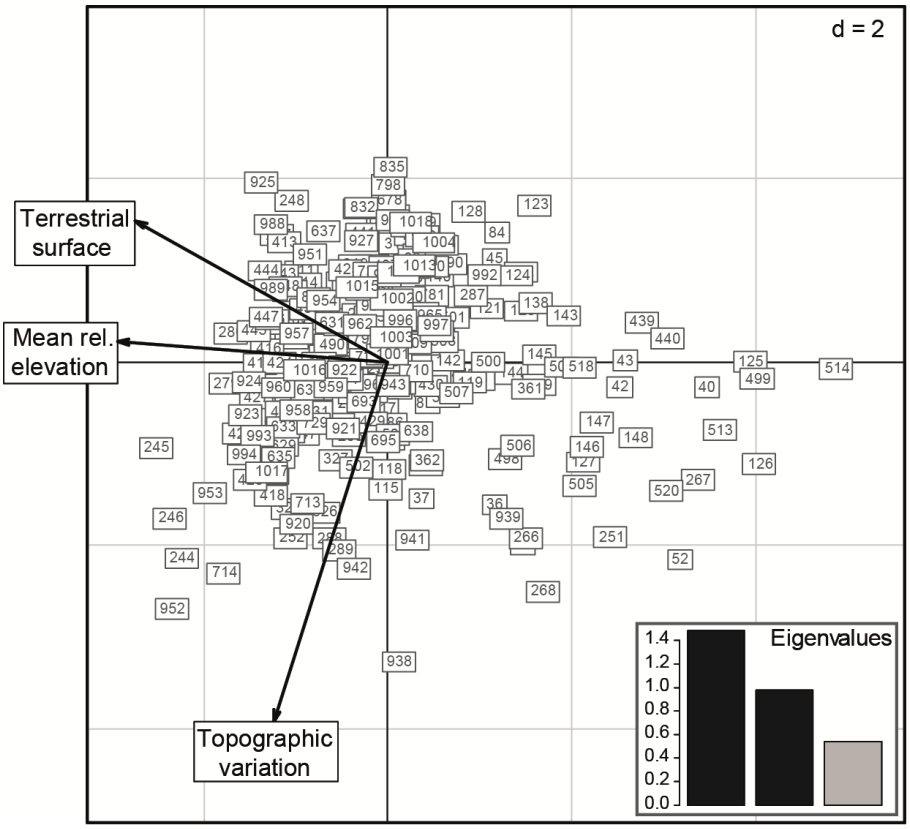

Figure IV–16: Results from Principal Components Analysis summarised in a factor map: the three input variables are depicted using black arrows, individual dike fields are represented by grey squares and their respective ID number. Barplots represent the eigenvalues of the first three dimensions.

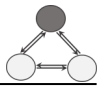

At the reach-scale we principally found a difference between PDR and the three other reaches (Figure IV–18). This was mainly based on the comparatively low terrestrialisation status of PDR dike fields, and the comparatively low relative elevations of their emerged surfaces (clusters 2 and 3 dominated, whereas cluster 7 was absent in this reach). This suggests that within-reach variability was higher than between-reach variability. Indeed, the between-reach / within-reach PCA revealed that the between-reach variability explained 15.9% of the total inertia, whereas the within-reach variability explained 84.1%.

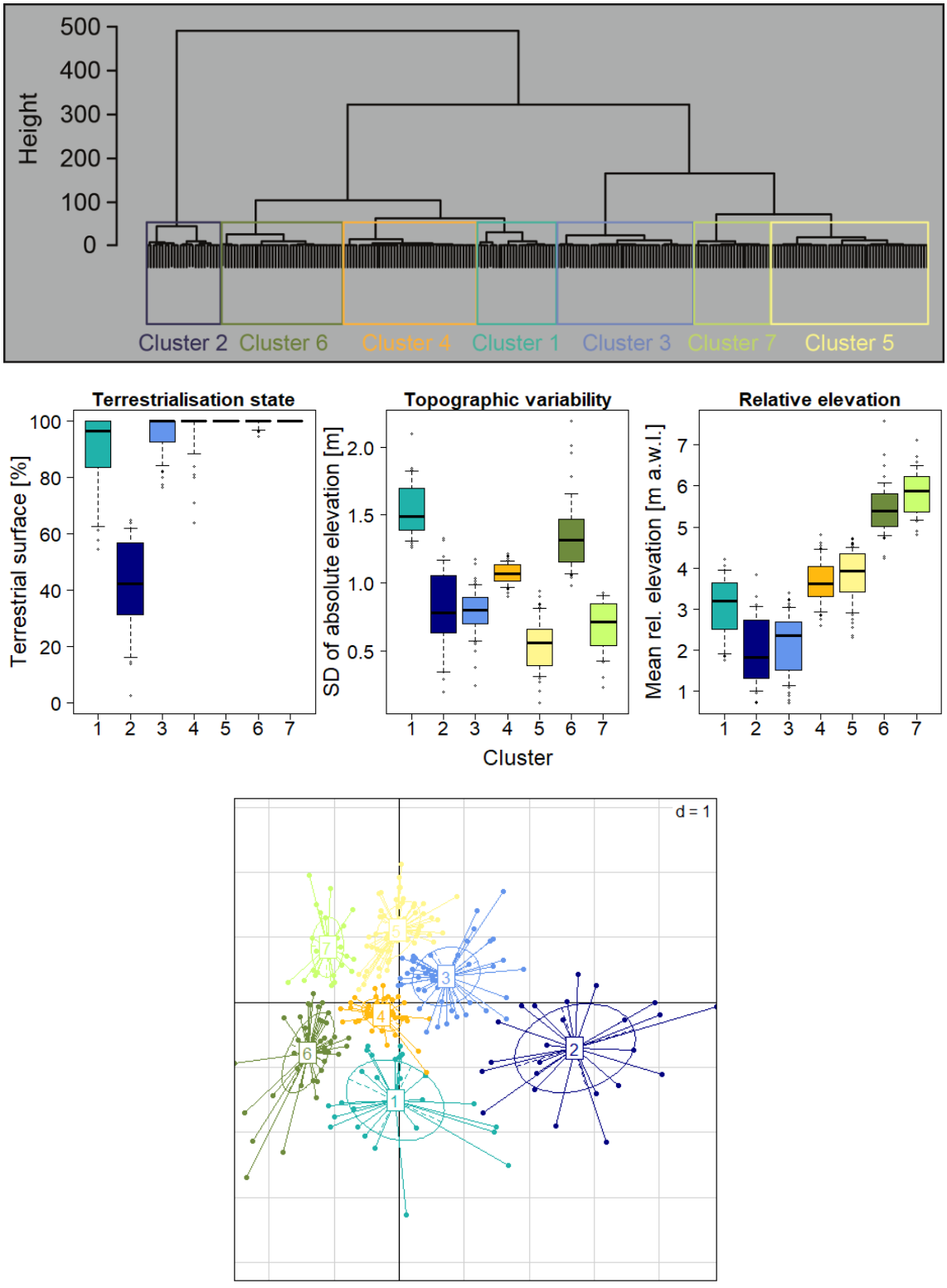

Figure IV–17: Results from hierarchical cluster analysis: dendrogram (top), comparison of the characteristics of the resulting clusters regarding the three PCA input variables (centre), and visualisation of the clusters on the PCA factor map (bottom).

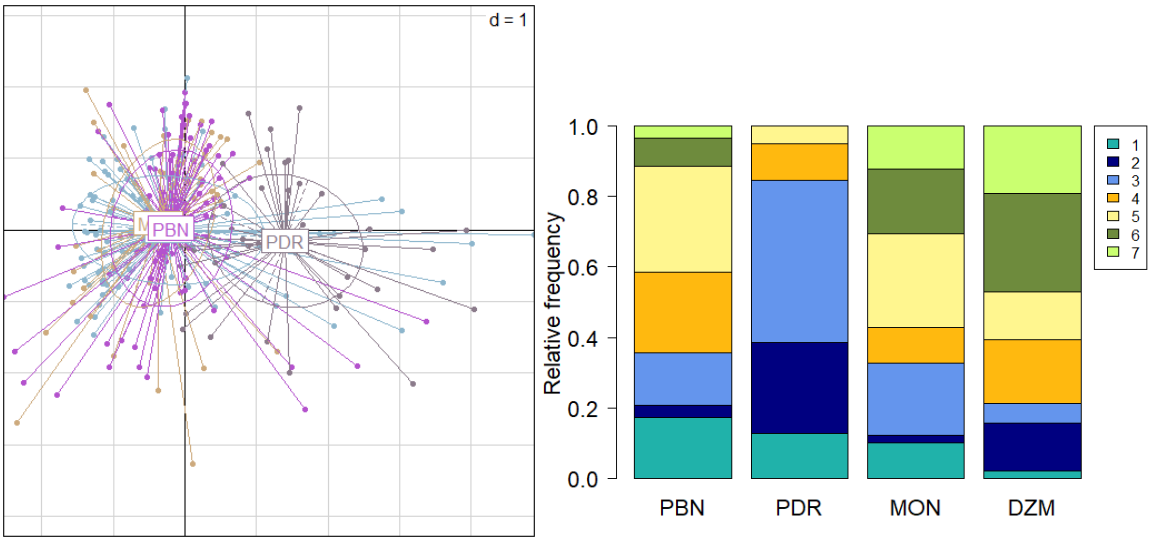

Figure IV–18: Reach-scale patterns behind the PCA and clustering results: colour coding the PCA factor map introduced in according to the study reach (left). Distribution of clusters between reaches (right).

3.3 Presentation of control factors

3.3.1 Connectivity

To describe the hydrological connectivity of the dike fields via their longitudinal dikes, we explored four variables: relative elevation of the dikes above the water level at a discharge of 100m³/s, dike submersion frequency, dike submersion duration, and the return frequency of the threshold discharge at which the dike is submerged (Figure IV–19). The analysis of the LiDAR data-based digital elevation model (DEM) revealed a range of mean relative heights of longitudinal dikes from 0.1 m to 6.7 m (mean = 3.3 m, SD = ±1.4 m) above the water level at a discharge of 100 m^3s^{-1} (Figure 16). Significant differences were observed between the reaches (Kruskal Wallis test, chi-squared = 123.67, df = 3, $p < .001$) and between upstream and downstream reaches (Mann-Whitney U test, W = 12,495, $p < .001$). Potentially, part of this difference is explained by the differences in construction height observed during the different construction periods (see section 1.1.1). For instance, we found that dikes were significantly higher at DZM (mean = 4.3 m, SD = ±1.3 m), where they had been constructed earlier (Figure 2), than in the other reaches. At PBN (mean = 3.1 m, SD = ±0.9 m) and MON (mean = 3.5 m, SD = ±1.1 m) the majority of longitudinal dikes had been constructed at approximately the same period and they showed indeed

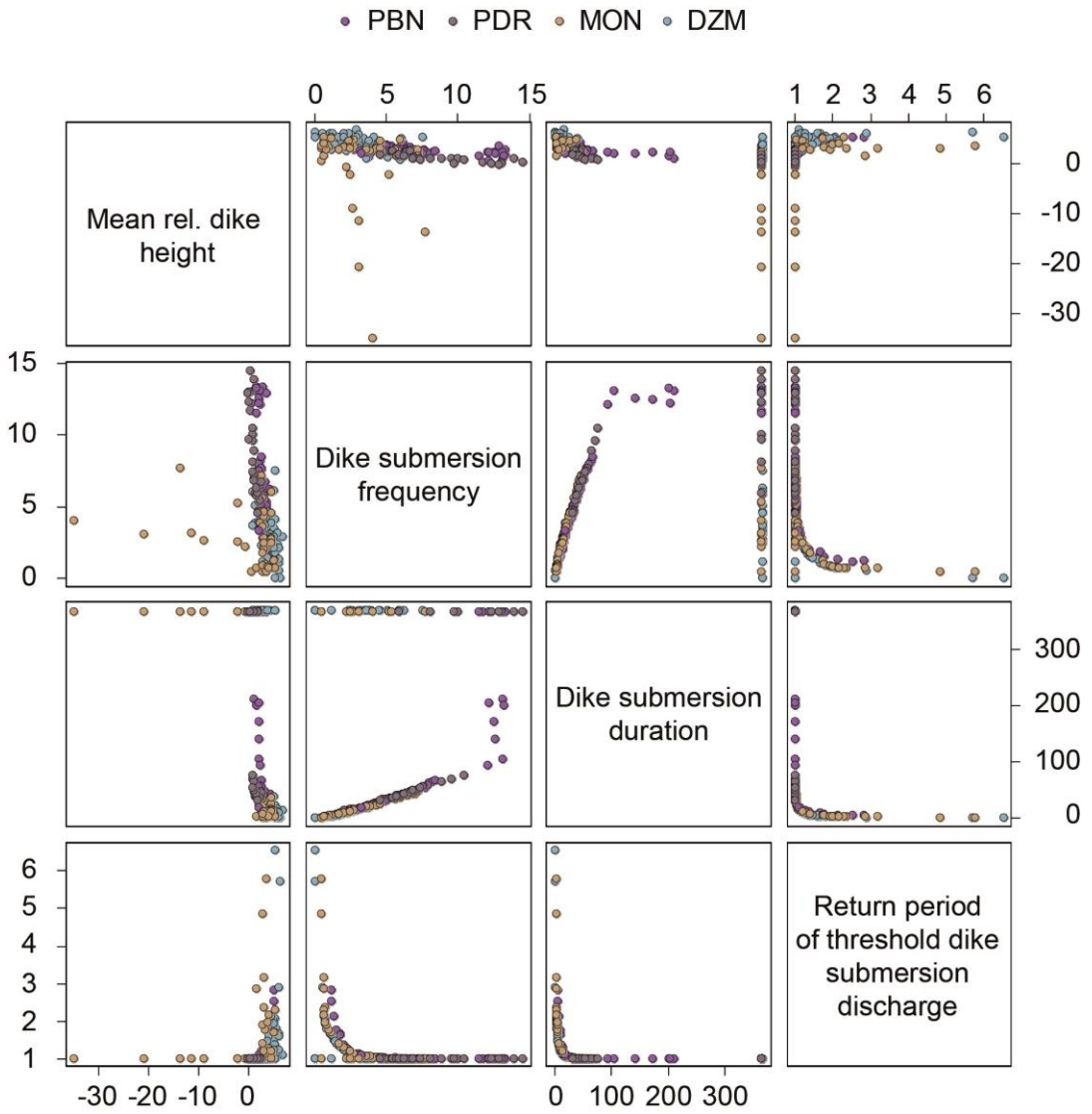

Figure IV–19: Bivariate relationships between the four variables used as proxies for hydrological connectivity of the dike fields.

comparative distribution patterns of relative dike heights. The dikes at PDR had been constructed at a later period. The DEM analysis confirmed that they were, on average, much lower (mean = 1.4 m, SD = ±0.7 m) compared to the other reaches. However, a straight forward link between original dike height above conventional low flow and the model derived relative elevations is restricted. The relative dike heights are influenced by the historical evolution of the channel geometry (see chapter XX) and to a minor extent by the deposition of sediments on the dike themselves.

We examined the relation between mean and minimum relative dike heights to estimate the presence of larger passages in the dikes. The water level at which such

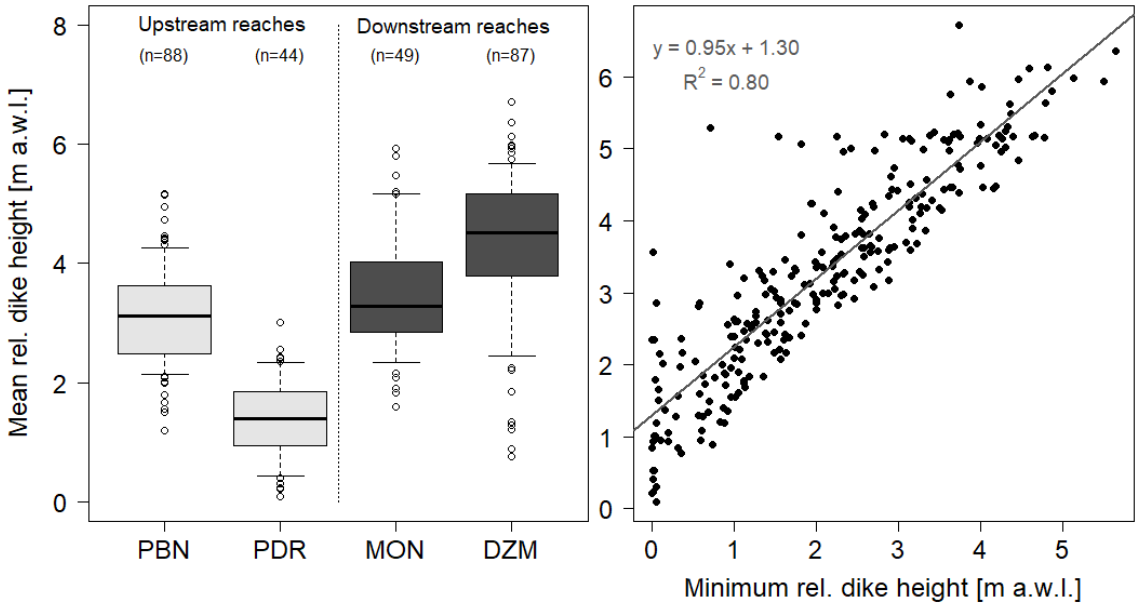

Figure IV–20: Inter-reach differences in mean longitudinal dike height (left). Relationship between minimum and mean relative longitudinal dike height (right).

dike fields are connected to their surrounding may be reduced with respect to the mean relative dike height. The regression model yielded a strong positive linear relationship between mean and minimum relative dike heights (R^2 = 0.80). Yet, the remaining variability may be partly related to passages and discontinuous dikes, and partly to digitisation inaccuracies or DEM resolution (= 2 m x 2 m), since the dikes are relatively thin elements. Small passages might not be detectable by the DEMs.

Longitudinal dikes were submerged between 0 and 365 days per year (mean = 89.2 d/yr, SD = ±133.0 d/yr, Figure IV–21). Submersion duration varied significantly between reaches (Kruskal-Wallis test, chi-squared = 38.47, df = 3, $p < .001$), as well as between upstream and downstream reaches (Mann-Whitney U test, W = 5,968.5, $p < .001$). PDR was significantly different from all other reaches, and DZM differed significantly from the two upstream reaches (Annexe). PBN and MON were similar to each other.

The return period of the dike submersion threshold discharge, i.e. the discharge at which the longitudinal dike is overflowed, varied between 1.0 and 6.5 years (Figure IV–22, mean = 1.2, SD = ±0.7). Consistently with relative dike height and submersion duration data, we found significant differences in return periods between study

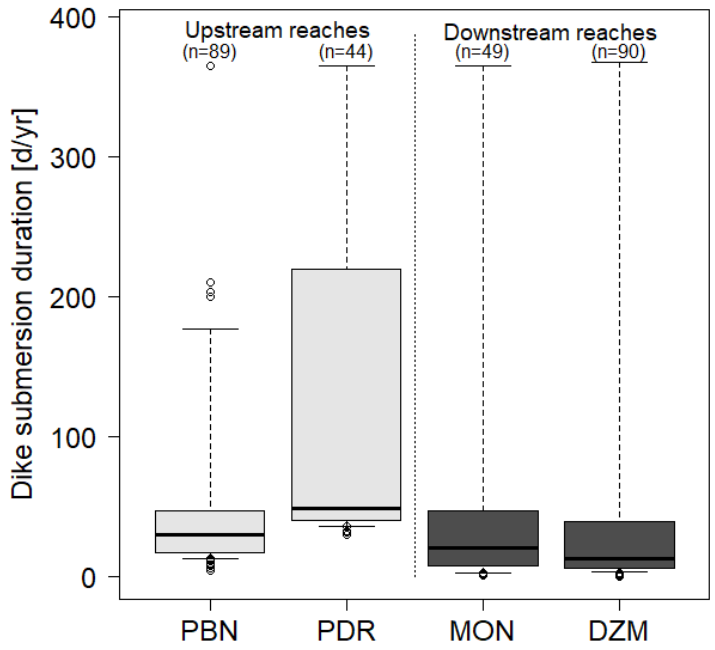

Figure IV–21: Comparison of longitudinal dike submersion durations between reaches.

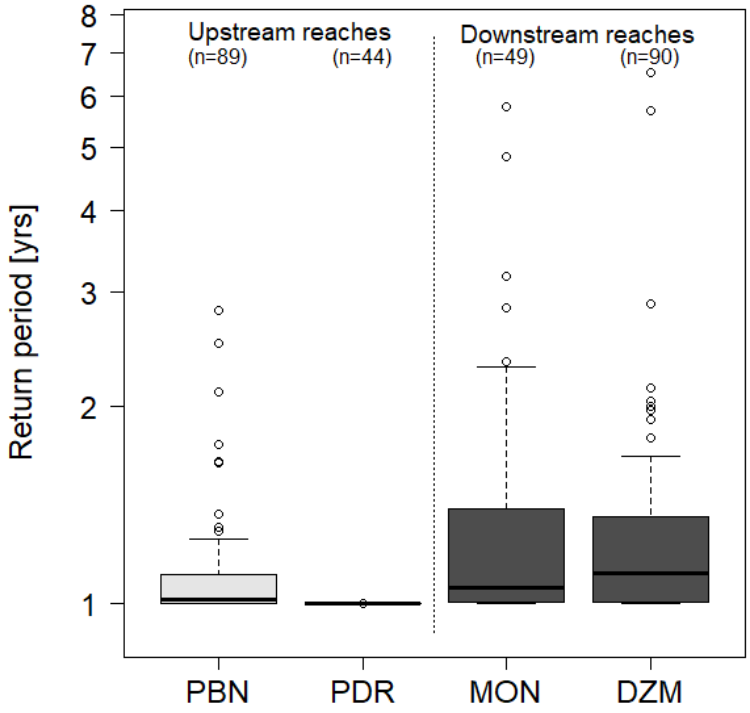

Figure IV– 22: Inter-reach comparison of the return period of the longitudinal dike submersion threshold discharge.

reaches (Kruskal-Wallis test, chi-squared = 104.59, df = 3, p < .0001) and between upstream and downstream reaches (Mann-Whitney U test, W = 14,253, p < .0001). Differences were significant between all pairwise combinations of the four reaches, except between MON and DZM (Annexe).

3.3.2 Land cover

Approximately 130 years after the installation of the first comprehensive engineering structures, the predominant land cover type in the Rhône dike fields consisted of trees and shrub land (denoted as "forest" in the following, 56.2% of the surface area of 357 studied dike fields). This totalled 181.10 ha. Open sites, i.e. sediment and herbaceous covers, made up 27.9% (89.99 ha), remaining water surfaces 11.7% (37.61 ha), agricultural land 3.5% (11.13 ha), and infrastructures 0.8% (2.50 ha).

The relative distribution of the five land cover types followed the same patterns in the four study reaches (Figure IV–23). At PBN, we found a significantly more important

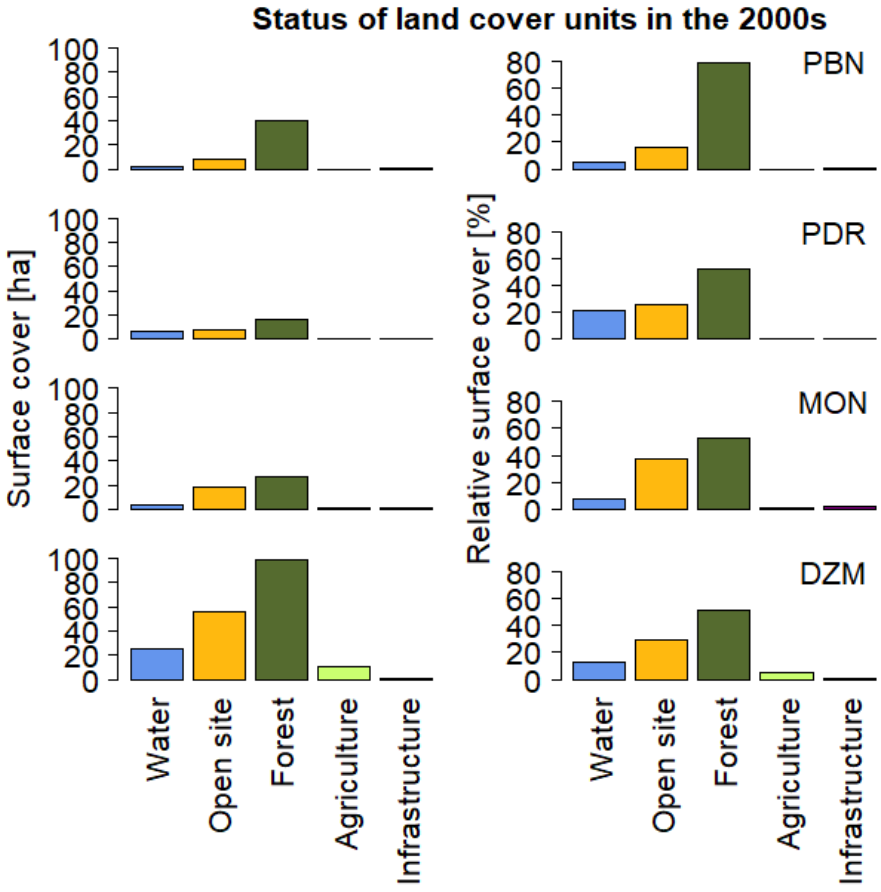

Figure IV–23: Contemporary distribution of land cover units in dike fields compared between the four reaches (N_{PBN} = 113, N_{PDR} = 73, N_{MON} = 62, N_{DZM} = 109).

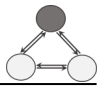

relative wood cover (total = 79.2%, mean = 79.9%, SD = ±22.4%) than in the other three reaches (Kruskal-Wallis test, chi-squared = 49.7, df = 3, $p < .001$), which featured similar values ($total_{PDR}$ = 52.3%, $mean_{PDR}$ = 54.5%, SD_{PDR} = ±31.0%; $total_{MON}$ = 52.2%, $mean_{MON}$ = 55.2%, SD_{MON} = ±34.1%; $total_{DZM}$ = 51.7%, $mean_{DZM}$ = 54.9%, SD_{DZM} = ±32.8%).

3.4 Individual roles and interplay of drivers with respect to sedimentation and terrestrialisation patterns

The multitude of drivers acting on large rivers, such as the Rhône, and their complex interactions hamper straight forward statements on the role of individual drivers regarding dike field terrestrialisation. We disentangled their effects based on several approaches. First, we extended our multivariate approach to identify possible interactions between dependent morpho-topographical (active inputs to the principal components analysis (PCA)) and independent control variables (supplementary inputs to the PCA) beyond the bivariate scale. Bivariate scatter plots showed almost no (linear) relationships between dependent and independent variables (Figure IV–24). When adding the driver variables to the factorial map established in section 3.2.3, we found significant correlations with the projected axes (Table IV–1, Figure IV–25). The connectivity of the dike fields to the main by-passed channel had a marked influence on dike field terrestrialisation status and the relative elevation of emerged surfaces to the water level at 100 m^3/s. Topographic variability seemed to be influenced by geometric characteristics of the dike fields. As evidenced in a between-reach vs. within-reach principal components analysis (PCA), differences within reaches account for 84.1% of the total inertia and thus of the morpho-topographical variability between dike fields, compared to only 15.9% for between reach differences. This confirms the importance of the local-scale drivers. To investigate drivers whose effect might be masked by these local phenomena, we carried out a comparative analysis of morpho-topographically variable clusters of dike fields which showed similar connectivity conditions. The organisation of the results follows our initial research questions and hypotheses regarding individual potential drivers.

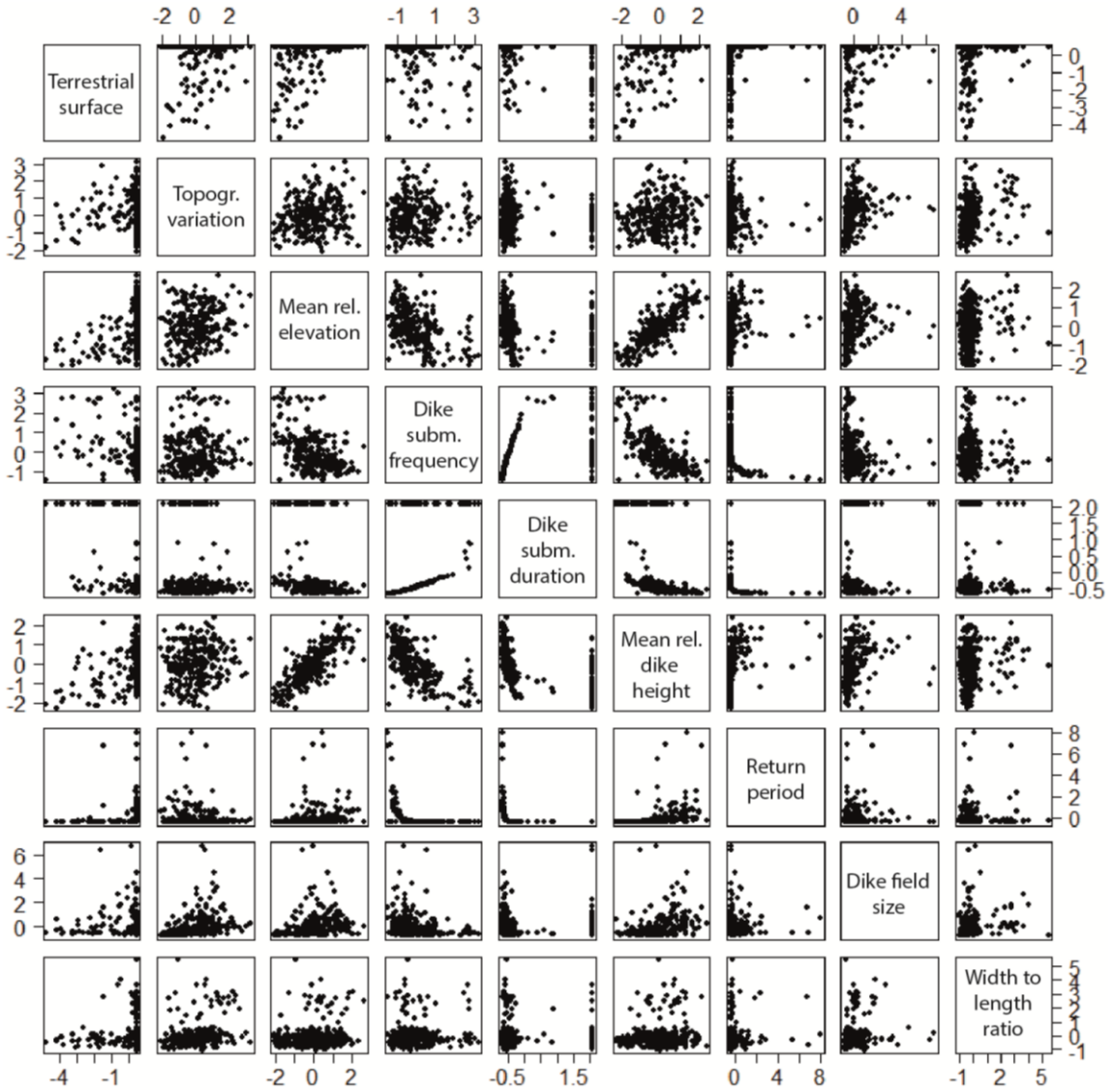

Figure IV–24: Bivariate analysis of all active and supplementary variables of the principal components analysis (PCA).

3.4.1 Connectivity as a major driver

Hypothesis H1: Connectivity between the dike field and the by-passed channel was negatively related to terrestrialisation.

We expected connectivity to be a major driver of the evolution of dike field sediment deposits, by controlling the influx of suspended sediment present in the main by-passed channel, as well as scour processes. This was confirmed by the principal components analysis, to which we added mean relative longitudinal dike height, dike submersion duration, dike submersion frequency, and the return period of the

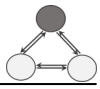

Table IV–1: Results (correlation coefficient and p-value) of a correlation analysis between all active and supplementary variables of the PCA and the three projected axes. Correlations which are statistically significant are marked with stars (* p < .05, ** p < .01, *** p < .001, **** p < .0001).

Variable	Correlation	p-value
Axis 1		
Mean rel. elevation of emerged dike field surfaces	0.85	1.18×10^{-74}****
Terrestrial surface	0.80	1.21×10^{-58}****
Mean rel. dike height	0.72	4.54×10^{-43}****
Topographic variability	0.36	1.71×10^{-09}****
Dike field size	0.19	1.95×10^{-03}**
Width to length ratio	0.20	1.21×10^{-03}**
Return period of dike submersion threshold discharge	0.12	4.71×10^{-02}*
Dike submersion frequency	-0.41	3.81×10^{-12}****
Dike submersion duration	-0.43	5.43×10^{-13}****
Axis 2		
Topographic variability	0.92	3.68×10^{-107}****
Dike field size	0.30	6.45×10^{-07}****
Width to length ratio	0.22	2.83×10^{-04}***
Dike submersion frequency	0.20	1.30×10^{-03}**
Return period	-0.12	4.71×10^{-02}*
Terrestrial surface	-0.36	1.51×10^{-09}****
Axis 3		
Terrestrial surface	0.49	4.81×10^{-17}****
Dike submersion frequency	0.24	8.85×10^{-05}****
Topographic variation	0.16	8.31×10^{-03}**
Return period	-0.12	4.57×10^{-02}*
Dike field size	-0.17	7.15×10^{-03}**
Mean rel. dike height	-0.39	7.37×10^{-11}****
Mean rel. elevation of emerged dike field surfaces	-0.52	5.85×10^{-20}****

threshold dike submersion discharge as supplementary variables (Figure IV–25 and section 3.2.3). The first three showed a strong positive ($r = 0.72$, $p < .0001$) and moderate negative ($r = -0.43$, $p < .001$ and $r = -0.41$, $p < .001$) correlation with regard to axis 1, respectively. The return period of the threshold submersion discharge was weakly positively correlated ($r = 0.12$, $p < .05$).

We note that connectivity was related to the rate of sedimentation / terrestrialisation, with dike submersion frequency and duration being negatively correlated to terrestrialisation state and mean relative elevation of emerged dike field surfaces. Mean relative dike height is positively correlated to mean relative elevation of emerged dike field surfaces and terrestrialisation state. The bivariate correlation between relative dike height and relative elevation of emerged surfaces (Figure IV–26) is likely in part explained by the effect of the evolution of the main by-passed channel geometry, since we consider values relative to the water level (see further chapter V). This partly masks the effect of sediment deposition on elevation. However, the remaining residual variation ($R^2 = 0.65$) still highlights variations in sediment deposition within the dike fields observed as elevation differences with reference to dike height (Figure IV–26).

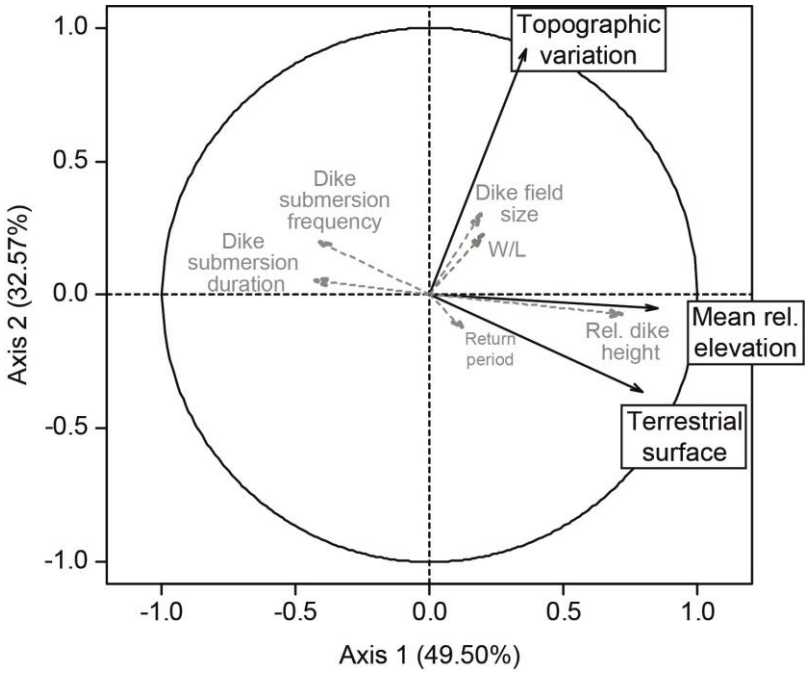

Figure IV–25: Variables factor map resulting from the principal components analysis. Black: active input variables. Grey: supplementary variables.

Some dike fields have accumulated deposits which surpass their dikes in elevation. Others still have depressional areas.

Analysis of the individual clusters, which resulted from the principal components analysis followed by hierarchical clustering, revealed a gradient of connectivity between clusters (Figure IV–27) with

cluster 2 > cluster 3 > clusters 1,4,5 > cluster 6 > cluster 7.

Clusters 1, 4, and 5 showing similar connectivity, we chose to analyse the dike fields of these three clusters to better distinguish the effects from connectivity and the other drivers on sedimentation and terrestrialisation. Statistical analysis revealed significant differences in the state of terrestrialisation between the three clusters (Kruskal-Wallis test, chi-squared = 35.94, df = 2, $p < .001$). Hence, although connectivity explained a large part of the variation in terrestrialisation patterns, other drivers seem to play a role, too.

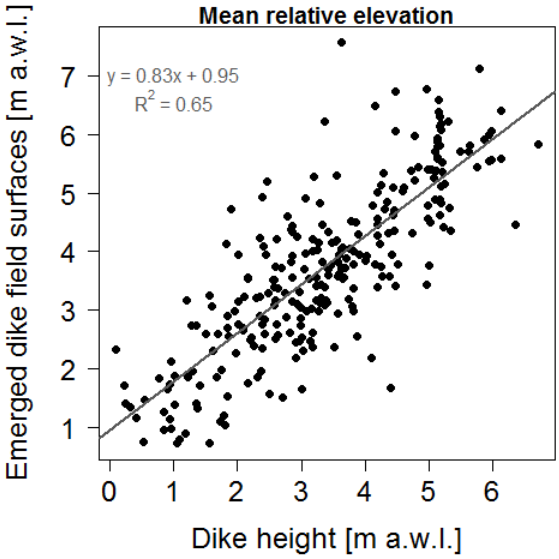

Figure IV–26: Relationshipt between dike height and emerged dike field sediment deposits.

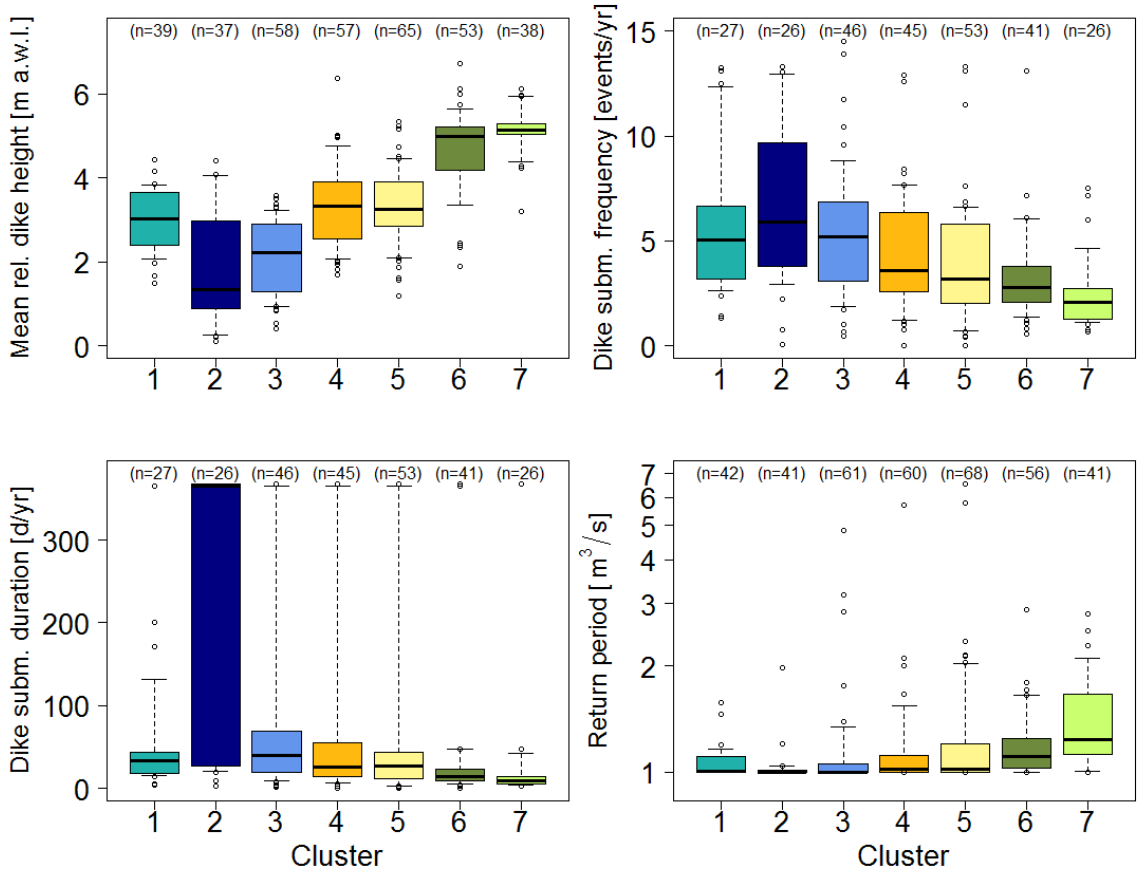

Figure IV–27: Comparison of connectivity variables between the seven morpho-topographical clusters.

3.4.2 For a given level of connectivity, local- and reach-scale drivers show an impact on sedimentation and terrestrialisation patterns

Having identified connectivity as a major control factor on dike field sedimentation and terrestrialisation, in the following we zoom to potential local (interior hydraulic conditions) and reach scale factors (suspended sediment flux and discharge regime). Clusters 1, 4, 5 represent 125 dike fields of similar connectivity conditions which shall be compared. The aim was to separate the effects from connectivity from other factors.

Hypothesis H2: For a given level of connectivity, differences in hydraulic conditions within the dike fields only partly affected terrestrialisation patterns.

- Variations in roughness conditions within dike fields, related to the dominant land cover type, were not related to significant differences in terrestrialisation patterns.

Land cover units with a high roughness value (e.g. forest) were expected to show higher sedimentation rates than units representing low roughness values (bare sediment / herbaceaous layer / pastures). This hypothesis could not be verified. The three clusters of similar connectivity (clusters 1, 4, 5) showed no significant differences in their terrestrialisation state between forest dominated and open site dominated dike fields (Figure IV–28 left, Mann-Whitney U test, W = 782, p = 0.57). In total, 97 dike fields were forest dominated (> 50% forest cover), 17 were open site dominated (> 50% open site cover), 11 did not correspond to any of the two groups. Likewise, we found no significant differences in topographic variability (SD of absolute altitude, Mann-Whitney U test, W = 742, p = 0.51) or mean relative elevation (Mann-Whitney U test, W = 787, p = 0.77) (Figure IV–28 centre and right).

- Dike fields of varying size showed differences in the topographic variability of overbank fine sediment deposits

As described above, from experiences with harbours and groyne fields, we expected the shape and surface area of the dike fields to have an effect on the hydraulic conditions within the dike fields and thus in turn on sedimentation and terrestrialisation patterns. The extended principal component analysis (PCA) showed that topographic variability was highly correlated to axis 2 (r = 0.92, p < .0001), which was also, although weakly, correlated to the control variables dike field size (r = 0.30, p < .0001) and width to length ratio (r = 0.22, p < .001) (Figure IV–29). Beyond this, the various clusters manifested a pattern of dike field size, width to length ratio, dike

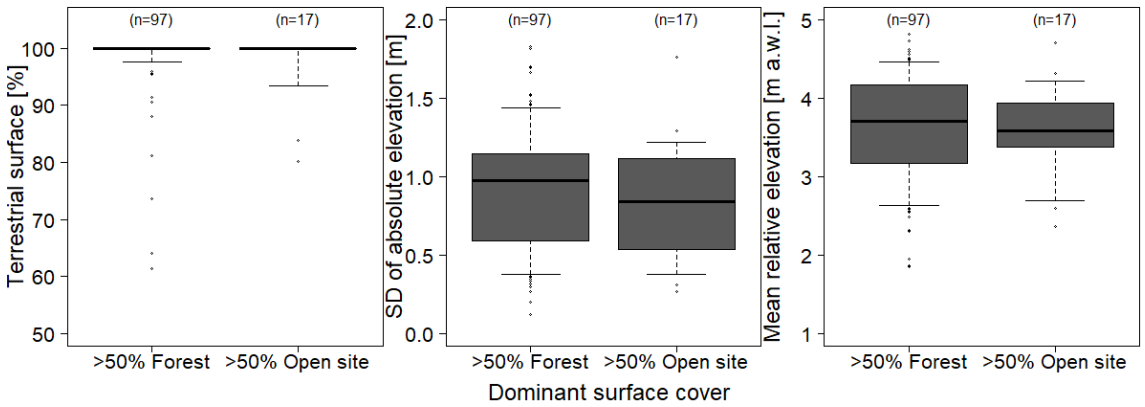

Figure IV–28: Comparison of forest- and open site-dominated dike fields in terms of sedimentation and terrestrialisation patterns.

length, and dike width which was very similar to topographic variability (compare Figure IV–17 and Figure IV–29): clusters 1, 4, and 6 generally showed higher values than clusters 2, 3, 5, and 7.

Hypothesis H3: For a given level of connectivity, higher fluxes of suspended sediments related to tributary inputs did not produce higher sediment deposition or a more advanced state of terrestrialisation.

Our third hypothesis suggested that at equal conditions of connectivity, high suspended sediment fluxes would imply strong sedimentation and terrestrialisation. We compared reaches upstream and downstream of the Isère River, the most important Rhône tributary in terms of suspended sediment input, in order to evaluate this factor. For dike fields of the three clusters of similar connectivity (1, 4, 5), we found that median terrestrialisation status was significantly higher in upstream reaches compared to downstream reaches (Figure IV–30a, Mann-Whitney U test, W = 1,620, $p < .05$). Significant differences were evidenced for the relative elevation of emerged deposits within dike fields (Figure IV–30b, Mann-Whitney U test, W = 2,587, $p < .001$), with deposits being higher in downstream reaches than in upstream reaches. Topographic variability did not differ between upstream and downstream reaches (Figure IV–30c, Mann-Whitney U test, W = 1,663, p = 0.22).

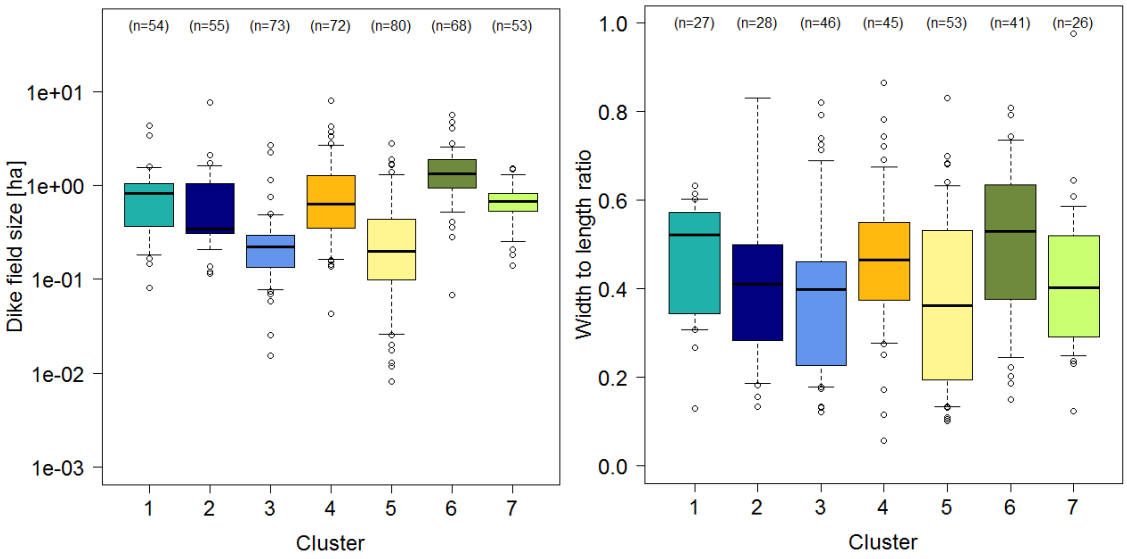

Figure IV–29: Dike field terrestrialisation patterns with respect to dike field geometry characteristics (left: dike field size, right: width to length ratio).

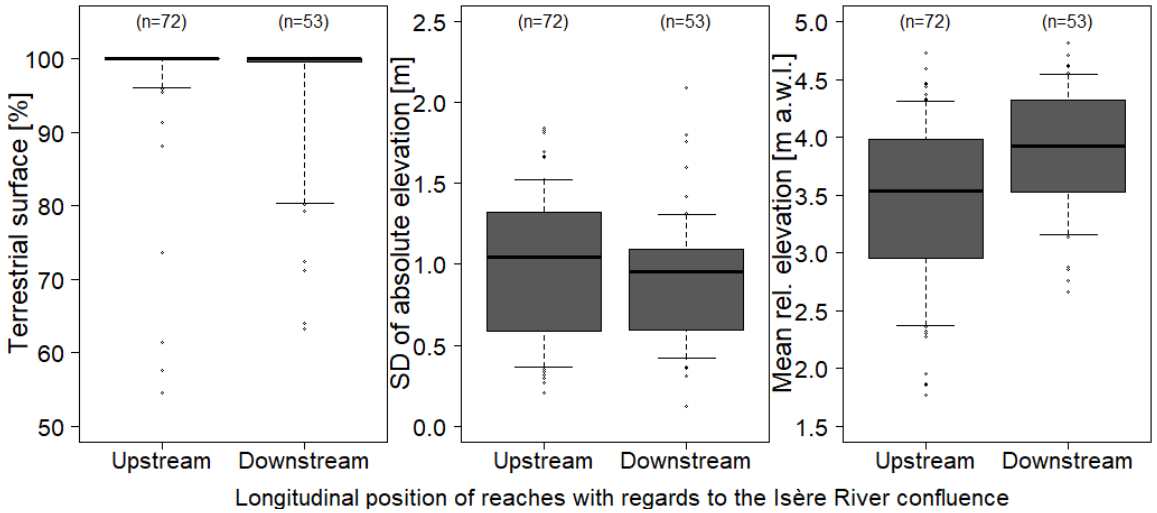

Figure IV–30: Comparison of sedimentation and terrestrialisation patterns between reaches upstream and downstream of the Isère River confluence. From left to right: planimetric terrestrialisation state, topographic variability, and mean relative elevation above the water level.

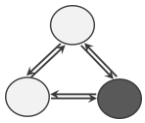

CHAPTER V HISTORICAL EVOLUTION OF DIKE FIELD DEPOSITS

Résumé du chapitre V : évolution historique des casiers

Pour mieux comprendre et interpréter les patrons de sédimentation et d'atterrissement observés dans le chapitre précédent, nous avons par la suite adopté une perspective diachronique. Appliquant la même approche comparative que pour l'analyse des patrons contemporains, nous avons noté deux aspects : dans les années 1940, environ 60 ans après la construction des premières digues, la variabilité des conditions intra-secteur était importante. A titre comparatif, la variabilité inter-secteur était moindre, seul celui de Montélimar (MON) montrait des pourcentages d'atterrissement plus forts par rapport aux autres secteurs d'étude. Ainsi, en comparant les conditions des années 1940 aux conditions en 2000, nous apercevons des trajectoires divergentes entre la période antérieure et précédant les années 1940. Nous avons également remarqué des patrons divergents entre les évolutions planimétrique et verticale des dépôts dans les quatre secteurs. Tandis que Pierre-Bénite (PBN) et MON montrent un fort atterrissement planimétrique dans les années 2000, nous constatons des épaisseurs de sédiments fins faibles comparé aux secteurs de DZM et PDR. Ces derniers, au contraire, ont un atterrissement planimétrique plus faible, caractérisé par un nombre plus important de surfaces restées en eau. Dans le même temps, leurs dépôts de sédiments sont importants. Nous émettons donc l'hypothèse que les processus d'atterrissement divergeaient entre les secteurs : à PBN et MON c'est l'assèchement (« *dewatering* ») qui predominait, à PDR et DZM la sédimentation était importante. L'analyse longitudinale des variables de réponse et des diverses variables de contrôle nous a permit à évaluer les liens à travers une autre échelle. Nous avons pu constater des patrons sinusoïdales pour les variables de réponse qui semblent correspondre relativement bien à la trajectoire de la contrainte tractrice dans le chenal principale du Rhône court-circuité. Ceci souligne le rôle des facteurs locaux.

1 Introduction

Space and time are the fundamental notions of fluvial geomorphology (Bravard, 1998). To better understand and interpret the patterns of sedimentation and terrestrialisation

that we observed in the dike fields in chapter IV, in a next step we took a diachronic perspective. Studying the evolutionary trajectory of the sediment deposits in the dike fields is fundamental if we want to derive the underlying processes and more fully understand the diverse drivers. We also know that some external conditions were not constant over time, including the geometry of the river bed (Parrot, 2015; Depret et al., 2017; Piégay et al., 1997) or discharge conditions.

2 Material and methods

2.1 Material

In the framework of the Rhône Sediment Observatory (‘*Observatoire des sediments du Rhône’*, OSR), 839 measures of overbank fine sediment have been carried out in the dike fields of PBN, PDR, and DZM by GeoPeKa and the CNRS (UMR 5600 EVS) (Piégay et al., 2018). Sedimentation rates have been calculated based on the year the dikes had been constructed.

We furthermore obtained shear stress values of the main by-passed channel from D. Vázquez Tarrío (University of Aix-Marseille) for flood discharges (Q_2 and Q_5). Using a 1-D hydraulic model (MAGE), local shear stresses along the river bank were calculated using the local water levels obtained from the model and the slope. Average values for each river bank were used.

2.2 Determining the evolutionary pattern of dike field sediment deposits

In the following sections, we present two analyses involving different study reaches: A first analysis was carried out on all reaches (PBN, PDR, MON, DZM). A second more detailed analysis covered the reaches of PDR and DZM, where we described 3 historical states of dike field evolution. Details of the dates and their purposes are available in Table III–2.

2.2.1 Planimetric evolution (PBN, PDR, MON, DZM): Terrestrialisation and land cover

For 343 dike fields, we mapped land cover units in the 1940s to describe the state of terrestrialisation, woody vegetation colonisation and other land uses prior to diversion and to compare them to contemporary conditions. Details of the procedure were described in chapter III section 2.2.1. The georeferenced aerial photographs from the

French National Geographic and Forestry Information Institute (Institut National de l'Information Géographique et Forestière, IGN) were selected as to cover the same point in time (PBN: 1945; PDR: 1948/9; MON: 1949; DZM: 1947) (Table III–2). This represented conditions approximately sixty years since the beginning of the major construction phase and just prior to the first diversions. Having calculated the percentage of terrestrial surfaces and the relative cover of individual land cover units per dike field for this period, too (chapter III section 2.2.1), we were further interested in the changes in terrestrialisation status and forest cover over time. We thus calculated the difference between the percent cover in the 2000s and the 1940s, as well as the rate of change per year:

$$\Delta\, T\ [\%] = T_{2000}[\%] - T_{1940}[\%], \qquad (Equ.V-1)$$

$$Rate\ of\ change\ \left[\frac{\%}{yr}\right] = \frac{\Delta\, T\ [\%]}{(Year_{2000s} - Year_{1940s})}, \qquad (Equ.V-2)$$

with T = terrestrial surface (or forest cover in vegetalisation analysis), ΔT = difference between terrestrial surface (or forest cover) in the 2000s and the 1940s.

Furthermore, we determined the relative change in terrestrialisation which took place between the 1940s and the 2000s, with reference to the available space in the 1940s:

$$T\ ratio = \frac{\Delta\, T\ [\%]}{(100\ [\%] - T_{1940}\ [\%])}, \qquad (Equ.V-3)$$

To minimise the digitisation error associated to sometimes imprecise georeferencing, instead of intersecting the land cover unit polygons of different dates, we calculated differences in surface cover.

2.2.2 Vertical evolution

For the analysis of the vertical evolution of the sediment deposits, we used the sediment sampling data presented in chapter III section 4.2.2. In a GIS environment, we determined the mean surface age for each sampling point based on aerial image interpretation. For this we identified the acquisition year of the latest aerial image on which the surface was still aquatic ($Year_{aqu}$) and of the earliest on which it had evolved to a terrestrial state ($Year_{terr}$). Then we calculated the mid-point of the period between the two images. The difference between this resulting year and the year 2014 was defined as the mean age of the surface:

$$Mean\ surface\ age\ [yrs] = 2014 - \left(\frac{Year_{aqu} - Year_{terr}}{2}\right), \qquad (Equ.V-4)$$

Based on these analyses, we could approximate average annual sedimentation rates by calculating the ratio between the overbank fine sediment thickness and the mean surface age (Citterio & Piégay, 2009):

$$Average\ annual\ sedim.rate\ \left[\frac{cm}{yr}\right] = \frac{Overbank\ fine\ sedim.thickness\ [cm]}{Mean\ surface\ age\ [yrs]}, \quad (Equ.V-5)$$

This parameter does not take into account the potentially high variability of sediment deposition through time, related to a) the stochastic and intermittent nature of the process of sediment transport, but also to b) the frequency of connection of the dike field, which itself was assumed to have changed over time. The normalisation facilitated a comparison of average longer-term trends in the relative evolution of sediment deposits between study reaches with different histories. Utilising the same time average method for both pre- and post-dam periods, the change in connectivity which had occurred at the installation of the diversion scheme is not taken into account. A comparison between the two periods is therefore limited.

Some potential errors related to the vertical data were identified. For the measurement of the overbank fine sediment thickness, we assumed that no important layers of gravel had been deposited after dike construction. Small local lenses of gravel in a sand or silt matrix might have introduced an error to these measurements in some instances. Our samples, as well as GPR measurements suggested that some small gravels were indeed locally present. Moreover, the accuracy of the mean surface age depended on the availability of aerial image series. Especially in the early years, but in some reaches over the entire period, relatively few series were available, which shows in the mean surface age distributions.

2.3 Analysis of the evolution of environmental conditions

We expected environmental conditions in- and outside of the dike fields which control sedimentation to be non-stationary and thus to have evolved over time. We had at our disposition several data sets that we analysed in a comparative approach between the four reaches (Table III–4): we examined water levels from the years 1902 and 2010 and determined the change in water level in proximity to each dike field. We assumed the two factors to have influenced water levels were the changes in the geometry of

the main by-passed channel and diversion. We analysed geometry changes separately utilised thalweg elevation change data obtained from Parrot (2015) for the pre-dam and post-dam periods (Table III–4).

2.4 Finer scale temporal evolution (2-D) (PDR, DZM)

The more detailed temporal analysis for the reaches of PDR and DZM included four dates, as introduced in Table III–2, with the aim to represent conditions prior to and directly following dam construction, as well as several decades later. We carried out the same analyses as for the coarser scale (two dates) described in section 2.2.1 of this chapter, including mapping of land cover units, determination of relative surface covers and calculation of terrestrialisation and vegetalisation rates (Equation V–1).

2.5 Explanatory analysis: drivers of terrestrialisation / sedimentation

Potential changes in environmental conditions over time were expected to have had an impact on the evolution of the sediment deposits in the dike fields. We analysed relationships in bivariate and multivariate approaches presented in the following.

2.5.1 Connectivity change and terrestrialisation

Having identified connectivity of the dike fields via their longitudinal dikes as a potentially important control factor of terrestrialisation, we were interested to know how the evolution of the water-level controlled connectivity. Regression analyses were carried out regarding relationships between water level change and the parameters describing the contemporary connectivity status. We furthermore hypothesised that also the state of the dike fields in the 1940s would have influenced their further development until the 2000s. To explain how the two parameters interacted with the evolution of the dike fields, we performed a multiple regression analysis. Finally, the respective contributions of diversion and geometric change of the main by-passed channel was examined, as described in the following two sections.

Contribution of diversion: Hypothesis 4a

Our assumption was that the diversion schemes and the implied sudden drop in the water level would have greatly accelerated the terrestrialisation of the dike fields by the process of dewatering. We also expected the decreased frequency of submersion to have reduced sedimentation rates.

The four study reaches have been subjected to diversion at different points in time, a comparative approach can therefore give some first insights on the impact from diversion. For PDR and DZM, the reaches with the latest and earliest diversion, respectively, we were in possession of data describing the terrestrialisation status just prior to and following the installation of the diversion scheme. First, we considered these patterns of planimetric change and any important shift in the rate of terrestrialisation. Second, we related overbank fine sediment depth and sedimentation rates to mean surface age to evidence potential abrupt changes in sedimentation over time.

Evolution of the channel geometry and its effects: Hypothesis 4b

Degradation of the main by-passed channel was presumed to accelerate terrestrialisation gradually along the process, disconnecting and thus slowly dewatering the dike fields. An aggradation of the main by-passed channel was expected to slow down terrestrialisation.

To approximate the vertical evolution of the channel bed in proximity to each dike field, we integrated the thalweg data from Parrot (2015) in our analyses. For this we applied the *Near* tool in ESRI ArcGIS (*Proximity* toolset in the *Analysis* toolbox), to relate the nearest point to each dike field. We used a) 'pre-dam thalweg elevation change', i.e. changes in the period between the installation of the dikes and dam construction, b) 'post-dam thalweg elevation change', corresponding to changes following dam construction, and c) 'net thalweg elevation change', which represents the sum of a) and b). This allowed us to analyse effects from potential channel degradation or aggradation on sedimentation patterns by acting on hydrological connectivity for each of the two river engineering measures.

First, we graphically related planimetric terrestrialisation patterns to local thalweg elevation changes in proximity to the dike fields. We did this a) for the net thalweg elevation change and terrestrialisation status in the 2000s, and b) for thalweg elevation change prior to diversion and terrestrialisation status in the 1940s. Second, we carried out a linear regression analysis to evaluate the influence of thalweg elevation change on the resulting water level for each reach individually and for all dike fields together. We also calculated the residuals and compared them between reaches, as an indicator of variability. Beyond this, we worked at the reach scale, where we

compared aggregated values of terrestrialisation and sedimentation patterns to mean/median thalweg elevation change values.

2.5.2 Within-reach spatial pattern analysis

Having evidenced the importance of local conditions on terrestrialisation and sedimentation patterns, we plotted all available data sets against downstream distance. The downstream distance of each dike field was determined based on river kilometre data using the *Create a simple route* tool from the *Editor* toolbox in ESRI ArcGIS. This allowed us to study the longitudinal distribution of phenomena for each reach individually and aid the interpretation of the role of individual drivers.

3 Results

3.1 Evolutionary trajectories of dike field overbank fine sediment deposition

3.1.1 Planimetric conditions in the 1940s and 2000s (PBN, PDR, MON, and DZM)

In the 1940s, approximately sixty years since the first Girardon measures and just prior to the first diversions, the planimetric state of terrestrialisation in the 343 studied dike fields ranged from 0% to 100%. Of these dike fields, 9.9% were terrestrial over more than 90% of their surface area (mean degree of terrestrialisation = 42.9%, SD = ±29.5%). Aquatic dike fields (terrestrial over less than 10% of their surface area) amounted to 14.9%. The terrestrialisation state of dike fields was heterogeneous within each of the four reaches, while between-reach variation was significant mainly due to a comparatively advanced state of terrestrialisation of MON dike fields (Figure V–1 left and Table A–II–1, Kruskal Wallis test, chi-squared = 58.50, df = 3, $p < .001$). On average, dike fields were 36.3% terrestrial (SD = ±26.7%) at PBN, 43.7% (SD = ±27.8%) at PDR, 69.5% (SD = ±26.3%) at MON, and 34.3% (SD = ±26.3) at DZM. In total at PBN, 43.4% of the total studied dike field surface was terrestrial, at PDR 39.6%, at MON 68.1%, and at DZM 34.4%. Upstream and downstream reaches showed a significant variation (Mann-Whitney U test, W = 16836, $p < .05$).

Trajectories of planimetric evolution were variable between individual dike fields, and terrestrialisation dynamics prior to 1940 were weakly related to dynamics in the

following period, until the 2000s (Figure V–1 right). The latter may indicate an important shift in the evolution of the dike fields following the 1940s, which is most likely related to diversion. To the lower left of the plot, we find dike fields which have remained aquatic over the entire investigation period (from the 1880s to the 2000s). Toward the upper left corner, we identify dike fields which had remained aquatic in the first period of observation (1880s–1940s), while having terrestrialised to a large degree by the 2000s. In the upper right corner, we find dike fields which have terrestrialised very early and have remained in these conditions since or continued advancing. The closer the dike fields are to the grey diagonal line, the less change they have undergone in their state of terrestrialisation between the 1940s and the 2000s. Some dike fields are located below the grey line. They featured an increase in water surfaces between the two dates. This may be related to an aggradation of the main by-passed channel, and therefore an increased connectivity, as we shall see in section 3.4.2.

The centres of gravity of the four reaches, and thus their average evolutionary trajectories, were relatively close. As we already saw in Figure IV–12, we may still identify two groups of clusters: concerning the 1940s conditions, PBN, PDR, and DZM

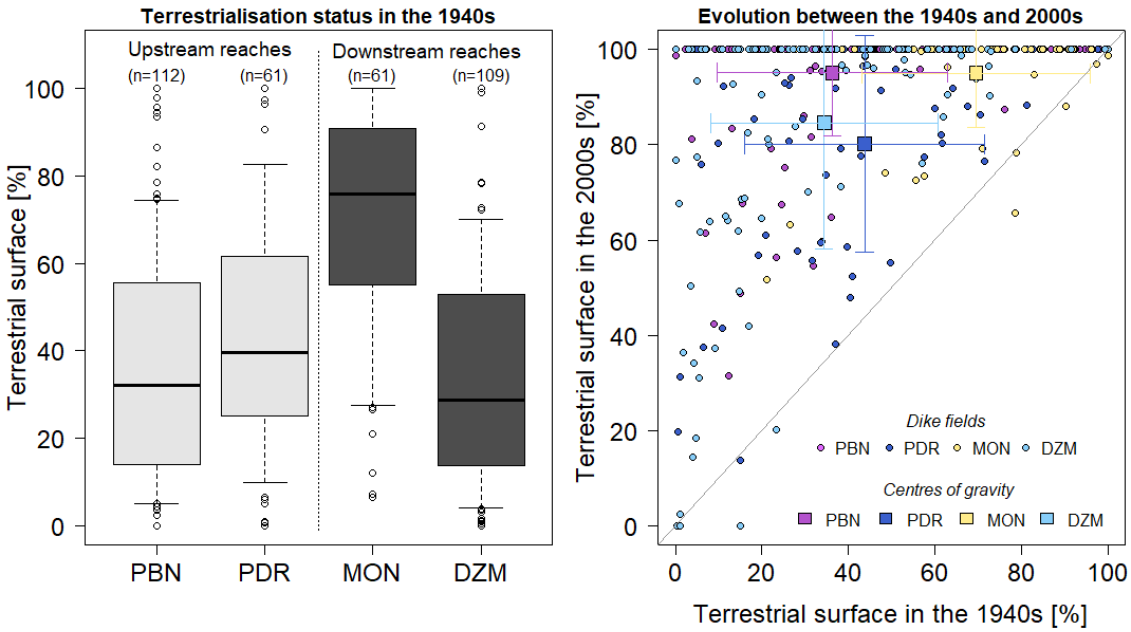

Figure V–1: Comparison of the dike field terrestrialisation status in the four study reaches in the 1940s (left). Relationship between the dike field terrestrialisation status in the 1940s and 2000s (right). The grey line provides a reference where x=y.

form one cluster with similar trajectories; and MON a second, featuring more advanced states of terrestrialisation. In the 2000s, we found one cluster composed of PBN and MON, and another comprising PDR and DZM. This re-grouping over time indicates that following the 1940s, changes in the trajectories of the different reaches potentially have taken place, which were themselves variable from one reach to another.

3.1.2 Strong vegetalisation trend

We discovered strong terrestrialisation and vegetalisation tendencies in the studied dike fields. In the 1940s, the predominant land cover type in the dike fields (N = 343) was water, covering 58.4% of the studied dike field surface, or 183.2 ha. Trees and shrubs (forest) covered 26.0%, or 81.5 ha and bare sediment / herbaceaous layers (open sites) another 15.5%, totalling 48.6 ha. Agricultural land made up 0.1% (0.4 ha) and infrastructures 0.1%, (0.2 ha). Due to the comparatively large dike field sizes at DZM, the largest water and forest surfaces were found in this reach (Figure V–2a). In relative terms, however, land cover patterns in this reach were comparable to other reaches (Figure V–2b): at PBN, PDR, and DZM water surfaces dominated. Conversely, at MON, open sites, water and forest were relatively equally represented (respectively 37.3%, 31.8%, and 29.6%). The extent of open surfaces and water surfaces might be influenced by discharge conditions. The more stable forest cover was significantly higher in the downstream than in the upstream reaches (Wilcoxon test, $W = 17{,}820$, $p < .001$).

The sample sizes of analysed dike fields in the 1940s and the 2000s were slightly different due to differences in the longitudinal coverage of the reaches by the available imagery. To describe evolutionary patterns of the dike fields between the two dates, we therefore compared average rates of change of the individual dike fields instead of reach wide differences. The water cover in the dike fields decreased on average by –0.77 %/yr (SD = ±0.48 %/yr), while the forest cover increased on average by 0.65 %/yr (SD = ±0.60 %/yr) in this period (between the 1940s and 2000s). Average evolution of open surfaces, agricultural surfaces, and infrastructures was 0.07 %/yr, 0.04 %/yr, and 0.01 %/yr, respectively. We observed approximately the same patterns of rates of change in the four reaches, although with varying magnitudes (Figure V–3): water surfaces featured primarily negative rates of change, forest surfaces primarily positive rates of change, and open surfaces both negative and positive rates of change.

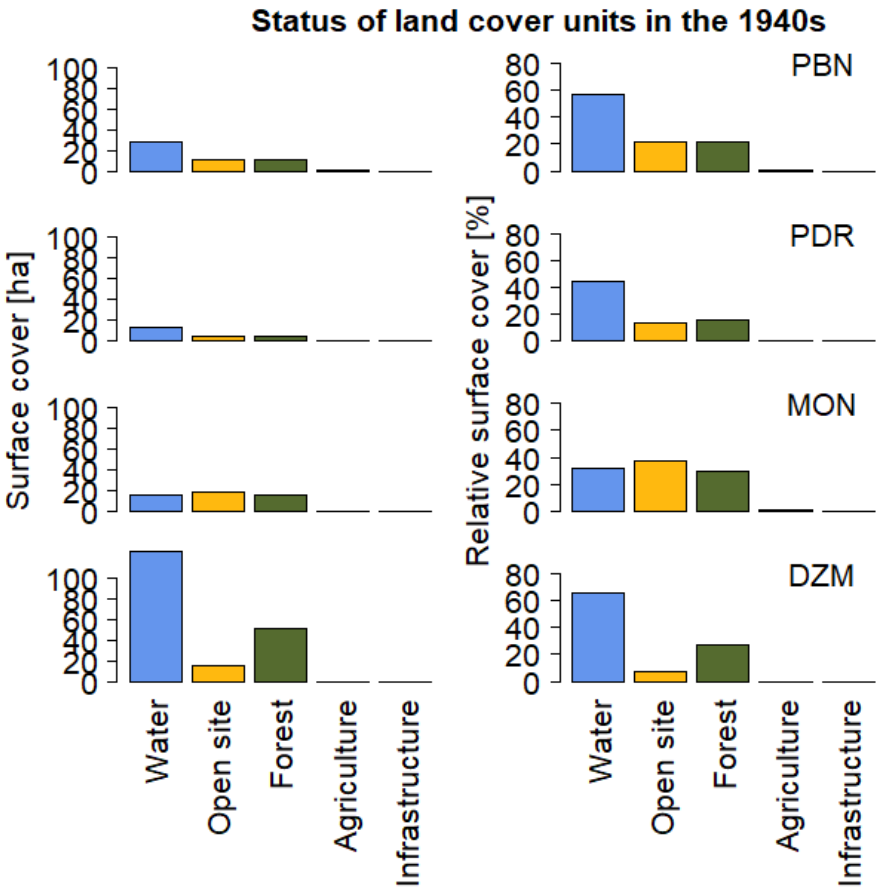

Figure V–2: Distribution of land cover units in dike fields of the four reaches prior to diversion (in the 1940s, i.e. ~60 years since construction of the dikes). Left: absolute surface cover. Right: relative surface cover. Note that the sample size is not the same as in the analysis of contemporary conditions (N_{PBN} = 112, N_{PDR} = 61, N_{MON} = 61, N_{DZM} = 109).

Agricultural surfaces and infrastructures primarily showed positive rates of change. Both evolved more strongly in the downstream reaches. At DZM, indeed, 60% of the historical active tract was cultivated in 2006 (Gaydou, 2013). The dike fields were not excluded from this evolution, yet these surfaces remained comparatively small compared to the other three land cover units. From visual inspection of additional aerial images, we know that especially agricultural surfaces underwent smaller-scale temporal changes which are not evident in this net analysis.

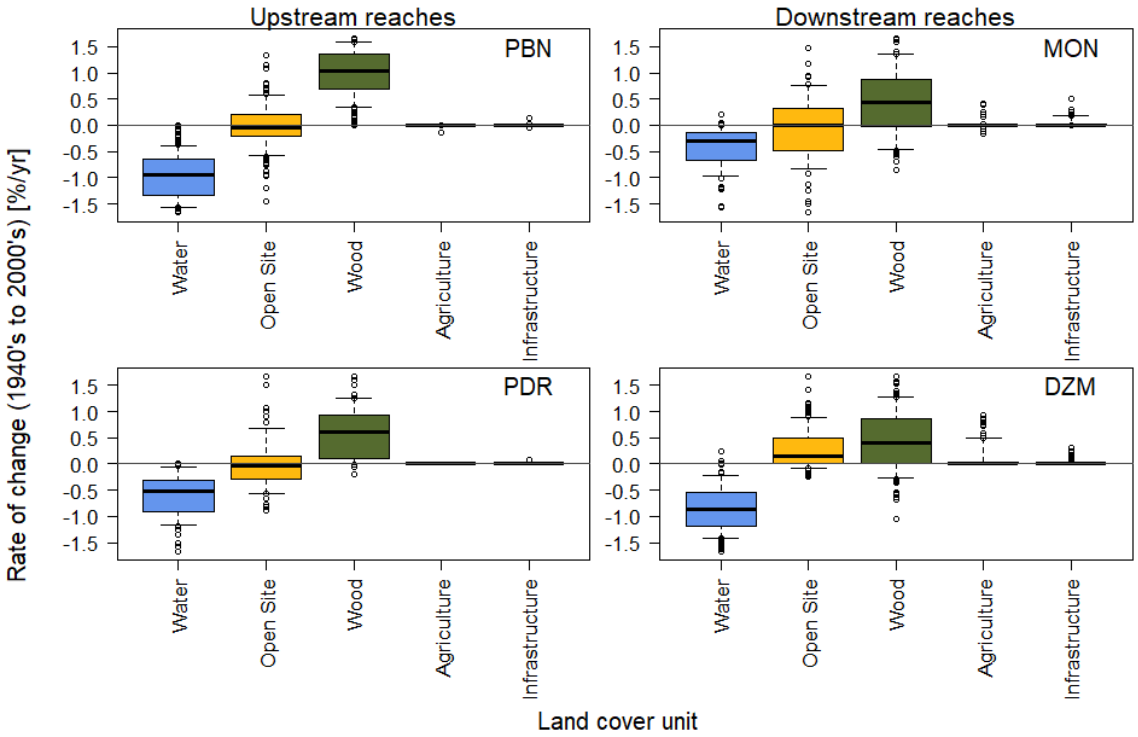

Figure V–3 Comparison of land cover rates of change between the four study reaches from the 1940s to the 2000s.

3.1.3 Variable vertical evolution of dike field overbank fine sediment deposits

Deposit thickness

Overbank fine sediment deposits of pre-diversion surfaces reached thicknesses ranging from 24 cm to 471 cm (Figure V–4a, mean = 276 cm, SD = ±125 cm). In these absolute terms, we stated that sedimentation was more important at PDR and DZM than at PBN and MON (Table V–1). However, we highlighted that deposition periods were longer for the upstream reaches (from approximately 1880 to at least 1966 and 1977 at PBN and PDR, respectively) than for downstream reaches (from approximately 1880 to 1956 and 1952 at MON and DZM, respectively). Post-diversion surfaces were characterised by sediment deposit thicknesses which ranged from 10 cm to 463 cm (Figure V–4b and Table V–1, mean = 210 cm, SD = ±113 cm). In absolute terms, downstream reaches featured mightier overbank fine sediment deposits than upstream reaches. Again, we need to consider, however, that the periods of deposition might have been shorter in the two upstream reaches, which were by-passed later than the downstream reaches.

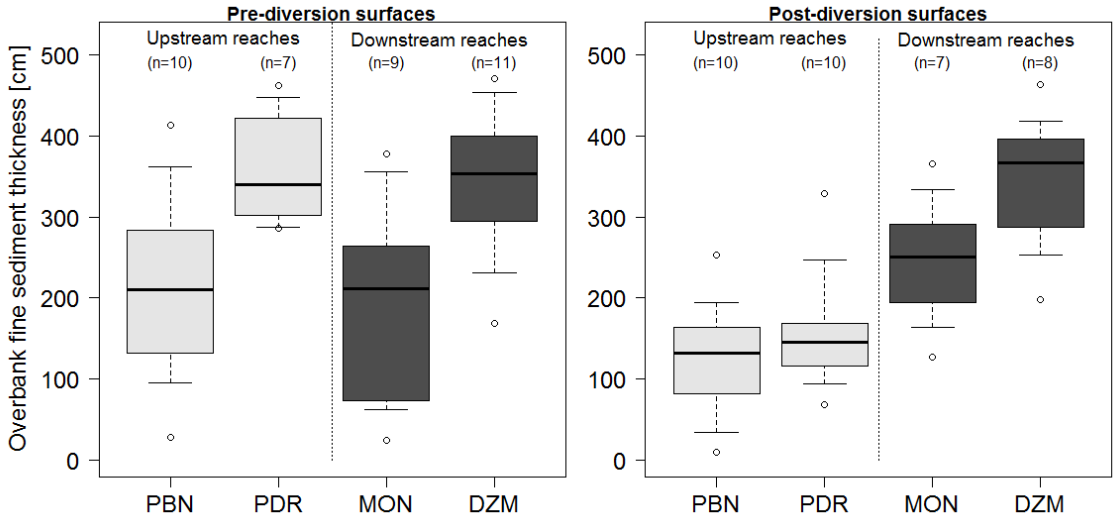

Figure V–4: Inter-reach comparison of measured overbank fine sediment thicknesses on (left) pre-diversion surfaces, and (right) post-diversion surfaces.

Table V–1: Summary statistics for overbank fine sediment depths in the four study reaches.

	Range [cm]		Mean (±1 SD) [cm]	
	Pre-diversion	Post-diversion	Pre-diversion	Post-diversion
PBN	28–413	10–253	218 (±117)	126 (±72)
PDR	286–462	69–329	362 (±72)	160 (±74)
MON	24–378	127–366	193 (±125)	245 (±81)
DZM	169–471	198–463	343 (±94)	345 (±84)

Sedimentation rates

In the following, we normalised thickness values by the mean number of years since terrestrialisation (Figure V–5) in order to compare vertical sedimentation patterns between reaches. The obtained average annual sedimentation rates ranged between 0.2 cm/yr and 6.5 cm/yr for pre-diversion surfaces (Figure V–6a, Table V–2, mean = 3.4 cm/yr, SD = ±1.6 cm/yr). They differed between reaches (Kruskal-Wallis test, chi-squared = 11.94, df = 3, $p < .01$), while variations were not significant between upstream and downstream reaches (Mann-Whitney U test, W = 173, p = 0.94). Instead, differences were significant between PBN and PDR, PBN and DZM, and PDR and MON (Table A–II–2).

On post-diversion surfaces, estimated average annual sedimentation rates ranged from 0.2 cm/yr to 10.8 cm/yr (Figure V–6b, mean = 5.2 cm/yr, SD = ±2.3 cm/yr). A

Kruskal Wallis test yielded significant differences between study reaches (chi-squared = 11.72, df = 3, $p < .01$). These differences were mainly related to low rates at PBN compared to the other reaches, and a significant difference between MON and DZM dike fields (Table A–II–2).

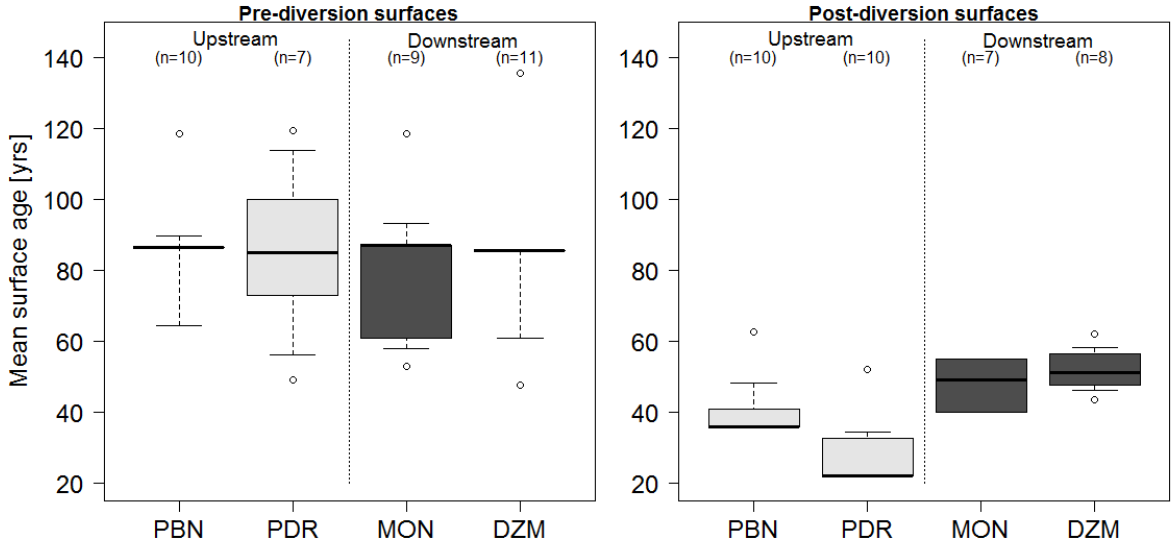

Figure V–5: Comparative representation of mean surface age for (left) pre-diversion surfaces, and (right) post-diversion surfaces of the four study reaches.

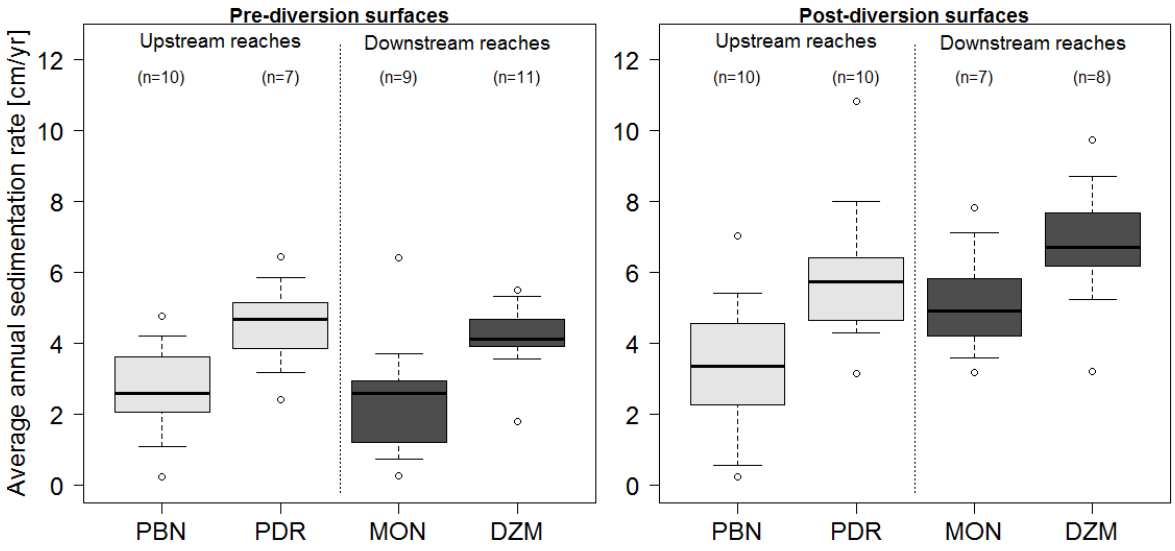

Figure V–6: Average annual sedimentation rates compared between the four reaches for (a) pre-diversion surfaces, and (b) post-diversion surfaces.

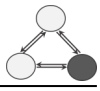

Table V–2: Summary statistics of average annual sedimentation rates for the four study reaches.

	Range [cm/yr]		Mean (±1 SD) [cm/yr]	
	Pre-diversion	Post-diversion	Pre-diversion	Post-diversion
PBN	0.2–4.8	0.2–7.0	2.7 (±1.4)	3.4 (±2.1)
PDR	2.4–6.4	3.1–10.8	4.5 (±1.3)	6.0 (±2.1)
MON	0.3–6.4	3.2–7.8	2.5 (±1.8)	5.1 (±1.6)
DZM	1.8–5.5	3.2–9.7	4.2 (±1.0)	6.8 (±1.9)

3.1.4 Summary of sediment deposit evolutionary dynamics

In summary, the planimetric data showed relatively heterogeneous conditions in the studied dike fields in the 1940s. Within the reaches, we then observed a simplification and homogenisation over time, amplifying in turn the importance of inter-reach differences in the period following the 1940s. Averaged vertical evolution rates of the overbank fine sediment deposits correspond to values in the literature in this regional context. For the Ain, for instance, Piégay et al. (2008) found rates between 0.11 and 2.4 cm/yr. In vegetation units at the Drôme, rates ranged between 0.2 and 10.1 cm/yr (Dufour et al., 2007) and for the Ain, Doubs, and Rhône, Citterio & Piégay (2009) noted values between 0 and 2.57 cm/yr.

When plotting planimetric versus vertical sedimentation and terrestrialisation data, we found no evident relationships (Figure V–7). On the one side, the planimetric values integrate the two processes of sedimentation and dewatering and the advanced state of terrestrialisation might mask potential differences in the evolutionary process. On the other side, also the averaged sedimentation rates even out potential changes of actual sedimentation rates over time. It is to be expected that environmental conditions in-and outside of the dike fields have undergone changes over time. In the following we shall analyse temporal changes of potential factors that we have identified in a literature review. To evaluate their impacts on sedimentation and terrestrialisation at the reach scale, we have summarised the preliminary findings of this chapter in Table V–3 as a basis for reach comparisons in the following.

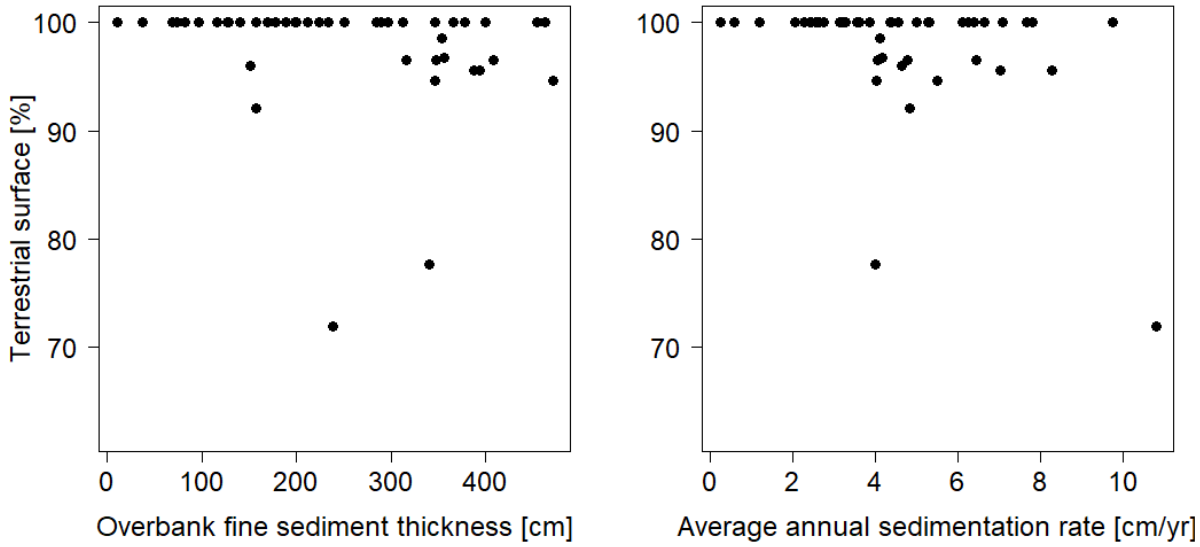

Figure V–7: Relationships between planimetric and vertical sedimentation patterns: (left) overbank fine sediment thickness and (right) average annual sedimentation rate per dike field.

Table V–3: Schematic summary of pre- and post-dam conditions in the four reaches (symbologies for average planimetric terrestrialisation state: – = 0%–25%, + = 25%–50%, ++ = 50%–75%, +++ = 75%–100%; for average vertical sediment accumulation: + = 0–3 cm/yr, ++ = 3–5 cm/yr, +++ = > 5 cm/yr).

Period	Variable	PBN	PDR	MON	DZM
Pre-dam (1940s)	Planimetric	+	+	++	+
	Vertical	++	+++	+++	+++
Post-dam (2000s)	Planimetric	+++	+++	+++	+++
	Vertical	+	+	++	++

3.2 Evolution of environmental conditions

Beyond changing sedimentary and terrestrialisation conditions inside the dike fields over time, we analysed the evolution of the drivers in order to explain changes in trajectories. In chapter IV we identified the connectivity of dike fields to the main by-passed channel as a major driver. We considered the geometric evolution of the main by-passed channel (Parrot, 2015), as well as the implementation of the diversion schemes. Both had an impact on water levels and thus potentially the frequency and duration of connection of the dike fields. The diversion schemes furthermore modified the discharge regime in the by-passed reaches (see chapter II).

3.2.1 Change in connectivity

The comparison of water levels from the years 1902 and approximately 2010 revealed an average decline in the order of –1.48 m (±1.37 m) in proximity to the studied dike fields. At PBN we noted the most important declines, whereas we found both declines and increases close to dike fields of MON and DZM (Table V–4, Figure V–8). Around PDR dike fields we observed relatively homogeneous conditions of change.

In the reach of PBN, the water level has lowered throughout the reach (Figure V–9). At PDR the weir of Peyraud locally increased the water level with regards to 1902 conditions. However, in this area we did not study any dike fields, which explains the lack of positive values in Table V–4 and Figure V–8. The backwater effect near the confluence of the old Rhône and the diversion canal at MON and DZM caused the water level in 2010 to be above the level of 1902, while in the upstream parts of the two reaches water levels have likewise lowered.

Table V–4: Descriptive statistics of water level change between 1902 and approximately 2010.

	Range [m]	Mean (±1 SD) [m]
PBN	min: –3.27, max: –1.19	–2.77 (±0.67)
PDR	min: –2.17, max: –0.10	–1.21 (±0.44)
MON	min: –2.38, max: 1.42	–0.85 (±1.44)
DZM	min: –2.19, max: 2.35	–0.75 (±1.36)

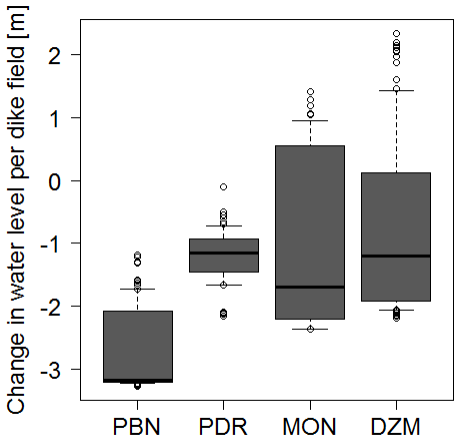

Figure V–8: Between-reach comparison of water level changes (WL_{2010}-WL_{1902}).

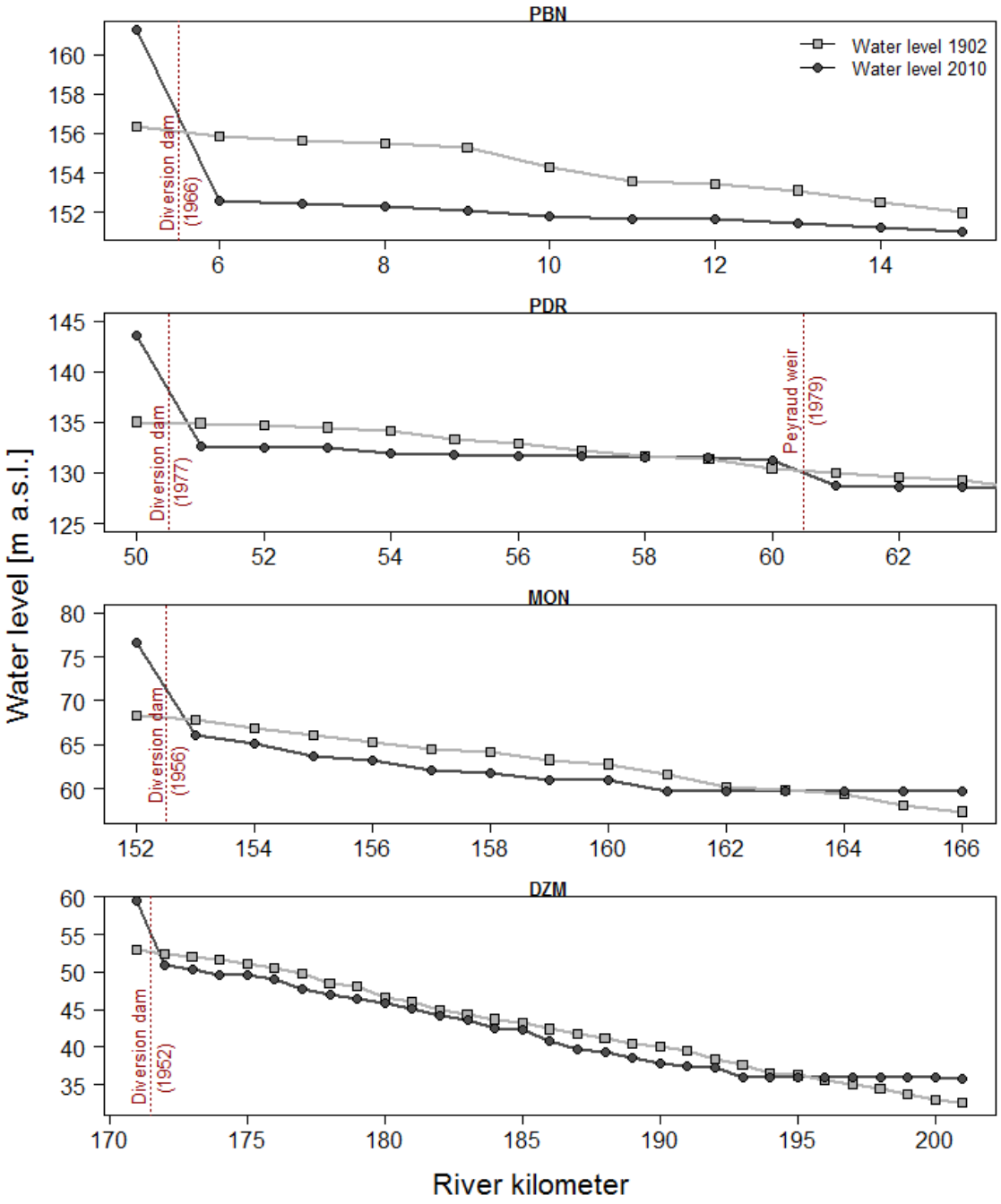

Figure V–9: Longitudinal pattern of water levels and their evolution (1902–approximately 2010) in the four study reaches.

Changing channel geometry

One factor which we expected to have an impact on the water level, and thus potentially on connectivity, is the evolution of the channel geometry. The available thalweg elevation change data from Parrot (2015) allowed us to analyse its effects on sedimentation and terrestrialisation both prior to and following diversion. In proximity

to the individual dike fields, we stated net changes over the investigation period which ranged from –6.27 m to 1.51 m (mean = –1.76 m, SD = ±1.63 m). Considerable changes in thalweg elevation occurred in the by-passed channels following the construction of the Girardon dike system (Parrot, 2015). Near the dike fields, we stated mainly incision (min = –3.46 m; mean incision = –1.32 m, SD = ±0.82 m) and in some parts aggradation (max = 2.73 m; mean aggradation = 0.37 cm, SD = ±0.61 cm) during this period. Following diversion, maximum incision was –5.42 m (mean = –1.45 m, SD = ±1.18 m), maximum aggradation 1.99 m (mean = 0.08 m, SD = ±0.31 m).

Net thalweg evolution over the entire study period was significantly different between the four reaches (Kruskal-Wallis test, chi-squared = 106.82, df = 3, $p < .001$). And also in each period individually, changes varied significantly between reaches (Figure V–10; Kruskal-Wallis tests, prior to diversion: chi-squared = 119.78, df = 3, $p < .001$; following diversion: chi-squared = 100.74, df = 3, $p < .001$). For thalweg elevation changes prior to diversion, Mann-Whitney U tests revealed significant differences between all reaches (Figure V–10a, Table A–II–3). At PBN, incision in proximity to the dike fields was strongest, with a mean ±1 SD of –1.50 m ±0.80 m. At PDR and MON values were –0.84 m ±1.12 m and –0.93 m ±0.69 m, respectively. In the reach of DZM, on average the channel rather aggraded in proximity to the dike fields (mean = 0.13 m, SD = ±0.90 m). Thalweg changes following diversion were likewise significantly different between all reach combinations (Figure V–10b, Table A–II–3). At PBN, incision continued and was even stronger than prior to diversion (mean = –1.75 m, SD = ±1.13 m). In the reaches of PDR and MON, incision on average continued, but it was less marked than prior to diversion ($mean_{PDR}$ = –0.13 m, SD_{PDR} = ±0.24 m; $mean_{MON}$ = –0.31 m, SD_{MON} = ±0.64 m). Thalweg evolution at DZM was reversed—we found strong incision following diversion (mean = –1.25 m, SD = ±1.37 m). Thalweg evolution within the PBN reach showed thus no change between the two periods (Wilcoxon test, V = 2167, $p = 0.20$), whereas we saw significant variations at PDR (Wilcoxon test, V = 83, $p < .001$), MON (Wilcoxon test, V = 273, $p < .001$), and DZM (Wilcoxon test, V = 2912, $p < .001$).

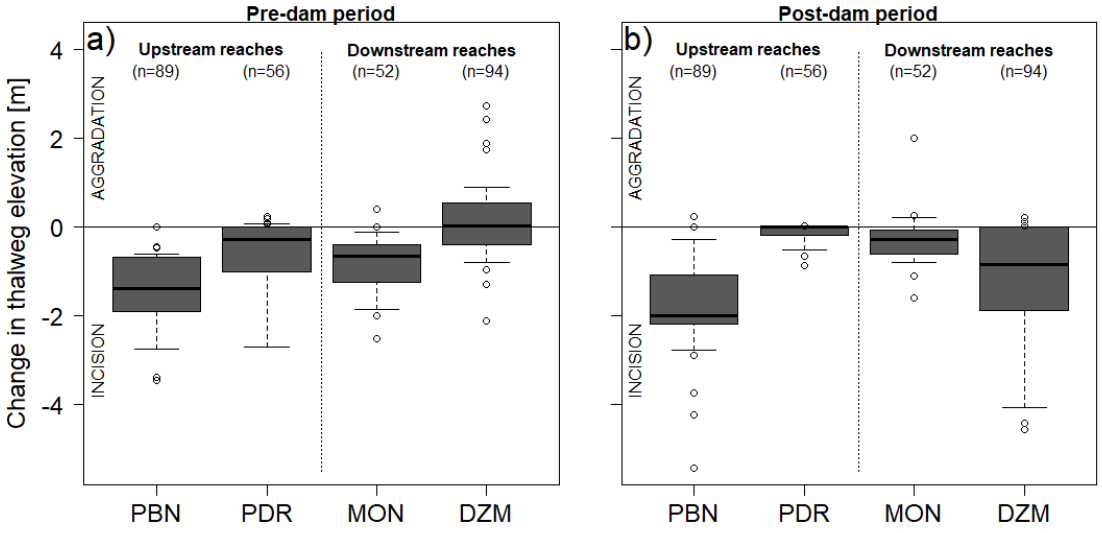

Figure V–10: Change in thalweg elevation in proximity to the dike fields compared between reaches for (a) the pre-dam period and (b) the post-dam period.

The strong trend of incision in the by-passed reach of PBN (mean net thalweg elevation change = –3.25 m, SD = ±1.39 m) potentially led to an early and then continued reduction in the connectivity of the dike fields to the main by-passed channel. The reaches of PDR and MON showed incision, yet less strong compared to PBN (mean net thalweg elevation change$_{PDR}$ = –0.98 m, SD$_{PDR}$ = ±1.18 m; mean net thalweg elevation change$_{MON}$ = –1.24 m, SD$_{MON}$ = ±0.72 m) and thus only moderate reductions in connectivity, especially over the second phase. DZM dike fields were well connected in the first phase, following an average aggradation trend. Strong incision followed diversion and may have led to a late and moderate average reduction in the connectivity of the dike fields (mean net thalweg elevation change = –1.12 m, SD = ±1.53 m).

3.3 Finer scale temporal patterns (PDR and DZM)

3.3.1 Evolution of sediment deposits (planimetric extent)

A closer look at evolution dynamics at PDR and DZM confirmed variable trajectories among the individual dike fields, but also a reach-wide homogenisation over time (Figure V–11). At both reaches, the terrestrialisation status of the dike fields is heterogeneous in the 1940s. At PDR discharge conditions may amplify this effect: for the major part of the reach, discharge conditions on the aerial image series were low.

A small part of the reach, covered by another image series, showed relatively high discharge conditions. The average (±1 standard deviation (SD)) terrestrialisation degree of the dike fields in 1948/49 amounted to 43.7% (±27.8%). In 1958, comparatively high discharge conditions on aerial images caused a marked decrease in terrestrial surfaces (mean = 28.8%, SD = ±25.0%) (Table A–II–4). We then identified a net advancement in terrestrialisation between 1958 and 1986 (mean = 74.9%, SD = ±25.4%), with the probability distribution shifting from a right-skewed to a left-skewed shape. The diversion scheme was realised in this period and put into operation in 1977. In 2006–9, we then stated an average terrestrialisation status of 80.2% and a standard deviation of ±22.8%.

At DZM, the diversion scheme was put into operation in 1952. Comparing the conditions between 1947 (mean = 34.3%, SD = ±26.3%) and 1954/5 (mean = 57.5%, SD = ±27.5%), we stated a distinct change in the state of terrestrialisation as a direct consequence of the drop in the water level (Table A–II–4). It is likewise in this period that we observed a shift from a right-skewed to a left-skewed probability distribution. We then noted continued significant advancement in terrestrialisation between 1954/5 and 1976 and between 1976 and the 2000s. Mean values in 1976 and the

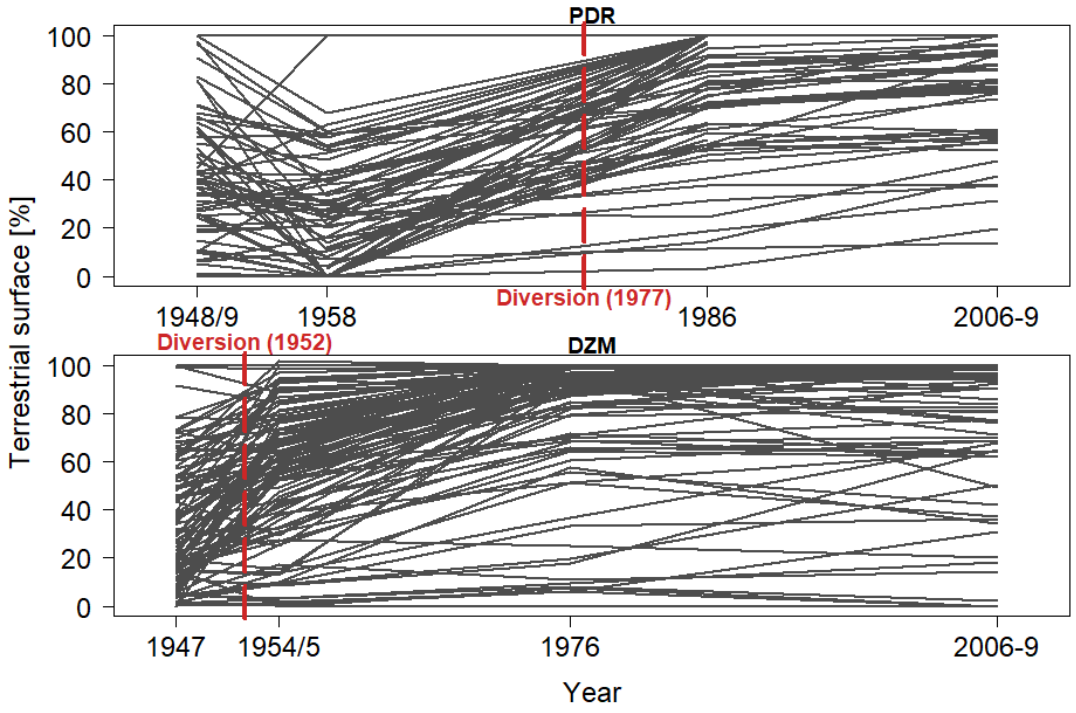

Figure V–11: Evolution of dike field surfaces at PDR (top) and DZM (bottom). Red dashed lines indicate the year when the diversion scheme was put into operation.

2000s were 82.9% and 84.6%, respectively, standard deviation respectively amounted to ±27.0% and ±26.5%.

Analysis of terrestrialisation rates revealed the significantly highest increases in the periods when the diversion schemes were put into operation in both reaches (Figure V–12, Table A–II–5). At PDR, this might have been slightly reinforced by the higher discharge in 1958. In following periods, terrestrialisation continued, however at significantly lower rates. In summary, diversion hence represented a major break in the evolutionary trajectory of the dike fields. And over time, we examined an increasing homogenisation of conditions within both reaches.

3.3.2 Vegetalisation patterns

We demonstrated marked changes in the evolution of the forest cover for both reaches during the study period (Figure V–13). In the 1940s, approximately 60 years since the construction of the dike system, an average forest cover of 18.0% (SD = ±19.9%) was recorded at PDR, and an average of 29.0% (SD = ±26.8%) at DZM. At PDR, this changed to an average 20.4% (SD = ±19.0%) in 1958, to 34.3% (28.0%) in 1986, and 54.6% (SD = ±32.7%) in the 2000s. Statistically significant were the changes between 1958 and 1986, when the by-passing occurred (1977), as well as between 1986 and 2006–09, i.e. between 9 and 29 to 32 years after by-passing (Table A–II–6). We believe that the impact of the higher discharge in 1958 was minor on forest cover compared to bare surfaces. At DZM, a statistically significant change in forest cover

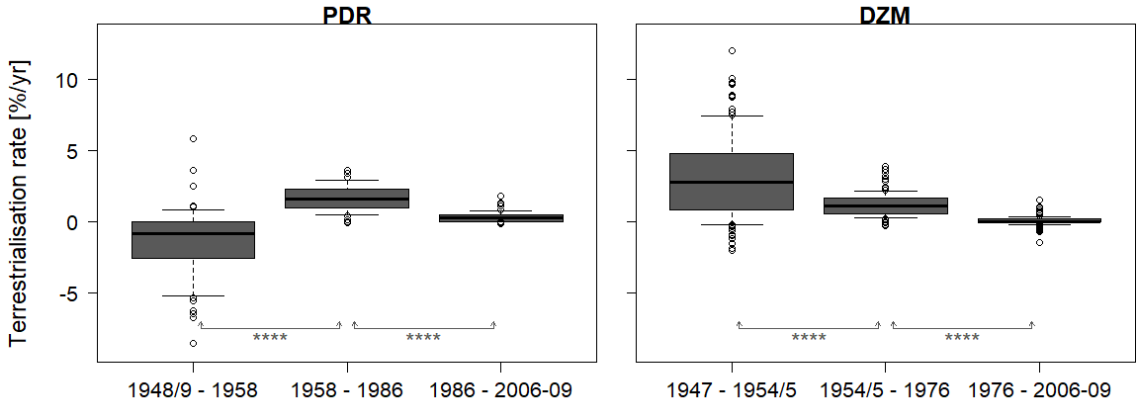

Figure V–12: Comparison of terrestrialisation rates between aerial image series. Stars indicate significance levels from paired Wilcoxon tests (* p < .05; ** p < .01; *** p< .001; **** p < .0001).

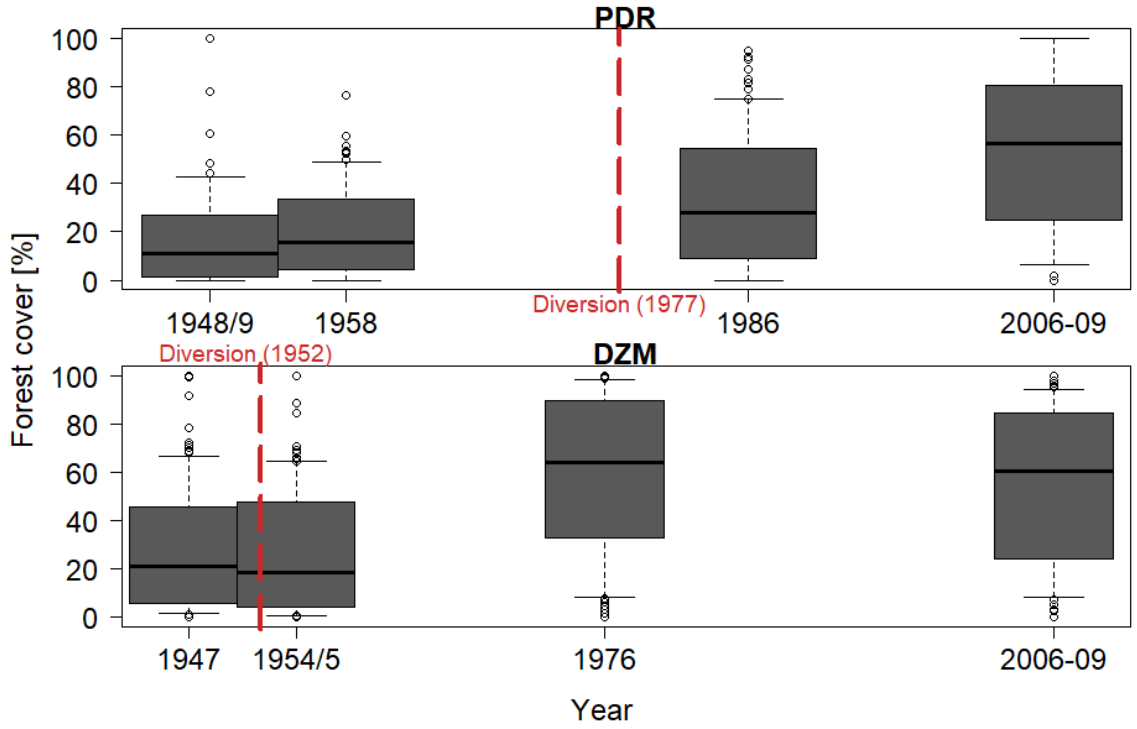

Figure V–13: Evolution of the forest cover in dike fields of PDR (top) and DZM (bottom). Red dashed lines indicate the year when the diversion scheme was put into operation.

took place between 1954/5 and 1976, thus between 2 to 3 and 24 years after by-passing (Table A–II–6). The average forest cover more than doubled in this period, going from 26.4% (SD = ±25.6%) to 59.2% (SD = ±32.7%). In the first and last period, changes were not significant.

In both reaches, we saw increasing interquartile ranges, indicating an increasing statistical dispersion of the forest cover distribution within each of the reaches. The most important changes are observed few decades after the diversions, the time probably for the forest to install on the newly emerged surfaces. This was likewise observed by Arnaud (2012) on the Rhine River, who studied the vegetalisation of groyne fields and the active channel only few years after dam constructions.

At PDR, rates of change in forest cover, referred to as vegetalisation rates in the following, continuously increased from an average 0.3%/yr (SD = ±2.1%/yr) in period 1 (1948/9 to 1958), to 0.5%/yr (SD = ±1.1%/yr) in period 2 (1958 to 1986, with diversion in 1977), and to 0.9%/yr (SD = ±1.3%/yr) in period 3 (1986 to 2006–9) (Figure V–14, Table A–II–7). Yet, pairwise differences were not significant between either combination of these periods. Contrarily, at DZM, we found significant

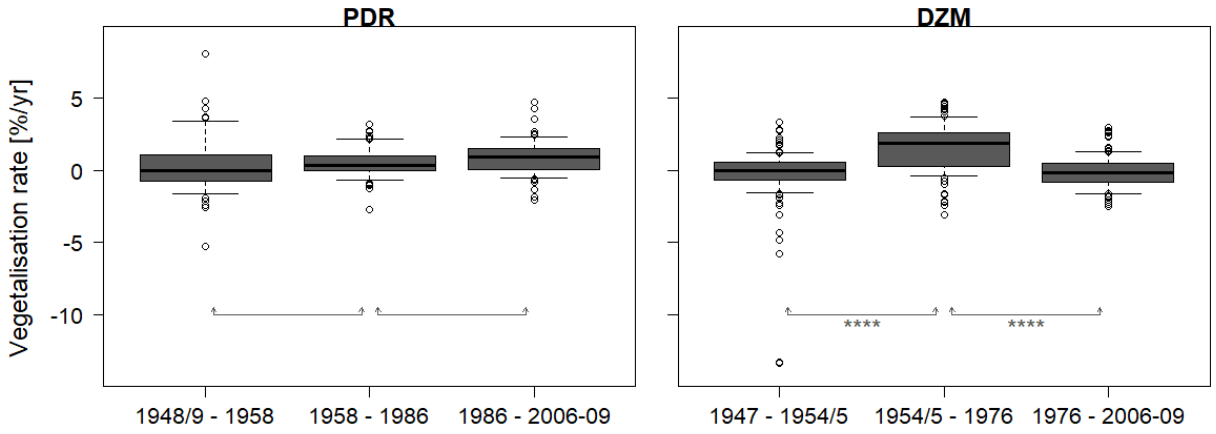

Figure V–14: Vegetalisation rates between analysed image series at PDR (left) and DZM (right). The stars indicate significant differences from pairwise comparisons using Mann-Whitney U tests.

differences between periods 1 and 2, as well as between periods 2 and 3, due to an important increase in vegetalisation rates in the second period, following diversion (1954/4 to 1976) (Table A–II–7). Rates in this reach were highest in period 2 (1954/5 to 1976) with an average 1.5%/yr (SD = ±1.7%/yr), compared to an average forest loss of -0.4%/yr (SD = ±2.2%/yr) between 1947 and 1954/5 and an average loss of –0.1%/yr (SD = ±1.1%/yr) between 1976 and 2006–9.

3.4 Synthesis and explanations

We expected that changing environmental conditions over time would have entailed changing conditions for sedimentation and terrestrialisation within dike fields. In the preceding sections, we stated that channel straightening, as well as damming and water diversion, implied important changes in the water level in the main by-passed channel. This has likely changed the connectivity of the dike fields to the main by-passed channel over time. Within the dike fields, roughness conditions have evolved with the changing land cover. Land cover evolution in the entire drainage basin, and consequently the evolution of suspended sediment loads in the Rhône and its tributaries, additionally implied potential changes in the sediment loads entering the dike fields.

In the following we shall investigate direct and indirect consequences on patterns of dike field evolution. The four reaches demonstrated varying trajectories in both sedimentation and terrestrialisation, which facilitated the disentangling of the effects of individual drivers. For this we furthermore used a spatial analysis of patterns within

the reaches. For the drainage basin wide drivers, a short literature review helped us identify potential larger scale breaks.

3.4.1 Changing dike field connectivity over time and its impacts

We found weak to moderate negative linear relationships between contemporary mean relative dike heights above the water level at a discharge of 100m³/s and the changes in water levels between 1902 and 2010 in the four reaches (Figure V–15). The connectivity of the dike fields to the main by-passed channel has thus been influenced in part by the combined effect of by-passing and the evolution of the channel geometry (Figure V–16 and Figure V–17).

The effects of changing water levels (1902 to 2010) on contemporary connectivity (described by relative dike heights, submersion duration and frequency) were not equal in the four reaches. MON showed the smallest effect (slope = –0.30, R^2 = 0.14), PBN almost double (slope = –0.56, R^2 = 0.19), DZM more than double (slope = –0.76, R^2 = 0.53), and PDR three times (slope = –0.92, R^2 = 0.40) as strong an effect on relative dike height, for instance. Submersion frequency showed a positive relationship to water level change at PDR and a negative relationship at MON.

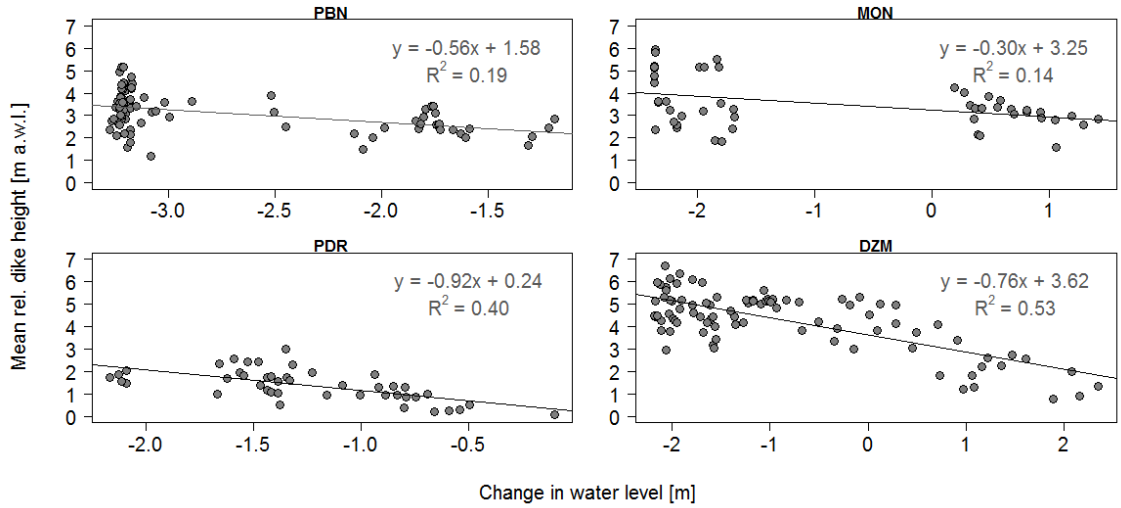

Figure V–15: Impact of changes in water level on relative elevation of dike crests.

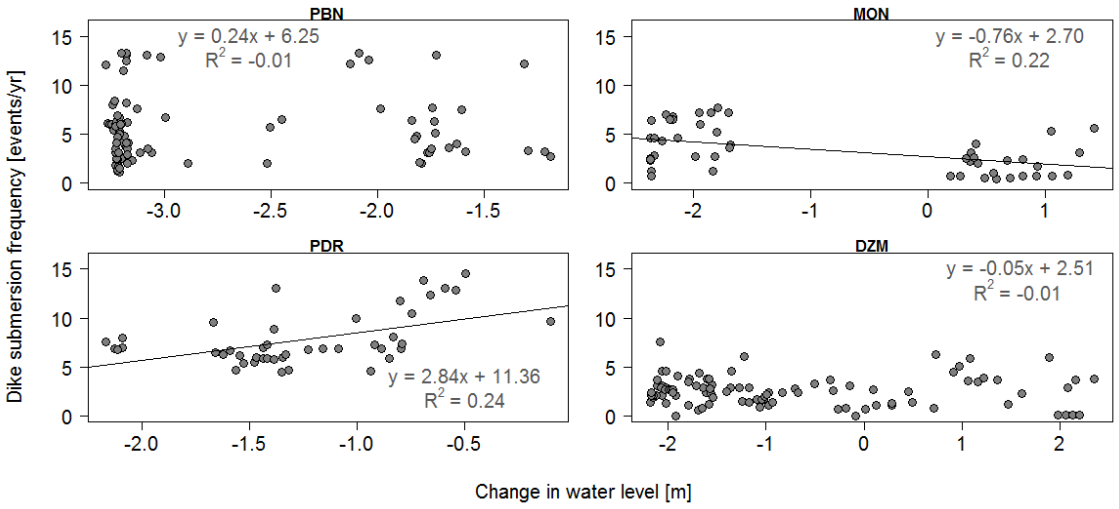

Figure V–16: Impact of changes in water level on dike submersion frequency.

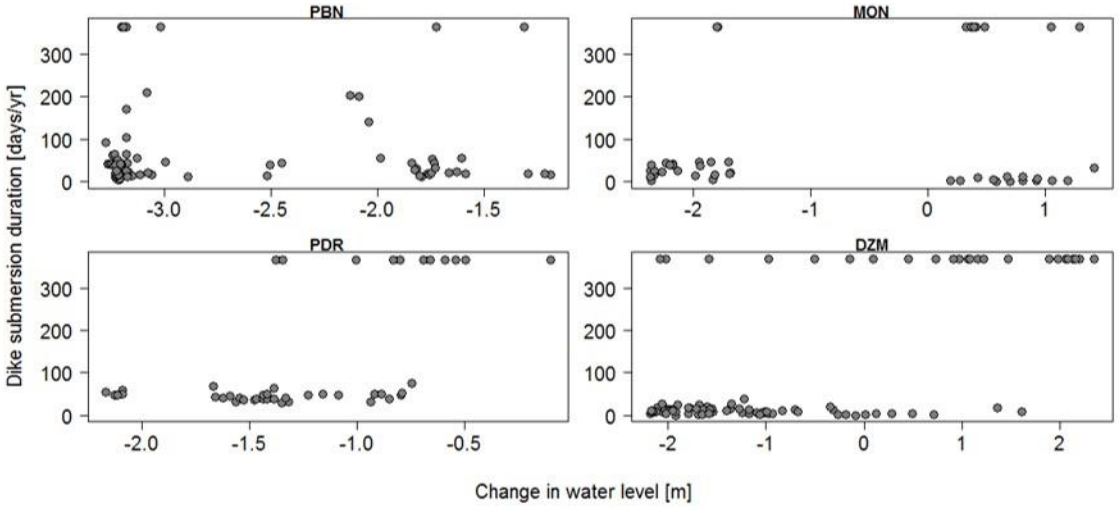

Figure V–17: Impact of changes in water level on dike submersion duration.

Multiple linear regression analysis revealed a certain linear relationship (R^2 = 0.16) between the logit-transformed ratio of terrestrialisation change with respect to available space (T ratio), and a) the change in water levels between 1902 and 2010, and b) the logit-transformed terrestrialisation state in the 1940s (Figure V–18):

$$T\ ratio = \frac{\Delta\ T_{2000s-1940s}}{Available\ space\ in\ 1940s},$$

$$T\ ratio = -0.53 \times \Delta\ Water\ level_{2010-1902} + 0.30\ \times T_{1940s}\ + 2.70$$

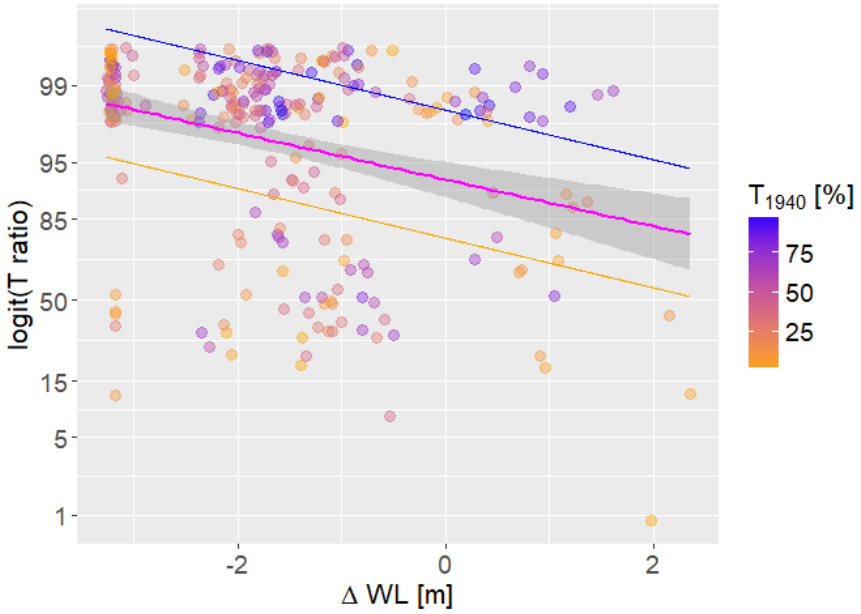

Figure V–18: Multiple regression model.

The models in orange and blue in Figure V–18 represent the two extreme cases where the terrestrialisation status in the 1940s was either 1 % or 99 %. The two parameters show to be two of a number of drivers acting on the system. The individual effects of diversion and changing channel geometry shall be analysed further in the following paragraphs.

The contribution of diversion

Hypothesis 4a: By-passing of the old Rhône reaches and the implied drop in the water level accelerated terrestrialisation in dike fields. Sedimentation rates remained constant or increased over time.

Our hypothesis was that the drop in water levels related to diversion accelerated the terrestrialisation process by rapid dewatering and thus exposure of sediment deposits. Indeed, we saw significant increases in 2-D terrestrialisation rates in the periods when the diversion schemes were put into operation at PDR and DZM (Figure V–12). The changes in the evolutionary trajectories of dike fields which we observed for the four reaches (Figure V–1) pointed in the same direction. The assumption, however, that the reduced frequency of connection between the dike fields and the main by-passed channel would have decreased overbank fine sediment deposition could not be confirmed. Instead, following diversion we found sedimentation rates of the same order of magnitude or higher than prior to diversion.

We plotted overbank fine sedimentation thickness and average annual sedimentation rates against surface age to reveal potential breaks in the trajectories (Figure V–19 and Figure V–20, respectively). Absolute thicknesses in the two upstream reaches showed a break at the time of the diversion, probably simply because of varying time spans over which sediment accumulated. In the two downstream reaches, the time spans prior to diversion and following diversion were relatively equal and we did not see any remarkable difference between the two periods. Normalised average annual sedimentation rates confirmed these assumptions. They even showed weak to moderate negative linear relationships with surface age, pointing out a rather continuous increase in sedimentation rates over time. If we considered that sedimentation had taken place over the entire period since construction of the dikes around 1860 in all sampled locations, sedimentation rates would not have increased with time, but would have remained constant, as is indicated by the error bars.

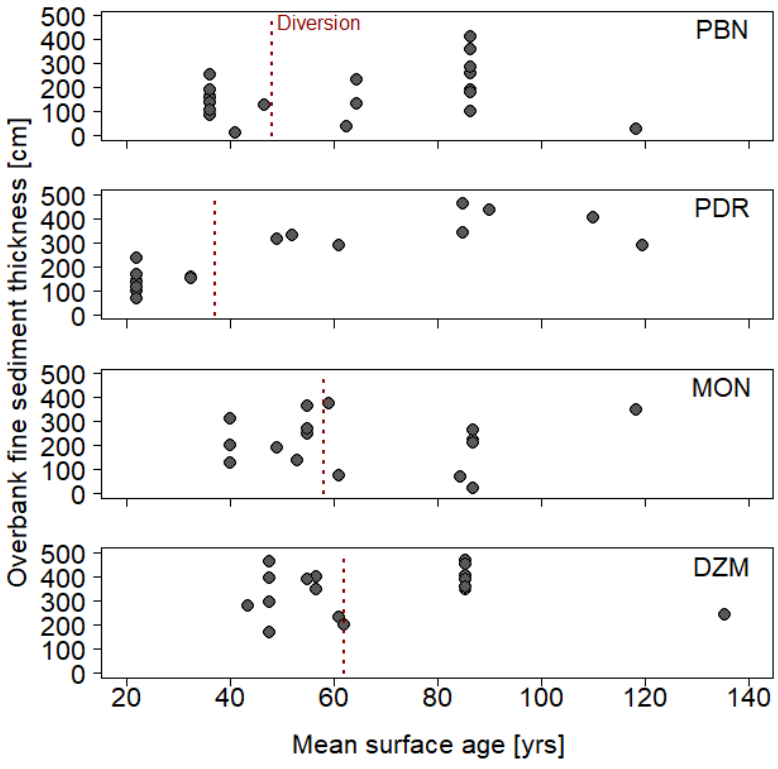

Figure V–19: Chronologic evolution of sedimentation dynamics in a space-for-time substitution approach: overbank fine sediment thickness.

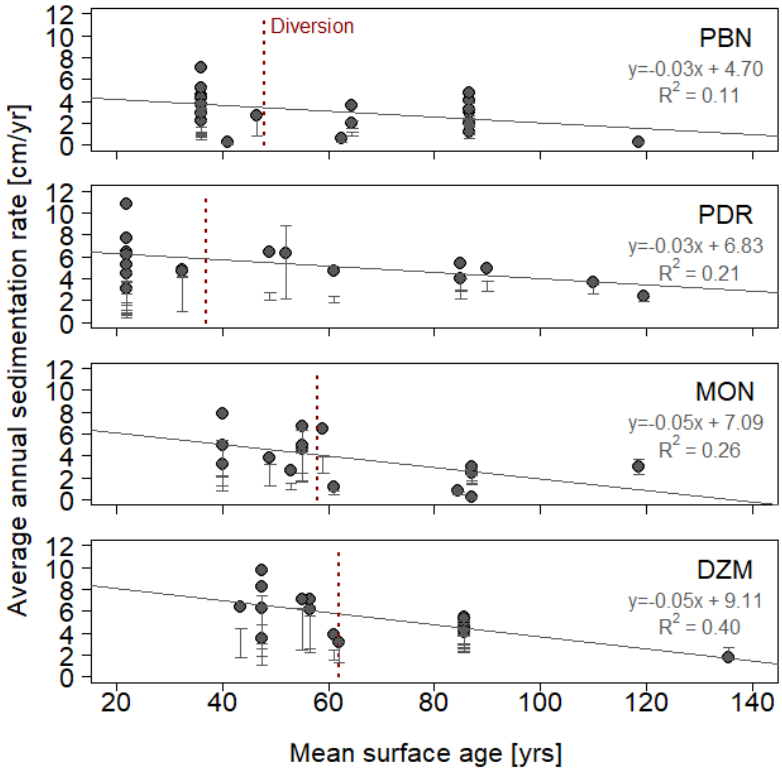

Figure V–20: Chronologic evolution of sedimentation dynamics in a space-for-time substitution approach: sedimentation rates. Error bars represent rates calculated with different approaches.

The contribution of changing channel geometry

Hypothesis 4b: Local incision and aggradation of the main by-passed channels did not show direct links to terrestrialisation. At the reach scale, however, we observed marked differences.

We found no direct link between the local evolution of the main by-passed channel and the terrestrialisation patterns in dike fields nearby (Figure V–21). In this analysis, however, we only considered elevation changes without accounting for initial conditions. Moreover, contrary to our expectations, we found negative linear relationships between net thalweg elevation change and water level change (between 1902 and 2010) for several of the study reaches (Figure V–22). For MON, this negative relationship was relatively strong, with an adjusted R^2 of 0.56, while for PBN and DZM it amounted to 0.14 and 0.10, respectively. Taking the dike fields of all four reaches together, we found a positive, yet extremely weak relationship (adjusted R^2 = 0.03). To investigate these patterns more in detail and to find possible explanations, we analysed the spatial patterns of terrestrialisation and environmental factors in section 3.4.2.

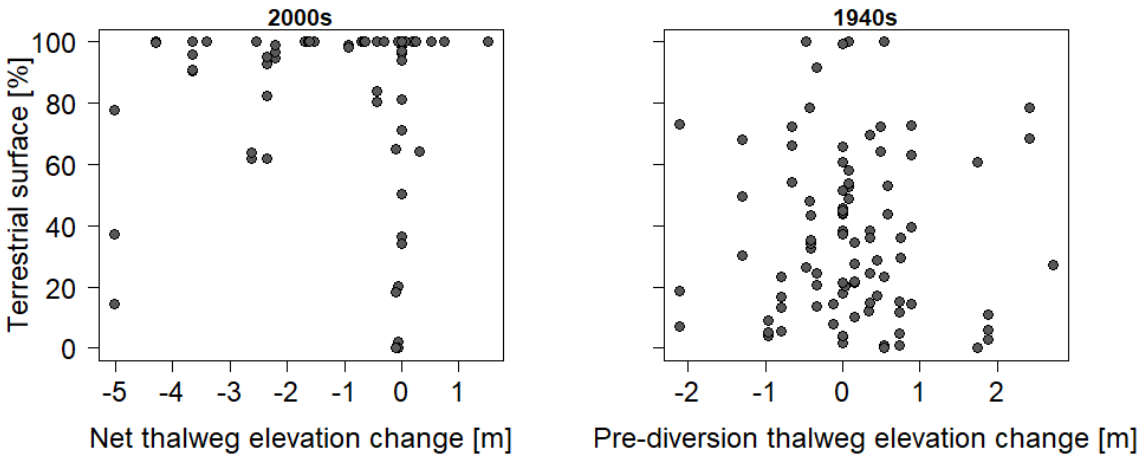

Figure V–21: Relationship between local thalweg elevation change in proximity of dike fields and the respective dike field terrestrialisation status. (left) Net thalweg change versus terrestrialisation status in the 2000s, (right) pre-diversion thalweg change versus terrestrialisation status in the 1940s.

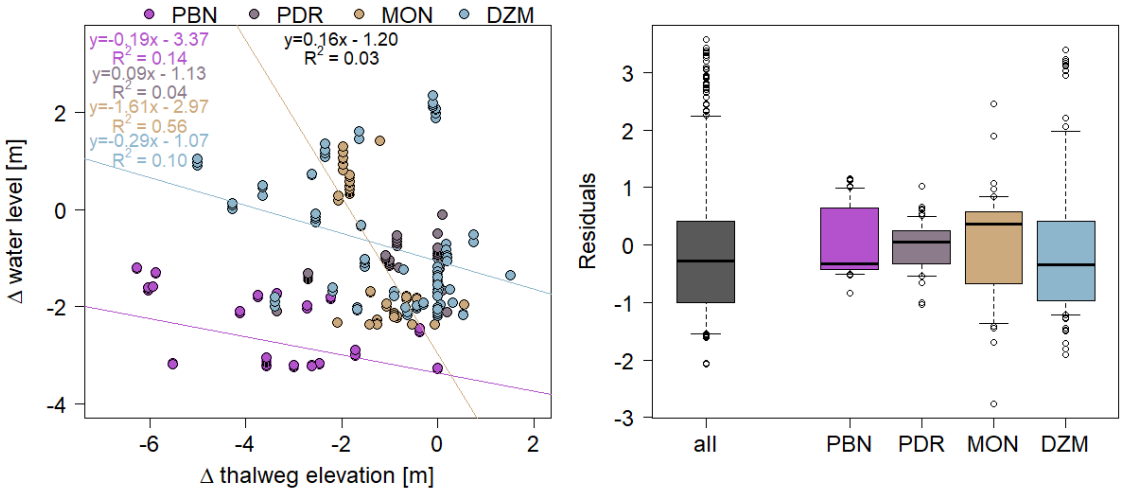

Figure V–22: Relationship between net thalweg elevation change and water level change over the entire study period (in black the overall regression equation including all dike fields) (left). Residuals of the linear regressions for all dike fields together and for each study reach separately (right).

At the reach-scale, patterns of thalweg elevation change yet seem to reflect and partly explain the terrestrialisation patterns summarised in Table V–3. Already in the pre-dam phase, strong incision at PBN led to a disconnection of the dike fields. This explains why they were highly advanced in their terrestrialisation status in the 2000s, while sedimentation rates were lowest compared to the other reaches. Although less marked than at PBN, early incision in MON was probably the reason why pre-dam sedimentation rates were very low in this reach, too. Howeverm following diversion, incision was less marked. As we shall see in the spatial pattern analysis, the locations

where incision was highest in this reach even experienced some aggradation in the post-dam period (section 3.4.2). At PDR, only minor changes in thalweg elevation occurred and at DZM the early aggradation trend, too, maintained the connection to the channel. The patterns in Figure V–22 were strongly masked by the diversion schemes and other local effects on the water levels, as we shall see in section 3.4.2. Comparing Figure V–8 and Figure V–10, we again see that at the reach-scale, thalweg elevation change very likely did play its role in influencing the change in water levels.

The impact of the time span since diversion

Hypothesis 5: The time span since diversion did not necessarily predict the terrestrialisation state

Depret et al. (2017) have shown the impact of the highly modified discharge regime from by-passing on terrestrialisation rates in abandoned channels. From this and from the natural tendency of abandoned channels to terrestrialise after cut-off (e.g. Citterio & Piégay, 2009; Constantine et al., 2010; Depret et al., 2017), we expected the degree of dike field terrestrialisation to reflect the time span since diversion. At equal conditions of connectivity, we expected terrestrialisation to be more advanced in reaches with a long time span since diversion. We had chosen our study reaches according to a gradient of time spans since diversion of DZM > MON > PBN > PDR. Terrestrialisation tendencies did not represent the same patterns (Figure V–23) and thus did not reflect these time spans. Topographic variability varied between PDR and DZM, and thus between the two reaches with the longest and shortest time spans. In contrast, elevations of emerged dike field surfaces showed the same gradient as time spans of DZM > MON > PBN > PDR. Differences between PBN and MON are not statistically significant, although the time span between the two diversions amounts to 10 years.

3.4.2 Within-reach spatial analysis

To aid the interpretation of the relationships between sedimentation / terrestrialisation and potential control factors, we examined their spatial patterns within each reach (Figure V–24, Figure V–25 and Annexe II). The longitudinal patterns of the sedimentation and terrestrialisation status of the dike fields, as well as of potential control factors, were diverse. On a first sight, mainly localised phenomena were evident

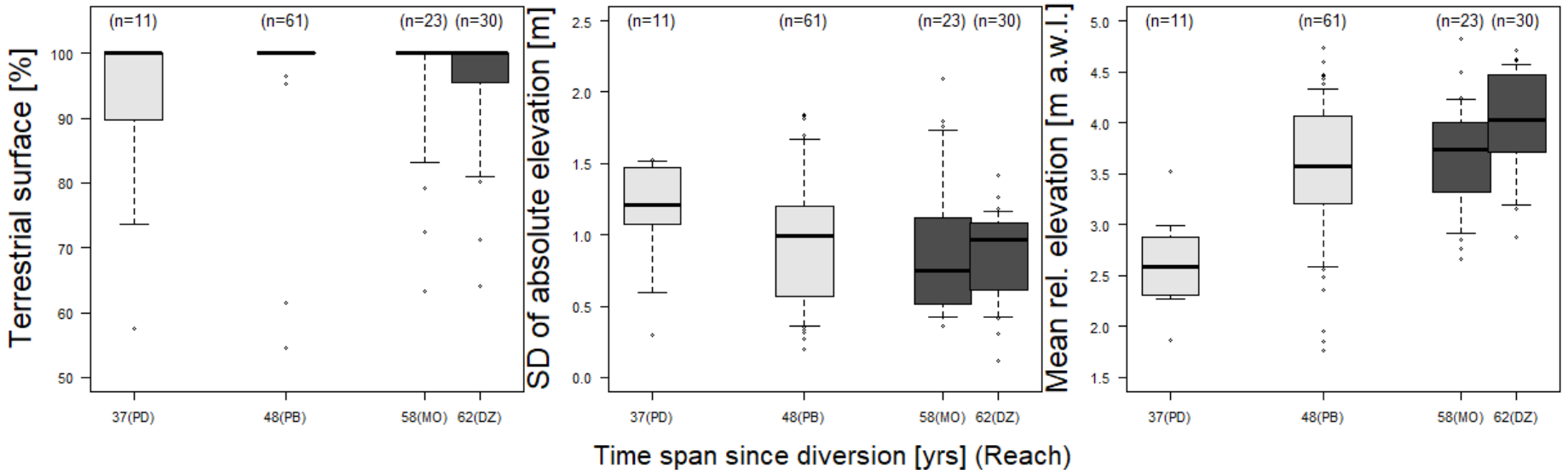

Figure V–23: Comparison of morphological and topographical variables regarding the time span since diversion.

for the four reaches, with an organisation rather at the scale of small sub-reaches. But even within these sub-reaches, we find a large local variability. This explains why we found strong differences in the evolution and contemporary status of the four reaches, but also in the respective roles of the different drivers, as we shall see further on.

The most upstream and most downstream parts of the reaches generally diverged from the global pattern. For instance, in all four reaches, incision was strongest toward the upstream and downstream ends. There is however no direct translation of these patterns in the water levels, due to specific local conditions. First, we noted the typical effect of dams on the water level, producing the strongest drop just downstream, close to the dam, and a more gradual effect further down. At the confluence between the diversion canal and the main by-passed channel, we observed strong backwater effects. They showed as a rise in water levels, especially at MON and DZM, or a gradual reduction in the drop of water level, such as at PBN. At PDR, the Peyraud weir just below river kilometre (RK) 60 likewise artificially changed the water level in its proximity. All these patterns masked the effects of incision or aggradation, at least locally, so that we found, for instance, highly connected aquatic dike fields at the downstream end of DZM, albeit strong incision. At MON, the dike fields situated downstream of the reach, in the backwater affected zone around RK 164, were already highly terrestrial in the 1940s, prior to dam construction and diversion. They remained principally terrestrial also in the 2000s. Potentially, the backwater effect which manifested after diversion, masked the effect from incision in this downstream reach, but did not re-initiate early terrestrialisation conditions, i.e. aquatic surfaces. At PDR, the situation seems more intuitive, as it combined the potentially lowest dikes (Figure IV–6 and Figure IV–20), with the least changes in channel bed elevation (Figure V–10) and highest connectivity until today (Figure IV–21). The diversion scheme was built very late in this reach, too (1977), so that the drop in water levels did not necessarily impede sedimentation from early onwards. Additionally, the Peyraud weir (1979) artificially increased the water levels over some distance of the reach. The Saint-Vallier diversion was put into operation in 1971 and has probably influenced downstream dike fields since then.

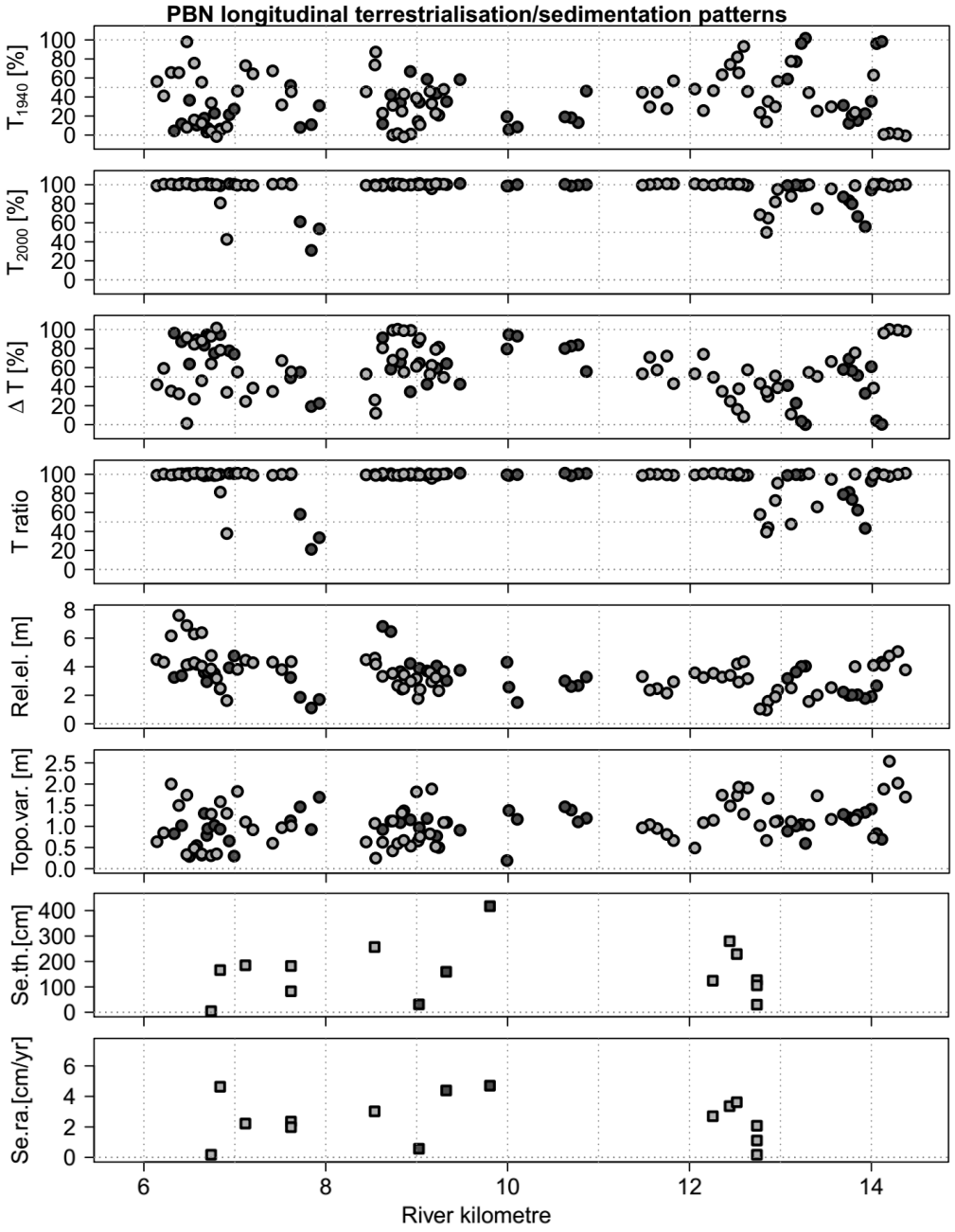

Figure V–24: Longitudinal patterns of terrestrialisation and sedimentation in the reach of PBN ($T_{1940/2000}$: Terrestrial surface in 1940s/2000s, respectively; $\Delta T = T_{2000} - T_{1940}$; T ratio = $\Delta T/(100\% - T_{1940})$; Rel.el. = Relative elevation of emerged surfaces above the water level at a discharge of 100m³/s; Topo.var. = Topographic variability; Se.th.= Overbank fine sediment thickness. Se.ra. = Sedimentation rate). Light grey: right bank, dark grey: left bank.

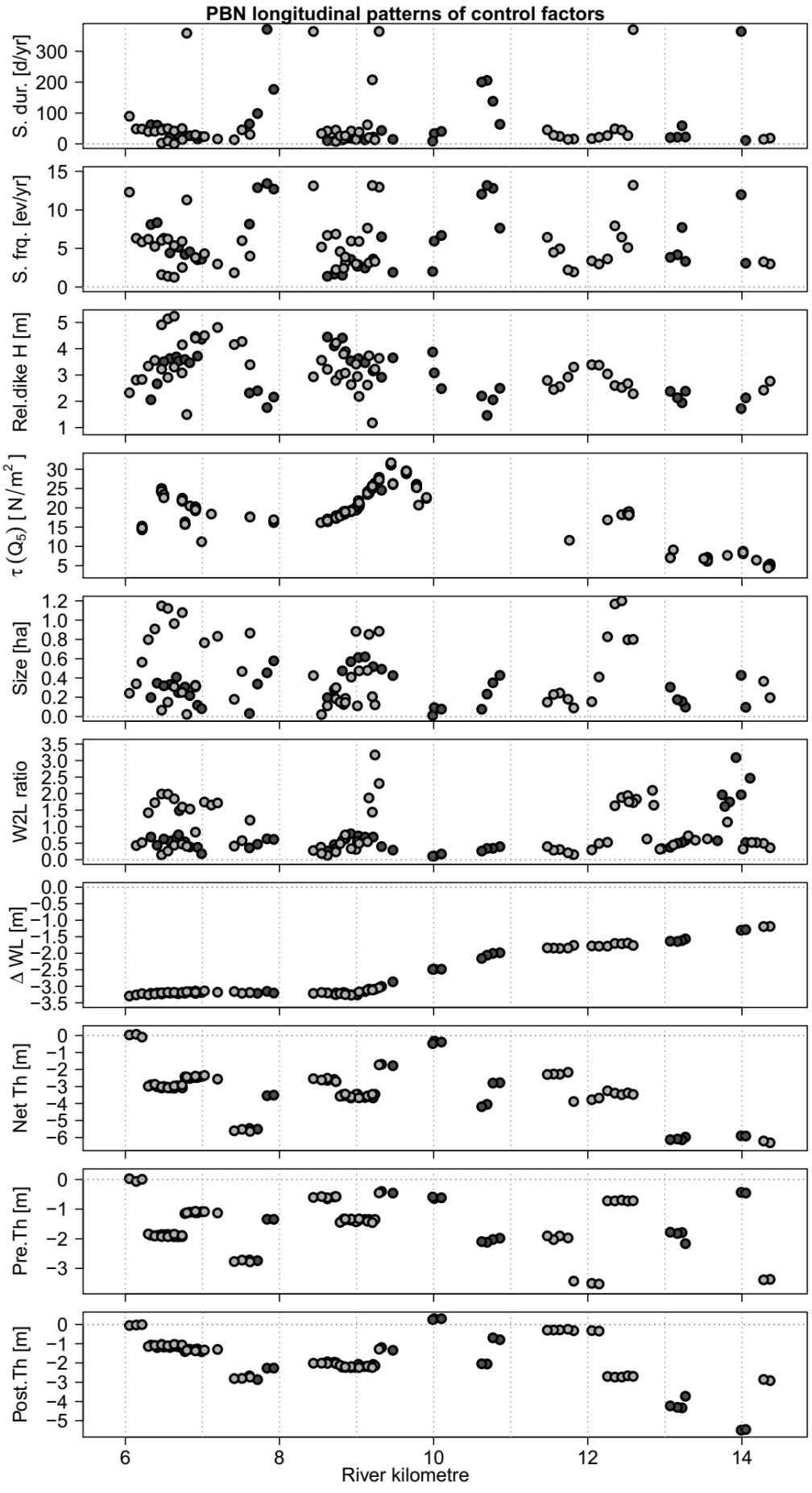
PBN longitudinal patterns of control factors
S. dur. [d/yr]
S. frq. [ev/yr]
Rel.dike H [m]
τ (Q5) [N/m2]
Size [ha]
W2L ratio
Δ WL [m]
Net Th [m]
Pre.Th [m]
Post.Th [m]
River kilometre

Figure V–25 (preceding page): Longitudinal patterns of environmental conditions in the reach of PBN (S.dur. = Submersion duration; S. frq. = Submersion frequency; Rel. dike H = Relative height of longitudinal dike with respect to the water level at a discharge of 100m^3/s; $\tau(Q_5)$ = Modelled shear stress at a discharge of a return period of 5 years. Size = Dike field size; W2L ratio = Dike field width to length ratio; Δ WL = Water $level_{2010}$ – Water $level_{1902}$; Net Th = Net thalweg elevation change; Pre. Th = Thalweg elevation change in pre-dam period; Post. Th = Thalweg elevation change in post-dam period).

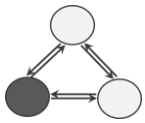

CHAPTER VI DIKE FIELD RIPARIAN FOREST STAND CHARACTERISTICS

Résumé du chapitre VI : caractéristiques de la ripisylve des casiers

Quelques études pilotes existent sur le potentiel écologique des casiers aquatiques, qui ont pu démontrer leur rôle comme annexe fluviales. Ils fonctionnent notamment comme sites de refuge et de nurseries pour des poissons et comme habitat pour des macroinvertébrés. En contrepartie, notre connaissance des casiers terrestres reste limitée, alors que ce sont les boisements qui couvrent aujourd'hui la plus grande surface des casiers. Ce chapitre vise à donner un premier aperçu plus détaillé de la structure et de la composition des ces milieux. Dans un premier temps, nous avons fait une analyse descriptive des milieux. Ensuite, nous avons effectué des analyses comparatives à la fois entre des surfaces qui ont émergé dans les phases pré- et post-dérivation, et entre les casiers et deux sites de références semi-naturels. Ces sites se situent aux deux extrémités d'un gradient de succession. Un de ces site, caractérisé par des îlots pionniers, est situé sur la rivière Drôme. L'autre site abrite des boisements matures de plaine alluviale dans la Réserve Naturelle des Iles de la Platière. Des analyses multivariées nous ont servi pour investiguer des patrons spatiaux plus globaux. Nous avons également caractérisé les conditions physiques qui contrôlent potentiellement ces boisements.

1 Introduction

In previous chapters, we saw that over time the studied dike fields have evolved from aquatic to primarily terrestrial habitats with a dominant forest cover. In the context of globally diminishing riparian zones, the question arises whether such newly evolving, 'artificial wetlands' may support a sustainable riparian forest. Do they provide an ecological potential, in the form of a dynamic riparian habitat? Could they replace some of the habitats that were lost as a result of river channelization and damming? Are environmental conditions favourable for such a development? Beyond this, do they provide any important ecosystem services (carbon sequestration, biomass)? The surface area represented by the dike fields is relatively small compared to the historical

extent of riparian zones. However, their occurrence along vast distances of the river could provide a relatively inter-connected corridor. So far, little research has been conducted focussing on such highly modified, artificial systems and their ecological potential.

In this general context, we pursued the following principal questions in this study: How do forest stands that colonize dike fields vary in their composition and structure, and compare to naturally regenerated riparian forests within the same biome and region? General structural and compositional characteristics of natural systems have already been discussed in chapter I. In this chapter, we first describe basic characteristics of dike field forest stands in terms of composition and structure in relation to physical characteristics and time since terrestrialisation. Secondly, we compare the dike field forests to two reference sites representing successional end points within more naturally-functioning riparian ecosystems within the region: (1) a mature floodplain forest site, situated in the Platière Nature Reserve at Péage de Roussillon (PDR); and (2) young riverine island sites within the Drôme River, a tributary of the Rhône in south-eastern France, which represents an early pioneer development stage.

2 Detailed research questions

The following detailed research questions guided the vegetation analyses and the structure of this chapter:

- Globally, what are the current structural and compositional characteristics of riparian forest stands in the studied dike fields?
  Structure
  - What are the overall diameter, basal area, height, and density characteristics?
  - What are the relative proportions of mature trees versus regeneration (seedlings and saplings) and what are their respective structural characteristics?

  Composition
  - Which species are present in dike field forest stands, at which life history stage?
  - What are the dominant species (pioneer, post-pioneer, and non-native)?
- How do the structural and compositional characteristics compare between by-passed reaches and between pre- and post-dam surfaces?

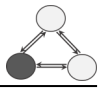

- Are variations in structural/compositional characteristics mainly significant …
  - …along a longitudinal gradient between upstream- and downstream reaches?
  - …along a lateral gradient between pre- and post-dam surfaces?
  - …at the local scale (marked between- and within-reach differences)?
- Are dominant species (pioneer, post-pioneer, and invasive) the same between reaches / management periods or do they vary?
- Do the respective structural characteristics of the dominant species vary between reaches / periods?

- How does the composition and structure of dike field forest stands compare to pioneer forest communities / mature forest communities in the same regional context?
- What are the environmental factors related to the compositional and structural characteristics of the dike field forest communities?
  - Do local effects dominate? i.e. do forest characteristics vary mainly with…
    - … the thickness of overbank fine sediments?
    - … the elevation above the water level, and with elevation-based hydrological metrics (submersion frequency and duration)?
  - Or are there potential latitudinal effects (comparison of upstream vs. downstream reaches) related to climate, which dominate?
- In conclusion, what is the likely future trajectory of dike field forest dynamics, and what are the implications for management? (see chapter VII)

3 Materials and methods

3.1 Data sources: external reference sites

Two data sets of reference sites external to the dike fields were available. An inventory of woody pioneer vegetation units on the Drôme River (hereafter DROM), south-eastern France was provided from S. Dufour from the University of Rennes (Table VI–1). This inventory was carried out in quadrats of 4 m^2 (2 m x 2 m) in which species and stem diameters (measured 5 cm above ground level) had been determined in August 2001 (Dufour et al., 2007). It was located on four pioneer vegetation islands within the active floodplain of the river. The quadrats were regularly distributed along 2-m wide belt transects perpendicular to the central lengthwise axis of each island.

An inventory of mature floodplain vegetation units within the Nature Reserve "Ile de la Platière" (hereafter PLAT), dating from the year 2013, was provided by B. Pont from the Reserve (Table VI–1). They executed the protocol of the National Forest Office (Office National des Forêts, ONF), on which we had likewise largely based our inventory, as described in the following. This common basis facilitated the comparison between sites.

Table VI–1: Overview of available data in the different study sites.

	Dike fields (present work)	PLAT (mature FP)	DROM (pioneer islands)
Stem density per ha	x	x	x
Diameter	x	x	x
Basal area per ha	x	x	x
Height	x	x	---
Species	x	x	x

3.2 Dike field forest inventory survey

In 2014, we surveyed in total, 5,022 stems in the 83 plots located in the forest stands of 61 of the studied dike fields, as presented in chapter III (Figure III–8). We recorded structural and compositional characteristics of all live and standing dead stems in the two nested circular plots of 10-m radius and 20-m radius. Trees were defined as woody stems with a diameter measured at breast height (DBH; measured 1.37 m above average ground surface) of ≥ 7.5 cm. Within a 20-m radius plot, all stems ≥ 30 cm DBH were inventoried and within a 10-m radius plot all stems 7.5 cm ≤ DBH < 30 cm. In the following the individual parameters shall be presented. The regeneration survey was carried out in 1.5-m radius sub-plots. There, we counted and identified to the species level all stems < 7.5 cm DBH. Diameters and heights were recorded in classes:

- Seedlings < 0.5 m
- Small saplings: 0.5 ≤ H < 1.5 m
- Medium saplings: H ≥ 1.5 m and DBH < 2.5 cm
- Tall saplings: 2.5 cm ≤ DBH < 7.5 cm

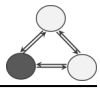

Our analyses were based on the three life history stages trees, saplings (including small, medium, and tall saplings), and seedlings, individually per plot. We calculated the parameters presented in the following both for each life history stage, as well as plot totals.

3.2.1 Structural parameters

The structural characteristics of the dike field forest stands were surveyed to give an overview of their size (diameter and height, as a proxy of age) and density distributions.

Diameter at breast height (DBH) and basal area

We measured stem diameter at breast height (1.37 m above average ground surface, DBH) using a measuring tape or a calliper for larger stems. We then calculated the basal area, i.e. the surface area that is occupied by the cross-section of each stem, using the equation

$$BA\,[cm^2] = \pi \times \left(\frac{DBH\,[cm]}{2}\right)^2, \qquad (Equ.VI-1)$$

with π = 3.14159. The total plot basal area was then derived using the following equation:

$$Total\ plot\ BA\left[\frac{cm^2}{ha}\right] = \sum_{i=1}^{N_{plot}} BA\,[cm^2] \times \frac{10{,}000}{plot\ area\,[m^2]}, \qquad (Equ.VI-2)$$

with plot areas corresponding to 1,257 m^2 for stems within the 20-m radius plots, 314 m^2 for stems within the 10-m radius plots, and 7 m^2 for stems within the 1.5-m radius sub-plots (see section 3), respectively. We also approximated basal areas for each life history stage, based on mean diameter values per class for seedlings and saplings.

Height

The height of all woody stems was visually estimated and recorded in 6 classes: (“< 2”) 0–2 m; (“< 4”) 2–4m; (“< 8”) 4–8m; (“< 15”) 8–15m; (“< 25”) 15–25m; (“> 25”) > 25m. Similarly, we calculated mean height values for each regeneration class.

Stem density

For each plot, we calculated total plot stem density per hectare as a structural parameter and to analyse the level of competition:

$$Total\ plot\ density\ \left[\frac{no.\ of\ stems}{ha}\right] = \sum_{i=1}^{N_{plot}} stem\ count \times \frac{10{,}000}{plot\ area\ [m^2]}, (Equ. VI-3)$$

with plot areas corresponding according to each stem individually, to the respective descriptions provided for equation VI–2. We also calculated plot densities for each life history stage following the same equation, including only the respective size classes.

Multivariate analysis on structural characteristics of trees

To identify potential spatial patterns in the overall structural characteristics of the trees in dike field forest stands we explored the data using a principal component analysis (PCA). This was accomplished using the function *dudi.pca* from the *ade4* package in R. We did not include the regeneration stages in this analysis due to the approximated DBH and height values.

3.2.2 Compositional characteristics

We identified all woody stems to the species level and calculated the following diversity indices for each life history stage, as well as plot totals:

- specific species richness, i.e. the number of species,
- Shannon diversity index $H' = -\sum_{i=1}^{S} p_i\, ln(p_i)$,
- and Simpson diversity index $D = 1 - \sum_{i=1}^{S} p_i^2$.

We used the function *diversity* of the *vegan* package in R to calculate the latter two (Oksanen et al., 2017).

To identify potential gradients in the composition data, we applied a detrended correspondence analysis (DCA) using the function *decorana* from the *vegan* package in R (Hill & Gauch, 1980; Oksanen et al., 2017). This multivariate ordination technique has a similar functioning than a correspondence analysis (CA), avoids however the so called ‘edge’ and ‘arch effects’ (Hill & Gauch, 1980). In this analysis we included all life history stages.

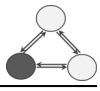

3.3 Comparative analysis between dike field forest stands and external reference sites

For the '*Platière*' mature floodplain data set (PLAT) we used and calculated the same parameters described for the dike field forest stands in section 3.2, as the same data were available. The '*Drôme*' pioneer vegetation unit data (DROM) did not contain any records of height. However, from the stem counts, diameter measurements and species records we likewise calculated plot densities, basal areas and diversity indices, as described in section 3.2. We conducted a DCA (see section 3.2.2), using all three data sets, to explore potential gradients between dike field, pioneer, and mature units.

3.4 Drivers of forest stand characteristics

We used data on frequency and duration of submersion and return frequency of the threshold submersion discharge to describe hydrological connectivity and the disturbance level. For this we applied the "Extract Values to Point" tool in ArcGIS to extract data at the plot centres from the data sets provided by Džubáková et al. (2015) (see chapter III, section 3.4). Moreover, we extracted the relative height above the water level at a discharge of 100 m^3/s from their data sets. Together with the overbank fine sediment thickness data determined at the plot centres, as described in chapter III section 4.2.2, this served as a proxy for the accessibility of resources, mainly water and nutrients.

3.5 Statistical analyses

We performed one-way Analysis of Variance (ANOVA) and Mann-Whitney U tests to test for significant differences in our comparative analyses. The control variables described in section 3.4 as supplementary variables in the PCA using the 'FactoMineR' package in R and fitted them onto the ordination from the DCA using the 'Vegan' tool to determine their influence on the vegetation patterns. In the PCA, this was done by vector fitting, whereas in the DCA we used surface fitting applying the function 'decorana'. We also related the control variables to the PCA sample scores.

Eventually we performed stepwise multiple logistic regressions based on an additive approach to analyse the combined effect of the various drivers on the distribution of the dominant species. Models were fit using the glm function in R. Akaike's Information Criteria (AIC) served us to develop and select the models. To detect multicollinearity we

calculated variance inflation factors (VIF). Literature based thresholds of VIF values between 5 and 10 were generally not exceeded.

4 Results

4.1 Dike field riparian forest stand characteristics

The following subsection presents in short general details of sampling plots, the stratified sampling approach, and forest stand characteristics to provide the reader with the general framework and specifically introduce the dike field forest stands. We will then directly follow up on the spatial analysis and the comparison to the reference sites, which are at the heart of this research.

4.1.1 Short overview of general structural and compositional characteristics

We found both, mature life history stages (trees, ≥ 7.5 cm DBH, 39.9% of all stems) and regeneration stages (saplings, 7.5 cm > DBH ≥ 0.5 cm, 10.5% of all stems, and seedlings, < 0.5 cm DBH, 49.5% of all stems) in the dike fields (Table VI–2). Regeneration stages were absent in some of the plots. Minimum forest stand age, determined based on a chronosequence of aerial images, ranged between 6 and 76 years. Stands were on average older on pre-dam than on post-dam surfaces, except at MON, where the average age was higher on post-dam surfaces. To describe the forest stands, five structural parameters, namely diameter, basal area, height, density, and the Shannon index were investigated. Summary statistics for each are presented in Table VI 3.

Overall, we encountered 34 woody riparian vegetation species in the studied dike fields (trees: 26, saplings: 23, seedlings: 20), as listed in Table VI 3. For our analyses, we regrouped *Populus nigra*, *Populus x canadensis*, and *Populus alba*, *Fraxinus angustifolia* and *Fraxinus excelsior* to *Populus spp*. and *Fraxinus spp*., respectively, to account for introgression. The dominant species (≥ 10% of the total stem count) thus included *Acer negundo* (53.3%) and *Populus spp.* (15%). Together they comprised 68.3% of all stems, while the remaining 36.3% were represented by 29 other species. The composition for each of the three life history stages separately is depicted in Figure VI–1: Trees were dominated to 91.5% by *Populus spp.*, *Acer negundo*, *Salix alba*,

Table VI–2: Set-up of the four study reaches.

	PBN		PDR		MON		DZM		Total
	Pre-dam	Post-dam	Pre-dam	Post-dam	Pre-dam	Post-dam	Pre-dam	Post-dam	
Average surface age [years, mean ±SD]	85 (±15)	40 (±9)	86 (±25)	27 (±10)	80 (±20)	48 (±8)	84 (±21)	52 (±6)	63(±27)
No. sampling plots	11	10	10	10	10	10	11	10	82
trees present in	11	10	10	10	10	10	11	10	82
saplings present in	11	7	8	6	10	9	11	9	71
seedlings present in	9	6	9	8	9	8	9	6	64
Minimum stand age [years, mean ±SD]	66 (±6)	22 (±11)	54 (±23)	22 (±6)	38 (±24)	44 (±3)	63 (±14)	43 (±11)	

Table VI 3: Summary table of forest structural and compositional characteristics (range, mean (±SD) of all sampled plots) for all stems, as well as for the three LHS separately.

	All stems	Life history stage (LHS)		
		Trees (DBH > 7.5 cm)	Saplings (DBH < 7.5 cm)	Seedlings (Height < 1 m)
Density [stems/ha]	55.7 – 1,702,095.0, 51,877.7 (±196,757.4)	55.7 – 1,169. 7, 470.9 (±251.1)	0.0 – 83,467.9, 9,016.6 (±12,874.8)	0 – 1,697,652.0, 42,390.2 (±197,189.2)
DBH [cm]	0.3 – 147.0, 23 (±21.9)	7.5 – 147.0, 32.0 (±20.6)	1 – 5, 2.3 (±1.5)*	0.3 – 0.3, 0.3 (0)*
Basal area [m^2/ha]	7.4 – 63.3, 32.3 (±12.0)	6.7 – 62.5, 27.8 (±11.5)	0.0 – 21.3, 4.4 (±5.2)*	0.0 – 8.3, 0.2 (±1.0)*
Height [m]	0.3 – 40.0, 18.8 (±14.1)	1 – 40, 22.1 (±13.0)	1 – 3, 1.9 (0.7)*	0.3 – 0.3, 0.3 (0)*
Species richness [No. species]	2 – 10, 6 (±2)	2 – 10, 5 (±1)	1 – 6, 3 (±1)	1 – 6, 2 (±1)
Shannon H’	0.2 – 1.8, 1.0 (±0.3)	0.2 – 1.4, 0.8 (±0.3)	0.0 – 1.1, 0.3 (±0.3)	0.0 – 1.5, 0.3 (±0.3)
Simpson D	0.1 – 0.8, 0.5 (±0.2)	0.1 – 0.7, 0.4 (±0.2)	0.0 - 0.6, 0.2 (±0.2)	0.0 – 0.8, 0.2 (±0.2)

*Classification, not measurement

Robinia pseudoacacia, and Fraxinus spp. At the sapling stage, *Cornus sanguinea* (27.2%), *Ligustrum vulgare* (16.8%), *Acer negundo* (12.7%), *Sambucus nigra* (10.6%), and *Fraxinus spp.* (10%) predominated. We found that seedlings consisted to 91.1% of *Acer negundo* and to 7.9% of 18 other species. Table VI–4 presents specific traits of each species. For instance, the species pool covered both pioneer and post-pioneer successional stages and indicated gradients of environmental conditions, here represented by soil moisture, light, and substrate texture indicators. Six species that we encountered are considered non-native to France/Europe, including the dominant *Acer negundo* and *Robinia pseudoacacia*. *Ailanthus altissima* and *Robinia pseudoacacia* are even among the 100 worst invasive species of Europe (DAISIE). None of the encountered species are considered threatened according to the Red list (UICN France et al., 2012).

The distribution of the dike field species and their relative frequencies were relatively similar between pre- and post-dam surfaces, although pre-dam surfaces were species-richer—29 species compared to 21 on post-dam surfaces (Figure VI–1). The tree stage was dominated by both pioneer and post-pioneer species, while regeneration is dominated by the non-native species *Acer negundo* and some understorey species. Although *Acer negundo* is a pioneer species, it is tolerant to both shade and low moisture conditions, which is why it often co-occurs with post-pioneer species (e.g. González-Muñoz et al., 2014). The dike fields seem to be in transition to a post-pioneer stage.

Table VI–4: Presentation and characteristics of species encountered in dike fields.

Species	Species traits						
	Plant life-form (1)	Ecological strategy type (2)	Soil moisture indicator value (3)	Light indicator value (3)	Substrate indicator value (texture) (3)	Origin (2)	Red list status (4)
Acer negundo	meso-phanerophyte	pioneer	7	8	2	introduced (North America)	---
Acer platanoides							---
Ailanthus altissima	macro-phanerophyte	pioneer	5	8	3	introduced (East Asia, China)	---
Celtis occidentalis						introduced (5)	---
Cornus sanguinea	nano- to micro-phanerophyte		5	6	2	Eurasia	---
Corylus avellana	micro-phanerophyte		5	5	3	Eurasia	---
Crataegus monogyna	nano- to meso-phanerophyte		5	7	3	Southern Eurasia	---
Euonymus europaeus	micro-phanerophyte		5	6	2	Eurasia	---
Ficus carica			4	7	3	introduced (West Asia)	---
Fraxinus angustifolia	meso- to macro-phanerophyte	post-pioneer,	7	8	2	Southern Europe	---
Fraxinus excelsior	macro-phanerophyte	post-pioneer,	7	7	2	Europe	---
Gleditsia triacanthos						introduced (North America)	---
Hedera helix	phanerophyte liana		5	5	8	Southern Eurasia	---
Juglans regia	meso- to macro-phanerophyte	post-pioneer	5	8	3	Southern Eurasia	---
Laurus nobilis			5	5	3	Mediterranean	---
Ligustrum vulgare	nano-phanerophyte		4	7	3	Eurasia	---
Morus alba	meso-phanerophyte		5	7	5	introduced (South Asia)	---
Platanus x hispanica	macro-phanerophyte		7	8	2	Europe	---
Populus alba	macro-phanerophyte	pioneer	7	8	1	Southern Europe	---

Populus nigra	macro-phanerophyte		7	8	2	Southern Europe	---
Populus x canadensis	meso- to macro-phanerophyte		7	8	2	Europe	---
Prunus avium	meso- to macro-phanerophyte	post-pioneer	5	7	3	Southern Eurasia	Least concern
Prunus domestica			5	7	3	temperate Eurasia	---
Quercus ilex	micro- to meso-phanerophyte	post-pioneer	5	7	3	Mediterranean	---
Quercus pubescens	meso- to macro-phanerophyte	post-pioneer,	4	8	2	Southern Europe	---
Quercus robur	macro-phanerophyte	post-pioneer,	5	7	3	Europe	---
Rhamnus cathartica	nano- to micro-phanerophyte		5	6	2	Eurasia	---
Robinia pseudoacacia	meso- to macro-phanerophyte	pioneer	5	8	3	introduced (North America)	---
Salix alba	meso- to macro-phanerophyte	pioneer	8	8	6	Eurasia	---
Sambucus nigra	micro- to meso-phanerophyte		5	5	3	Southern Eurasia	---
Tilia platyphyllos	macro-phanerophyte	post-pioneer,	5	8	3	Europe	---
Ulmus laevis	macro-phanerophyte	post-pioneer,	7	7	2	Europe	---
Ulmus minor	macro-phanerophyte	post-pioneer,	5	7	2	Europe	---

(1) Rameau et al., 1989, modified after Raunkiær, 1934; Julve, 1998ff
(2) Rameau et al., 1989, Julve, 1998ff
(3) Julve, 1998ff, modified after Ellenberg et al., 1992
(4) UICN France, FCBN & MNHN, 2012
(5) DAISIE European Invasive Alien Species Gateway (http://www.europe-alines.org), last accessed 10/04/2018.

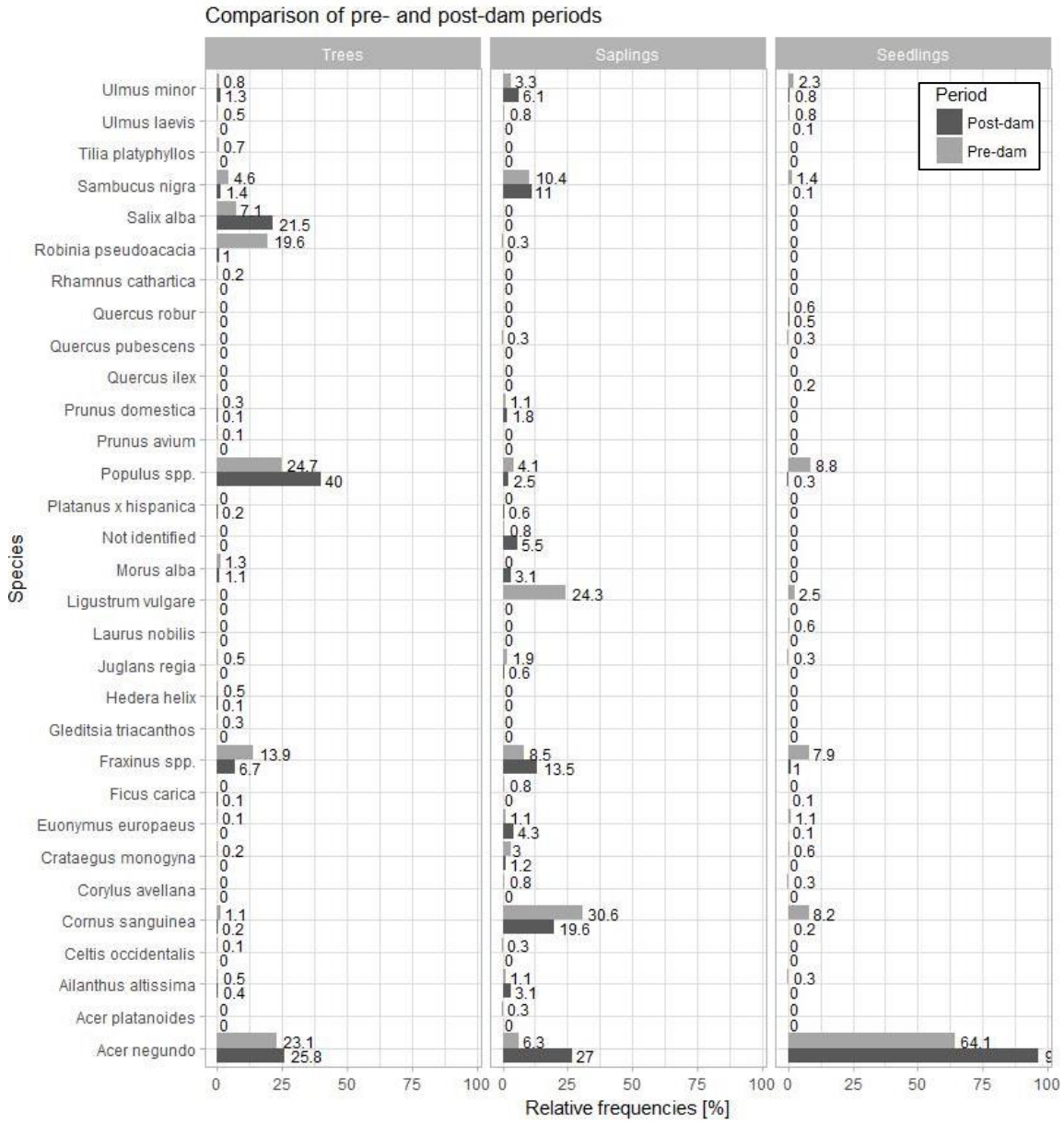

Figure VI–1: Bar plots comparing relative frequencies of species at the three life history stages between pre- and post-dam surfaces. Relative frequency of Acer negundo seedlings on post-dam surfaces was 96.7%.

4.1.2 Comparing spatial and chronological patterns of structural characteristics

After having identified some of the general characteristics of dike field forest stands, our focus was on their spatial and chronological patterns. This analysis not only provided information on the basic functioning of dike fields as habitats, but its comparative character may serve as an indicator for explanatory analyses. Beyond the comparison between the various dike fields themselves, we additionally considered external sites functioning as references to better classify the status of the rather

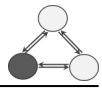

'artificial' dike field forest units. The reference site PLAT corresponds to a rather mature floodplain unit, while DROM represents relatively young pioneer island units (Table VI–5). We note, that at PLAT, seedlings had not been surveyed.

At PLAT, 24 species were counted, among which both post-pioneers and some pioneers. *Fraxinus spp.*, *Crataegus monogyna*, and *Populus nigra* were the most frequent trees, at the sapling stage understorey species dominated. *Salix spp.* were not found among live trees anymore and neither *Populus* nor *Salix* occurred at the sapling stage, thus their regeneration is probably very low to non-existent. Non-native *Acer negundo* and *Robinia pseudoacacia* were present but not among the dominant species, neither at the tree nor at the sapling stage. At DROM, vegetation stands were dominated by pioneer Salicaceae species (*Populus* and *Salix*) in all three life history stages. Among the 11 species identified, two non-native, namely *Robinia pseudoacacia* and *Buddleja davidii*, were present. However, they occurred principally at the tree stage.

Table VI–5: Plot characteristics, as well as structural and compositional forest stand characteristics (range, mean (±SD) at the two reference sites.

	Mature floodplain (FP) PLAT	Pioneer islands DROM
Total no. of plots	46	103
in which trees are present	42	17
in which saplings are present	46	103
in which seedlings are present	---	43
Total stem count	3,049	2,240
of which trees	952	23
of which saplings	2,097	2,069
of which seedlings	---	148
Density [stems/ha]	7,082.2 – 150,905.6, 65,131.44 (±24,608.4)	2,500 – 262,500, 54,368.9 (±45,028.2)
only trees	0.0 – 1,432.4, 560.7 (±326.8)	0.0 – 10,000.0, 558.3 (±1,523.2)
only saplings	7,082.2 – 150,141.6, 64,570.8 (±24,521.6)	2,500.0 – 217,500.0, 50,218.5 (±40,522.2)
only seedlings	---	0.0 – 45,000.0, 3,592.2 (±7,222.6)
DBH [cm]	1.0 – 107.0, 13.1 (±15.8)	0.1 – 16.0, 1.8 (±1.5)
only trees	8.0 – 107.0, 20.7 (±16.7)	7.5 – 16.0, 9.8 (±2.0)
only saplings	1.0 – 5.0	0.5 – 7.4,

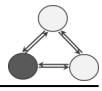

		2.0 (±1.4)		1.8 (±1.3)
only seedlings		---		0.1 – 0.4, 0.3 (±0.1)
Basal area [m^2/ha]	3.6 –64.4, 34.1 (±12.4)		0.1 – 117.2, 23.7 (±19.6)	
only trees		0.0 – 40.7, 16.0 (±9.6)		0.0 – 94.2, 4.4 (±12.8)
only saplings		3.6 – 36.8, 18.1 (±8.2)		0.1 – 62.2, 19.3 (±13.6)
only seedlings		---		0.0 – 0.5, 0.0 (±0.1)
Height [m]	1 – 41, 10 (±10)		---	
only trees		1 – 41, 16 (±10)		---
only saplings		1 – 3, 2 (±1)		---
only seedlings		---		---
Species richness [No. species]	2 – 13, 8 (±2)		1 – 7, 3 (±1)	
only trees		1 – 9, 6 (±2)		1 – 3, 1 (±0)
only saplings		2 – 10, 6 (±2)		1 – 8, 3 (±2)
only seedlings		---		1 – 5, 2 (±1)
Shannon H’	0.0 – 1.4, 1.1 (±0.2)		0.0 – 0.5, 0.1 (±0.1)	
only trees		0.0 – 0.9, 0.5 (±0.2)		0.0 – 0.1, 0.0 (±0.0)
only saplings		0.0 – 1.2, 0.8 (±0.2)		0.0 – 0.5, 0.1 (±0.1)
only seedlings		---		0.0 – 0.1, 0.0 (±0.0)
Simpson D	0.0 – 0.7, 0.5 (±0.1)		0.0 – 0.3, 0.1 (±0.1)	
only trees		0.0 – 0.4, 0.2 (±0.1)		0.0 – 0.0, 0.0 (±0.0)
only saplings		0.0 – 0.6, 0.4 (±0.1)		0.0 – 0.3, 0.1 (±0.1)
only seedlings		---		0.0 – 0.1, 0.0 (±0.0)

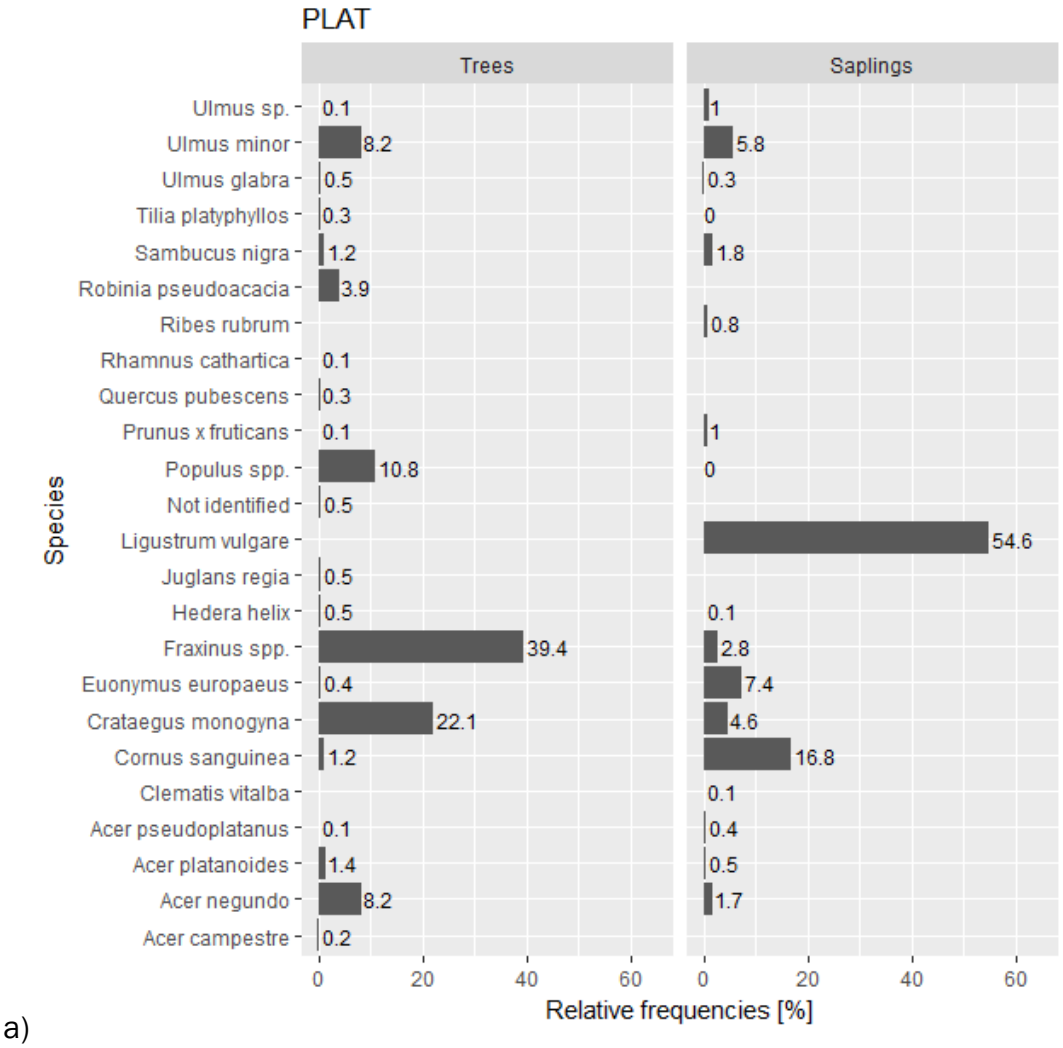

a)

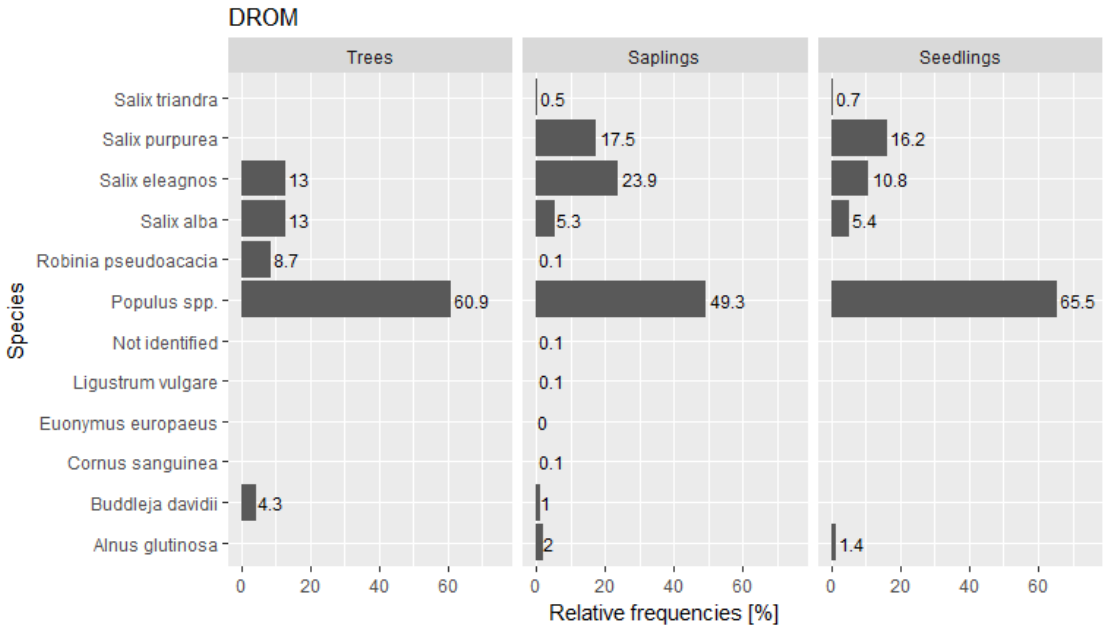

b)

Figure VI–2: Bar plots comparing relative frequencies of species at the three life history stages between a) PLAT (seedlings have not been surveyed at this detail) and b) DROM.

Stem frequency and density

While we observe the typical right-skewed distributions for the three dike field and reference sites (Figure VI–3a), we notice two particularities in the dike fields: they showed the largest DBH values, as well as two distinct peaks for the tree stage at approximately 7.5–15 cm and 30–35 cm DBH (Figure VI–3b). At PLAT and DROM, small tree diameters were the most frequent.

The total density of woody plants in the surveyed plots, including all life history stages, ranged from 55.7 to 1,702,095.0 stems/ha (median = 14,393.7 stems/ha, IQR = 22,483.69 stems/ha, Figure VI–4a). No significant differences were detected between or within reaches (Table A–III–1), however the inter-quartile range and thus the variability of the total density differed: at PBN we found a comparatively diverse pattern (pre- dam: median = 14,433.5 stems/ha; IQR = 27,479.4 stems/ha; post-dam:

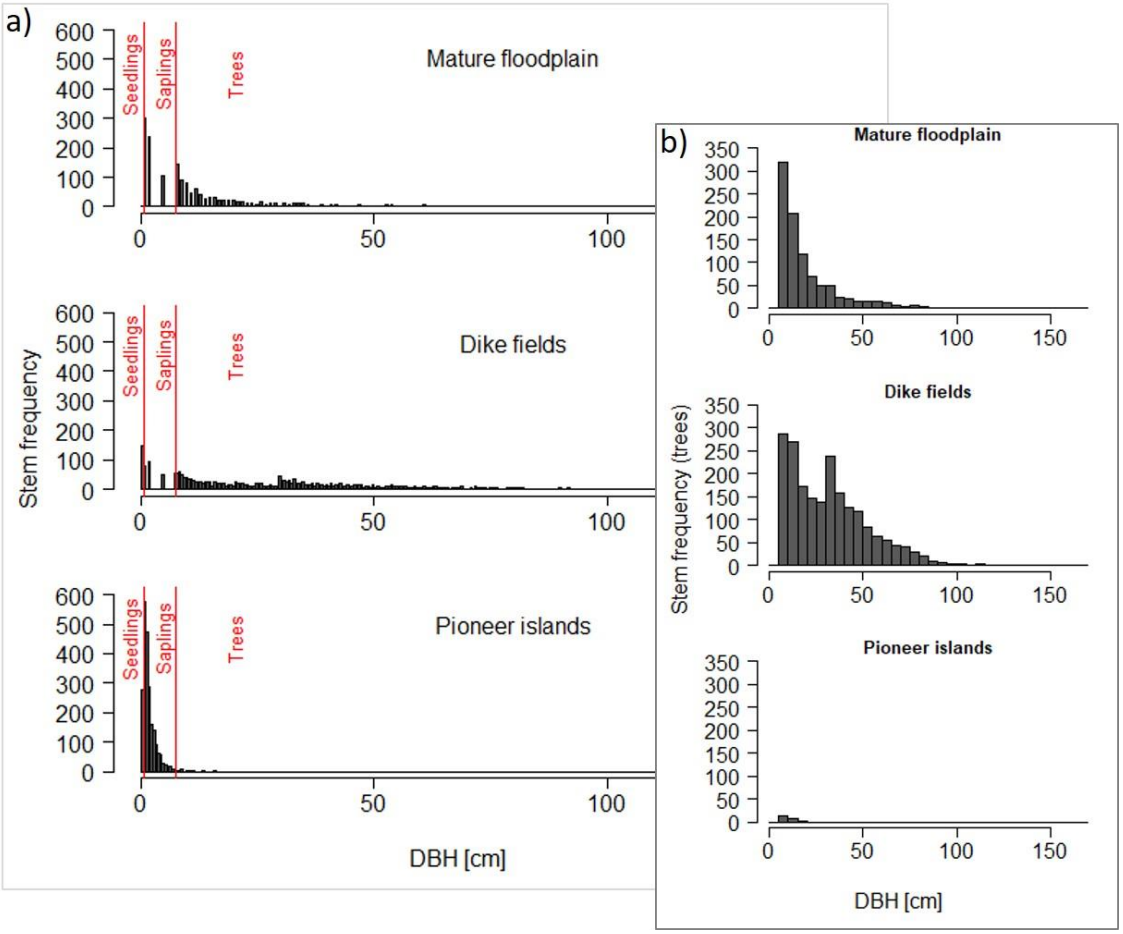

Figure VI–3: Stem frequencies of the different life history stages a) all life history stages b) zoom to trees only.

median = 9,164.5 stems/ha, IQR = 22,730.8 stems/ha), while conditions were more homogeneous at MON (pre-dam: median = 18,093.6 stems/ha, IQR = 10,962.5 stems/ha; post-dam: median = 23,609.3 stems/ha, IQR = 19,218.0 stems/ha). Both reference sites demonstrated significantly higher total densities and higher variability compared to the dike fields, which is not evident from Figure VI–4a, due to the logarithmic scale of the y-axis (PLAT: median = 66,182.4 stems/ha, IQR = 30,841.2 stems/ha; DROM: median = 45,000.0 stems/ha, IQR = 42,500.0 stems/ha). Only PBN-C showed some similarity with DROM. Total PLAT densities were furthermore significantly higher than total DROM densities.

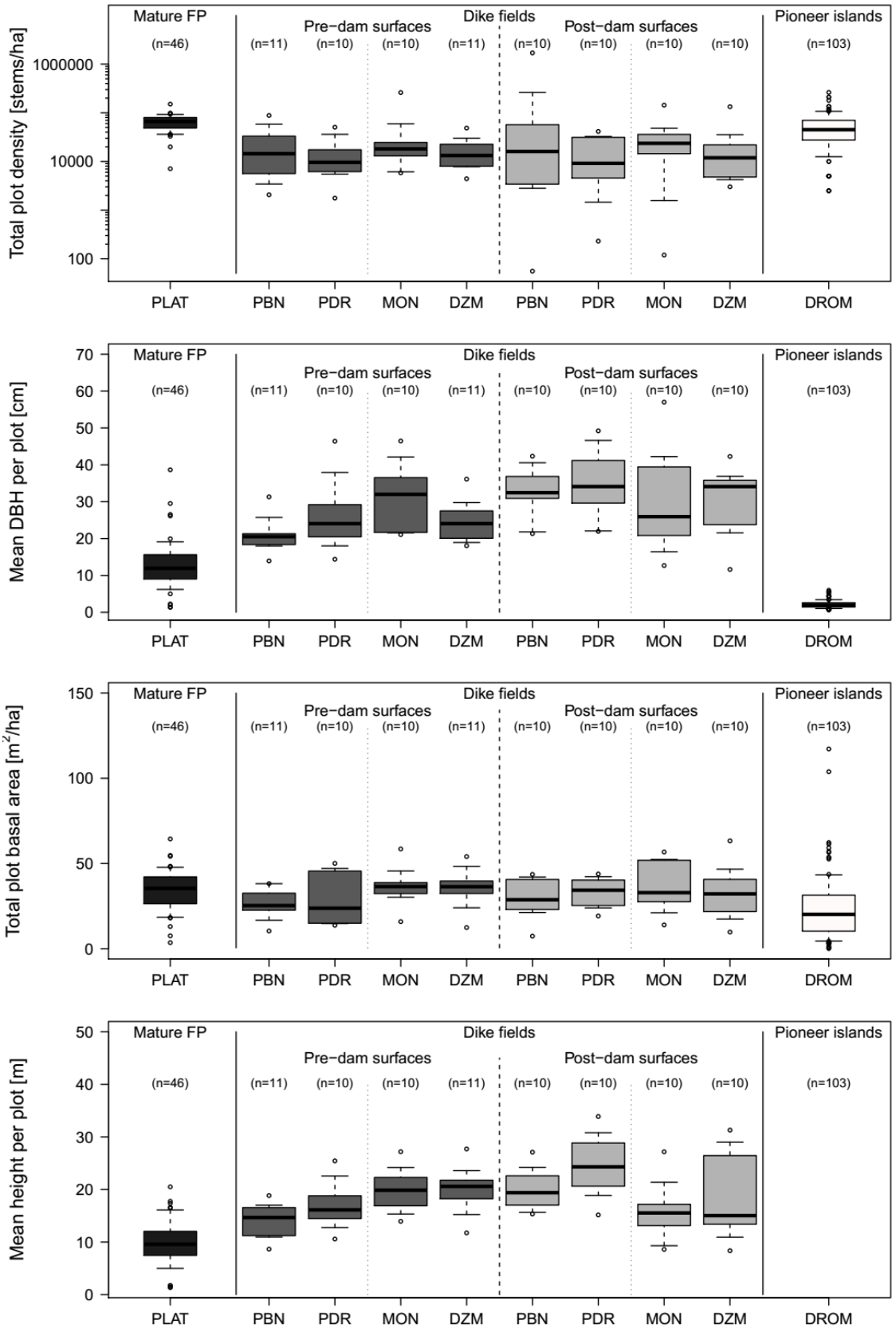

Figure VI–4: Comparison of structural forest stand characteristics between dike fields and between dike fields and reference sites. From top to bottom: total plot stem density, mean diameter at breast height (DBH), total plot basal area, mean plant height.

Tree density sub-totals in dike fields ranged from 55.7 to 1,169.7 stems/ha in the various plots (median = 417.7 stems/ha, IQR = 306.4 stems/ha, Figure A–III–1). Differences between, as well as within reaches were not significant, although their variability varied slightly (Table A–III–2; PBN-B: median = 477.4 stems/ha, IQR = 238.7 stems/ha; PBN-C: median = 294.3 stems/ha, IQR = 185.0 stems/ha; PDR-B: median = 441.6 stems/ha, IQR = 141.2 stems/ha; PDR-C: median = 326.2 stems/ha, IQR = 300.3 stems/ha; MON-B: median = 409.7 stems/ha, IQR = 276.5 stems/ha; MON-C: median = 477.4 stems/ha, IQR = 336.2 stems/ha; DZM-B: median = 692.2 stems/ha, IQR = 501.3 stems/ha; DZM-C: median = 481.3 stems/ha, IQR = 252.6 stems/ha). The comparison with the reference sites revealed that tree density sub-totals in dike fields differed significantly from DROM tree densities. Very few trees were present in DROM plots, with only a few exceptions (median = 0 stems/ha, IQR = 0 stems/ha), which is not completely evident from Figure A–III–1, due to the logarithmic scale of the y-axis. Contrarily, the distributions of tree density sub-totals in dike fields proved to be similar to PLAT (median = 533.2 stems/ha, IQR = 391.9 stems/ha). As an exception, PBN-C was different from both reference sites.

Sapling and seedling sub-totals of densities ranged from 0.0 to 83,467.9 stems/ha (median = 4,244.13 stems/ha, IQR = 9,903.0 stems/ha), and from 0.0 to 1,697,652.0 stems/ha (median = 5658.8 stems/ha, IQR = 197,189.2 stems/ha) in the dike fields, respectively (Figure A–III–1). Sapling densities were significantly higher on pre-dam surfaces (median = 7073.6 stems/ha, IQR = 8488.3 stems/ha) than on post-dam surfaces (Mann-Whitney U test, W = 1,164, $p < .01$), all reaches considered together. In contrast, seedling densities showed no such difference (Mann-Whitney U test, W = 712.5, $p = .24$), which evokes the question of whether recruitment conditions were less favourable on post-dam surfaces than on pre-dam surfaces. Significant pairwise differences in the density distributions of saplings were due to relatively low central tendencies at PDR-C (median = 1,414.7 stems/ha, IQR = 2,475.7 stems/ha) and a relatively low variability at DZM-B (median = 8,488.3 stems/ha, IQR = 9,195.6 stems/ha) (Table A–III–3). Regarding seedlings, merely the distribution of MON-B densities differed significantly from PBN-B (median = 4,244.1 stems/ha, IQR = 3,536.8 stems/ha) and DZM-B (median = 2,829.4 stems/ha, IQR = 1,414.7 stems/ha), due to a distribution characterised by high central tendencies and high compactness (median = 9,195.6 stems/ha, IQR = 11,671.4 stems/ha) (Table A–III–4). In the dike fields, sapling densities were consistently significantly lower than in the

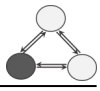

two reference sites (PLAT: median = 65,155.8 stems/ha, IQR = 30,453.3 stems/ha; DROM: median = 45,000 stems/ha, IQR = 37,500 stems/ha), which were themselves significantly different from each other. Unexpectedly, seedling densities were significantly higher in dike fields than on pioneer islands (DROM: median = 0 stems/ha; IQR = 2,500 stems/ha). For MON-B and DZM-C the difference was not statistically significant, however they strongly showed the same tendencies.

Diameter at breast height (DBH)

Mean plot diameters at breast height (DBH) showed significant differences within and between some study reaches (Figure VI–4b, Table A–III–5). Mean plot DBH was lower on pre-dam surfaces compared to post-dam surfaces for PBN (pre-dam: median = 20.5 cm, IQR = 2.9 cm; post-dam: median = 32.4 cm, IQR = 4.8 cm), PDR (pre-dam: median = 24.0 cm, IQR = 7.5 cm; post-dam: median = 34.1 cm, IQR = 10.1 cm), and DZM (pre-dam: median = 24.1 cm, IQR = 7.4 cm; post-dam: median = 34.1 cm, IQR = 10.2 cm). At MON an inverse tendency showed (pre-dam: median = 32.0 cm, IQR = 14.1 cm; post-dam: median = 25.9 cm, IQR = 15.9 cm). These differences between pre- and post-dam periods were significant for the two upstream reaches. The variability of mean plot DBH was comparatively low at PBN and comparatively high at MON (see IQRs above). Finally, mean plot DBH were significantly higher in dike fields (median = 27.0 cm, IQR = 14.4 cm) than in the reference sites (Mann-Whitney U test, $W = 445$, $p < 0.0001$). This is unexpected with regards to the mature floodplain sites, especially since no seedlings had been included in the survey at these sites (PLAT, median = 11.9 cm, IQR = 6.2 cm). Pioneer islands (DROM) showed the lowest mean plot DBH and the lowest variability (median = 2.0 cm, IQR = 1.2 cm), as expected.

These patterns were driven by the trees in the study plots, which show approximately the same configuration in terms of mean plot DBH (Figure A–III–2, Table A–III–6): we found significant differences between pre- and post-dam surfaces (Mann-Whitney U test, $W = 496.5$, $p < .01$) and between some of the reaches. The same pattern of higher post-dam mean DBH compared to pre-dam mean DBH at PBN (pre-dam: median = 20.3 cm, IQR = 3.2 cm; post-dam: median = 32.3 cm, IQR = 4.8 cm), PDR (pre-dam: median = 23.7 cm, IQR = 7.8 cm; post-dam: median = 34.1 cm, IQR = 10.1 cm), and DZM (pre-dam: median = 23.8 cm, IQR = 7.3 cm; post-dam: median = 34.0 cm, IQR = 10.2 cm) versus the inverse trend at MON (pre-dam: median = 31.8 cm, IQR = 14.1 cm; post-dam: median = 25.7 cm, IQR = 15.8 cm) stood out. Likewise, dike fields showed older

trees (median = 26.7 cm, IQR = 14.2 cm) than both PLAT (median = 11.1 cm, IQR = 6.2 cm) and DROM (median = 0.0 cm, IQR = 0.0 cm) plots. Saplings seemed to show the opposite trend, being smaller in dike fields than at reference sites (Figure A–III–2). However, these values do not reflect detailed field measures but size classes, except for the pioneer island plots at the Drôme River. The same is the case for seedlings, which correspond to one single size class.

Basal area

In terms of total plot basal area, dike fields showed a high similarity both within (pre-dam versus post-dam surfaces: Mann-Whitney U test, W = 822, p-value = .87) and between reaches (Kruskal-Wallis test, chi-squared = 5.5254, df = 3, p = .14), as well as with mature floodplain plots at PLAT (Mann-Whitney U test, W = 2,082, p = .33) (Figure VI–4c, Table A–III–7). Yet, pre-dam surfaces at PBN (median = 25.3 m^2/ha, IQR = 10.0 m^2/ha) proved to be significantly different from both downstream pre-dam surfaces (MON: median = 36.5 m^2/ha, IQR = 5.8 m^2/ha; DZM: median = 36.4 m^2/ha, IQR = 7.3 m^2/ha). Pre-dam surfaces at PBN, MON, and DZM presented low variability (see IQR values above) compared to the high heterogeneity at PDR-B (IQR = 30.3 m^2/ha), but also compared to the post-dam surfaces (PBN: IQR = 14.2 m^2/ha, PDR: IQR = 12.8 m^2/ha, MON: IQR = 21.3 m^2/ha, DZM: 17.2 m^2/ha). PBN-B plots were the only dike field plots which were significantly different from mature floodplain (PLAT) plots (median = 35.4 m^2/ha, IQR = 15.3 m^2/ha). Total DROM basal areas were significantly lower (median = 20.2 m^2/ha, IQR = 21.1 m^2/ha) than most dike fields—except PBN-B, PDR-B (median = 23.8 m^2/ha), and PBN-C (median = 28.7 m^2/ha, IQR = 14.2 m^2/ha)—and also than PLAT plots.

Considering subtotals of tree basal area per plot, the dike field analysis revealed that pre-dam surfaces at PBN (median = 19.1 m^2/ha, IQR = 12.3 m^2/ha) were significantly different from pre-dam surfaces at MON (median = 30.0 m^2/ha, IQR = 6.7 m^2/ha) and post-dam surfaces at PDR (median = 33.8 m^2/ha, IQR = 12.1 m^2/ha) (Figure A–III–3, Table A–III–8). We found larger differences in the variability of basal areas on pre-dam (PBN-B: see above; PDR-B: IQR = 21.8 m^2/ha; MON-B: see above; DZM-B: IQR = 13.1 m^2/ha) than on post-dam surfaces (PBN-C: IQR = 9.2 m^2/ha; PDR-C: see above; MON-C: IQR = 12.3 m^2/ha; DZM-C: IQR = 16.4 m^2/ha). PBN-B and PDR-B tree stands were similar in their basal area distributions to PLAT tree stands (median = 15.5 m^2/ha, IQR = 8.4 m^2/ha), unlike all other dike field stands, which showed significantly higher basal

areas. All tree stands in dike fields showed basal areas which were significantly higher than stands on pioneer islands (DROM: median = 0.0 m^2/ha, IQR = 0.0 m^2/ha). Indeed, in 86 out of 103 pioneer island plots, trees were absent (Table VI–5). We noticed that the variability of tree basal areas in the two reference sites was generally lower than in the dike fields.

Throughout all dike field plots, subtotals of sapling basal area seemed to be much lower than both the mature floodplain plots and the pioneer island plots (Figure A–III–3). Saplings were therefore either younger or less frequent, in 11 (13%) plots they were absent (Table VI–2). The variation in plot subtotal basal areas was lower in dike fields than in the reference sites (DROM: median = 17.2 m^2/ha, IQR = 16.8 m^2/ha). Seedlings were absent from 18 (22%) dike field plots (Table VI–2) and from 60 (58%) pioneer island plots, and they were not measured at PLAT (Table VI–5). The variation in seedling basal area in dike field plots was high.

Height

The analysis of mean plant heights per plot on pre- and post-dam surfaces revealed contrasting upstream versus downstream patterns in dike fields. (Figure VI–4d, Table A–III–9). In the upstream reaches, mean heights were significantly lower on pre-dam than on post-dam surfaces (PBN-B: median = 14.7 m, IQR = 5.4 m; PBN-C: median = 19.4 m, IQR = 5.0 m; PDR-B: median = 16.1, IQR = 3.9; PDR-C: median = 24.3 m, IQR = 8.2 m). We observed the inverse trend in the downstream reaches, although the difference was not significant for DZM, which showed a comparatively high variability on post-dam surfaces and a right-skewed distribution (MON-B: median = 19.9 m, IQR = 5.0 m; MON-C: median = 15.5 m, IQR = 3.8 m; DZM-B: median = 20.6 m, IQR = 3.5 m; DZM-C: median = 15.0 m, IQR = 12.3 m). Significant between-reach differences were dominated by particular stand characteristics on pre-dam surfaces of PBN and post-dam surfaces of MON, i.e. comparatively low mean DBH (Table A–III–9). PDR tended to have comparatively high mean DBH, as well as some plots at DZM. Plants were significantly taller in dike fields than on the mature floodplain (median = 9.6 m, IQR = 4.3 m), even though the latter did not include seedlings in the analysis.

In the separate tree analysis, we found approximately the same patterns already described above for the entire woody assemblage (Figure A–III–4, Table A–III–10), with the following characteristic values for the different sites: PLAT-A: median = 8.9 m, IQR = 4.5 m PBN-B: median = 14.6 m, IQR = 5.2 m; PBN-C: median = 19.2 m, IQR = 5.0 m;

PDR-B: median = 16.0 m, IQR = 3.8 m; PDR-C: median = 24.2 m, IQR = 8.2 m; MON-B: median = 19.6 m, IQR = 5.1 m; MON-C: median = 15.3 m, IQR = 4.0 m; DZM-B: median = 20.4 m, IQR = 3.5 m; DZM-C: median = 15.0 m, IQR = 12.3 m.

4.1.3 Spatial and chronological patterns of species composition

Species diversity

Given the strong linear relationship between Shannon and Simpson indices (Figure VI–5; Spearman's rank correlation rho = 0.98, p < .0001; R^2 = 0.97, $y = 0.50x + 0.00$), further analyses will focus on Shannon H' and exclude Simpson D, as we can assume they follow the same patterns. We note that DROM is relatively distinct from the other sites in terms of species diversity, while PLAT seems to be relatively close to the dike fields.

Species richness was significantly different on pre-dam compared to post-dam dike field surfaces (Mann-Whitney U test, W = 1,192, p < .001). In the pairwise analysis per reach, we saw that it was higher on pre-dam surfaces for all reaches except MON, where we saw an opposite tendency (Figure VI–6; median values: PBN-B: 7, PBN-C: 4, PDR-B: 6, PDR-C: 5, MON-B: 5, MON-C: 5.5, DZM-B: 7, DZM-C: 4.5). The pairwise differences were significant only at PBN and DZM (Table A–III–11). The variability of the distributions was relatively constant, with MON-C and PDR-B showing slightly lower and higher variability, respectively (IQR values: PBN-B: 3, PBN-C: 1.5; PDR-B: 2, PDR-C: 1.5, MON-B: 1.75, MON-C: 1, DZM-B: 2, DZM-C: 1.75). Species richness was significantly lower in dike fields compared to the mature floodplain sites and higher compared to the pioneer islands (Mann-Whitney U tests, PLAT: W = 3,106.5, p < .0001; DROM: W = 852, p < .0001). In the pairwise analysis only PBN-B and DZM-B were not significantly different from PLAT (Table A–III–11).

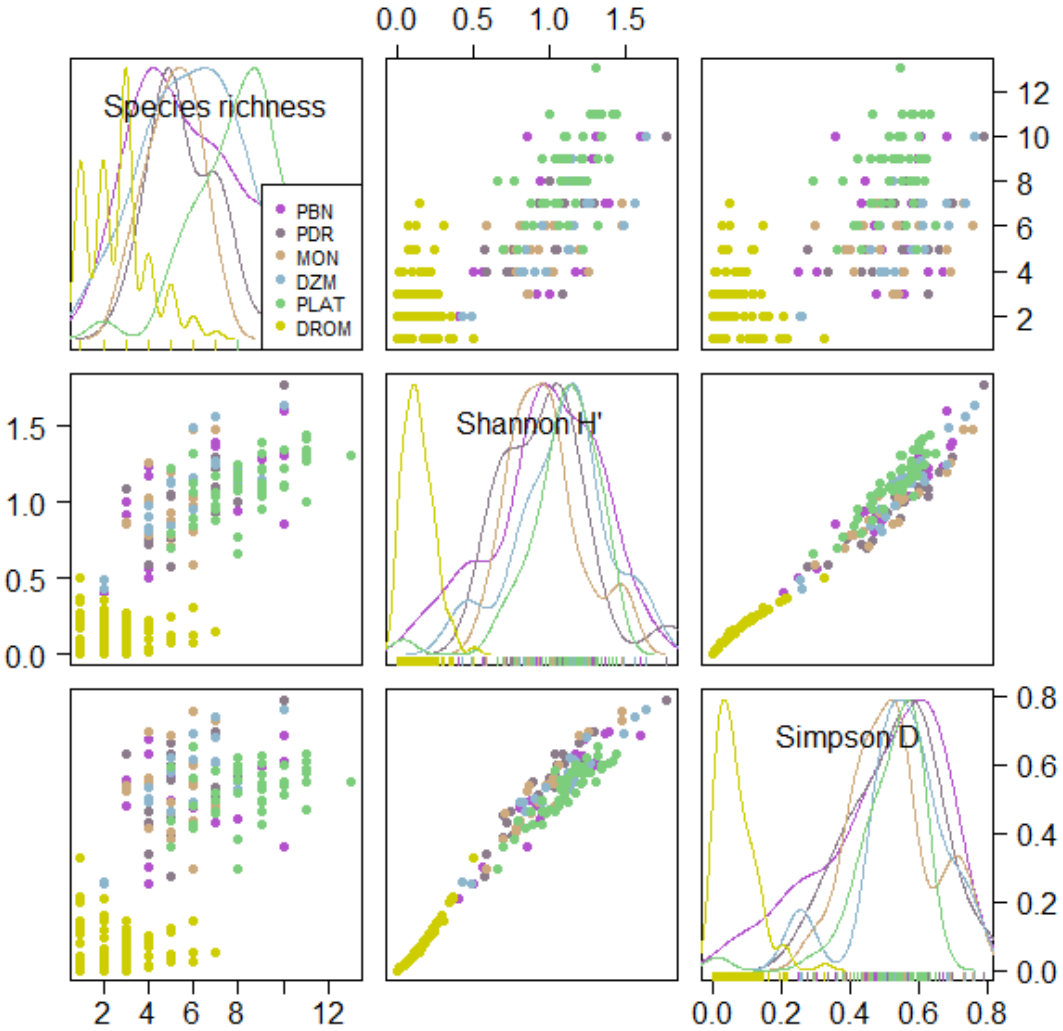

Figure VI–5: Scatter plots showing the relationships of the three variables describing the species richness of the six sites. The diagonal line represents density plots of each variable per site.

In contrast to species richness, Shannon and Simpson indices did not differ between pre- and post-dam surfaces (Mann-Whitney U tests: Shannon H': W = 926, p =.43; Simpson D: W = 837, p = .98, Figure A–III–7). Both indices indicated similarities between dike fields and mature floodplain sites in general (Mann-Whitney U tests: Shannon H': W = 2,376, p < .05; Simpson D: W = 1,824, p =.76) and for all pairwise comparisons (Table A–III–15 and Table A–III–19), and inversely significant differences to the pioneer island sites in general (Mann-Whitney U tests: Shannon H': W = 50, p < .0001; Simpson D: W = 65, p < .0001) and for all pairwise comparisons.

Species diversity was higher for mature trees than for regeneration stages, as highlighted by all three indices. Trees furthermore showed almost no within- or between-reach differences in dike fields, similarities in species richness with mature floodplain sites (Figure A–III–5, Table A–III–12), while Shannon and Simpson indices were different both from mature and pioneer sites (Figure A–III–6 and Figure A–III–8, Table A–III–16, and Table A–III–20). In terms of species richness, saplings differed between pre- and post-dam surfaces (Mann-Whitney U test, W = 1,259.5, p < .0001), they were significantly lower than mature floodplain sites (median = 6.5, IQR = 2), and similar to pioneer islands (median = 3, IQR = 2) (Table A–III–13). Seedlings, in turn, were similar within and between dike fields of the various reaches and higher than DROM sites (median = 1, IQR = 1), except PBN-C (median = 2, IQR = 2) and DZM-C (median = 2, IQR = 1) (Table A–III–14). For Shannon and Simpson indices,

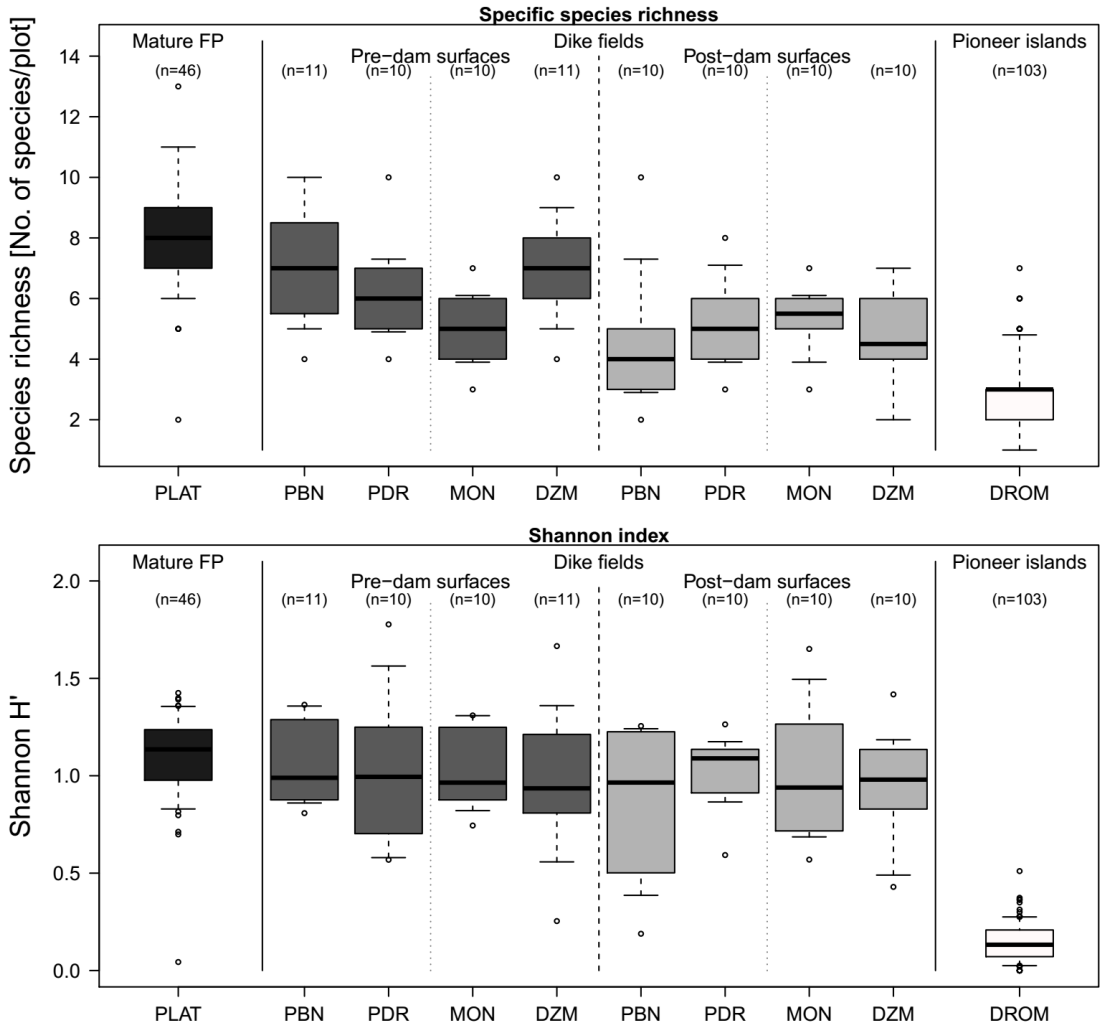

Figure VI–6: Comparison of compositional forest stand characteristics between dike fields and between dike fields and reference sites. Top: species richness, bottom: Shannon diversity index.

we found a few pairwise differences for dike fields for both saplings (Table A–III–17, Table A–III–21) and seedlings (Table A–III–18, Table A–III–22). For saplings, we identified significant higher diversity at mature floodplain sites (Shannon H': median = 0.8, IQR = 0.2; Simpson D: median = 0.4, IQR = 0.1) than in dike fields, while relative to pioneer islands (Shannon H': median = 0.1, IQR = 0.1; Simpson D: median = 0.0, IQR = 0.1), similarities were evidenced for PBN-B (Shannon H': median = 0.3, IQR = 0.7; Simpson D: median = 0.1, IQR = 0.4), PBN-C (Shannon H': median = 0.1, IQR = 0.3; Simpson D: median = 0.1, IQR = 0.1), PDR-C (Shannon H': median = 0.1, IQR = 0.2; Simpson D: median = 0.0, IQR = 0.1), and DZM-C (Shannon H': median = 0.3, IQR = 0.3; Simpson D: median = 0.1, IQR = 0.2). For seedlings both indices were significantly higher in dike fields compared to pioneer island sites (Shannon H': median = 0.0, IQR = 0.0; Simpson D: median = 0.0, IQR = 0.0).

4.1.4 Multivariate gradients of forest stand characteristics

Structure

For a structural classification of dike field forest stands, we analysed the interplay of five of the parameters previously presented. The focus was here on the life history stage 'trees', for which we had measured all of the parameters. The individual parameters showed some linear relationships, for instance as expected between mean tree diameter and mean tree height while residual variations were generally important (Figure VI–7). In the following, the results from the multivariate approach shall be examined, which has the potential to reveal more complex patterns which do not necessarily show in simple bivariate relationships.

The Principal Component Analysis (PCA) revealed an age or growth performance gradient of the trees along factorial axis 1 (F1) and a density gradient along factorial axis 2 (F2) (Figure VI–8a). Together these two axes explained 74.5% of the total inertia. In detail, axis F1 was significantly correlated at an alpha level of $p < .0001$ to mean tree diameter (rho = 0.9), mean tree height (rho = 0.8), and tree basal area (rho = 0.7). Axis F2 was correlated at the same alpha level to tree density (rho = 0.9).

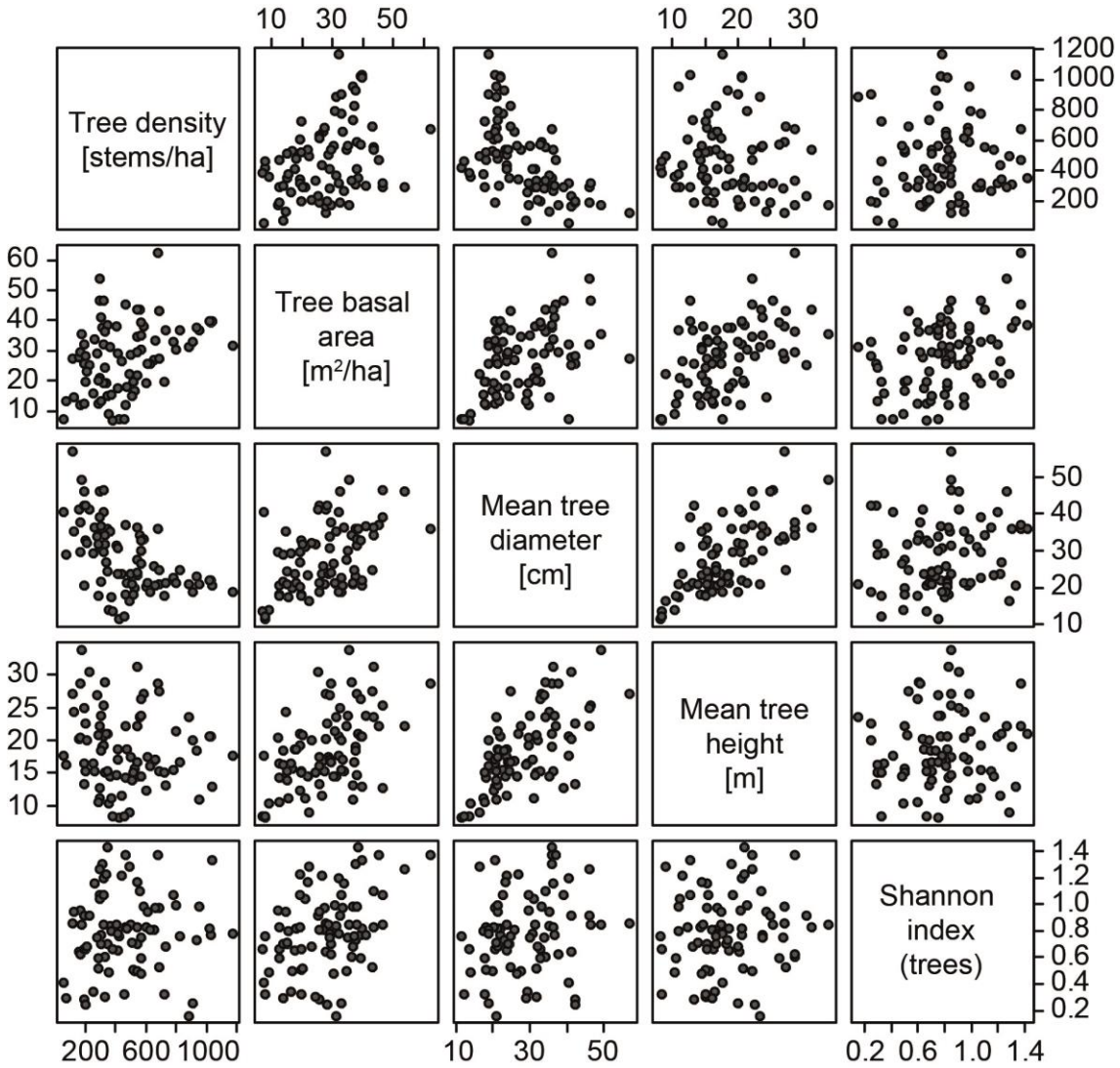

Figure VI–7: Bivariate relationships between PCA input variables.

Despite an overall similarity and thus overlapping, the age gradient was also detectable when plotting the distribution of the reaches and their respective pre- and post-dam surfaces (Figure VI–8b), although contrary to our expectations: post-dam surfaces (predominantly on the upper left) exhibited characteristics of older stands while pre-dam surfaces (predominantly on the lower right) showed characteristics of comparatively younger stands. MON was an exception. Diversity tended to be higher in downstream than in upstream reaches and slightly higher on pre-dam compared to post-dam surfaces, although overlapping indicates many similarities between plots throughout the reaches and periods.

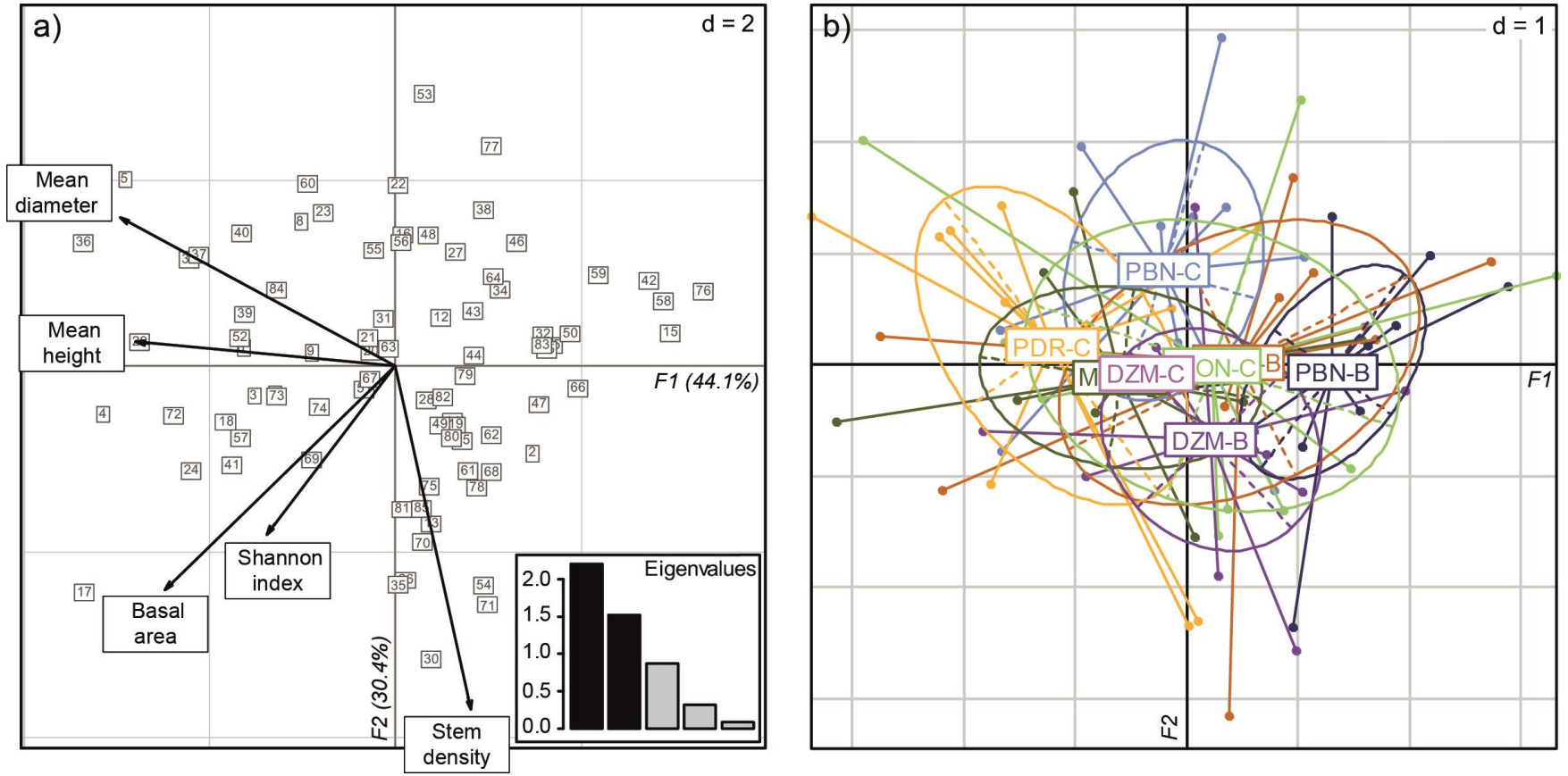

Figure VI–8: Results of the PCA on structural forest stand parameters. a) Factor map. b) Representation of the individual plots coloured by the study reach and period they belong to on the factor map. The four labels in the centre of the plot, which overlap, are from left to right: MON-B (dark green), DZM-C (light violet), MON-C (light green), and PDR-B (dark orange).

Based on the dendrogram resulting from hierarchical clustering, we identified five clusters of distinct structural characteristics (Figure VI–9). We found a cluster of high species diversity and average values for all other parameters (Cluster 1). Cluster 2 likewise showed high species diversity and average to low stem densities. However, basal areas were high, as the tree stands seemed to be older, evident from both high mean diameters and mean heights. Cluster 3 grouped older tree stands of low diversity and density, resulting in average basal areas. Clusters 4 and 5 consisted of younger tree stands, both of average species diversity. While cluster 4 stands were of average density and low basal areas, cluster 5 stands showed high densities and high basal areas. We state that clusters 1 and 2 covered most of the reaches and periods, confirming the relative similarity of plots between sites and a certain variability within sites (Figure VI–10). Clusters 3 to 5 were fairly site specific: cluster 3 was dominated by plots from post-dam surfaces at PBN (50% of the plots samples at this site), cluster 4 by pre-dam surfaces of the two upstream reaches, and cluster 5 mainly by DZM-B.

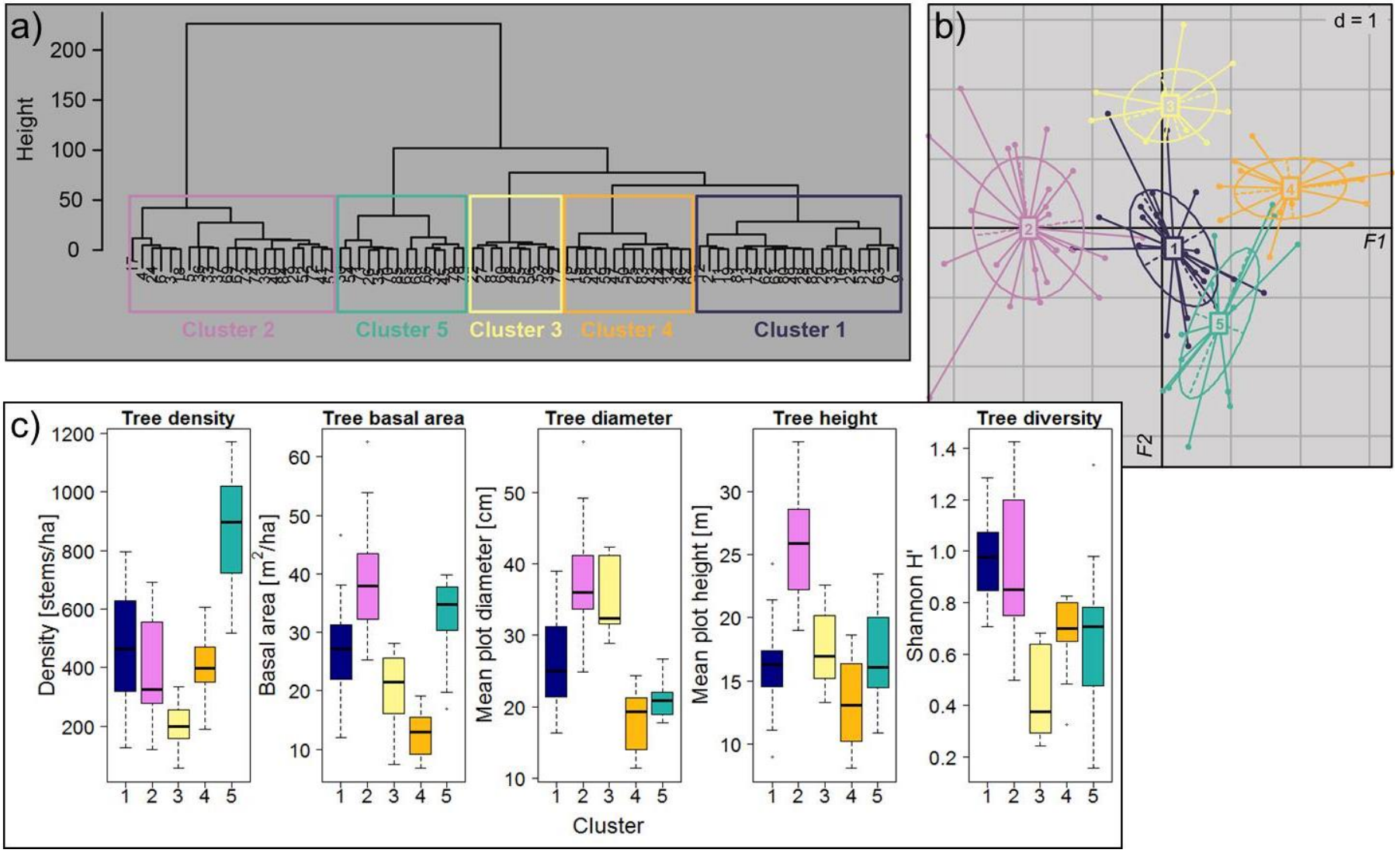

Figure VI–9: Results of clustering analysis following PCA. a) Dendrogram with clusters, b) biplot with colour code according to clusters, c) comparison of structural forest stand characteristics between clusters.

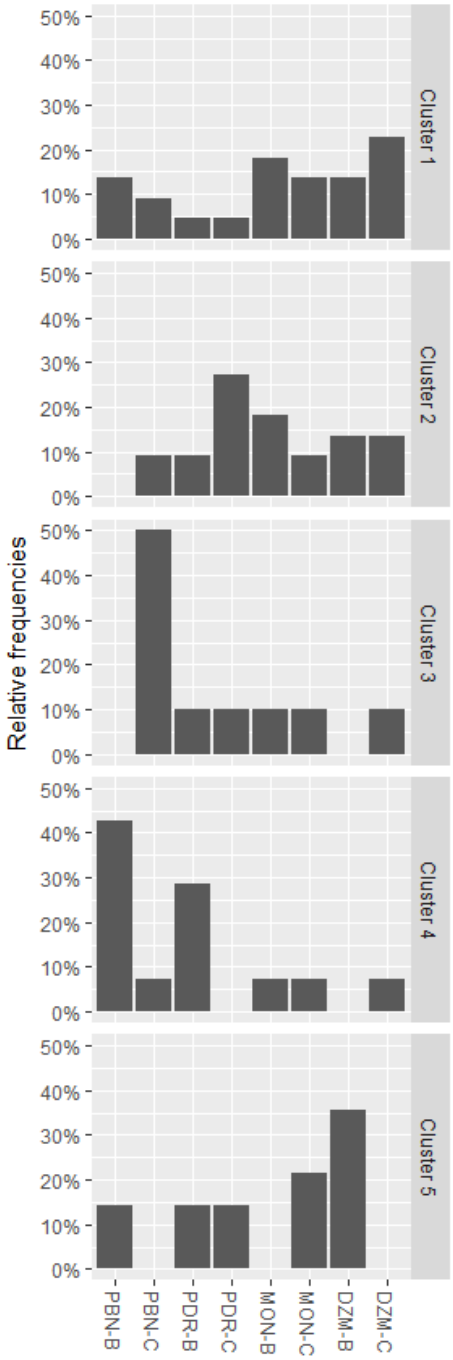

Figure VI–10: Distribution of the clusters resulting from the PCA and hierarchical clustering among the dike field sites.

Species composition

The first detrended correspondence analysis (DCA) included all life history stages, except seedlings at PLAT, which had not been surveyed at this detail. It yielded a relatively distinct spatial organisation of species abundances. On the species biplot, we observed mainly post-pioneer species at the far-left, including genera such as

Quercus, *Ulmus*, *Acer* or *Fraxinus*. To the far-right, pioneer species prevailed, with genera such as *Salix*, *Alnus*, or *Populus* (Figure VI–11). When colour coding the sampling plots on the biplot by site, a spatial gradient in species abundances from mature floodplain (PLAT) plots over dike fields in the centre, to pioneer island (DROM) plots was apparent along axis 1 (DCA1) (Figure VI–12). Dike field plots were relatively distinct from the two reference sites, despite some overlappings. With the exception of MON-B, a gradient from pre-dam to post-dam sites of dike fields (from left to right in the biplot) was observed: Plots from PBN-B, PDR-B, or DZM-B were situated closer to PLAT, while the post-dam surfaces and MON-B were in the centre of the two reference sites, with some plots being located closer to DROM. It is notable that many non-native species are concentrated around the dike field plots in the centre of the biplot, indicating high abundances in these systems. These include, for instance, *Acer negundo*, *Robinia pseudoacacia*, or *Morus alba*. PLAT plots form a dense cluster with maximum variation along axis 1. Dike fields and DROM plots proved less dense, with maximum variations along axis 2 (DCA2). Axis 2 seemed to partly represent an upstream-downstream gradient, with the gravity centres of PLAT, PBN, and PDR being located above the centre line and DROM, MON, and DZM below. However, this gradient showed a lot of noise.

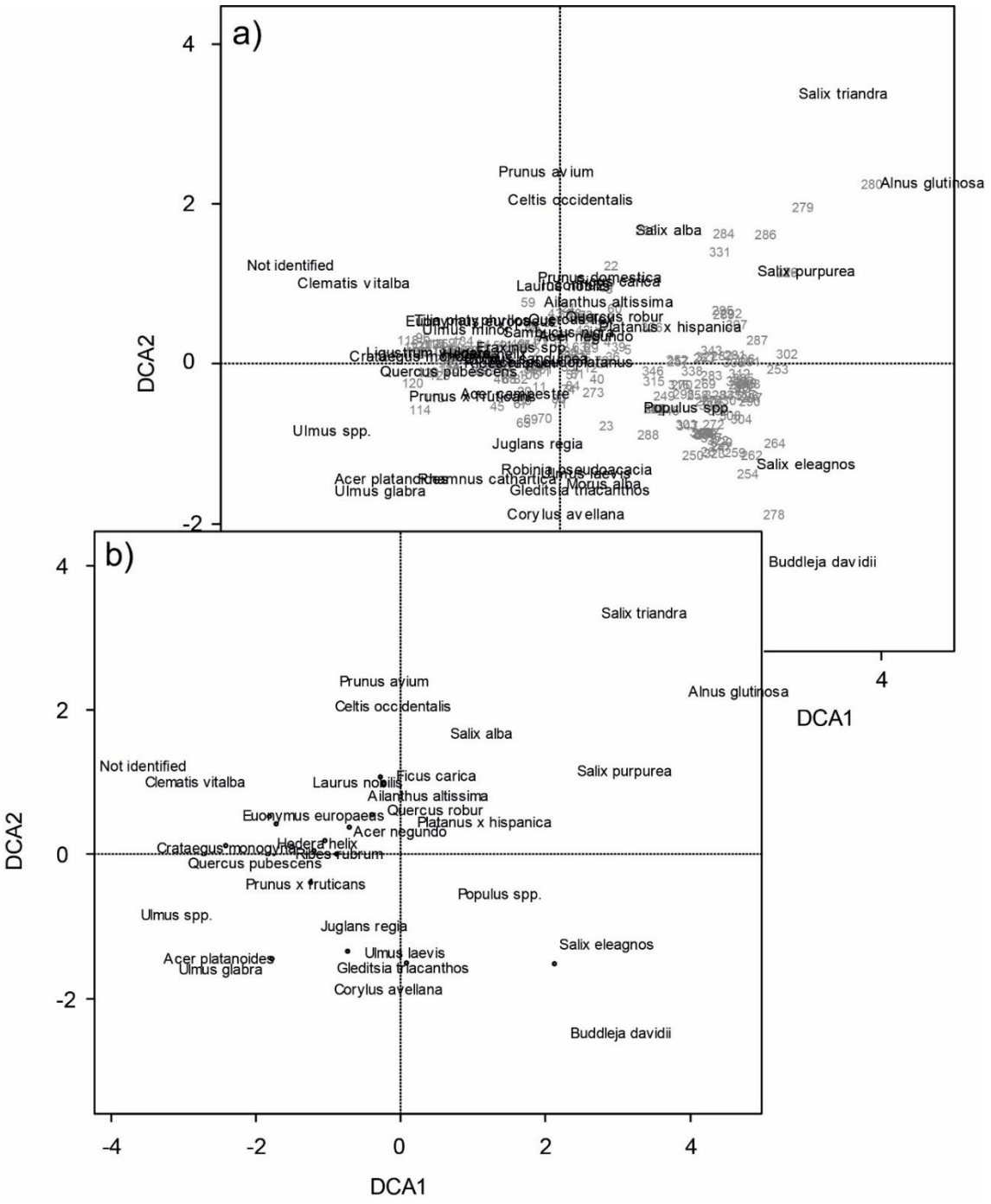

Figure VI–11: Results from a DCA on both dike fields and reference sites: biplots with a) species and samples, and b) a zoom on species for improved readability (overlapping labels deleted).

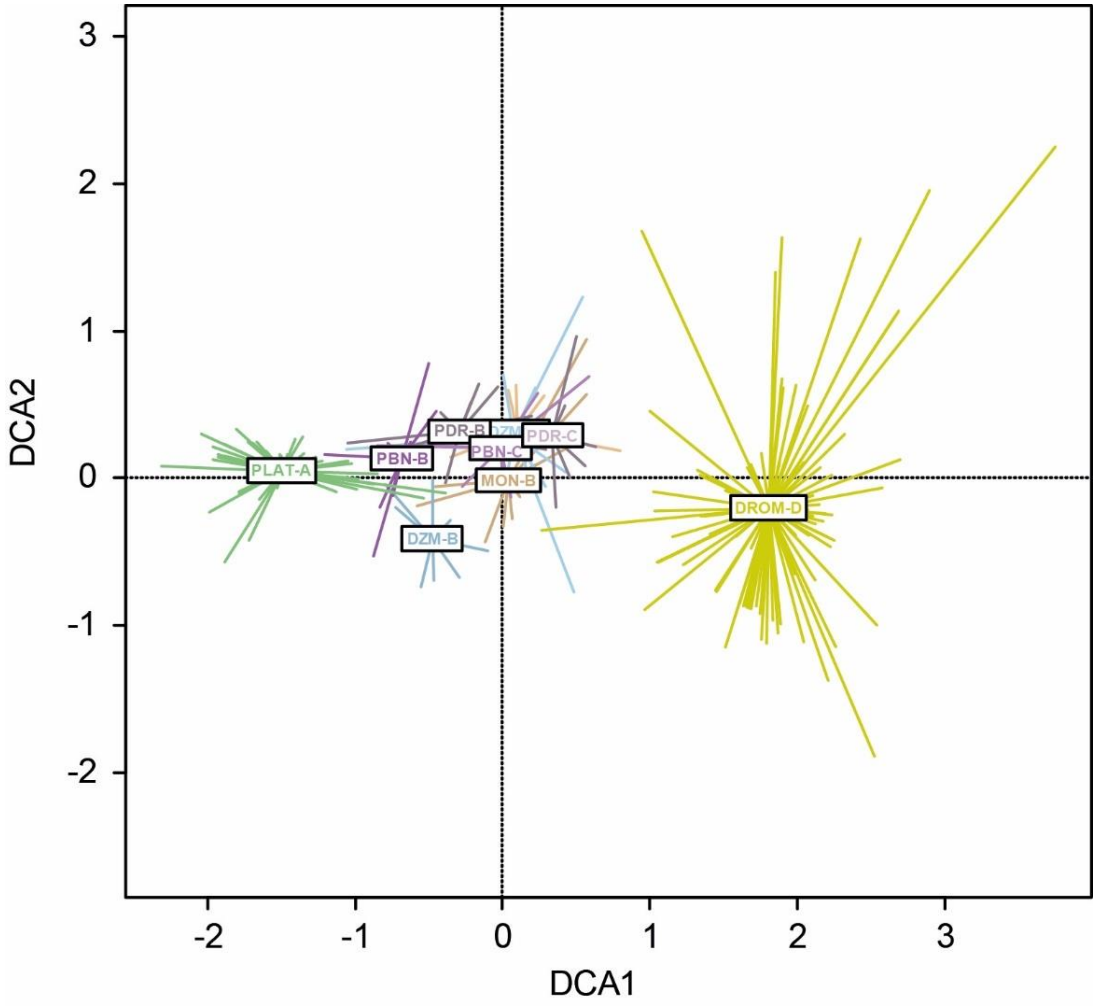

Figure VI–12: Results from a DCA on both dike fields and reference sites: sample biplot with colour coding by site.

A second DCA concentrated in detail on the set of dike field plots only (Figure VI–13). The sample biplot marked a relatively tight cluster around the centre of the plot, with some more or less distinct sub-clusters (Figure VI–13a). Colour coding the sample plots revealed an upstream-downstream organisation of the species from the top to the bottom (Figure VI–13b). Indeed, while post-dam surface plots showed yet a high similarity and thus a relatively tight cluster to the left, we observe a more marked divergence between upstream and downstream reaches on pre-dam surfaces (to the right). Toward the bottom we therefore find more Mediterranean species (e.g. *Ficus carica*, *Laurus nobilis*, etc.), toward the top more continental species (*Cornus sanguinea*, *Ligustrum vulgare*, etc.). The non-native post-pioneer *Acer negundo* and native *Populus spp.* take up a central position on the biplot, which coincides approximately with the centre of the sample cluster, indicating that these species were

abundant in many of the plots. Other species were particularly abundant in certain sites, such as *Corylus avellana*, *Robinia pseudoacacia*, *Juglans regia*, or *Gleditsia triacanthos* at DZM-B, or *Morus alba*, *Ficus carica*, in downstream reaches. But also *Rhamnus cathartica* or *Ligustrum vulgare* at PBN-B. *Salix alba*, a short-lived pioneer tree species, and *Platanus x hispanica* seemed to be particularly abundant on post-dam surfaces, but also post-pioneer species, such as *Quercus robur* or *Ulmus minor*.

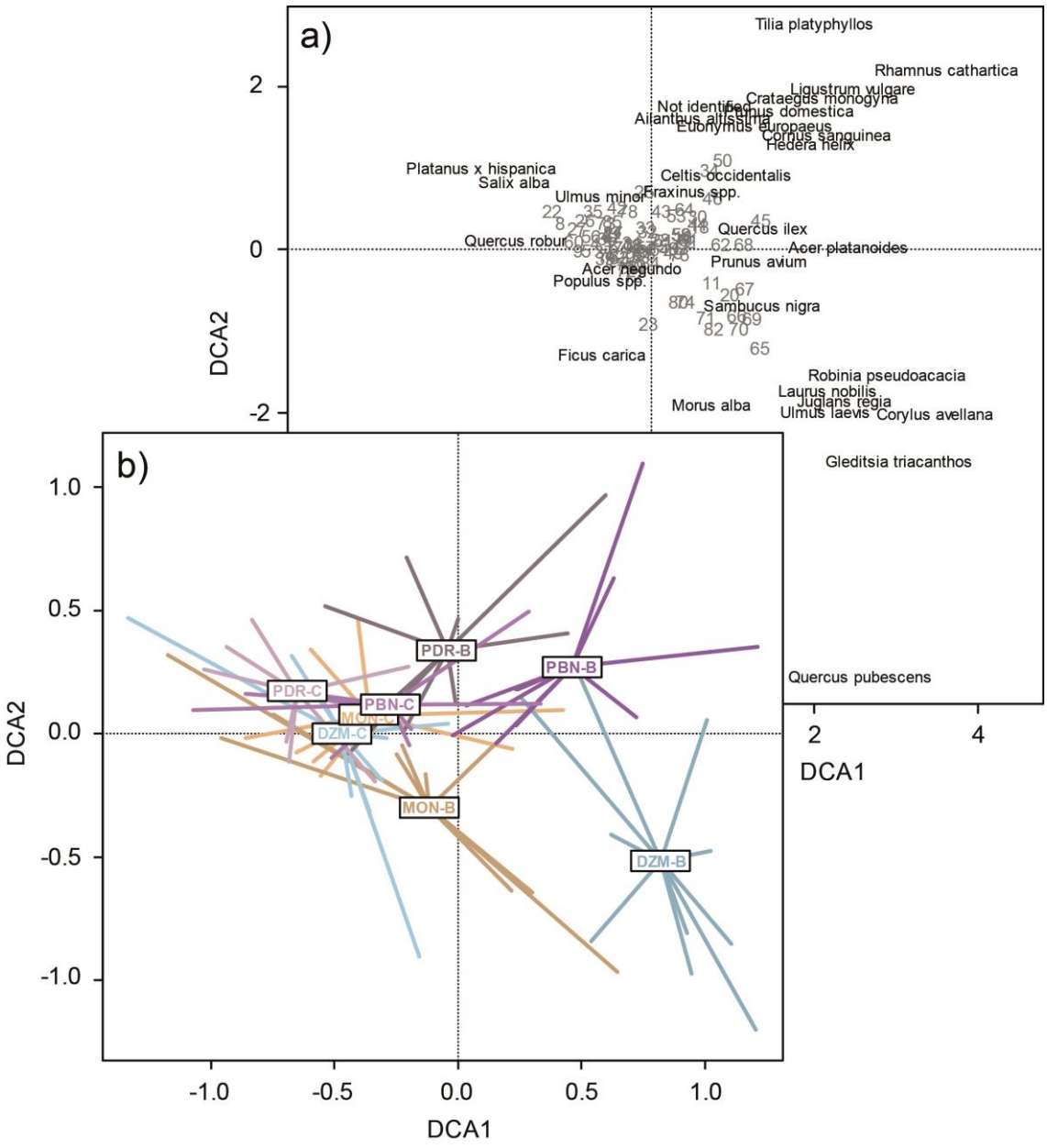

Figure VI–13: Results from a DCA on dike fields only: biplots with a) species and samples and b) samples coded by reach and pre- vs. post-dam surfaces.

4.1.5 Dominant species: structural characteristics and spatio-temporal patterns

We identified dominant (> 10% of stems, see Figure VI–1 and Figure VI–2) pioneer (native *Populus* and *Salix spp*., as well as non-native *Acer negundo*, *Robinia pseudoacacia*), post-pioneer (Fraxinus *spp*.) and understorey species (*Crataegus monogyna*, *Cornus sanguinea, Ligustrum vulgare*) in the dike fields and reference sites to describe their structural characteristics more in detail. In the reference sites, we found typical early successional (DROM) and late successional (PLAT) characteristics regarding the relative frequency of the dominant species (Figure VI–14a): at DROM the dominant species constituted mainly native pioneers at all life history stages, as well as some *Robinia pseudoacacia* (trees/saplings), and some understorey species at the sapling stage (Figure A–III–9). Although *Populus nigra*, *Salix alba* and *eleagnos* made up 88.4% of the tree stems at DROM (Figure VI–2), their average relative frequency was only 8.5% for *Populus spp.* and 5.1% for *Salix spp.*, since trees were absent in 84.5% of the study plots. Average relative frequencies for *Populus* saplings was 51.5% and *Salix* saplings 42.9%, *Populus* seedlings 27.6%, and *Salix* seedlings 13.5%. *Populus* saplings were present in 88.3% of the plots, *Salix* saplings in 76.7%, *Populus* seedlings in 33.0%, and *Salix* seedlings in 17.5%.

At PLAT, native *Populus spp.* were still present at the tree stage (11.6% mean relative frequency, present in 52.2% of the study plots) and in one out of 46 study plots at the sapling stage (0.0% mean relative frequency). Seedlings had not been surveyed at this site. Shorter-lived *Salix spp.* were already completely absent among live trees and saplings. Both trees and saplings were dominated by post-pioneer *Fraxinus spp.* (mean relative frequency: 34.3% trees, 3.0% saplings) and abundant understory species, notably *Crataegus monogyna* trees (18.8%), and *Ligustrum vulgare* (51.2%) and *Cornus sanguinea* (17.6% plot average) saplings. Non-native pioneers were found to be cohabiting with these native species, yet at lower relative frequencies: *Acer negundo* made up 9.2% and 1.9% of trees and saplings, respectively, *Robinia pseudoacacia* 3.3% of trees, no saplings were found.

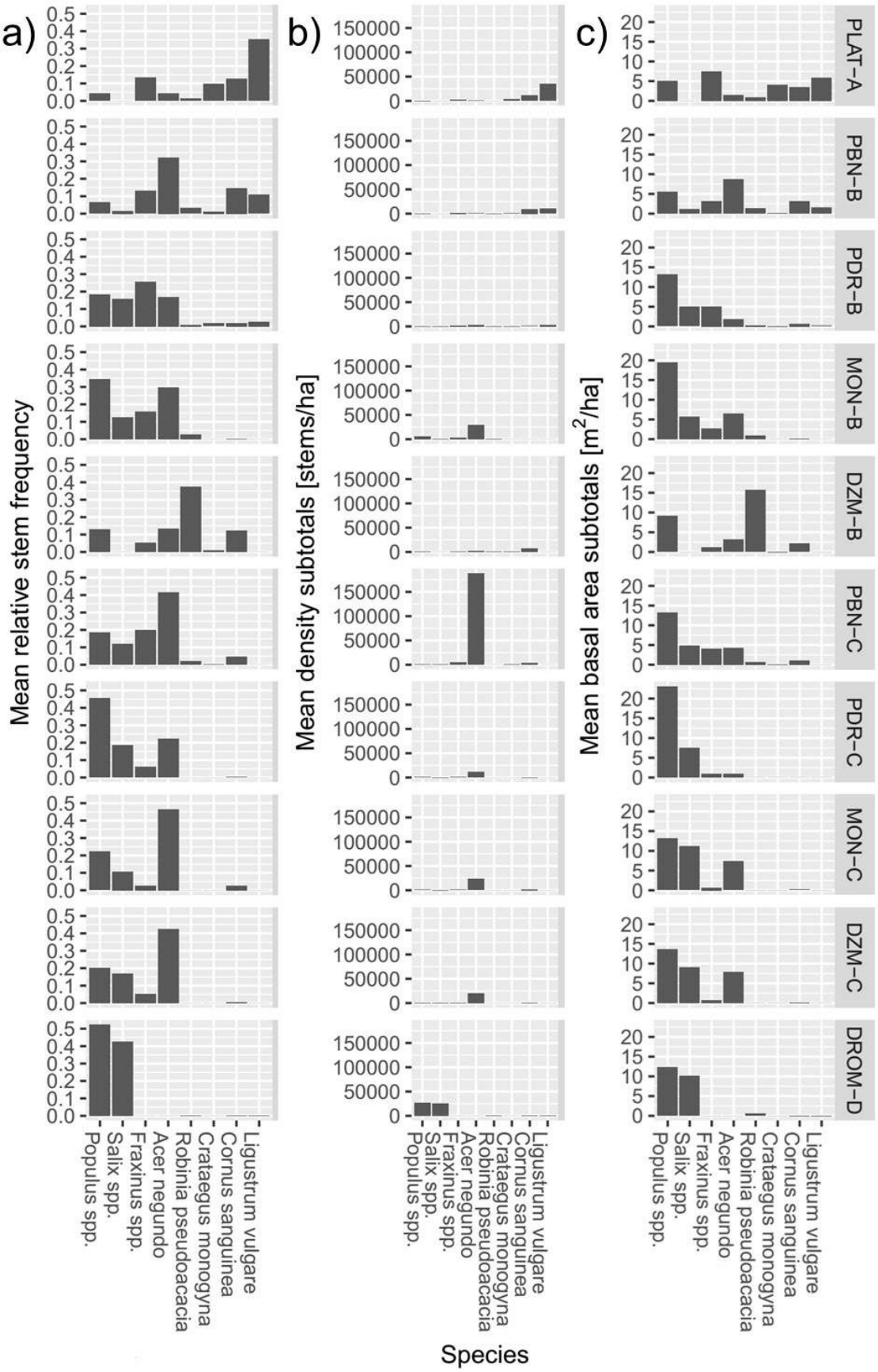

Figure VI–14: Structural characteristics of dominant species (all life history stages included, for each LHS separately, see Appendix III): mean relative frequency (a), mean density (b), mean basal area (c). At PLAT, no seedlings had been surveyed.

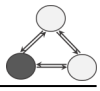

The vegetation in dike fields was at an intermediary state between DROM and PLAT in terms of native pioneer species, with *Populus spp.* being present mainly at the tree stage, and regeneration being rare and restricted to a few sites (MON-B, PDR-C, MON-C). MON-B was an exception with more abundant regeneration (on average 21.9% of all saplings in a plot and 19.3% of seedlings). No more regeneration was noted for *Salix spp.*, and mature trees were still present on post-dam surfaces but getting rare on pre-dam surfaces—at DZM-B live *Salix* were already absent. *Fraxinus* were regenerating, especially on pre-dam surfaces, and in several of the sites we recorded important relative frequencies of trees, as well (e.g. PDR-B: 25.3%, PBN-C: 19.9%). Especially pre-dam surfaces in dike fields presented an important understorey—with the exception of MON-B—but some post-dam surfaces likewise did. Indeed, at MON-B, except for some few mature *Cornus sanguinea* (making up on average 0.4% of tree stems per plot), the three understorey species were not represented. We furthermore noted that *Crataegus monogyna* and *Ligustrum vulgare* were relatively confined, *Crataegus* to pre-dam surfaces and PBN-C, whereas *Ligustrum* only occurred on the pre-dam surfaces of the two upstream reaches. *Cornus sanguinea* was ubiquitous, throughout all the dike field sites at least a few stems were found. At PBN-B and DZM-B the entire understorey was best developed. In terms of non-native species, dike fields showed patterns that diverged from both reference sites: *Robinia pseudoacacia* showed a strong local peak at DZM pre-dam surfaces, making up on average 48.3% of the trees in these plots. It occurred in 100% of the DZM-B plots, compared to an average 22.7% of plots on the other pre-dam sites. This was likely related to nearby plantations along the railway tracks. *Acer negundo* was notable as it was frequent in dike fields throughout all reaches and management phases, but particularly on post-dam sites. It occurred as trees in 82.9% of all dike field plots, as saplings in 30.5% and as seedlings in 47.6%. Its regeneration was particularly strong, compared to other species.

We found similar patterns in terms of mean stem densities (Figure VI–14b) and mean basal areas (Figure VI–14c). In dike fields, densities of non-native trees were generally high, while high basal areas were generally connected to native species, especially *Populus* and *Salix spp*. This is due to differences in diameters, and thus age (although different characteristic growth patterns might play a role, too), with native species being generally dominated by older individuals in dike fields (Figure VI–15).

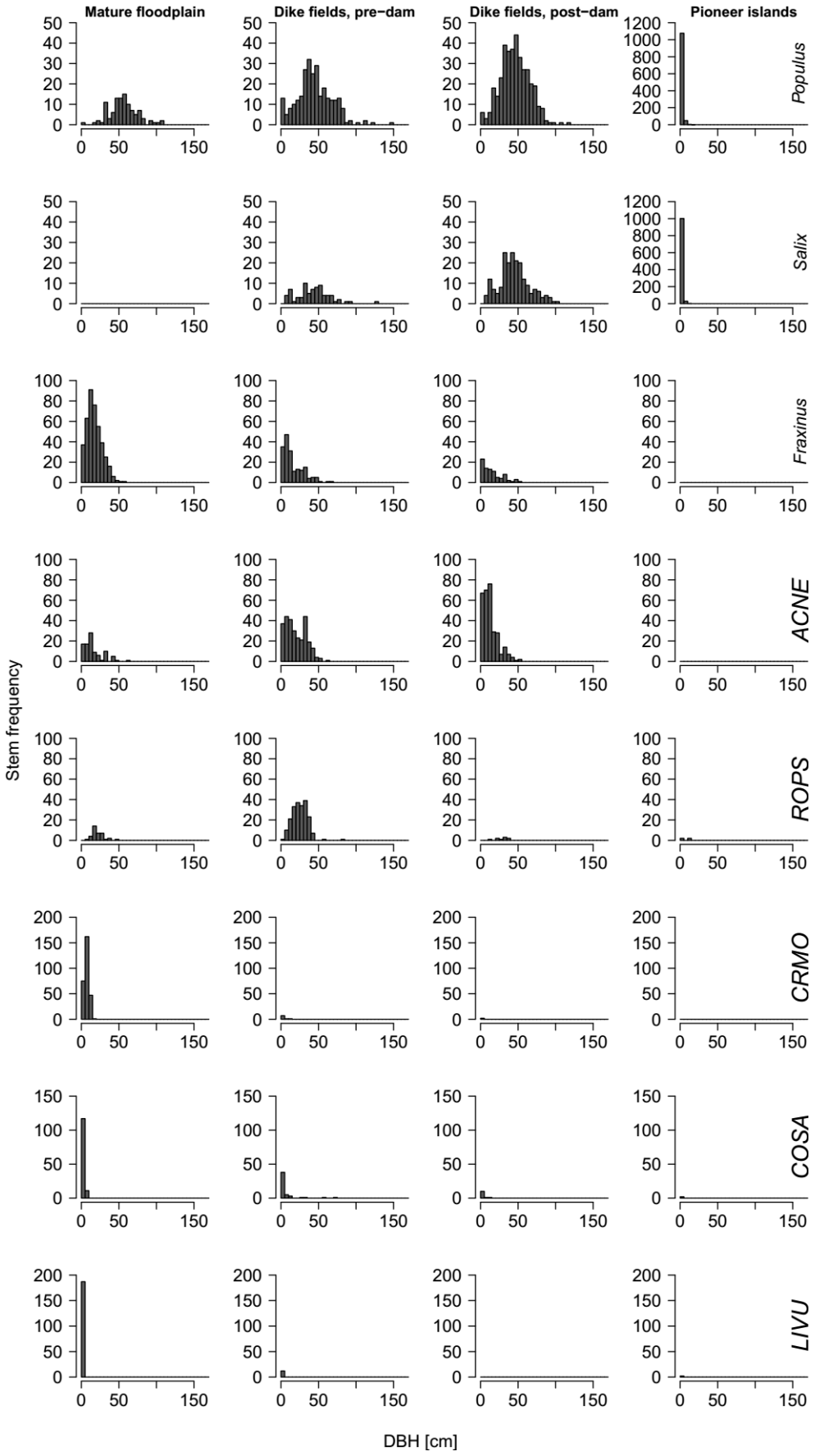

Figure VI–15: Between-site comparison of diameter at breast height (DBH) frequency distributions among dominant species.

Both, sapling densities and basal areas were comparatively low for individual dominant species in dike fields with respect to the reference sites. We already saw such a pattern for the entire species pool (Figure A–III–3). In the reference sites, we noted that it were certain individual species (native pioneers at DROM and understorey species at PLAT) which presented high values for both parameters. In dike fields, values for individual species were much lower.

To sum up the preliminary findings on the structure and composition of dike field forest stands:

- We found distinct structural and compositional differences within (pre- vs. post-dam surfaces) and between reaches:
  - Stem diameter at breast height and stem height presented marked differences between pre- and post-dam surfaces, while total plot density and basal area did not
  - Pre-dam surfaces showed a latitudinal effect, with continental species in the upstream reaches and Mediterranean species in the downstream reaches. These differences did not dominate post-dam surfaces.
- At MON the structural and compositional patterns were generally inversed between pre- and post-dam surfaces, which was probably due to higher minimum stand ages on post-dam surfaces compared to pre-dam surfaces
- In comparison to reference sites: dike field forest stands
  - were structurally apart from both reference sites, their compositional characteristics lay in between the two, yet showed more similarities with the PLAT mature reference
  - showed lower stem densities, higher DBH, similar basal areas, and taller stems than reference sites, when considering all life history stages together
- Non-native species were particularly abundant in dike fields, especially *Acer negundo*, which dominated the regeneration stage and was abundant throughout all sites. *Robinia pseudoacacia* was locally dominant, especially at DZM-B. But also other non-native species were inventoried, such as *Ailanthus altissima*

4.2 Drivers of forest stand characteristics

In the organisation of the structural and compositional characteristics of the dike field forest stands, we already highlighted some spatial differences, which might be related to latitudinal effects. In the following, we were therefore interested in investigating further potential drivers behind these patterns. First, we shall present drivers acting at the local scale and their spatial patterns, which could then be compared to the vegetation patterns described earlier. Eventually, we analysed in how far these drivers could explain the variation in structural and compositional patterns by relating them directly to one another.

4.2.1 Spatial analysis of environmental conditions related to the sampling plots

As expected, hydrological connectivity conditions, and thus potentially the magnitude and frequency of disturbance and resource supply, were spatially variable. For instance, relative elevations of the sampled plots above the water level at a discharge of 100 m^3/s varied between reaches and between pre- and post-dam surfaces (Figure VI–16). Over all plots together, they ranged from 0.57 m to 7.23 m a.w.l. (median = 4.01 m, IQR = 2.54 m). Within-reach differences, in terms of pre- vs. post-dam surfaces, were significant for all four reaches and more pronounced than between-reach differences, which were not always significant. We also noticed that pre- versus post-dam differences were more marked in the two upstream reaches, where by-passing occurred much later than in the downstream reaches.

We recorded largely corresponding patterns for plot submersion duration and frequency (Figure VI–16). Overall, plot submersion duration ranged from 0.0 to 46.1 d/yr (median = 2.6 d/yr, IQR = 15.7 d/yr). On pre-dam surfaces, which were all relatively disconnected, we recorded little within-reach variation (IQR: PBN-B = 1.31 d/yr, PDR-B = 1.54 d/yr, MON-B = 2.00 d/yr, DZM-B = 0.01 d/yr) and little between-reach variation (median: PBN-B = 0.00 d/yr, PDR-B = 2.44 d/yr, MON-B = 2.68 d/yr, DZM-B = 0.00 d/yr). On post-dam surfaces, on the other hand, we find a much higher variability both within most reaches and between reaches: the IQR ranged from 1.82 d/yr at DZM-C, 7.17 d/yr at MON-C, 10.93 d/yr at PDR-C, to 22.04 d/yr at PBN-C. Median tendencies amounted to 16.48 d/yr at PBN- C, 27.82 d/yr at PDR-C, 6.42 d/yr at MON-C, and 0.46 d/yr at DZM-C.

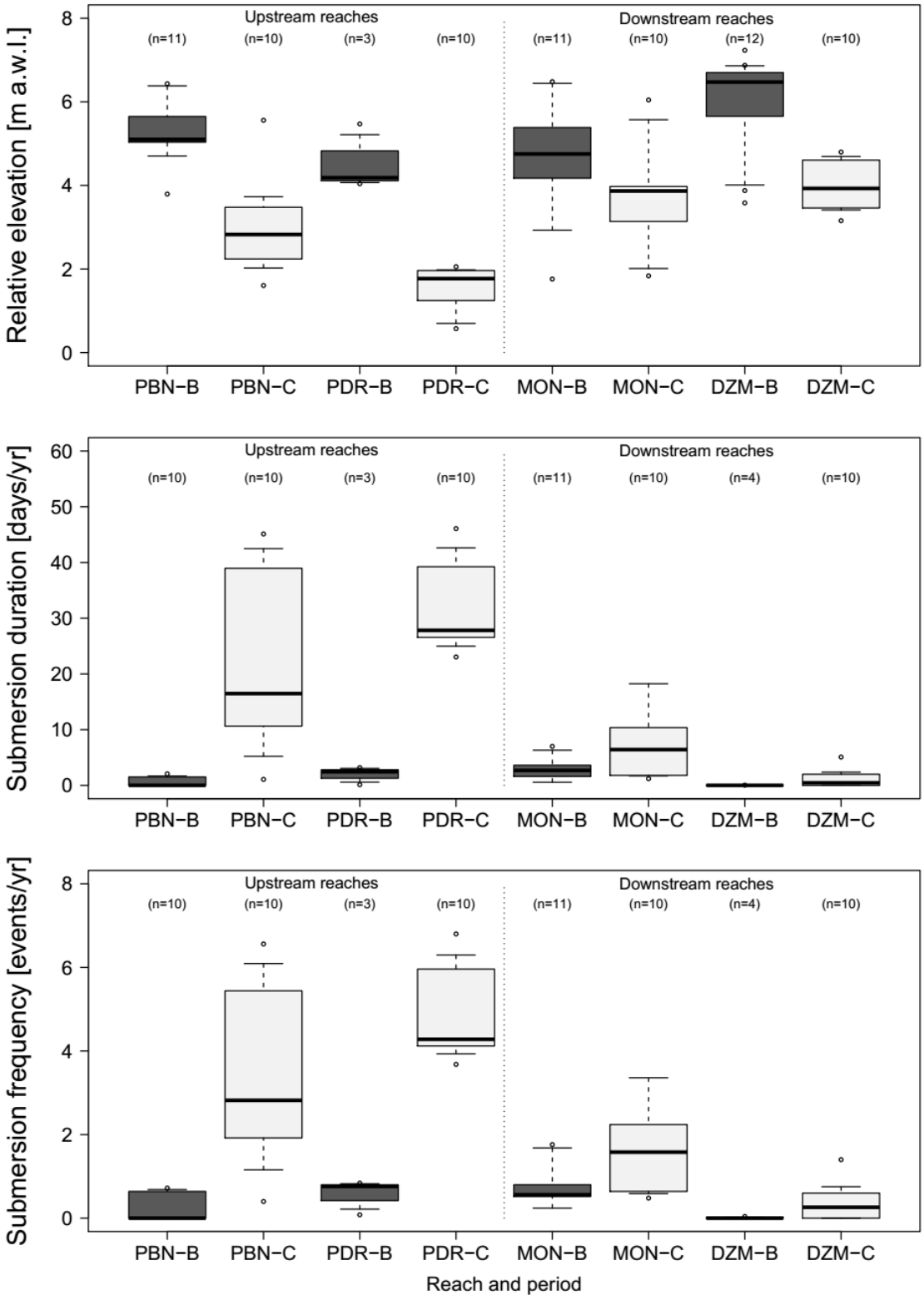

Figure VI–16: Spatial patterns of, from top to bottom: relative sampling plot elevations above the water level at a discharge of 100 m^3/s, sampling plot submersion duration, sampling plot submersion frequency, surface age at the sampling plot location, overbank fine sediment thicknesses measured at the sampling plot centre, the distance of sampling plots to the longitudinal dike (see following page).

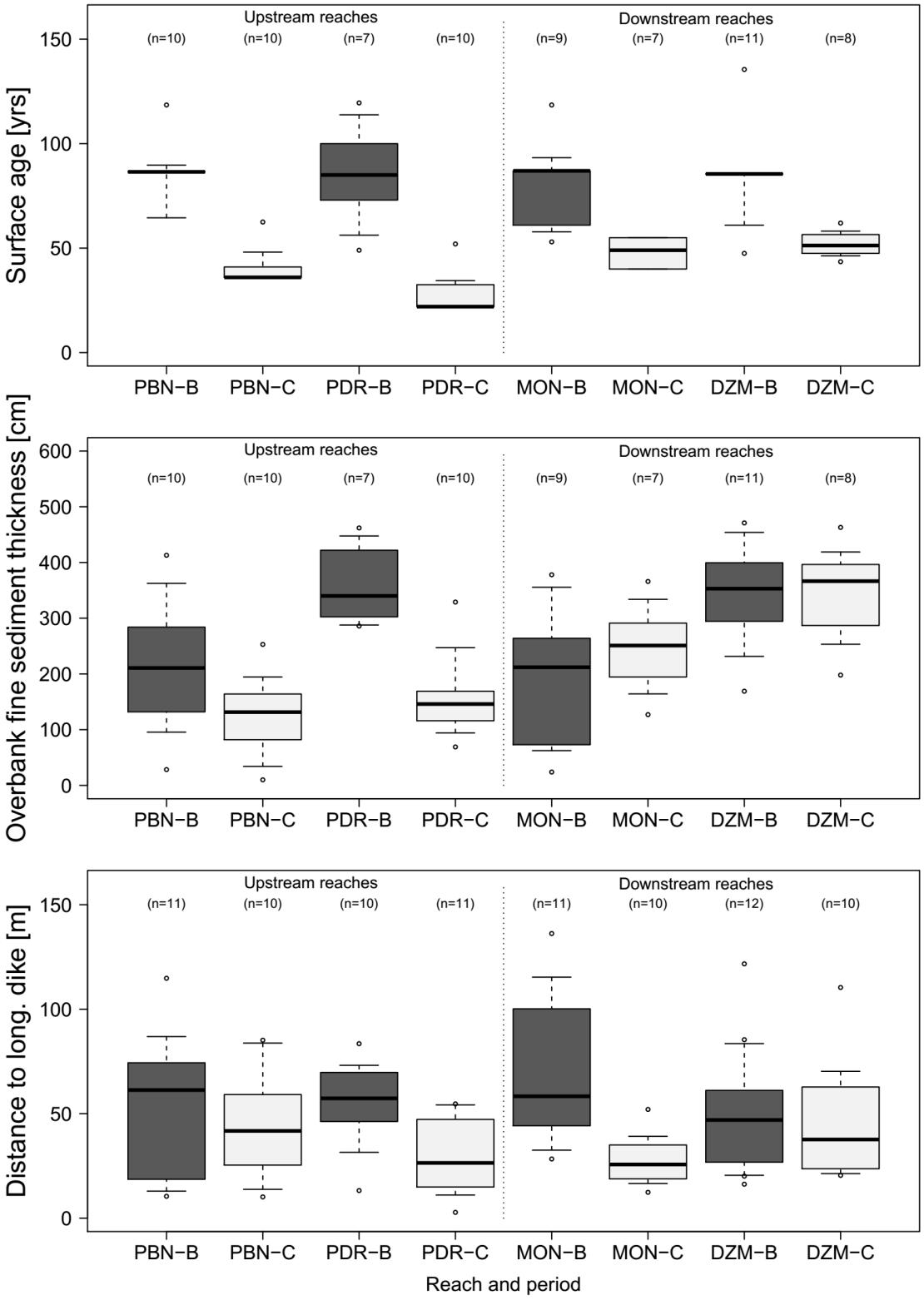

(Figure VI−16 continued)

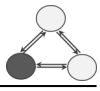

Plot submersion frequency ranged from 0.00 to 6.80 events/yr (median = 0.68 events/yr, IQR = 2.53 events/yr, Figure VI–16). The patterns being the same as for plot submersion duration, we shall only list the descriptive values for this parameter in the following. On pre-dam surfaces, the median plot submersion frequency values were 0.00 events/yr at PBN-B, 0.76 events/yr at PDR-B, 0.56 events/yr at MON-B, 0.00 events/yr at DZM-B. The IQR was 0.55 events/yr at PBN-B, 0.38 events/yr at PDR-B, 0.28 events/yr at MON-B, and 0.01 events/yr at DZM-B. On post-dam surfaces we noted median values of 2.82 events/yr at PBN-C, 4.28 events/yr at PDR-C, 1.58 events/yr at MON-C, and 0.26 events/yr at DZM-C. For the IQR we found 2.87 events/yr at PBN-C, 1.50 events/yr at PDR-C, 1.38 events/yr at MON-C, and 0.59 events/yr at DZM-C.

Mean plot surface ages ranged from 22 years to 136 years (median = 58 years, IQR = 46 years, Figure VI–16). Pre-dam plot surface ages were on average equal between reaches (median: PBN-B = 87 yrs, PDR-B = 85 yrs, MON-B = 87 yrs, DZM-B = 86 yrs). Variation was higher at PDR and MON than at PBN and DZM (IQR: PBN-B = 0 yrs, PDR-B = 27 yrs, MON-B = 26 yrs, DZM-B = 0 yrs). Post-dam mean surface ages were less variable within each reach (IQR: PBN-C = 4 yrs, PDR-C = 8 yrs, MON-C = 15 yrs, DZM-C = 9 yrs). Median values ranged, corresponding to the order of the timing of diversion, from 51 yrs at DZM-C, over 49 yrs at MON-C, 36 yrs at PBN-C to 22 yrs at PDR-C.

Accumulated overbank fine sediment reached important depths, with a median value of 241 cm (IQR = 207 cm), and up to 471 cm maximum (Figure VI–16). The minimum depth was 10 cm. We found the on average deepest layers on pre-dam surfaces of PDR (median = 340 cm, IQR = 120 cm) and DZM (median = 353 cm, IQR = 105 cm), and on post-dam surfaces of DZM (median = 367 cm, IQR = 103 cm). Median values of pre-dam surfaces at PBN (211 cm, IQR = 134 cm) and MON (212 cm, IQR = 191 cm) and on post-dam surfaces of MON (251 cm, IQR = 97 cm) were intermediate. The lowest median values were measured on the post-dam surfaces of the two upstream reaches (PBN: median = 132 cm, IQR = 74 cm; PDR: median = 146 cm, IQR = 45 cm). Pre- and post-dam surfaces showed less differences in the two downstream reaches than in the two upstream reaches, probably at least partly due to the similarities in time of accumulation downstream and inversely the differences upstream.

We measured distances of the plot centres to the longitudinal dikes of between 3 m and 136 m (median = 45 m, IQR = 39 m; Figure VI–16). Median values were similar

between reaches on pre-dam surfaces (PBN-B = 61 m, PDR-B = 57 m, MON-B = 58 m, DZM-B = 47 m) and lower on post-dam surfaces and a little more varied on post-dam surfaces (median: PBN-C = 42 m, PDR-C = 26 m, MON-C = 26 m, DZM-C = 38 m). The variability was higher on pre-dam (PBN-B = 56 m, PDR-B = 23 m, MON-B = 56 m, DZM-B = 30 m) than on post-dam surfaces (PBN-C = 31 m, PDR-C = 32 m, MON-C = 14 m, DZM-C = 36 m).

4.2.2 Relationships between drivers

To better understand the environmental variables and their interactions we likewise explored their bivariate relationships. Plot submersion duration and frequency were, for instance, highly correlated (Spearman's rank correlation rho = 0.99, $p < .0001$), showing a strong positive linear relationship (Figure VI–17, $R^2 = 0.98$, $y = 0.14x + 0.28$). In the following, we therefore focused our analyses on submersion duration, whose patterns were then assumed to be equally true for frequency and thus to acceptably describe hydrological connectivity phenomena.

The relationship between surface age and plot submersion duration (Figure VI–18a) confirmed the disconnection of pre-dam surface plots and a negative linear gradient in the hydrological connectivity of pre-dam surface plots. Pre-dam surfaces were higher (Figure VI–18b) and therefore less connected. Overbank fine sedimentation showed no particular pattern with regard to surface age (Figure VI–18c). We therefore assumed that similar patterns of sedimentation have taken place but have shifted spatially following diversion. However, as Figure VI–18d reveals, this shift was potentially not always simply in lateral direction toward the longitudinal dike or thus generally the channel.

We identified a tendency of increasing overbank fine sedimentation with elevation on pre-dam surfaces (Figure VI–18e). A similar trend is also detected for post-dam surfaces, with similar slopes but at lower elevations. Similar to observations in the literature (e.g. Walling & He, 1998), we did not find any particular pattern between overbank fine sediment thickness and lateral distance from the longitudinal dike as a proxy to lateral distance to the channel (Figure VI–18f).

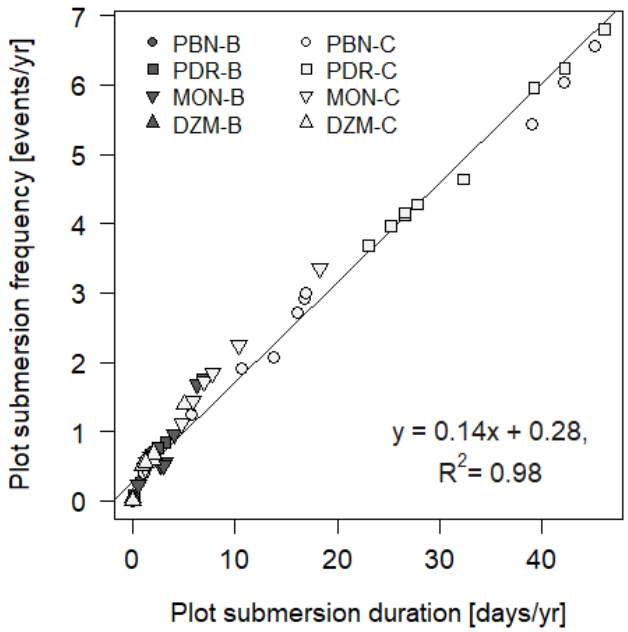

Figure VI–17: Relationship between plot submersion duration and frequency.

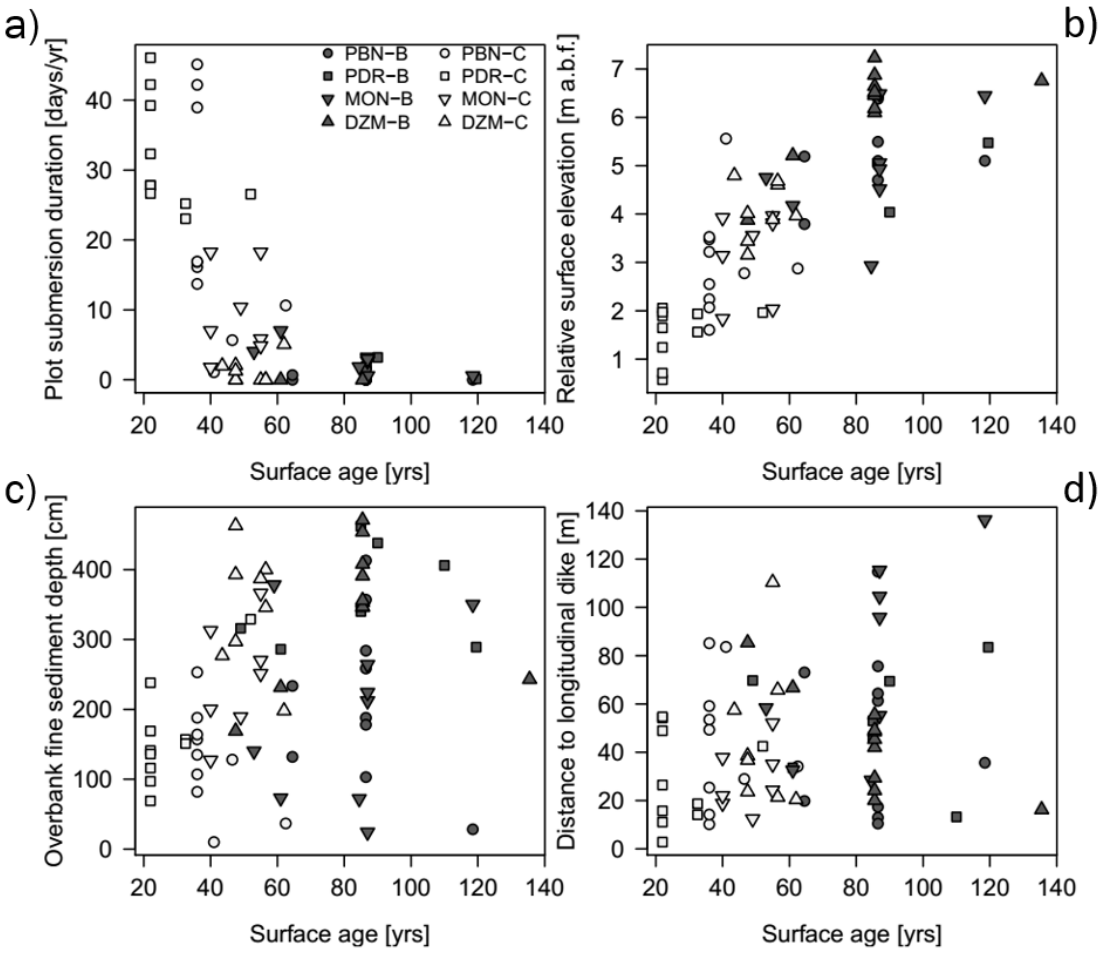

Figure VI–18: Bivariate relationships between drivers.

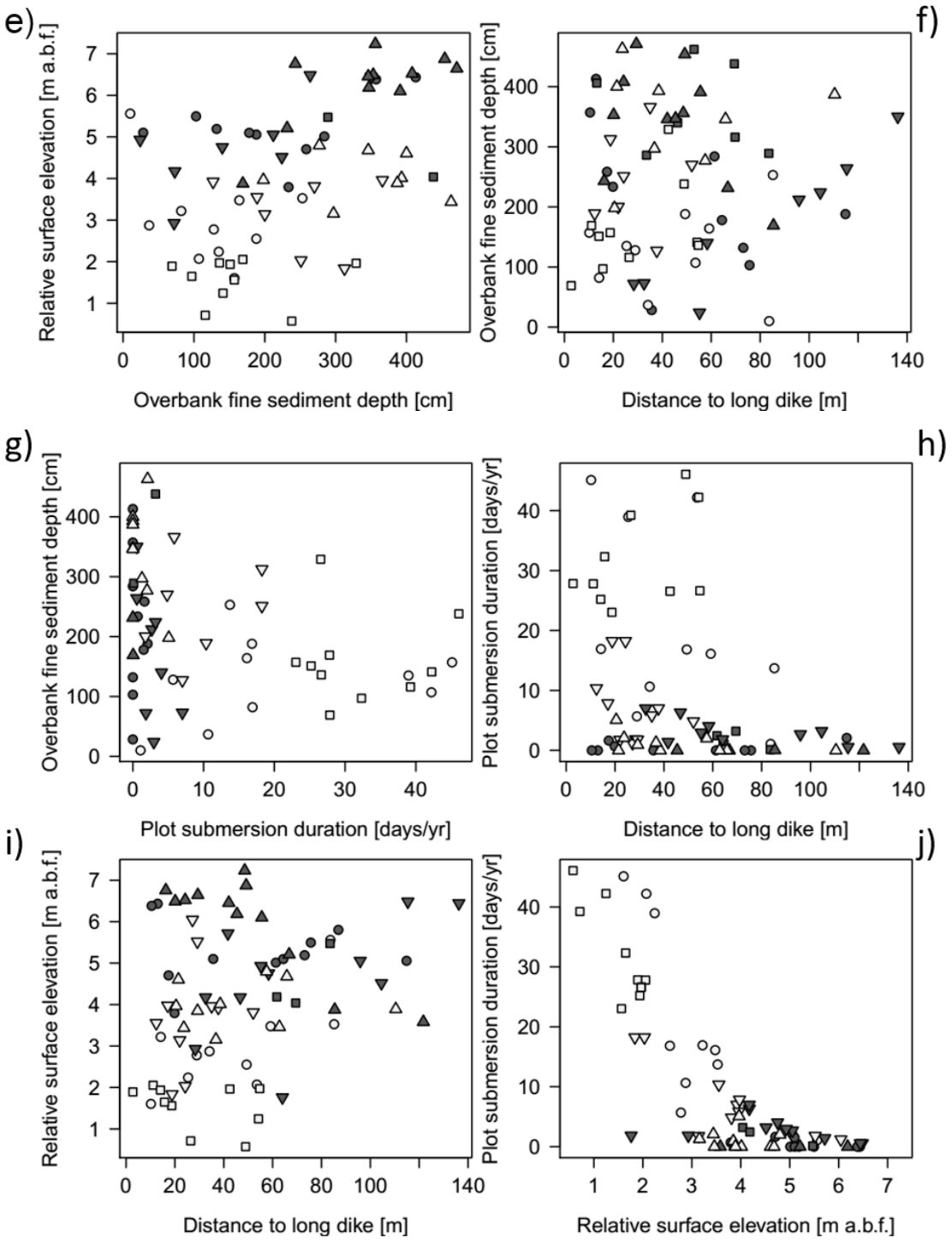

(Figure VI–18 continued)

Overbank fine sediment thicknesses were rather heterogeneous regarding plot submersion duration (Figure VI–18g). We simply noticed a reduction in variability with increasing duration. Plot submersion duration is low for pre-dam surfaces over the entire lateral distance gradient (Figure VI–18h). At smaller distances to the longitudinal

dike, the variability of relative elevations above the water level was very high and no particular pattern observable. At farther distances, approximately 70 m and more, we found higher relative elevations (Figure VI–18i).

4.2.3 Linking physical conditions and vegetation characteristics

In the preliminary analyses of this chapter, we stated marked within-reach differences, particularly between pre-dam and post-dam surfaces, in both structural and compositional dike field forest stand characteristics. Beyond this, we saw compositional differences between pre-dam surfaces of upstream and downstream reaches, which were probably indicative of latitudinal effects. In the following, we investigated the influence of the potential local controls, which have been introduced in this section, and their role in comparison to the regional factors. First, we integrated them into the multivariate analyses, then we added more detailed analyses.

Variation of forest stand structure according to local environmental factors

Overall, we state that local factors seemed to be masked by the major impact of dam construction. We see this in Figure VI–19, where the pre- vs. post-dam patterns predominate the organisation over the local patterns, since dam construction profoundly influenced sediment deposition dynamics and connectivity. For instance, we observed a tendency of linearly rising score values for rising relative elevation of the plots above the water level, although the variation remains important (Figure VI–19a). The distribution of the sites was relatively distinct, and pre- and post-dam surfaces were relatively well discriminated at PBN, PDR, and DZM—post-dam surfaces showed both lower scores and relative elevation values than post-dam surfaces. In contrast, at MON, the distinction according to relative elevations is not evident. Concerning plot submersion (Figure VI–19b), we likewise found a distinct gradient between pre- (lower submersion duration and higher scores) and post-dam surfaces (higher submersion duration and generally lower scores). For the upstream reaches, the distinction is more evident than for the downstream reaches. Regarding surface age, we noted a positive linear tendency until an age of approximately 70 years, including mainly post-dam surfaces, followed by a slight downward tendency, mainly related to pre-dam surfaces (Figure VI–19c). Overbank fine sediment thickness was only distinctly different at the within-reach level at PDR, with lower scores and sediment thicknesses on post-dam surfaces and higher scores and thicknesses on pre-dam

surfaces (Figure VI–19d). Concerning sedimentation rates, these patterns were even less evident and for lateral distances from the longitudinal dike, we found no relationship (Figure VI–19e and f, respectively). Overbank fine sediment thickness and distance to longitudinal dike thus seemed to follow more complex patterns related not only to dam construction but probably local phenomena.

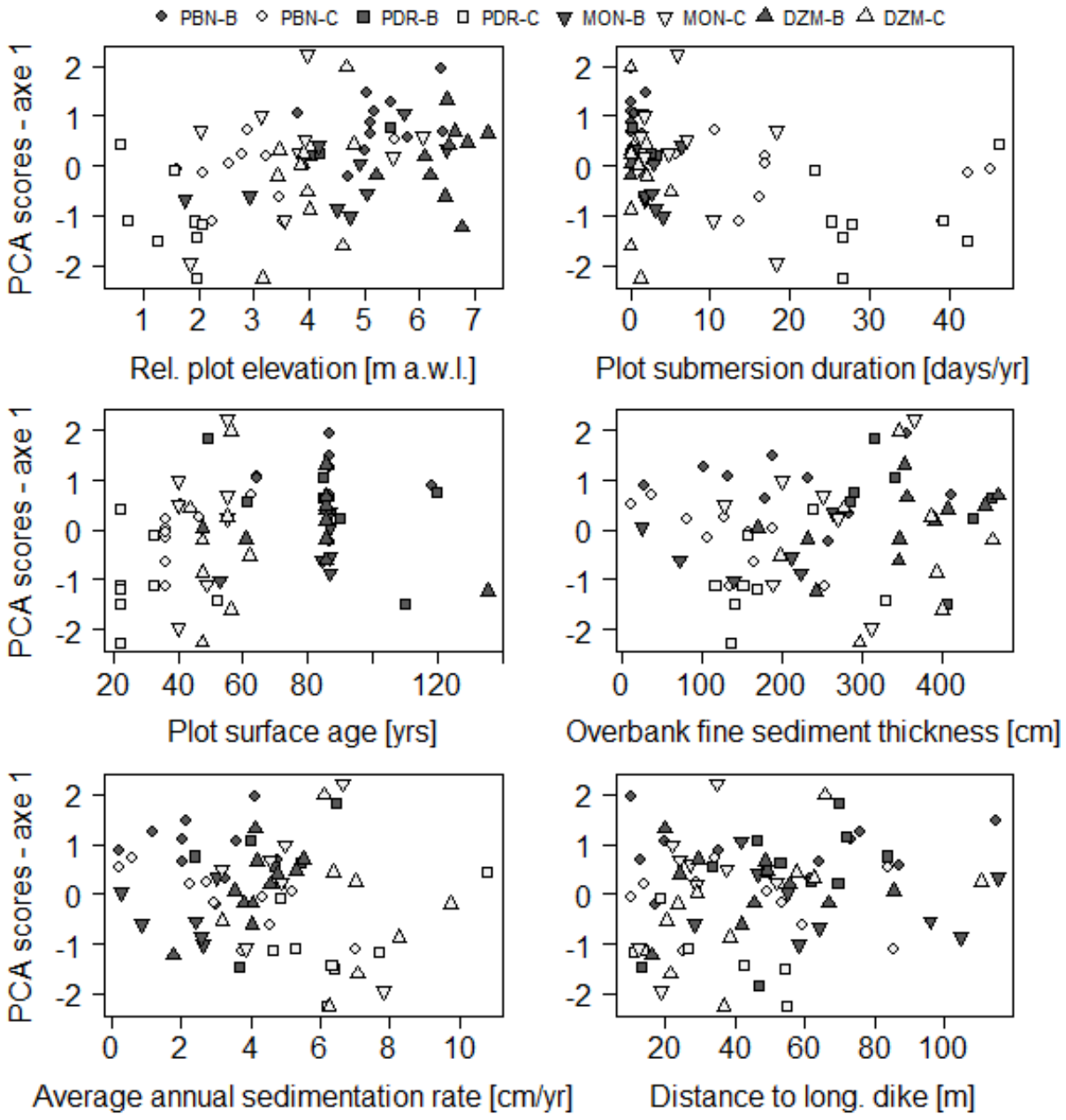

Figure VI–19: Relationship between control variables and PCA scores on axis 1.

Variation of forest stand composition according to local environmental factors

By adding environmental variables to the DCA on dike fields using surface fitting we were able to display two gradients determining the distribution of the species (Figure VI–20): A first gradient approximately traverses the scatter plot from left to right, along axis 1. It implies an increasing hydrological disconnection of the plots here represented by conditions of elevation relative to the water level at a discharge of 100 m^3/s, plot submersion duration (whose gradient is not linear), and surface age. This seems logic and corresponds to the distribution of the pre- and post-dam plots on the biplot from left to right (Figure VI–13). A second gradient was distinguished from top to bottom, and thus along axis 2, indicating increasing overbank fine sediment thicknesses. For *Robinia pseudoacacia*, situated at the bottom of the biplot, this corresponds to its preferences: it can tolerate the dry season of the Mediterranean region, is however not adapted to frequent flood stress or high ground water tables (Vítková et al., 2017). Important overbank fine sediment deposits at high elevation plots provide sufficient soil moisture and nutrients while the ground water table can be relatively far. In the following we investigated in more detail the impact of these factors on the presence or absence of the dominant species using logistic regression analysis.

Indeed, logistic regression models yielded relatively distinct preferences, for some species, regarding the environmental gradients observed in dike fields (e.g. *Robinia pseudoacacia*, *Salix alba*). Other species proved rather flexible (e.g. *Acer negundo*, *Populus spp.*) and occurred in a wide range of conditions. The best models per species were defined by the lowest AIC value following stepwise addition of variables (in bold in Table VI– 6). The dominant drivers in the best models were not the same for the different species: the presence of *Populus nigra* was best described by relative plot elevation, however this variable was not significant. Independent variables which were not significant were added to the model when they improved the model by decreasing AIC values. For *Populus alba*, the best descriptors were plot submersion duration ($p < .05$) and overbank fine sediment thickness, which both showed negative slopes. *Salix alba* was more likely to be present on younger surfaces than on older ($p < .01$). *Fraxinus spp*. and *Fraxinus angustifolia* presence were best described by distance to the longitudinal dike ($p < .01$) and overbank fine sediment thickness. The best model for

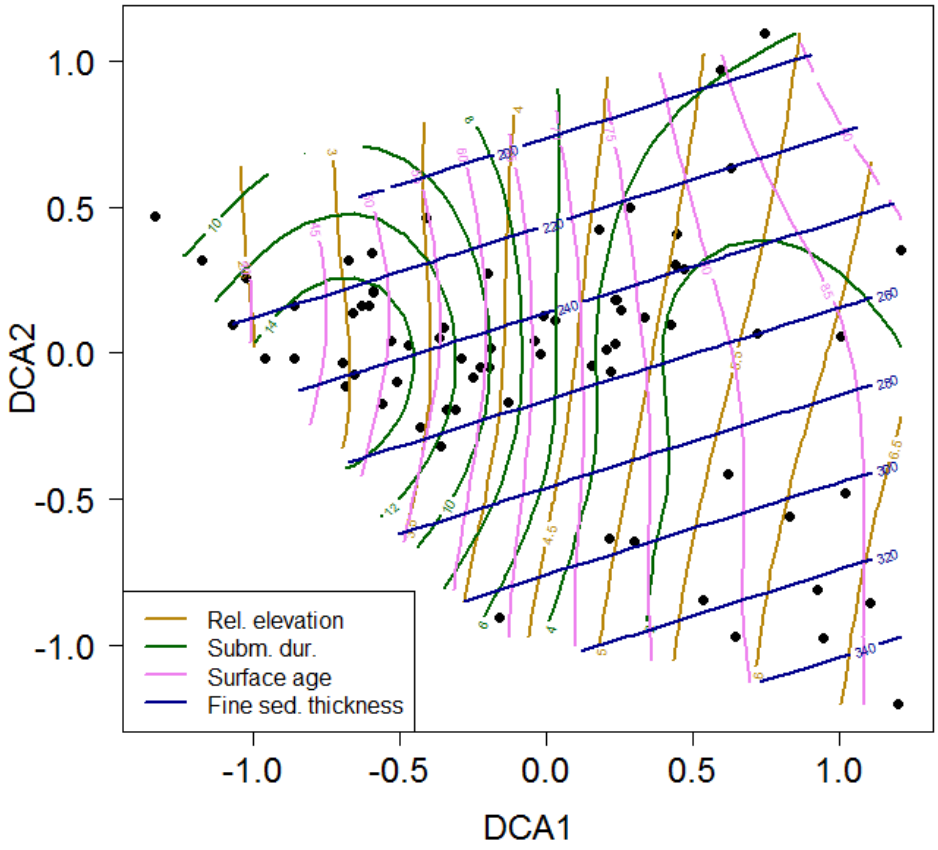

Figure VI–20: Surfaces of environmental variables fitted to ordinations of the DCA.

Fraxinus excelsior included overbank fine sediment thickness ($p < 0.01$), distance to the longitudinal dike ($p < .05$), relative plot elevation ($p < .05$) and plot submersion duration. *Robinia pseudoacacia* presence was best fitted by relative plot elevation, overbank fine sediment thickness, plot submersion duration and distance to the longitudinal dike, none of which were however significant. The models for *Acer negundo* and *Populus spp*. could not be improved by addition of the available control variables with reference to the null model. As we already saw, these species occurred over many plots, with the difference that *Acer negundo* presented a strong regeneration phase, whereas *Populus* was mainly represented by older individuals. Multicollinearity between the independent variables in the best models was not considered a serious issue, as all VIF values were < 5 (for all except 2 variables it was < 2), while as a rule of thumb a threshold value of 10 is generally considered in the literature. Akaike weights ranged between 0.29 and 0.60 for the best models of all species, showing low to moderate conditional probabilities for the models being favourable compared to the others. Pseudo R^2 values were low for most models, indicating a relatively low model fit.

Table VI–6: Results of logistic regressions per species using stepwise addition of multiple independent variables.

	Null Deviance	Residual Deviance	AIC	ΔAIC	Akaike weights
Populus spp.					
NULL	**9.96**	**9.96**	**11.96**	**0.00**	**0.60**
FineSed.Thickn.	9.96	9.74	13.74	1.78	0.25
FineSed.Thickn.+Subm.Dur.	9.96	9.63	15.63	3.67	0.10
FineSed.Thickn.+Subm.Dur.+Rel.El.100	9.96	9.32	17.32	5.36	0.04
FineSed.Thickn.+Subm.Dur.+Rel.El.100+Surf.Age	9.96	9.25	19.25	7.29	0.02
FineSed.Thickn.+Subm.Dur.+Rel.El.100+Surf.Age+Distance2L.Dike	9.96	9.21	21.21	9.25	0.01
Populus nigra					
NULL	41.65	41.65	43.65	2.30	0.11
Rel.El.100	**41.65**	**37.36**	**41.36**	**0.00**	**0.36**
Rel.El.100+Distance2L.Dike	41.65	35.57	41.57	0.22	0.32
Rel.El.100+Distance2L.Dike+Subm.Dur.	41.65	35.24	43.24	1.88	0.14
Rel.El.100+Distance2L.Dike+Subm.Dur.+FineSed.Thickn.	41.65	35.13	45.13	3.78	0.05
Rel.El.100+Distance2L.Dike+Subm.Dur.+FineSed.Thickn.+Surf.Age	41.65	35.12	47.12	5.76	0.02
Populus alba					
NULL	67.27	67.27	69.27	2.81	0.079
Subm.Dur.	67.27	63.13	67.13	0.67	0.23
Subm.Dur. (*) +FineSed.Thickn.	**67.27**	**60.46**	**66.46**	**0.00**	**0.32**
Subm.Dur.+FineSed.Thickn.+Rel.El.100	67.27	59.42	67.42	0.96	0.20
Subm.Dur.+FineSed.Thickn.+Rel.El.100+Distance2L.Dike	67.27	58.45	68.45	1.99	0.12
Subm.Dur.+FineSed.Thickn.+Rel.El.100+Distance2L.Dike+Surf.Age	67.27	58.32	70.32	3.86	0.05
Salix alba					
NULL	74.56	74.56	76.56	11.60	0.00
Surf.Age (**)	**74.56**	**60.96**	**64.96**	**0.00**	**0.35**
Surf.Age+FineSed.Thickn.	74.56	59.17	65.17	0.21	0.31
Surf.Age+FineSed.Thickn.+Distance2L.Dike	74.56	57.99	65.99	1.03	0.21

Surf.Age+FineSed.Thickn.+Distance2L.Dike+Rel.El.100	74.56	57.50	67.50	2.54	0.10
Surf.Age+FineSed.Thickn.+Distance2L.Dike+Rel.El.100+Subm.Dur.	74.56	57.47	69.47	4.51	0.04
Fraxinus spp.					
NULL	59.61	59.61	61.61	5.62	0.03
Distance2L.Dike	59.61	54.07	58.07	2.08	0.17
Distance2L.Dike (*) +FineSed.Thickn.	**59.61**	**49.99**	**55.99**	**0.00**	**0.48**
Distance2L.Dike+FineSed.Thickn.+Subm.Dur.	59.61	49.81	57.81	1.82	0.19
Distance2L.Dike+FineSed.Thickn.+Subm.Dur.+Surf.Age	59.61	49.29	59.29	3.30	0.09
Distance2L.Dike+FineSed.Thickn.+Subm.Dur.+Surf.Age+Rel.El.100	59.61	49.22	61.22	5.23	0.04
Fraxinus angustifolia					
Null	59.609	59.609	61.609	5.62	0.03
Distance2L.Dike	59.609	54.066	58.066	2.08	0.17
Distance2L.Dike (*) + FineSed.Thickn.	**59.609**	**49.986**	**55.986**	**0.00**	**0.48**
Distance2L.Dike+FineSed.Thickn.+Subm.Dur.	59.609	49.808	57.808	1.82	0.19
Distance2L.Dike+FineSed.Thickn.+Subm.Dur.+Surf.Age	59.609	49.290	59.29	3.30	0.09
Distance2L.Dike+FineSed.Thickn.+Subm.Dur.+Surf.Age+Rel.El.100	59.609	49.216	61.216	5.23	0.04
Fraxinus excelsior					
NULL	68.74	68.74	70.74	7.19	0.01
FineSed.Thickn.	68.74	60.51	64.51	0.95	0.18
FineSed.Thickn.+Distance2L.Dike	68.74	57.81	63.81	0.26	0.25
FineSed.Thickn.+Distance2L.Dike+Rel.El.100	68.74	56.68	64.68	1.12	0.16
FineSed.Thickn. (**) +Distance2L.Dike (*) +Rel.El.100 (*) +Subm.Dur.	**68.74**	**53.56**	**63.56**	**0.00**	**0.29**
FineSed.Thickn.+Distance2L.Dike+Rel.El.100+Subm.Dur.+Surf.Age	68.74	53.45	65.45	1.90	0.11
Acer negundo					
NULL	**41.65**	**41.65**	**43.65**	**0.00**	**0.51**
FineSed.Thickn.	41.65	41.05	45.05	1.40	0.25
FineSed.Thickn.+Rel.El.100	41.65	40.79	46.79	3.14	0.11
FineSed.Thickn.+Rel.El.100+Surf.Age	41.65	39.19	47.19	3.54	0.09
FineSed.Thickn.+Rel.El.100+Surf.Age+Subm.Dur.	41.65	39.18	49.18	5.52	0.03

FineSed.Thickn.+Rel.El.100+Surf.Age+Subm.Dur.+Distance2L.Dike	41.65	39.17	51.17	7.51	0.01
	Robinia Pseudoacacia				
NULL	45.30	45.30	47.30	16.51	8.91×10^{-05}
Rel.El.100	45.30	32.11	36.11	5.32	0.02
Rel.El.100+FineSed.Thickn.	45.30	27.21	33.21	2.42	0.10
Rel.El.100+FineSed.Thickn.+Subm.Dur.	45.30	23.26	31.26	0.46	0.27
Rel.El.100+FineSed.Thickn.+Subm.Dur.+Distance2L.Dike	**45.30**	**20.79**	**30.79**	**0.00**	**0.34**
Rel.El.100+FineSed.Thickn.+Subm.Dur.+Distance2L.Dike+Surf.Age	45.30	19.35	31.35	0.56	0.26

CHAPTER VII SYNTHESIS AND DISCUSSION

Résumé du chapitre VII : synthèse et discussion

Nous avons pu démontrer dans les chapitres précédents que les conditions de sédimentation et de l'atterrissement dans les casiers sont spatialement et temporellement complexes. Dans le chapitre VII, nous discutons d'abord la question de la diversité d'habitats dans les casiers. Les conditions planimetriques ne ressemblent pas aux conditions d'habitats complexes, surtout au sein de chaque secteur d'étude nous apercevons plutôt une homogeneisation des conditions. Rares sont les casiers aquatiques dont nous savons de la litérature qu'ils peuvent satisfaire certaines fonctions écologiques pour les poissons ou les macroinvertébrés. En revanche, en termes de topographie, les dépôts de sédiments des casiers sont relativement hétérogènes, indiquant des processus de sédimentation variables et potentiellement des héritages de processus à la fois du passé et plus récents. Les patrons d'atterrissement que nous avons observé peuvent être liées à différents processus, notamment la sédimentation et l'assèchement par abaissement de la ligne d'eau. Selon les casiers et les secteurs, les deux processus n'ont pas la même importance. Outre ces processus, nous avons vu que l'erosion joue également un rôle dans la modelisation de ces paysages de casier. Dans une analyse longitudinale, nous enregistrons des patrons locaux hétérogènes, similaire à ce que l'on avait pu souligner dans les chapitres précedents. Nous avons trouvé notamment des patrons sinusoïdals, qui ressortaient également dans une analyse à travers des trains de casiers.

Nos analyses comparatives à l'échelle des secteurs ainsi que les analyses multivariées ont montré une certaine importance des facteurs locaux. Surtout la connectivité des casiers au chenal court-circuité principal et les facteurs qui contrôlent cette connectivité. Les relations bivariées signalent tout de même des conditions plus complexes. L'analyse des patrons longitudinales dans chaque secteur nous a donné des éléments de clarification sur le rôle complexe de l'interaction des divers facteurs de contrôle tant dans l'espace que dans le temps. Ainsi, nous avons pu expliquer en partie l'hétérogénéité locale des patrons de sédimentation et d'atterrissement.

Malgré les conditions topographiques variables, nous avons observé une évolution relativement unidirectionnelle vers le boisement des casiers terrestres. Ces

boisements sont, en termes de composition, en transition de stades pionniers à des stades post-pionniers, à situer entre les deux sites de référence. Concrètement, les espèces pionnières, comme celles de la famille des Salicacées, sont présentes surtout parmi des strates plus vieilles, avec des diamètres plus importants, ainsi que dans le bois mort sur pied. A l'inverse, ce sont des espèces post-pionnières comme les frênes, des pionniers exogènes comme l'érable negundo (*Acer negundo*), et des espèces de sous-bois comme le cornouiller sanguin (*Cornus sanguinea*) ou le troène commun (*Ligustrum vulgare*) qui constituent les strates de régénération. Au longterme, un renouvellement des milieux est empêché par le manque de dynamique latérale. Ainsi il est très peu probable que de nouveaux habitats pionniers pourraient être créés sans intervention. En outre, les espèces exogènes prennent une place remarquable dans ces milieu anthropo-construits. *A. negundo* étant relativement résistant au stresse hydrique et aux conditions d'ombrage, il faut s'attendre donc à ce que les conditions dans les casiers pourraient être favorables pour cette espèce. D'autres espèces exogènes présentes, comme *Robinia pseudoacacia*, semblent être moins persistantes sur le long-termes sans intervention, mais pourraient éventuellement retrouver des conditions favorables lors d'une intervention.

1 Introduction

The results obtained in the context of this research provided a first broad overview of the present-day conditions (chapter IV) and the evolution (chapter V) of overbank fine sediment deposits within Rhône River dike fields. We could show that the complex planimetric and vertical patterns of sedimentation and terrestrialisation were related to varying processes during the evolution of the dike fields. In our comparative analysis, we could then shed some light on the drivers behind these patterns (chapters IV and V). For instance, we evidenced the varying roles of local and reach-scale drivers. We also saw that the non-stationary nature of the environmental conditions added to the complexity of the resulting patterns. The analysis of the forest stands was essential in that it provides a first more detailed description of the most prominent land cover type encountered in these ecosystems in their actual state (chapters IV and VI).

In this chapter we shall synthesise the most important findings and discuss them against the background of current research findings but also of the restoration and

mitigation works which have started being carried out. We shall also put the issue of the future of the dike fields in the wider perspective of these measures.

2 Dike field evolution: sustainable diverse habitats or homogenisation trend?

Both the literature review (especially Girardon, 1894; Bethemont, 1972; Salvador, 1983; Poinsart & Salvador, 1993) and the analysis of the dikes suggested that the construction of the final dike field units generally took several decades. During these periods, construction guidelines evolved along with the observed results. Especially over the first decades, hydraulic and morphological responses often diverged from the intended outcome. This guided following measures but has likely also left a legacy on the current morphology (Downs & Gregory, 2014; Brierley et al., 2010). It is difficult to take into account and to separate such imprints from the natural channel conditions prior to engineering works. In any case it must be expected that the sedimentation in the dike fields was also influenced by the hydraulic effects of these first engineering structures, which sometimes induced profound scour holes behind the dikes (Poinsart & Salvador, 1993). This was confirmed by GPR profiles carried out in 2017 in the framework of the 4th Rhône sediment observatory project (OSR4, '*Observatoire des Sédiments du Rhône*') (Piégay et al., 2018). The dike network resulting from this empirical 'learning-by-doing approach' is very heterogeneous, which also showed in the geometry of the dike fields in their present-day configuration (Figure II–4). Even more so when Girardon abandoned the systematic approach of constant dike geometries and configurations in 1884 (Girardon, 1894). But also as he was obliged to add his new approach to the existing heterogeneous engineering infrastructure. Experiences from the literature on the effects of tidal harbour, groyne field, spur dike fields, lateral cavity, and abandoned channel entrance geometry effects (Langendoen, 1992; Uijttewaal et al., 1999; Uijttewaal et al., 2001; Sukhodolov et al., 2002; Le Coz et al., 2010; Mignot et al., 2013), as well as on the effects from different design characteristics of the engineering structures themselves (Vaghefi et al., 2009; Henning & Hentschel, 2013;) led us to expect heterogeneous hydraulic conditions and consequently diverse sedimentation and erosion patterns. If this was the case, would such heterogeneous conditions provide any potential habitats which would otherwise remain lost if no further interventions were carried out? Or are conditions rather

homogenising over time as natural processes which could rework the actual state are inhibited? Similar as on other large rivers, huge areas of floodplain on the Rhône River have been completely lost due to conversion to agricultural land, settlement or industry. In the remaining, spatially very restricted floodplains, including the dike fields, the natural processes and functioning have been heavily modified as a consequence of the two major engineering phases (Fruget, 2003). In chapter I, we had shortly described the diversity of habitat and ecotone conditions in natural floodplains (Figure I–1). The two-scale approach we have adopted in our work allows us to evaluate the question of potential habitat diversity related to the dike fields from two points of view: based on our results, first, we shall describe whether this distinct morphological unit, which is extensively present along the entire Middle and Lower Rhône, has in itself a potential to offer diverse, natural, representative, rare or specific habitat conditions (conservation values *sensu* Dunn, 2004; Muhar et al., 2011). This part focuses on our comparison of dike fields among each other. Second, in a more global context of restoration and mitigation actions currently carried out along the Rhône, do dike fields contribute to a diverse riparian zone and/or as a migratory axis to the green infrastructure? Here, we build the bridge between dike fields and other natural/artificial geomorphic units (remaining and restored islands, abandoned channels, mature floodplains), reflecting also the inherent conditions of the reaches. This is based on a more global perspective of habitat variability along the entire Rhône corridor, to which we can contribute with our inter-reach analysis results. Both reflections are fed by our interpretations of potential pattern-process relationships and the respective roles of the analysed control factors.

2.1 Inter- and intra-reach habitat variability

The planimetric analysis of the dike fields revealed a gradient of conditions in the years 2000 between fully aquatic and fully terrestrial. However, the relative abundance of fully terrestrial dike fields was high, while semi-terrestrial and fully aquatic dike fields were rare. Overall, there is thus an obvious trend of a homogenisation of planimetric conditions, diverging from the initially aquatic toward fully terrestrial conditions. This trend culminated in a dense vegetation cover, primarily forest stands, in most dike fields (Figure IV–23 and chapter V). These findings are consistent with observations from Piégay et al. (1997) at PBN and Gaydou (2013) along the Middle and Lower Rhône. Adding the historical dimension, we saw that in the 1940s, the variability in

terrestrialisation stage was highest within each of the four reaches. In contrast, in the 2000s, reach-scale conditions were so advanced and homogenised that between-reach differences were accentuated: PBN and MON were more advanced than DZM, and there was a particularly marked difference to PDR, which still showed some more aquatic patches (Figure IV–12 and Figure V–1). Several studies on aquatic and semi-aquatic dike fields of the Total Rhône and in the by-passed reach of PDR revealed a potential of these artificial wetlands as nursery sites, refuge during disturbance events, and feeding grounds for fish and macroinvertebrates (Franquet et al., 1995; Nicolas & Pont, 1995; Poizat & Pont, 1996; Nicolas & Pont, 1997; Franquet, 1999; Gandouin et al., 2006; Thorel et al., 2018). Thorel et al. (2018) highlighted the link between macroinvertebrate α-diversity and hydrological connectivity. The dike fields also provide a habitat for phytoplankton (Thorel et al., 2018). Thermal conditions are generally higher in the lentic dike fields than in the main channel of the Rhône, although some showed rare colder spots, which were probably related to upwelling groundwater (Thorel et al., 2018). Aquatic zones in dike fields might therefore contribute to a diversification of conditions. Similar observations regarding potential ecological functions of engineering structures have been made in spur dike fields on the Missouri River and Mississippi River (Burch et al., 1984; Shields, 1995), related to individual groynes on the Blackledge River and Salmon River (Thomson, 2002), or groyne fields along the Elbe River (Wirtz, 2004; Henning & Hentschel, 2013) and the Danube (Tritthart et al., 2009).

Although planimetric conditions in the dike fields were thus rather homogeneous, field observations suggested that morphological processes and resulting reliefs still showed some heterogeneity. The topographic characteristics extracted from the LiDAR-data-based DEM indeed showed more diverse patterns. In some dike fields, sediment deposits had filled up the entire space homogeneously without much relief or only one major slope between pre- and post-dam surfaces (Figure VII–1). Others showed heterogeneous reliefs. For instance, some dike fields demonstrated a distinct legacy from original channel conditions, especially the imprint of former side arms was often still well distinguishable. In others, the hydraulic conditions which prevailed since the installation of the dikes left distinct patterns in the form of scour holes or overbank flood channels and distinct localised deposits. Brierley (2010) emphasises the influence of the ‘landscape memory’, with both its natural (geologic and climatic) and anthropogenic components, in shaping contemporary form-process relationships. We

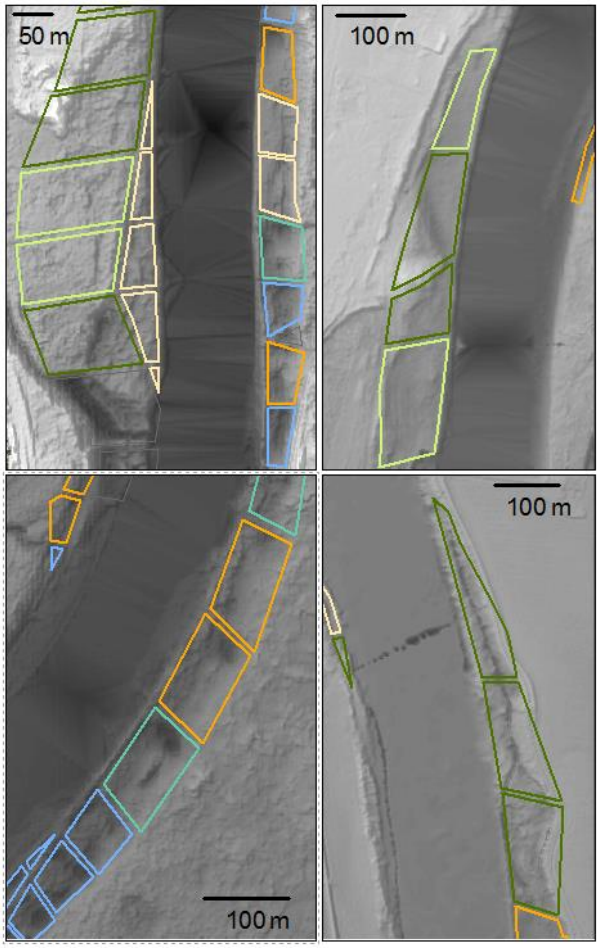

Figure VII–1: Topographic variability of sediment deposits in dike fields illustrated by digital elevation models. The colours of the dike fields correspond to the clusters from the combined PCA and clustering analyses. Top left: Organisation of the clusters in short sub-units of larger sequences. Top right: homogeneous planar deposits in the two light green dike fields (cluster 7). Bottom left: several dike fields with plunge pools below the upstream lateral dikes. Bottom right: dike fields with probably unidirectional flow within flood channels.

shall discuss this notion in more detail in section 3 where we focus on the drivers of sediment deposition.

Regarding topographical aspects of the dike field deposits, within-reach variability was more pronounced than between-reach variability. The longitudinal analysis of terrestrialisation patterns opened up some more insights on the spatial organisation of the remaining variability. Instead of finding an initially expected pattern which would follow the concavities and convexities of the river channel, it highlights recurring sinuous patterns of smaller extent than the river bends. When considering longitudinal patterns of terrestrialisation along all individual dike field sequences, we again encountered certain sinuous patterns (Figure VII–2). These patterns were not the same in the four reaches, and neither between variables. However, the sinuous patterns also

seem to be in accordance with our principal component analysis (PCA) and hierarchical clustering results: the spatial distribution of dike fields belonging to the various clusters has likewise shown an organisation of similar conditions over short sequences of a few dike fields (Appendix IV: Figure A–IV–2). Such patterns are also observed in other works currently carried out on the dike fields (Seignemartin, in prep).

A pilot analysis of twenty surface sediment samples taken from the sampling plot centres during our field campaign revealed generally that generally sandy-silts prevailed but that conditions were relatively variable (Appendix IV: Figure A–IV–1). Qualitative observations during sampling (throughout the vertical profiles from the surface to the gravel layer) suggested that this variability prevailed both horizontally within and between dike fields, and vertically through the profiles. Preliminary findings from a more detailed analysis of the samples by Seignemartin (in prep.) point into the same direction. Beyond this, our observations are in accordance with results from Clozel-Leloup et al. (2013) on a dike field at PDR and from Roditis & Pont (1993) on dike fields along the Total Rhône near Arles.

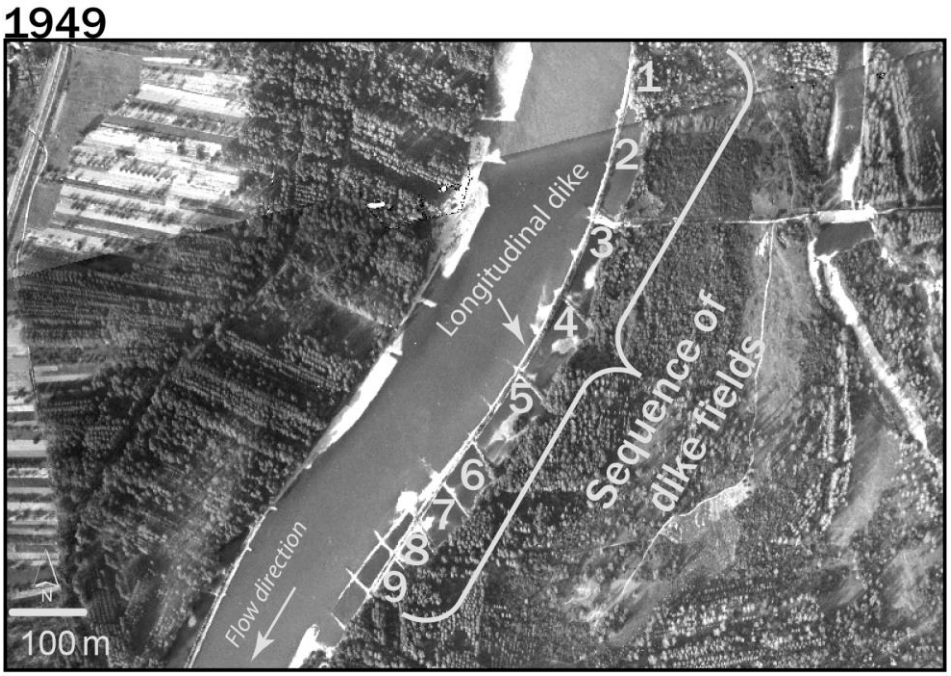

Figure VII–2: Concept of a sequence of dike fields.

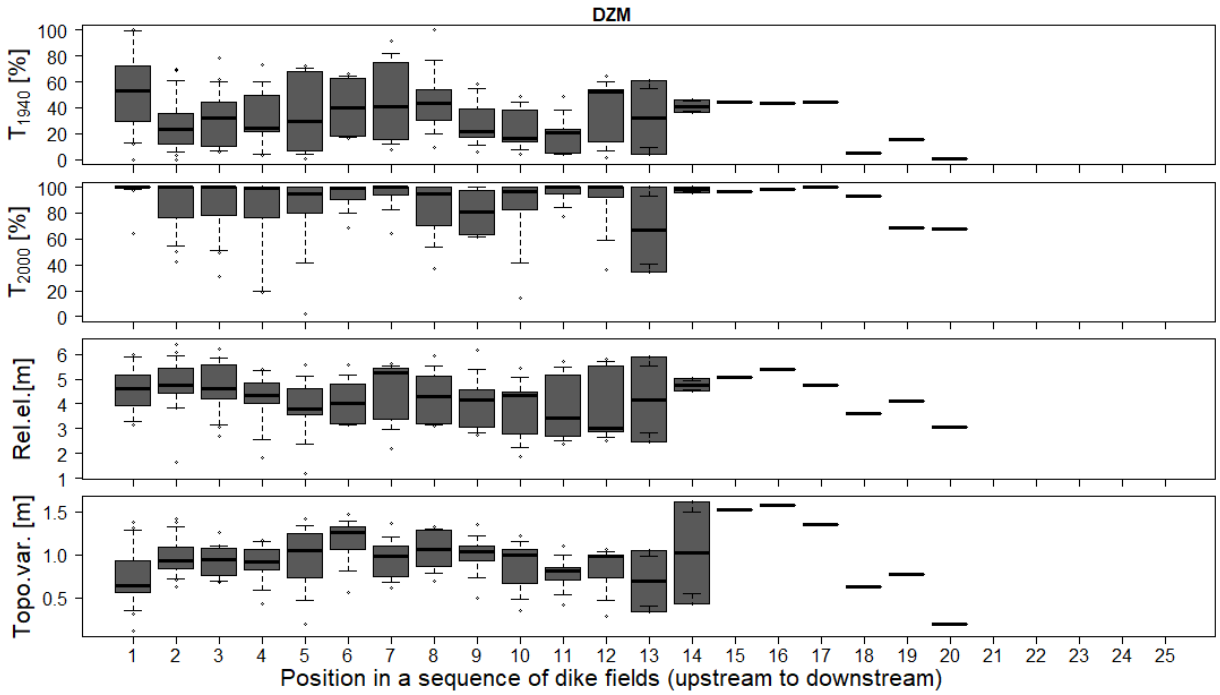

Figure VII–3: Longitudinal analysis of sedimentation and terrestrialisation patterns along sequences of dike fields (position 1=farthest upstream, position n = farthest downstream). Example of DZM (for the other study reaches see Appendix IV, Figure A–IV–3).

In summary, we saw that the largest part of the dike fields was completely terrestrial in the 2000s and only rarely on a gradient between aquatic and semi-aquatic. From a connectivity and habitat successional stage perspective (Amoros et al., 1987), most of the dike fields therefore do not seem to contribute to diversify conditions along the Rhône River. Neither to the within- nor the between-reach habitat diversity. Inversely, the lateral connectivity and resulting ecological conditions were indeed variable between the few aquatic dike fields (Thorel et al., 2018). Since we found higher amounts of aquatic dike fields at PDR and DZM than at PBN and MON, this local diversity might not only play a role between different dike fields within a reach, but also at the between-reach-scale.

2.2 From pattern to process

The reach-scale analyses manifested patterns of terrestrialisation which led to the hypothesis of varying evolutionary processes. In particular, we saw that PBN and MON dike fields were highly terrestrial in the 2000s, while the thickness of their sediment deposits remained noticeably below that of the reaches of PDR and DZM. The latter two reaches, instead, were characterised by more frequent remaining aquatic

surfaces, while their sediment deposits were considerable. We assume that at PBN and MON the high terrestrialisation state was accelerated mainly by the process of dewatering related to dropping water levels and only secondarily due to sediment accretion. Depret et al. (2017) observed corresponding processes in abandoned channels situated in by-passed channels. At PDR and DZM, sediment accretion played a more important role in the terrestrialisation process, next to dewatering from water level decreases. At high connectivity, we further hypothesise that erosion processes might locally predominate over sedimentation processes, creating permanent scour holes. However, we saw that the topography of the deposits was influenced by several factors, including legacies from past processes. Moreover, the LiDAR data-derived digital elevation models would not take into account the bathymetry of the aquatic dike fields. We are thus currently unable to establish direct relationships between the degree of terrestrialisation and topographic patterns. Studies on groynes however strongly suggest that according to the water level and thus the degree of emersion or submersion of engineering structures, hydraulic conditions may change from jet-like circulation currents to wake-type turbulent structures (Huang & Dong, 1999; Uijttewaal et al., 2001; Sukhodolov, 2014). Scour and sedimentation in the two circumstances do not occur in the same spatial arrangement. We believe that both the lateral and longitudinal dikes strongly influenced the spatial patterns of erosion and sedimentation in the dike fields, depending on the dominant processes of connection—submersion, passages, seepage (Figure IV–8).

Similarly, the variability of topographic patterns between dike fields is an indicator that both sedimentation and erosion processes occurred within the dike fields. Their patterns seem complex and not necessarily played the same roles, respectively, in each dike field. Several authors underlined the influence of the local microtopography and related inundation times, flow direction and velocities, as well as water column depth on sedimentation rates (Asselman & Middelkoop, 1995; Walling & He, 1998; Thonon et al., 2007). There is thus likely a complex interaction between historical bed forms (legacy from former fluvial processes and first engineering infrastructure; Brierley, 2010) and contemporary processes of sedimentation and erosion. Intrigued by the high spatial variation of topographic forms and potentially related processes within the reaches, we initiated an analysis of intra-dike field patterns to assess the localisation of remaining water surfaces or depressions. Some preliminary results are summarised in Appendix IV.

3 Individual roles and interactions of the various drivers

Two aspects made direct relationships between terrestrialisation patterns and the studied drivers little evident: first, the cumulative impact of several drivers, as well as their own evolution through time. We saw that drivers can have synergistic, antagonistic, or additive effects (Tockner et al., 2010), which was confirmed in the longitudinal analyses, which also stresses the chronologic sequence of influences. Second, the highly advanced terrestrialisation state of the dike fields inhibited the distinction of finer nuances in the process-form relationship. Using the comparative approach facilitated the disentangling of the effects and aided our interpretation of patterns and processes.

3.1 Reach-scale drivers

Several authors found differences in the terrestrialisation rates of abandoned side arms on the Rhône between sites upstream and downstream of the Isère, which contributes an important amount of suspended sediment to the Rhône (Depret et al., 2017; Riquier et al., in prep.). These analyses included three of the by-passed reaches of our study. With these results, the authors highlighted the influence of the suspended sediment flux to the by-passed reaches. In the dike fields, we did not observe such a pattern. Instead, we saw in section 2.2 that the two process-patterns (1. high planimetric terrestrialisation status + low vertical sedimentation (PBN, MON) and 2. low planimetric terrestrialisation status + high vertical sedimentation (PDR, DZM)) were each found in reaches located upstream as well as downstream of the Isère River. Le Coz (2007) observed at the example of PBN, that downstream of the confluence of the Rhône River and the Saône River, the suspended sediment load contributed by the Saône during a flood did not directly mix with the Rhône water. Instead, the load was carried in a distinct current over several kilometres, a phenomenon well known from other rivers, such as the Rio Negro and the Rio Solimões which after their confluence form the Amazon River. The Saône sediment flux was almost entirely injected into the by-passed channel of PBN, located a few kilometres downstream of the confluence. Conditions at the diversion dams on the Rhône, where the flows are routed into either the by-passed channels or the diversion canal, are probably complex and depend on several factors, including specific local conditions as well as prevailing discharge conditions.

3.2 Local factors

The importance of the lateral connectivity between the river channel and its floodplain for the natural functioning of the latter has often been stressed in the literature (Junk et al., 1989; Ward, 1998; Tockner & Stanford, 2002; Wiens, 2002; Opperman et al., 2009 and 2010). As river channels adjust their geometry as a response to river training (generally by degradation), diversion, or aggregate mining, the frequency of this connection is reduced, limiting interactions and reducing sedimentation (e.g. Kondolf, 1997; Wyżga, 2001b). This phenomenon seems to be at the root of the patterns we observed at PBN and MON, which showed high terrestrialisation and low sedimentation. Indeed, we have shown that in both reaches the by-passed channels degraded early on, following the installation of the dikes (Figure V–10a). At PBN this was particularly pronounced as degradation continued also following diversion (Figure V–10b). The related drop in the water level could obviously explain the dewatering of the surfaces and the reduced sedimentation compared to the other two reaches. The latter also experienced diversion, as did PBN and MON, however degradation was less pronounced and they even locally experienced aggradation (Figure V–10a,b). This could partly explain why sedimentation was more substantial at PDR and DZM. Through the reach-scale analyses we hence gained some first insights concerning the drivers of terrestrialisation patterns. However, the weak bivariate relationships between drivers and response variables (e.g. Figure V–21) indicated a much more complex picture. It was only with the combined investigation of local-scale spatio-temporal patterns in a longitudinal analysis that we could further unravel and explain some of this complexity (Figure V–24, Figure V–25, Appendix II). In particular, we could show that conditions are spatially highly variable and highly dependent on the specific history and generally the combined effects from several drivers. The various drivers could override the effects of each other over time and depending on the location and chronology of events this could even lead to inversed tendencies within one and the same reach. These aspects explain the weak bivariate relationships between drivers and responses. Still not all patterns could be explained by the drivers we analysed, and some discrepancies and divergence remain, especially in the longitudinal analysis. Two patterns from this analysis shall be discussed in the following: first, local conditions seemed to play an important role, as we just mentioned. Second, we recurrently observed sinuous patterns suggesting gradients of comparable conditions over small sub-units of a sequence of dike fields, as mentioned in section 2.1 of this chapter. Considering other

geomorphic units which have a functioning similar to that of dike fields might aid our understanding of the local controls.

For instance, the evolution of restored side channels on the Rhône River in terms of sedimentation rates and grain size characteristics, can today be relatively well predicted based on the duration of lotic functioning of the channel [days/yr], maximum recorded shear stress since restoration and backflow capacity (Riquier et al., 2015, 2017). In dike fields, flow conditions are potentially more complex, as indicated our topographical analyses and field observations. In some of them, predominately unidirectional flows seem to occur (Figure VII–1, bottom right) as is also the case in side channels. Others which show homogeneous deposits perhaps rather resemble vertically accreting floodplains and the diffuse flows related to them (Figure VII–1, top right). Hydraulic conditions in the main by-passed channel seemed to follow the sinuous patterns of the sedimentation / terrestrialisation variables from the dike fields (Figure V–24, Figure V–25, Appendix II). Next to the aspect ratio (=width to length ratio) which controls the hydraulic conditions within groyne fields, Uijttewaal (1999) pointed out the role of the position of a groyne field in a sequence of groynes. He found that "[t]he shear layer present at the interface between the river and the groyne field broadens with downstream position, partly due to large turbulence structures that are generated in the shallow shear flow, and leads to a more smooth exchange flow." (Uijttewaal, 1999, p. 1). Uijttewaal et al. (2001) confirmed these results, as well as later studies (Constantinescu et al., 2009; Sukhodolov, 2014). These observations may not be directly applicable to the Rhône dike fields, due to the combined effect of the longitudinal and lateral dikes. Yet perhaps larger-scale hydraulic structures might also be generated by them. This could further be influenced by the fact that longitudinal dikes were, at least in later periods, adapted in height from their ends towards the centre (Girardon, 1894). And also the local passages discovered on many dikes might add some complexity to this. The wave patterns did not follow the same up and down movement in the four reaches. However, the authors of the groyne field studies suggested that the mixing layer increased from the first to approximately the third or fifth groyne field. Downstream of approximately the fifth field, this growth ceases (Uijttewaal et al., 2001; McCoy et al., 2008; Constantinescu et al., 2009). Further analyses are necessary to evaluate the potential existence of such broader hydraulic structures along longitudinal dikes on the Rhône, as well as their implications for sedimentation patterns.

In the principal component analysis (PCA) we saw a relationship between the topographic variability of the overbank fine sediment deposits and the size of dike fields (Figure IV–25). This relationship might be a result of the legacy of former channel patterns, as we found larger dike fields in the main channel than in the former side channels (Figure VII–4). Since variability increases with dike size rather than decreases, we suppose that it is not related to the impact of the dikes, which may produce local scour depending on how they are emerged or submerged and when (Yossef & de Vriend, 2010; Sukhodolov, 2014). Instead, findings from the literature on similar geomorphic units suggest that unit geometry influences the number of vortices produced within a field, notably the width to length ratio (Uijttewaal et al., 1999; Uijttewaal et al., 2001; Sukhodolov et al., 2002; Le Coz et al., 2010). These studies also showed that the relationship was not linear, as seems to be suggested by our PCA.

3.3 Temporal dimensions

The chronology of events seems to play an important role for the evolution of the dike fields and we saw that the four study reaches do not show the same order of events, nor the same drivers (Figure VII–5). The longitudinal analysis showed that according to the initial conditions in and around the dike field, the nature of the drivers, and the chronologic order of the inset of each driver the responses would not be the same. Additionally, the duration of the impact probably also plays a role.

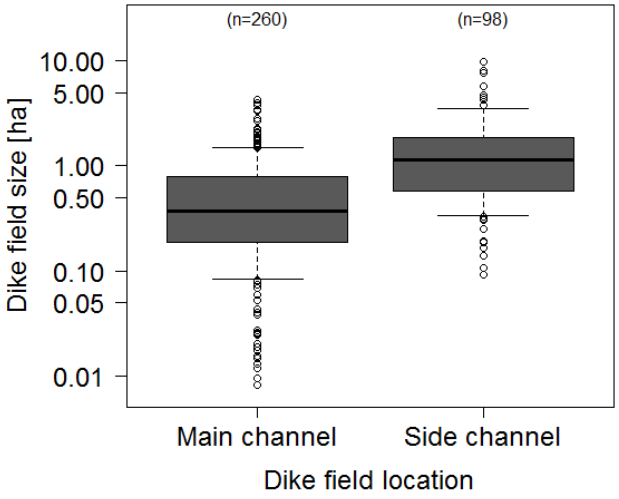

Figure VII–4: Comparison of dike field size between main channel and side channel locations.

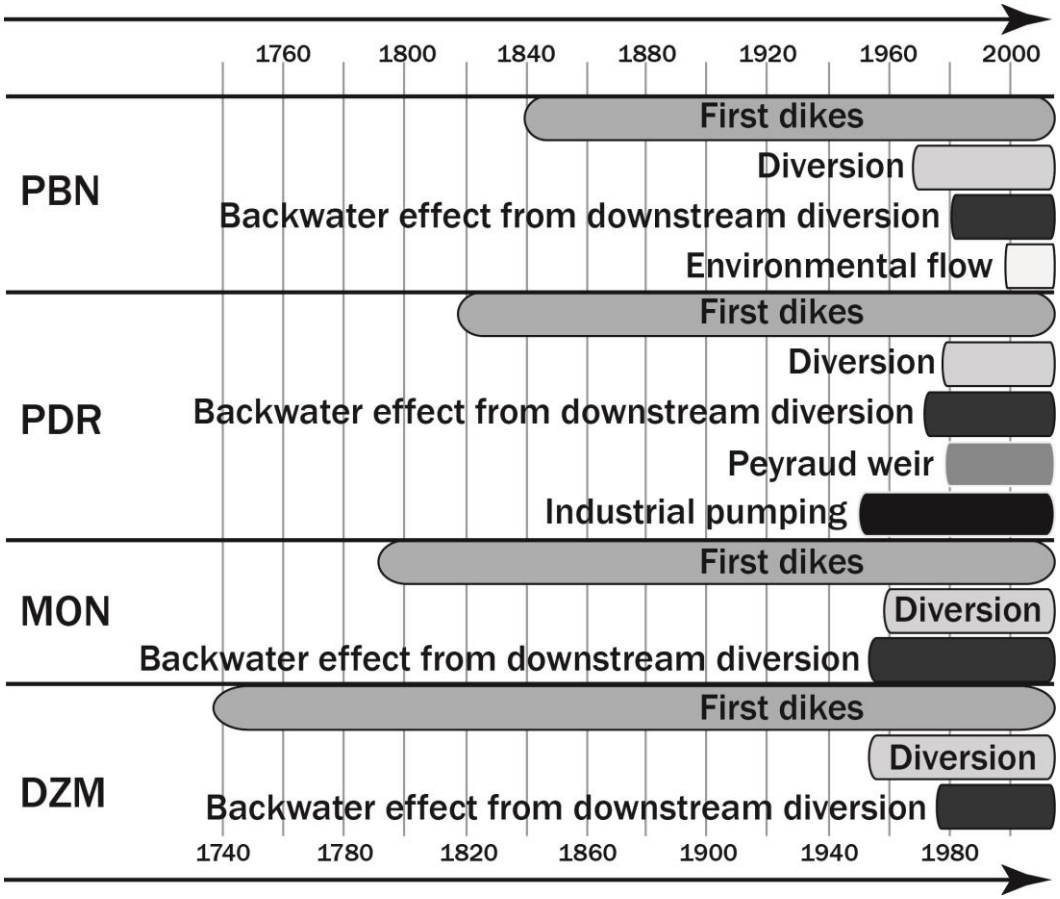

Figure VII–5: Chronologic order of some of the drivers identified to act in the various reaches.

3.4 Refining the conceptual model

In summary, our analyses confirmed that bed level change, diversion and dam operation, local water level controls played a role on the local scale in the evolution of the dike fields. They influenced the connectivity characteristics, but also shear stresses associated to connecting flows. In addition, we saw that also the backwater effects from downstream diversion schemes and especially the historical dimension. The literature strongly suggests that also the other drivers of our model play their role. Instead of a fixed hierarchy in the drivers, we observed varying relationships which were highly dependent on the specific location and chronological history of environmental conditions (Figure VII–6).

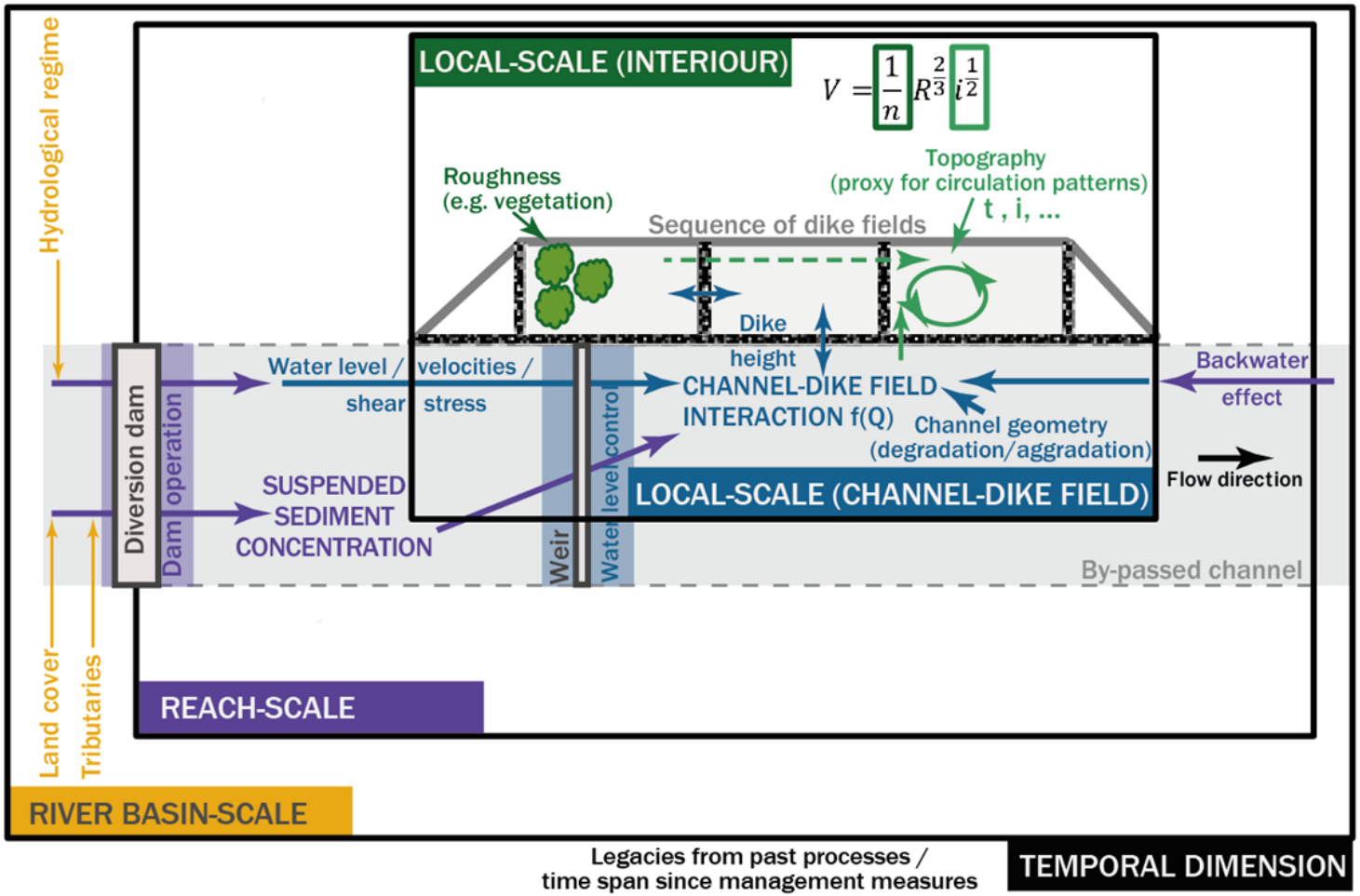

Figure VII–6: Conceptual model of potential drivers of sedimentation and terrestrialisation.

4 Dike field forest stands: closer to novel than to near-natural ecosystems

The sets of comparative and multivariate analyses of dike field forest stand structure and composition revealed several peculiarities. Mean stem diameters and mean stem heights, as proxies of age, were larger and higher, respectively in dike fields compared to both mature and pioneer references. Moreover, they were larger and higher, respectively, on younger, i.e. post-dam surfaces than on older pre-dam surfaces. Inversely, total plot densities were lower in dike fields, than in reference sites. There was no difference between pre- and post-dam surfaces. Furthermore, pioneer species in dike fields were present primarily in mature stages and rare or non-existent in the regeneration stage. Instead, post-pioneer species and a strong presence of non-native species were recorded. Beyond this, the composition of dike field forests resembled mature reference sites more than pioneer sites, yet several gradients were detectable throughout the dike fields, as depicted by the multivariate analyses: a) the composition of pre-dam surfaces (except MON) was closest to mature units, while post-dam surfaces had a more central position between mature and pioneer references.

4.1 In transition to post-pioneer stages

The dike fields seem to be in transition from pioneer to post-pioneer stages. First, we saw in the descriptive and multivariate analyses that the species pool was made up of both pioneer and post-pioneer species (Figure VI-1). Second, analysing diameter at breast height (DBH) frequency distributions of the dominant species (Figure VI-15) evidenced patterns of aging stems for native pioneers and primarily young stems for native post-pioneers: we found principally bell-shaped distributions for *Populus spp*., with maximum frequencies around 40 cm DBH on pre-dam surfaces and 50 cm DBH on post-dam surfaces. A similar pattern was shown for *Salix alba*. *Fraxinus spp.* in contrast showed right-skewed and reverse J-shaped distributions on the two surfaces, respectively. Third, we registered the upcoming of understorey species, such as *Cornus sanguinea*, *Crataegus monogynya,* and *Ligustrum vulgare*, primarily on pre-dam surfaces but starting also on post-dam surfaces. Indeed, in the same plots over the four study reaches, Gruel (2014) found that median soil cover values of the shrub layer ranged between approximately 40% (at PDR) and 70% (at DZM) on pre-dam surfaces.

On post-dam surfaces median values ranged between 5% (at PDR) and 25% (at MON). He also found that median liana coverage of the trees was between approximately 20% (at MON) and 50% (at DZM) on pre-dam surfaces and between approximately 0% (at PBN and PDR) and 30% (at DZM) on post-dam surfaces. The lianas consisted primarily of *Hedera helix* and *Vitis vinifera*. These observations stand for stabilising conditions on pre-dam surfaces, with similar tendencies on post-dam surfaces. In summary, we thus see dense multi-layered canopies, especially on pre-dam surfaces, but potentially initiating also on post-dam surfaces.

Hence, some evidence is given for pre-dam surfaces in dike fields to be in an established forest phase (*sensu* Muñoz-Mas et al., 2017): The canopy cover is potentially high (Modrak, 2013) and it is multi-layered. Our field observations also suggest that disturbance frequency is reduced, evident from the often thick herbaceous layer on the ground, and a soil A horizon was often observed on top of the overbank fine sediment (Figure VII–7a). The tree layer is dominated by macrophanerophyte *Populus* and *Fraxinus*, although next to *Acer negundo* and *Robinia pseudoacacia*. A shift in the understorey toward shade tolerant and slow-growing species, including *Ulmus* and *Quercus* is likewise observed (Figure VI–1). Differences to the mature forest phase were evidenced in the comparative and multivariate analyses between dike fields and mature reference sites. They suggested that total plot stem densities in dike fields were still lower than in the mature reference (Figure VI–4), particularly due to lower sapling stem densities (Appendix III: Figure A–III–1). Species diversity was likewise slightly lower, although not significantly (Figure VI–6). Some particularities however remain: the biomass of individual stems might be higher than in mature sites, as suggested diameter at breast height (DBH) and height data (Figure VI–4). Considering the stem density particularity just mentioned, the total plot biomass may as a result still be comparable between dike fields and mature sites, however based on two different structural patterns. Additionally, species richness was higher on pre-dam than on post-dam surfaces, except at MON. The opposite is generally the case (Trémolière et al., 1998). Another particularity might be the mortality of trees in the dike fields. Naiman et al. (2005) related the coexistence of large living old trees, large dead standing trees and dead logs to the mature forest stage. Indeed, a large range of stem diameters is noticed for standing dead stems in dike fields (Figure VII–8). Particularly on pre-dam surfaces, we see many stems of low DBH, and thus potentially low age, which have declined, but we also find significantly larger stems.

Pioneer species have obviously been present more abundantly and have started to decline. We find evidence of *S. alba* amongst the dead standing trees, which is no longer present amongst living trees on pre-dam surfaces of some sites. But also some non-native species show high mortality. Most standing dead stems were counted at DZM-B and PBN-B. Lowest frequencies were recorded for PBN-C and PDR-C. For all four reaches, mortality was distinctly higher on pre-dam than on post-dam surfaces, even at MON. The detrended correspondence analysis (DCA) confirmed that pre-dam sites were close but still distinct in their composition to the mature reference. MON pre-dam sites were still further apart.

Post-dam surfaces can probably likewise be characterised as being in the established forest phase (*sensu* Muñoz-Mas et al., 2017). Yet, on a gradient, they would be situated further at the beginning of this phase compared to pre-dam surfaces. This classification

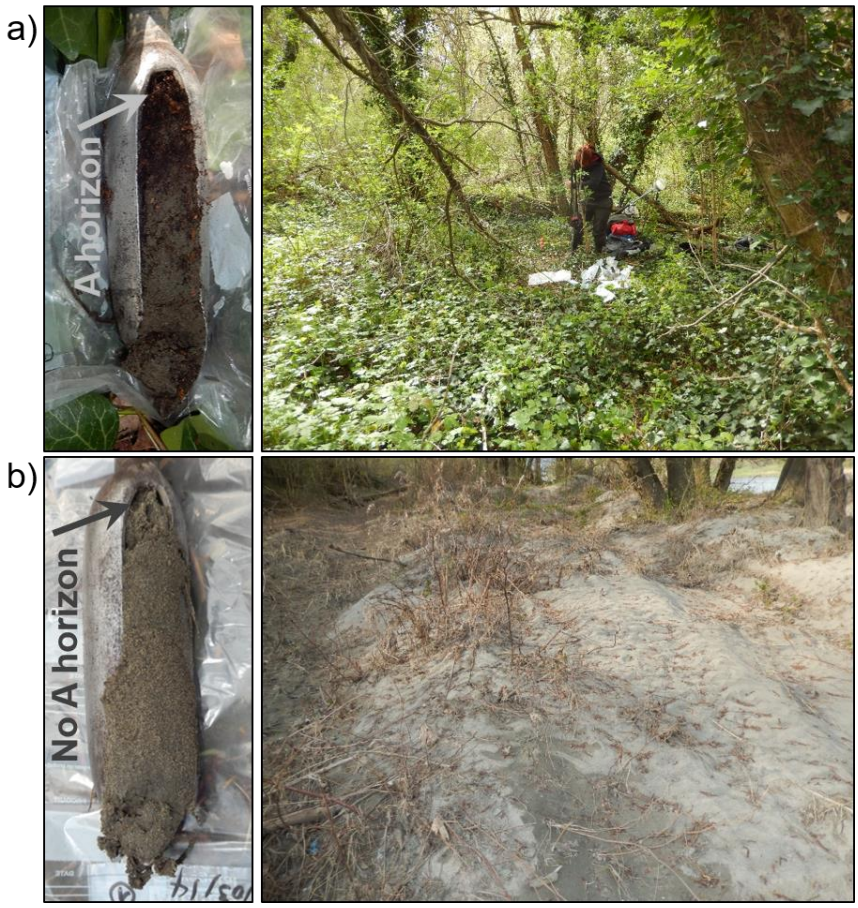

Figure VII–7: a) Example of pre-dam surface conditions (DZM reach). Left: Surface sample from a sampling plot centre. Right: ground surface conditions in the same plot. b) Example of post-dam surface conditions (MON reach). Left: Surface sample from a sampling plot centre. Right: ground surface conditions in the same dike field. All four photos were taken in the course of two days in mid-March 2014.

is evident in terms of composition from the principal component analysis (PCA), where post-dam sites were rather centred between mature and pioneer sites. They still show a beginning understorey shift with *Ulmus* and *Quercus* starting to be present particularly in the regeneration stages (Figure VI–1). The canopy is also starting to be multi-layered and the tree layer is dominated by the single-stem macrophanerophytes *Populus spp*., *S. alba*, and mesophanerophyte *Acer negundo*. However, stem densities, DBH, and stem height were still relatively distinct from both pre-dam surfaces and mature reference sites (Figure VI–4 and Appendix III: Figure A–III–1). DBH and height were higher, while densities were comparable to or only slightly lower than pre-dam dike field surfaces. Furthermore, disturbance is often still evident on the ground surface and an A horizon is not often observed (Figure VII–7b). These factors again point out the peculiarities of the dike fields, although some characteristics overlap with reference systems. Mortality seemed to be equally frequent for different DBH classes and thus age classes on post-dam surfaces. *R. pseudoacacia* dead stems were rare (Figure VII–8), and we saw in chapter VI that it was not abundant amongst living trees either (Figure VI–1).

Although we saw evidence of some sort of fluvial dynamics in dike fields, particularly on post-dam surfaces, and even local scouring processes (Figure VII–1), an actual reworking and turnover of deposits and related forest stands is impeded in these fixed environments (Fruget, 2003). Apart from the terrestrialisation of the last remaining aquatic surfaces in the dike fields, no further suitable pioneer vegetation habitat is expected to be created. We saw in chapter I that it requires bare moist sediment for pioneers such as Salicaceae species to successfully establish. On braided rivers, floodplain turnover rates can be in the order of a few years or decades, creating regularly suitable pioneer habitat and a mosaic of vegetation patches of very young mean age (Beechie et al., 2006, Ward et al., 2001; Surian et al., 2015). Meandering rivers show intermediate turnover rates, generally in the order of several decades (Beechie et al., 2006). Both channel patterns were formerly encountered on the Rhône River. Instead, since the major engineering works, we saw a one-sided trend of floodplain encroachment by vegetation in the dike fields, followed by a succession trend. This trend of disappearing pioneer habitats is observed along the entire Rhône corridor (Bourdin, 2004, cited by Dufour 2005 p. 181).

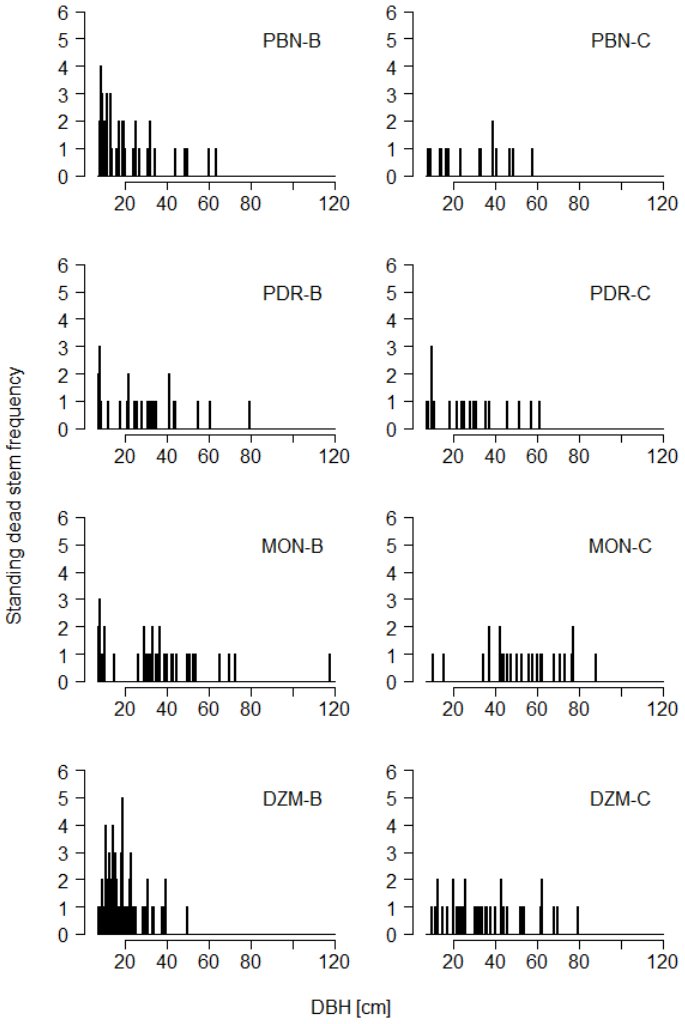

a)

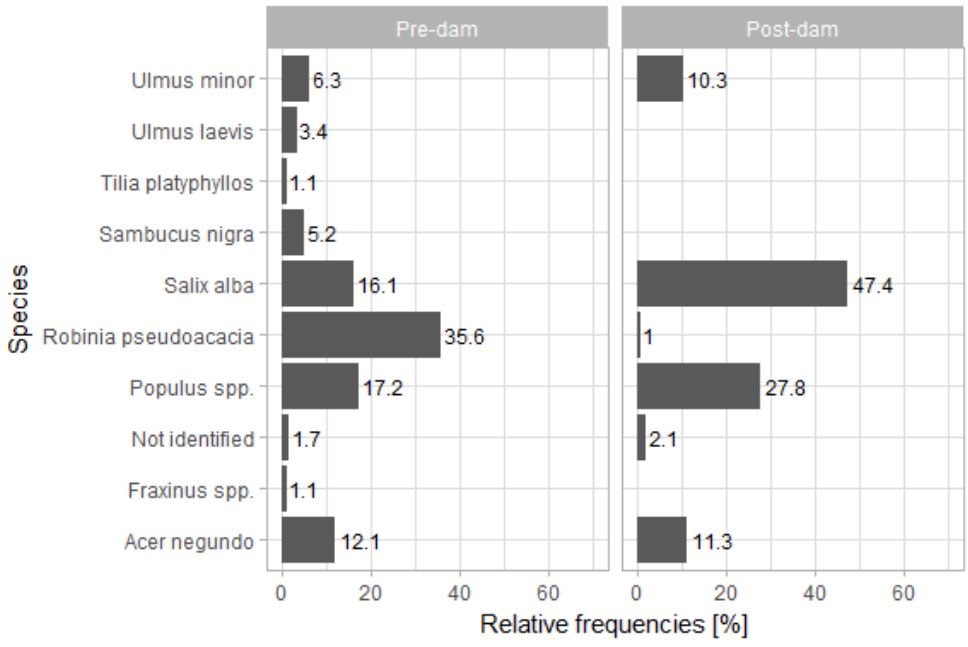

b)

Figure VII–8: a) Stem frequency distributions according to DBH classes. b) Comparison of the occurrence of standing dead stems per species between pre- and post-dam surfaces.

4.2 Spread of non-native species

One notable pattern in the dike fields is the spreading of non-native tree species. Such spreading has been documented for other anthropogenically impacted river systems (Glenn & Nagler, 2005; González-Muños et al., 2014). The most prominent non-native species in the dike fields was by far *Acer negundo* (Box alder). This species was strongly represented in all three life history stages and it made up the largest part of all seedlings (Figure VI–1, 64.1% of all seedlings on pre-dam surfaces and 96.7% on post-dam surfaces). Frequency distributions of diameter classes demonstrated that at the tree life history stage, it was represented primarily by young trees (bimodal distribution on pre-dam surfaces, right-skewed or reverse J-shaped distribution on post-dam surfaces, both with diameters primarily < 50 cm). Logistic regression showed no specific habitat preferences for *A. negundo*. Indeed, it was present in 92% of all study plots and therefore covered almost the entire range of conditions of the input variables. González-Muños et al. (2014) demonstrated that this species does not necessarily show any superior characteristics over native species. However, under certain environmental conditions, such as declining water tables and reduced irradiance in regulated systems, their seedlings showed to be more resistant than those of native species. Over the long-term *A. negundo* might thus benefit from altered conditions in anthropogenically impacted systems. As nutrients are generally abundant in riparian areas, rather shade and water stress will be the limiting variables and thus decisive for species composition of riparian forests, especially in Mediterranean sites (González et al., 2010). In the pioneer reference site, *A. negundo* was absent, while in the mature reference site it was present but not dominant in tree and sapling stages (seedlings were not included in the analysis). Reports from the nature reserve 'Ile de la Platière' in which the mature reference plots are located however indicate a spread of *A. negundo*, too, particularly in regeneration stages (e.g. Pont et al., 2009). We know that counter-active management measures had been taken within the nature reserve, at some moment, such as girdling practices, where the bark is removed from a part of the stem, inducing the decay of the tree above this intervention spot. However, these measures have now been reduced as they were not fruitful. Both dike field plots and mature reference plots are located in the by-passed reach of PDR and therefore underlie the same modified hydrological regime. Dike fields still seem to provide more beneficial conditions for this species. This might be an indication that other stresses act on the pioneer species, which make them less competitive (González-Muños et al.,

2014). The timing relative to engineering measures and the succession stage at which the forest stands were when *A. negundo* started to spread might have to be considered as a factor as well.

Another dominant non-native species in dike fields is *Robinia pseudoacacia* (Black locust). Unlike *A. negundo*, however, *R. pseudoacacia* occurred primarily in the tree life history stage and in particularly high frequency, density and basal area on pre-dam surfaces of the DZM reach (Appendix III: Figure A–III–9, Figure A–III–10, Figure A–III–11). We expect plantations to play a role regarding this local pattern, either directly in the dike fields or nearby, in the latter case functioning as seed sources (e.g. Vítková et al., 2017). *R. pseudoacacia* also occurred on post-dam surfaces, and in both mature and pioneer reference sites, however not in comparable relative frequencies. The concentration of *R. pseudoacacia* on pre-dam surfaces might also be influenced by habitat preferences, as logistic regression suggests: it occurred preferentially on higher relative surface elevations characterised by low submersion duration and extensive fine sediment deposits. None of the variables was significant in the model and the results are partly in line with observations from the literature. The fact that it occurs primarily on higher less frequently inundated sites corresponds to its general characteristics (Vítková et al., 2017). However, being a nitrogen-fixing species, it is not necessarily dependent on abundant fine sediment and generally rather colonises hostile substrates (Akamatsu et al., 2011). The low regeneration rates are probably related to a lack of disturbance in dike fields, as *R. pseudoacacia* is light-demanding and does not readily regenerate under closed canopy (Terwei et al., 2013; Höfle et al., 2014). Additionally, it has a relatively short life span. On the one hand, competition and lack of disturbance are therefore limiting factors for this species under the current conditions in dike fields. On the other hand, *R. pseudoacacia* are characterised by a high fruit production and its seeds are viable over an extended period of time, so that seed banks are created (Castro-Díez et al., 2014). This distinguishes them from short lived *Salicaceae* seeds. Under unfavourable light conditions, *R. pseudoacacia* can furthermore form bud banks (Kowarik, 1996). Both these mechanisms, together with high growth rates at an early age allow it to benefit quickly from future disturbance events which provide space in the canopy (Vítková et al., 2017). This raises the question of whether interventions in light of a rehabilitation of the system might provide favourable conditions for this species.

Next to these dominant species, we also found other non-native species in the dike fields (Table VI–4), including *Ailanthus altissima* or *Morus alba* among several others. Although individually they were not among the dominant species, all non-native species together make up a certain part of the forest stands. And further changes in conditions in the dike fields, also related to future climatic change, could produce more favourable conditions for their further spread in the future. They should therefore be included in risk assessments and management measures. The same is true for herbaceaous species, which were not considered in this work. However, our field observations showed that for instance *Fallopia japonica* (Japanese knotweed) was likewise abundant (Modrak, 2013; Gruel, 2014).

4.3 Multiple pressures and controls

Several dike field forest stand characteristics diverged from our initial expectations, which had been based on natural and flow regulation related colonisation and succession processes. Among those characteristics, particularly the diameter at breast height (DBH) and height distributions are to be mentioned. Median values for both variables proved to be higher on younger surfaces than on older, and higher in dike fields than in both reference sites. Additionally, we would expect total plot densities to decrease as the aboveground biomass of individual stems increases through a natural succession process, and basal area to increase (Naiman et al., 2005). Instead, densities in Rhône dike fields were comparable between pre- and post-dam surfaces and remained below both reference sites. Basal areas were comparable between pre- and post-dam sites and with the mature reference, while slightly above the pioneer reference sites. On another regulated system, the Rhine River, Trémolière et al. (1998) observed increased tree densities in a hardwood forest which experienced a disconnection from the channel. This was explained by an increase in sapling densities in these sites. In the dike fields, we hypothesise that there are four potential explanations to the observed patterns of younger trees on pre-dam surfaces and older trees on post-dam surfaces: 1. Selective logging and clear-cutting. 2. Water stress on higher pre-dam surfaces induced from water table decline related to channel degradation, diversion, and, in the case of PDR, industrial pumping. 3. Management of invasive species (*A. negundo*, *R. pseudoacacia*), e.g. by girdling. 4. Ecological effects, such as competition due to an accelerated succession, which led to mortality and fast installation of saplings.

Since 1933, the dike fields lie at least in part within the French 'public fluvial domain' ('*domaine public fluvial*') and are managed by the National Rhône Company (CNR, '*Compagnie Nationale du Rhône*', see also chapter II). The overall task of the CNR is to ensure human requirements regarding the river, including the management of flood risks related to the operation of the diversion schemes. On the river margins, including the dike fields, this involves managing vegetation installation by clearance to reduce hydraulic resistance and increase flow velocities. Overbank fine sediment deposits are dredged. Initially this was regardless of any environmental objectives (Savey, 1992), and today still, it is difficult to know the details of CNR interventions (Pont, 2018, personal communication). From inspection of the available aerial images it was possible for a few sites to deduce actions of vegetation clear-cutting where this was done over areas which were sufficiently large to be identifiable. It was however difficult to unambiguously identify such processes when larger time spans were not covered by aerial images, as was often the case. Beyond this, it is very likely that interventions from private persons were and are frequent (Pont, 2017; Pont, 2018, personal communication), which would rather involve selective logging and would not be identifiable on aerial images. Liébault & Piégay (2002) showed that deforestation was common in the region prior to the 1960s and then decreased.

In chapter V we evidenced the drop in water levels in the four by-passed reaches related to channel degradation and diversion. Stella et al. (2013) demonstrated the impacts of water stress on radial growth, mortality, and crown loss, particularly for phreatophytic species, such as *Populus nigra*. We analysed the species composition of standing dead stems in the dike fields to get a first impression concerning mortality conditions (Figure VII–8). Yet this analysis does not provide any information on the health status of living trees or on woody debris on the ground. We saw that most dead stems are made up of pioneer species, primarily *S.*, *Populus spp.*, and *R. pseudoacacia*. *R. pseudoacacia* is known for its tolerance to extremely dry soils and high mortality is generally rather associated to competition or age as it is naturally short-lived (Vítková et al., 2015; Vítková et al., 2017). Indeed, this species showed highest mortality in plots where it was most abundant. A hypothesis is thus that these sites are undergoing succession, with increasing competition.

The fact that both *R. pseudoacacia* and *Acer negundo* are well represented amongst standing dead stems (Figure VII–8) could theoretically be an indication of localised

management measures against invasive species. During field sampling, we saw some local evidence of girdling practice. However, we did not observe this as a wide-spread practice and to our knowledge, such interventions have been reduced, due to counter-active reactions in some plants, such as increased seed dispersal.

While we had expected compositional differences between upstream and downstream reaches due to their position in different hydro-ecoregions, this proved to be the case only for pre-dam surfaces but not for post-dam surfaces (Figure VI–13). Indeed, pre-dam surfaces presented continental species in the upstream reaches, including e.g. *Cornus sanguinea*, *Ligustrum vulgare*, and several Mediterranean species, such as *Ficus carica* or *Laurus nobilis* in the downstream reaches. In contrast, post-dam surfaces showed an azonal vegetation pattern, with few differences between upstream and downstream sites. Based on the literature, one would expect this to be an indication that on post-dam surfaces the influence of hydrological conditions still predominate over the influence of climatic conditions, which only has a secondary role (Ozenda, 1994).

Another unexpected pattern was that the MON reach showed almost constantly median values of structural parameters which were inversed between pre- and post-dam surfaces compared to the other three reaches. For compositional parameters this was generally not the case. Based on the available aerial images, we estimated forest stand age for most of the sampling plots (Figure VII–9). We found that surface ages were generally a little higher than forest ages, a typical lag effect between emergence of a surface and vegetation installation. The detailed analysis of the reaches of PDR and DZM support this pattern and Arnaud (2012) observed this trend on the Rhine River. There was still some scatter, particularly toward lower surface ages. Indeed, at MON, we recorded that it was mainly the pre-dam surfaces which caused the divergence, with either younger or even-aged stands compared to post-dam surfaces, and a wide range in minimum ages. The issue of logging and clear cutting described in this section might have influenced the age distribution. This issue however needs to be explored more in detail, since compositional data do not show the same trends.

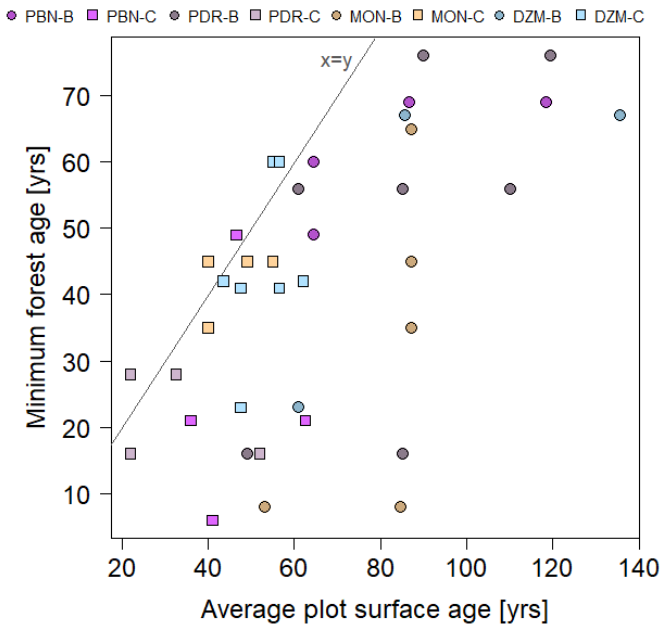

Figure VII–9: Relationship between surface age and forest age. The reference line represents x = y conditions.

CHAPTER VIII CONCLUSIONS ET PERSPECTIVES

Dans le cadre de la Directive Cadre sur l'Eau (DCE) les états membre ont initié l'application de mesures de mitigation à leurs masses d'eau fortement modifiées ou artificielles. Relativement peu d'études existent encore aujourd'hui sur ce type de masses d'eau pour guider de telles actions. Pour conclure les interprétations de nos travaux, nous faisons le lien entre les connaissances acquises sur les casiers Girardon et de potentielles interventions à venir sur eux-mêmes. Nous évaluons notamment les potentiels de diverses actions de préservation, ainsi que les potentiels et les risques liés au démantèlement des digues. Nous nous plaçons également dans une perspective plus globale des mesures de gestion qui sont menées le long du corridor rhodanien.

Concernant les résultats de cette étude et des études plus détaillées sur les casiers aquatiques sur le Rhône, nous concluons que de potentielles actions de gestion devraient dans un premier temps faire la distinction entre les casiers aquatiques et semi-aquatiques (< 90% de surface atterrie) d'un côté, et les casiers terrestres (≥ 90% de surface en plan atterrie) de l'autre, conformément à une approche proposée par Thorel et al. (2018). Dans un second temps, les potentiels et les risques sont à investiguer et à pondérer réciproquement dans un contexte d'interdisciplinarité.

1 Les risques liés à la conservation et au démantèlement des casiers

Les casiers représentent une partie de la plaine alluviale récente des secteurs court-circuités étudiés. Ceux qui sont terrestres montrent un atterrissement par aggradation de sédiments fins ainsi que par assèchement. Les boisements ont des fortes tendances vers une maturation graduelle, ainsi que la propagation d'espèces ligneuses non-endémiques, voire invasives. Tout cela est le reflet d'une perte substantielle de la dynamique latérale et, par la suite, de la modification des conditions stationnelles envers des sites plus secs et moins perturbés. Ceci présente des potentiels très limités pour une régénération d'espèces pionnières endémiques, qui ont commencé à décliner. Certaines espèces exogènes, au contraire, montraient une tolérance élevée à ces conditions, notamment l'érable négundo (*Acer negundo*). A long-terme, cette espèce pourrait éventuellement profiter de cette situation.

Inversement, en cas d'une intervention, des espèces comme le robinier faux-acacia (*Robinia pseudoacacia*), pourraient potentiellement coloniser rapidement de nouveaux espaces. Etant plutôt sur le déclin dans les conditions actuelles vers des stades post-pionniers, ils pourraient se rétablir grâce à des adaptations présentées en chapitre VII, en particulier si, dans le même temps les conditions défavorisent des espèces pionnières endogènes. En outre, les sédiments stockés à l'intérieur des casiers sont probablement pollués avec des PCBs ('*poly-chlorinated biphenyls*'), des métaux, des nutriments, des pesticides ou d'autres substances chimiques et physiques (Comby et al., 2014 ; Thorel et al., 2018 ; Seignemartin, en prép.). Tout d'abord, beaucoup de polluants sont associés à la fraction fine des sédiments fluviales. Deuxièmement, les phases de sédimentation dans les casiers correspondent en partie à des périodes importantes de flux (pour les PCB il s'agit p.ex. des années 1970/1980, Piégay et al., 2018). Une remobilisation de tels stocks pourrait avoir des effets dévastateurs pour des écosystèmes en aval et présente donc un risque. Cependant, Thorel et al. (2018) suggèrent que les patrons spatio-temporels des contaminants dans les casiers sont très variables.

2 Les potentiels liés à la conservation ou au démantèlement complet/partiel

Les casiers aquatiques peuvent avoir, selon leurs caractéristiques spécifiques, une fonction de zone d'alimentation ou de refuge pour les poissons et d'habitat pour les macroinvertébrés ainsi que pour le phytoplancton. Dans ces conditions, ils remplacent potentiellement des habitats de plaine alluviale qui ont été définitivement perdus lors d'une urbanisation, d'usages agricoles ou autres. Surtout dans les secteurs où le chenal principal présente par ailleurs des conditions homogénéisées à cause des aménagements multiples. Un démantèlement partiel pourrait potentiellement diversifier encore plus ces conditions et les rendre plus pérennes.

Les potentiels des casiers terrestres, quant à eux, devraient être évalués au niveau inter-secteurs, pouvant potentiellement constituer un élément d'un réseau interconnectant des écosystèmes éloignés. Leur étendue sur de longues distances semble important pour des espèces migratrices et afin de faciliter l'échange génétique entre différents pools dans un paysage de plus en plus fragmenté. En outre, des

services écosystémiques comme la production de la biomasse ou le stockage de carbone sont en cours d'évaluation (p.ex. projet OHM de John Stella & Virginia Matzek).

3 Implications pour la gestion des casiers

Nos résultats et les interprétations discutés par la suite ont montré que la sélection des casiers pour chacun des divers types d'interventions de préservation ou de réhabilitation doit se faire selon des critères interdisciplinaires. Thorel et al. (2018) ont établi un modèle conceptuel de type 'arbre de décisions' dans ce but. Comme indiqué en début du chapitre, celui-ci part de la distinction entre casiers terrestres et aquatiques/semi-aquatiques. Quant à leur potentiel écologique, les casiers aquatiques ne devraient *a priori* pas être les unités prioritaires pour un démantèlement complet. Mais au contraire, si leurs caractéristiques spécifiques le suggèrent (qualité de l'eau, présence d'espèces rares, absence d'espèces non-endémiques, etc.), ils pourraient faire partie de mesures de préservation. Notamment dans des secteurs pauvres en habitats diversifiés, où de grands travaux de restauration ne sont pas envisagés, ces casiers pourraient jouer un rôle. *A priori*, la connectivité au chenal principal semble jouer un rôle primordial pour les conditions à l'intérieur du casier, avec des niveaux intermédiaires produisant des diversités α les plus hautes dans des études de macroinvertébrés. Ceci rejoint le concept de l''*Intermediate Disturbance Hypothesis*' (Connell, 1978). En reconnectant des casiers à faible connectivité au chenal principal ou alors à d'autres casiers, leur biodiversité pourrait être augmentée à de moindre coûts. Thorel et al. (2018) incluent également la qualité thermique des casiers dans ces réflexions. Ils diversifient également les interventions d'un simple démantèlement complet vers des options de démantèlement partiel, la création de bras secondaires artificiels par une reconnexion au chenal uniquement par l'aval et/ou entre les casiers eux-mêmes. Outre le seul regard sur la maximisation de la biodiversité on pourrait rajouter des réflexions par rapport à d'autres valeurs de préservation, comme indiqué par exemple par Dunn (2004). Ici, l'étude à plusieurs échelles spatiales (du secteur ou de plusieurs secteurs et prenant en compte divers unités géomorphologiques) apportera des éléments additionnels par rapport à la décision du type d'intervention, comme le font remarquer Thorel et al. (2018) également. Au lieu de créer les mêmes conditions intermédiaires de connectivité, il est souhaitable de préserver la diversité des conditions aquatiques, si les risques le permettent.

Le but d'un démantèlement, surtout des casiers terrestres, serait de ré-initier le remodelage régulier des paysages afin de créer une mosaïque de tâches d'habitats de différents âges, des habitats pionniers inclus. Certains travaux ont cependant montré que pour une destruction effective de la végétation établie, à la fois des apports hydrologiques et de la mobilité sédimentaire sont nécessaires (p.ex. Jourdain, 2017). Dans les secteurs court-circuités, ceci nécessiterait donc, au-delà du démantèlement, une réhabilitation du débit liquide, ainsi que des apports en sédiments grossiers.

4 Perspectives

Ce travail s'inscrit dans un cadre avec plusieurs autres études autour des casiers Girardon actuellement menés. Grace à une approche multi-échelle, nos analyses ont fourni des éléments de base qui serviront à des analyses plus spécifiques ainsi qu'à une localisation spatiale plus adaptée pour ceux-ci. Les études concernent notamment la pollution liée aux dépôts de sédiments (thèse de doctorat de Gabrielle Seignemartin ; Seignemartin, en prépa.), le fonctionnement écologique des casiers aquatiques (projet OHM Evelyne Franquet, PostDoc Maxine Thorel ; Thorel et al., 2018) ainsi que les trajectoires successionnelles des boisements (PostDoc Philippe Janssen). Alors que nous avons pu démêler certains des facteurs potentiels de contrôle agissant sur les conditions sédimentaires dans les casiers, d'autres analyses seront nécessaires afin de permettre à prédire des trajectoires, notamment par rapport aux conditions hydrauliques à la fois à l'intérieur des casiers ainsi que dans la zone d'échange entre le chenal principal et le casier.

BIBLIOGRAPHIE / REFERENCES

Acreman MC & MJ Dunbar (2004) Defining environmental river flow requirements—A review. *Hydrology and Earth System Sciences* 8(5):861–876.

Akamatsu F, Ide K, Shimano K & H Toda (2011) Nitrogen stocks in a riparian area invaded by N-fixing black locust (Robinia pseudoacacia L.). *Landscape and Ecological Engineering* 7(1):109–115.

Allix A (1930) Corrections et aménagements actuels du Rhône. *Les Études rhodaniennes* 6(2):189–193.

Ambert J (2013) *Etude diachronique de l'évolution bathymétrique du Rhône*. Bachelor thesis, University of Lyon 3, 40 p.

American Rivers (2017) *American Rivers Dam Removal Database*. figshare.

Amoros C, Richardot-Coulet M & G Pautou (1982) Les « ensembles fonctionnels » : des entités écologiques qui traduisent l'évolution de l'hydrosystème en intégrant la géomorphologie et l'anthropisation (exemple du Haut-Rhône français). *Revue de géographie de Lyon* 57(1):49–62.

Amoros C, Roux AL, Reygrobellet JL, Bravard J-P & G Pautou (1987) A method for applied ecological studies of fluvial hydrosystems. *Regulated Rivers* 1:17–36.

Amoros C & GE Petts (1993) Bases conceptuelles. In: Amoros C & GE Petts [eds] *Hydrosystèmes fluviaux*. Collection d'écologie 24. Masson, Paris, pp. 3–17.

Amoros C & G Bornette (2002) Connectivity and biocomplexity in waterbodies of riverine floodplains. *Freshwater Biology* 47(4):761–776.

Arnaud F (2012) *Approches géomorphologiques historique et expérimentale pour la restauration de la dynamique sédimentaire d'un tronçon fluvial aménagé : le cas du Vieux Rhin entre Kembs et Breisach (France, Allemagne)*. PhD thesis, University of Lyon 2, 280p.

Arnaud F, Piégay H, Béal D, Collery P, Vaudor L & AJ Rollet (2017) Monitoring gravel augmentation in a large regulated river and implications for process-based restoration. *Earth Surface Processes and Landforms* 42(13):2147–2166.

Asselman NEM & H Middelkoop (1995) Floodplain sedimentation: quantities, patterns and processes. *Earth Surface Processes and Landforms* 20(6):481–499.

Barthélémy C & Y Souchon (2009) La restauration écologique du fleuve Rhône sous le double regard du sociologue et de l'écologue. *Nature Sciences Sociétés* 17:113–121.

Baxter RM (1977) Environmental effects of dams and impoundments. *Annual Review of Ecology and Systematics* 8(1):255–283.

Beckstead G & GW Samide (1975) *Design considerations for stream groynes*. Hydraulic engineering report. Alberta Department of the Environment, Environmental engineering support services. 152p.

Beechie TJ, Liermann M, Polloc, MM, Baker S & J Davies (2006). Channel pattern and river-floodplain dynamics in forested mountain river systems. *Geomorphology* 78(1–2):124–141.

Bellmore JR, Duda JJ, Craig LS, Greene SL, Torgersen CE, Collins MJ & K Vittum (2017) Status and trends of dam removal research in the United States. *Wiley Interdisciplinary Reviews: Water 4*(2):1–13.

Bertoldi W, Drake NA & AM Gurnell (2011) Interactions between river flows and colonizing vegetation on a braided river: Exploring spatial and temporal dynamics in riparian vegetation cover using satellite data. *Earth Surface Processes and Landforms* 36:1474–1486.

Bethemont J (1972) *Le thème de l'eau dans la vallée du Rhône*. Essai sur la genèse d'un espace hydraulique. Le feuillet blanc, Saint-Etienne, 642p.

Bethemont J (2000) *Les grands fleuves. Entre nature et société*. 2nd edition, Armand Colin, Paris, 255p.

Bethemont J & J-P Bravard (2016) *Pour saluer le Rhône.* Libel, Lyon, 399p.

Betin C & L Cottet-Dumoulins (1999) Mémoire fluviale, planification stratégique. Le cas d'Oullins dans l'agglomération lyonnaise. *Les Annales de la recherche urbaine* 82:118–129.

Bligh WG (1915) *Dams and weirs. An analytical and practical treatise on gravity dams and weirs; arch and buttress dams; submerged weirs; and barrages*. American technical society, Chicago, 206p.

Bloesch J (2003) Flood plain conservation in the Danube River Basin, the link between hydrology and limnology: summary report on the 34th IAD-conference, August 27–30, 2002, in Tulcea (Romania) and the 21st IHP/UNESCO-hydrological conference, September 2–6, 2002, in Bucharest (Romania). *Archiv für Hydrobiologie Supplement* 147(3–4):347–362 (Large Rivers 14/3–4).

Boon PJ (1992) Essential elements in the case for river management. In: Boon PJ, Calow P & GE Petts [eds] *River conservation and management*. Wiley, Chichester, pp. 11–32.

Boon PJ (2012) Revisiting the case for river conservation. In: Boon PJ & PJ Raven [eds] *River conservation and management*, Wiley, Chichester, pp. 1–14.

Bourdin L (2004) *Les rivières en tresses sur le bassin Rhône-Méditerranée-Corse, bilan et perspective de gestion*. MSc thesis, ENGREF, 60p.

Braatne JH, Rood S & PE Heilman (1996) Life history, ecology, and conservation of riparian cottonwoods in North America. In: Stettler RF, Bradshaw HD, Heilman PE & Hinckley TM [eds] *Biology of Populus and its implications for management and conservation (Part I)*. NRC Press, pp. 17–67.

Bradley CE & DG Smith (1986) Plains cottonwood recruitment and survival on a prairie meandering river floodplain, Milk River, southern Alberta and northern Montana. *Canadian Journal of Botany* 64:1433–1442.

Brandt SA (2000) Classification of geomorphological effects downstream of dams. *Catena* 40(4):375–401.

Bravard J-P (1987) *Le Rhône. Du Léman à Lyon.* La Manufacture, Lyon, 451p.

Bravard J-P & J-L Perry (1993) La disparition du tressage fluvial dans les Alpes françaises sous l'effet de l'aménagement des cours d'eau (19–20ème siècle). *Zeitschrift für Geomorphologie*, Supplementband 88:67–79.

Bravard J-P (1994) L'incision des lits fluviaux: du phénomène morphodynamique naturel et réversible aux impacts irréversibles / The incision of river beds: from a natural and reversible morphodynamic phenomenon to irreversible impacts. *Revue de géographie de Lyon* 69(1):5–10.

Bravard, J-P (1998) Le temps et l'espace dans les systèmes fluviaux, deux dimensions spécifiques de l'approche géomorphologique. *Annales de géographie* 3–15.

Bravard J-P (2001) Le Rhône amont. In: Grand Lyon Mission Prospective et Stratégie d'agglomération. *Les cahiers millénaires trois* 25:11–14.

Bravard J-P & A Clémens [eds] (2008) *Le Rhône en 100 Questions*. Graie, Lyon, 289p.

Bravard J-P, Doutriaux E, Bethemont J & P Allard (2008a) Quels sont les principaux aménagements présents sur le fleuve et dans sa vallée ? In: Bravard J-P & A Clémens [eds] *Le Rhône en 100 Questions*. Graie, Lyon, pp. 70–73.

Bravard J-P, Provansal M, Arnaud-Fassetta G, Chabbert S, Gaydou P, Dufour S, Richard F, Valleteau S, Melun G & P Passy (2008b) Un atlas du paléo-environnement de la

plaine alluviale du Rhône de la frontière suisse à la mer. Collection EDYTEM – *Cahiers de Géographie* 6:101–116.

Bravard J-P (2010) Discontinuities in braided patterns: the River Rhône from Geneva to the Camargue delta before river training. *Geomorphology* 117:219–233.

Bravard J-P & P Gaydou (2015) Historical development and integrated management of the Rhône River floodplain, from the Alps to the Camargue delta, France. In: Hudson PF & H Middelkoop [eds] *Geomorphic Approaches to Integrated Floodplain Management of Lowland Fluvial Systems in North America and Europe.* Springer, pp. 289–320.

Bréthaut C (2015) Analyse des facteurs contribuant à l'émergence d'une nouvelle gouvernance transfrontalière de l'eau : le cas du Rhône. In: Reynard E, Evéquoz-Dayen M & G Borel [eds] *Le Rhône, entre nature et société*. Cahiers de Vallesia 29, Sion, pp. 327–338.

Bréthaut C & G Pflieger (2015) The shifting territorialities of the Rhone River's transboundary governance: a historical analysis of the evolution of the functions, uses and spatiality of river basin governance. *Regional Environmental Change* 15(3):549–558.

Brierley GJ & EJ Hickin (1992) Floodplain development based on selective preservation of sediments, Squamish River, British Columbia. *Geomorphology* 4(6):381–391.

Brierley GJ (2010) Landscape memory: the imprint of the past on contemporary landscape forms and processes. *Area* 42(1):76–85.

Brookes A (1988, repr. 1992) *Channelized rivers. Perspectives for environmental management*. Wiley, Chichester. 326p.

Brookes A, Gregory KJ & FH Dawson (1983) An assessment of river channelization in England and Wales. *Science of the Total Environment* 27(2–3):97–111.

Brown AG (1996) Floodplain palaeoenvironments. In: Anderson MG, Walling DE & PD Bates [eds] *Floodplain processes*. Wiley, Chichester, pp. 95–138.

Brown AG, Tooth S, Bullard JE, Thomas DSG, Chiverrell RC, Plater AJ, Murton J, Thorndycraft VR, Tarolli P, Rose J, Wainwright J, Downs P & R Aalto (2017) The geomorphology of the Anthropocene: emergence, status and implications. *Earth Surface Processes and Landforms* 42:71–90.

Bruns DA, Minshall GW, Cushing CE, Cummins KW, Brock JT & Vannote RL (1984) Tributaries as modifiers of the river continuum concept: analysis by polar ordination and regression models. *Archiv für Hydrobiologie* 99(2):208–220.

Buijse AD, Coops H, Staras M, Jans LH, Van Geest GJ, Grift RE, Ibelings BW, Oosterberg W & FCJM Roozen (2002) Restoration strategies for river floodplains along large lowland rivers in Europe. *Freshwater biology* 47(4):889–907.

Burch CW, Abell PR, Stevens MA, Dolan R, Dawson B & FD Shields Jr (1984) *Environmental guidelines for dike fields*. Environmental and water quality operational studies, Technical Report E-84-4. 236p.

Castañeda RA, Avlijas S, Simard MA & A Ricciardi (2014) Microplastic pollution in St. Lawrence river sediments. *Canadian Journal of Fisheries and Aquatic Sciences* 71(12):1767–1771.

Castro-Díez P, Valle G, González-Muñoz N & Á Alonso (2014) Can the life-history strategy explain the success of the exotic trees Ailanthus altissima and Robinia pseudoacacia in Iberian floodplain forests?. *PloS ONE* 9(6):12p.

Cazenave P (1997) L'utilisation des groupes bulbes dans les aménagements de basse chute. *La Houille Blanche*. 3:25–31.

Chambers JC (1995) Relationships between seed fates and seedling establishment in an alpine ecosystem. *Ecology* 76(7):2124–2133.

Chessel D, Dufour AB & J Thioulouse (2004) The ade4 package-I- One-table methods. *R News* 4:5–10.

Church M (2015) *The regulation of Peace River. A case study for river management*. Wiley, Chichester, 296p.

Citterio A & H Piégay (2009) Overbank sedimentation rates in former channel lakes: characterization and control factors. *Sedimentology* 56(2):461–482.

Clozel-Leloup B, Roux G & C Moiroud (2013) *Caractérisation casier Girardon vis-à-vis des PCB - Elaboration de propositions de méthodes d'échantillonnage transposables aux autres casiers en vue de la redynamisation des marges alluviales du fleuve Rhône.* Rapport I. BRGM/RC-60367-FR, 154p.

Comby E, Le Lay YF & H Piégay (2014) How chemical pollution becomes a social problem. Risk communication and assessment through regional newspapers during the management of PCB pollutions of the Rhône River (France). *Science of the Total Environment* 482–483:100–115.

Comby E (2015) *Pour qui l'eau ? Les contrastes spatio-temporels des discours sur le Rhône (France) et le Sacramento (Etats-Unis).* PhD thesis, University of Lyon, 721p.

Compagnie Nationale du Rhône (CNR) (2000) *Etude globale pour une stratégie de réduction des risques dus aux crues du Rhône. Modélisation hydraulique hors delta. Histoire de l'aménagement du fleuve Montélimar (1950 – 1957)*. Unpublished report, Lyon, 47p.

Compagnie Nationale du Rhône (CNR) (2012) *Réhabilitation des lônes du vieux-Rhône de Péage de Roussillon. Dossier d'autorisation au titre de la Loi sur l'Eau et les Milieux Aquatiques et dossier d'enquête publique Bouchardeau*. 298p.

Connell JH (1978) Diversity in tropical rainforests and coral reefs. *Science* 199(4335):1302–1310.

Constantine JA, Dunne T, Piégay H & GM Kondolf (2010) Controls on the alluviation of oxbow lakes by bed-material load along the Sacramento River, California. *Sedimentology* 57(2):389–407.

Constantinescu G, Sukhodolov A & A McCoy (2009) Mass exchange in a shallow channel flow with a series of groynes: LES study and comparison with laboratory and field experiments. *Environmental fluid mechanics*, 9(6):587–615.

Convention on Wetlands of International Importance especially as Waterfowl Habitat, 1971, amended in 1982 and 1987 (Ramsar Convention).

Cooper DJ, Merritt DM, Andersen DC & RA Chimner (1999) Factors controlling the establishment of Fremont cottonwood seedlings on the Upper Green River, USA. *River Research and Applications* 15:419–440.

Cooper DJ, Andersen DC & RA Chimner (2003) Multiple pathways for woody plant establishment on floodplains at local to regional scales. *Journal of Ecology* 91:182–196.

Corenblit D, Tabacchi E, Steiger J & AM Gurnell (2007) Reciprocal interactions and adjustments between fluvial landforms and vegetation dynamics in river corridors: A review of complementary approaches. *Earth-Science Reviews* 84:56–86.

Corenblit D, Baas ACW, Bornette G, Darrozes J, Delmotte S, Francis RA, Gurnell AM, Julien F, Naiman RJ & J Steiger (2011) Feedbacks between geomorphology and biota controlling earth surface processes and landforms: A review of foundation concepts and current understandings. *Earth-Science Reviews* 106:307–311.

Corenblit D, Steiger J, González E, Gurnell AM, Charrier G, Darrozes J, Dousseau J, Julien F, Lambs L, Larrue S, Roussel E, Vautier F & O Voldoire (2014) The biogeomorphological life cycle of poplars during the fluvial biogeomorphological succesion: A special focus on Populus nigra L. *Earth Surface Processes and Landforms* 39:546–563.

Cortier B & B Couvert (2001) Causes et conséquences du blocage actuel de la dynamique fluviale et du transit sédimentaire du Rhône. *La Houille Blanche* 8:72–78.

Council Directive 92/43/EEC of 21 May 1992 on the conservation of natural habitats and of wild fauna and flora (Habitats Directive).

Crutzen PJ (2002) Geology of mankind. *Nature* 415(3):23.

DAISIE European Invasive Alien Species Gateway (http://www.europe-alines.org), last access 10/04/2018.

Decamps H, Fortune M, Gazelle F & G Pautou (1988) Historical influence of man on the riparian dynamics of a fluvial landscape. *Landscape ecology* 1(3):163–173.

Depret T, Riquier J & H Piégay (2017) Evolution of abandoned channels: Insights on controlling factors in a multi-pressure river system. *Geomorphology* 294:99–118.

des Chatelliers D (1995) *Etude géomorphologique. Bilan du transit, de l'érosion et du dépôt de la charge solide. Réserve naturelle de la Platière ; Rhône court-circuité de Péage de Roussillon.* Etude réalisée pour le compte de l'Agence de l'Eau RM&C. Avec la participation de la CNR. 59p.

Directive 79/409/EEC, amended in 2009: Directive 2009/147/EC of the European Parliament and of the Council of 30 November 2009 on the conservation of wild birds (Birds Directive).

Directive 2000/60/EC of the European Parliament and of the Council of 23 October 2000 establishing a framework for Community action in the field of water policy (EU WFD).

Direction Régionale de l'Environnement Rhône-Alpes, Délégation de Bassin Rhône-Méditerranée (DIREN) [ed] (2007) *Cartographie du paléo-environnement de la plaine alluviale du Rhône de la frontière suisse à la mer*. 73p.

Downs PJ & KJ Gregory (2004, repr. 2014) *River channel management Towards Sustainable Catchment Hydrosystems*. Routledge, New York, USA, 395p.

Doyle MW, Stanley EH, Havlick DG, Kaiser MJ, Steinbach G, Graf WL, Galloway GE & Riggsbee JA (2008) Aging infrastructure and ecosystem restoration. *Science* 319(5861):286–287.

Droppo IG & ED Ongley (1994) Flocculation of suspended sediment in rivers of southeastern Canada. *Water Research* 28(8):1799–1809.

Duda JJ, Wieferich DJ, Bristol RS, Bellmore JR, Hutchison VB, Vittum KM, Craig L & JA Warrick (2016) *Dam Removal Information Portal (DRIP)—A map-based resource linking scientific studies and associated geospatial information about dam removals*. U.S. Geological Survey Open-File Report 2016-1132, 14 p.

Dudgeon D (2000) Large-Scale Hydrological Changes in Tropical Asia: Prospects for Riverine Biodiversity: The construction of large dams will have an impact on the biodiversity of tropical Asian rivers and their associated wetlands. *BioScience* 50(9):793–806.

Dudgeon D, Arthington AH, Gessner MO, Kawabata ZI, Knowler DJ, Lévêque C, Naiman RJ, Prieur-Richard AH, D Soto D, Stiassny MLJ & CA Sullivan (2006) Freshwater biodiversity: importance, threats, status and conservation challenges. *Biological Reviews* 81(2):163–182.

Dufour S (2005) *Contrôles naturels et anthropiques de la structure et de la dynamique des forêts riveraines des cours d'eau du bassin rhodanien (Ain, Arve, Drôme et Rhône)*. PhD thesis, University of Lyon 3, 244p.

Dufour S, Barsoum N, Muller E & H Piégay (2007) Effects of channel confinement on pioneer woody vegetation structure, composition and diversity along the River Drôme (SE France). *Earth Surface Processes and Landforms* 32(8):1244–1256.

Dufour S & H Piégay H (2009) From the myth of a lost paradise to targeted river restoration: forget natural references and focus on human benefits. *River Research and Applications* 25(5):568–581.

Dufour S, Rinaldi M, Piégay H & A Michalon (2015) How do river dynamics and human influences affect the landscape pattern of fluvial corridors? Lessons from the Magra River, Central–Northern Italy. *Landscape and Urban Planning* 134:107–118.

Dunn H (2004) Defining the ecological values of rivers: the views of Australian river scientists and managers. *Aquatic Conservation: Marine and Freshwater Ecosystems* 14(4):413–433.

Dykaar BB & PJ Wigington Jr (2000) Floodplain formation and cottonwood colonization patterns on the Willamette River, Oregon, USA. *Environmental Management* 25(1):87–104.

Dynesius M & C Nilsson (1994) Fragmentation and flow regulation of river systems in the Northern Third of the World. *Science*, New Series 266(5186):753–762.

Džubáková K, Piégay H, Riquie, J & M Trizna (2015) Multi-scale assessment of overflow-driven lateral connectivity in floodplain and backwater channels using LiDAR imagery. *Hydrological Processes* 29(10):2315–2330.

Egger G, Drescher A, Hohensinner S & M Jungwirth (2007) Riparian vegetation model of the Danube River (Machland, Austria): changes of processes and vegetation patterns. *Proceedings of the 6th International Symposium on Ecohydraulics* 18:263–266.

Ellenberg H, Weber HE, Dull R, Wirth V, Werner W & D Paulissen (1992) Zeigerwerte von Pflanzen in Mitteleuropa. *Scripta Geobotanica* 18:1-258.

Erskine WD, Terrazzolo N & RF Warner (1999) River rehabilitation from the hydrogeomorphic impacts of a large hydro-electric power project: Snowy River, Australia. *Regulated Rivers: Research & Management* 15(1–3):3–24.

Escudié B, Combe JM & J Payen [eds] (1991) *Vapeurs sur le Rhône. Histoire scientifique et technique de la navigation à vapeur de Lyon à la mer*. Editions du CNRS, Paris. Presses Universitaires de Lyon, Lyon, 462p.

European Commission Directorate-General for Environment (DG Env) (2011) *Links between the Water Framework Directive (WFD 2000/60/EC) and Nature Directives (Birds Directive 2009/147/EC and Habitats Directive 92/43/EEC). Frequently Asked Questions*. 31p.

European Commission (2012) *Report from the Commission to the European Parliament and the Council on the implementation of the Water Framework Directive (2000/60/EC) River Basin Management Plans*. SWD 379. Brussels, 14p.

European Sediment Research Network (SedNet) (2004) *Contaminated sediments in European River Basins*. 80p.

Everitt BL (1968) Use of the cottonwood in an investigation of the recent history of a flood plain. *American Journal of Science* 266:417–459.

Ferrar AA, O'Keeffe JH & BR Davies (1988) *The river research programme*. Foundation for research development, Republic of South Africa, 28p.

Florsheim JL, Mount JF & A Chin (2008) Bank erosion as a desirable attribute of rivers. *BioScience* 58(6):519–529.

Francis RA, Gurnell AM, Petts GE & JE Peter (2005) Survival and growth responses of Populus nigra, Salix elaeagnos and Alnus incana cuttings to varying levels of hydric stress. *Forest Ecology and Management* 210:291–301.

Franquet E, Cellot B, Pont D & M Bournaud (1995) Environmental and macroinvertebrate dynamics in the Lower Rhone River and a lateral dike field: a study matching two functioning descriptors. *Hydrobiologia* 308:207–217.

Franquet E (1999) Chironomid assemblage of a Lower-Rhône dike field: relationships between substratum and biodiversity. *Hydrobiologia* 397:121–131.

Friedman JM, Osterkamp WR & WM Lewis Jr (1996) Channel narrowing and vegetation development following a Great Plains flood. *Ecology* 77(7):2167–2181.

Fruget JF & JL Michelot (1997) Dérives écologiques et gestion du milieu fluvial rhodannien / Ecological evolution and management of the natural environment of the Rhône valley. *Revue de géographie de Lyon* 72(1):35–48.

Fruget (2003) Changements environnementaux, dérives écologiques et perspectives de restauration du Rhône français: bilan de 200 ans d'influences anthropiques. *VertigO – La revue en sciences de l'environnement* 4(3):17p.

Fryirs K, Brierley GJ & WD Erskine (2012) Use of ergodic reasoning to reconstruct the historical range of variability and evolutionary trajectory of rivers. *Earth Surface Processes and Landforms* 37(7):763–773.

Gage EA & DJ Cooper (2005) Patterns of willow seed dispersal, seed entrapment, and seedling establishment in a heavily browsed montane riparian ecosystem. *Canadian Journal of Botany* 83:678–687.

Galay VJ (1983) Causes of river bed degradation. *Water resources research* 19(5):1057–1090.

Gandouin E, Maasri A, Van Vliet-Lanoë B & E Franquet (2006) Chironomid (Insecta: Diptera) assemblages from a gradient of lotic and lentic waterbodies in river floodplains of France: a methodological tool for paleoecological applications. J*ournal of Paleolimnology* 35:149–166.

Garbrecht G (1985, 1997, 2016) Sadd el-Kafara, the world's oldest large dam. In: Jackson DC [ed] *Dams*. Routledge, London/New York, 364p (1985 Wilmongton Publishing, 1997 Ashgate Publishing, 2016 Routledge).

Gaydou P (2013) *Observatoire des Sédiments du Rhône (OSR) : Schéma directeur de ré-activation de la dynamique fluviale des marges du Rhône*. Version du 28 février 2013. Rapport de synthèse. 92p.

Geerling GW, Kater E, Van den Brink C, Baptist MJ, Ragas AMJ & AJM Smits (2008) Nature rehabilitation by floodplain excavation: The hydraulic effect of 16 years of sedimentation and vegetation succession along the Waal River, NL. *Geomorphology* 99(1–4):317–328.

Girardon H (1894) *L'amélioration des rivières en basses eaux.* VIème Congrès International de Navigation Intérieure, La Haye, 85p.

Glenn EP & PL Nagler (2005) Comparative ecophysiology of Tamarix ramosissima and native trees in western US riparian zones. *Journal of Arid Environments* 61(3):419–446.

Glymph LM (1954) Studies of sediment yields from watersheds. *International Association of Hydrological Sciences Publication* 36:178–191.

González E, González-Sanchis M, Cabezas Á, Comín FA & E Muller (2010) Recent changes in the riparian forest of a large regulated Mediterranean river: implications for management. *Environmental Management* 45(4):669–681.

González-Muñoz N, Castro-Díez P & O Godoy (2014) Lack of superiority of invasive over co-occurring native riparian tree seedling species. *Biological invasions* 16(2):269–281.

Goudie A, Atkinson BW, Gregory KJ, Simmons IG, Stoddart DR & D Sugden (1994, repr. 1999) *The encyclopedic dictionary of physical geography*. 2nd edition, Blackwell, Oxford, 611p.

Graf WL (2001) Damage control: restoring the physical integrity of America's rivers. *Annals of the Association of American Geographers* 91(1):1–27.

GRAIE–Groupe de Recherche Rhône-Alpes sur les Infrastructures et l'Eau [ed] (2016) *Le suivi scientifique de la restauration hydraulique et écologique du Rhône 2000–2015. RhôneEco. Evaluer et comprendre pour mieux agir*. Lyon, 24p.

Grandjean P (1990) *La régularisation du Lac Léman. Hydrology in mountainous regions, I–Hydrological measurements; the water cycle*. Proceedings of two Lausanne Symposia. IAHS Publ. 193.

Grizzetti B, Pistocchi A, Liquete C, Udias A, Bouraoui F & W van de Bund (2017) Human pressures and ecological status of European rivers. *Nature Scientific Reports*, 7(1):205.

Gruel CR (2014) *Etude de la structure et de la dynamique forestière dans les casiers Girardon du Rhône : analyses écologiques et spatio-temporelles comparées sur quatre secteurs court-circuités Pierre-Bénite, Péage-de-Roussillon, Montélimar et Donzère-Mondragon – Diagnostique fonctionnel permettant de définir une politique de conservation ou de restauration de ces écosystèmes anthropo-construits*. MSc thesis, University of Lyon 2, 85p.

Guertault L, Camenen B, Peteuil C & A Paquier (2014) Long term evolution of a dam reservoir subjected to regular flushing events. *Advances in Geosciences* 39:89–94.

Guilloy-Froget H, Muller E, Barsoum N & FMR Hughes (2002) Dispersal, germination, and survival of Populus nigra L. (Salicaceae) in changing hydrologic conditions. *Wetlands* 22(3):478–488.

Gurnell AM, Petts GE, Hannah DM, Smith BP, Edwards PJ, Kollmann J, Ward JV & K Tockner (2001) Riparian vegetation and island formation along the gravel-bed Fiume Tagliamento, Italy. *Earth Surface Processes and Landforms* 26(1):31–62.

Gurnell AM, Goodson JM, Angold PG, Morrisse YIP, Petts GE & J Steiger (2004) Vegetation propagule dynamics and fluvial geomorphology. In: Bennett SJ & A Simon [eds] *Riparian vegetation and fluvial geomorphology: Hydraulic, hydrologic, and geotechnical interactions*. Water Science and Application 8. American Geophysical Union, pp. 209–219.

Gurnell AM, Tockner K, Edwards P & G Petts (2005) Effects of deposited wood on biocomplexity of river corridors. *Frontiers in Ecology and the Environment* 3(7):377–382.

Habersack H, Haspel D, Muhar S & H Waidbacher (2014) Preface: Impact of human activities on biodiversity of large rivers. *Hydrobiologia* 729(1):1–2.

Hannappel S & B Piepho (1996) Cluster analysis of environmental data which is not interval scaled but categorical. Evaluation of aerial photographs of groyne fields for the determination of representative sampling sites. *Chemosphere* 33(2):335–342.

Haond M (2008) D'où vient l'eau du Rhône ? In: Bravard JP & A Clémens [eds] *Le Rhône en 100 questions*. Graie, Lyon, 289p.

Heiler G, Hein T, Schiemer F & G Bornette (1995) Hydrological connectivity and flood pulses as the central aspects for the integrity of a river-floodplain system. *Regulated Rivers: Research and Management* 11(3–4):351–361.

Hein T, Schwarz U, Habersack H, Nichersu I, Preiner S, Willby N & G Weigelhofer (2016) Current status and restoration options for floodplains along the Danube River. *Science of the Total Environment* 543:778–790.

Henning M, & B Hentschel (2013) Sedimentation and flow patterns induced by regular and modified groynes on the River Elbe, Germany. *Ecohydrology* 6(4):598–610.

Hill MO & HG Gauch (1980) Detrended correspondence analysis: an improved ordination technique. *Vegetatio* 42:47–58.

Hinkel J (1999) *Die Ermittlung vegetationsfreier Flächen entlang der Elbeufer aus Luftbildern und ihre Korrelation mit der Flußgeometrie und dem Uferverbau*. Diplomarbeit, Technical University of Karlsruhe, 98p.

Hobbs RJ, Higgs E & JA Harris (2009) Novel ecosystems: implications for conservation and restoration. *Trends in Ecology and Evolution* 24(11):599–605.

Höfle R, Dullinger S & F Essl (2014) Different factors affect the local distribution, persistence and spread of alien tree species in floodplain forests. *Basic and Applied Ecology* 15(5):426–434.

Hohensinner S, Jungwirth M, Muhar S & S Schmutz (2011) Spatio-temporal habitat dynamics in a changing Danube River landscape 1812–2006. *River Research and Applications* 27:939–955.

Hollander M & DA Wolfe (1973) *Nonparametric Statistical Methods.* Wiley, New York, 503p.

Howard AD (1996) Modelling channel evolution and floodplain morphology. In: Anderson MG, Walling DE & PD Bates [eds] *Floodplain processes*. Wiley, Chichester, pp. 15–62.

Huang CJ & CM Dong (1999) Wave deformation and vortex generation in water waves propagating over a submerged dike. *Coastal Engineering* 37(2):123–148.

International Commission on Large Dams (2011) *Constitution status*. Previous edition 2002, 21p.

International Sediment Initiative (ISI) (2011) *Sediment issues & sediment management in large river basins. Interim case study synthesis report*. UNESCO, Beijing, 82p.

James CS (1985) Sediment transfer to overbank sections. *Journal of Hydraulic Research* 23(5):435–452.

Janauer GA, Albrecht J & L Stratmann (2015) Synergies and conflicts between Water Framework Directive and Natura 2000: legal requirements, technical guidance and experiences from practice. In: Ignar S & M Grygoruk [eds] *Wetlands and Water Framework Directive, protection, management and climate change. GeoPlanet: Earth and Planetary Sciences*, Springer, Cham, pp. 9–29. doi:10.1007/978-3-319-13764-3_2.

Johnson WC (1994) Woodland expansion in the Platte River, Nebraska: Patterns and causes. *Ecological Monographs* 64:45–84.

Jones KB, Slonecker ET, Nash MS, Neale AC, Wade TG & S Hamann (2010) Riparian habitat changes across the continental United States (1972–2003) and potential implications for sustaining ecosystem services. *Landscape Ecology* 25(8):1261–1275.

Jourdain C (2017) *Action des crues sur la dynamique sédimentaire et végétale dans un lit de rivière à galets: l'Isère en Combe de Savoie*. PhD thesis, University of Grenoble, 283p.

Julve P (1998ff) *Baseflor. Index botanique, écologique et chorologique de la flore de France*. Version: "2017". http://perso.wanadoo.fr/philippe.julve/catminat.htm.

Jungwirth M, Haidvogl G, Moog O, Muhar S & S Schmutz (2003) *Angewandte Fischökologie an Fließgewässern*. Facultas UTB, Wien, 547p.

Junk WJ, Bayley PB & RE Sparks (1989) The flood pulse concept in river-floodplain systems. In: Dodge DP [ed] *Proceedings of the International Large River Symposium. Canadian Special Publication of Fisheries and Aquatic Sciences* 106:110–127.

Kantoush SA & T Sumi (2010) *River morphology and sediment management strategies for sustainable reservoir in Japan and European Alps*. Annuals of Disaster Prevention Research Institute, Kyoto University, No. 53B, pp. 821–839.

Karrenberg S, Edwards PJ & J Kollmann (2002) The life history of Salicaceae living in the active zone of floodplains. *Freshwater Biology* 47:733–748.

Kellerhals R (1982) Effect of river regulation on channel stability. In: Hey RD, Bathurst JC & Thoren CR [eds] *Gravel-bed Rivers.* Wiley, Chichester, 685–715.

Klasz G, Krouzecky N, Reckendorfer W, Schmalfuß R & R Schlögl (2009) Neue wasserbauliche Wege: Uferrückbau und Buhnenumgestaltung an der Donau östlich von Wien. New hydro-engineering approaches: river bank renaturation and groyne redesign along the Danube east of Vienna *Österreichische Ingenieur-und Architekten-Zeitschrift* 154:109–118.

Klingeman PC, Bravard J-P & Y Giuliani (1994) Les impacts morphodynamiques sur un cours d'eau soumis à un aménagement hydroélectrique à dérivation : le Rhône en Chautagne (France) / Morphodynamic impacts on a river affected by a hydro-electric diversion scheme : the Rhône in the Chautagne region of France. *Revue de géographie de Lyon* 69(1):73–87.

Klingeman PC, Bravard J-P, Giuliani Y, Olivier JM & G Pautou (1998) Hydropower reach by-passing and dewatering impacts in gravel-bed rivers. In: Klingeman PC, Beschta R, Komar P & J Bradley [eds] *Gravel Bed Rivers in the Environment*, Water Resources Publications, Littleton, pp. 313–344.

Kondolf GM (1997) Hungry water: effects of dams and gravel mining on river channels. *Environmental Management* 21(4):533–551.

Kondolf GM, Smeltzer MW & SF Railsback (2001) Design and performance of a channel reconstruction project in a coastal California gravel-bed stream. *Environmental Management* 28(6):761–776.

Kondolf GM, Gao Y, Annandale GW, Morris GL, Jiang E, Zhang J, Cao Y, Carling P, Fu K, Guo Q, Hotchkiss R, Peteuil C, Sumi T, Wang HW, Wang Z, Wei A, Wu B, Wu C & CT Yang (2014) Sustainable sediment management in reservoirs and regulated rivers: experiences from five continents. *Earth's Future* 2:256–280.

Kowarik I (1996) Funktionen klonalen Wachstums von Bäumen bei der Brachflächen-Sukzession unter besonderer Beachtung von Robinia pseudoacacia. *Verhandlungen der Gesellschaft für Ökologie 26*:173–181.

Lamouroux N, Gore JA, Lepori F & B Statzner (2015) The ecological restoration of large rivers needs science-based, predictive tools meeting public expectations: an overview of the Rhone project. *Freshwater Biology* 60:1069–1084.

Landon N & H Piegay (1994) L'incision d'affluents méditerranéens du Rhône: la Drôme et l'Ardèche / The incision of two sub-mediterranean tributaries of the Rhône: the Drôme and the Ardèche. *Revue de géographie de Lyon* 69(1):63–72.

Lane EW (1955) *The importance of fluvial morphology in hydraulic engineering*. Proceedings of the American Society of Civil Engineers, paper no. 745, vol. 81, 17p.

Langendoen EJ (1992) *Flow patterns and transport of dissolved matter in tidal harbours*. PhD thesis, Technical University of Delft, 187p.

Launay M (2014) *Flux de matières en suspension, de mercure et de PCB particulaires dans le Rhône, du Léman à la Méditerranée*. PhD thesis, University of Lyon, 432p.

Lave R (2009) The controversy over natural channel design: substantive explanations and potential avenues for resolution. *Journal of the American Water Resources Association* 45(6):1519–1532.

Lê S, Josse J & F Husson (2008) FactoMineR: An R Package for Multivariate Analysis. *Journal of Statistical Software* 25(1):1–18.

Lechner A, Keckeis H, Lumesberger-Loisl F, Zens B, Krusch R, Tritthart M, Glas M & E Schludermann (2014) The Danube so colourful: a potpourri of plastic litter outnumbers fish larvae in Europe's second largest river. *Environmental Pollution* 188:177–181.

Le Coz J (2007) *Fonctionnement hydro-sédimentaire des bras morts de rivière alluviale*. PhD thesis, Ecole Centrale of Lyon, 308p.

Le Coz J, Michalkova M, Hauet A, Comaj M, Dramais G, Holubová K, Piégay H & A Paquier (2010) Morphodynamics of the exit of a cutoff meander: experimental

findings from field and laboratory studies. *Earth Surface Processes and Landforms*, 35(3):249–261.
Leopold LB, Wolman MG & JP Miller (1964, republ. 1995) *Fluvial processes in geomorphology*. Dover, New York, 522p.
Lewin J (1978) Floodplain geomorphology. *Progress in Physical Geography* 2:408–437.
Lewin J (2013) Enlightenment and the GM floodplain. *Earth Surface Processes and Landforms* 38(1):17–29.
Liébault F & H Piégay (2002) Causes of 20th century channel narrowing in mountain and piedmont rivers of southeastern France. *Earth Surface Processes and Landforms* 27(4):425–444.
Loizeau J-L (1991) La sédimentation récente dans le delta du Rhône, Léman : processus et évolution. PhD thesis, University of Geneva, 210p.
Magilligan FJ, Graber BE, Nislow KH, Chipman JW, Sneddon CS & CA Fox (2016) River restoration by dam removal: Enhancing connectivity at watershed scales. *Elementa: Science of the Anthropocene* 4:1–14.
Mahoney JM & SB Rood (1998) Streamflow requirements for cottonwood seedling recruitment—An integrative model. *Wetlands* 18(4):634–645.
Mandier P (1984) *Le relief de la moyenne vallée du Rhône au Tertiaire et au Quartenaire. Essai de synthèse paléogéographique*. Bureau de Recherches Géologiques et Miniers, Orléans, 653p.
Maniak U (1997, 2010) *Hydrologie und Wasserwirtschaft. Eine Einführung für Ingenieure.* 6th edition, Springer, Heidelberg, 686p.
Mann ME (2002) Little Ice Age. Volume 1, The Earth system: physical and chemical dimensions of global environmental change. In: MacCracken MC, Perry JS & T Munn [eds] *Encyclopedia of Global Environmental Change*. Wiley, Chichester, pp. 504–509.
Marriott S (1992) Textural analysis and modelling of a flood deposit: River Severn, U.K. *Earth Surface Processes and Landforms* 17(7):687–697.
Mathieu L (2013) *Etude diachronique de l'évolution bathymétrique du Rhône 1897-2010. Contribution pour des recherches sur les dynamiques fluviales*. BSc thesis, University of Lyon 3, 50 p.
McCoy A, Constantinescu G & LJ Weber (2008) Numerical investigation of flow hydrodynamics in a channel with a series of groynes. *Journal of Hydraulic Engineering* 134(2):157–172.
Miall AD (1985) Architectural-element analysis: A new method of facies analysis applied to fluvial deposits. *Earth-Science Reviews* 22:261–308.
Michelot JL (1983) Evolution des paysages fluviaux de la vallée du Rhône dans le secteur du Péage-de-Roussillon *Revue de géographie de Lyon* 58(4):307–322.
Mignot E, Wei C, Escauriaz C & Rivière N (2013) *Analyse expérimentale et numérique du champ de vitesse dans des cavités latérales de différents rapports d'aspect*. Proceedings of the 21ème Congrès Français de Mécanique, Bordeaux, 9p.
Modrak P (2013) *Spatio-temporal characterisation of riparian habitats on an embanked and by-passed Rhône River reach – Vegetation dynamics to support river bank rehabilitation*. MSc thesis, Radboud University Nijmegen & University of Duisburg-Essen, 121p.
Morris GL & J Fan (1998) *Reservoir Sedimentation Handbook: Design and Management of Dams, Reservoirs and Watersheds for Sustainable Use*. McGraw-Hill Book Co., New York, 805p. available at: www.reservoirsedimentation.com.
Morritt D, Stefanoudis PV, Pearce D, Crimmen OA & PF Clark (2014) Plastic in the Thames: a river runs through it. *Marine Pollution Bulletin* 78(1):196–200.

Morse NB, Pellissier PA, Cianciola EN, Brereton RL, Sullivan MM, Shonka NK, Wheeler TB & WH McDowell (2014) Novel ecosystems in the Anthropocene: a revision of the novel ecosystem concept for pragmatic applications. *Ecology and Society* 19(2):12p.

Muhar S, Schmutz S & M Jungwirth M (1995) River restoration concepts—goals and perspectives. In: Schiemer F, Zalewski M & JE Thorpe [eds] *The Importance of Aquatic-Terrestrial Ecotones for Freshwater Fish*. Kluwer, Dordrecht, pp. 183–194.

Muhar S, Poppe M, Preis S, Jungwirth M & S Schmutz (2011) Schutz und Sicherung ökologisch sensibler Fließgewässerstrecken: Anforderungen, Kriterien, Implementierungsprozess. *Österreichische Wasser-und Abfallwirtschaft* 63(9–10):196–204.

Müller M, Bieri M, Boillat JL & A Schleiss (2010) Barrage de Lavey–Modélisations physique et numérique des écoulements et du transport solide dans le Rhône. *Wasser Energie Luft—eau énergie air—Acqua energia aria* 102:327–332.

Muñoz-Mas R, Garófano-Gómez V, Andrés-Doménech I, Corenblit D, Egger G, Francés F, Ferreira MT, García-Arias A, Politti E, Rivaes R, Rodríguez-González PM, Steiger J, Vallés-Morán FJ & F Martínez-Capel (2017) Exploring the key drivers of riparian woodland successional pathways across three European river reaches. *Ecohydrology*:1–19.

Murray QW (1955) Water from the desert: some ancient Egyptian achievements. *The Geographical Journal* 121(2):171–181.

Naiman RJ, Décamps H & ME McClain (2005) *Riparia. Ecology, conservation, and management of streamside communities*. Elsevier, Amsterdam, 430p.

Nanson GC & JC Croke (1992) A genetic classification of floodplains. *Geomorphology* 4(6):459–486.

Netzband A (2007) Sediment management: an essential element of river basin management plans. *Journal of Soils and Sediments* 7(2):117–132.

Newson M & J Lewin (1991) Climatic change, river flow extremes and fluvial erosion-scenarios for England and Wales. *Progress in Physical Geography* 15(1):1–17.

Nicolas Y & D Pont (1995) Importance d'annexes latérales artificielles pour le recrutement en juvéniles de poissons dans un fleuve aménagé, le bas-Rhône. *Bulletin Français de la Pêche Piscicole* 337/338/339:249–257.

Nicolas Y & D Pont (1997) Hydrosedimentary classification of natural and engineered backwaters of a large river, the lower Rhône: possible applications for the maintenance of high fish biodiversity. *Regulated Rivers: Research & Management* 13:417–431.

Nilsson C & M Dynesius (1994) Ecological effects of river regulation on mammals and birds: a review. *River Research and Applications*, 9(1):45–53.

Nilsson C & K Berggren (2000) Alterations of Riparian Ecosystems Caused by River Regulation: Dam operations have caused global-scale ecological changes in riparian ecosystems. How to protect river environments and human needs of rivers remains one of the most important questions of our time. *American Institute of Biological Sciences Bulletin*, 50(9):783–792.

Nilsson C, Reidy CA, Dynesius M & C Revenga (2005) Fragmentation and flow regulation of the world's large river systems. *Science* 308(5720):405–408.

O'Connor JE, Dud, JJ & GE Grant (2015) 1000 dams down and counting. *Science* 348(6234):496–497.

Oliver CD & BC Larson (1996) *Forest stand dynamics*. Wiley, New York, 544p.

Olivier JM, Carrel G, Lamouroux N, Dole-Olivier M-J, Malard F, Bravard JP & C Amoros (2009) The Rhône River basin. In: Tockner K, Uehlinger U & T Robinson [eds] *Rivers of Europe*. Academic Press, San Diego, 728p.

Opperman JJ, Galloway GE, Fargione J, Mount JF, Richter BD & S Secchi (2009) Sustainable floodplains through large-scale reconnection to rivers. *Science* 326(5959):1487–1488.

Opperman JJ, Luster R, McKenney BA, Roberts M & AW Meadows (2010) Ecologically functional floodplains: connectivity, flow regime, and scale. *Journal of the American Water Resources Association* 46(2):211–226.

Oksanen J, Blanchet FG, Friendly M, Kindt R, Legendre P, McGlinn D, Minchin PR, O'Hara RB, Simpson GL, Solymos P, Stevens MHH, Szoecs E & H Wagner (2017) *vegan: Community Ecology Package*. R package version 2.4-3. https://CRAN.R-project.org/package=vegan.

Ortmann-Ajkai A, Lóczy D, Gyenizse P & E Pirkhoffer (2014) Wetland habitat patches as ecological components of landscape memory in a highly modified floodplain. *River Research and Applications 30*(7):874–886.

Owens PN (2005) Models and budgets for sediment management at the river basin scale. *Journal of Soils and Sediments* 5(4):201–212.

Owens PN, Batalla RJ, Collins AJ, Gomez B, Hicks DM, Horowitz AJ, Kondolf GM, Marden M, Page MJ, Peacock DH, Petticrew EL, Salomons W & NA Trustrum (2005) Fine-grained sediment in river systems: environmental significance and management issues. *River Research and Applications* 21:693–717.

Owens PN (2007) Introduction. Background and summary of this issue on sediment linkages. *Journal of Soils and Sediments* 7(5):273–276.

Ozenda P (1994) *Végétation du continent européen*. Delachaux et Niestlé, Lausanne, 271p.

Paine DM (1985) 'Ergodic' reasoning in geomorphology: time for a review of the term? *Progress in Physical Geography* 9(1):1–15.

Pardé M (1925) Le régime du Rhône. *Revue de géographie alpine* 13(3):459–547.

Parrot E (2015) *Analyse spatio-temporelle de la morphologie du chenal du Rhône du Léman à la Méditerranée*. PhD thesis, University of Lyon 3, 469p.

Petts GE (1994) *Impounded rivers: perspectives for ecological management*. Wiley, Chichester, 326p.

Petts GE (1999) River regulation. In: Alexander DE [ed] *Environmental Geology*. Encyclopedia of Earth Science. Springer, Dordrecht.

Petts GE & AM Gurnell (2005) Dams and geomorphology: research progress and future directions. *Geomorphology* 71(1–2):27–47.

Pfarr U, Kuhn S, Huppmann O & G Klaiber (1996) *Rahmenkonzept des Landes Baden-Württemberg zur Umsetzung des Integrierten Rheinprogramms*. Oberrheinagentur, Lahr, 94p.

Pickett STA (1989) Space-for-time substitution as an alternative to long-term studies. In: Lickens GE [ed] *Long-term studies in ecology*. Springer, New York, pp. 110-135.

Piégay H, Joly PB, Foussadier R, Mourier V & G Pautou G (1997) Principes de réhabilitation des marges du Rhône à partir d'indicateurs géomorphologiques, phyto-écologiques et batrachologiques (cas du Rhône court-circuité de Pierre-Bénite) / Principles for the rehabilitation of the banks of the Rhône, using geomorphological, phyto-ecological and batrachological indicators. *Revue de géographie de Lyon* 72(1):7–22.

Piégay H & SA Schumm (2003) System approaches in fluvial geomorphology. In: Kondolf GM & H Piégay [eds] *Tools in fluvial geomorphology*. Wiley, Chichester, 688p.

Piégay H, Hupp CR, Citterio A, Dufour S, Moulin B & DE Walling (2008) Spatial and temporal variability in sedimentation rates associated with cutoff channel infill deposits: Ain River, France. *Water Resources Research* 44(5):1–18.

Piégay H (2016) The spatial framework: Emphasizing spatial structure and nested character of fluvial forms. In: Kondolf GM & H Piégay [eds] *Tools in fluvial geomorphology*. 2nd edition. Wiley, Chichester, 541p.

Piégay H, Seignemartin G, Tena-Pagan A, Räpple B, Barra A, Berger J-F, Roux G, Tal M, Vazquez D & T Winiarski (2018) *Stocks sédimentaires des marges actives – Approche comparée inter-sites DZM – PDR – PBN*. Report OSR 4, No. 2, Action II.2 and Action II.4., 92p.

Pizzuto JE (1987) Sediment diffusion during overbank flows. *Sedimentology* 34(2):301–317.

Poff NL & DD Hart (2002) How dams vary and why it matters for the emerging science of dam removal. *BioScience* 52(8):659–668.

Poff NL, Allan JD, Bain MB, Karr JR, Pestegaard KL, Richter BD, Sparks RE & JC Stromberg (1997) The natural flow regime: A paradigm for river conservation. *BioScience* 47(11):769–784.

Poinsart D (1992) *Effets des aménagements fluviaux sur les débits liquides et solides. L'exemple du Rhône dans les plaines de Miribel-Jonage et Donzère-Mondragon*. PhD thesis, University of Lyon 3, 501p.

Poinsart D & PG Salvador (1993) Histoire de l'endiguement du Rhône à l'aval de Lyon (XIXè siècle). In: Piquet F [eds] *Le fleuve et ses métamorphoses*, Actes du colloques qui s'est tenu à Lyon, du 13 au 15 May 1992, Didier Erudition, Paris, pp299–313.

Poizat G et D Pont (1996) Multi-scale approach to species–habitat relationships: juvenile fish in a large river section. *Freshwater Biology* 36:611–622.

Polzin ML & SB Rood (2006) Effective disturbance: seedling safe sites and patch recruitment of riparian cottonwoods after a major flood of a mountain river. *Wetlands* 26(4):965–980.

Pont B, Mathieu M, Bazin N, Aguiard C & AS Pillard (2009) *Plan de gestion Réserve Naturelle de l'Ile de la Platière, période 2008–2017*. 154p.

Pont B (2017) *Evolution des boisements de l'Ile des Graviers et des marges alluviales du RCC de Péage de Roussillon*. 3p.

Pont B (2018) Personal communication, 30/03/2018.

Ponts and Chaussées (1910) *Monographie du Rhône de la frontière suisse à la mer*. Imp. Réunies, Lyon, 32p.

Przedwojski B, Błażejewski R & KW Pilarczyk (1995) *River training techniques. Fundamentals, design and applications*. Balkema, Rotterdam, 629p.

R Development Core Team (2016). *R: A language and environment for statistical computing*. R Foundation for Statistical Computing, Vienna, Austria, http://www.R-project.org.

Rameau JC, Mansion D, Dumé G, Timbal J, Lecointe A, Dupont P & R Keller (1989) *Flore forestière française. Guide écologique illustré. Vol 1 Plaines et collines*. Institut pour le developpement forestier, Paris, 1785p.

Rameye L, Kiener A, Spiellmann CP & J Biousse (1976) Aspect de la biologie de l'alose du Rhône. Pêche et difficultés croissantes de ses migrations. *Bulletin Français de Pisciculture* 263:50–76.

Räpple B, Piégay H, Stella JC & D Mercier (2017) What drives riparian vegetation encroachment in braided river channels at patch to reach scales? Insights from annual airborne surveys (Drôme River, SE France, 2005–2011). *Ecohydrology* 10(8):16p.

Raunkiær C (1934) *The life forms of plants and statistical plant geography. Being the collected papers of C. Raunkiær*. Clarendon Press, Oxford, 632p.

Reckendorfer W, Schmalfuss R, Baumgartner C, Habersack H, Hohensinner S, Jungwirth M & F Schiemer (2005) The Integrated River Engineering Project for the

free-flowing Danube in the Austrian Alluvial Zone National Park: contradictory goals and mutual solutions. *Archiv für Hydrobiologie Supplement* 155(1–4):613–630.

Reynard E, Arnaud-Fassetta G, Laigre, L & P Schoeneich (2009) Le Rhône alpin vu sous l'angle de la géomorphologie : état des lieux. In: Reynard E, Evéquoz-Dayen M & P Dubuis [eds] *Le Rhône : dynamique, histoire et société*. Cahiers de Vallesia, Sion, pp 75–102.

Rhoads BL, Lewis QL & W Andresen (2016) Historical changes in channel network extent and channel planform in an intensively managed landscape: Natural versus human-induced effects. *Geomorphology* 252:17–31.

Rinaldi M, Wyżga B & N Surian (2005) Sediment mining in alluvial channels: physical effects and management perspectives. *River Research and Applications* 21(7):805–828.

Riquier J, Piégay H & M Sulc Michalkova (2015) Hydromorphological conditions in eighteen restored floodplain channels of a large river: linking patterns to processes. *Freshwater Biology* 60:1085–1103.

Riquier J, Piégay H, Lamouroux N & L Vaudor (2017) Are restored side channels sustainable aquatic habitat features? Predicting the potential persistence of side channels as aquatic habitats based on their fine sedimentation dynamics. *Geomorphology* 295:507–528.

Riquier J, Piégay H & L Vaudor (in prep.) Prediction of sedimentation rates in restored and unrestored floodplain channels of the Rhône River based on their hydrodynamic conditions.

Roditis PS & D Pont (1993) Dynamiques fluviales et milieux de sédimentation du Rhône à l'amont immédiat de son delta. *Méditerranée* 78(3–4) La Camargue et le Rhône, hommes et milieux:5–18.

Rohde S, Hostmann M, Peter A & KC Ewald (2006) Room for rivers: An integrative search strategy for floodplain restoration. *Landscape and Urban Planning* 78(1–2):50–70.

Rollet AJ, Piégay H, Dufour S, Bornette G & H Persat (2014) Assessment of consequences of sediment deficit on a gravel river bed downstream of dams in restoration perspectives: application of a multicriteria, hierarchical and spatially explicit diagnosis. *River Research and Applications* 30(8):939–953.

Rood SB, Hillman C, Sanche T & JM Mahoney (1994) Clonal reproduction of riparian cottonwoods in southern Alberta. *Canadian Journal of Botany* 72:766–1774.

Rosgen DL (2008) Discussion: "Critical evaluation of how the Rosgen classification and associated "natural channel design" methods fail to integrate and quantify fluvial processes and channel response" by Simon A, Doyle M, Kondolf M, Shields FD, Rhoads B & M McPhillips. *Journal of the American Water Resources Association* 44(3):782–792.

Salvador P-G (1983) *Les impacts de l'aménagement du Rhône à l'aval de Pierre-Bénite (Km 1 à 16). L'évolution du fleuve et des paysages de la vallée (1838-1980)*. Maîtrise thesis, University of Lyon 3, 120p.

Salvador P-G, Vérot-Bourrély A, Bravard J-P, Franc O & S Macé (2002) Les crues du Rhône à l'époque gallo-romaine dans la région lyonnaise. In: Bravard J-P & M Magny [eds] *Les paléoenvironnements fluviatiles et lacustres en France depuis 15 000 ans*. Errance, Paris, pp. 215–222.

Salvador P-G, Berger J-F, Gauthier E & B Vannière (2004) Holocene fluctuations of the Rhône River in the alluvial plain of the Basses Terres (Isère, Ain, France) / Fluctuations du Rhône à l'Holocène dans la plaine alluviale de Basses Terres (Isère, Ain, France). *Quaternaire* 15(1–2):177–186.

Sarriquet PE, Bordenave P & P Marmonier (2007) Effects of bottom sediment restoration on interstitial habitat characteristics and benthic macroinvertebrate assemblages in a headwater stream. *River Research and Applications* 23(8):815–828.

Savey P (1992) La gestion environnementale du Rhône / Environmental Management of the Rhône. *Revue de géographie de Lyon* 67(4):285–292.

Scheikl S, Seliger C, Loach A, Preis S, Schinegger R, Walder C, Schmutz S & S Muhar (2016) Schutz ökologisch sensibler Fließgewässer: Konzepte und Fallbeispiele. Protecting ecologically sensitive river stretches: concepts and case studies. *Österreichische Wasser-und Abfallwirtschaft* 68(7–8):288–300.

Schleiss AJ & CD Oehy (2002) Verlandung von Stauseen und Nachhaltigkeit. *Wasser Energie Luft—eau énergie air—Acqua energia aria* 95(7/8):227–234.

Schmidt JC & PR Wilcock (2008) Metrics for assessing the downstream effects of dams. *Water Resources Research* 44(4):1–119.

Schmitt RJP, Bizzi S, Castelletti A & GM Kondolf (2018) Improved trade-offs of hydropower and sand connectivity by strategic dam planning in the Mekong. *Nature Sustainability* 1(2):96–104.

Schnitzler A (1994) Conservation of biodiversity in alluvial hardwood forests of the temperate zone. The example of the Rhine valley. *Forest Ecology and Management* 68(2–3):385–398.

Schumm SA (1977) *The fluvial system*. Wiley, Chichester, 338p.

Schumm SA (1969) River metamorphosis. *Journal of the Hydraulics division* 95(1):255–274.

Schwartz R & HP Kozerski (2003) Entry and deposits of suspended particulate matter in groyne fields of the Middle Elbe and its ecological relevance. *Acta hydrochimica hydrobiologica* 31(4–5):391–399.

Scott ML, Friedman JM & GT Auble (1996) Fluvial process and the establishment of bottomland trees. *Geomorphology* 14:327–339.

Seidel M (2008) *Entwicklungsmaßnahmen von Tieflandbächen mit Holz – Vergleich von Einbauvarianten im Ruhlander Schwarzwasser*. Diploma Thesis, Brandenburg University of Technology Cottbus, 64 p.

Seignemartin G (2014) *Etude préliminaire en deux phases : Compréhension et analyse spatiale de l'évolution des marges aménagées du Rhône par l'étude diachronique du tracé de l'interface lit mineur / lit majeur ; Etude de l'occupation du sol dans les aménagements Girardon en vue d'une caractérisation opérationnelle ; Sur les secteurs court-circuités de Pierre-Bénite, Le-Péage-de-Roussillon, Montélimar et Donzère Mondragon*. MSc thesis, University of Lyon 2, 95p.

Seignemartin G (in prep) Geohistoire de la sédimentation fine et des contaminations métalliques sur les marges construites du Rhône. PhD thesis, University of Lyon 2.

Shields Jr. FD (1995) Fate of Lower Mississippi River habitats associated with river training dikes. *Aquatic Conservation: Marine and Freshwater Ecosystems* 5(2):97–108.

Simon A, Doyle M, Kondolf M, Shields FD, Rhoads B & M McPhillips (2007) Critical evaluation of how the Rosgen classification and associated "natural channel design" methods fail to integrate and quantify fluvial processes and channel response. *Journal of the American Water Resources Association* 43(5):1117–1131.

Simons JH, Bakker C, Schropp MH, Jans LH, Kok FR & RE Grift (2001) Man-made secondary channels along the River Rhine (The Netherlands); results of post-project monitoring. *Regulated Rivers: Research and Management* 17(4–5):473–491.

Slattery MC & Burt TP (1997) Particle size characteristics of suspended sediment in hillslope runoff and stream flow. *Earth Surface Processes and Landforms* 22:705–719.

Stein JL, Stein JA & HA Nix (2002) Spatial analysis of anthropogenic river disturbance at regional and continental scales: identifying the wild rivers of Australia. *Landscape and Urban Planning* 60(1):1–25.

Stella JC, Battles JJ, Orr BK & JR McBride (2006) Synchrony of seed dispersal, hydrology and local climate in a semi-arid river reach in California. *Ecosystems* 9:1200–1214.

Stella JC, Hayden MK, Battles JJ, Piégay H, Dufour S & AK Fremier (2011) The role of abandoned channels as refugia for sustaining pioneer riparian forest ecosystems. *Ecosystems* 14(5):776–790.

Stella JC, Riddle J, Piégay H, Gagnage M & M-L Trémélo (2013) Climate and local geomorphic interactions drive patterns of riparian forest decline along a Mediterranean Basin river. *Geomorphology* 202:101–114.

Stroffek S, Amoros C & M Zylberblat (1996) La logique de réhabilitation physique appliquée à un grand fleuve : le Rhône / A methodology for physical restoration applied to a major river: the Rhône. *Revue de géographie de Lyon* 71(4):287–296.

Stromberg JC, Tiller R & B Richter (1996) Effects of groundwater decline on riparian vegetation of semiarid regions: the San Pedro, Arizona. *Ecological Applications* 6(1):113–131.

Sukhodolov A, Uijttewaal WS & C Engelhardt (2002) On the correspondence between morphological and hydrodynamical patterns of groyne fields. *Earth Surface Processes and Landforms* 27(3):289–305.

Sukhodolov AN (2014) Hydrodynamics of groyne fields in a straight river reach: insight from field experiments. *Journal of Hydraulic Research* 52(1):105–120.

Surian N & M Rinaldi (2003) Morphological response to river engineering and management in alluvial channels in Italy. *Geomorphology* 50(4):307–326.

Surian N, Barban M, Ziliani L, Monegato G, Bertoldi W & F Comiti (2015) Vegetation turnover in a braided river: Frequency and effectiveness of floods of different magnitude. *Earth Surface Processes and Landforms* 40:542–558.

Syvitski JP, Vörösmarty CJ, Kettner AJ & P Green (2005) Impact of humans on the flux of terrestrial sediment to the global coastal ocean. S*cience* 308(5720):376–380.

Ten Brinke WBM, Schulze FH & P van Der Veer (2004) Sand exchange between groyne-field beaches and the navigation channel of the Dutch Rhine: the impact of navigation versus river flow. *River Research and Applications* 20(8):899–928.

Terwei A, Zerbe S, Zeileis A, Annighöfer P, Kawaletz H, Mölder I & C Ammer (2013) Which are the factors controlling tree seedling establishment in North Italian floodplain forests invaded by non-native tree species? *Forest Ecology and Management* 304:192–203.

Thompson DM (2002) Long-term effect of instream habitat-improvement structures on channel morphology along the Blackledge and Salmon Rivers, Connecticut, USA. *Environmental Management* 29(2):250–265.

Thonon I, Middelkoop H & M Van Der Perk (2007) The influence of floodplain morphology and river works on spatial patterns of overbank deposition. *Netherlands Journal of Geosciences* 86(1):63–75.

Thorel M, Piégay H, Barthelemy C, Räpple B, Gruel CR, Marmonier P, Winiarski T, Bedell J-P, Arnaud F, Roux G, Stella JC, Seignemartin G, Tena-Pagan A, Wawrzyniak V, Roux-Michollet D, Oursel B, Fayolle S, Bertrand C & E Franquet (2018) Socio-environmental implications of process-based restoration strategies in large rivers: should we remove novel ecosystems along the Rhône (France)? *Regional Environmental Change*:1–13.

Thorne C, Hey R & M Newson (1997) *Applied fluvial geomorphology for river engineering and management*. Wiley, 376p.

Tockner K & JA Stanford (2002) Riverine flood plains: present state and future trends. *Environmental Conservation* 29(3):308–330.

Tockner K, Pusch M, Borchardt D & MS Lorang (2010) Multiple stressors in coupled river–floodplain ecosystems. *Freshwater Biology* 55(suppl. 1):135–151.

Trémolières M, Sánchez-Pérez JM, Schnitzler A & D Schmitt (1998) Impact of river management history on the community structure, species composition and nutrient status in the Rhine alluvial hardwood forest. *Plant Ecology* 135(1):59–78.

Tricart J & J-P Bravard (1991) L'aménagement des trois plus grands fleuves européens : Rhin, Rhône et Danube. Problèmes et méfaits. *Annales de Géographie* 100(561–562):668–713.

Tritthart M, Liedermann M & H Habersack (2009) Modelling spatio-temporal flow characteristics in groyne fields. *River Research and Applications* 25(1):62–81.

UICN France, FCBN & MNHN (2012) *La Liste rouge des espèces menacées en France - Chapitre Flore vasculaire de France métropolitaine : premiers résultats pour 1 000 espèces, sous-espèces et variétés.* Dossier électronique, 23p.

Uijttewaal WSJ (1999) Groyne field velocity patterns determined with particle tracking velocimetry. *Proceedings of the 28th IAHR Congress*, Graz, 8p.

Uijttewaal WSJ, Lehmann DV & AV Mazijk (2001). Exchange processes between a river and its groyne fields: Model experiments. *Journal of Hydraulic Engineering* 127(11):928–936.

Vaghefi M, Ghodsian M & SAA Salehi Neyshaboori (2009) Experimental study on the effect of a T-shaped spur dike length on scour in a 90 channel bend. *Arabian Journal for Science and Engineering* 34(2):337–348.

Van Looy K, Honnay O, Bossuyt B & M Hermy (2003) The effects of river embankment and forest fragmentation on the plant species richness and composition of floodplain forests in the Meuse valley, Belgium. *Belgian Journal of Botany* 136(2):97–108.

Vannote RL, Minshall GW, Cummins KW, Sedell JR & CE Cushing (1980) The river continuum concept. *Canadian Journal of Fisheries and Aquatic Sciences* 37:130–137.

Vanoni VA (1946) Transport of suspended sediment by water. *Transactions of the American Society of Civil Engineers* 111:67–133.

Verhoeven JT, Soons MB, Janssen R & N Omtzigt (2008) An operational landscape unit approach for identifying key landscape connections in wetland restoration. *Journal of Applied Ecology* 45(5):1496–1503.

Villet O (2014) *Etude de la sédimentation fine associée aux ouvrages Girardon du Vieux Rhône de Montélimar*. MSc thesis, University of Lyon 3, 49p.

Vítková M, Tonika J & J Müllerová (2015) Black locust—Successful invader of a wide range of soil conditions. *Science of the Total Environment* 505:315–328.

Vítková M, Müllerová J, Sádlo J, Pergl J & P Pyšek (2017) Black locust (Robinia pseudoacacia) beloved and despised: A story of an invasive tree in Central Europe. *Forest Ecology and Management* 384:287–302.

Vörösmarty CJ, Meybeck M, Fekete B, Sharma K, Green P & JP Syvitski (2003) Anthropogenic sediment retention: major global impact from registered river impoundments. *Global and planetary change* 39(1–2):169–190.

Walling DE & Q He (1998) The spatial variability of overbank sedimentation on river floodplains. *Geomorphology* 24:209–223.

Walling, D. E. (1999). Linking land use, erosion and sediment yields in river basins. Hydrobiologia 410:223-240 (originally In: Garnier J & JM Mouchel [eds] *Man and River Systems*, Kluwer, Dordrecht).

Walling DE & D Fang (2003) Recent trends in the suspended sediment loads of the world's rivers. *Global and planetary change* 39(1–2):111–126.

Wang ZY, Wu B & G Wang (2007) Fluvial processes and morphological response in the Yellow and Weihe Rivers to closure and operation of Sanmenxia Dam. *Geomorphology* 91(1–2):65–79.

Walling D (2008) The changing sediment loads of the world's rivers. Proceedings of Sediment Dynamics in Changing Environments symposium, IAHS Publ. 325, Christchurch 39, 323–338.

Ward JV (1998) Riverine landscapes: biodiversity patterns, disturbance regimes, and aquatic conservation. *Biological Conservation 83*(3):269–278.

Ward JV, Tockner K, Edwards P, Kollmann J, Bretschko G, Gurnell A, Petts GE & B Rossaro (1999) A reference river system for the Alps: the 'Fiume Tagliamento'. *Regulated Rivers: Research and Management* 15(1–3):63–75.

Ward JV, Tockner K, Uehlinger U & F Malard (2001) Understanding natural patterns and processes in river corridors as the basis for effective river restoration. *River Research and Applications* 17(4–5):311–323.

Ward JV, Tockner K, Arscott DB & C Claret (2002) Riverine landscape diversity. *Freshwater Biology* 47:517–539.

Wasson JG, Malavoi JR, Maridet L, Souchon Y & L Paulin (1995) *Impacts écologiques de la chenalisation des rivières*. Rapport final, Commande DE 30/93. 166p.

Wasson JG (1996) Structure régionale du bassin de la Loire. *La Houille Blanche* 6/7:25–31.

Wasson JG, Chandesris A, Pella H & L Blanc (2004) Les hydro-écorégions : une approche fonctionnelle de la typologie des rivières pour la Directive cadre européenne sur l'eau. *Ingénieries* 40:3–10.

Wasson JG, Chandesris A, Garcia-Bautista A, Pella H & BVilleneuve (2007) REBECCA : *Relationships between ecological and chemical status of surface waters - European Hydro-Ecoregions*. EU 6th Framework Programme, Contract No. SSPI-CT-2003-502158, 44p.

Waters CN, Zalasiewicz J, Summerhayes C, Barnosky AD, Poirier C, Gałuszka A, Cearreta A, Edgeworth M, Ellis EC, Ellis M, Jeandel C, Leinfelder R, McNeill JR, Richter DdeB, Steffen W, Syvitski J, Vidas D, Wagreich M, Williams M, Zhisheng A, Grinevald J, Odada E, Oreskes N, AP Wolfe (2016) The Anthropocene is functionally and stratigraphically distinct from the Holocene. *Science* 351(6269):137–148.

Webb JA, Little SC, Miller KA, Stewardson MJ, Rutherfurd ID, Sharpe AK, Patulny L & NL Poff (2015). A general approach to predicting ecological responses to environmental flows: making best use of the literature, expert knowledge, and monitoring data. *River Research and Applications* 31(4):505–514.

Weitbrecht V (2004) *Influence of dead-water zones on the dispersive mass transport in rivers?* PhD thesis, University of Karlsruhe, 129p.

Weitbrecht V, Socolofsky SA & GH Jirka (2008) Experiments on mass exchange between groin fields and main stream in rivers. *Journal of Hydraulic Engineering* 134(2):173–183.

Wieferich DJ, Bristol RS, Bellmore JR, Vittum KM, Duda J & L Craig (2016) *National Dam Removal Science Database*, U.S. Geological Survey Data Release.

Wiens JA (2002) Riverine landscapes: taking landscape ecology into the water. *Freshwater Biology* 47(4):501–515.

Wilcox AC, O'Connor JE & JJ Major (2014) Rapid reservoir erosion, hyperconcentrated flow, and downstream deposition triggered by breaching of 38 m tall Condit Dam, White Salmon River, Washington. *Journal of Geophysical Research: Earth Surface* 119(6):1376–1394.

Williams AT & SL Simmons (1996) The degradation of plastic litter in rivers: implications for beaches. *Journal of Coastal Conservation* 2(1):63–72.

Wirtz C (2004) *Hydromorphologische und morphodynamische Analyse von Buhnenfeldern der unteren Mittelelbe im Hinblick auf eine ökologische Gewässerunterhaltung*. PhD Thesis, University of Berlin (FU), 291p.

Wolman MG & LB Leopold (1957) *River flood plains: some observations on their formation*. US Geological Survey Professional Paper 282–C. United States Government Printing Office, Washington, pp. 87–107.

Wood PJ & PD Armitage (1997) Biological effects of fine sediment in the lotic environment. *Environmental Management* 21(2):203–217.

World Commission on Dams (2000) *Dams and development. A new framework for decision making*. Report. Earthscan, London, Sterling, 404p.

Wyżga B (1991) Present-day downcutting of the Raba River channel (Western Carpathians, Poland) and its environmental effects. *Catena* 18:551–566.

Wyżga B (2001a) A geomorphologist's criticism of the engineering approach to channelization of gravel-bed rivers: case study of thRaba River, Polish Carpathians. *Environmental Management* 28(3):341–358.

Wyżga B (2001b) Impact of the channelization-induced incision of the Skawa and Wisłoka Rivers, southern Poland, on the conditions of overbank deposition. *Regulated Rivers: Research & Management* 17(1):85–100.

Xiaoqing Y (2003) *Manual on sediment management and measurement*. Operational Hydrology Report No. 47/WMO-No. 948, World Meteorological Organization, Geneva, 158p.

Yossef MFM (2005) *Morphodynamics of rivers with groynes*. PhD Thesis, Technical University of Delft, 225p.

Yossef MF & HJ de Vriend (2010) Sediment exchange between a river and its groyne fields: mobile-bed experiment. *Journal of Hydraulic Engineering* 136(9):610–625.

Zarfl C, Lumsdon AE, Berlekamp J, Tydecks L & K Tockner (2015) A global boom in hydropower dam construction. *Aquatic Sciences* 77(1):161–170.

Zsugyel M, Szabó KG, Kiss ZM, Józsa J, Ciraolo G, Nasello C, Napoli E & T Tél (2012) Detecting the chaotic nature of advection in complex river flows. *Periodica Polytechnica, Civil Engineering* 56(1):97–106.

APPENDICES

Appendix I: Supplementary material Chapter IV

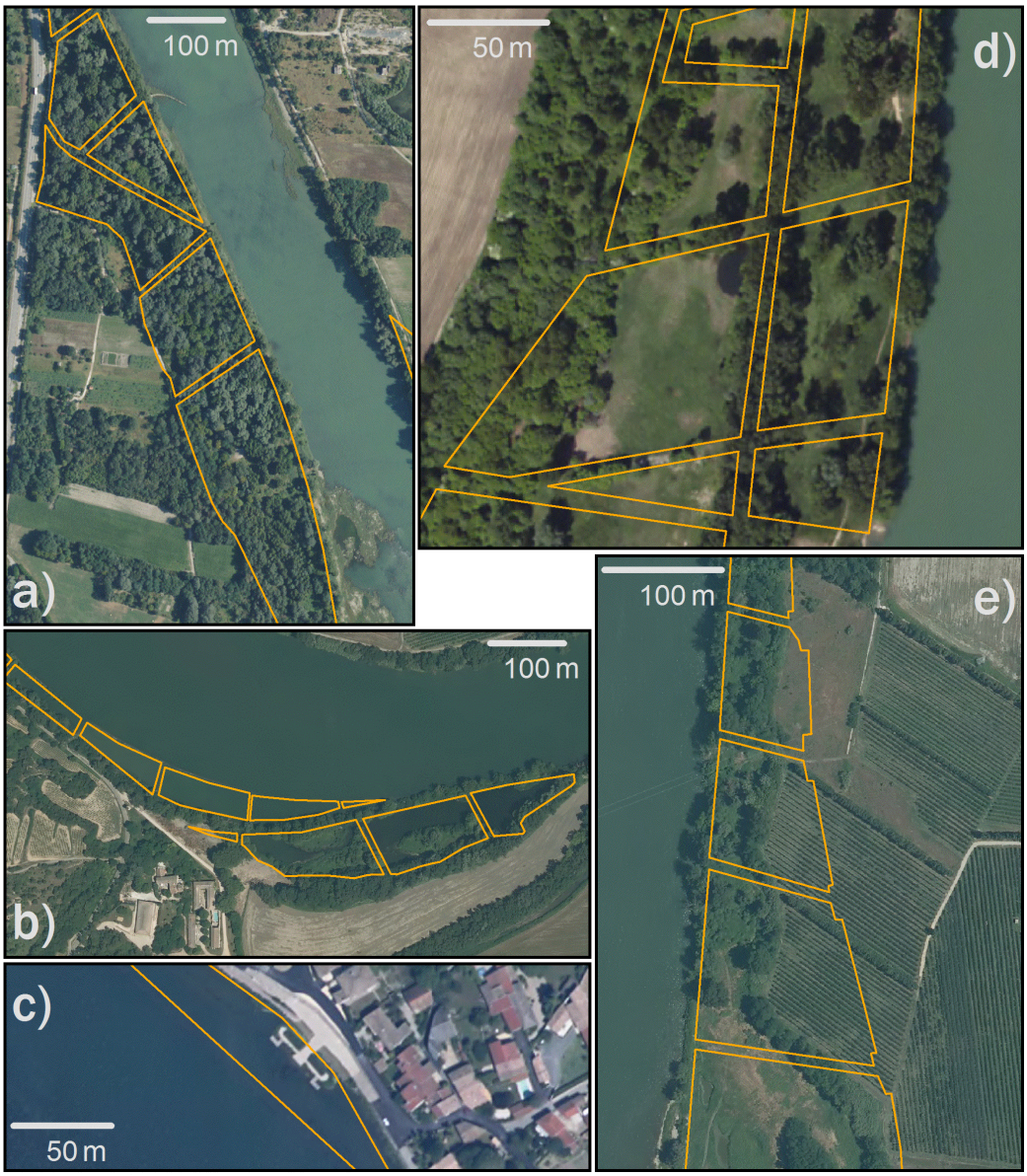

Figure A–I–1: Examples of different land cover units: a) forest, b) water, c) human infrastructure, d) open sites, and e) agriculture.

Figure A–I–2: Examples of different dike construction materials with potentially different seepage potential.

Appendix II: Supplementary material Chapter V

Table A–II–1: Results of Mann-Whitney U tests on terrestrialisation status in the 1940 compared between study reaches.

	PBN	PDR	MON
PDR	W = 2864.5, p = 0.07999	---	---
MON	W = 5502, p = 3.426×10^{-11} (***)	W = 2800, p = 1.51×10^{-06} (***)	---
DZM	W = 6344.5, p = 0.6135	W = 3978.5, p = 0.03375 (*)	W = 1181, p = 3.331×10^{-12} (***)

Table A–II–2: Results of Mann-Whitney U tests on average annual sedimentation rates compared between study reaches.

	PBN	PDR	MON
		Pre-dam surfaces	
PDR	W = 32, p = 0.03579(*)	---	---
MON	W = 72, p = 0.4165	W = 18, p = 0.0009019 (***)	---
DZM	W = 160, p = 0.03957(*)	W = 54, p = 0.06594	W = 109, p = 0.3175
		Post-dam surfaces	
PDR	W = 22, p = 0.0002587(***)	---	---
MON	W = 117, p = 0.00768(**)	W = 59, p = 1	---
DZM	W = 148, p = 0.000166(***)	W = 110, p = 0.06569	W = 110, p = 0.003562(**)

Table A–II–3: Thalweg elevation change prior to and following diversion compared between reaches using Mann-Whitney U tests.

	PBN	PDR	MON
		Pre-dam	
PDR	W = 1405.5, p = 2.928 x 10^{-06} (***)	---	---
MON	W = 3351.5, p = 8.941 x 10^{-06} (***)	W = 1155.5, p = 0.0339 (*)	---
DZM	W = 7749.5, p < 2.2 x 10^{-16} (***)	W = 4070.5, p = 2.753 x 10^{-07} (***)	W = 4120.5, p = 6.831 x 10^{-12} (***)
		Post-dam	
PDR	W = 358.5, p < 2.2 x 10^{-16} (***)	---	---
MON	W = 4064.5, p = 6.629 x 10^{-14} (***)	W = 941.5, p = 0.0004825 (***)	---
DZM	W = 5572.5, p = 0.0001026 (***)	W = 1305.5, p = 3.259 x 10^{-08} (***)	W = 1599.5, p = 0.0005497 (***)

Table A–II–4: Pairwise Wilcoxon test results of changes in terrestrialisation state between two dates.

		PDR	
	1948/9	*1958*	*1986*
1958	V = 1398, p < .001	---	---
1986	---	V = 1, p < .001	---
2006/7/9	---	---	V = 25, p < .001
		DZM	
	1947	*1954/5*	*1976*
1954/5	V = 286, p < .001	---	---
1976	---	V = 34, p < .001	---
2006/7/9	---	---	V = 1158, p < .05

Table A–II–5: Results of pairwise Wilcoxon tests on terrestrialisation rates.

	PDR	
	1948/9 – 1958	*1958 – 1986*
1958 – 1986	V = 104, p = 6.08 x 10^{-09}	---
1986 – 2006/7/9	---	V = 1589, p = 1.41 x 10^{-09}
	DZM	
	1947 – 1954/5	*1954/5 – 1976*
1954/5 – 1976	V = 4581, p = 1.46 x 10^{-07}	---
1976 – 2006/7/9	---	V = 5622, p < 2.20 x 10^{-16}

Table A–II–6: Pairwise Wilcoxon test results.

		PDR	
	1948/9	*1958*	*1986*
1958	V = 574, p = 0.54	---	---
1986	---	V = 406.5, p = 0.0001098 (***)	---
2006/7/9	---	---	V = 231, p = $3.82 * 10^{-06}$ (***)
		DZM	
	1947	*1954/5*	*1976*
1954/5	V = 3115, p = 0.48 (**)	---	---
1976	---	V = 644.5, p = $1.14 * 10^{-12}$ (***)	---
2006/7/9	---	---	V = 3469, p = 0.11

Table A–II–7: Vegetalisation rates, pairwise Wilcoxon test results.

	PDR	
	1948/9 – 1958	*1958 – 1986*
1958 – 1986	V = 568, p = 0.27	---
1986 – 2006/7/9	---	V = 668, p = 0.21
	DZM	
	1947 – 1954/5	*1954/5 – 1976*
1954/5 – 1976	V = 908, p = $2.69 * 10^{-10}$	---
1976 – 2006/7/9	---	V = 4944, p = $4.02 * 10^{-09}$

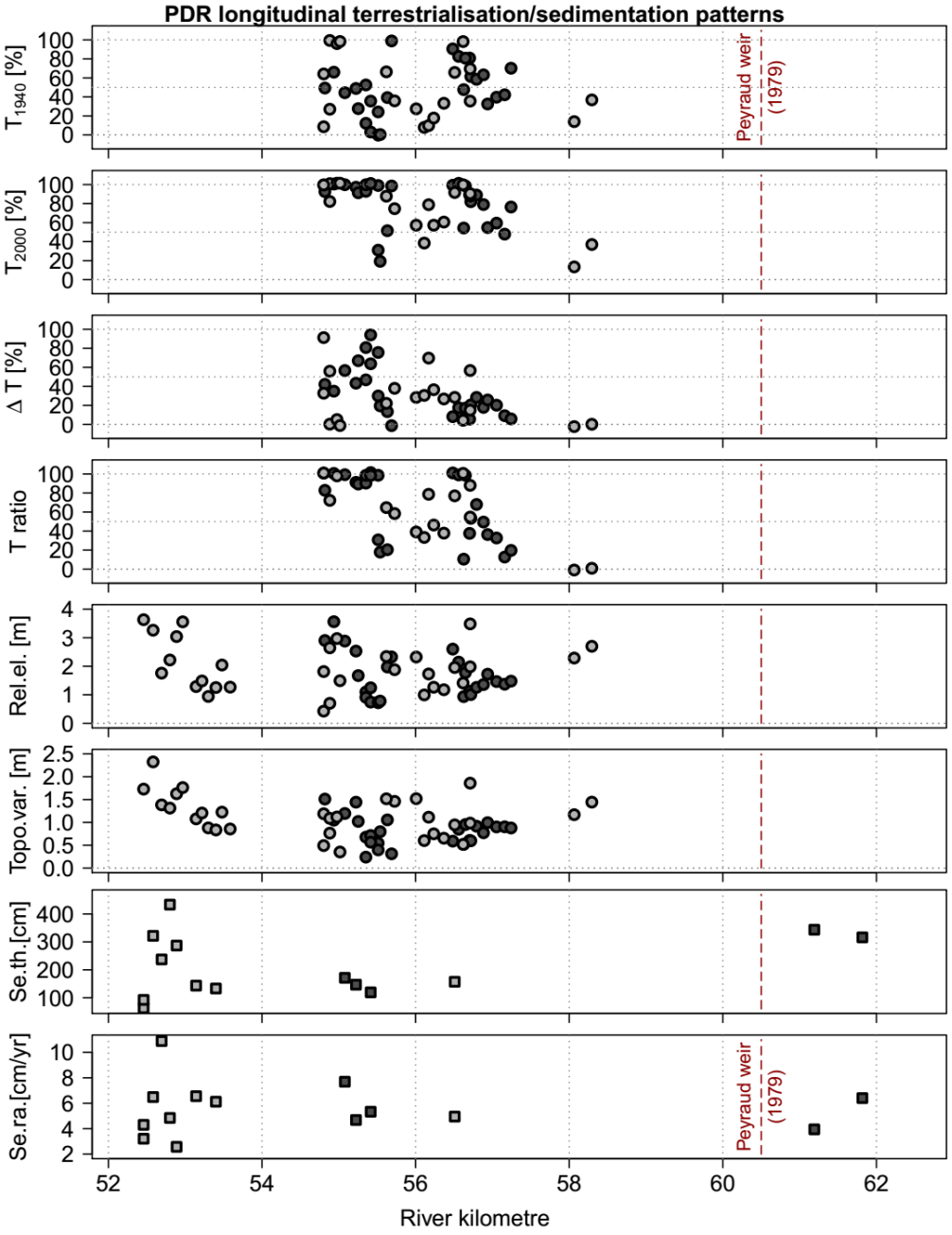

Figure A–II–1: Longitudinal patterns of terrestrialisation and sedimentation in the reach of PDR. For a detailed description of the variables see Figure V–24.

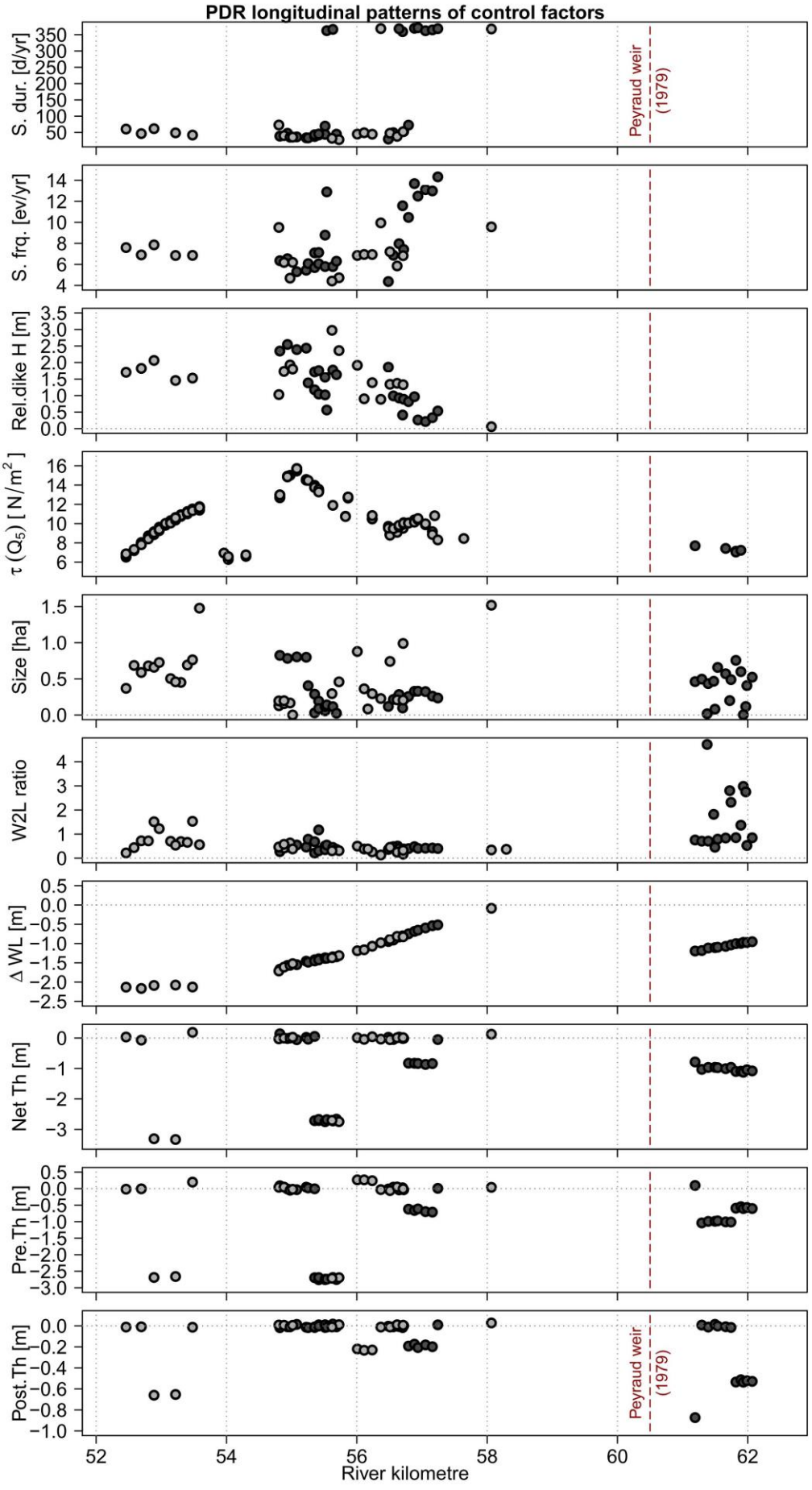
PDR longitudinal patterns of control factors
S. dur. [d/yr]
S. frq. [ev/yr]
Rel.dike H [m]
τ (Q5) [N/m2]
Size [ha]
W2L ratio
Δ WL [m]
Net Th [m]
Pre.Th [m]
Post.Th [m]
Peyraud weir
(1979)
River kilometre

Figure A–II–2 (preceding page): Longitudinal patterns of environmental conditions in the reach of PDR. For a detailed description of the variables see Figure V–25.

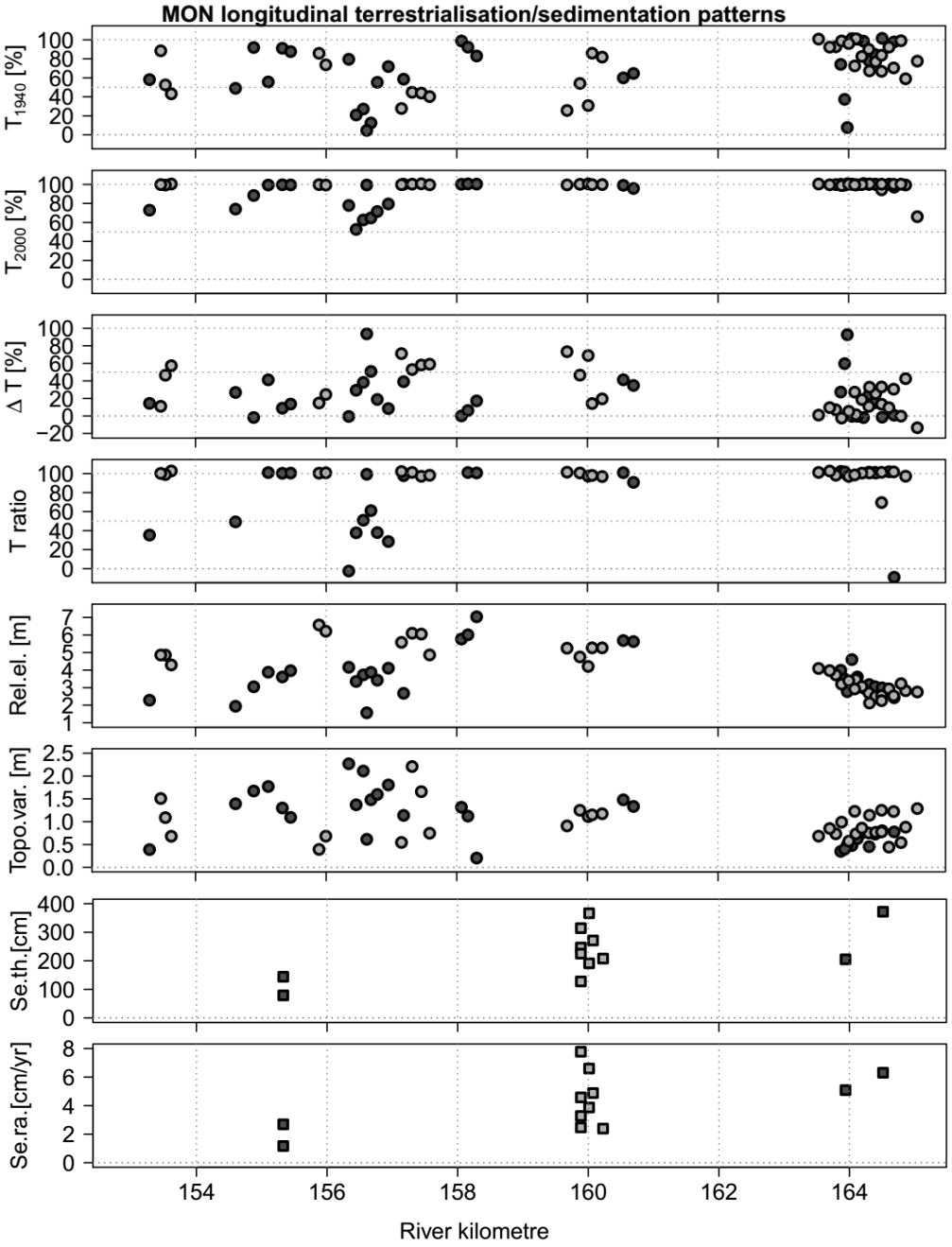

Figure A–II–3: Longitudinal patterns of terrestrialisation and sedimentation in the reach of MON. For a detailed description of the variables see Figure V–24.

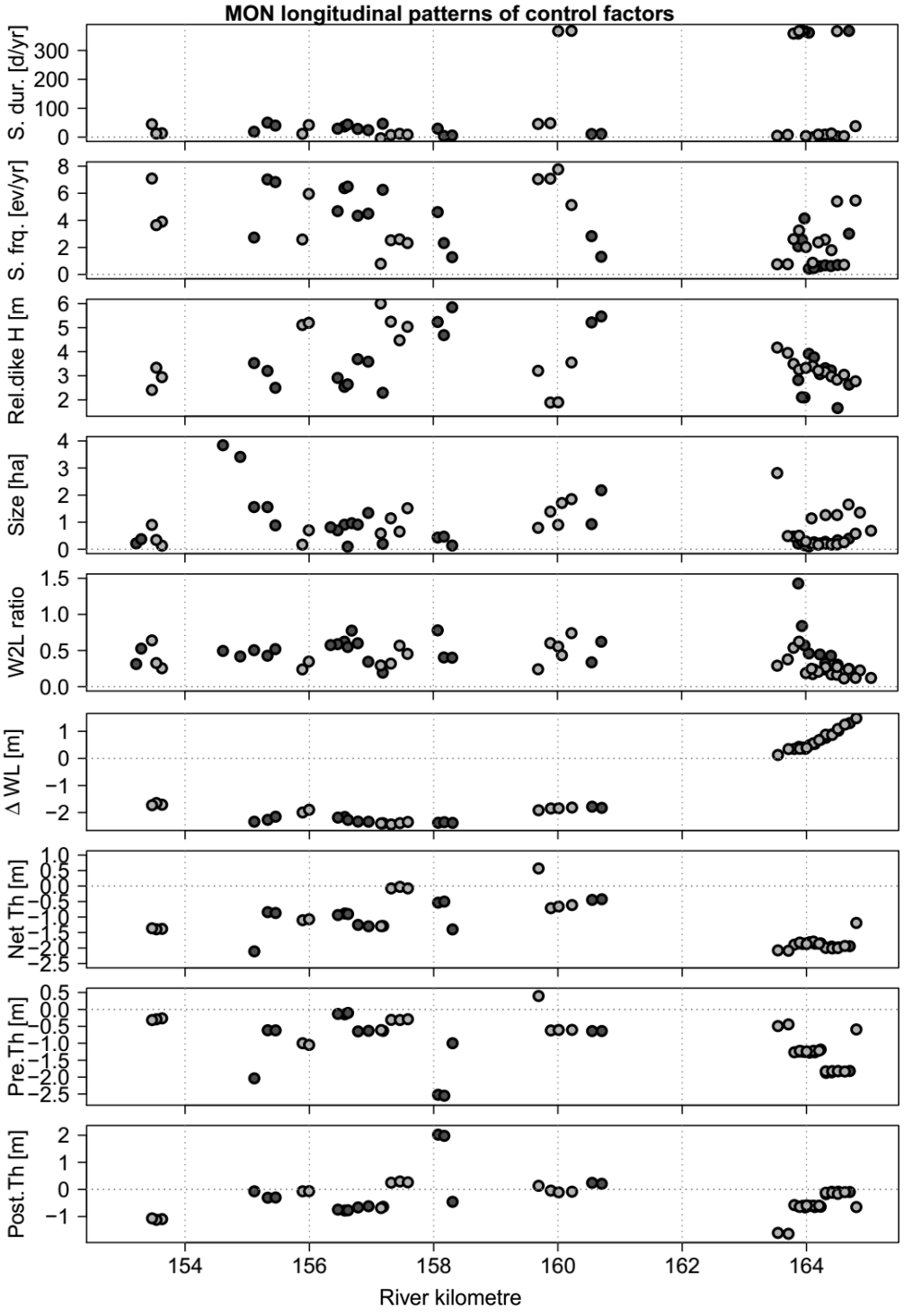

Figure A–II–4: Longitudinal patterns of environmental conditions in the reach of MON. For a detailed description of the variables see Figure V–25.

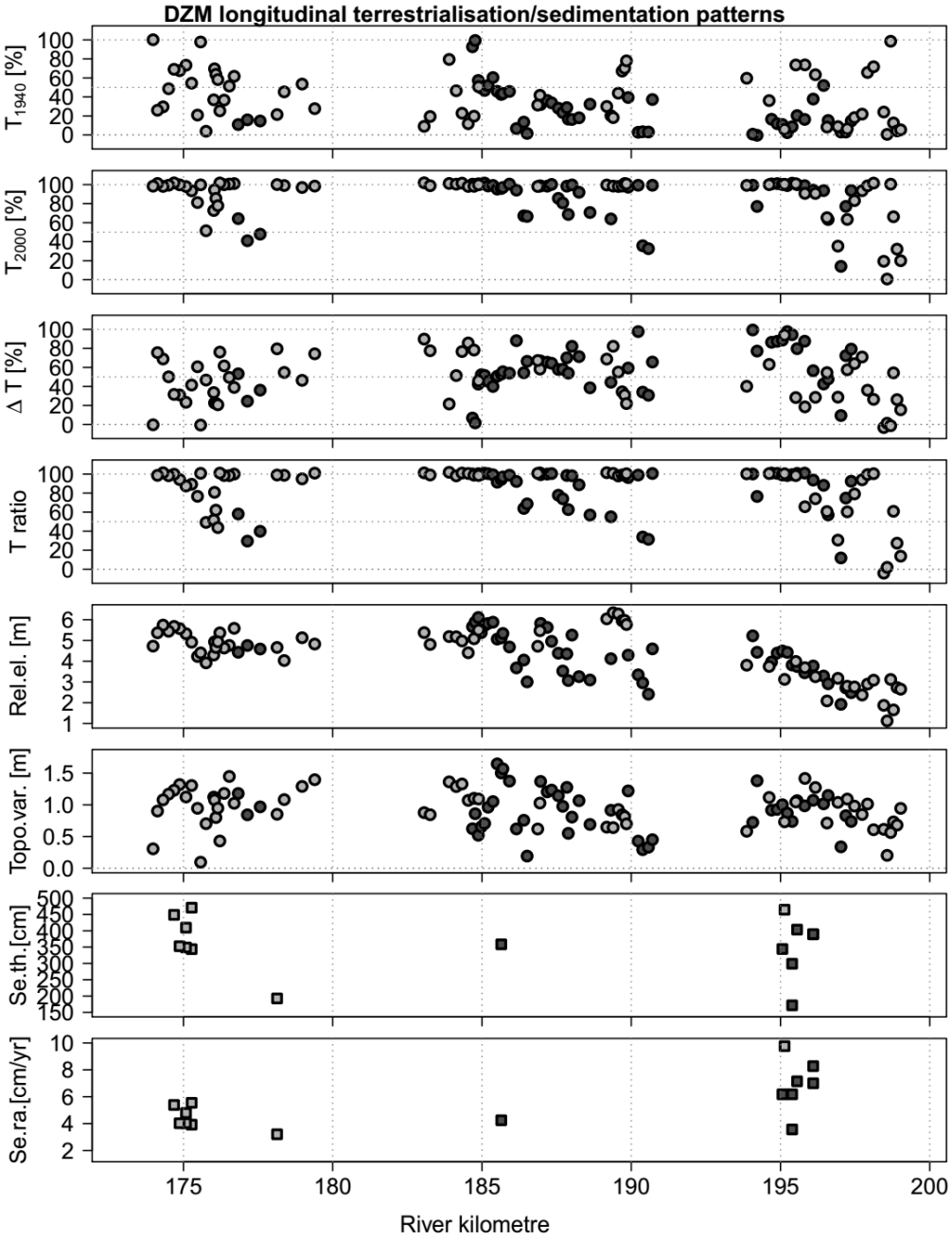

Figure A–II–5: Longitudinal patterns of terrestrialisation and sedimentation in the reach of DZM. For a detailed description of the variables see Figure V–24.

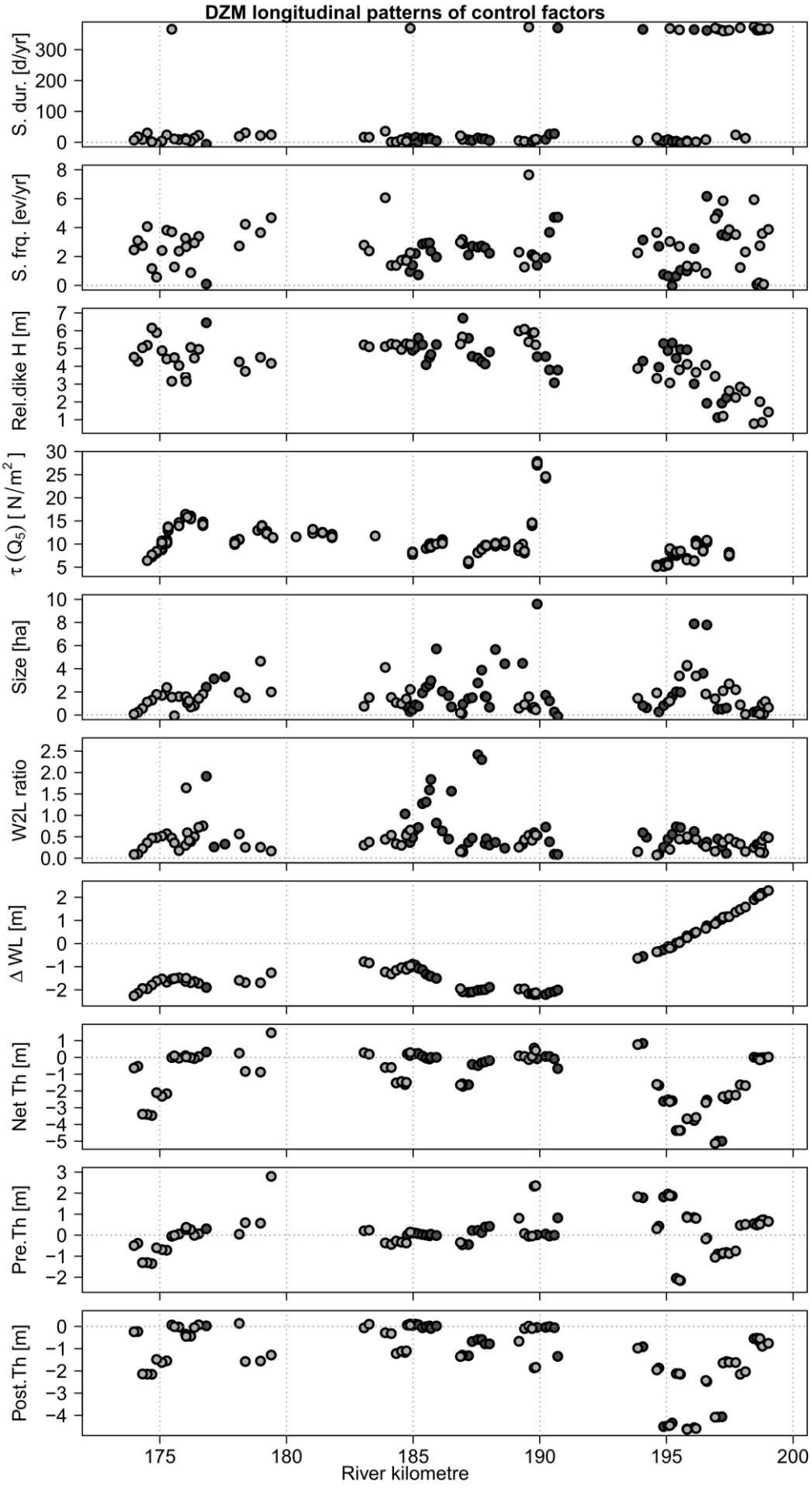
DZM longitudinal patterns of control factors
S. dur. [d/yr]
S. frq. [ev/yr]
Rel.dike H [m]
τ (Q5) [N/m2]
Size [ha]
W2L ratio
Δ WL [m]
Net Th [m]
Pre.Th [m]
Post.Th [m]
River kilometre

Figure A–II–6 (preceding page): Longitudinal patterns of environmental conditions in the reach of DZM. For a detailed description of the variables see Figure V–25.

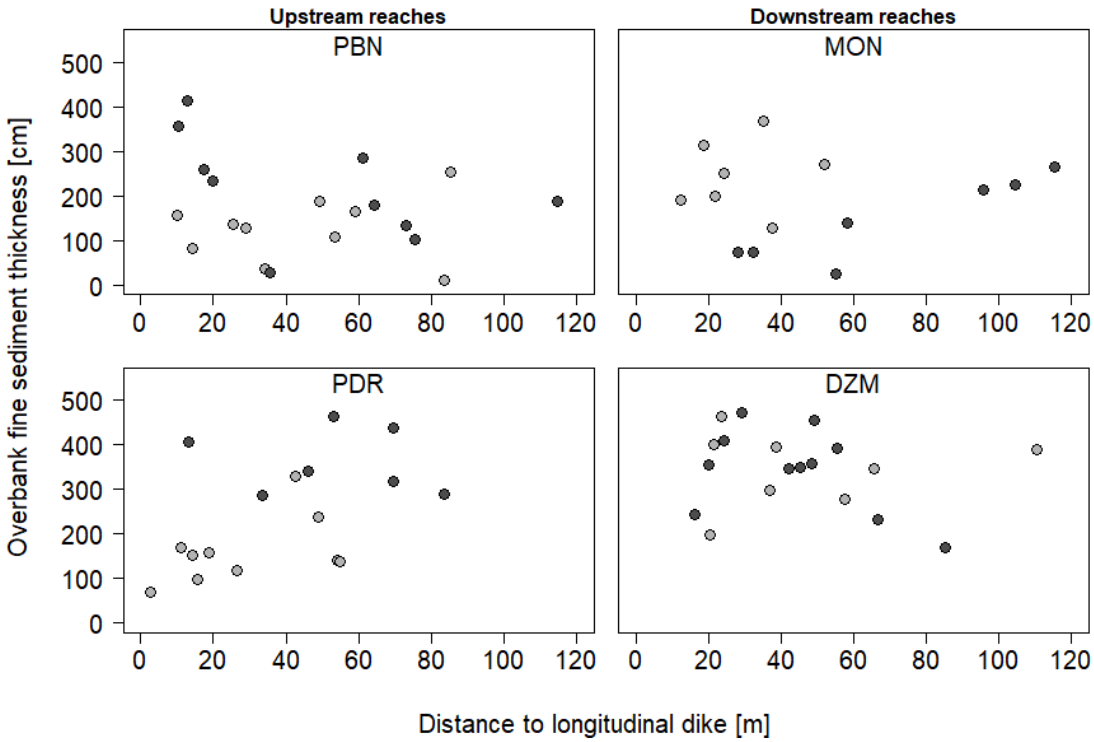

Figure A–II–7: Lateral patterns of overbank fine sediment thickness. Dark grey: pre-dam surfaces, light grey: post-dam surfaces.

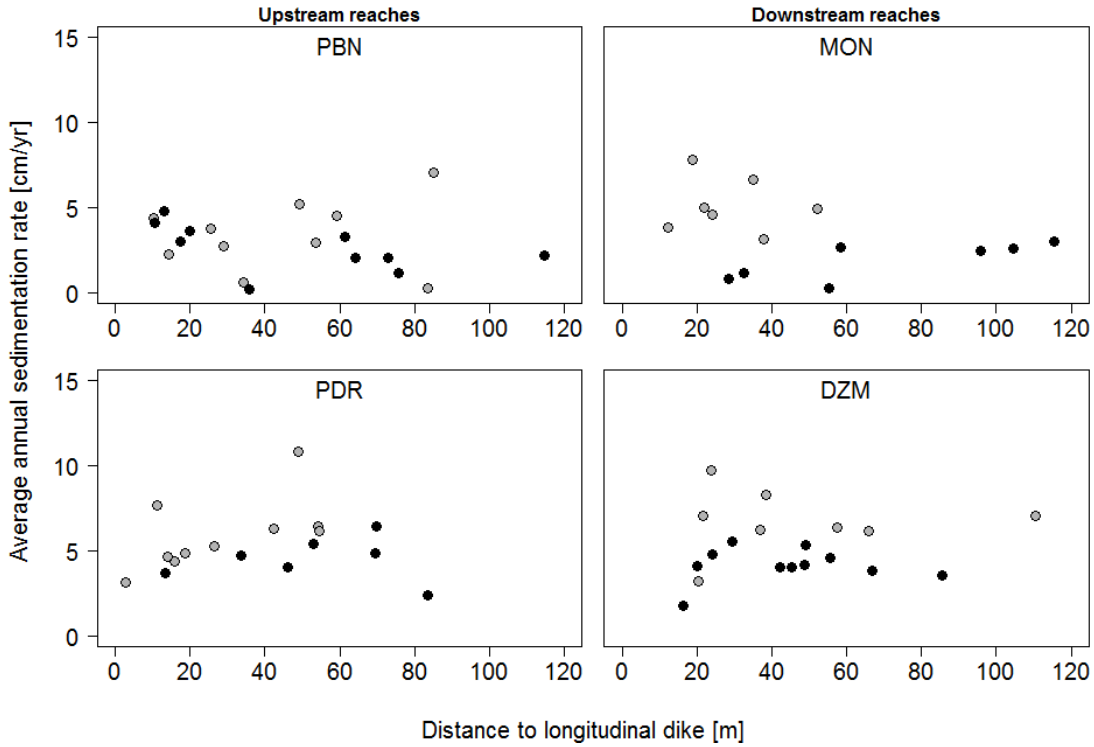

Figure A–II–8: Lateral patterns of average annual sedimentation rates. Dark grey: pre-dam surfaces, light grey: post-dam surfaces.

Appendix III: Supplementary material Chapter VI

Table A–III–1: Results of pairwise Mann-Whitney U tests (significant differences in bold print, α-levels: * p < .05; ** p < .01; *** p < .001; **** p < .0001) for plot density, **all plants**. Grey: Between and within reach comparisons of dike fields (within-reach comparisons, i.e. comparison of pre- and post-dam surfaces within each reach, are underlined). White: Comparisons between dike fields and external sites (MFP = mature floodplain; PI = pioneer islands).

		PBN-B	PDR-B	MON-B	DZM-B	PBN-C	PDR-C	MON-C	DZM-C	PLAT-A
				Pre-dam				*Post-dam*		*MFP*
PDR-B	*Pre-dam*	W = 61, p = 0.70	---	---	---	---	---	---	---	---
MON-B	*Pre-dam*	W = 51, p = 0.81	W = 33, p = 0.22	---	---	---	---	---	---	---
DZM-B	*Pre-dam*	W = 63, p = 0.90	W = 50, p = 0.76	W = 64, p = 0.56	---	---	---	---	---	---
PBN-C	*Pre-dam*	W = 52, p = 0.86	W =39, p = 0.44	W = 52, p = 0.91	W = 48, p = 0.65	---	---	---	---	---
PDR-C	*Post-dam*	W = 64, p = 0.56	W = 55, p = 0.74	W = 64, p = 0.32	W = 57, p = 0.92	W = 62, p = 0.39	---	---	---	---
MON-C	*Post-dam*	W = 50, p = 0.76	W = 33, p = 0.22	W = 44, p = 0.68	W = 40, p = 0.31	W = 48, p = 0.91	W = 37, p = 0.35	---	---	---
DZM-C	*Post-dam*	W = 60, p = 0.76	W = 45, p = 0.74	W = 67, p = 0.22	W = 60, p = 0.76	W = 56, p = 0.68	W = 46, p = 0.80	W = 66, p = 0.25	---	---
PLAT-A	*MFP*	**W = 68, p = 6.2 x 10^{-5} (****)**	**W = 21, p = 1.7 x 10^{-7} (****)**	**W = 61, p = 1.1 x 10^{-4} (***)**	**W = 24, p = 7.0 x 10^{-8} (****)**	**W = 122, p = 0.02 (*)**	**W = 15, p = 3.7 x 10^{-8} (****)**	**W = 62, p = 1.2 x 10^{-4} (***)**	**W = 53, p = 4.1 x 10^{-5} (****)**	---
DROM-D	*PI*	**W = 287, p = 7.4 x 10^{-3} (**)**	**W = 167, p = 4.4 x 10^{-4} (***)**	**W = 264, p = 0.01 (*)**	**W = 189, p = 3.0 x 10^{-4} (***)**	W = 361, p = 0.12	**W = 159, p = 3.2 x 10^{-4} (***)**	**W = 296, p = 0.03 (*)**	**W = 188, p = 9.6 x 10^{-4} (***)**	**W = 3,172, p = 9.7 x 10^{-4} (***)**

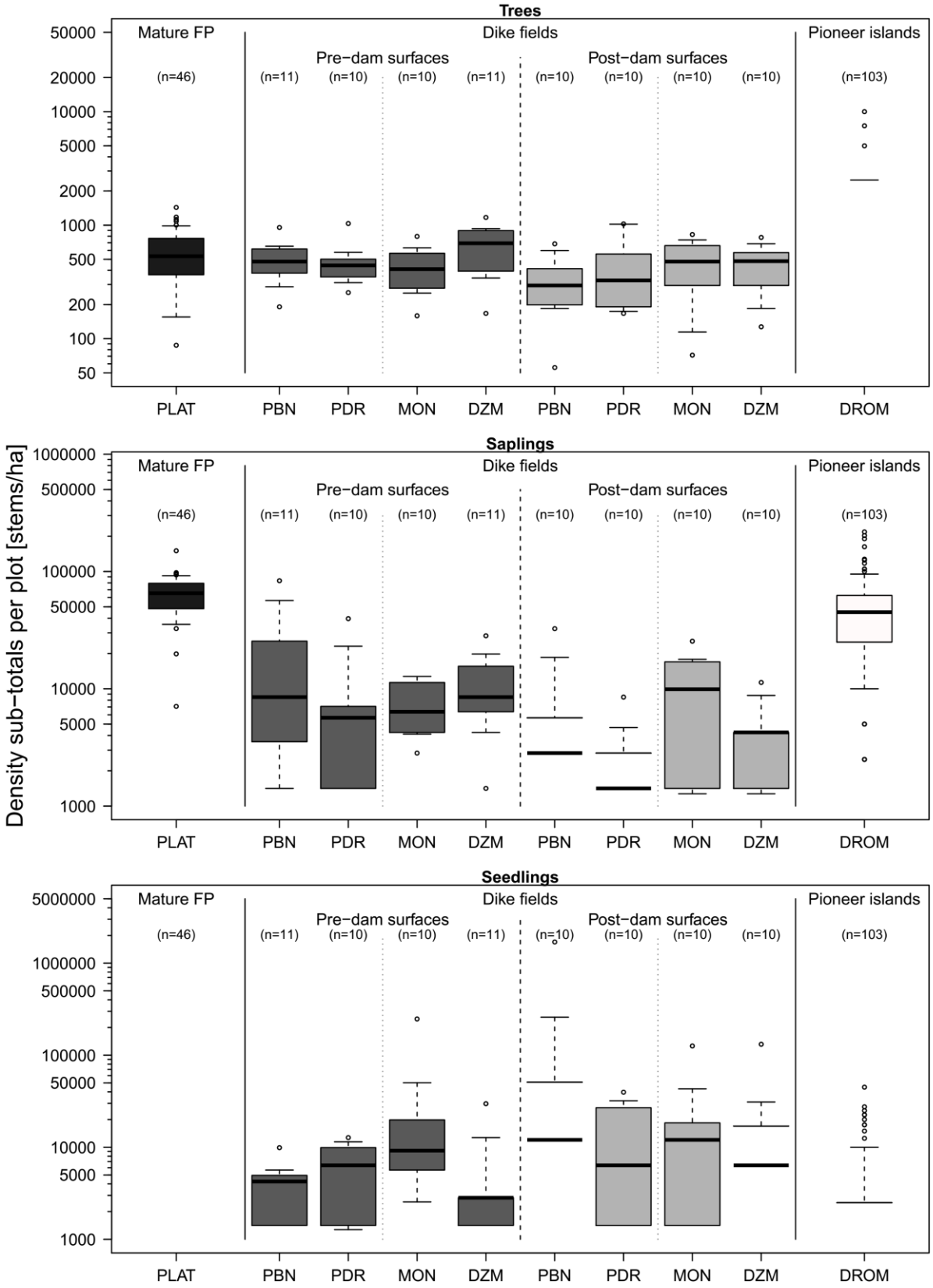

Figure A–III–1: Comparison of density sub-totals per plot between dike fields and between dike fields and reference sites for **each LHS** separately.

Table A–III–2: Results of pairwise Mann-Whitney U tests (significant differences in bold print, α-levels: * p < .05; ** p < .01; *** p < .001; **** p < .0001) for **tree** density. Grey: Between and within reach comparisons of dike fields (within-reach comparisons, i.e. comparison of pre- and post-dam surfaces within each reach, are underlined). White: Comparisons between dike fields and external sites (MFP = mature floodplain; PI = pioneer islands).

		PBN-B	PDR-B	MON-B	DZM-B	PBN-C	PDR-C	MON-C	DZM-C	PLAT-A
				Pre-dam				*Post-dam*		*MFP*
PDR-B	*Pre-dam*	W = 64, p = 0.56	---	---	---	---	---	---	---	---
MON-B	*Pre-dam*	W = 66, p = 0.47	W = 52, p = 0.91	---	---	---	---	---	---	---
DZM-B	*Pre-dam*	W = 44, p = 0.3	W = 37, p = 0.22	W = 30, p = 0.08	---	---	---	---	---	---
PBN-C		<u>W = 80, p = 0.08</u>	W = 75, p = 0.06	W = 64, p = 0.32	W = 91, p = 0.01	---	---	---	---	---
PDR-C	*Post-dam*	W = 73.5, p = 0.20	<u>W = 67, p = 0.22</u>	W = 54, p = 0.80	W = 79, p = 0.10	W = 44, p = 0.68	---	---	---	---
MON-C	*Post-dam*	W = 58, p = 0.86	W = 49.5, p = 1	<u>W = 45, p = 0.74</u>	W = 76, p = 0.15	W = 33, p = 0.22	W = 46, p = 0.80	---	---	---
DZM-C	*Post-dam*	W = 60, p = 0.76	W = 45, p = 0.74	W = 46, p = 0.80	<u>W = 76, p = 0.15</u>	W = 35, p = 0.28	W = 42, p = 0.58	W = 49, p = 0.97	---	---
PLAT-A	*MFP*	W = 216, p = 0.46	W = 180, p = 0.29	W = 169, p = 0.20	W = 292, p = 0.44	**W = 112, p = 0.01 (*)**	W = 157, p = 0.12	W = 188, p = 0.37	W = 181, p = 0.30	---
DROM-D	*PI*	**W = 946, p = 1.4 x 10^{-6} (****)**	**W = 860, p = 3.1 x 10^{-6} (****)**	**W = 860, p = 3.1 x 10^{-6} (****)**	**W = 946, p = 1.4 x 10^{-6} (****)**	**W = 860, p = 3.1 x 10^{-6} (****)**	**W = 860, p = 3.1 x 10^{-6} (****)**	**W = 860, p = 3.1 x 10^{-6} (****)**	**W = 860, p = 3.1 x 10^{-6} (****)**	**W = 3,784, p = 4.5 x 10^{-11} (****)**

Table A–III–3: Results of pairwise Mann-Whitney U tests (significant differences in bold print, α-levels: * p < .05; ** p < .01; *** p < .001; **** p < .0001) for **sapling** density. Grey: Between and within reach comparisons of dike fields (within-reach comparisons, i.e. comparison of pre- and post-dam surfaces within each reach, are underlined). White: Comparisons between dike fields and external sites (MFP = mature floodplain; PI = pioneer islands).

		PBN-B	PDR-B	MON-B	DZM-B	PBN-C	PDR-C	MON-C	DZM-C	PLAT-A
				Pre-dam				*Post-dam*		*MFP*
PDR-B	*Pre-dam*	W = 72, p = 0.24	---	---	---	---	---	---	---	---
MON-B	*Pre-dam*	W = 62, p = 0.64	W = 39, p = 0.42	---	---	---	---	---	---	---
DZM-B	*Pre-dam*	W = 62, p = 0.95	W = 33.5, p = 0.14	W = 39.5, p = 0.29	---	---	---	---	---	---
PBN-C		W = 80, p = 0.08	W = 59.5, p = 0.49	W = 72, p = 0.10	**W = 84.5, p = 0.04 (*)**	---	---	---	---	---
PDR-C	*Post-dam*	**W = 95, p = 4.9 x 10^{-3} (**)**	W = 71, p = 0.11	**W = 90.5, p = 2.3 x 10^{-3} (**)**	**W = 100.5, p = 1.4 x 10^{-3} (**)**	W = 64, p = 0.29	---	---	---	---
MON-C	*Post-dam*	W = 66.5, p = 0.44	W = 40, p = 0.47	W = 43.5, p = 0.65	W = 61, p = 0.70	W = 35, p = 0.27	**W = 19, p = 0.02 (*)**	---	---	---
DZM-C	*Post-dam*	W = 78, p = 0.11	W = 57, p = 0.62	W = 75.5, p = 0.05	**W = 89.5, p = 0.02 (*)**	W = 44.5, p = 0.70	W = 26, p = 0.07	W = 68.5, p = 0.17	---	---
PLAT-A	*MFP*	**W = 59, p = 9.1 x 10^{-5} (****)**	**W = 8, p = 2.1 x 10^{-6} (****)**	**W = 4, p = 1.4 x 10^{-6} (****)**	**W = 7, p = 6.8 x 10^{-7} (****)**	**W = 3, p = 1.3 x 10^{-6} (****)**	**W = 1, p = 1.0 x 10^{-6} (****)**	**W = 7, p = 1.9 x 10^{-6} (****)**	**W = 2, p = 1.1 x 10^{-6} (****)**	---
DROM-D	*PI*	**W = 258, p = 3.1 x 10^{-3} (**)**	**W = 102, p = 3.0 x 10^{-5} (****)**	**W = 78, p = 1.0 x 10^{-5} (****)**	**W = 130, p = 2.8 x 10^{-5} (****)**	**W = 78, p = 1.0 x 10^{-5} (****)**	**W = 16, p = 4.6 x 10^{-7} (****)**	**W = 104, p = 3.3 x 10^{-5} (****)**	**W = 40, p = 1.6 x 10^{-6} (****)**	**W = 3,309, p = 1.1 x 10^{-4} (***)**

Table A–III–4: Results of pairwise Mann-Whitney U tests (significant differences in bold print, α-levels: * p < .05; ** p < .01; *** p < .001; **** p < .0001) for **seedling** density. Grey: Between and within reach comparisons of dike fields (within-reach comparisons, i.e. comparison of pre- and post-dam surfaces within each reach, are underlined). White: Comparisons between dike fields and external sites (MFP = mature floodplain; PI = pioneer islands).

		PBN-B	PDR-B	MON-B	DZM-B	PBN-C	PDR-C	MON-C	DZM-C	PLAT-A
				Pre-dam				*Post-dam*		*MFP*
PDR-B	*Pre-dam*	W = 35, p = 0.17	---	---	---	---	---	---	---	---
MON-B	*Pre-dam*	**W = 21, p = 0.02 (*)**	W = 34, p = 0.24	---	---	---	---	---	---	---
DZM-B	*Pre-dam*	W = 70, p = 0.55	W = 71.5, p = 0.25	**W = 84, p = 0.04 (*)**	---	---	---	---	---	---
PBN-C		W = 40.5, p = 0.32	W = 40.5, p = 0.49	W = 50.5, p = 1	W = 44, p = 0.45	---	---	---	---	---
PDR-C	*Post-dam*	W = 35.5, p = 0.18	W = 43.5, p = 0.65	W = 57, p = 0.62	W = 35.5, p = 0.18	W = 52.5, p = 0.88	---	---	---	---
MON-C	*Post-dam*	W = 34.5, p = 0.16	W = 36, p = 0.31	W = 51, p = 0.97	W = 37, p = 0.21	W = 49, p = 0.97	W = 48.5, p = 0.94	---	---	---
DZM-C	*Post-dam*	W = 47, p = 0.59	W = 49, p = 0.97	W = 61, p = 0.42	W = 50, p = 0.75	W = 56, p = 0.67	W = 57.5, p = 0.59	W = 59, p = 0.51	---	---
PLAT-A	*MFP*	NA	NA	NA	NA	NA	NA	NA	NA	---
DROM-D	*PI*	**W = 754, p = 0.05 (*)**	**W = 767, p = 5.5 x 10^{-3} (**)**	**W = 855, p = 1.8 x 10^{-4} (***)**	W = 748, p = 0.06	**W = 708, p = 0.03 (*)**	**W = 770, p = 4.8 x 10^{-3} (**)**	**W = 782, p = 3.1 x 10^{-3} (**)**	W = 676, p = 0.07	NA

Table A–III–5: Results of pairwise Mann-Whitney U tests (significant differences in bold print, α-levels: * p < .05; ** p < .01; *** p < .001; **** p < .0001) for mean DBH, **all plants**. Grey: Between and within reach comparisons of dike fields (within-reach comparisons, i.e. comparison of pre- and post-dam surfaces within each reach, are underlined). White: Comparisons between dike fields and external sites (MFP = mature floodplain; PI = pioneer islands).

		PBN-B	PDR-B	MON-B	DZM-B	PBN-C	PDR-C	MON-C	DZM-C	PLAT-A
				Pre-dam				*Post-dam*		*MFP*
PDR-B		W = 36, p = 0.20	---	---	---	---	---	---	---	---
MON-B	*Pre-dam*	**W = 12, p = 1.5 x 10^{-3} (**)**	W = 30, p = 0.14	---	---	---	---	---	---	---
DZM-B		W = 37, p = 0.13	W = 55, p = 1	W = 81, p = 0.07	---	---	---	---	---	---
PBN-C		**W = 6, p = 1.7 x 10^{-4} (***)**	W = 26, p = 0.08	W = 46, p = 0.80	**W = 19, p = 0.01 (*)**	---	---	---	---	---
PDR-C		**W = 5, p = 1.1 x 10^{-4} (***)**	**W = 23, p = 0.04 (*)**	W = 38, p = 0.39	**W = 19, p = 0.01 (*)**	W = 40, p = 0.48	---	---	---	---
MON-C	*Post-dam*	W = 32, p = 0.11	W = 41, p = 0.53	W = 59, p = 0.53	W = 48, p = 0.65	W = 66, p = 0.25	W = 70, p = 0.14	---	---	---
DZM-C		**W = 16, p = 4.8 x 10^{-3} (**)**	W = 34, p = 0.25	W = 50, p = 1	W = 29, p = 0.07	W = 50, p = 1	W = 57, p = 0.63	W = 41, p = 0.53	---	---
PLAT-A	*MFP*	**W = 449, p = 1.7 x 10^{-5} (****)**	**W = 419, p = 7.6 x 10^{-6} (****)**	**W = 440, p = 1.4 x 10^{-7} (****)**	**W = 468, p = 1.0 x 10^{-6} (****)**	**W = 446, p = 2.8 x 10^{-8} (****)**	**W = 447, p = 2.1 x 10^{-8} (****)**	**W = 420, p = 6.5 x 10^{-6} (****)**	**W = 422, p = 4.7 x 10^{-6} (****)**	---
DROM-D	*PI*	**W = 1,133, p = 5.6 x 10^{-8} (****)**	**W = 1,030, p = 2.0 x 10^{-7} (****)**	**W = 1,030, p = 2.0 x 10^{-7} (****)**	**W = 1,133, p = 5.6 x 10^{-8} (****)**	**W = 1,030, p = 2.0 x 10^{-7} (****)**	**W = 1,030, p = 2.0 x 10^{-7} (****)**	**W = 1,030, p = 2.0 x 10^{-7} (****)**	**W = 1,030, p = 2.0 x 10^{-7} (****)**	**W = 4,488, p < 2.2 x 10^{-16} (****)**

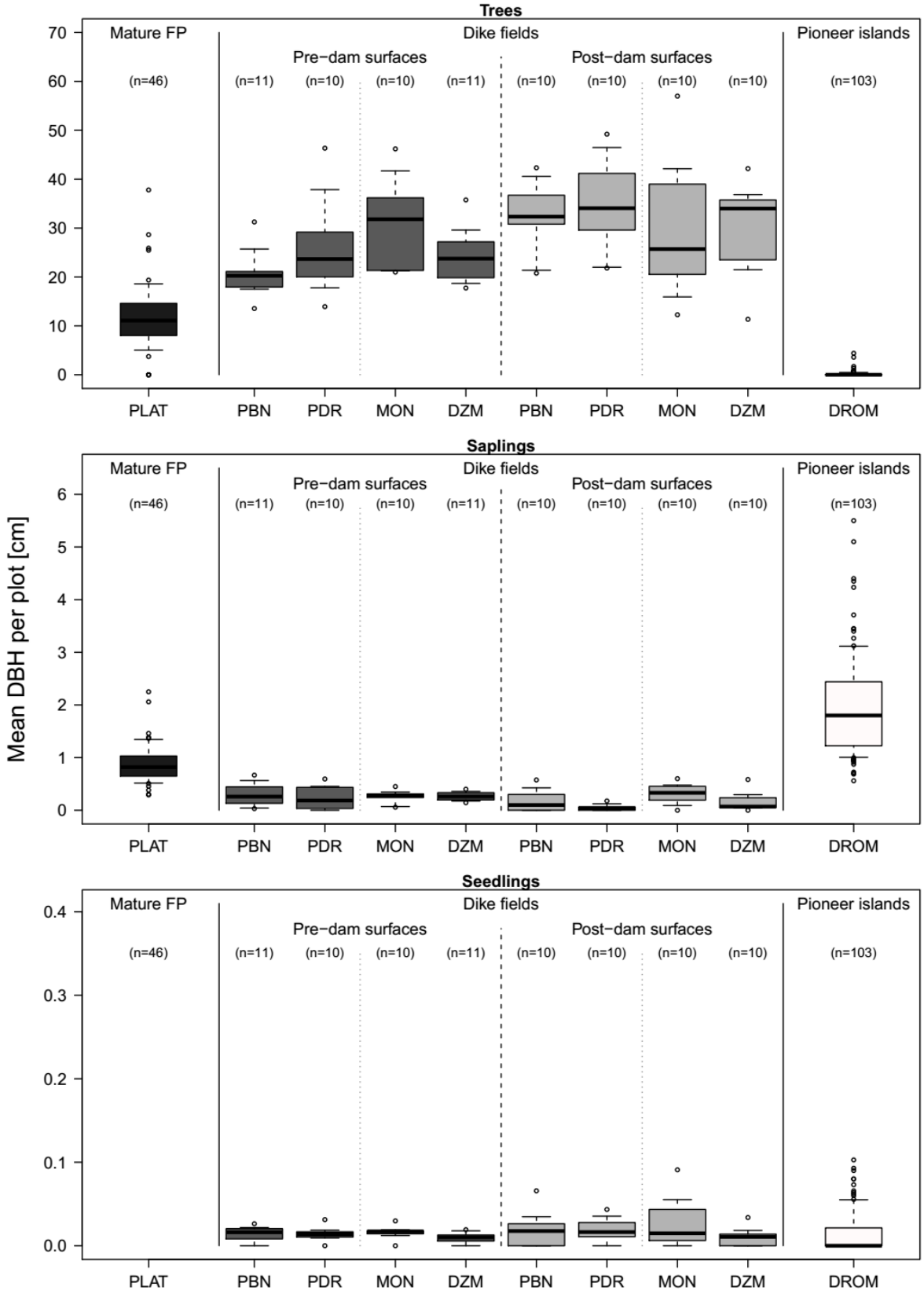

Figure A–III–2: Comparison of mean DBH per plot between dike fields and between dike fields and reference sites for **each LHS** separately. Sapling and seedling DBH based on classes.

Table A–III–6: Results of pairwise Mann-Whitney U tests (significant differences in bold print, α-levels: * p < .05; ** p < .01; *** p < .001; **** p < .0001) for mean **tree** DBH. Grey: Between and within reach comparisons of dike fields (within-reach comparisons, i.e. comparison of pre- and post-dam surfaces within each reach, are underlined). White: Comparisons between dike fields and external sites (MFP = mature floodplain; PI = pioneer islands).

		PBN-B	PDR-B	MON-B	DZM-B	PBN-C	PDR-C	MON-C	DZM-C	PLAT-A
				Pre-dam				*Post-dam*		*MFP*
PDR-B		W = 36, p = 0.20	---	---	---	---	---	---	---	---
MON-B	*Pre-dam*	**W = 11, p = 1.1 x 10^{-3} (**)**	W = 32, p = 0.19	---	---	---	---	---	---	---
DZM-B		W = 34, p = 0.09	W = 55, p = 1	W = 82, p = 0.06	---	---	---	---	---	---
PBN-C		**W = 7, p = 2.6 x 10^{-4} (***)**	W = 26, p = 0.08	W = 47, p = 0.85	**W = 20, p = 0.01 (*)**	---	---	---	---	---
PDR-C		**W = 5, p = 1.1 x 10^{-4} (***)**	**W = 23, p = 0.04 (*)**	W = 38, p = 0.39	**W = 18.5, p = 0.01 (*)**	W = 39, p = 0.44	---	---	---	---
MON-C	*Post-dam*	W = 32, p = 0.11	W = 42, p = 0.58	W = 61, p = 0.44	W = 48, p = 0.65	W = 66, p = 0.25	W = 70, p = 0.14	---	---	---
DZM-C		**W = 16, p = 4.8 x 10^{-3} (**)**	W = 35, p = 0.28	W = 49, p = 0.97	W = 29, p = 0.07	W = 50, p = 1	W = 57, p = 0.63	W = 41, p = 0.53	---	---
PLAT-A	*MFP*	**W = 450, p = 7.1 x 10^{-5} (****)**	**W = 421, p = 4.6 x 10^{-5} (****)**	**W = 440, p = 7.4 x 10^{-6} (****)**	**W = 468, p = 1.4 x 10^{-5} (****)**	**W = 446, p = 4.0 x 10^{-6} (****)**	**W = 447, p = 3.6 x 10^{-6} (****)**	**W = 421, p = 4.6 x 10^{-5} (****)**	**W = 426, p = 2.9 x 10^{-5} (****)**	—
DROM-D	*PI*	**W = 1,133, p = 6.5 x 10^{-13} (****)**	**W = 1,030, p = 3.5 x 10^{-12} (****)**	**W = 1,030, p = 3.5 x 10^{-12} (****)**	**W = 1,133, p = 6.5 x 10^{-13} (****)**	**W = 1,030, p = 3.5 x 10^{-12} (****)**	**W = 1,030, p = 3.5 x 10^{-12} (****)**	**W = 1,030, p = 3.5 x 10^{-12} (****)**	**W = 1,030, p = 3.5 x 10^{-12} (****)**	**W = 4,497, p < 2.2 x 10^{-16} (****)**

Table A–III–7: Results of pairwise Mann-Whitney U tests (significant differences in bold print, α-levels: * p < .05; ** p < .01; *** p < .001; **** p < .0001) for plot basal area, **all plants**. Grey: Between and within reach comparisons of dike fields (within-reach comparisons, i.e. comparison of pre- and post-dam surfaces within each reach, are underlined). White: Comparisons between dike fields and external sites (MFP = mature floodplain; PI = pioneer islands).

		PBN-B	PDR-B	MON-B	DZM-B	PBN-C	PDR-C	MON-C	DZM-C	PLAT-A
				Pre-dam				*Post-dam*		*MFP*
PDR-B	*Pre-dam*	W = 53, p = 0.92	---	---	---	---	---	---	---	---
MON-B	*Pre-dam*	**W = 25, p = 0.04 (*)**	W = 39, p = 0.44	---	---	---	---	---	---	---
DZM-B	*Pre-dam*	**W = 27, p = 0.03 (*)**	W = 44, p = 0.47	W = 56, p = 0.97	---	---	---	---	---	---
PBN-C	*Post-dam*	W = 43, p = 0.43	W = 49, p = 0.97	W = 70, p = 0.14	W = 73, p = 0.22	---	---	---	---	---
PDR-C	*Post-dam*	W = 31, p = 0.10	W = 44, p = 0.68	W = 59, p = 0.53	W = 63, p = 0.60	W = 40, p = 0.48	---	---	---	---
MON-C	*Post-dam*	W = 33, p = 0.13	W = 35, p = 0.28	W = 56, p = 0.68	W = 57, p = 0.92	W = 35, p = 0.28	W = 45, p = 0.74	---	---	---
DZM-C	*Post-dam*	W = 40, p = 0.31	W = 46, p = 0.80	W = 59, p = 0.53	W = 64, p = 0.56	W = 44, p = 0.68	W = 53, p = 0.85	W = 58, p = 0.58	---	---
PLAT-A	*MFP*	**W = 149, p = 0.04 (*)**	W = 193, p = 0.44	W = 244, p = 0.78	W = 272, p = 0.71	W = 174, p = 0.24	W = 211, p = 0.70	W = 241, p = 0.83	W = 206, p = 0.62	---
DROM-D	*PI*	W = 714, p = 0.16	W = 646, p = 0.19	**W = 803, p = 3.7 x 10^{-3} (**)**	**W = 859, p = 5.1 x 10^{-3} (**)**	W = 696, p = 0.07	**W = 771, p = 9.8 x 10^{-3} (**)**	**W = 776, p = 8.5 x 10^{-3} (**)**	**W = 722, p = 0.04 (*)**	**W = 3,471, p = 6.0 x 10^{-6} (****)**

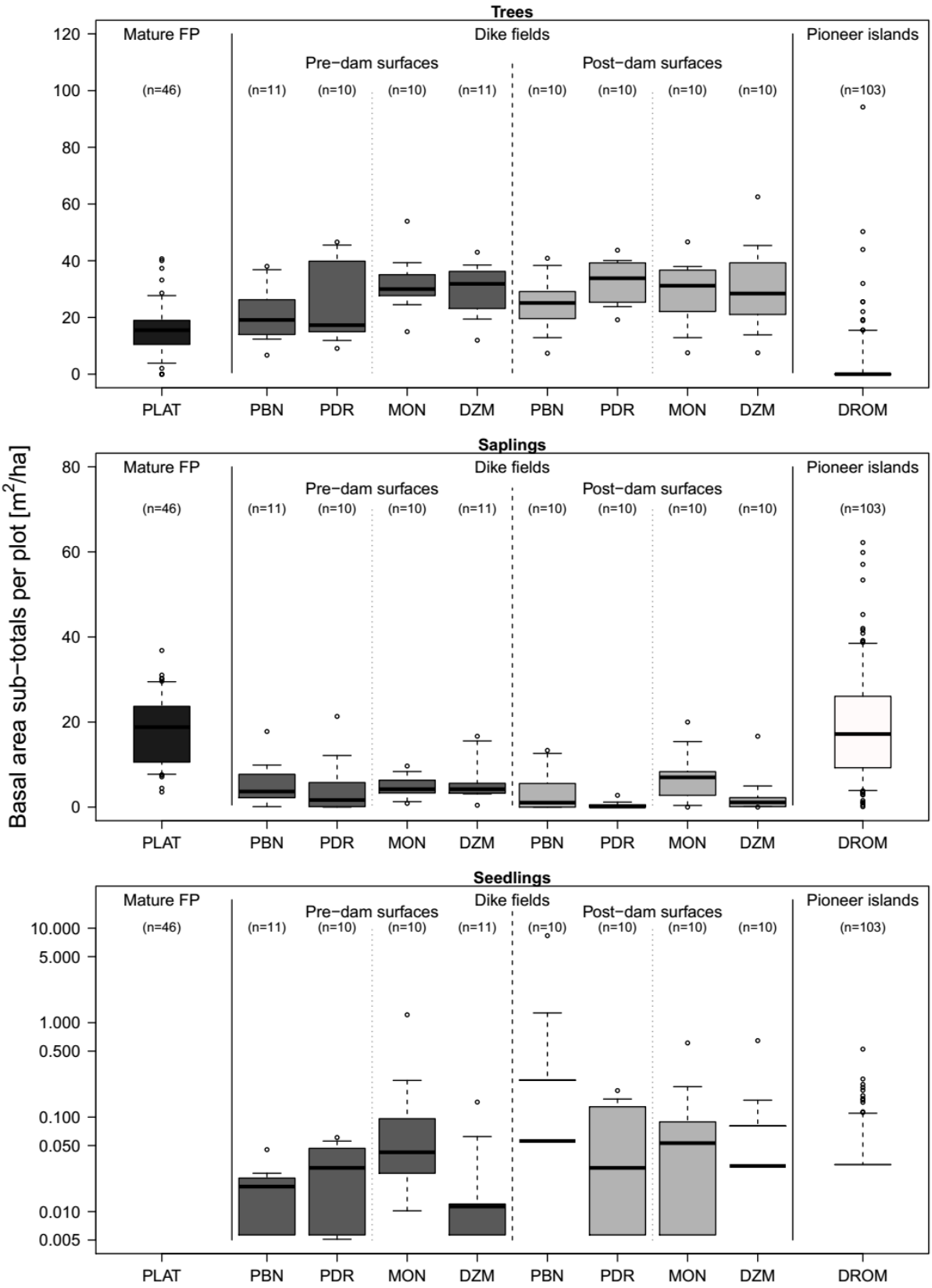

Figure A–III–3: Comparison of basal area sub-totals per plot between dike fields and between dike fields and reference sites for **each LHS** separately.

Table A–III–8: Results of pairwise Mann-Whitney U tests (significant differences in bold print, α-levels: * p < .05; ** p < .01; *** p < .001; **** p < .0001) for plot basal area, **trees**. Grey: Between and within reach comparisons of dike fields (within-reach comparisons, i.e. comparison of pre- and post-dam surfaces within each reach, are underlined). White: Comparisons between dike fields and external sites (MFP = mature floodplain; PI = pioneer islands).

		PBN-B	PDR-B	MON-B	DZM-B	PBN-C	PDR-C	MON-C	DZM-C	PLAT-A
				Pre-dam				*Post-dam*		*MFP*
PDR-B	*Pre-dam*	W = 51, p = 0.81	---	---	---	---	---	---	---	---
MON-B	*Pre-dam*	**W = 24, p = 0.03 (*)**	W = 33, p = 0.22	---	---	---	---	---	---	---
DZM-B	*Pre-dam*	W = 31, p = 0.06	W = 41, p = 0.35	W = 54, p = 0.97	---	---	---	---	---	---
PBN-C		W = 37, p = 0.22	W = 46, p = 0.80	W = 70, p = 0.14	W = 70, p = 0.31	---	---	---	---	---
PDR-C	*Post-dam*	**W = 21, p = 0.02 (*)**	W = 32, p = 0.19	W = 43, p = 0.63	W = 46, p = 0.56	W = 28, p = 0.11	---	---	---	---
MON-C	*Post-dam*	W = 33, p = 0.13	W = 41, p = 0.53	W = 55, p = 0.74	W = 58, p = 0.86	W = 38, p = 0.39	W = 59, p = 0.53	---	---	---
DZM-C	*Post-dam*	W = 33, p = 0.13	W = 41, p = 0.53	W = 56, p = 0.68	W = 57, p = 0.92	W = 39, p = 0.44	W = 59, p = 0.53	W = 52, p = 0.91	---	---
PLAT-A	*MFP*	W = 334, p = 0.10	W = 307, p = 0.10	**W = 403, p = 2.2 x 10^{-4} (***)**	**W = 430, p = 3.6 x 10^{-4} (***)**	**W = 348, p = 0.01 (*)**	**W = 418, p = 6.0 x 10^{-5} (****)**	**W = 362, p = 4.9 x 10^{-3} (**)**	**W = 358, p = 6.4 x 10^{-3} (**)**	---
DROM-D	*PI*	**W = 1,033, p = 3.2 x 10^{-9} (****)**	**W = 945, p = 6.4 x 10^{-9} (****)**	**W = 987, p = 1.8 x 10^{-10} (****)**	**W = 1,075, p = 1.1 x 10^{-10} (****)**	**W = 958, p = 2.2 x 10^{-9} (****)**	**W = 988, p = 1.7 x 10^{-10} (****)**	**W = 968, p = 9.5 x 10^{-10} (****)**	**W = 967, p = 1.0 x 10^{-9} (****)**	**W = 4,031, p = 1.1 x 10^{-14} (****)**

Table A–III–9: Results of pairwise Mann-Whitney U tests (significant differences in bold print, α-levels: * p < .05; ** p < .01; *** p < .001; **** p < .0001) for mean plot height, **all plants**. Grey: Between and within reach comparisons of dike fields (within-reach comparisons, i.e. comparison of pre- and post-dam surfaces within each reach, are underlined). White: Comparisons between dike fields and external sites (MFP = mature floodplain; PI = pioneer islands).

		PBN-B	PDR-B	MON-B	DZM-B	PBN-C	PDR-C	MON-C	DZM-C	PLAT-A
				Pre-dam				*Post-dam*		*MFP*
PDR-B		W = 36, p = 0.20	---	---	---	---	---	---	---	---
MON-B	*Pre-dam*	**W = 13, p = 2.1 x 10^{-3} (**)**	W = 30, p = 0.14	---	---	---	---	---	---	---
DZM-B	*Pre-dam*	**W = 14, p = 1.4 x 10^{-3} (**)**	W = 32, p = 0.11	W = 52, p = 0.86	---	---	---	---	---	---
PBN-C		**W = 11, p = 1.1 x 10^{-3} (**)**	W = 29, p = 0.12	W = 50, p = 1	W = 59, p = 0.81	---	---	---	---	---
PDR-C	*Post-dam*	**W = 5, p = 1.1 x 10^{-4} (***)**	**W = 15, p = 6.8 x 10^{-3} (**)**	W = 25, p = 0.06	W = 30, p = 0.08	W = 26, p = 0.08	---	---	---	---
MON-C	*Post-dam*	W = 45, p = 0.51	W = 57, p = 0.63	**W = 77, p = 0.04 (*)**	**W = 85, p = 0.04 (*)**	**W = 77, p = 0.04 (*)**	**W = 87, p = 3.9 x 10^{-3} (**)**	---	---	---
DZM-C		W = 41, p = 0.35	W = 48, p = 0.91	W = 59, p = 0.53	W = 63, p = 0.60	W = 61, p = 0.44	W = 72, p = 0.11	W = 42, p = 0.58	---	---
PLAT-A	*MFP*	**W = 401, p = 2.9 x 10^{-3} (**)**	**W = 409, p = 1.3 x 10^{-4} (***)**	**W = 439, p = 8.2 x 10^{-6} (****)**	**W = 484, p = 3.1 x 10^{-6} (****)**	**W = 441, p = 6.7 x 10^{-6} (****)**	**W = 452, p = 2.2 x 10^{-6} (****)**	**W = 370, p = 2.8 x 10^{-3} (**)**	**W = 381, p = 1.3 x 10^{-3} (**)**	---
DROM-D	*PI*	NA	NA	NA	NA	NA	NA	NA	NA	NA

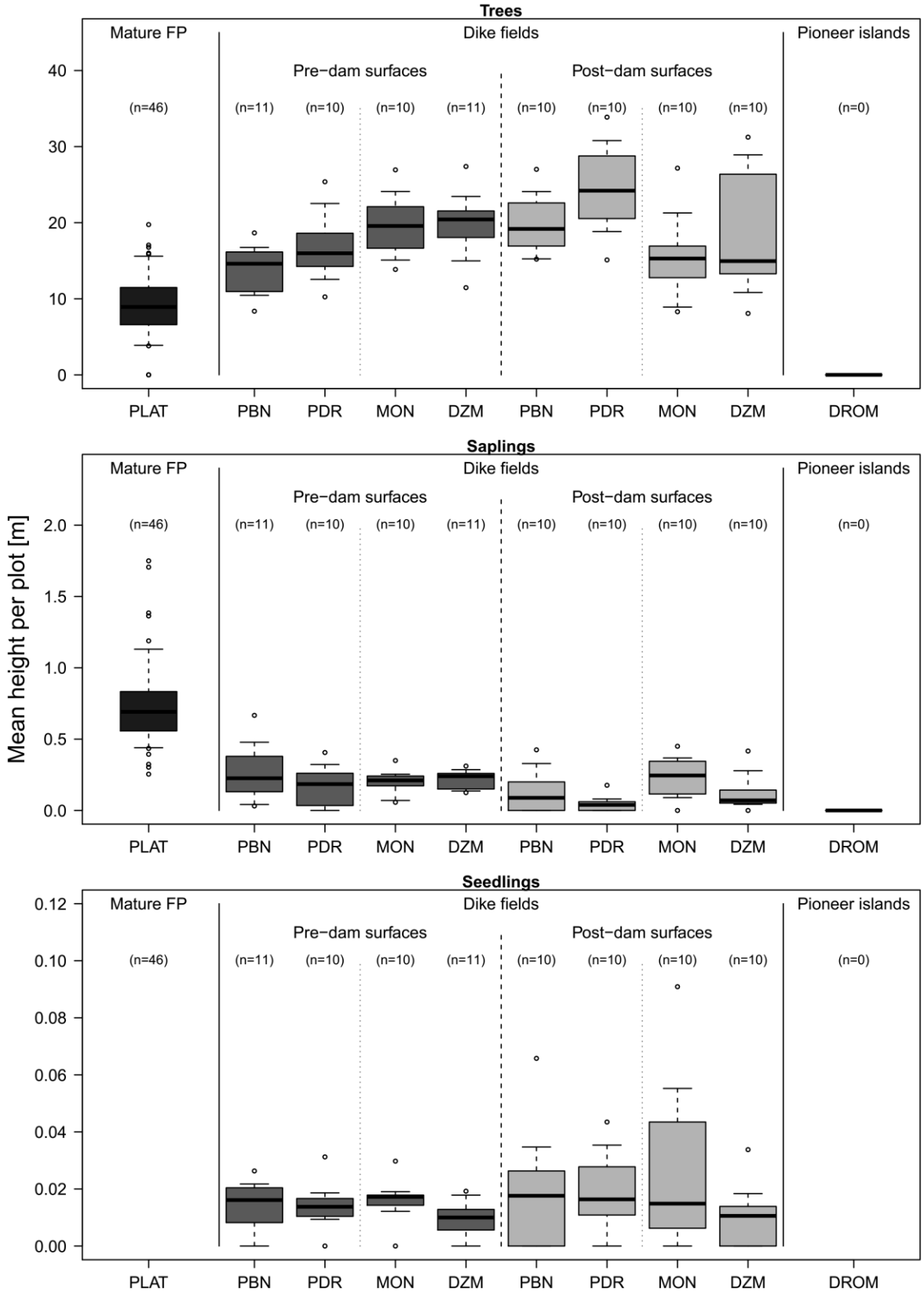

Figure A–III–4: Comparison of mean heights per plot between dike fields and between dike fields and reference sites for **each LHS** separately. Sapling and seedling height based on classes.

Table A–III–10: Results of pairwise Mann-Whitney U tests (significant differences in bold print, α-levels: * p < .05; ** p < .01; *** p < .001; **** p < .0001) for mean **tree** height. Grey: Between and within reach comparisons of dike fields (within-reach comparisons, i.e. comparison of pre- and post-dam surfaces within each reach, are underlined). White: Comparisons between dike fields and external sites (MFP = mature floodplain; PI = pioneer islands).

		PBN-B	PDR-B	MON-B	DZM-B	PBN-C	PDR-C	MON-C	DZM-C	PLAT-A
				Pre-dam				*Post-dam*		*MFP*
PDR-B		W = 34, p = 0.15	---	---	---	---	---	---	---	---
MON-B	*Pre-dam*	**W = 13, p = 2.1 x 10^{-3} (**)**	W = 31, p = 0.17	---	---	---	---	---	---	---
DZM-B	*Pre-dam*	**W = 14, p = 1.4 x 10^{-3} (**)**	W = 33, p = 0.13	W = 52, p = 0.86	---	---	---	---	---	---
PBN-C	*Pre-dam*	**W = 11, p = 1.1 x 10^{-3} (**)**	W = 30, p = 0.14	W = 49, p = 0.97	W = 59, p = 0.81	---	---	---	---	---
PDR-C	*Post-dam*	**W = 4, p = 6.8 x 10^{-5} (****)**	**W = 15, p = 6.8 x 10^{-3} (**)**	W = 25, p = 0.06	W = 28, p = 0.06	W = 26, p = 0.08	---	---	---	---
MON-C	*Post-dam*	W = 45, p = 0.51	W = 59, p = 0.53	W = 76, p = 0.05	**W = 85, p = 0.04 (*)**	**W = 78, p = 0.04 (*)**	**W = 87, p = 3.9 x 10^{-3} (**)**	---	---	---
DZM-C	*Post-dam*	W = 40, p = 0.31	W = 48, p = 0.91	W = 58, p = 0.58	W = 63, p = 0.60	W = 60, p = 0.48	W = 72, p = 0.11	W = 41, p = 0.53	---	---
PLAT-A	*MFP*	**W = 407, p = 1.9 x 10^{-3} (**)**	**W = 413, p = 9.4 x 10^{-5} (****)**	**W = 441, p = 6.7 x 10^{-5} (****)**	**W = 486, p = 2.6 x 10^{-6} (****)**	**W = 444, p = 4.9 x 10^{-6} (****)**	**W = 453, p = 1.9 x 10^{-6} (****)**	**W = 375, p = 2.0 x 10^{-3} (**)**	**W = 393, p = 5.1 x 10^{-4} (***)**	---
DROM-D	*PI*	NA	NA	NA	NA	NA	NA	NA	NA	NA

Table A–III–11: Results of pairwise Mann-Whitney U tests (significant differences in bold print, α-levels: * p < .05; ** p < .01; *** p < .001; **** p < .0001) for species richness, **all plants**. Grey: Between and within reach comparisons of dike fields (within-reach comparisons, i.e. comparison of pre- and post-dam surfaces within each reach, are underlined). White: Comparisons between dike fields and external sites (MFP = mature floodplain; PI = pioneer islands).

		PBN-B	PDR-B	MON-B	DZM-B	PBN-C	PDR-C	MON-C	DZM-C	PLAT-A
				Pre-dam				*Post-dam*		*MFP*
PDR-B	*Pre-dam*	W = 69.5, p = 0.31	---	---	---	---	---	---	---	---
MON-B	*Pre-dam*	**W = 90, p = 0.01 (*)**	W = 72.5, p = 0.09	---	---	---	---	---	---	---
DZM-B	*Pre-dam*	W = 59.5, p = 0.97	W = 37, p = 0.21	**W = 17, p = 7.5 x 10^{-3} (**)**	---	---	---	---	---	---
PBN-C	*Post-dam*	**W = 90.5, p = 0.01 (*)**	**W = 78.5, p = 0.03 (*)**	W = 64, p = 0.29	**W = 90, p = 0.01 (*)**	---	---	---	---	---
PDR-C	*Post-dam*	**W = 84.5, p = 0.04 (*)**	W = 66, p = 0.22	W = 45, p = 0.73	**W = 87.5, p = 0.02 (*)**	W = 32.5, p = 0.19	---	---	---	---
MON-C	*Post-dam*	**W = 84, p = 0.04 (*)**	W = 63.5, p = 0.31	W = 39, p = 0.41	**W = 88, p = 0.02 (*)**	W = 30, p = 0.13	W = 44, p = 0.67	---	---	---
DZM-C	*Post-dam*	**W = 90, p = 0.01 (*)**	W = 73.5, p = 0.07	W = 54.5, p = 0.76	**W = 92.5, p = 8.4 x 10^{-3} (**)**	W = 44, p = 0.67	W = 59.5, p = 0.49	W = 62.5, p = 0.35	---	---
PLAT-A	*MFP*	W = 171.5, p = 0.10	**W = 96, p = 3.9 x 10^{-3} (**)**	**W = 36.5, p = 3.1 x 10^{-5} (****)**	W = 165.5, p = 0.07	**W = 58, p = 2.2 x 10^{-4} (***)**	**W = 51, p = 1.1 x 10^{-4} (***)**	**W = 47.5, p = 8.4 x 10^{-5} (****)**	**W = 39.5, p = 4.1 x 10^{-5} (****)**	—
DROM-D	*PI*	**W = 1,097.5, p = 1.8 x 10^{-7} (****)**	**W = 981.5, p = 1.4 x 10^{-6} (****)**	**W = 913, p = 3.7 x 10^{-5} (****)**	**W = 1,103, p = 1.4 x 10^{-7} (****)**	**W = 808.5, p = 2.3 x 10^{-3} (**)**	**W = 924.5, p = 2.2 x 10^{-5} (****)**	**W = 941, p = 1.0 x 10^{-5} (****)**	**W = 825, p = 1.3 x 10^{-3} (**)**	**W = 4,631.5, p < 2.2 x 10^{-16} (****)**

Table A–III–12: Results of pairwise Mann-Whitney U tests (significant differences in bold print, α-levels: * p < .05; ** p < .01; *** p < .001; **** p < .0001) for species richness of **trees**. Grey: Between and within reach comparisons of dike fields (within-reach comparisons, i.e. comparison of pre- and post-dam surfaces within each reach, are underlined). White: Comparisons between dike fields and external sites (MFP = mature floodplain; PI = pioneer islands).

		PBN-B	PDR-B	MON-B	DZM-B	PBN-C	PDR-C	MON-C	DZM-C	PLAT-A
				Pre-dam				*Post-dam*		*MFP*
PDR-B	*Pre-dam*	W = 60.5, p = 0.71	---	---	---	---	---	---	---	---
MON-B	*Pre-dam*	W = 70.5, p = 0.26	W = 59, p = 0.48	---	---	---	---	---	---	---
DZM-B	*Pre-dam*	W = 59, p = 0.95	W = 49.5, p = 0.71	W = 43, p = 0.40	---	---	---	---	---	---
PBN-C	*Post-dam*	W = 79.5, p = 0.08	W = 71.5, p = 0.09	W = 66.5, p = 0.20	W = 74.5, p = 0.17	---	---	---	---	---
PDR-C	*Post-dam*	W = 77, p = 0.12	W = 66.5, p = 0.19	W = 59.5, p = 0.47	W = 74.5, p = 0.17	W = 46, p = 0.78	---	---	---	---
MON-C	*Post-dam*	W = 79.5, p = 0.07	W = 69, p = 0.11	W = 62.5, p = 0.31	W = 75, p = 0.15	W = 43.5, p = 0.63	W = 50, p = 1	---	---	---
DZM-C	*Post-dam*	W = 79.5, p = 0.08	W = 69.5, p = 0.13	W = 62.5, p = 0.34	W = 76, p = 0.14	W = 49, p = 0.97	W = 51.5, p = 0.94	W = 53, p = 0.84	---	---
PLAT-A	*MFP*	W = 250, p = 0.96	W = 203.5, p = 0.57	W = 167.5, p = 0.17	W = 259.5, p = 0.90	W = 140, p = 0.05	W = 147.5, p = 0.07	**W = 134, p = 0.04 (*)**	W = 140, p = 0.05	---
DROM-D	*PI*	**W = 1,133, p = 5.7 x 10^{-13} (****)**	**W = 1,030, p = 3.1 x 10^{-12} (****)**	**W = 1,030, p = 3.1 x 10^{-12} (****)**	**W = 1132.5, p = 6.0 x 10^{-13} (****)**	**W = 1,021, p = 7.1 x 10^{-12} (****)**	**W = 1020.5, p = 7.5 x 10^{-12} (****)**	**W = 1029.5, p = 3.2 x 10^{-12} (****)**	**W = 1,029, p = 3.4 x 10^{-12} (****)**	**W = 4,498, p < 2.2 x 10^{-16} (****)**

Table A–III–13: Results of pairwise Mann-Whitney U tests (significant differences in bold print, α-levels: * p < .05; ** p < .01; *** p < .001; **** p < .0001) for species richness of **saplings**. Grey: Between and within reach comparisons of dike fields (within-reach comparisons, i.e. comparison of pre- and post-dam surfaces within each reach, are underlined). White: Comparisons between dike fields and external sites (MFP = mature floodplain; PI = pioneer islands).

		PBN-B	PDR-B	MON-B	DZM-B	PBN-C	PDR-C	MON-C	DZM-C	PLAT-A
				Pre-dam				*Post-dam*		*MFP*
PDR-B	*Pre-dam*	W = 67, p = 0.40	---	---	---	---	---	---	---	---
MON-B	*Pre-dam*	W = 63.5, p = 0.56	W = 45.5, p = 0.76	---	---	---	---	---	---	---
DZM-B	*Pre-dam*	W = 51.5, p = 0.56	W = 37, p = 0.20	W = 40, p = 0.29	---	---	---	---	---	---
PBN-C		**W = 85, p = 0.03 (*)**	W = 65, p = 0.26	W = 70.5, p = 0.11	**W = 92, p = 8.2 x 10^{-3} (**)**	---	---	---	---	---
PDR-C	*Post-dam*	**W = 97.5, p = 2.0 x 10^{-3} (**)**	**W = 75.5, p = 0.05 (*)**	**W = 82, p = 0.01 (*)**	**W = 104, p = 4.4 x 10^{-4} (***)**	W = 61, p = 0.39	---	---	---	---
MON-C	*Post-dam*	W = 71.5, p = 0.24	W = 53, p = 0.85	W = 56.5, p = 0.64	W = 79.5, p = 0.08	W = 33.5, p = 0.21	**W = 20.5, p = 0.02 (*)**	---	---	---
DZM-C	*Post-dam*	**W = 89.5, p = 0.01 (**)**	W = 67, p = 0.19	W = 71.5, p = 0.07	**W = 99.5, p = 1.1 x 10^{-3} (**)**	W = 47.5, p = 0.87	W = 33.5, p = 0.17	W = 70, p = 0.11	---	---
PLAT-A	*MFP*	**W = 37.5, p = 9.5 x 10^{-6} (****)**	**W = 22, p = 6.4 x 10^{-6} (****)**	**W = 33.5, p = 2.0 x 10^{-5} (****)**	**W = 47.5, p = 2.5 x 10^{-5} (****)**	**W = 12, p = 2.3 x 10^{-6} (****)**	**W = 3.5, p = 9.3 x 10^{-7} (****)**	**W = 9.5, p = 1.8 x 10^{-6} (****)**	**W = 5.5, p = 1.1 x 10^{-6} (****)**	---
DROM-D	*PI*	W = 645, p = 0.44	W = 478.5, p = 0.71	W = 519, p = 0.97	W = 710.5, p = 0.16	**W = 315.5, p = 0.04 (*)**	**W = 205, p = 1.3 x 10^{-3} (**)**	W = 445, p = 0.47	**W = 286, p = 0.02 (*)**	**W = 4,382, p < 2.2 x 10^{-16} (****)**

Table A–III–14: Results of pairwise Mann-Whitney U tests (significant differences in bold print, α-levels: * p < .05; ** p < .01; *** p < .001; **** p < .0001) for species richness of **seedlings**. Grey: Between and within reach comparisons of dike fields (within-reach comparisons, i.e. comparison of pre- and post-dam surfaces within each reach, are underlined). White: Comparisons between dike fields and external sites (MFP = mature floodplain; PI = pioneer islands).

		PBN-B	PDR-B	MON-B	DZM-B	PBN-C	PDR-C	MON-C	DZM-C	PLAT-A
				Pre-dam				*Post-dam*		*MFP*
PDR-B	*Pre-dam*	W = 61.5, p = 0.65	---	---	---	---	---	---	---	---
MON-B	*Pre-dam*	W = 57.5, p = 0.88	W = 45.5, p = 0.74	---	---	---	---	---	---	---
DZM-B	*Pre-dam*	W = 75.5, p = 0.31	W = 64, p = 0.51	W = 68.5, p = 0.32	---	---	---	---	---	---
PBN-C	*Post-dam*	W = 69, p = 0.31	W = 59, p = 0.49	W = 62, p = 0.35	W = 58, p = 0.85	---	---	---	---	---
PDR-C	*Post-dam*	W = 61, p = 0.68	W = 51, p = 0.97	W = 54.5, p = 0.75	W = 48.5, p = 0.65	W = 42, p = 0.55	---	---	---	---
MON-C	*Post-dam*	W = 54.5, p = 1	W = 47, p = 0.84	W = 49.5, p = 1	W = 45.5, p = 0.50	W = 38, p = 0.37	W = 45.5, p = 0.75	---	---	---
DZM-C	*Post-dam*	W = 74, p = 0.17	W = 66, p = 0.21	W = 68.5, p = 0.15	W = 65.5, p = 0.45	W = 54, p = 0.78	W = 63, p = 0.32	W = 65.5, p = 0.23	---	---
PLAT-A	*MFP*	NA	NA	NA	NA	NA	NA	NA	NA	---
DROM-D	*PI*	**W = 851.5, p = 2.5 x 10^{-3} (**)**	**W = 779, p = 3.1 x 10^{-3} (**)**	**W = 797.5, p = 1.6 x 10^{-3} (**)**	**W = 790.5, p = 0.02 (*)**	W = 644, p = 0.15	**W = 739.5, p = 0.01 (*)**	**W = 754.5, p = 7.2 x 10^{-3} (**)**	W = 612.5, p = 0.27	NA

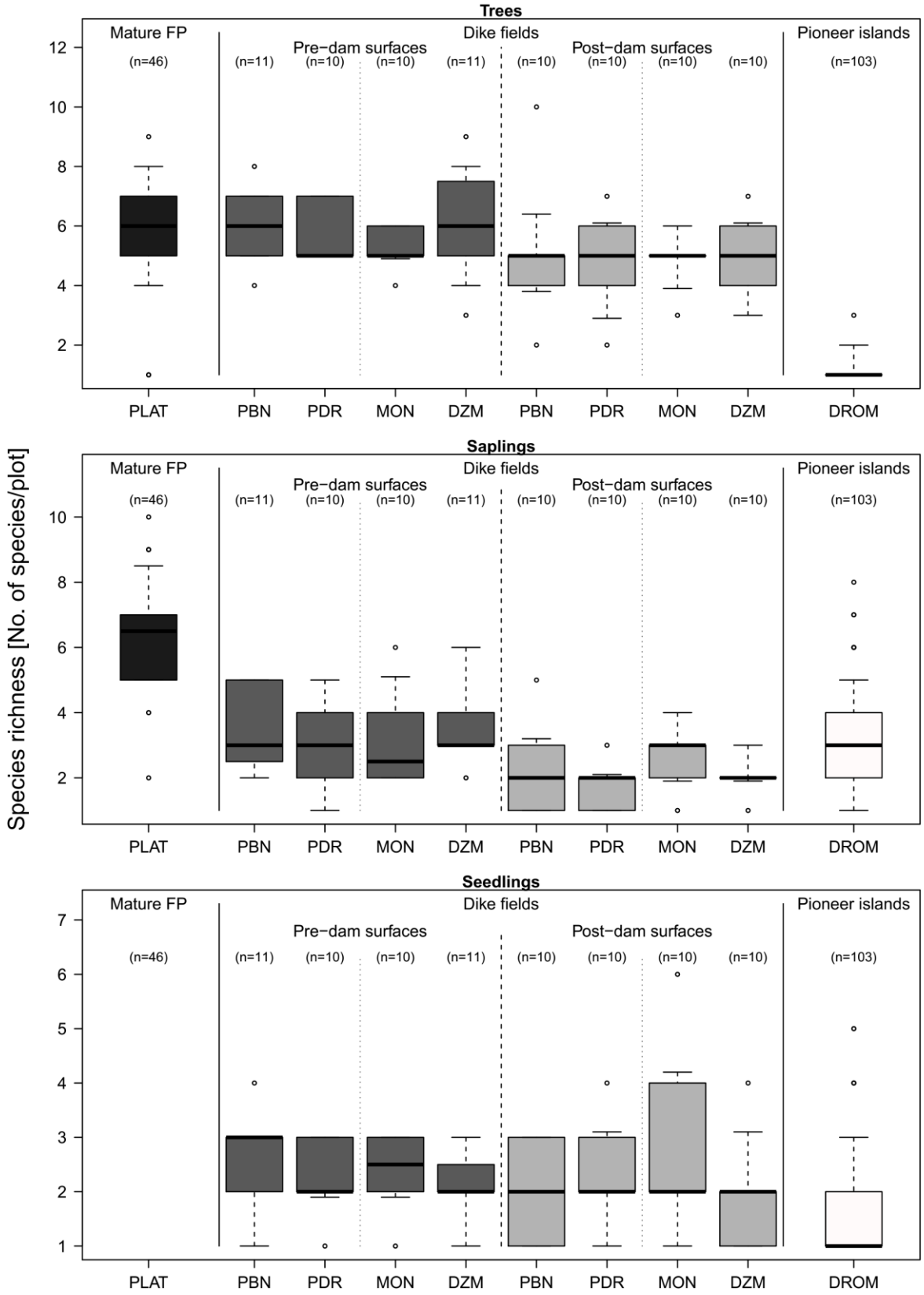

Figure A–III–5: Comparison of species richness per plot between dike fields and between dike fields and reference sites for **each LHS** separately.

Table A–III–15: Results of pairwise Mann-Whitney U tests (significant differences in bold print, α-levels: * p < .05; ** p < .01; *** p < .001; **** p < .0001) for Shannon H', **all plants**. Grey: Between and within reach comparisons of dike fields (within-reach comparisons, i.e. comparison of pre- and post-dam surfaces within each reach, are underlined). White: Comparisons between dike fields and external sites (MFP = mature floodplain; PI = pioneer islands).

		PBN-B	PDR-B	MON-B	DZM-B	PBN-C	PDR-C	MON-C	DZM-C	PLAT-A
				Pre-dam				*Post-dam*		*MFP*
PDR-B	*Pre-dam*	W = 64, p = 0.56	---	---	---	---	---	---	---	---
MON-B	*Pre-dam*	W = 61, p = 0.70	W = 45, p = 0.74	---	---	---	---	---	---	---
DZM-B	*Pre-dam*	W = 71, p = 0.52	W = 58, p = 0.86	W = 59, p = 0.81	---	---	---	---	---	---
PBN-C		W = 73, p = 0.22	W = 64, p = 0.32	W = 62, p = 0.39	W = 63, p = 0.60	---	---	---	---	---
PDR-C	*Post-dam*	W = 60, p = 0.76	W = 47, p = 0.85	W = 49, p = 0.97	W = 44, p = 0.47	W = 38, p = 0.39	---	---	---	---
MON-C	*Post-dam*	W = 65, p = 0.51	W = 51, p = 0.97	W = 55, p = 0.74	W = 54, p = 0.97	W = 38, p = 0.39	W = 58, p = 0.58	---	---	---
DZM-C	*Post-dam*	W = 69, p = 0.35	W = 56, p = 0.68	W = 59, p = 0.53	W = 55, p = 1	W = 46, p = 0.80	W = 61, p = 0.44	W = 53, p = 0.85	---	---
PLAT-A	*MFP*	W = 226, p = 0.60	W = 185, p = 0.35	W = 181, p = 0.30	W = 176, p = 0.12	W = 140, p = 0.05	W = 167, p = 0.18	W = 174, p = 0.24	W = 147, p = 0.08	---
DROM-D	*PI*	**W = 1,133, p = 5.6 x 10^{-8} (****)**	**W = 1,030, p = 2.0 x 10^{-7} (****)**	**W = 1,030, p = 2.0 x 10^{-7} (****)**	**W = 1,116, p = 1.4 x 10^{-7} (****)**	**W = 999, p = 1.0 x 10^{-6} (****)**	**W = 1,030, p = 2.0 x 10^{-7} (****)**	**W = 1,030, p = 2.0 x 10^{-7} (****)**	**W = 1,028, p = 2.2 x 10^{-7} (****)**	**W = 4,654, p < 2.2 x 10^{-16} (****)**

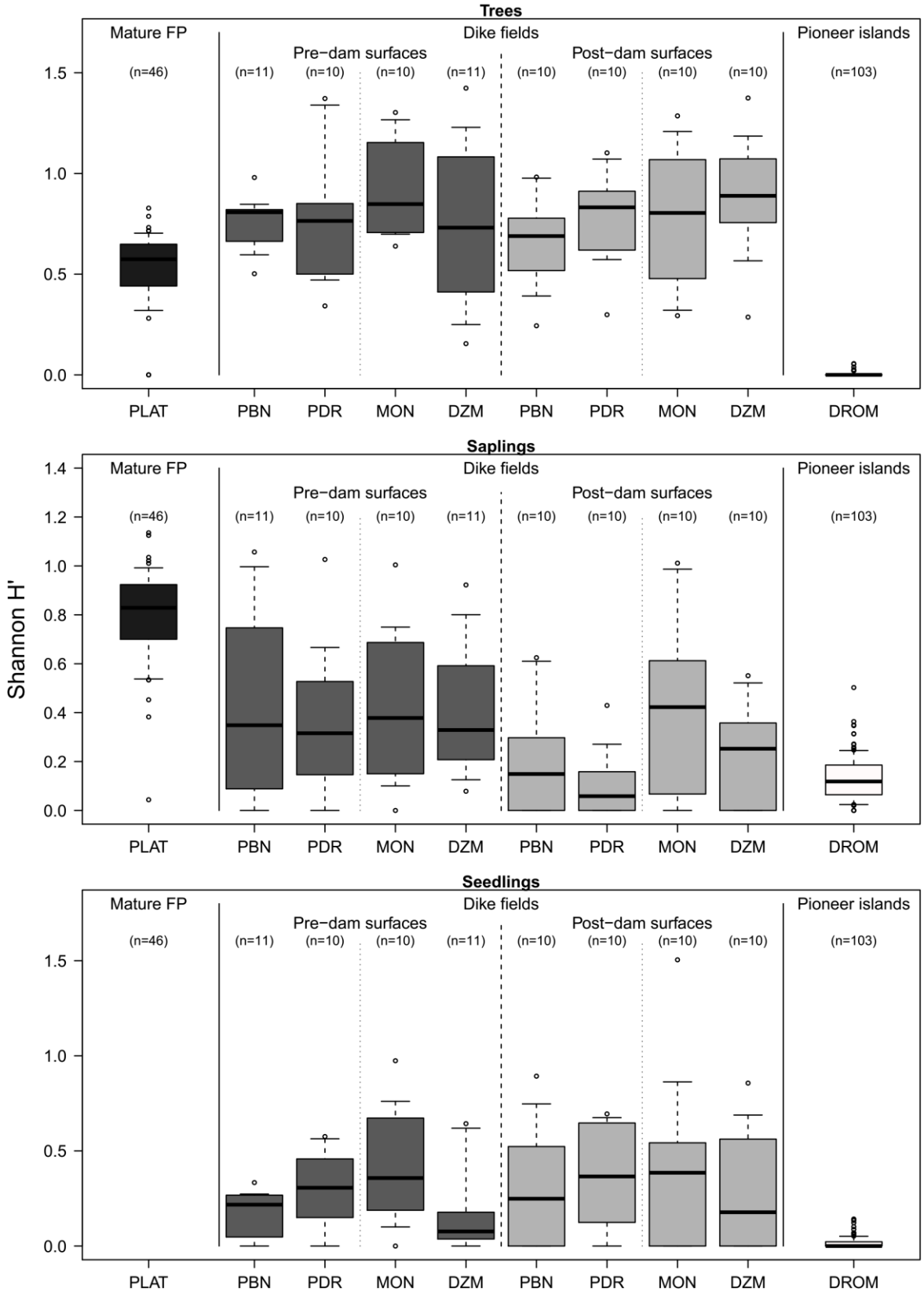

Figure A–III–6: Comparison of Shannon index per plot between dike fields and between dike fields and reference sites for **each LHS** separately.

Table A–III–16: Results of pairwise Mann-Whitney U tests (significant differences in bold print, α-levels: * p < .05; ** p < .01; *** p < .001; **** p < .0001) for Shannon H', **trees**. Grey: Between and within reach comparisons of dike fields (within-reach comparisons, i.e. comparison of pre- and post-dam surfaces within each reach, are underlined). White: Comparisons between dike fields and external sites (MFP = mature floodplain; PI = pioneer islands).

		PBN-B	PDR-B	MON-B	DZM-B	PBN-C	PDR-C	MON-C	DZM-C	PLAT-A
				Pre-dam				*Post-dam*		*MFP*
PDR-B	*Pre-dam*	W = 53, p = 0.92	---	---	---	---	---	---	---	---
MON-B	*Pre-dam*	W = 38, p = 0.25	W = 37, p = 0.35	---	---	---	---	---	---	---
DZM-B	*Pre-dam*	W = 69, p = 0.61	W = 61, p = 0.70	W = 70, p = 0.31	---	---	---	---	---	---
PBN-C		<u>W = 68, p = 0.39</u>	W = 58, p = 0.58	W = 75, p = 0.06	W = 59, p = 0.81	---	---	---	---	---
PDR-C	*Post-dam*	W = 43, p = 0.43	<u>W = 46, p = 0.80</u>	W = 61, p = 0.44	W = 48, p = 0.65	W = 34, p = 0.25	---	---	---	---
MON-C	*Post-dam*	W = 49, p = 0.70	W = 50, p = 1	<u>W = 59, p = 0.53</u>	W = 51, p = 0.81	W = 39, p = 0.44	W = 49, p = 0.97	---	---	---
DZM-C	*Post-dam*	W = 32, p = 0.11	W = 38, p = 0.39	W = 48, p = 0.91	<u>W = 42, p = 0.39</u>	W = 26, p = 0.08	W = 41, p = 0.53	W = 43, p = 0.63	---	---
PLAT-A	*MFP*	**W = 430, p = 3.6 x 10^{-4}(***)**	**W = 339, p = 0.02 (*)**	**W = 432, p = 1.6 x 10^{-5} (****)**	W = 316, p = 0.21	**W = 325, p = 0.04 (*)**	**W = 383, p = 1.1 x 10^{-3}(**)**	**W = 338, p = 0.02 (*)**	**W = 398, p = 3.4 x 10^{-4}(***)**	---
DROM-D	*PI*	**W = 1,133, p = 9.4 x 10^{-16} (****)**	**W = 1,030, p = 5.4 x 10^{-15} (****)**	**W = 1,030, p = 5.4 x 10^{-15} (****)**	**W = 1,133, p = 9.4 x 10^{-16} (****)**	**W = 1,030, p = 5.4 x 10^{-15} (****)**	**W = 1,030, p = 5.4 x 10^{-15} (****)**	**W = 1,030, p = 5.4 x 10^{-15} (****)**	**W = 1,030, p = 5.4 x 10^{-15} (****)**	**W = 4,512, p < 2.2 x 10^{-16} (****)**

Table A–III–17: Results of pairwise Mann-Whitney U tests (significant differences in bold print, α-levels: * p < .05; ** p < .01; *** p < .001; **** p < .0001) for Shannon H', **saplings**. Grey: Between and within reach comparisons of dike fields (within-reach comparisons, i.e. comparison of pre- and post-dam surfaces within each reach, are underlined). White: Comparisons between dike fields and external sites (MFP = mature floodplain; PI = pioneer islands).

		PBN-B	PDR-B	MON-B	DZM-B	PBN-C	PDR-C	MON-C	DZM-C	PLAT-A
				Pre-dam				*Post-dam*		*MFP*
PDR-B	*Pre-dam*	W = 60, p = 0.75	---	---	---	---	---	---	---	---
MON-B	*Pre-dam*	W = 49, p = 0.70	W = 40, p = 0.47	---	---	---	---	---	---	---
DZM-B	*Pre-dam*	W = 57, p = 0.84	W = 48, p = 0.65	W = 56, p = 0.97	---	---	---	---	---	---
PBN-C		W = 71, p = 0.27	W = 64, p = 0.30	W = 73, p = 0.09	W = 80.5, p = 0.08	---	---	---	---	---
PDR-C	*Post-dam*	W = 79, p = 0.09	**W = 77, p = 0.04 (*)**	**W = 80.5, p = 0.02 (*)**	**W = 94, p = 6.4 x 10^{-3} (**)**	W = 63.5, p = 0.31	---	---	---	---
MON-C	*Post-dam*	W = 57, p = 0.92	W = 45, p = 0.73	W = 51, p = 0.97	W = 55, p = 1	W = 35, p = 0.27	**W = 23, p = 0.04 (*)**	---	---	---
DZM-C		W = 69, p = 0.34	W = 60, p = 0.47	W = 66.5, p = 0.22	W = 71, p = 0.27	W = 44.5, p = 0.70	W = 29.5, p = 0.12	W = 64, p = 0.30	---	---
PLAT-A	*MFP*	**W = 131, p = 0.01 (*)**	**W = 60, p = 2.9 x 10^{-4} (***)**	**W = 78, p = 6.6 x 10^{-4} (***)**	**W = 76, p = 1.5 x 10^{-4} (***)**	**W = 21, p = 8.2 x 10^{-6} (****)**	**W = 6, p = 1.7 x 10^{-6} (****)**	**W = 99, p = 5.2 x 10^{-3} (**)**	**W = 15, p = 4.5 x 10^{-6} (****)**	---
DROM-D	*PI*	W = 733, p = 0.11	**W = 743, p = 0.02 (*)**	**W = 812, p = 2.7 x 10^{-3} (**)**	**W = 955, p = 2.0 x 10^{-4} (***)**	W = 559, p = 0.66	W = 379, p = 0.17	**W = 728, p = 0.03 (*)**	W = 668, p = 0.12	**W = 4,652, p < 2.2 x 10^{-16} (****)**

Table A–III–18: Results of pairwise Mann-Whitney U tests (significant differences in bold print, α-levels: * p < .05; ** p < .01; *** p < .001; **** p < .0001) for Shannon H', **seedlings**. Grey: Between and within reach comparisons of dike fields (within-reach comparisons, i.e. comparison of pre- and post-dam surfaces within each reach, are underlined). White: Comparisons between dike fields and external sites (MFP = mature floodplain; PI = pioneer islands).

		PBN-B	PDR-B	MON-B	DZM-B	PBN-C	PDR-C	MON-C	DZM-C	PLAT-A
				Pre-dam				*Post-dam*		*MFP*
PDR-B	*Pre-dam*	W = 35, p = 0.17	---	---	---	---	---	---	---	---
MON-B	*Pre-dam*	**W = 23.5, p = 0.03 (*)**	W = 40, p = 0.47	---	---	---	---	---	---	---
DZM-B	*Pre-dam*	W = 72.5, p = 0.45	W = 73, p = 0.21	**W = 85.5, p = 0.03 (*)**	---	---	---	---	---	---
PBN-C		W = 44, p = 0.45	W = 51.5, p = 0.94	W = 60, p = 0.47	W = 47, p = 0.59	---	---	---	---	---
PDR-C	*Post-dam*	W = 30, p = 0.08	W = 43, p = 0.62	W = 56.5, p = 0.65	W = 31, p = 0.10	W = 46, p = 0.79	---	---	---	---
MON-C	*Post-dam*	W = 29.5, p = 0.07	W = 46, p = 0.79	W = 52.5, p = 0.88	W = 38.5, p = 0.25	W = 44, p = 0.67	W = 50, p = 1	---	---	---
DZM-C	*Post-dam*	W = 47.5, p = 0.61	W = 55, p = 0.73	W = 62.5, p = 0.36	W = 53.5, p = 0.94	W = 53, p = 0.84	W = 58, p = 0.56	W = 56.5, p = 0.64	---	---
PLAT-A	*MFP*	NA	NA	NA	NA	NA	NA	NA	NA	---
DROM-D	*PI*	**W = 917, p = 1.1 x 10^{-4} (***)**	**W = 892, p = 1.3 x 10^{-5} (****)**	**W = 957, p = 3.8 x 10^{-7} (****)**	**W = 902, p = 2.2 x 10^{-4} (***)**	**W = 754, p = 5.1 x 10^{-3} (**)**	**W = 889, p = 1.5 x 10^{-5} (****)**	**W = 823, p = 3.4 x 10^{-4} (***)**	**W = 685, p = 0.04 (*)**	NA

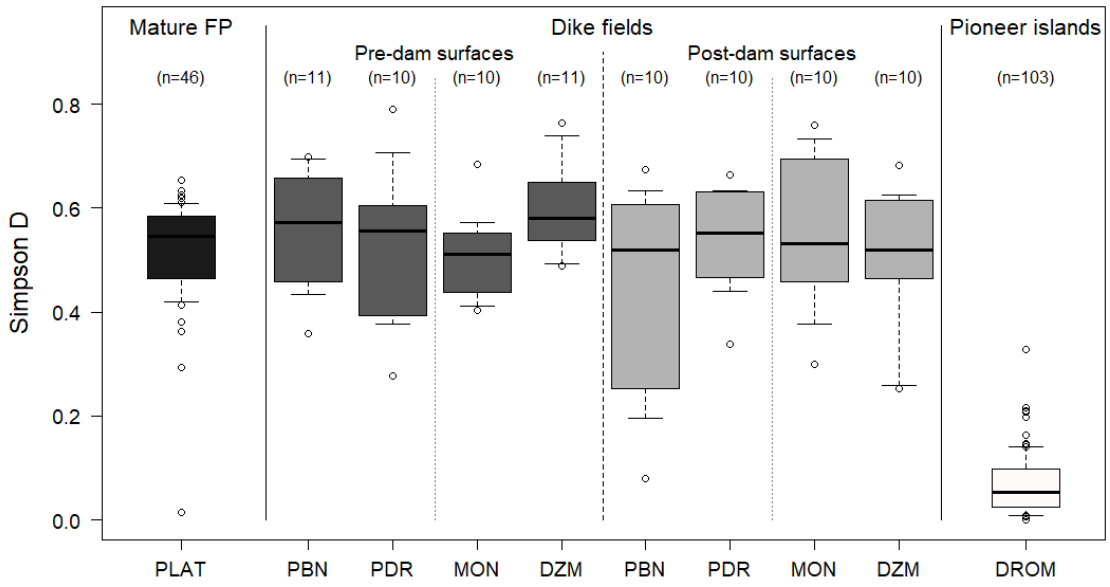

Figure A–III–7: Comparison of Simpson index per plot between dike fields and between dike fields and reference sites for **all plants** together.

Table A–III–19: Results of pairwise Mann-Whitney U tests (significant differences in bold print, α-levels: * p < .05; ** p < .01; *** p < .001; **** p < .0001) for Simpson D, **all plants**. Grey: Between and within reach comparisons of dike fields (within-reach comparisons, i.e. comparison of pre- and post-dam surfaces within each reach, are underlined). White: Comparisons between dike fields and external sites (MFP = mature floodplain; PI = pioneer islands).

		PBN-B	PDR-B	MON-B	DZM-B	PBN-C	PDR-C	MON-C	DZM-C	PLAT-A
				Pre-dam				*Post-dam*		*MFP*
PDR-B	*Pre-dam*	W = 56, p = 0.97	---	---	---	---	---	---	---	---
MON-B	*Pre-dam*	W = 54, p = 0.97	W = 44, p = 0.68	---	---	---	---	---	---	---
DZM-B	*Pre-dam*	W = 80, p = 0.22	W = 65, p = 0.51	W = 77, p = 0.13	---	---	---	---	---	---
PBN-C		<u>W = 72, p = 0.25</u>	W = 64, p = 0.32	W = 64, p = 0.32	W = 58, p = 0.86	---	---	---	---	---
PDR-C	*Post-dam*	W = 51, p = 0.81	<u>W = 47, p = 0.85</u>	W = 48, p = 0.91	W = 36, p = 0.20	W = 32, p = 0.19	---	---	---	---
MON-C	*Post-dam*	W = 52, p = 0.86	W = 48, p = 0.91	<u>W = 50, p = 1</u>	W = 37, p = 0.22	W = 36, p = 0.32	W = 54, p = 0.80	---	---	---
DZM-C	*Post-dam*	W = 58, p = 0.86	W = 55, p = 0.74	W = 54, p = 0.80	<u>W = 43, p = 0.43</u>	W = 41, p = 0.53	W = 61, p = 0.44	W = 54, p = 0.80	---	---
PLAT-A	*MFP*	W = 278, p = 0.63	W = 248, p = 0.71	W = 265, p = 0.47	W = 180, p = 0.14	W = 199, p = 0.52	W = 287, p = 0.23	W = 248, p = 0.71	W = 243, p = 0.79	---
DROM-D	*PI*	**W = 1,133, p = 5.6 x 10^{-8} (****)**	**W = 1,029, p = 2.1 x 10^{-7} (****)**	**W = 1,030, p = 2.0 x 10^{-7} (****)**	**W = 1,111, p = 1.8 x 10^{-7} (****)**	**W = 991, p = 1.5 x 10^{-6} (****)**	**W = 1,030, p = 2.0 x 10^{-7} (****)**	**W = 1,029, p = 2.1 x 10^{-7} (****)**	**W = 1,028, p = 2.2 x 10^{-7} (****)**	**W = 4,653, p < 2.2 x 10^{-16} (****)**

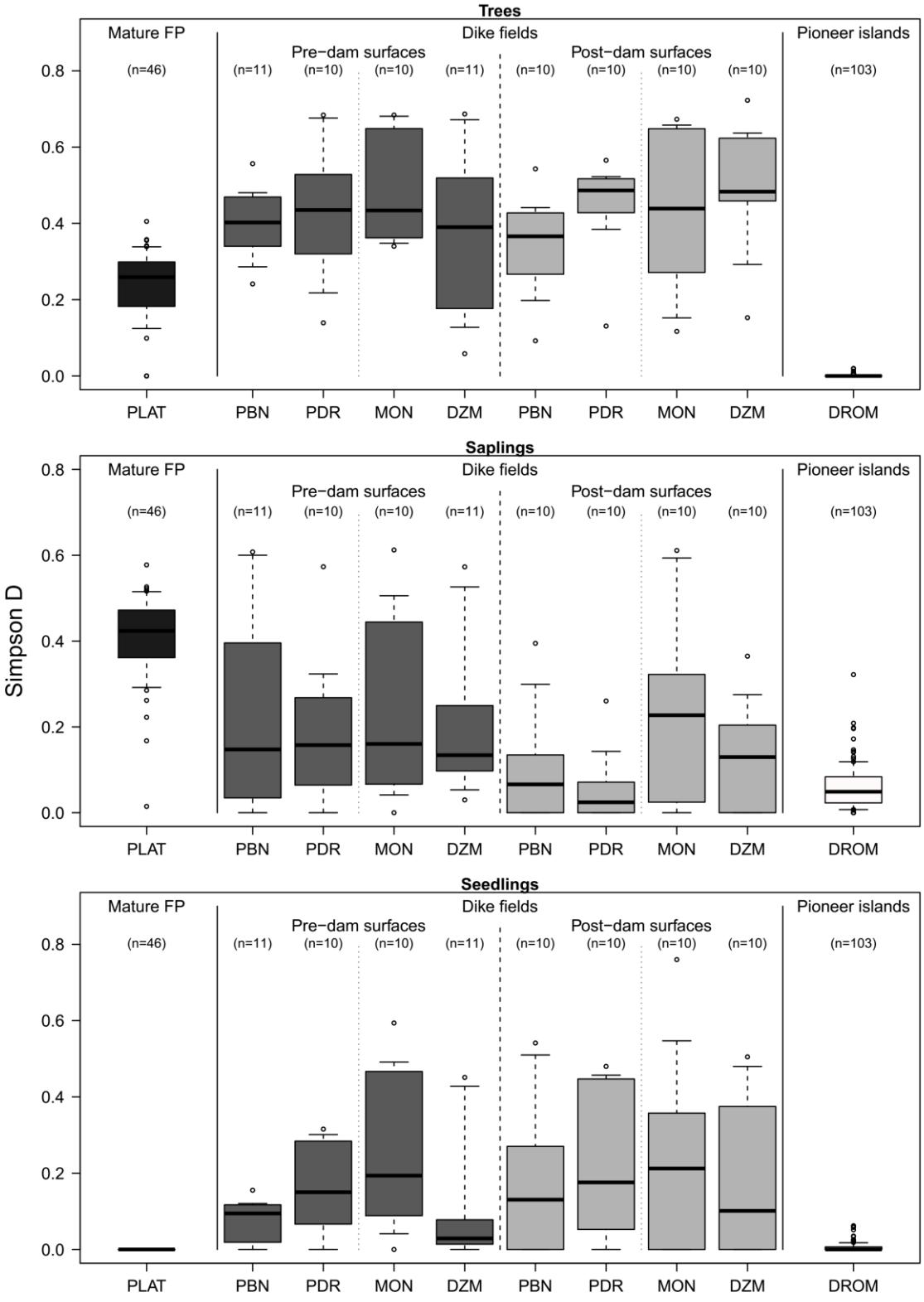

Figure A–III–8: Comparison of Simpson index per plot between dike fields and between dike fields and reference sites for **each LHS** separately.

Table A–III–20: Results of pairwise Mann-Whitney U tests (significant differences in bold print, α-levels: * p < .05; ** p < .01; *** p < .001; **** p < .0001) for Simpson D, **trees**. Grey: Between and within reach comparisons of dike fields (within-reach comparisons, i.e. comparison of pre- and post-dam surfaces within each reach, are underlined). White: Comparisons between dike fields and external sites (MFP = mature floodplain; PI = pioneer islands).

		PBN-B	PDR-B	MON-B	DZM-B	PBN-C	PDR-C	MON-C	DZM-C	PLAT-A
				Pre-dam				*Post-dam*		*MFP*
PDR-B	*Pre-dam*	W = 47, p = 0.60	---	---	---	---	---	---	---	---
MON-B	*Pre-dam*	W = 41, p = 0.35	W = 43.5, p = 0.65	---	---	---	---	---	---	---
DZM-B	*Pre-dam*	W = 68, p = 0.65	W = 65, p = 0.51	W = 70, p = 0.31	---	---	---	---	---	---
PBN-C		W = 69, p = 0.35	W = 64, p = 0.32	W = 72, p = 0.11	W = 58, p = 0.86	---	---	---	---	---
PDR-C	*Post-dam*	W = 29, p = 0.07	W = 45, p = 0.74	W = 45, p = 0.74	W = 40, p = 0.31	**W = 20, p = 0.02 (*)**	---	---	---	---
MON-C	*Post-dam*	W = 49, p = 0.70	W = 52, p = 0.91	W = 57, p = 0.63	W = 46, p = 0.56	W = 35, p = 0.28	W = 52, p = 0.91	---	---	---
DZM-C	*Post-dam*	W = 30, p = 0.08	W = 42, p = 0.58	W = 45, p = 0.74	W = 33, p = 0.13	**W = 20, p = 0.02 (*)**	W = 40, p = 0.48	W = 44, p = 0.68	---	---
PLAT-A	*MFP*	**W = 451, p = 6.5 x 10^{-5} (****)**	**W = 376, p = 1.9 x 10^{-3} (**)**	**W = 451, p = 2.4 x 10^{-6} (****)**	W = 324, p = 0.15	**W = 358, p = 6.4 x 10^{-3} (**)**	**W = 419, p = 5.5 x 10^{-5} (****)**	**W = 358, p = 6.4 x 10^{-3} (**)**	**W = 409, p = 1.3 x 10^{-4} (***)**	---
DROM-D	*PI*	**W = 1,133, p = 9.4 x 10^{-16} (****)**	**W = 1,030, p = 5.4 x 10^{-15} (****)**	**W = 1,030, p = 5.4 x 10^{-15} (****)**	**W = 1,133, p = 9.4 x 10^{-16} (****)**	**W = 1,030, p = 5.4 x 10^{-15} (****)**	**W = 1,030, p = 5.4 x 10^{-15} (****)**	**W = 1,030, p = 5.4 x 10^{-15} (****)**	**W = 1,030, p = 5.4 x 10^{-15} (****)**	**W = 4,512, p < 2.2 x 10^{-16} (****)**

Table A–III–21: Results of pairwise Mann-Whitney U tests (significant differences in bold print, α-levels: * p < .05; ** p < .01; *** p < .001; **** p < .0001) for Simpson D, **saplings**. Grey: Between and within reach comparisons of dike fields (within-reach comparisons, i.e. comparison of pre- and post-dam surfaces within each reach, are underlined). White: Comparisons between dike fields and external sites (MFP = mature floodplain; PI = pioneer islands).

		PBN-B	PDR-B	MON-B	DZM-B	PBN-C	PDR-C	MON-C	DZM-C	PLAT-A
				Pre-dam				*Post-dam*		*MFP*
PDR-B	*Pre-dam*	W = 59, p = 0.80	---	---	---	---	---	---	---	---
MON-B	*Pre-dam*	W = 45, p = 0.50	W = 43, p = 0.62	---	---	---	---	---	---	---
DZM-B	*Pre-dam*	W = 58, p = 0.90	W = 49, p = 0.70	W = 55, p = 1	---	---	---	---	---	---
PBN-C		W = 71, p = 0.27	W = 64, p = 0.30	W = 73, p = 0.09	W = 77.5, p = 0.12	---	---	---	---	---
PDR-C	*Post-dam*	W = 79, p = 0.09	**W = 77, p = 0.04 (*)**	**W = 79.5, p = 0.03 (*)**	**W = 92, p = 9.7 x 10^{-3} (**)**	W = 63.5, p = 0.31	---	---	---	---
MON-C	*Post-dam*	W = 57, p = 0.92	W = 42, p = 0.57	W = 52, p = 0.91	W = 52, p = 0.86	W = 35, p = 0.27	W = 25, p = 0.06	---	---	---
DZM-C	*Post-dam*	W = 67, p = 0.42	W = 59, p = 0.52	W = 63.5, p = 0.32	W = 66, p = 0.46	W = 41.5, p = 0.54	W = 29.5, p = 0.12	W = 63, p = 0.34	---	---
PLAT-A	*MFP*	**W = 144, p = 0.03 (*)**	**W = 59, p = 2.6 x 10^{-4} (***)**	**W = 137, p = 0.05 (*)**	**W = 106, p = 2.2 x 10^{-3} (**)**	**W = 26, p = 1.3 x 10^{-5} (****)**	**W = 7, p = 1.9 x 10^{-6} (****)**	**W = 110, p = 0.01 (*)**	**W = 23, p = 1.0 x 10^{-5} (****)**	---
DROM-D	*PI*	W = 738, p = 0.10	**W = 741, p = 0.02 (*)**	**W = 790, p = 5.5 x 10^{-3} (**)**	**W = 940, p = 3.4 x 10^{-4} (***)**	W = 558, p = 0.67	W = 385, p = 0.19	**W = 729, p = 0.03 (*)**	W = 671, p = 0.12	**W = 4,644, p < 2.2 x 10^{-16} (****)**

Table A–III–22: Results of pairwise Mann-Whitney U tests (significant differences in bold print, α-levels: * p < .05; ** p < .01; *** p < .001; **** p < .0001) for Simpson D, **seedlings**. Grey: Between and within reach comparisons of dike fields (within-reach comparisons, i.e. comparison of pre- and post-dam surfaces within each reach, are underlined). White: Comparisons between dike fields and external sites (MFP = mature floodplain; PI = pioneer islands).

		PBN-B	PDR-B	MON-B	DZM-B	PBN-C	PDR-C	MON-C	DZM-C	PLAT-A
				Pre-dam				*Post-dam*		*MFP*
PDR-B	*Pre-dam*	W = 32, p = 0.11	---	---	---	---	---	---	---	---
MON-B	*Pre-dam*	**W = 22.5, p = 0.02 (*)**	W = 40, p = 0.47	---	---	---	---	---	---	---
DZM-B	*Pre-dam*	W = 71.5, p = 0.49	W = 73, p = 0.21	**W = 85.5, p = 0.03 (*)**	---	---	---	---	---	---
PBN-C		W = 44, p = 0.45	W = 52.5, p = 0.88	W = 59, p = 0.52	W = 47, p = 0.59	---	---	---	---	---
PDR-C	*Post-dam*	**W = 26, p = 0.04 (*)**	W = 44, p = 0.68	W = 55.5, p = 0.70	W = 32, p = 0.11	W = 46, p = 0.79	---	---	---	---
MON-C	*Post-dam*	W = 28.5, p = 0.06	W = 44, p = 0.68	W = 51.5, p = 0.94	W = 38.5, p = 0.25	W = 44, p = 0.67	W = 47, p = 0.85	---	---	---
DZM-C	*Post-dam*	W = 47.5, p = 0.61	W = 52, p = 0.91	W = 61.5, p = 0.40	W = 53.5, p = 0.94	W = 53, p = 0.84	W = 56, p = 0.67	W = 57.5, p = 0.58	---	---
PLAT-A	*MFP*	NA	NA	NA	NA	NA	NA	NA	NA	---
DROM-D	*PI*	**W = 918, p = 1.1 x 10^{-4} (***)**	**W = 892, p = 1.3 x 10^{-5} (****)**	**W = 957, p = 3.8 x 10^{-7} (****)**	**W = 899, p = 2.5 x 10^{-4} (***)**	**W = 754, p = 5.1 x 10^{-3} (**)**	**W = 889, p = 1.5 x 10^{-5} (****)**	**W = 823, p = 3.4 x 10^{-4} (***)**	**W = 685, p = 0.04 (*)**	NA

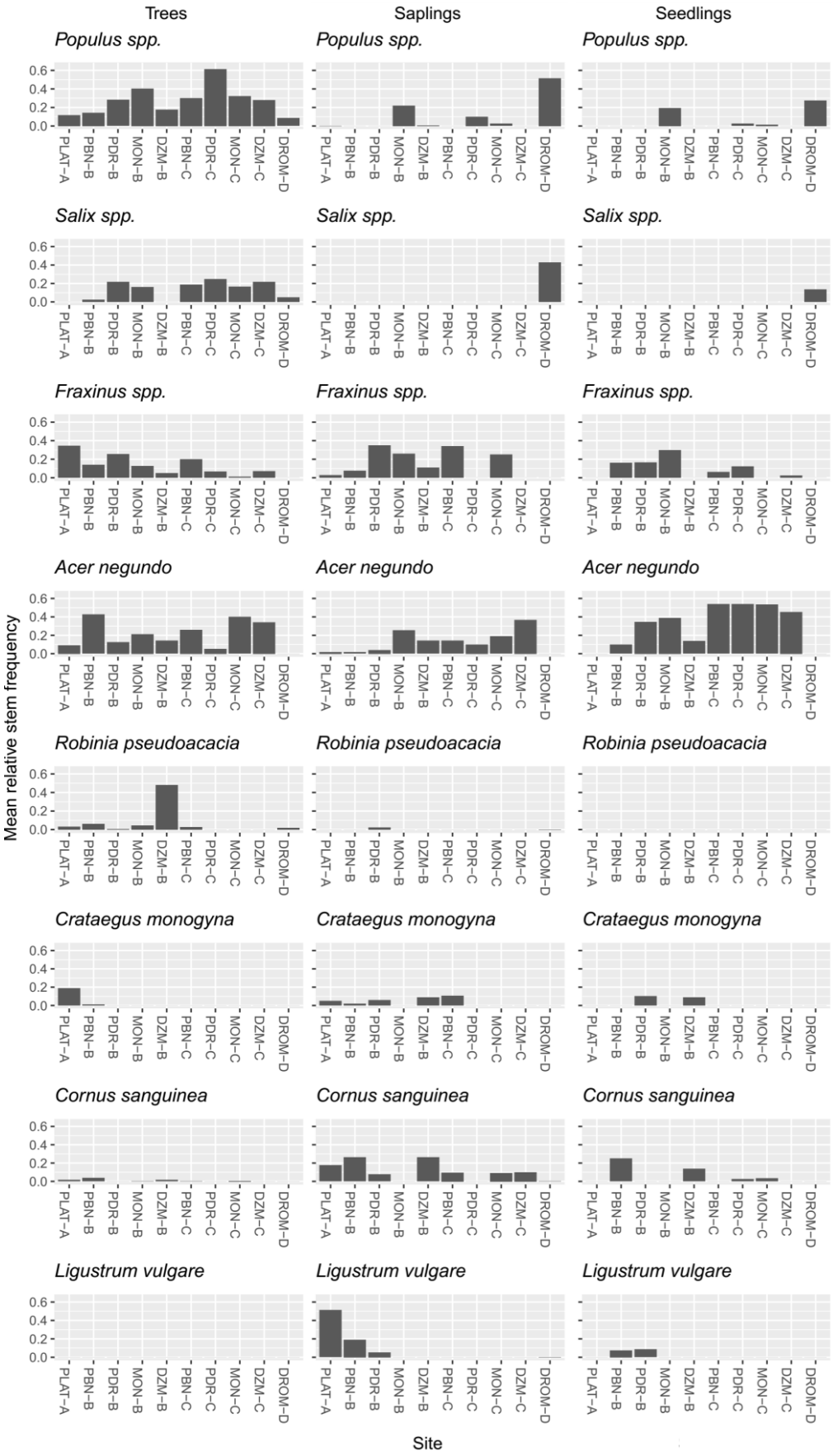

Figure A–III–9: Between-site comparison of mean relative frequencies of dominant species at each life history stage. At PLAT, no seedlings had been surveyed.

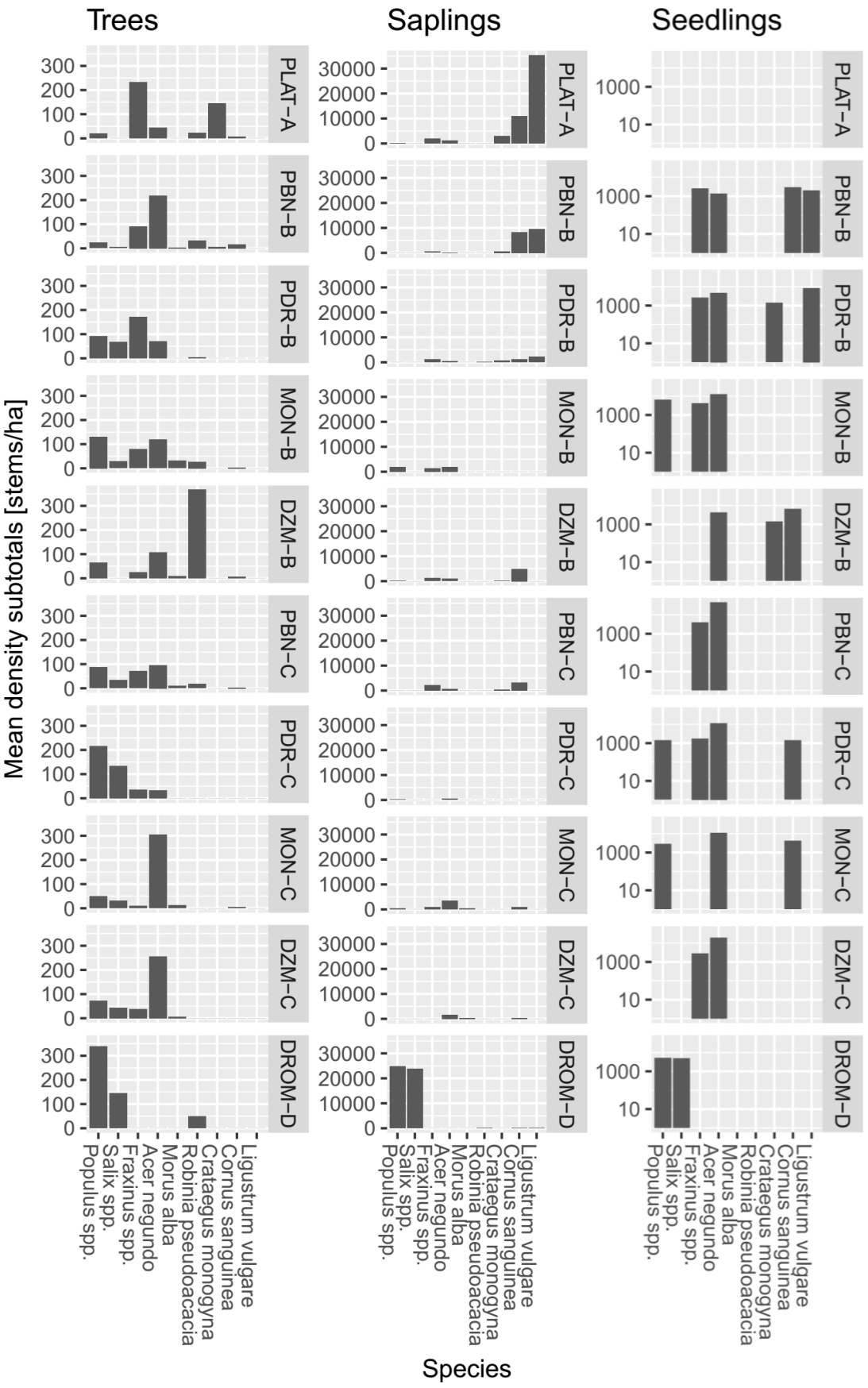

Figure A–III–10: Between-site comparison of mean density subtotals of dominant species at each life history stage. At PLAT, no seedlings had been surveyed.

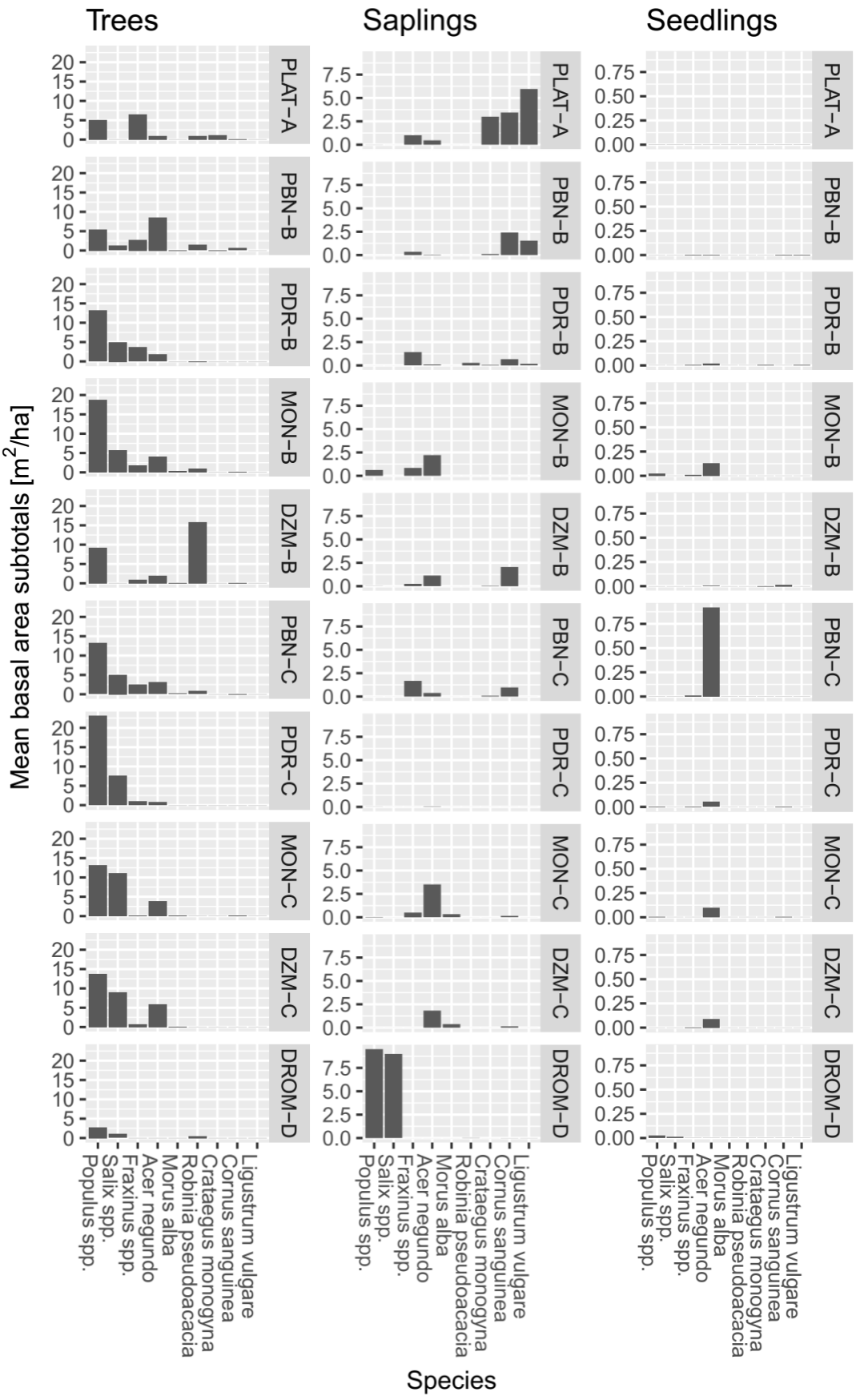

Figure A–III–11: Between-site comparison of mean basal area subtotals of dominant species at each life history stage. At PLAT, no seedlings had been surveyed.

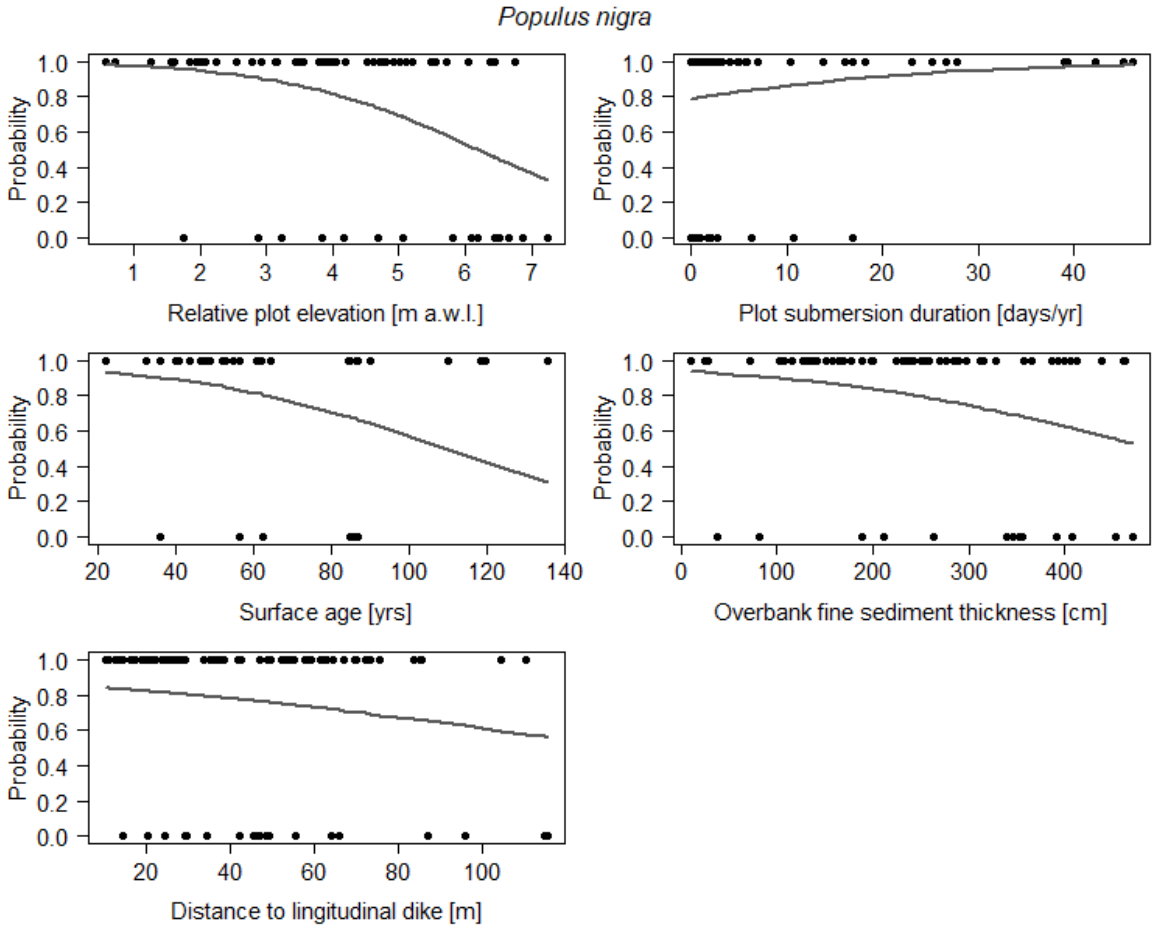

Figure A–III–12: Logistic regression models of individual drivers concerning *Populus nigra*. Relative elevation $p<0.01$, $\text{logit}(E(y)) = -0.43 x + 2.67$. Surface age $p < .05$, $\text{logit}(E(y)) = -0.02 x + 2.05529$. Sediment depth $p < .05$, $\text{logit}(E(y)) = -0.004 x + 1.92$.

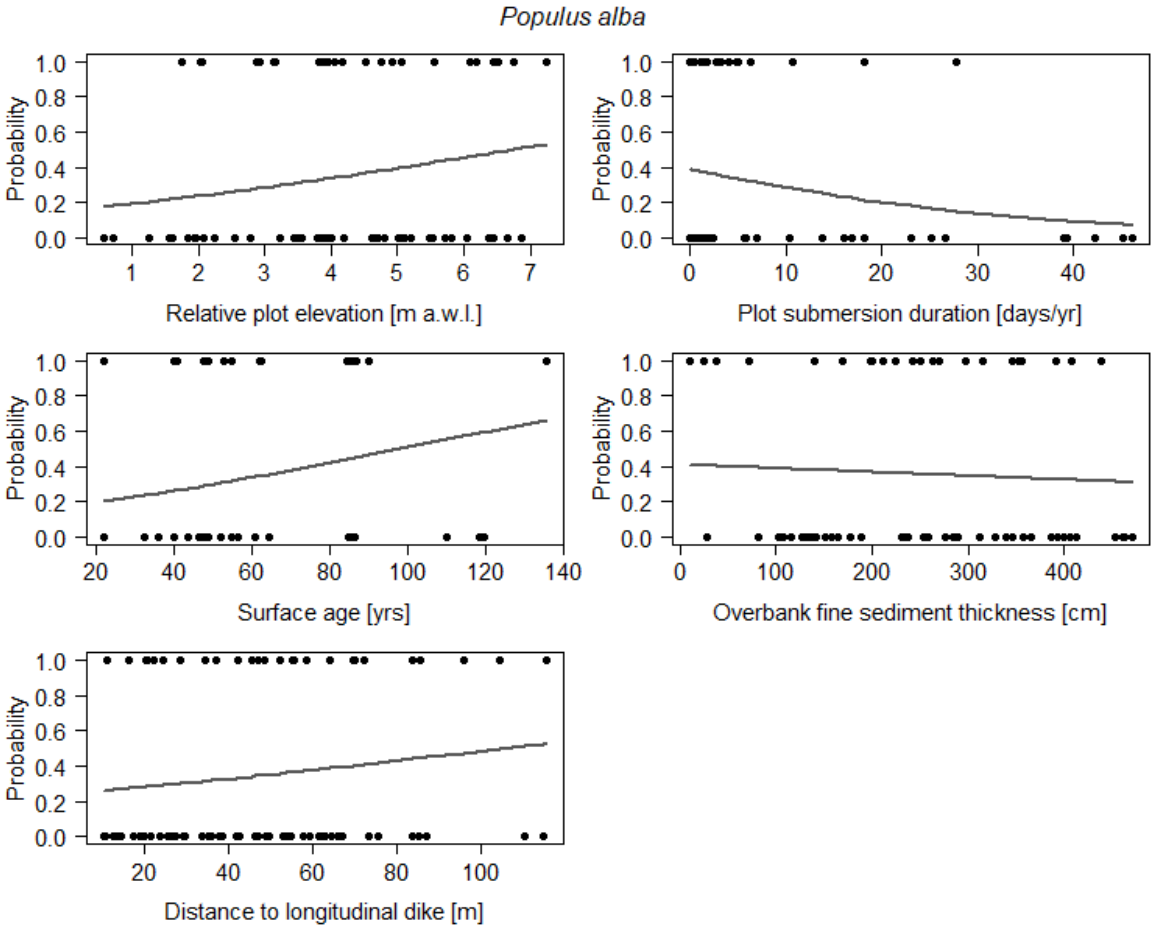

Figure A–III–13: Logistic regression models of individual drivers concerning *Populus alba*. Surface age $p < .05$, $\text{logit}(E(y)) = 0.02 x - 1.74$.

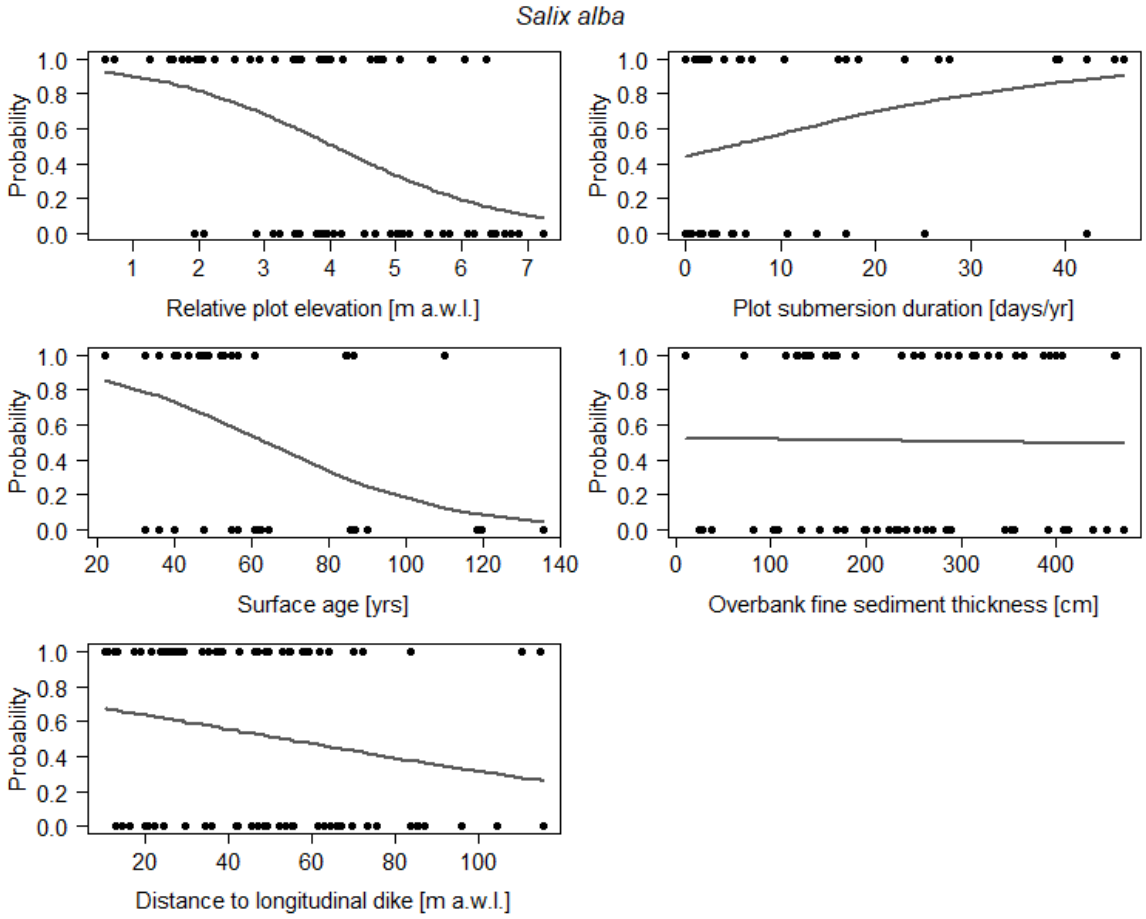

Figure A–III–14: Logistic regression models of individual drivers concerning *Salix alba*. Surface age $p < .0001$, $\text{logit}(E(y)) = -0.04 x + 2.90$. Relative elevation $p < .0001$, $\text{logit}(E(y)) = -0.73 x + 3.19$. Submersion duration $p < .05$, $\text{logit}(E(y)) = 0.04 x + 0.03$.

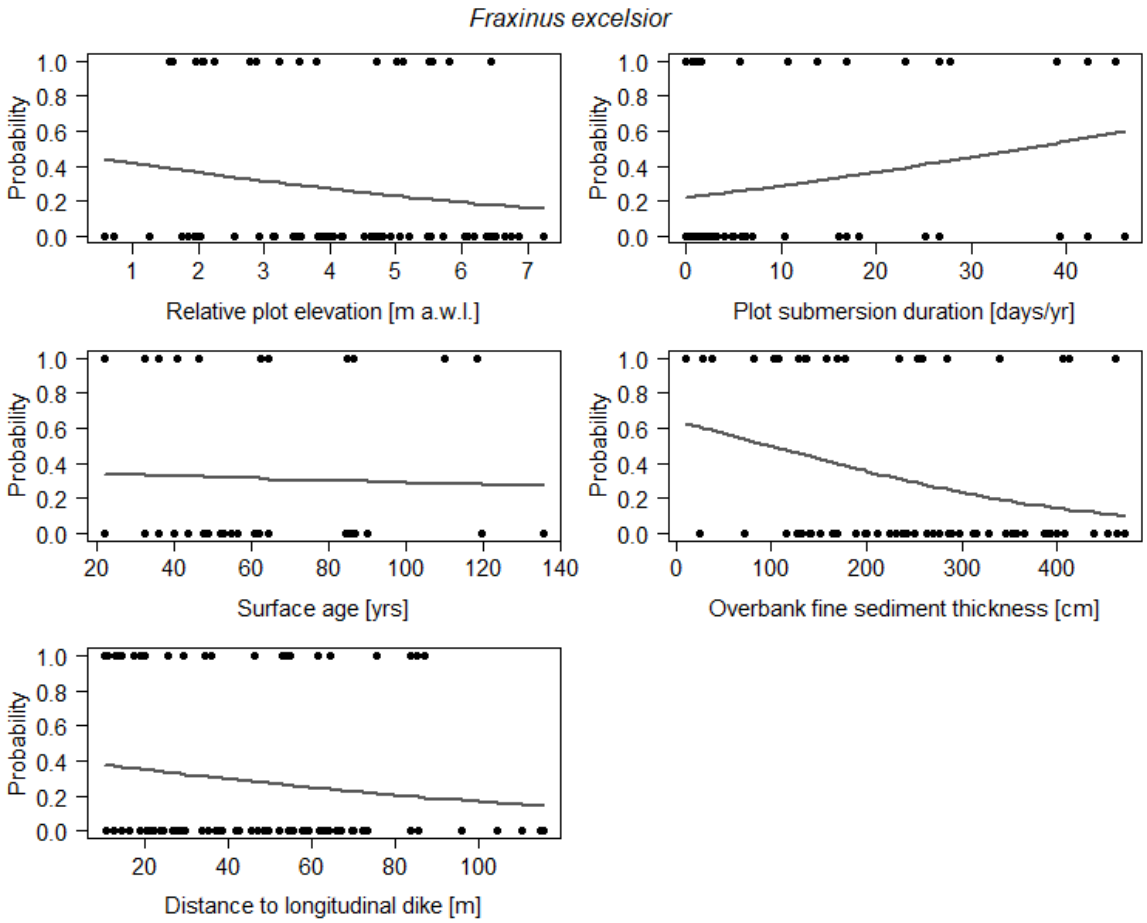

Figure A–III–15: Logistic regression models of individual drivers concerning *Fraxinus excelsior*. Sediment depth $p < .01$, $\text{logit}(E(y)) = -0.006 x + 0.58$. Submersion duration $p < .05$, $\text{logit}(E(y)) = 0.04 x - 1.27$.

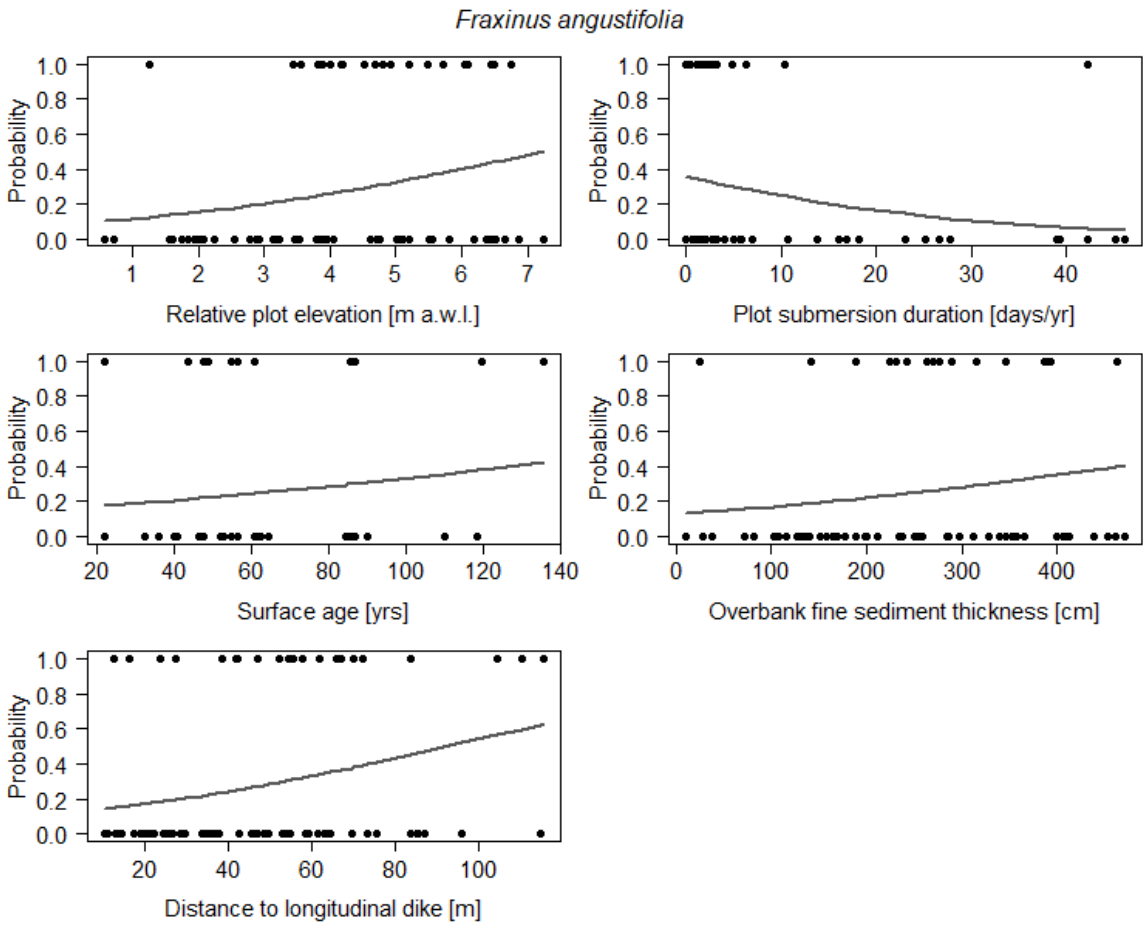

Figure A–III–16: Logistic regression models of individual drivers concerning *Fraxinus angustifolia*. Lateral distance to the longitudinal dike $p < .01$, $\text{logit}(E(y)) = 0.02 \times - 2.02$. Relative elevation $p < .05$, $\text{logit}(E(y)) = 0.3248 \times - 2.35$.

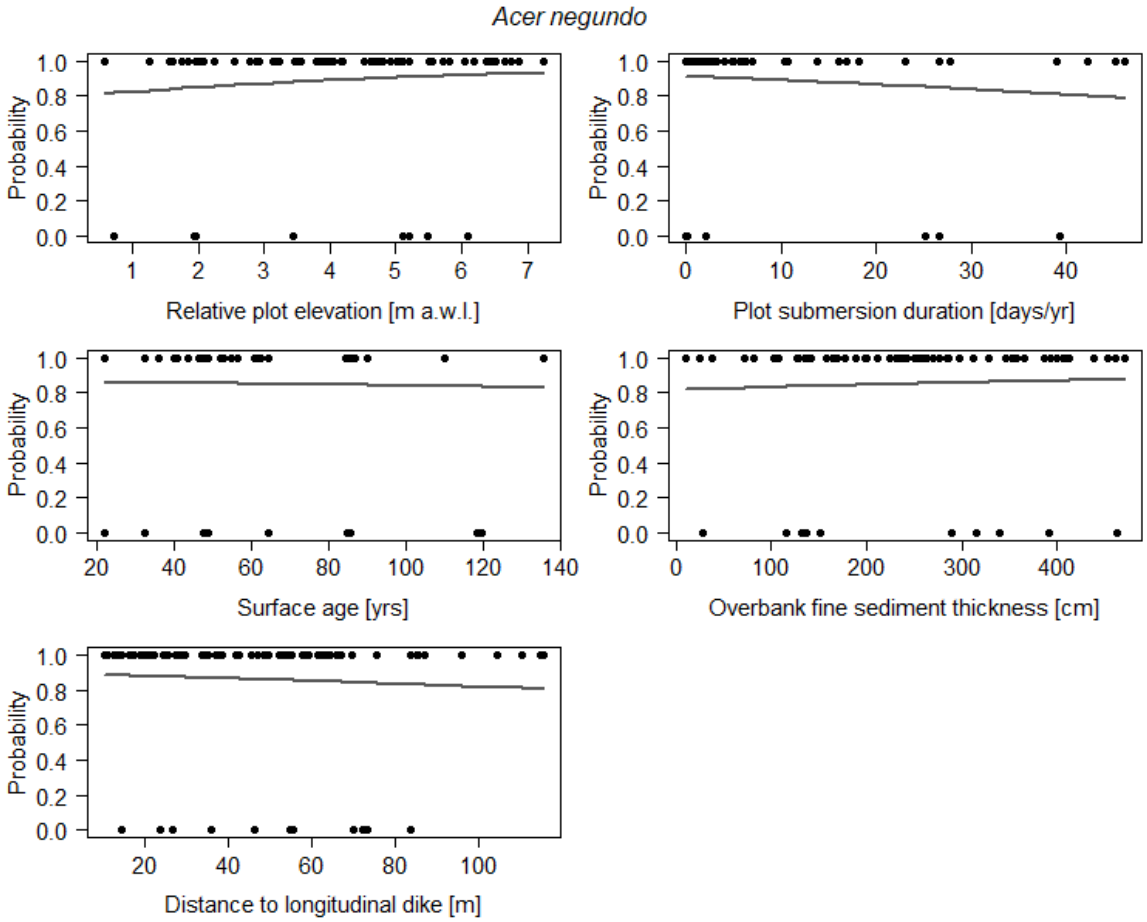

Figure A–III–17: Logistic regression models of individual drivers concerning *Acer negundo*. No significant gradients were found for the tested control variables.

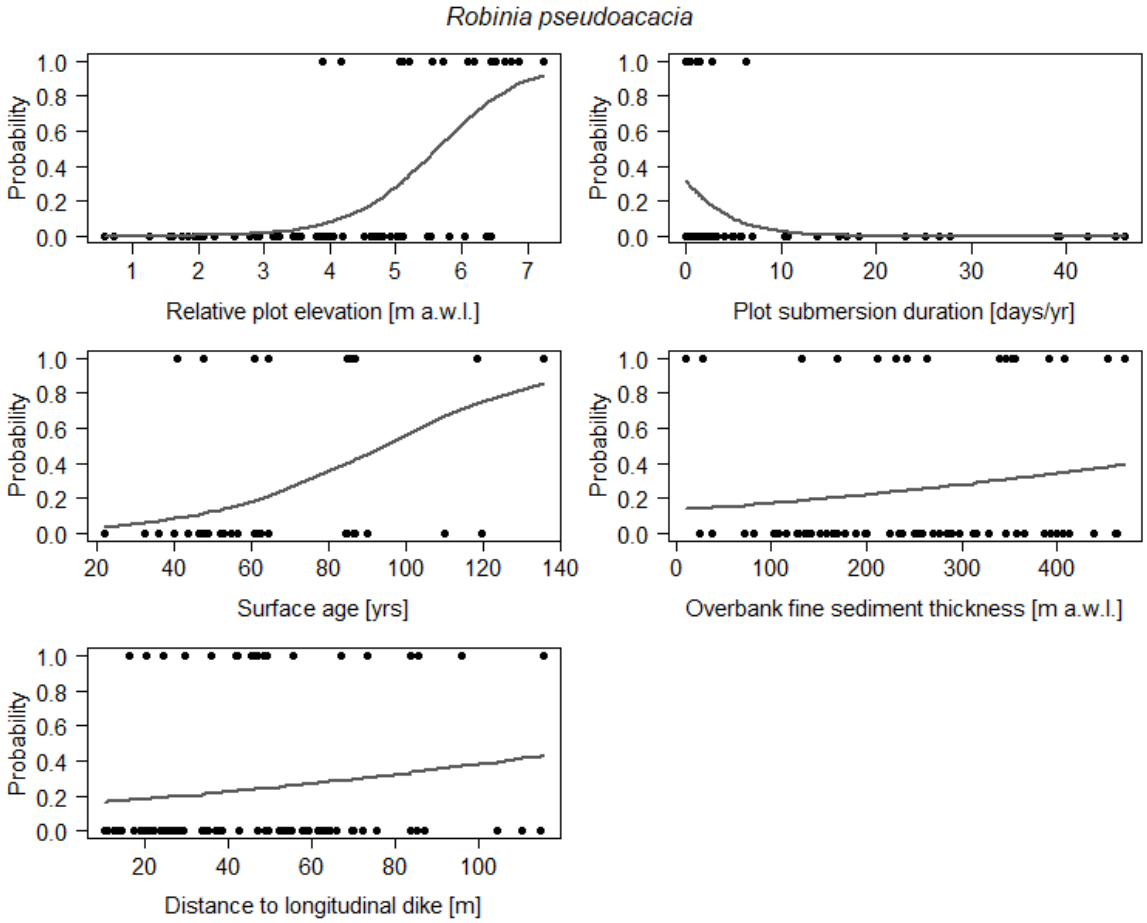

Figure A–III–18: Logistic regression models of individual drivers concerning *Robinia pseudoacacia*. Surface age $p < .001$, $\text{logit}(E(y)) = 0.04 \times - 3.89$. Submersion duration $p < .05$, $\text{logit}(E(y)) = -0.28 \times - 0.53$. Relative elevation $p < .0001$, $\text{logit}(E(y)) = 1.39 \times - 7.63$.

Appendix IV: Supplementary material Chapter VII

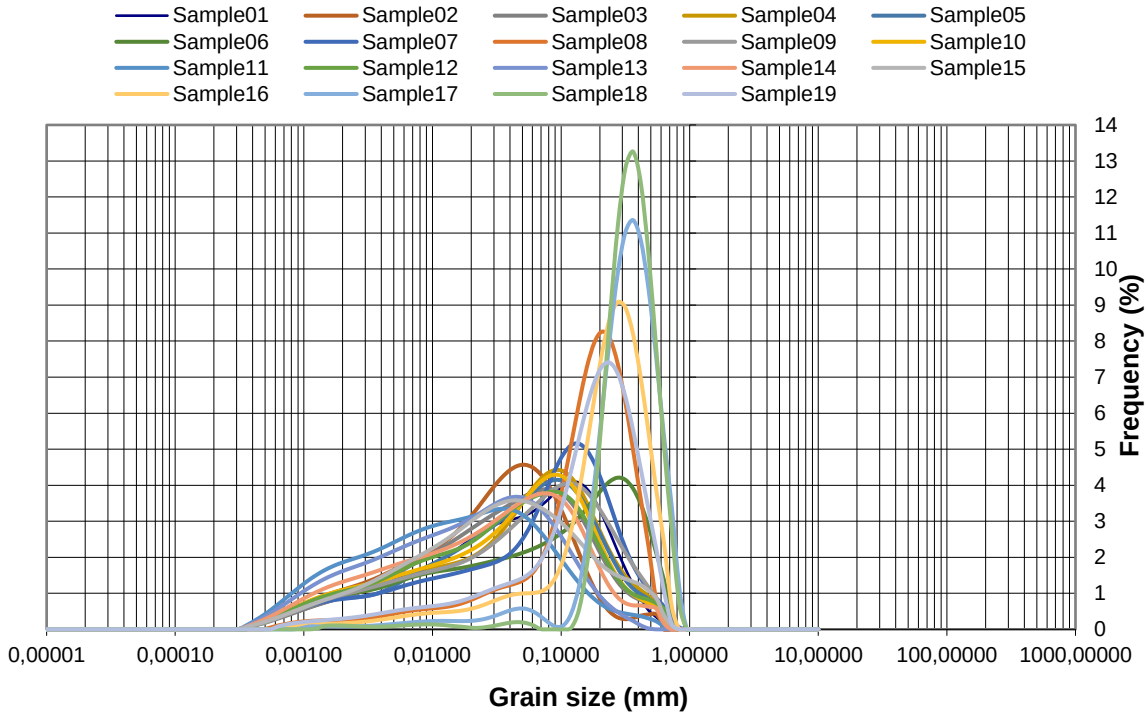

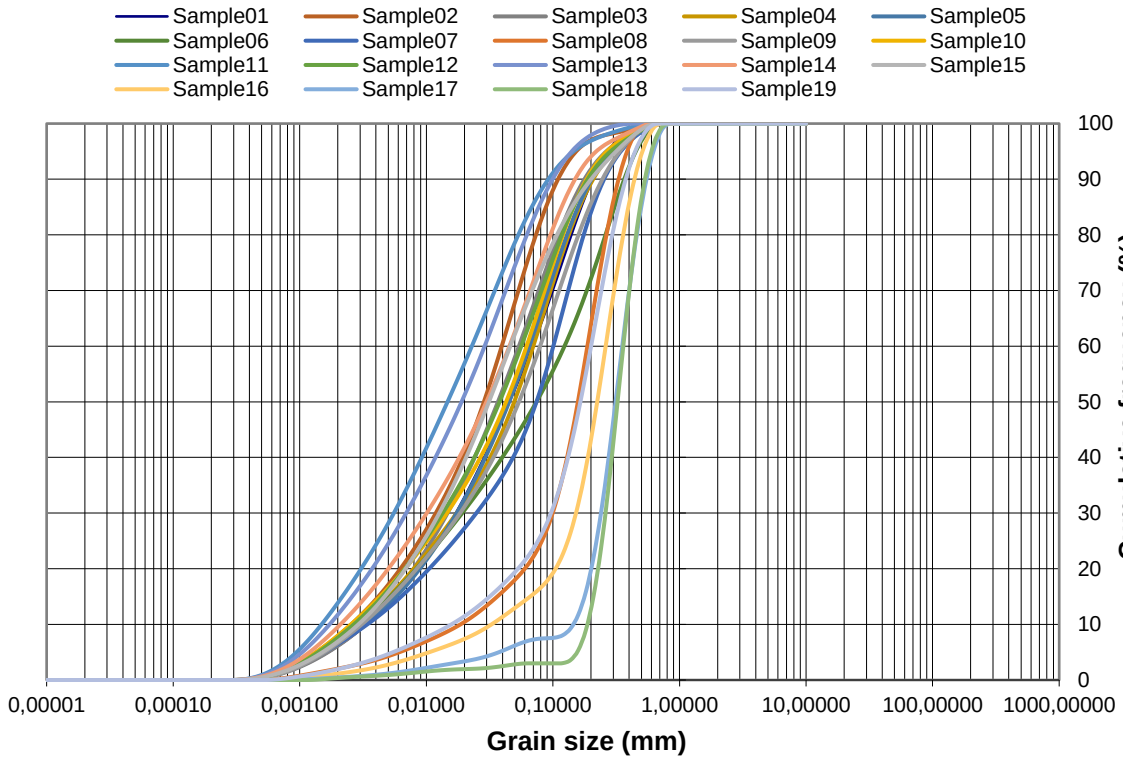

Figure A–IV–1: Results from granulometric laser analysis of 20 surface sediment samples (top: grain size curve, bottom: cumulative grain size curve).

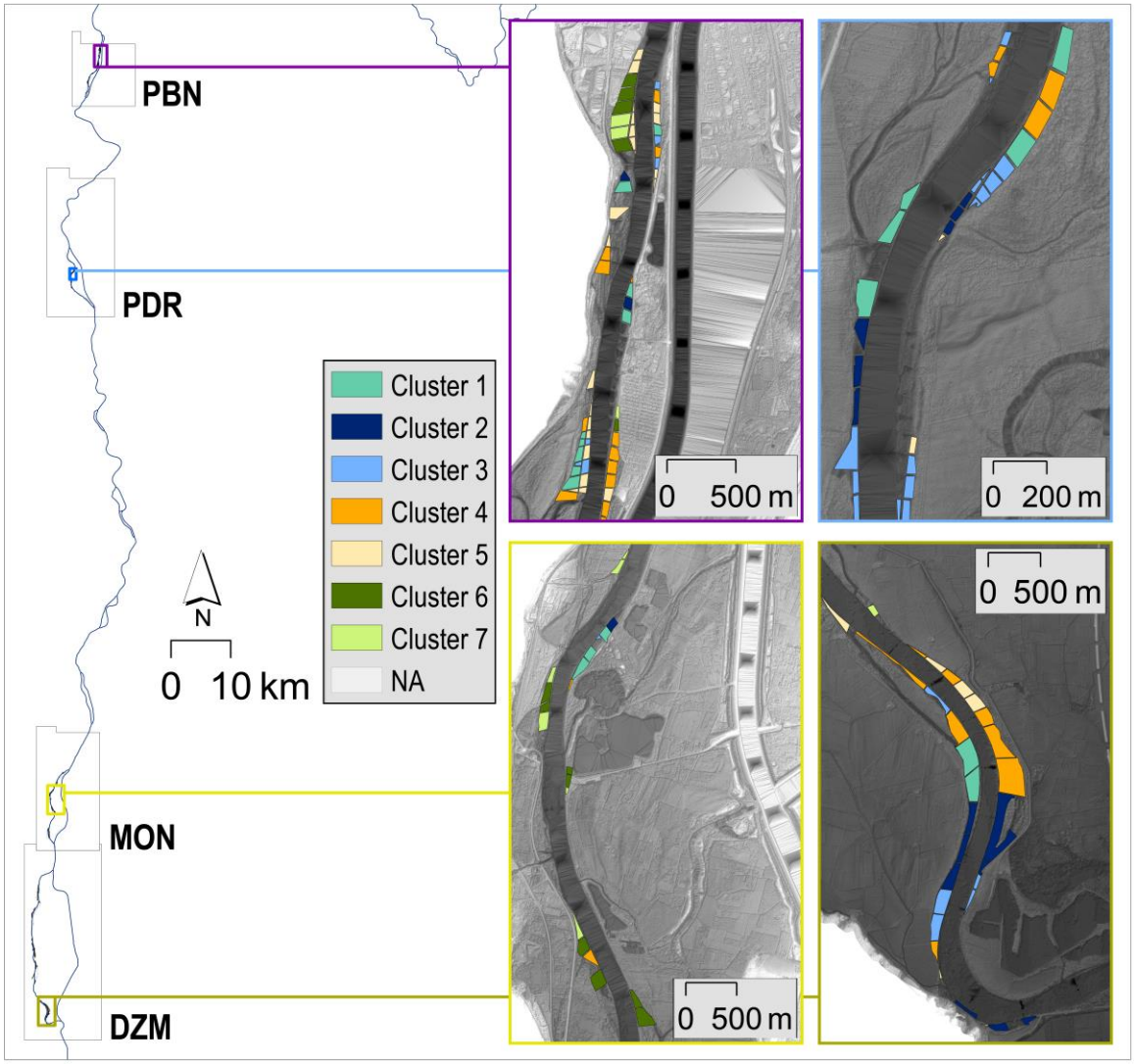

Figure A–IV–2: Spatial distribution of dike field types resulting from the combined principal component analysis and hierarchical clustering presented in chapter V. We note a local organisation in small entities, notably sub-entities of dike field sequences.

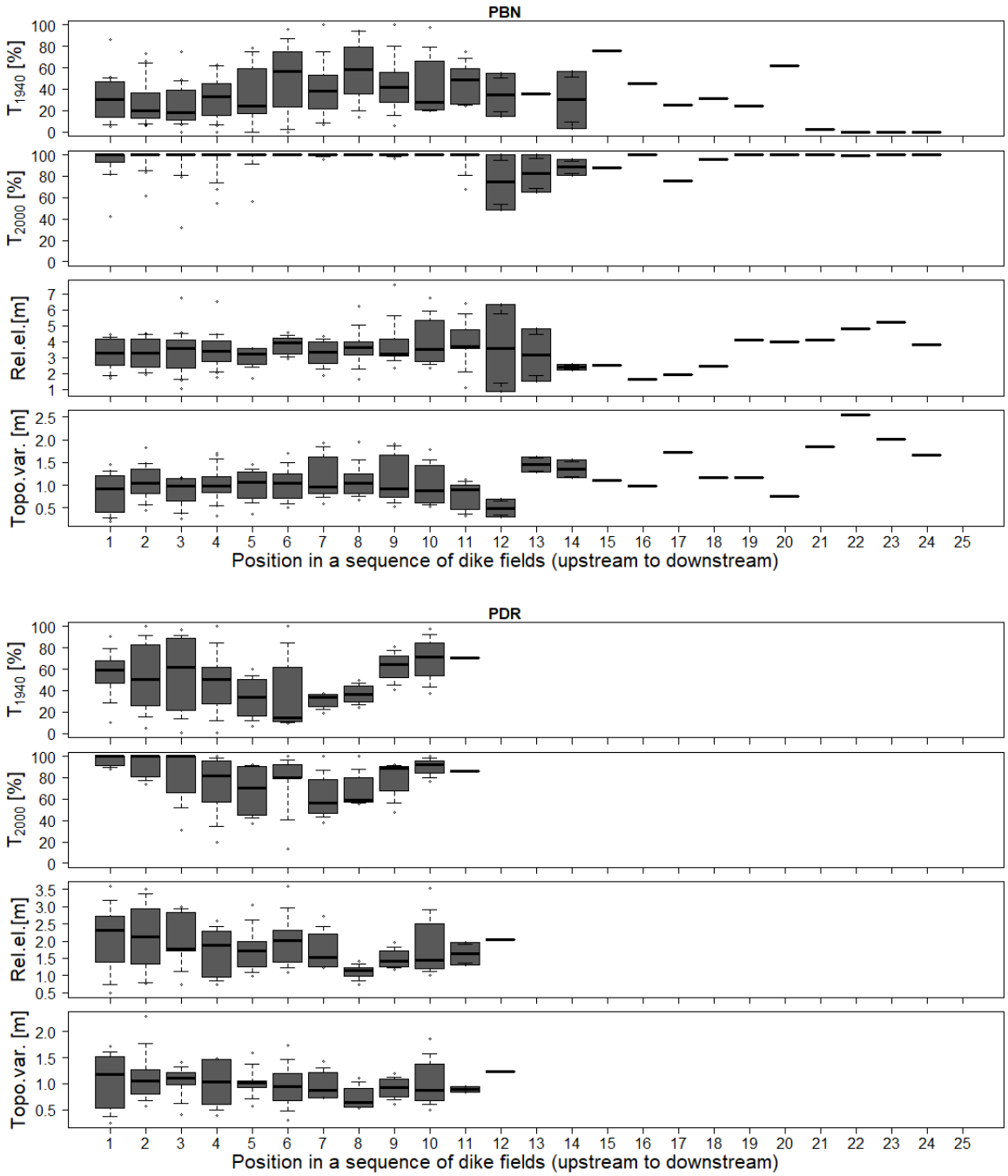

Figure A–IV–3: Patterns of sedimentation and terrestrialisation within sequences of dike fields of the various study reaches (1= most upstream dike field, n = most downstream dike field).

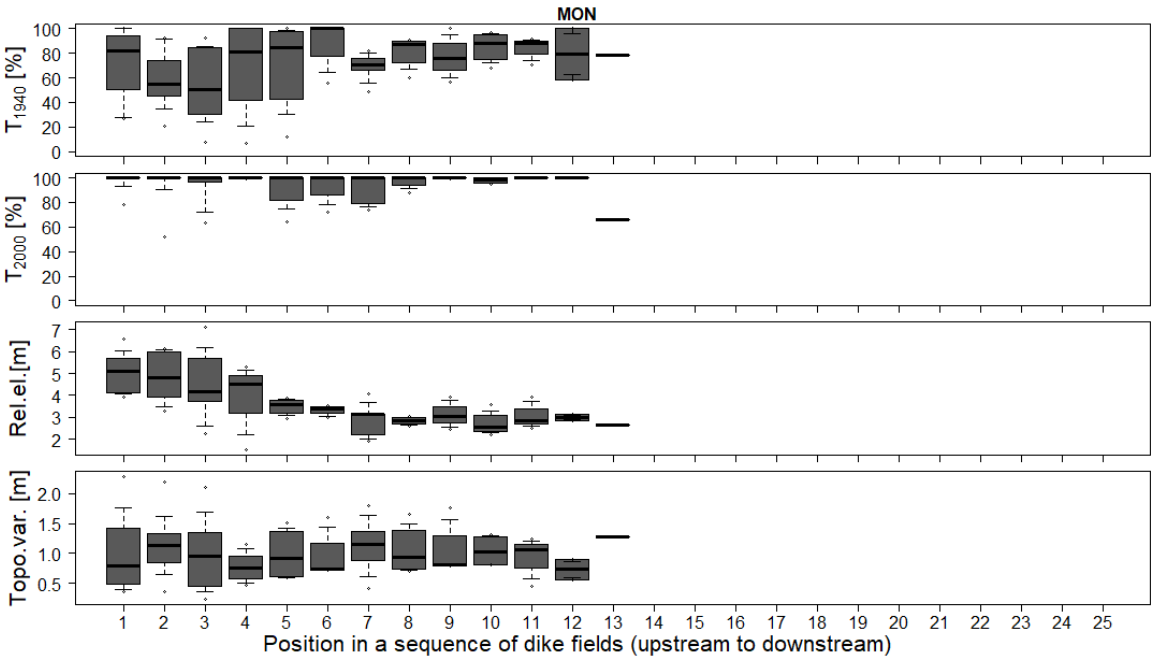

(**Figure A–IV–3 continued**)

Intra-dike field analysis

We used belt transects perpendicular to the dikes to analyse longitudinal patterns of sedimentation and terrestrialisation within each dike field. For this we first created small transects along the crest of the dikes, which were 4 m in length and 2 m on both sides of the crest. The transects were then extended into the dike fields (Figure A–IV–4). We quantified the percentage of aquatic and terrestrial pixels per transect as an information of the terrestrialisation status in each transect. We also extracted the mean relative elevation above a water level at 100 m^3/s and topographic variability from the LiDAR data based DEMs.

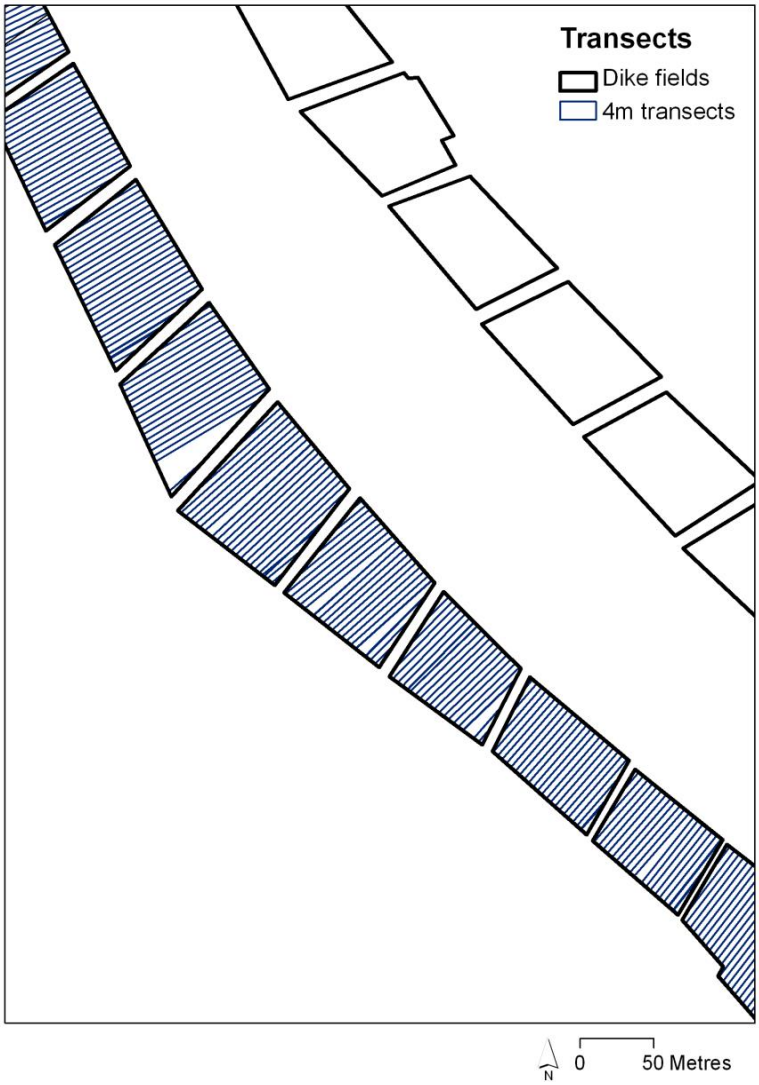

Figure A–IV–4: Schematic view of transects in dike fields.

Figure A–IV–5 (following pages): Longitudinal patterns of (a) terrestrialisation status (pp 335–347), (b) mean relative elevation above a water level at 100 m^3/s (pp 348–360), and (c) topographic variability (pp 361–373) in the individual dike fields. The colour code illustrates the four study reaches (pink: PBN, dark violet: PDR, golden: MON, light blue: DZM).

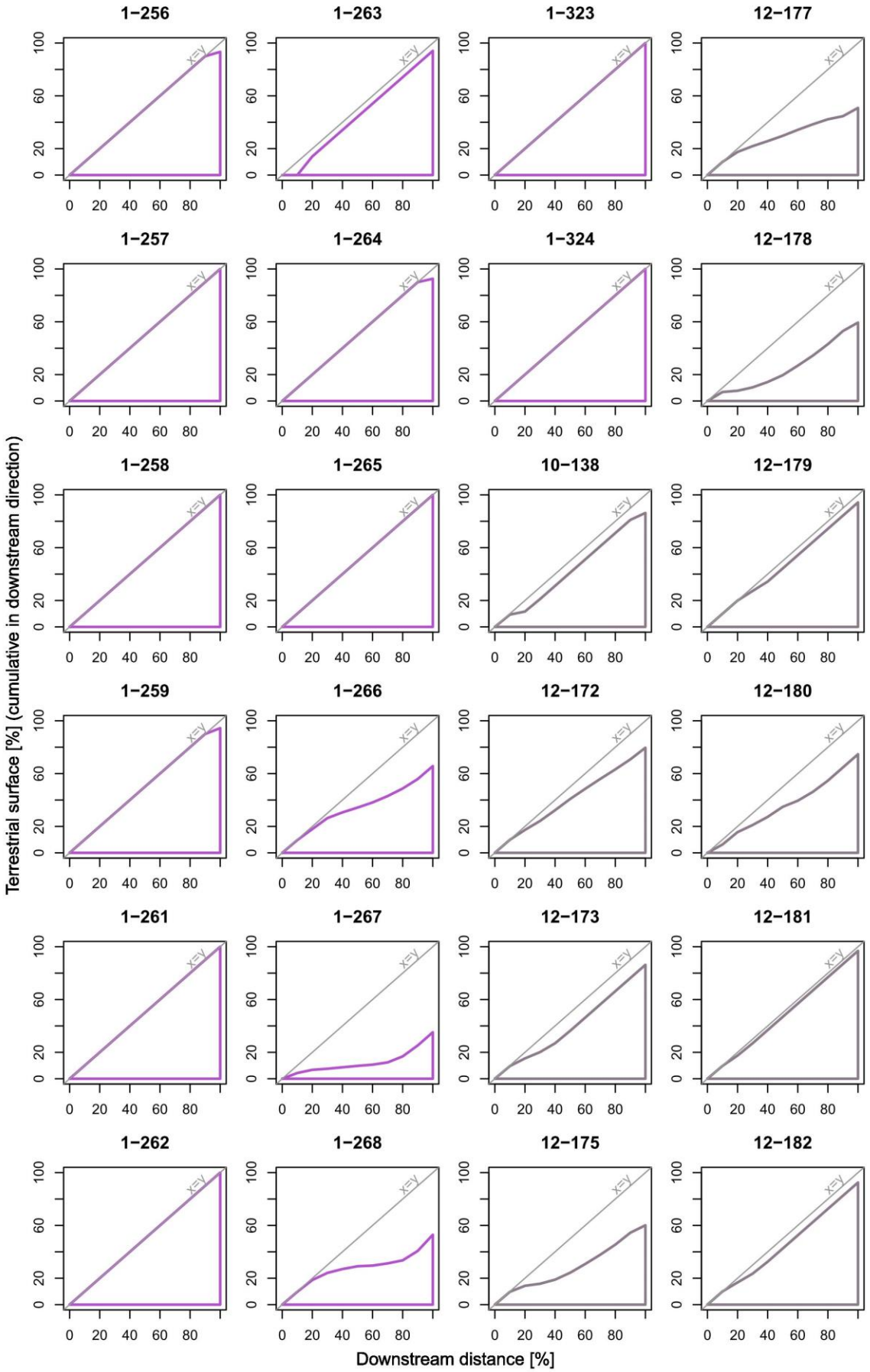

(Figure A-IV-5a)

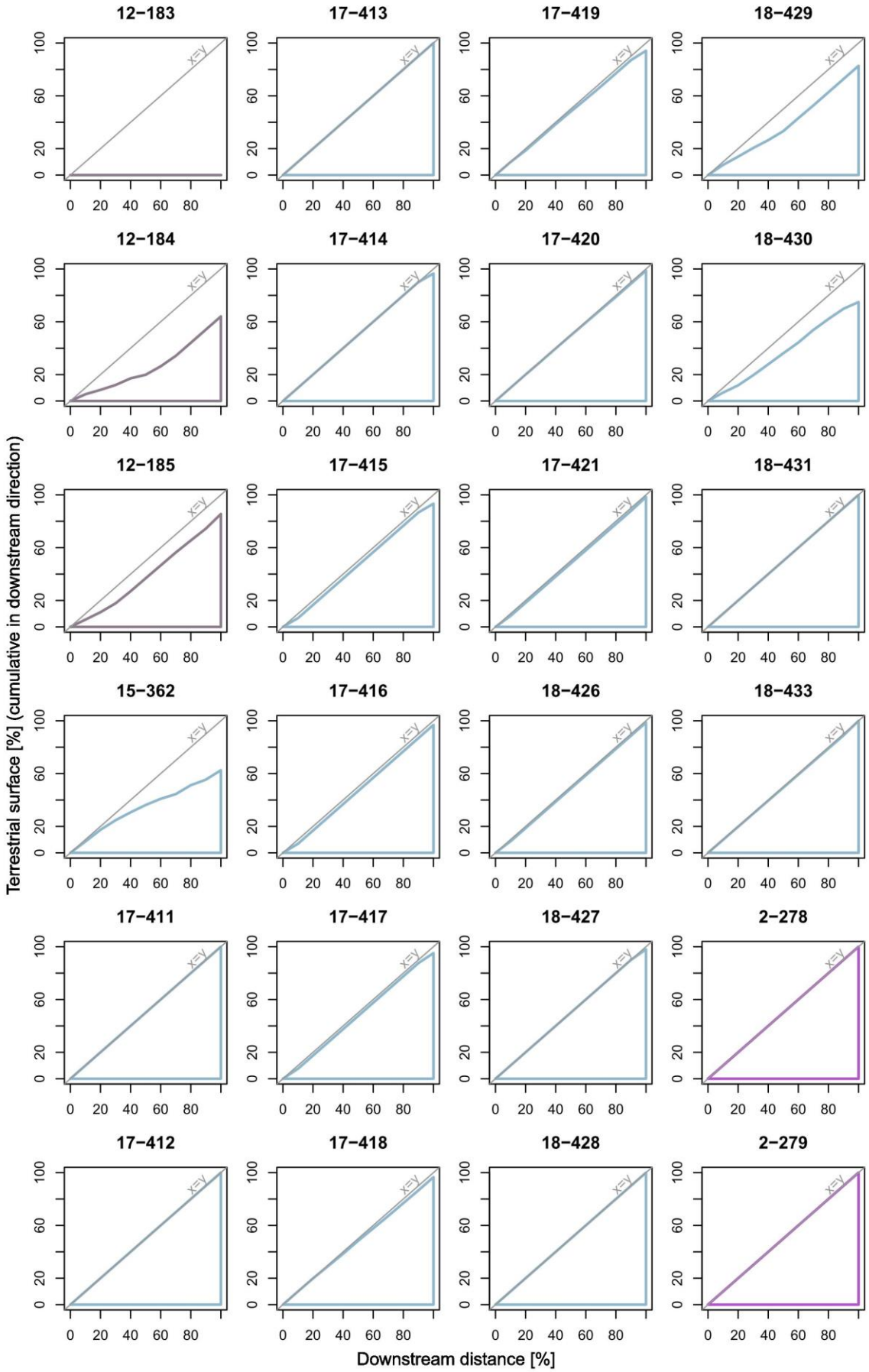

(Figure A–IV–5a continued)

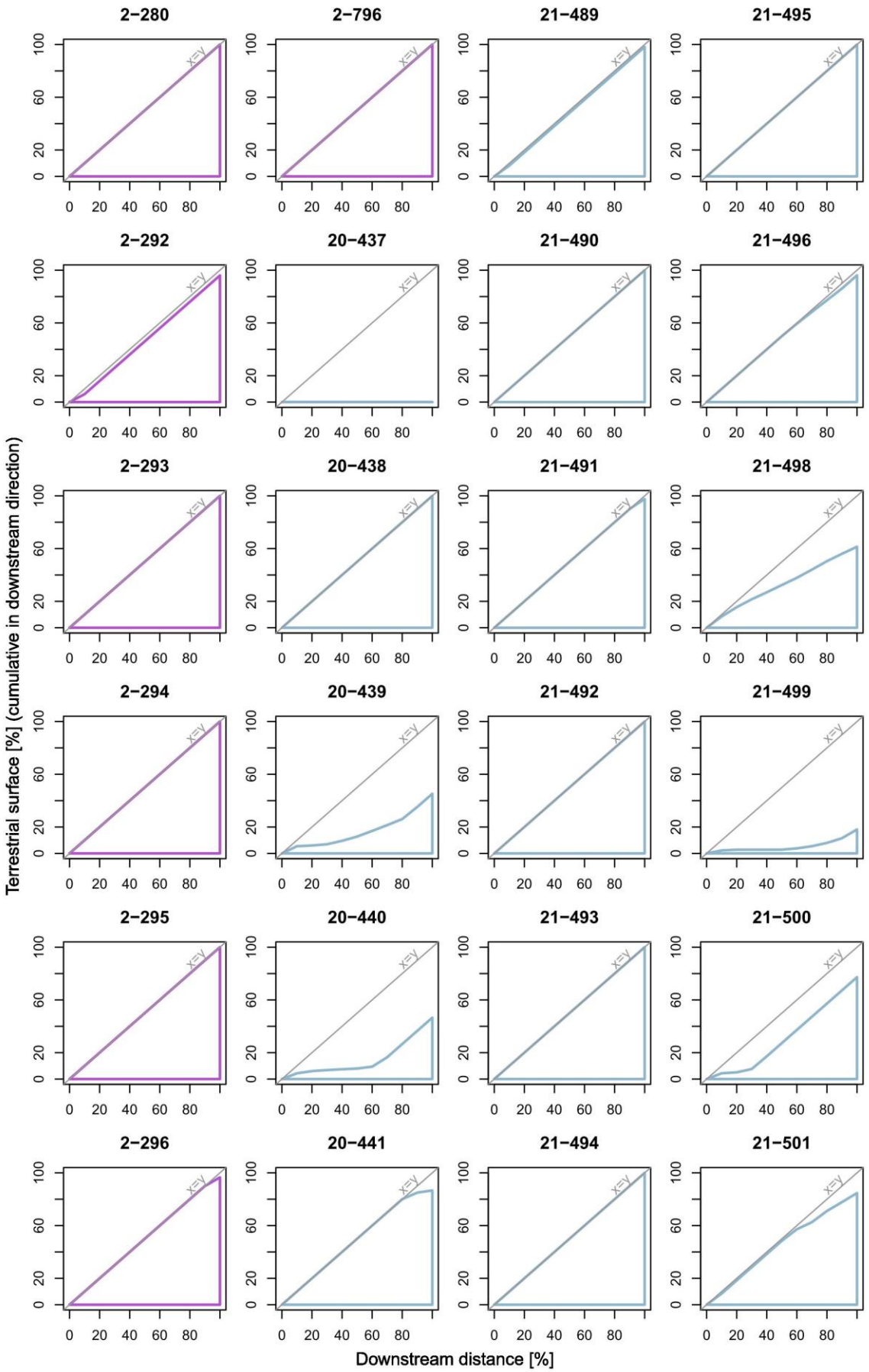

(Figure A–IV–5a continued)

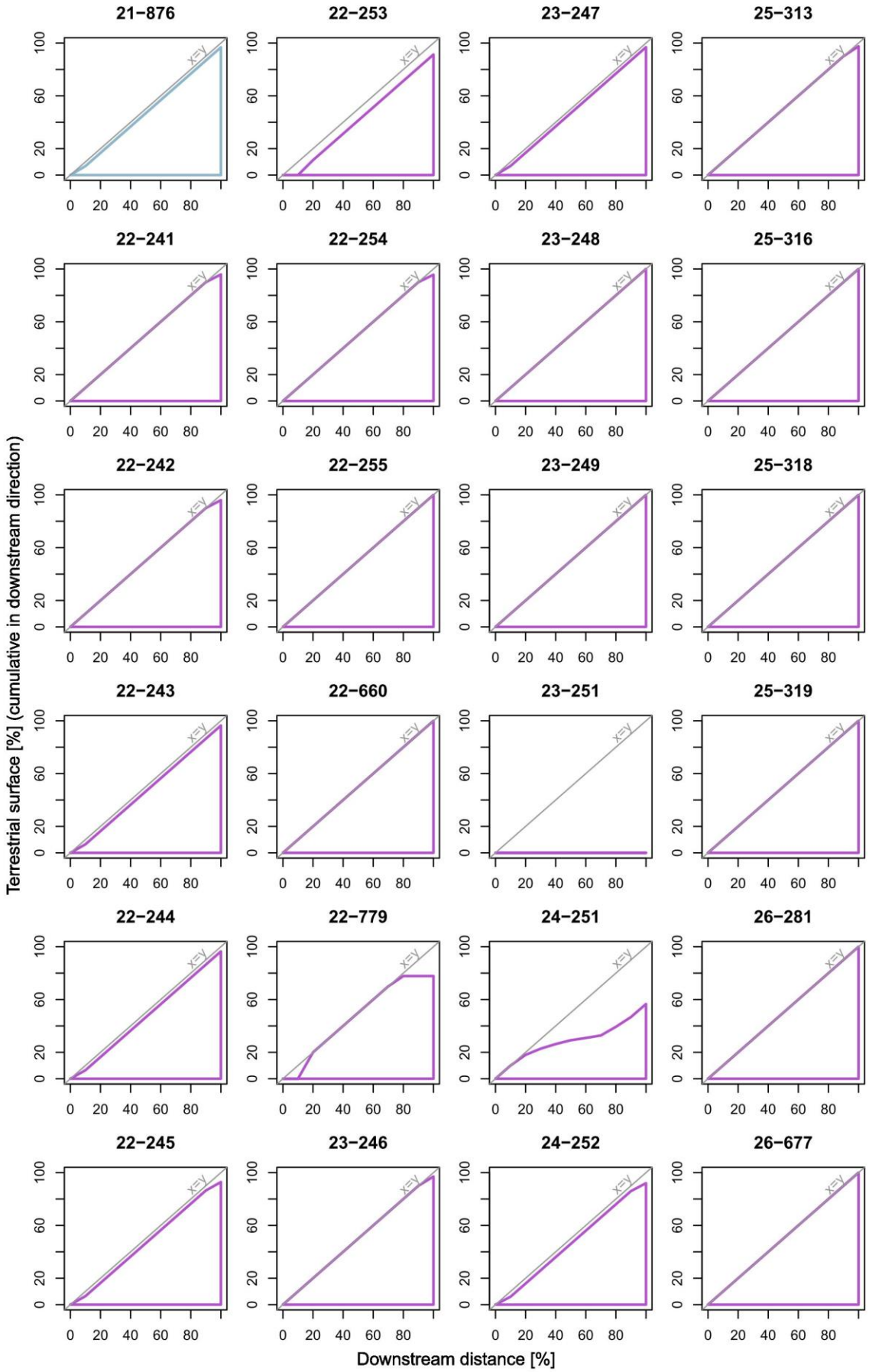

(Figure A–IV–5a continued)

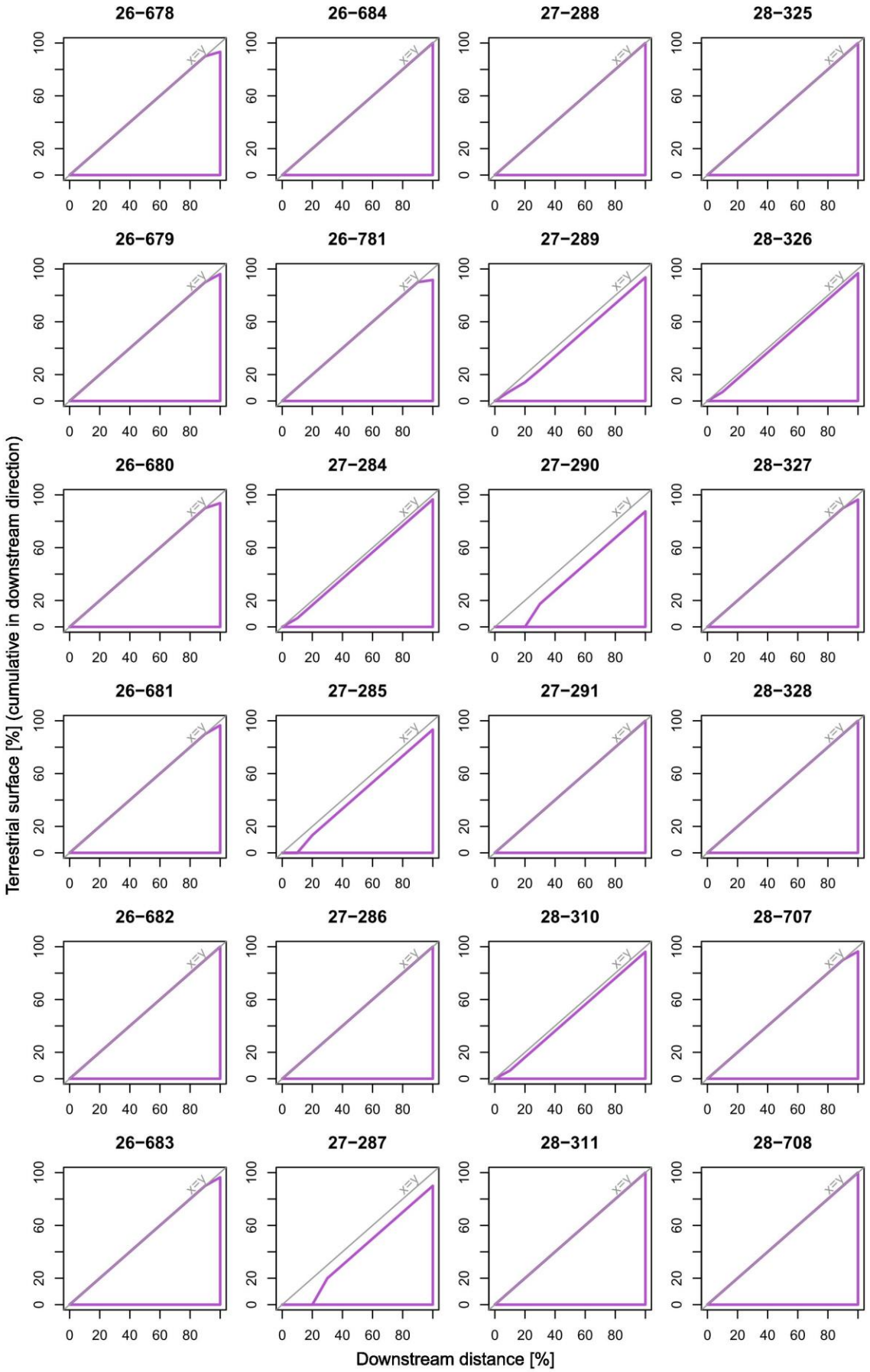

(Figure A–IV–5a continued)

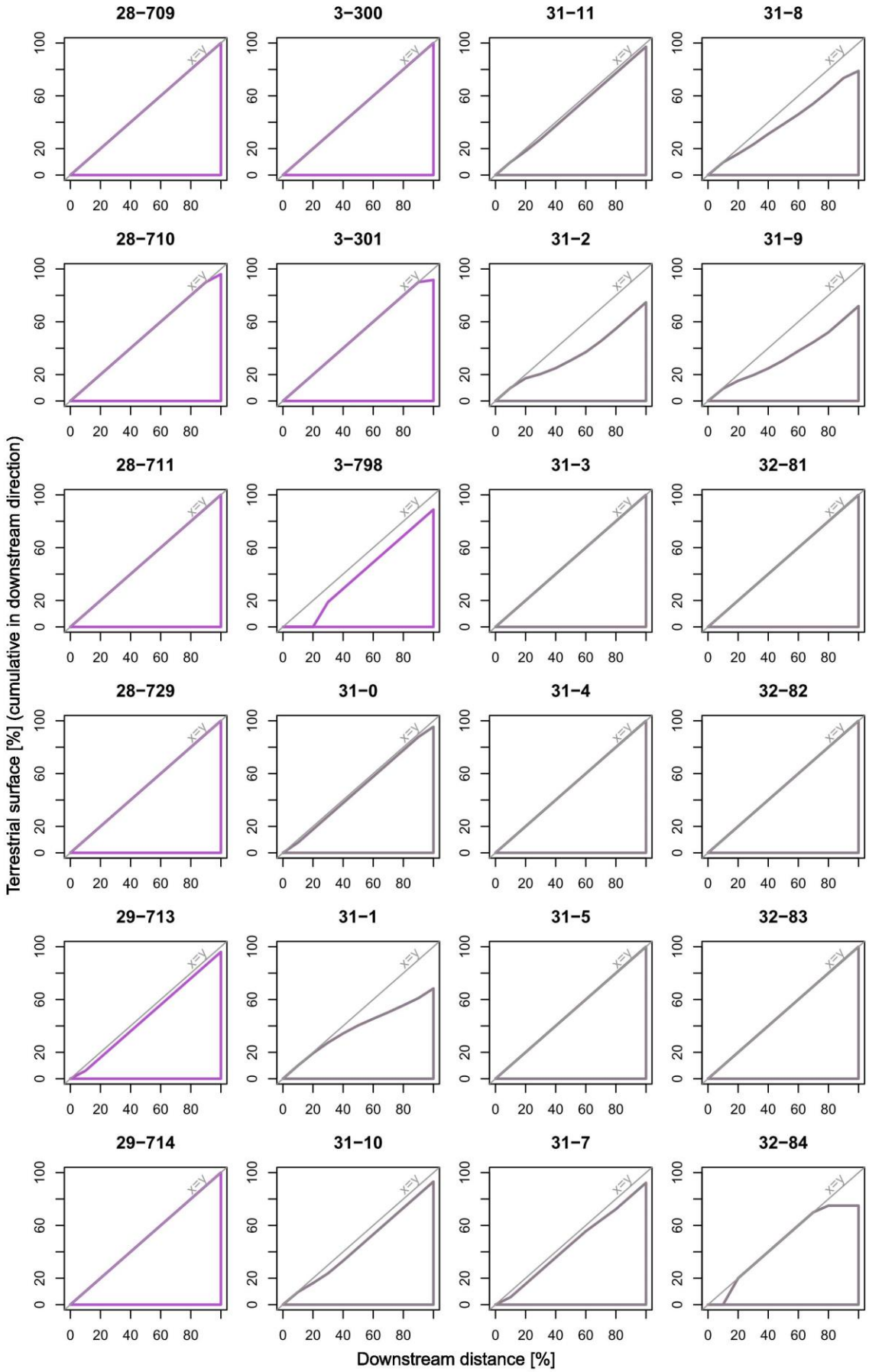

(Figure A–IV–5a continued)

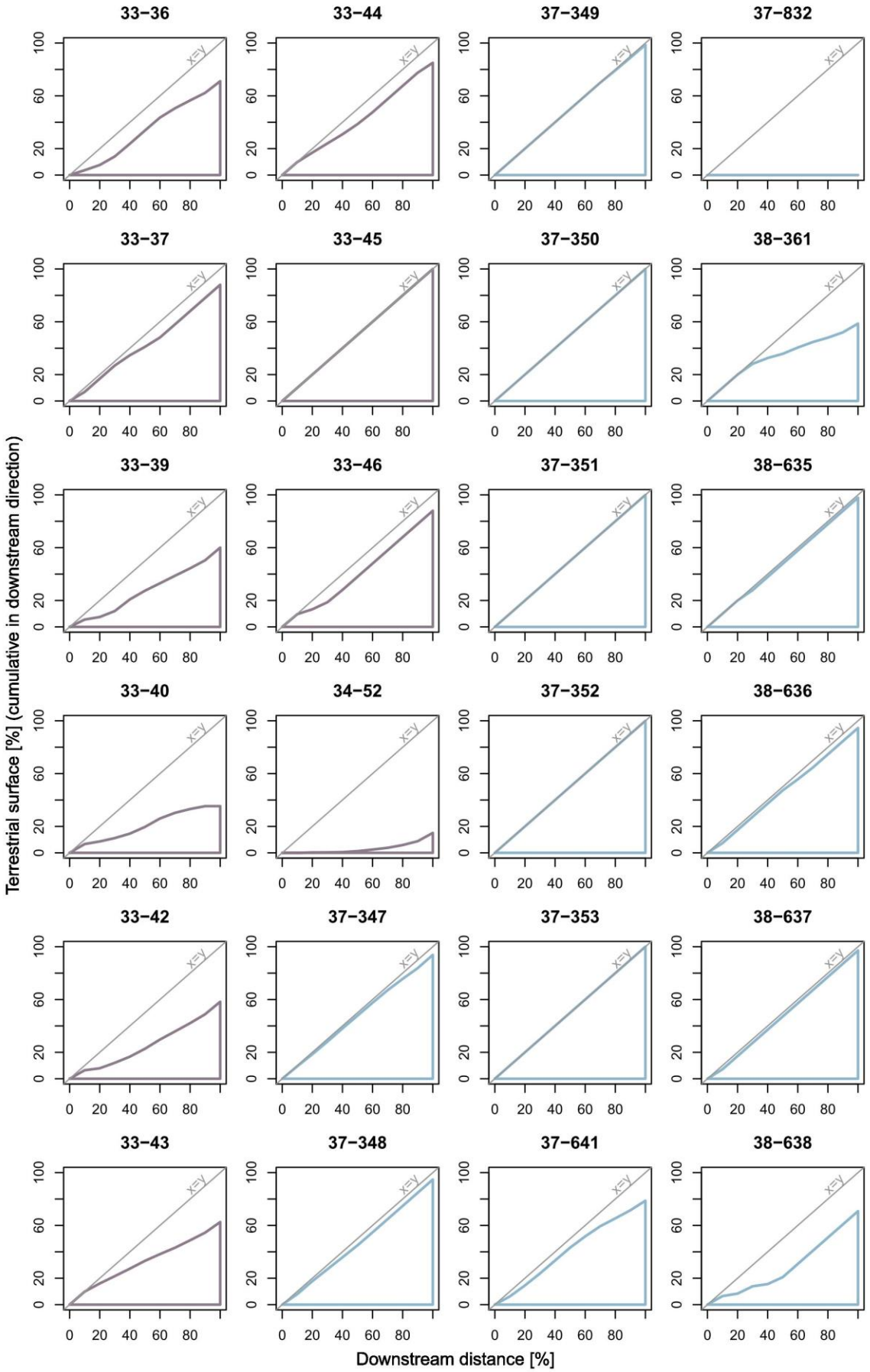

(Figure A–IV–5a continued)

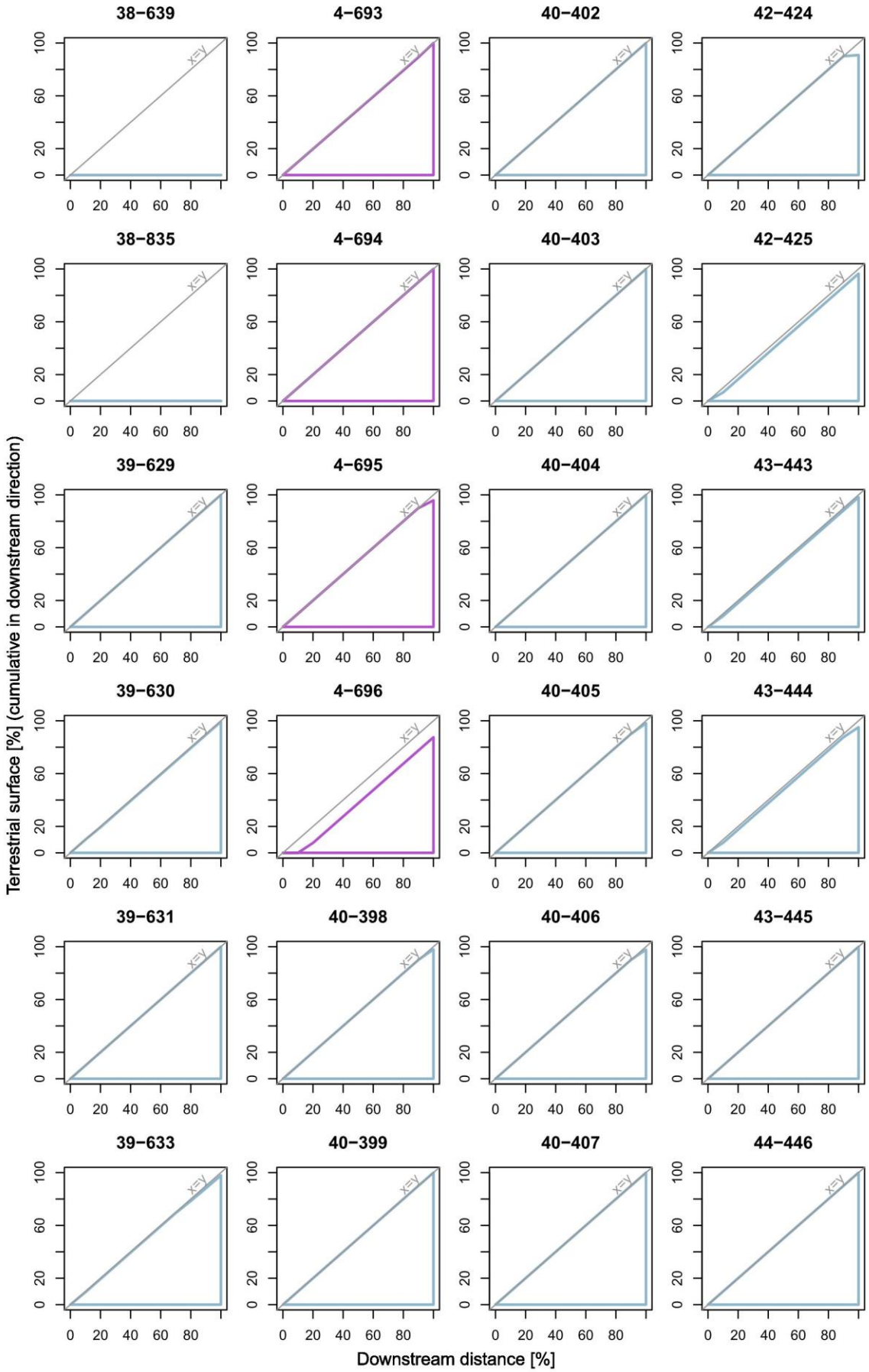

(Figure A–IV–5a continued)

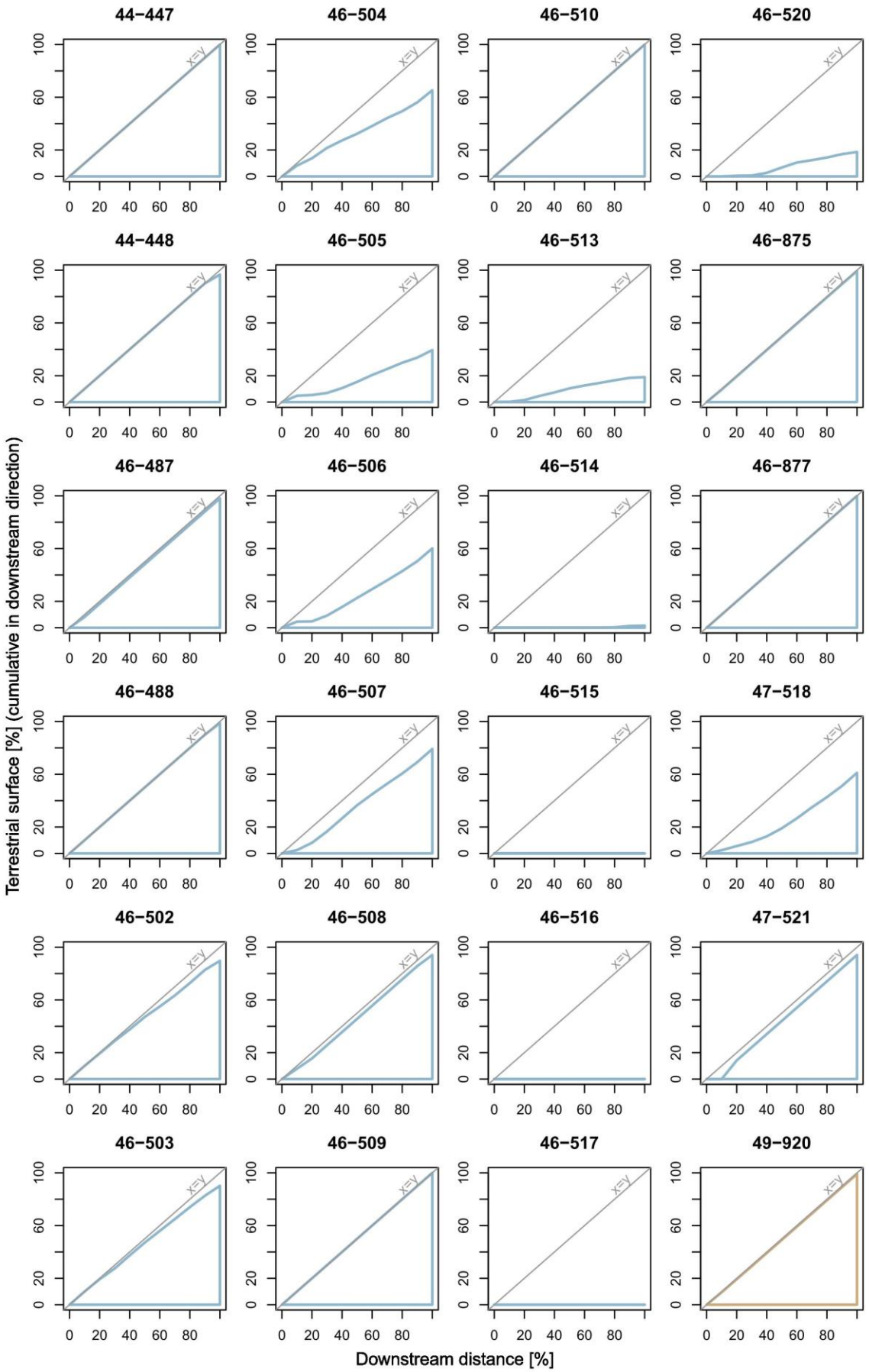

(Figure A-IV-5a continued)

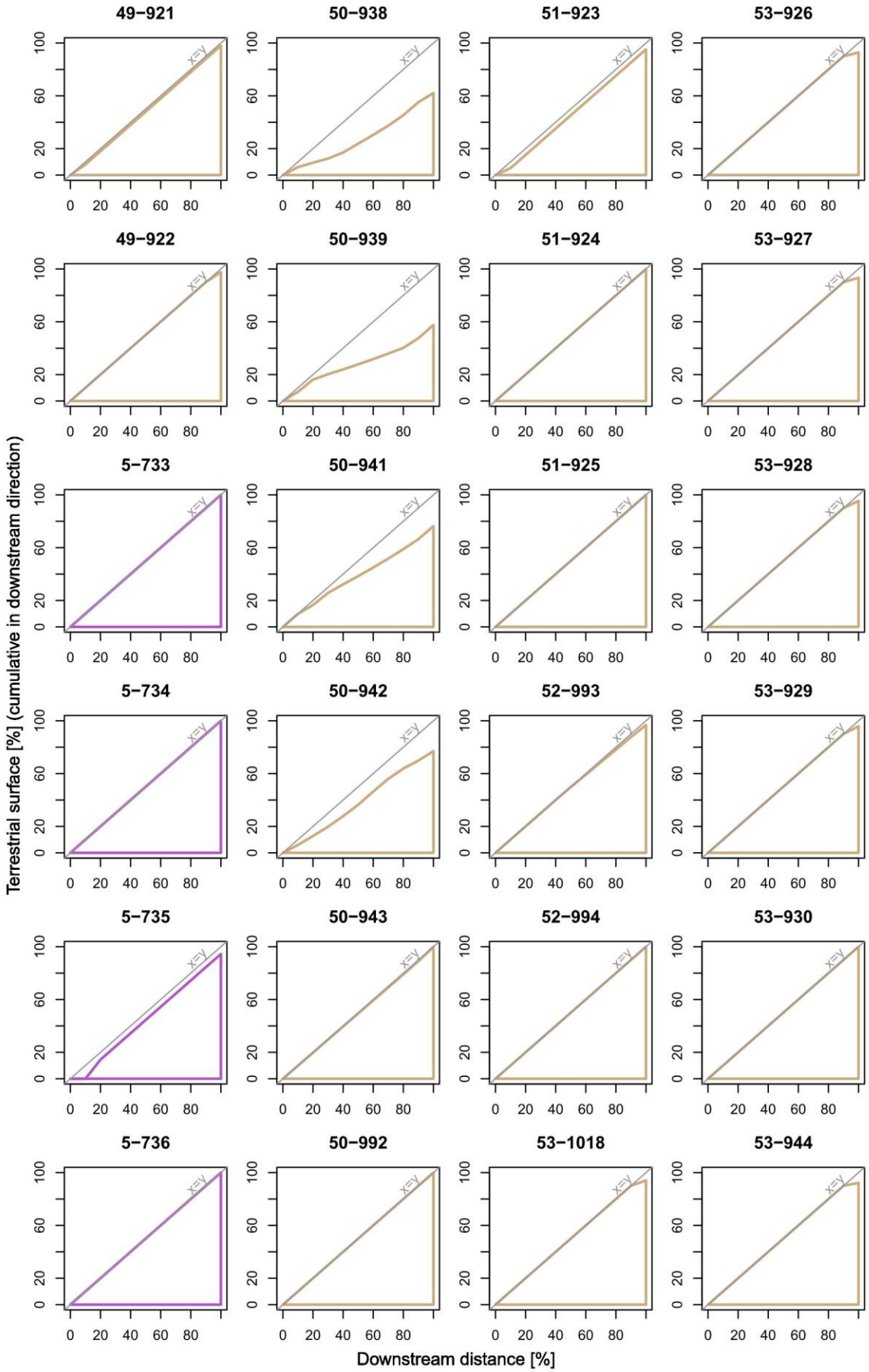

(Figure A–IV–5a continued)

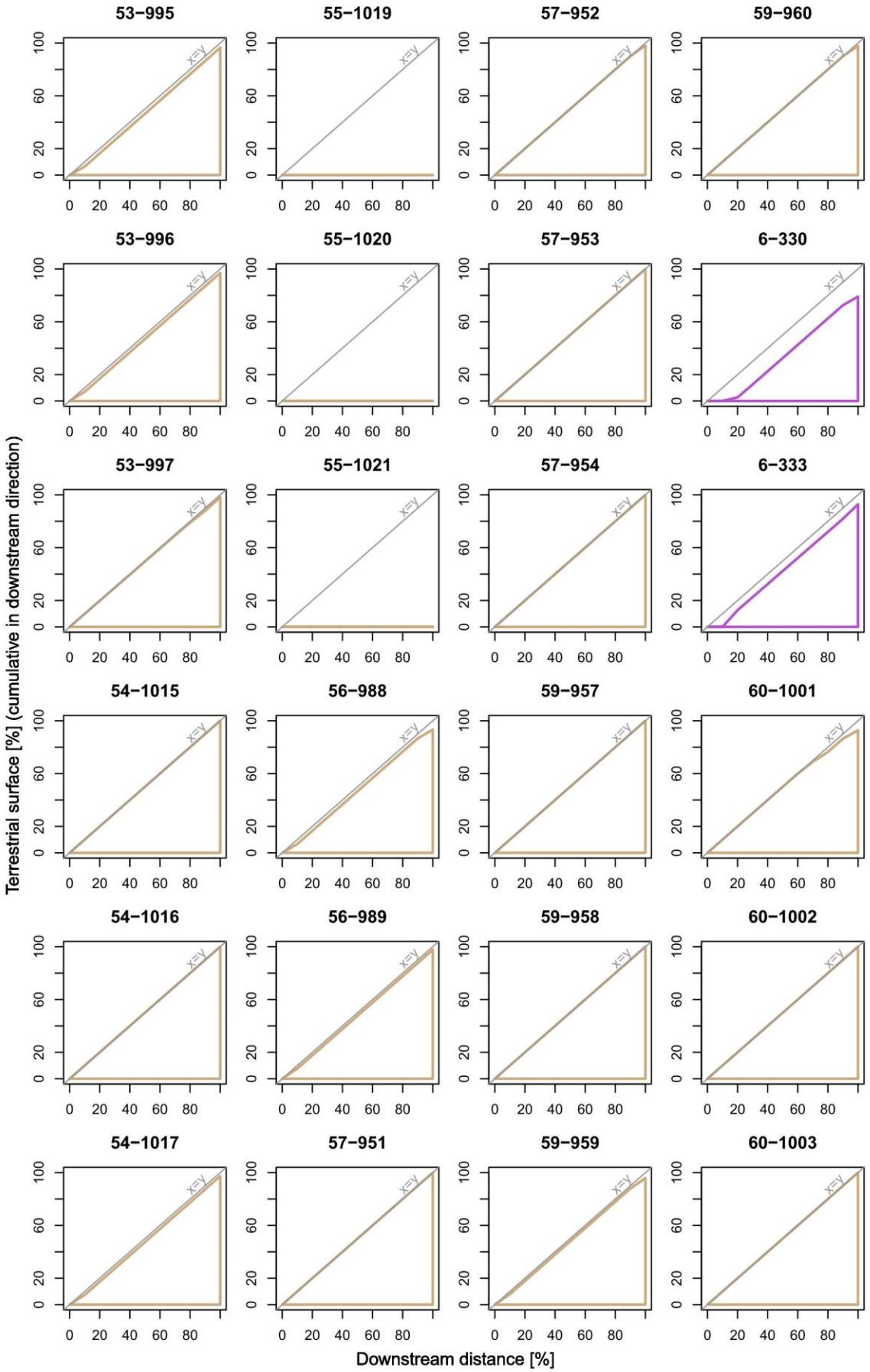

(Figure A–IV–5a continued)

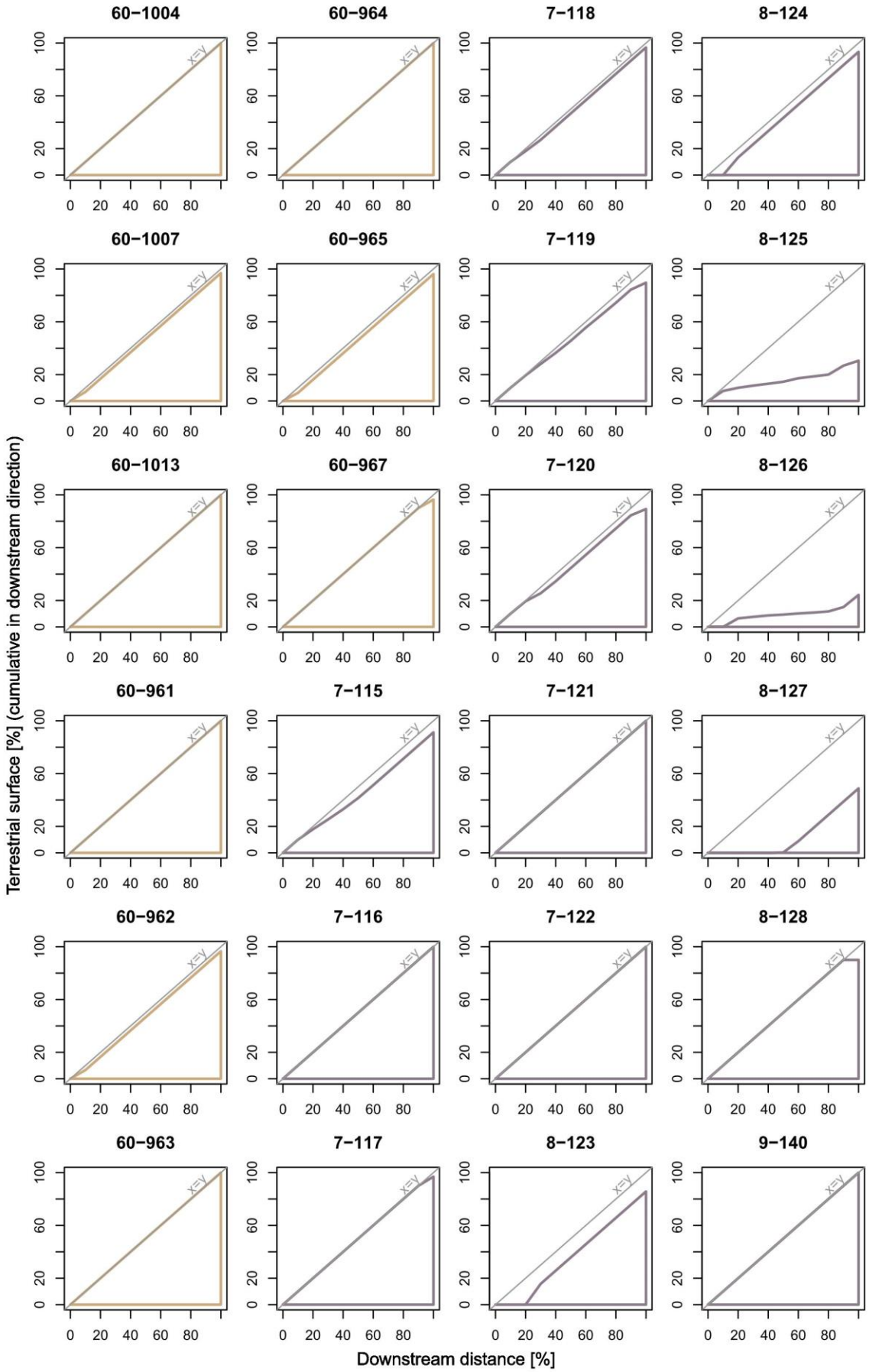

(Figure A–IV–5a continued)

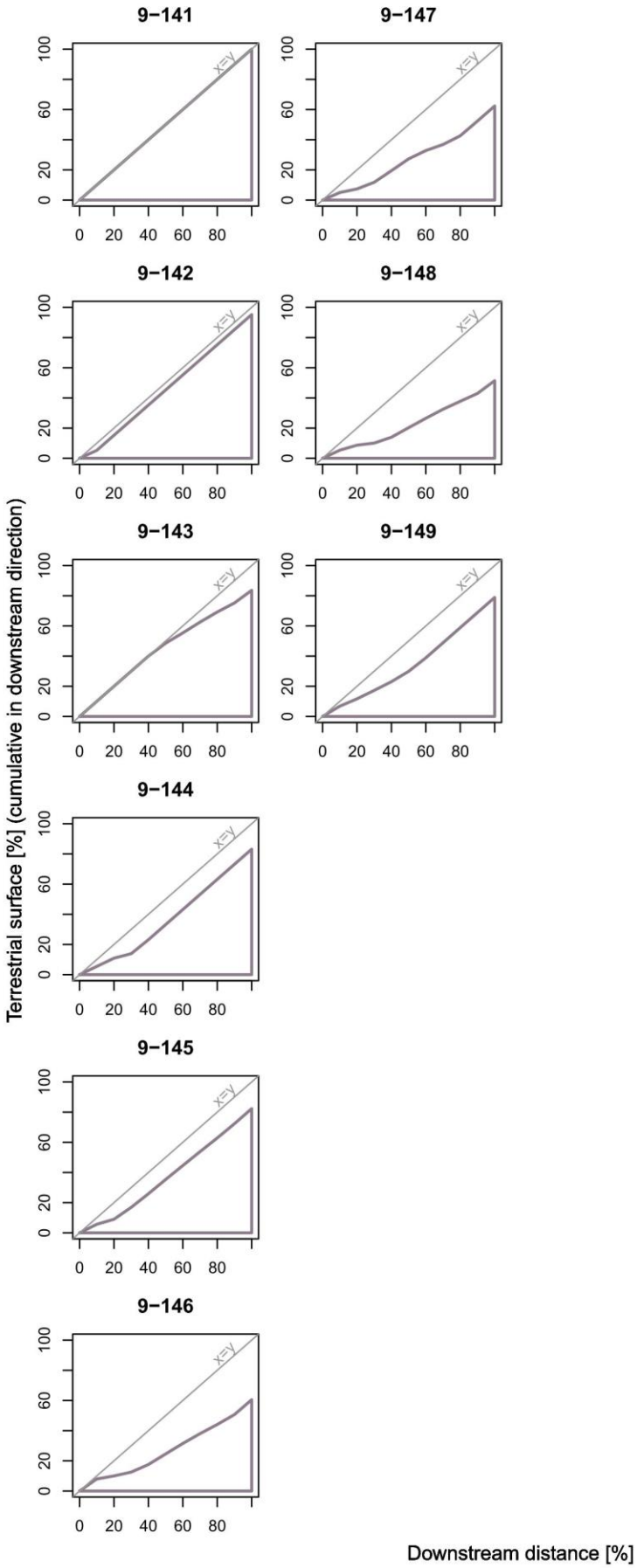

(Figure A–IV–5a continued)

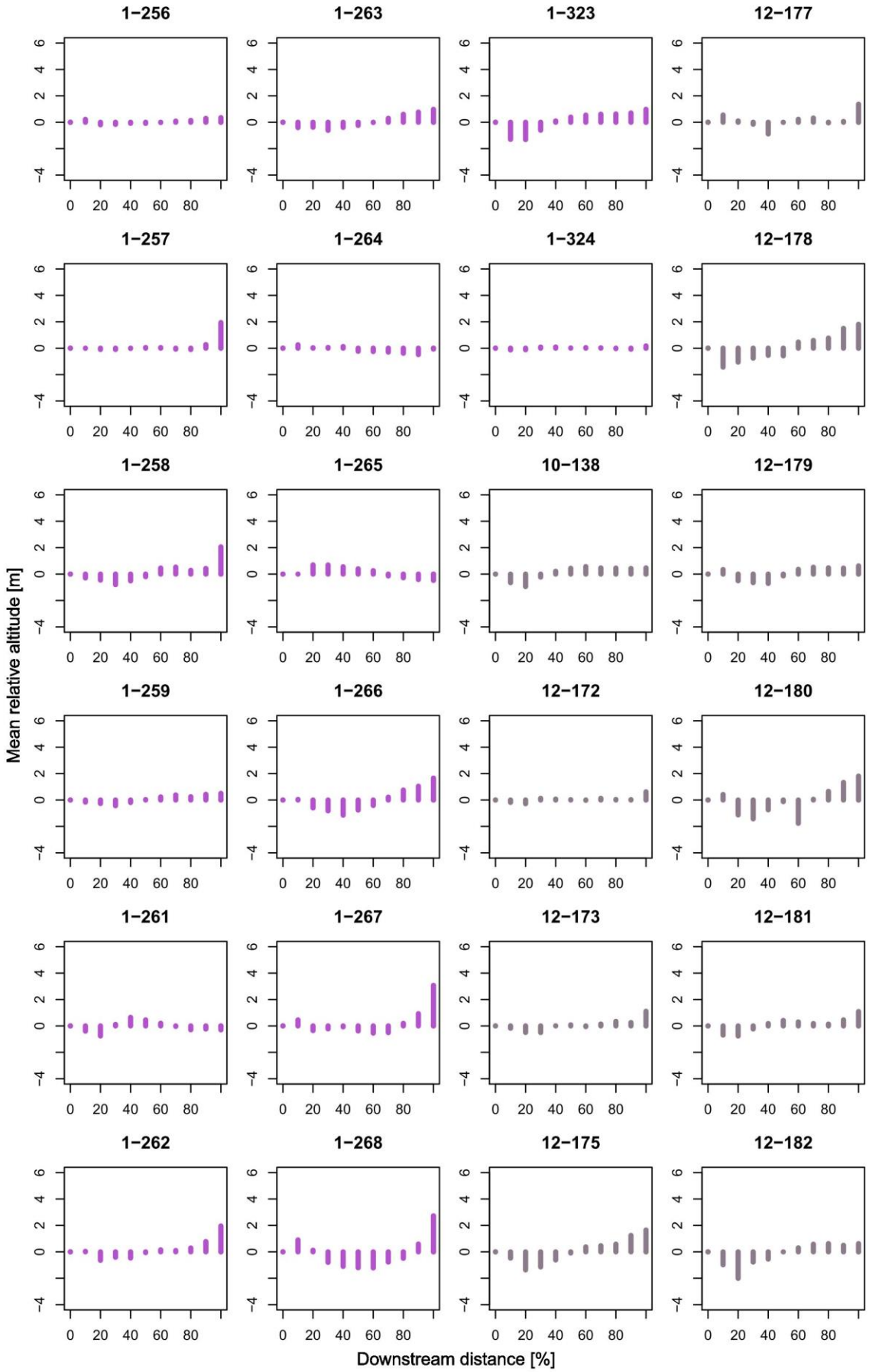

(Figure A–IV–5b)

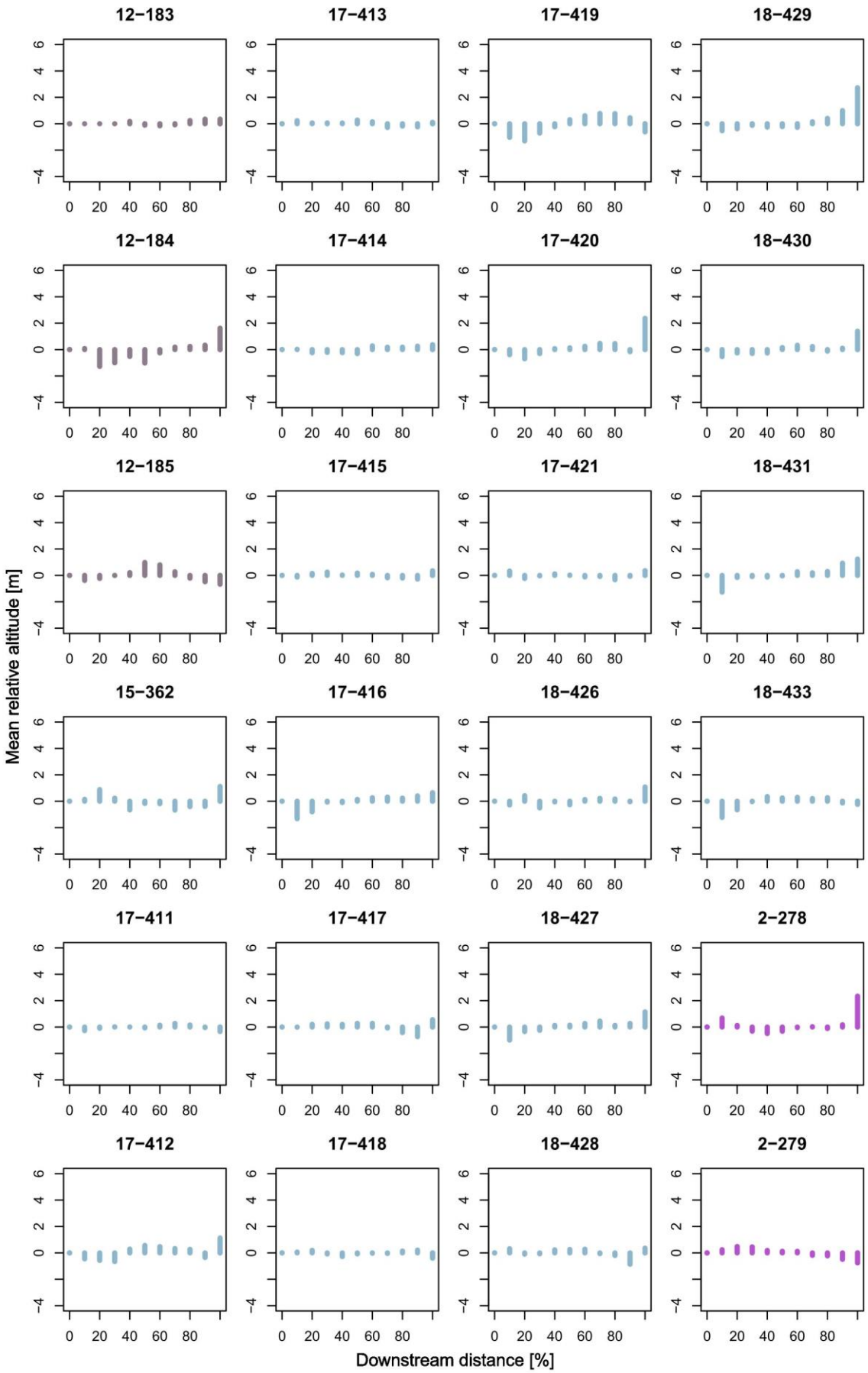

(Figure A–IV–5b continued)

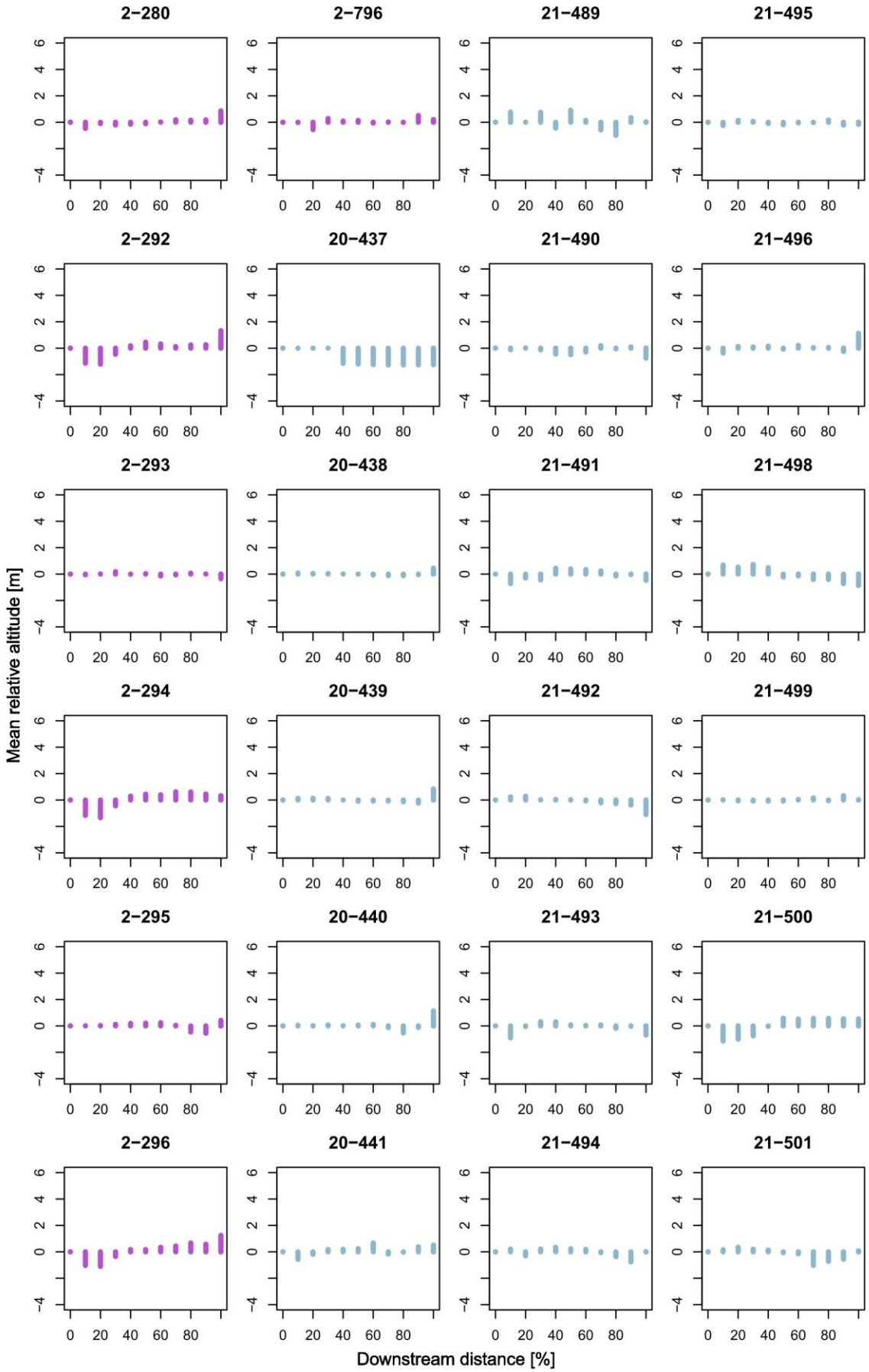

(Figure A–IV–5b continued)

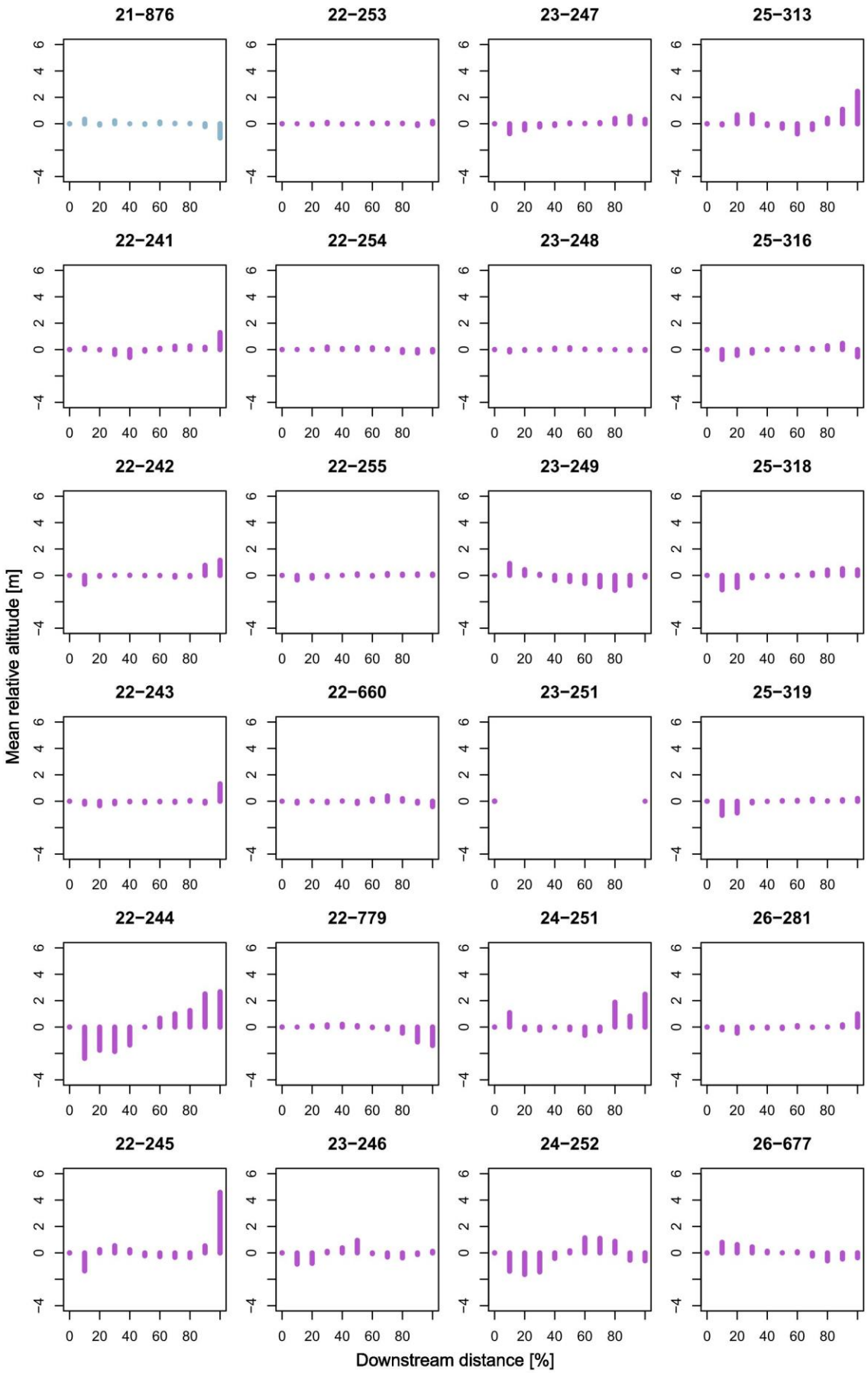

(Figure A–IV–5b continued)

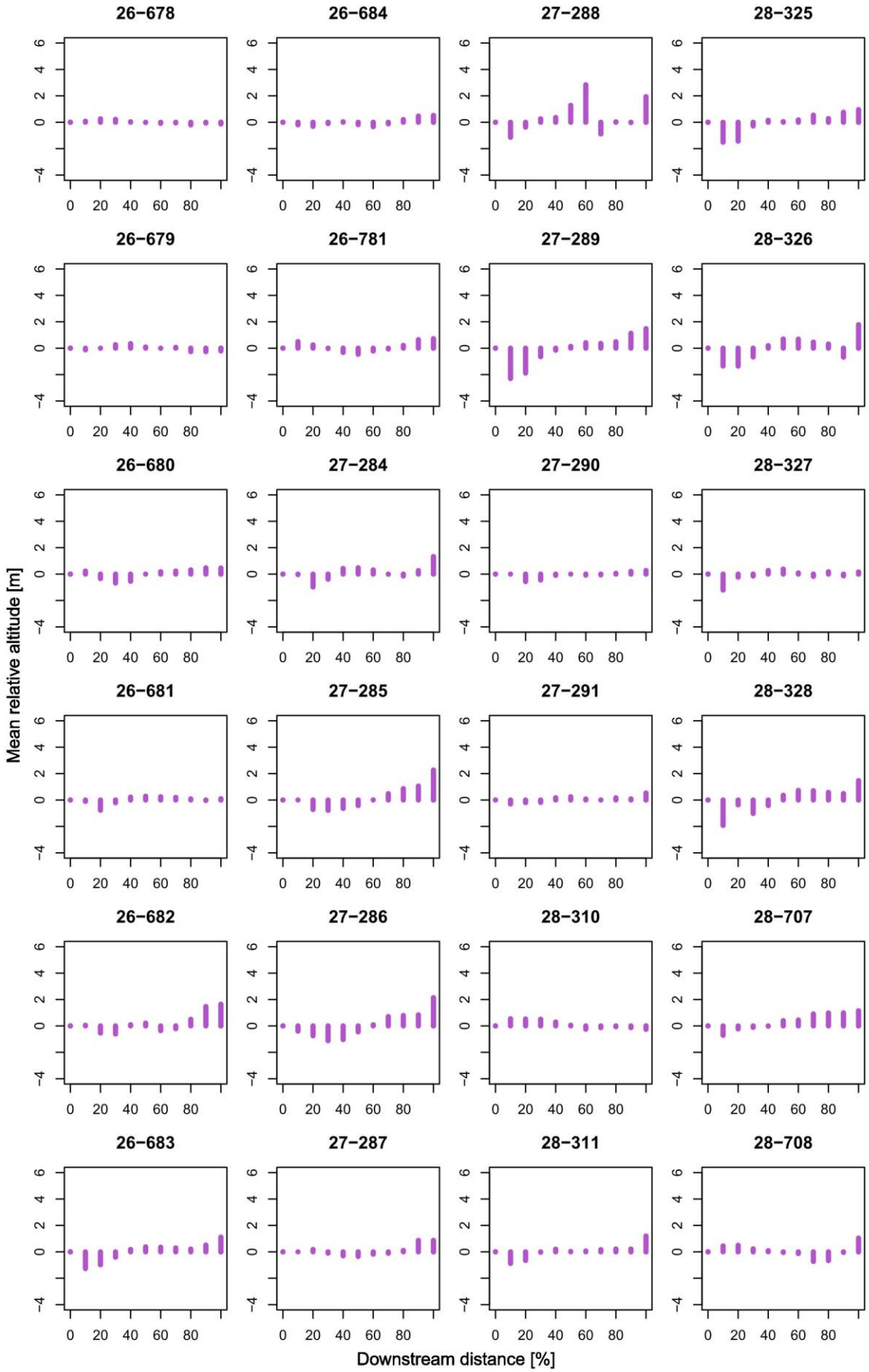

(Figure A–IV–5b continued)

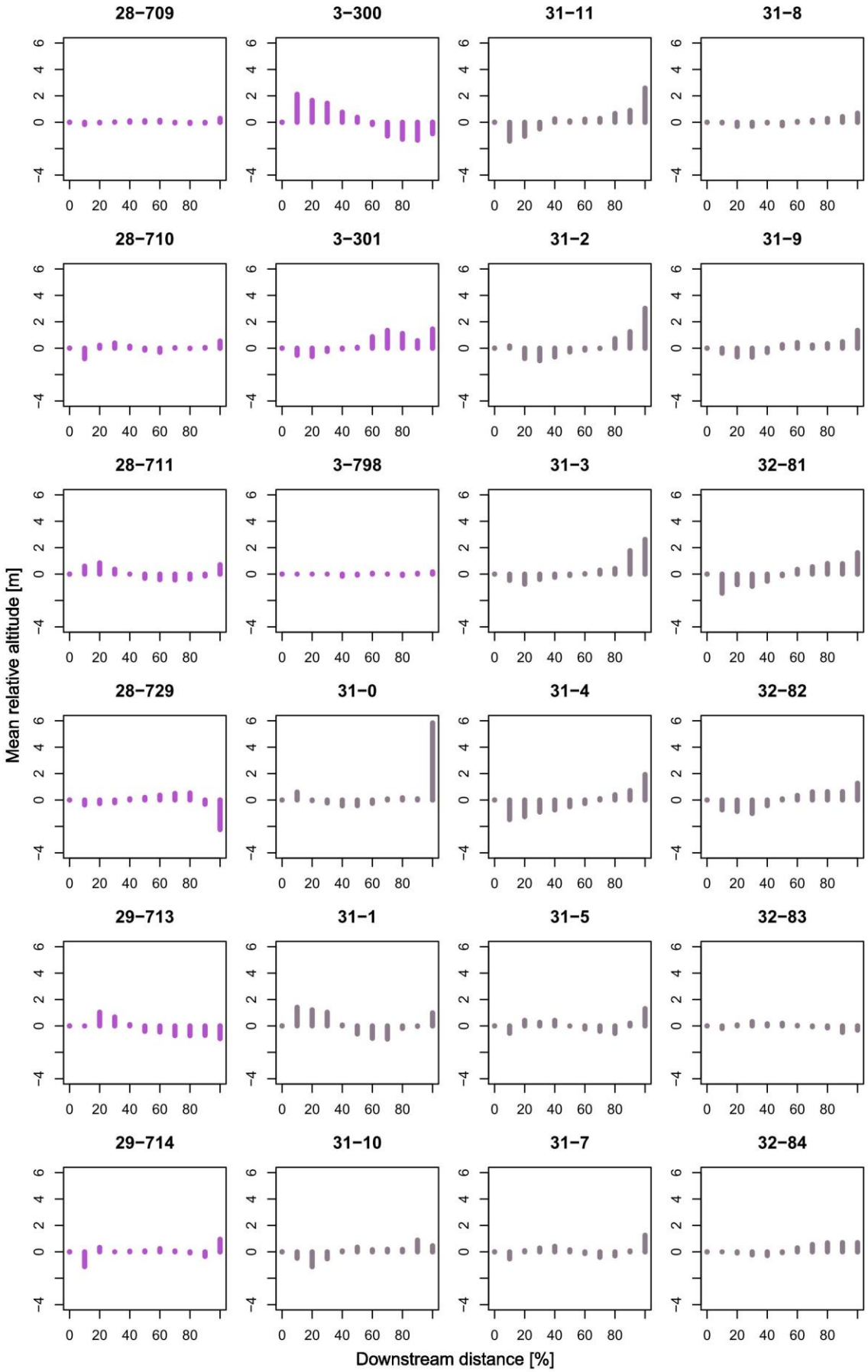

(Figure A–IV–5b continued)

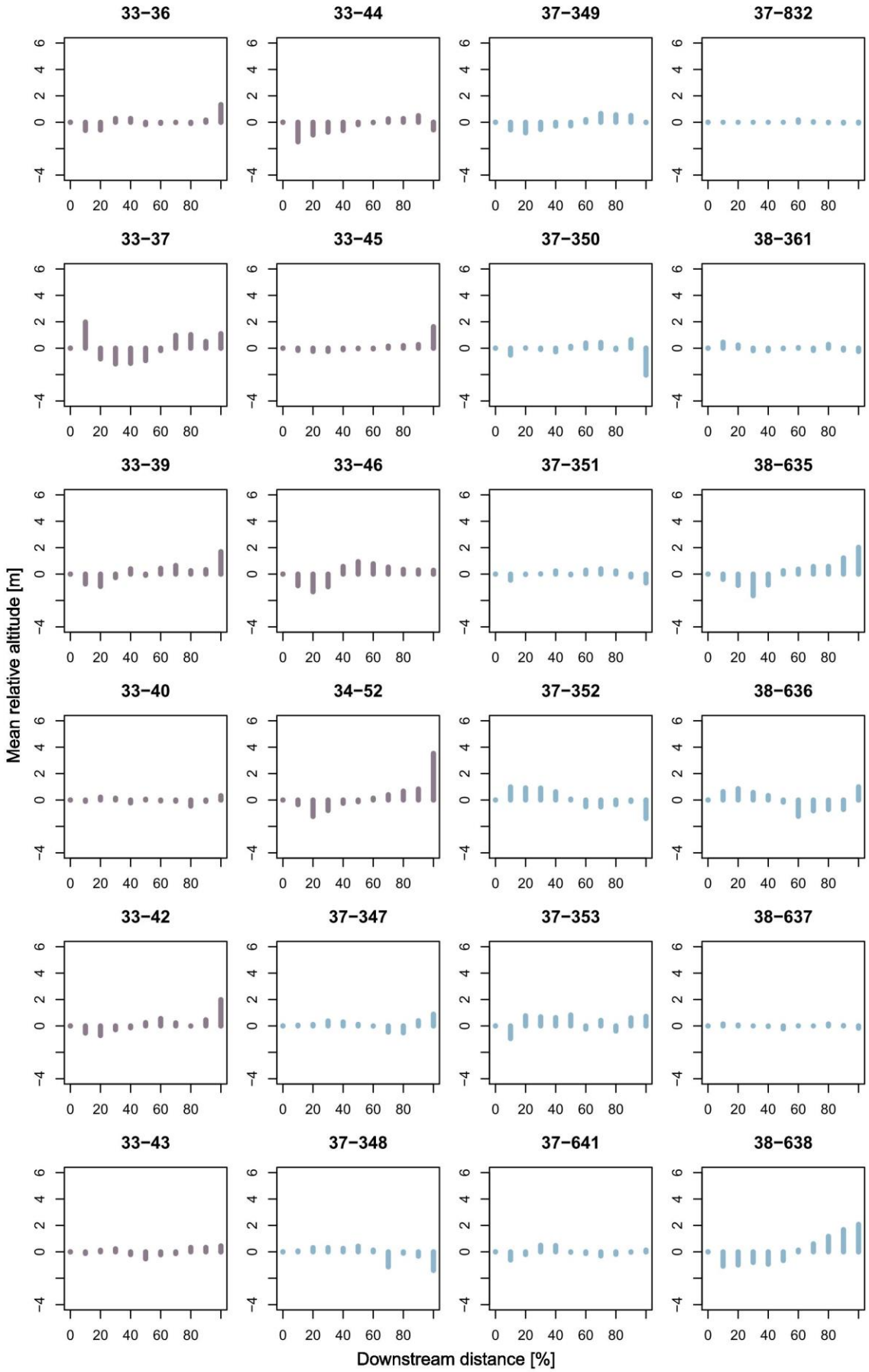

(Figure A–IV–5b continued)

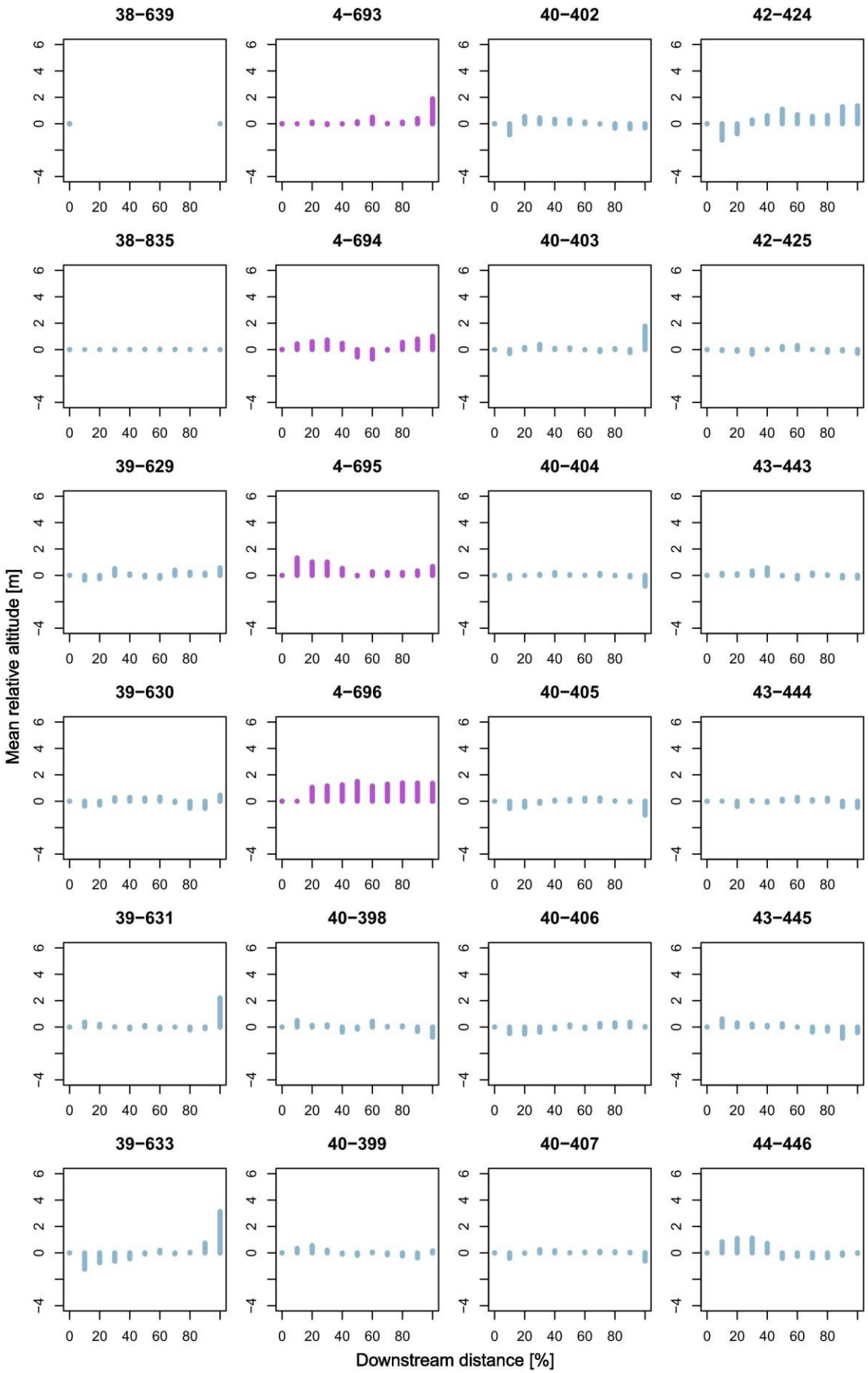

(Figure A–IV–5b continued)

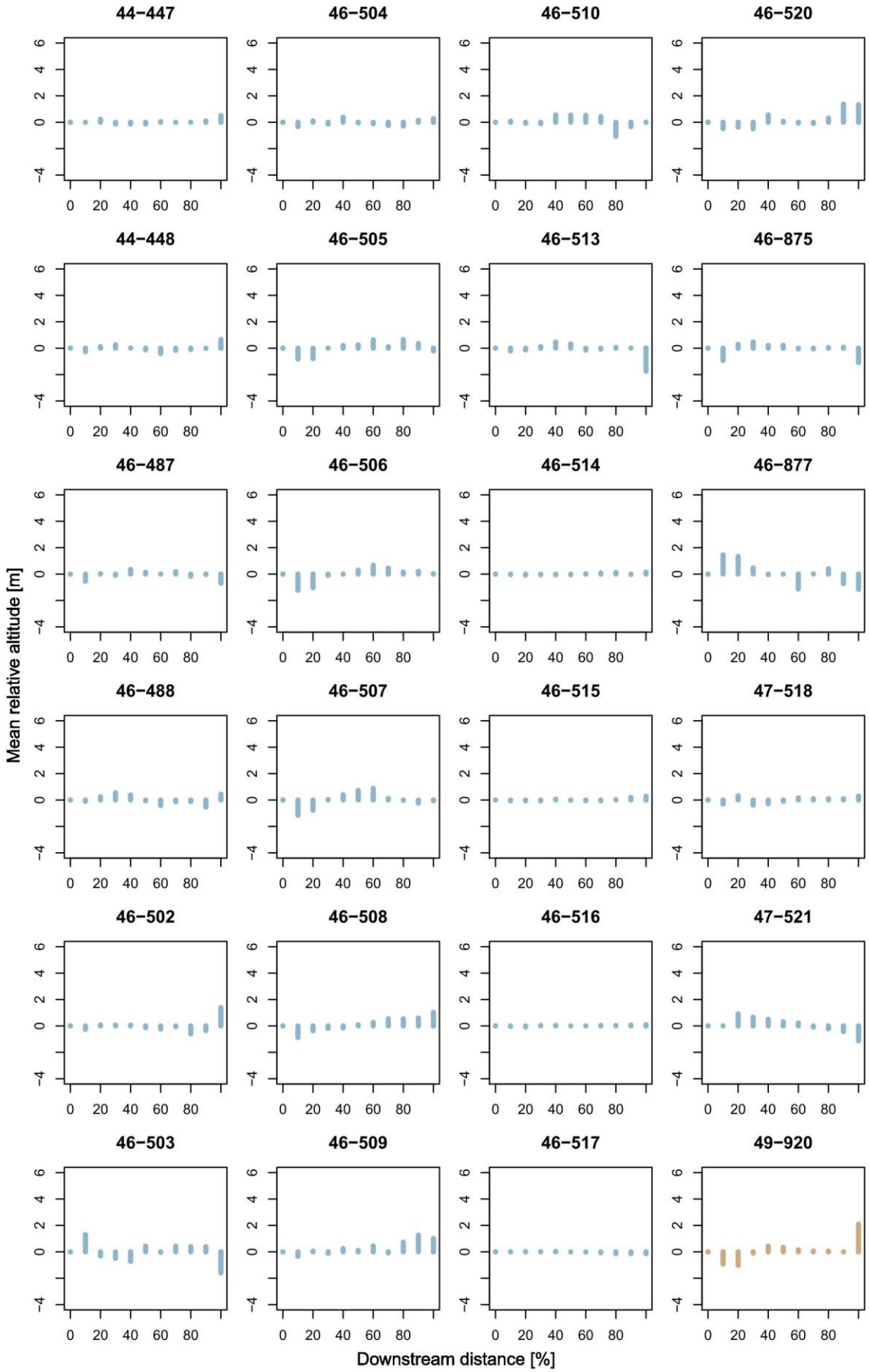

(Figure A–IV–5b continued)

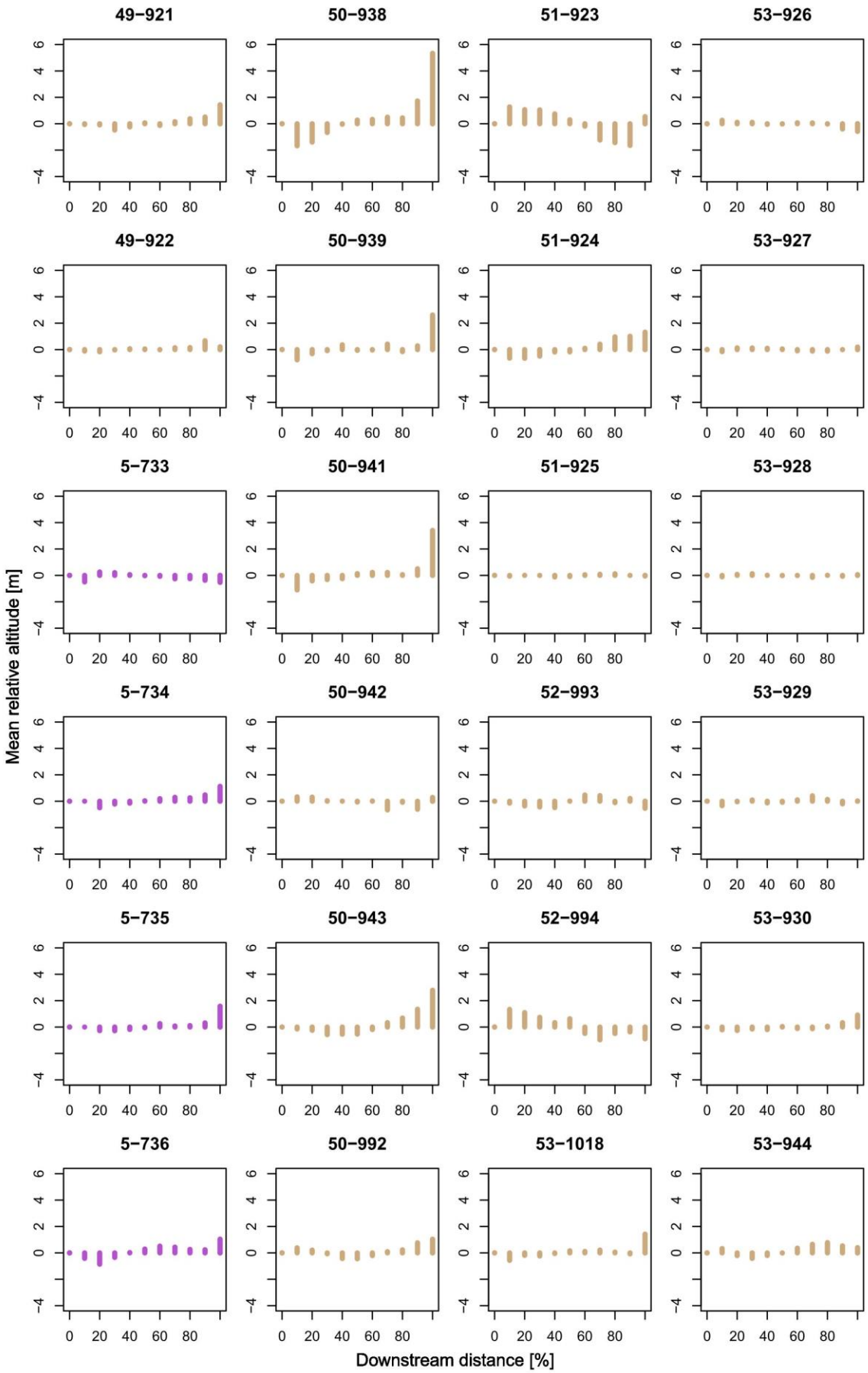

(Figure A–IV–5b continued)

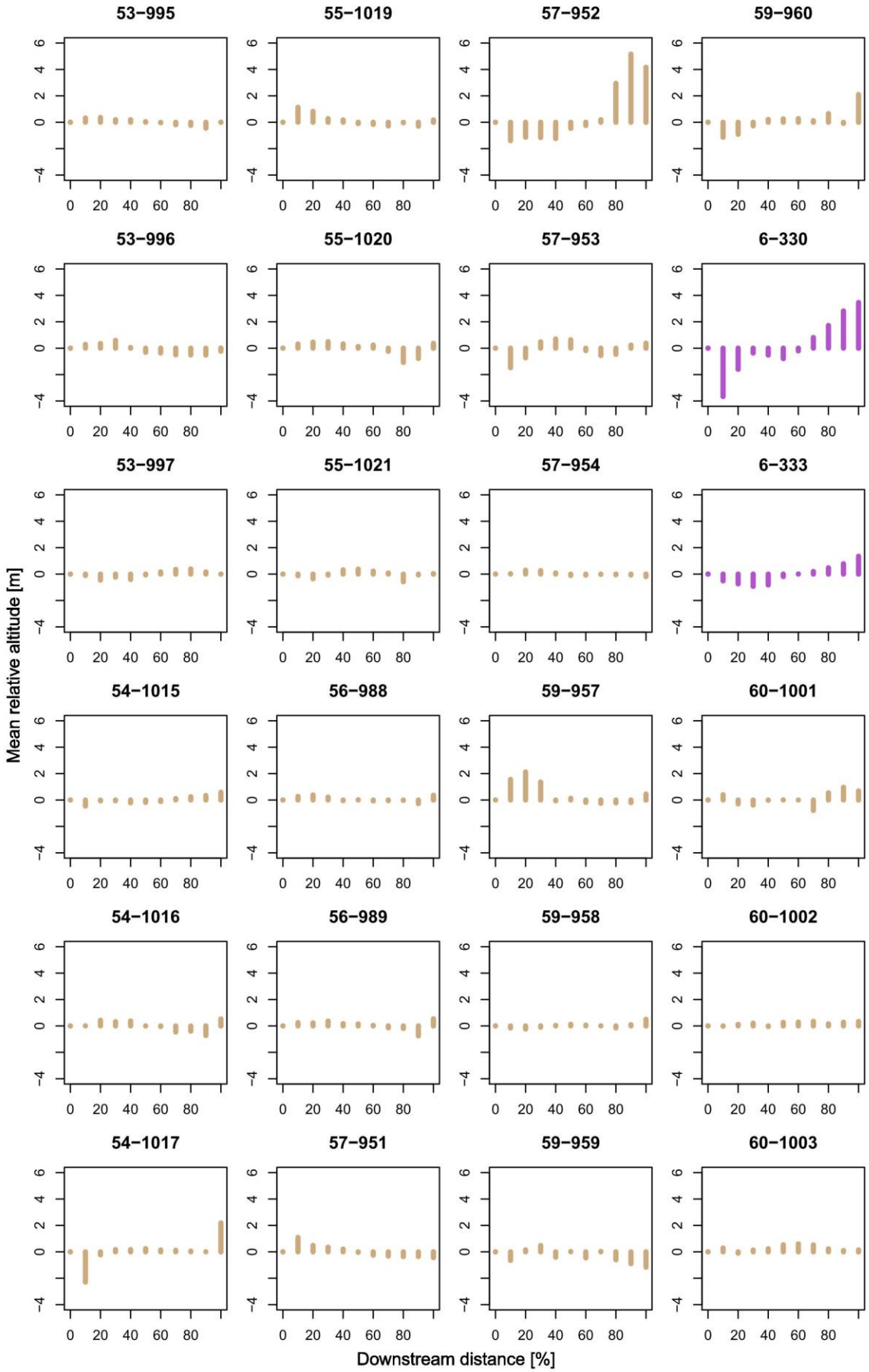

(Figure A–IV–5b continued)

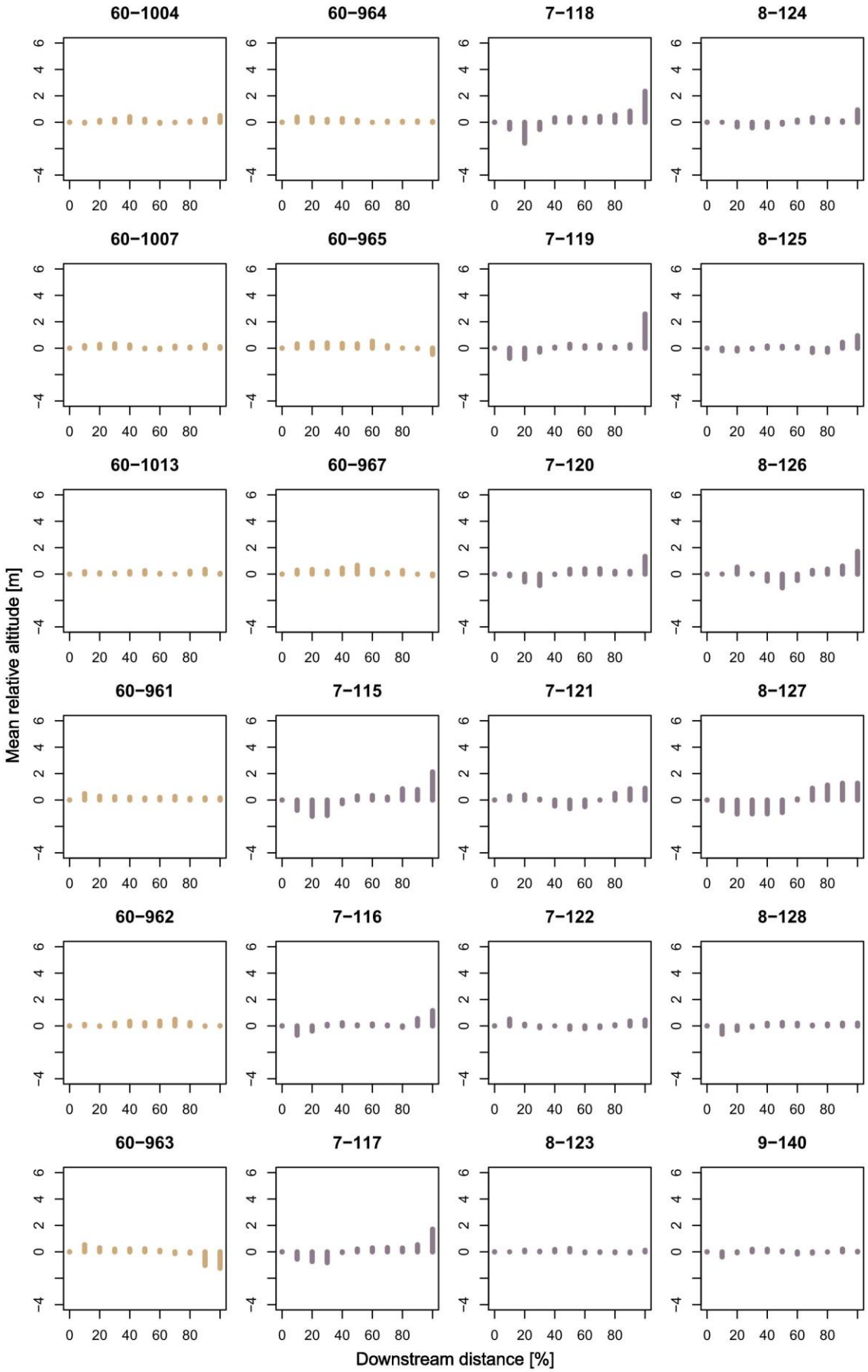

(Figure A–IV–5b continued)

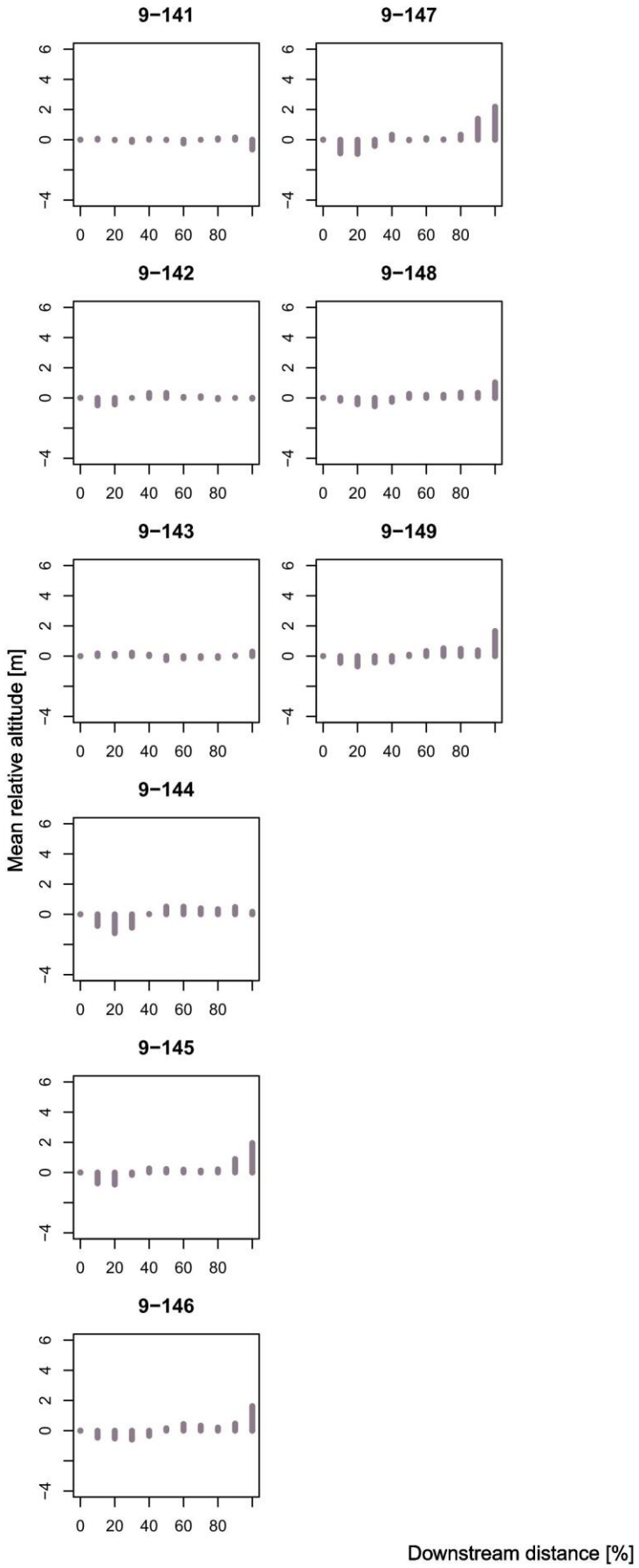

(Figure A–IV–5b continued)

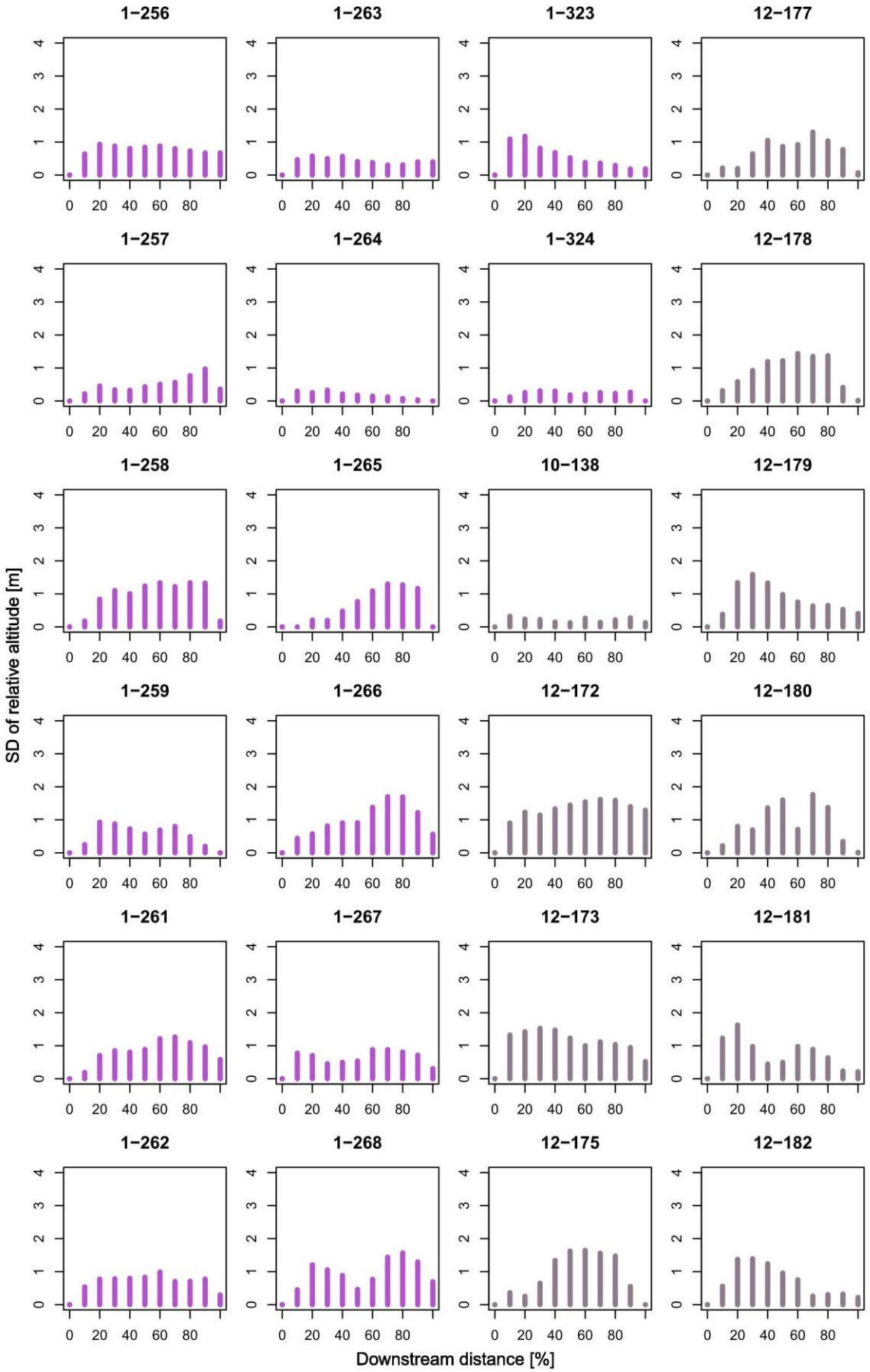

(Figure A–IV–5c)

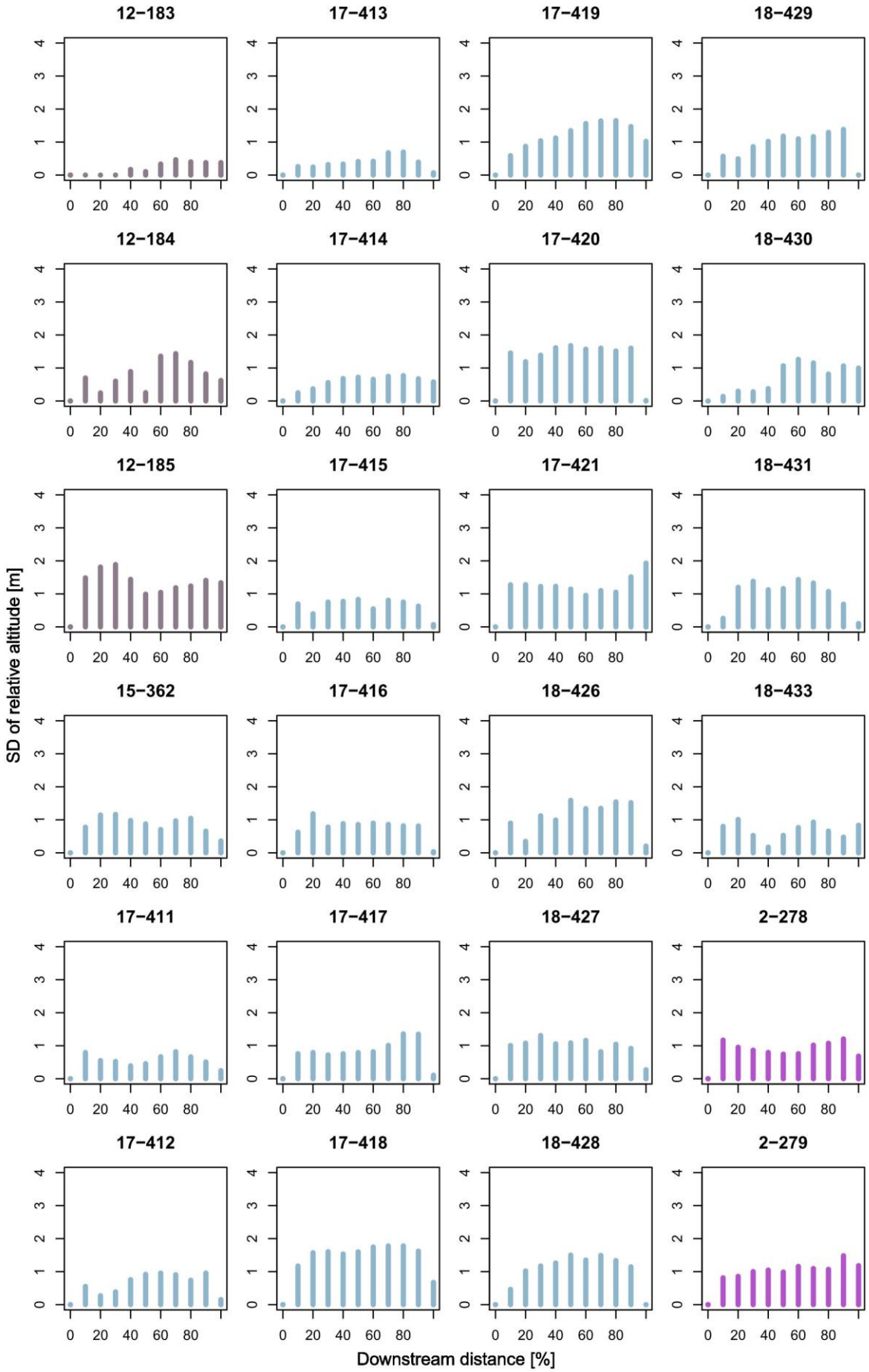

(Figure A–IV–5c continued)

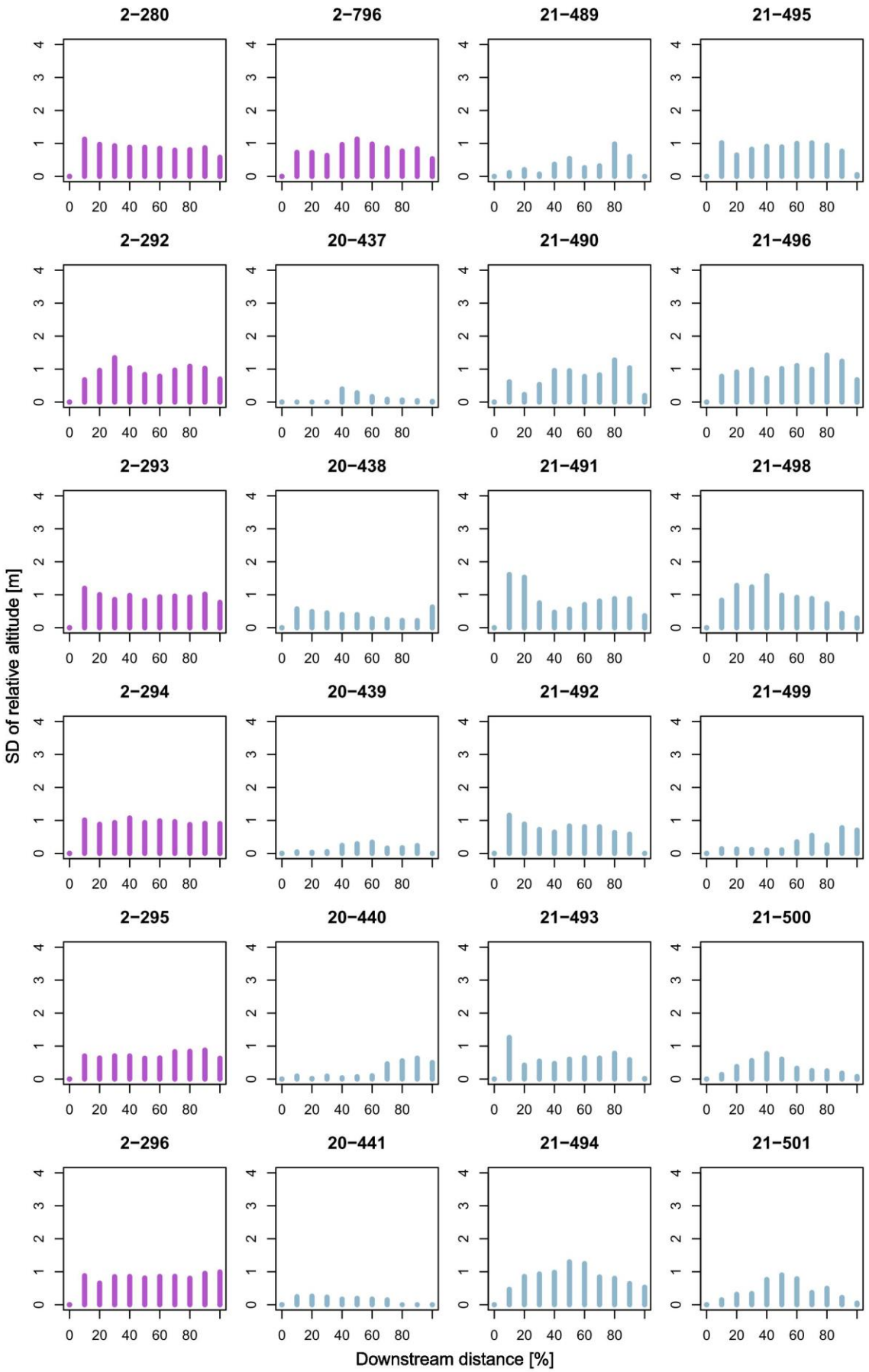

(Figure A–IV–5c continued)

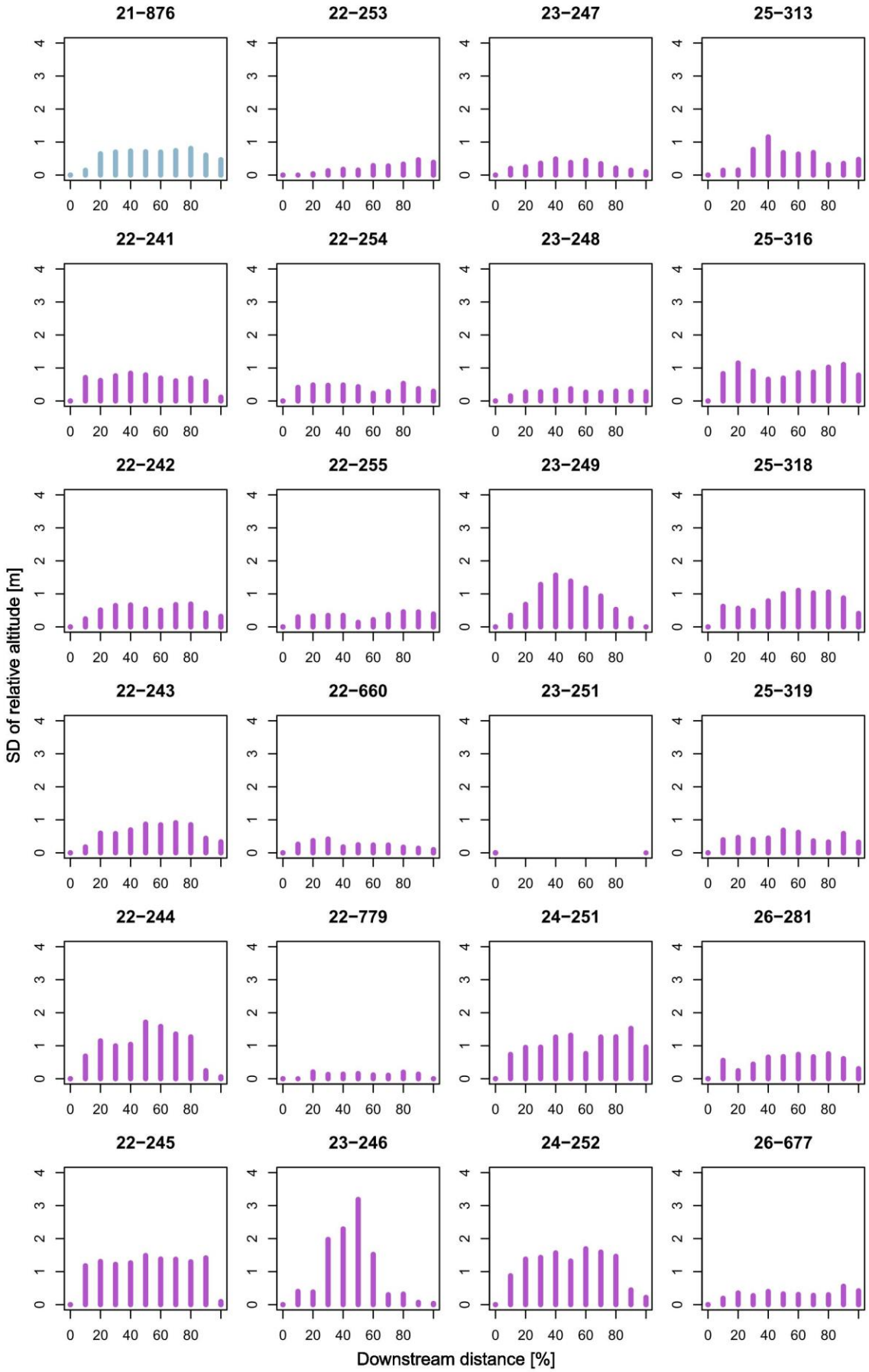

(Figure A–IV–5c continued)

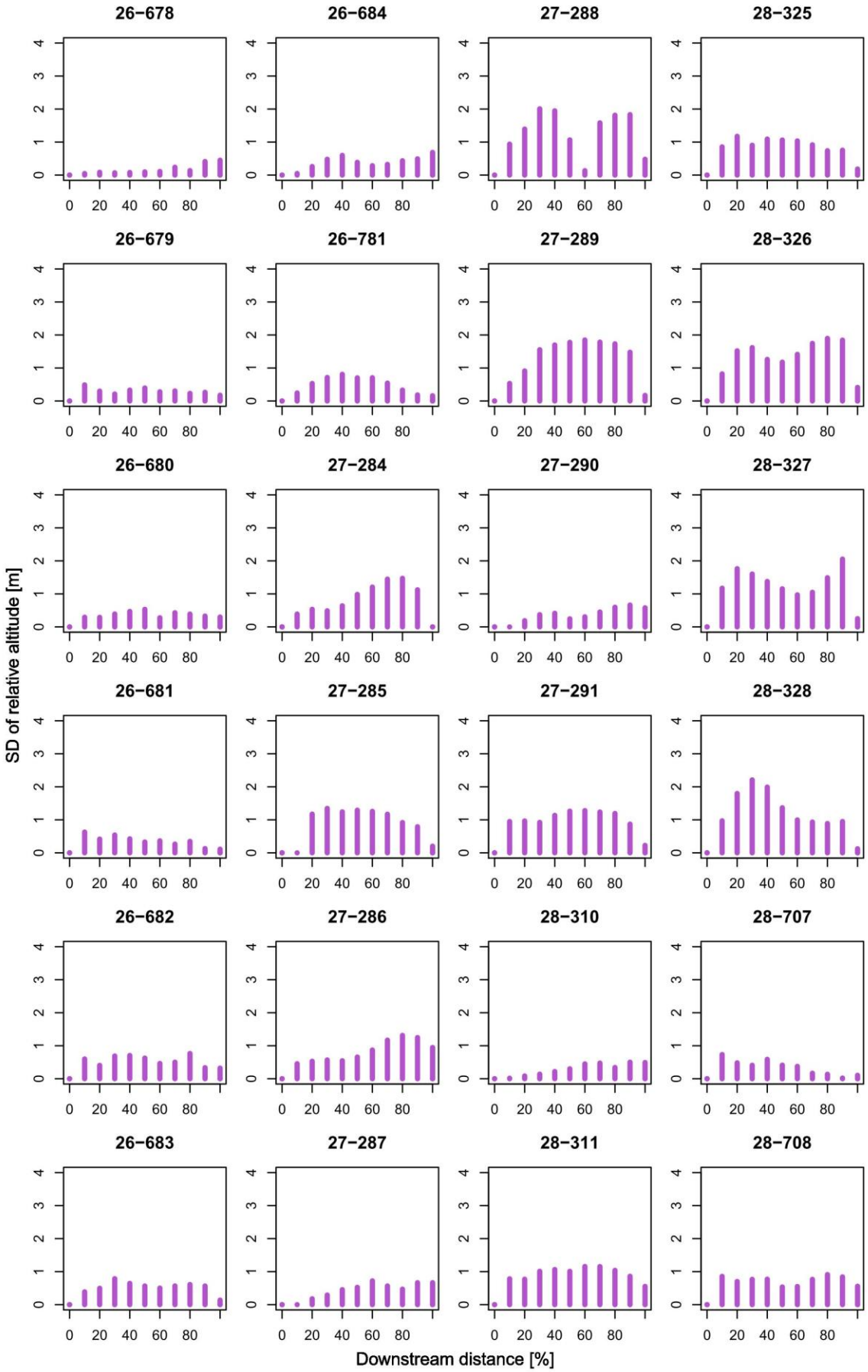

(Figure A–IV–5c continued)

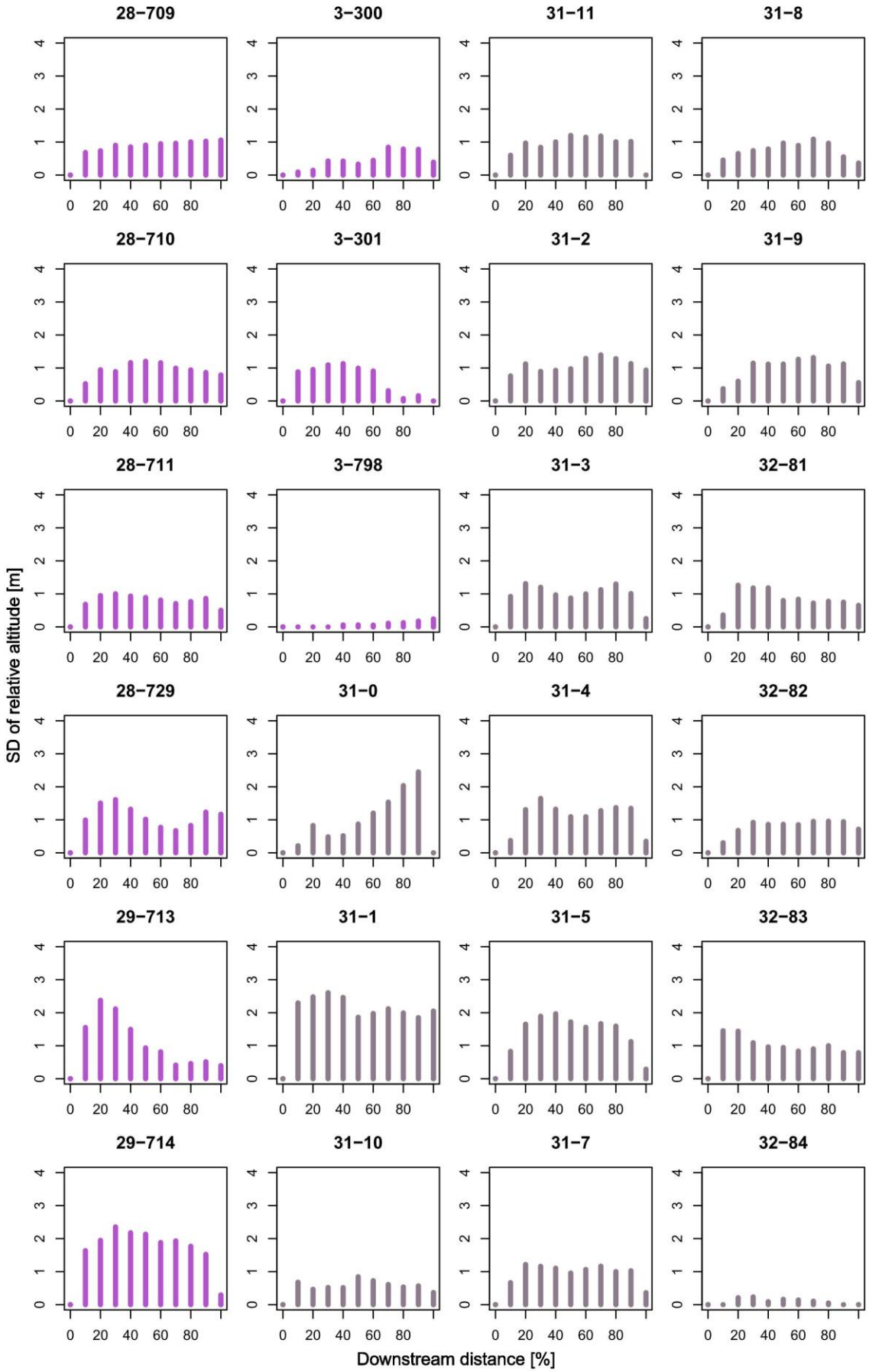

(Figure A–IV–5c continued)

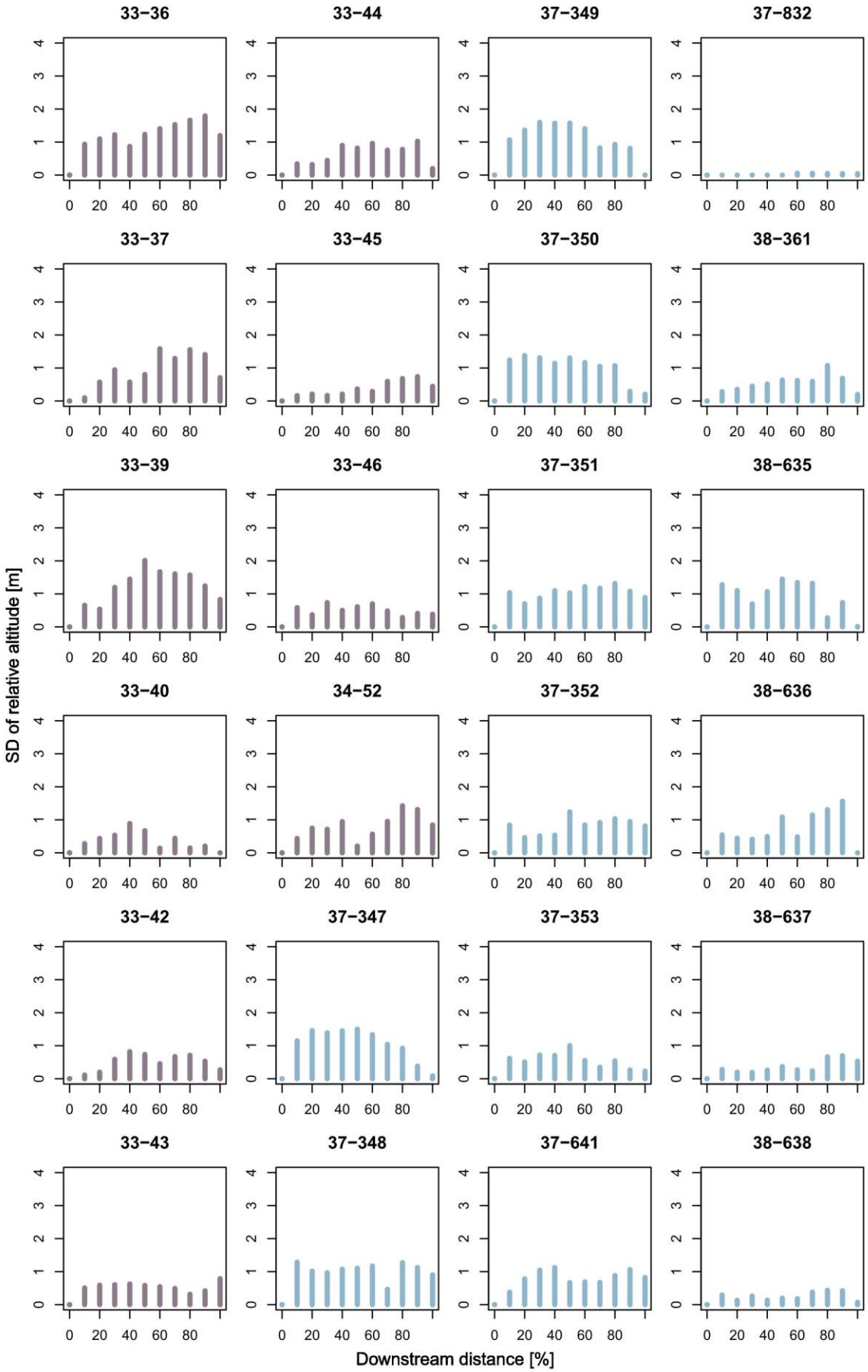

(Figure A–IV–5c continued)

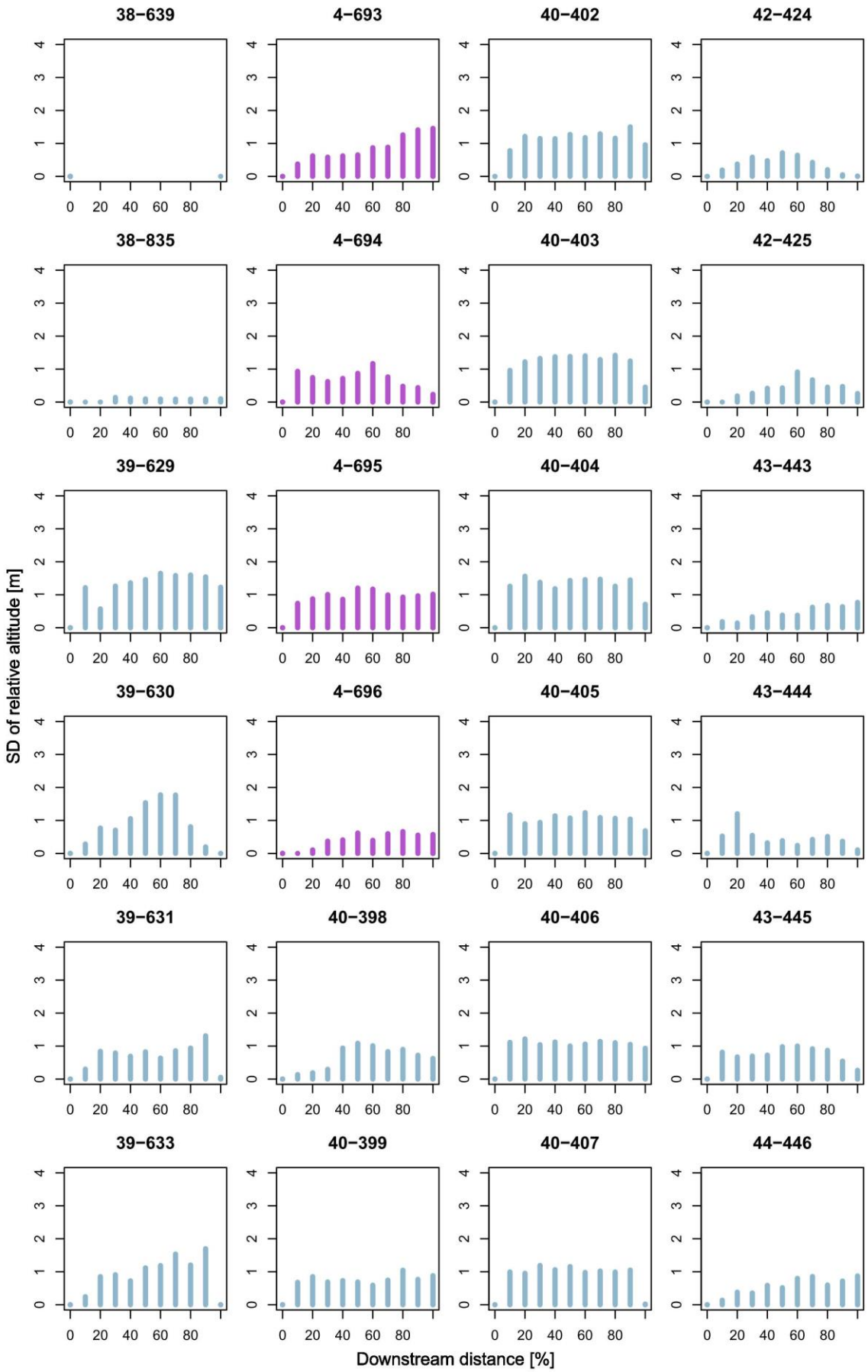

(Figure A–IV–5c continued)

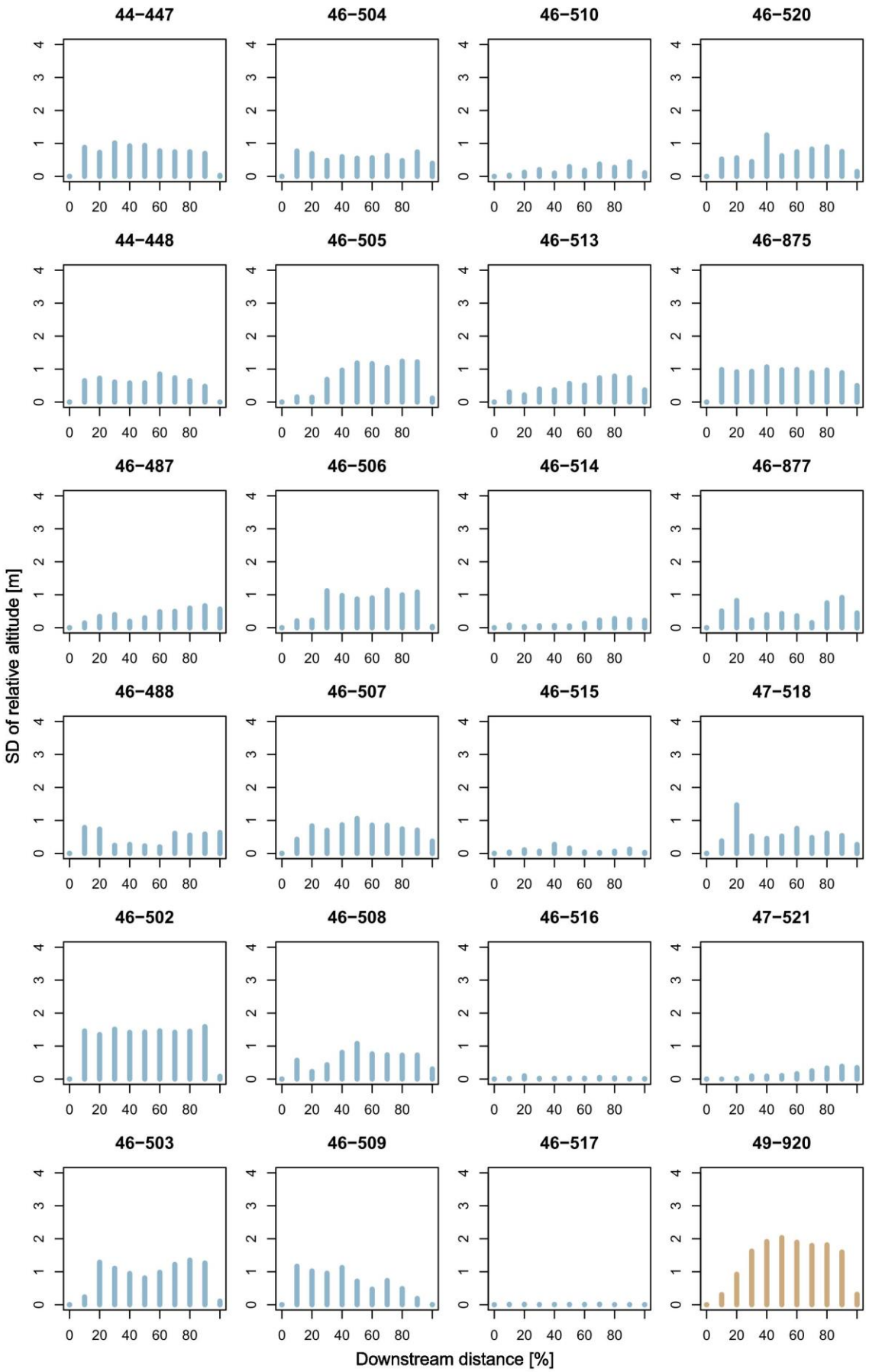

(Figure A–IV–5c continued)

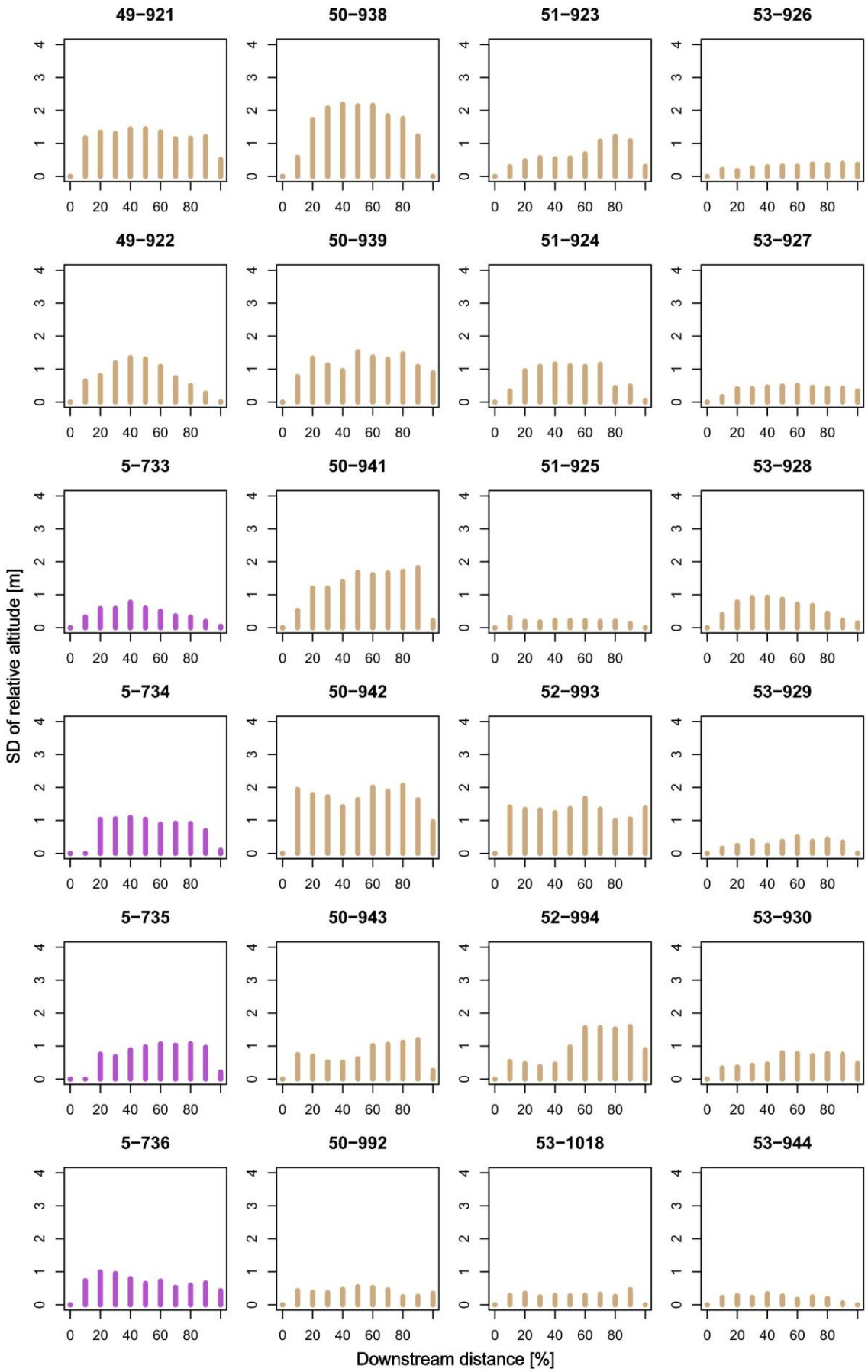

(Figure A–IV–5c continued)

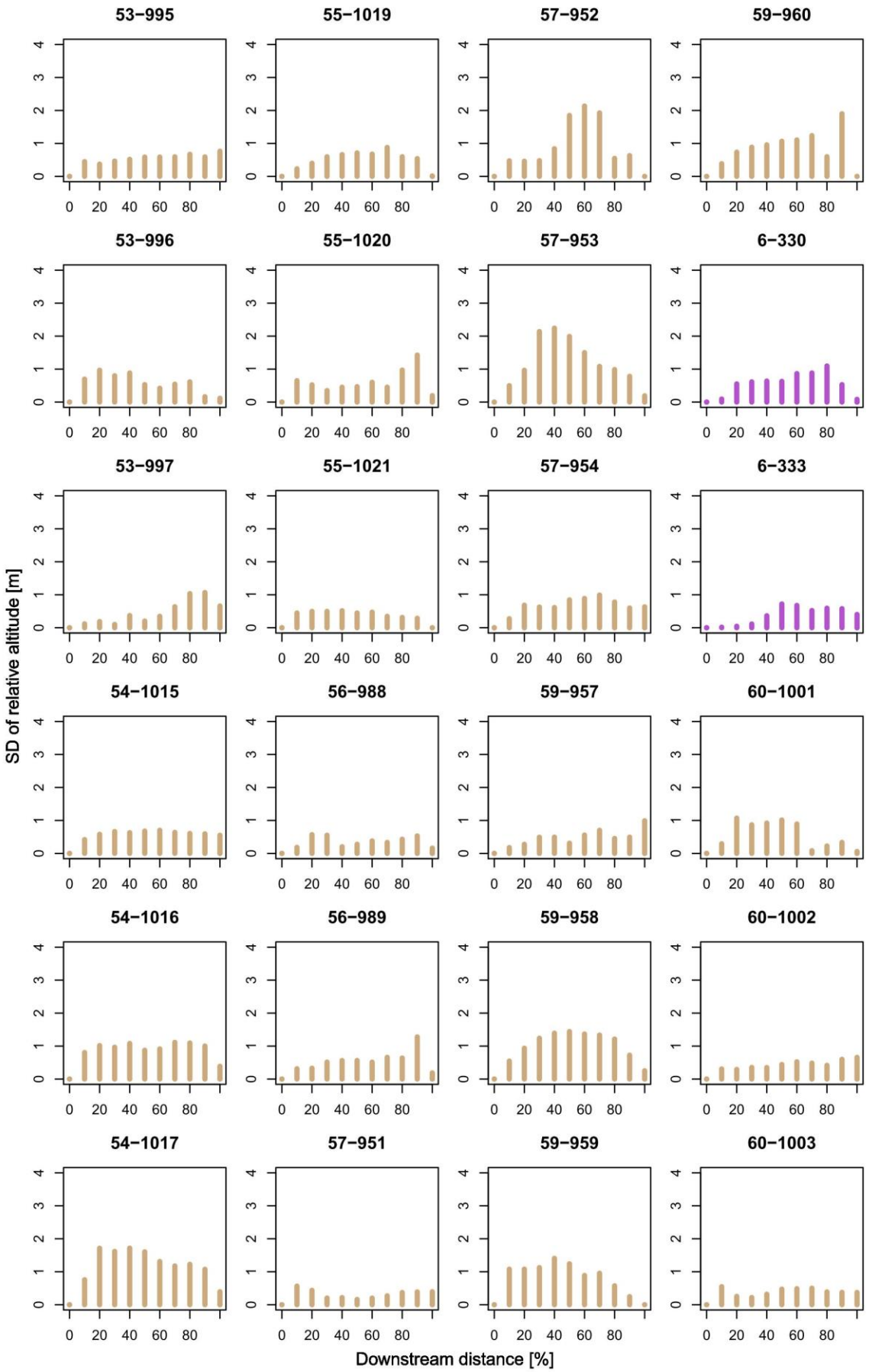

(Figure A–IV–5c continued)

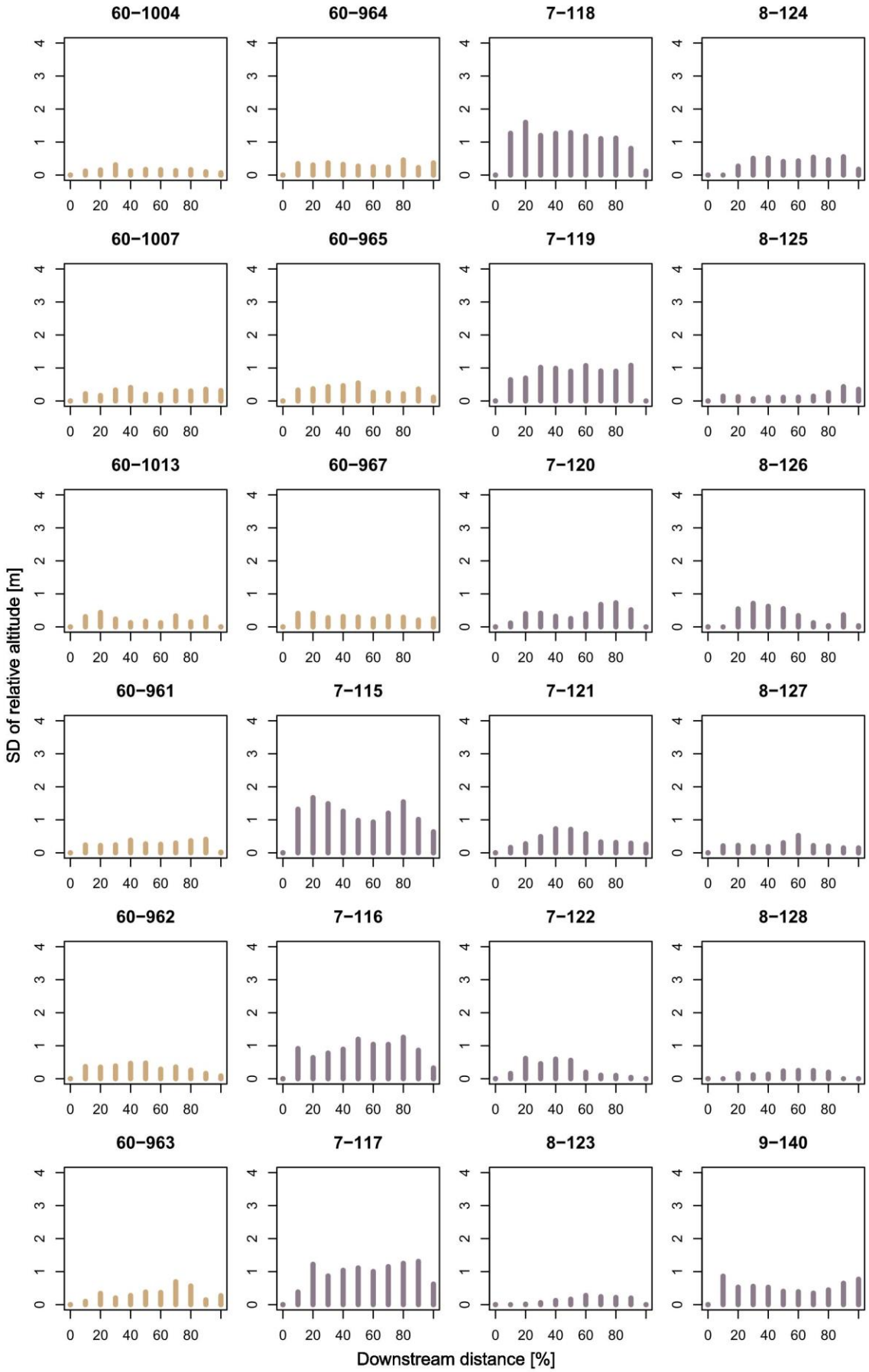

(Figure A–IV–5c continued)

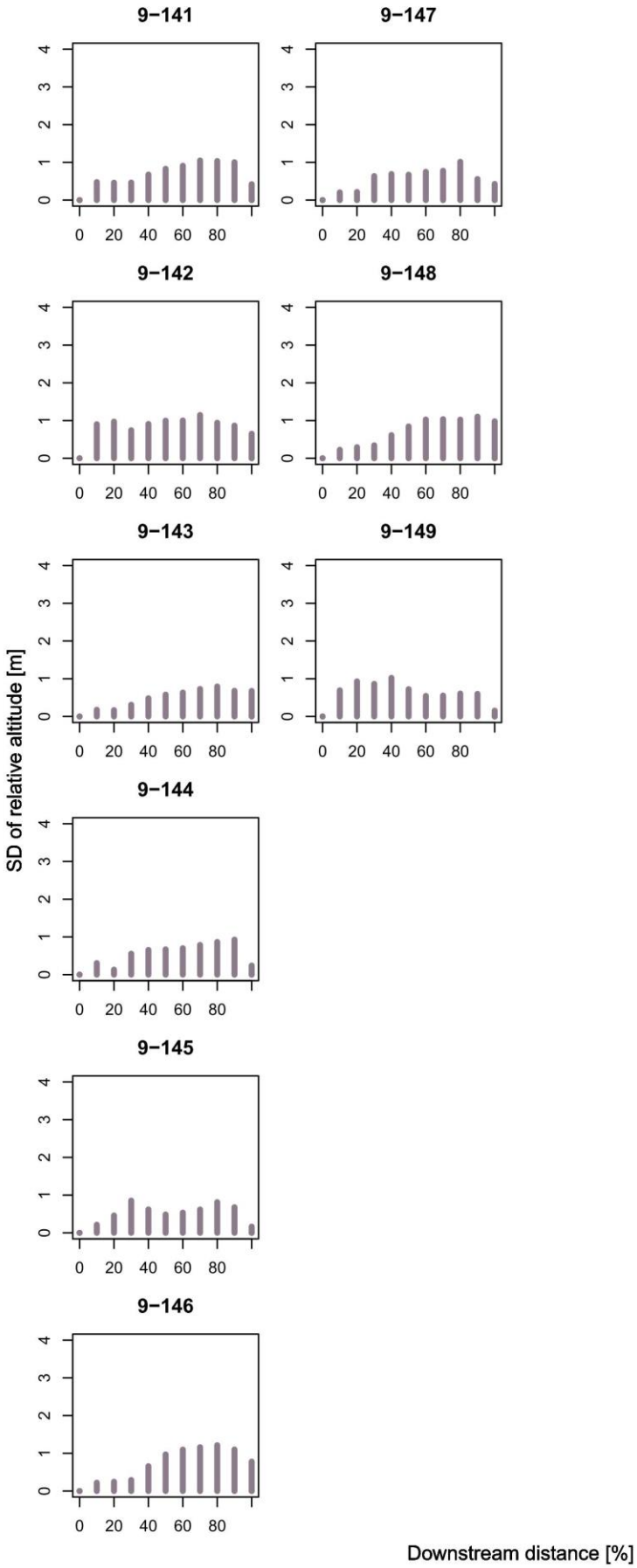

(Figure A–IV–5c continued)

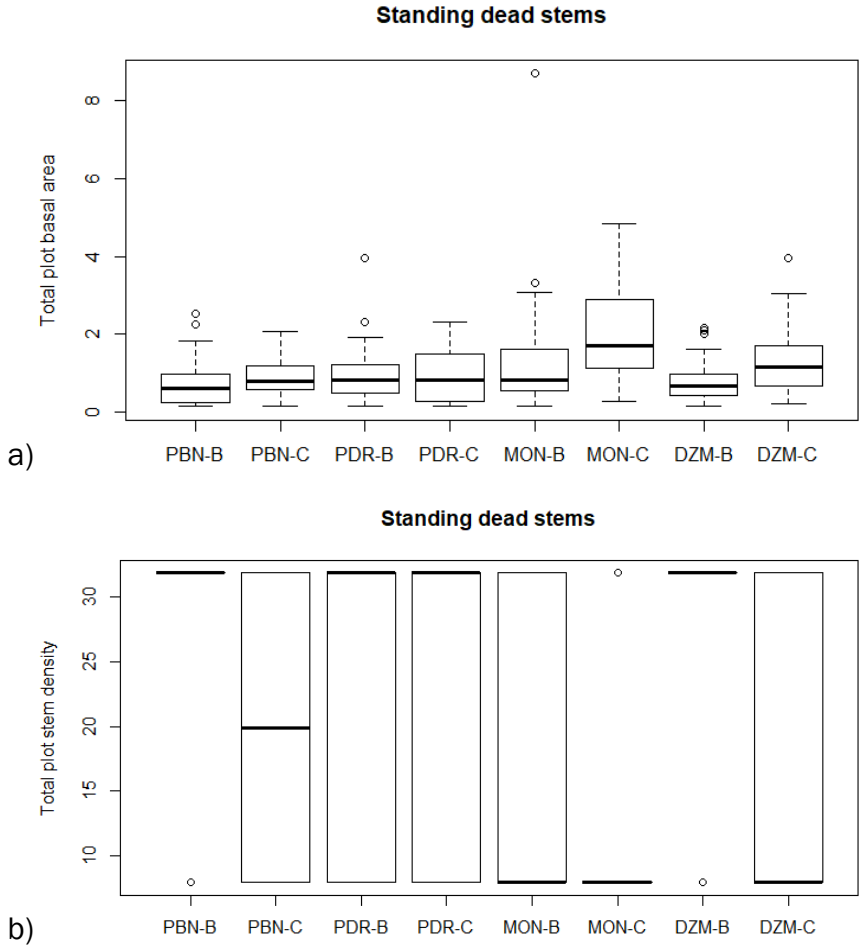

Figure A–IV–6: Standing dead stem characteristics compared between the various reaches and management phases: a) Total plot basal area, b) total plot stem density.

Appendix V: Complementary research work

Wawrzyniak V, Räpple B, Piégay H, Michel K, Parmentier H & A Couturier (2014) Analyse multi-temporelle des marges fluviales fréquemment inondées à partir d'images satellites Pléiades. *Revue Française de Photogrammétrie et de Télédétection* 208, Pléiades Days 2014, 1st Part:69–75.

Thorel M, Piégay H, Barthelemy C, Räpple B, Gruel CR, Marmonier P, Winiarski T, Bedell J-P, Arnaud F, Roux G, Stella JC, Seignemartin G, Tena-Pagan A, Wawrzyniak V, Roux-Michollet D, Oursel B, Fayolle S, Bertrand C & E Franquet (2018) Socio-environmental implications of process-based restoration strategies in large rivers: should we remove novel ecosystems along the Rhône (France)? *Regional Environmental Change*:1–13.

ABSTRACT

The multiple uses made of large rivers, such as the Rhône in south-eastern France, have provoked profound modifications of their fluvial dynamics. As a consequence, the hydro-sedimentary and ecological functioning of their channels and floodplains are highly altered. Integrated restoration programmes struggle in defining potentials and risks related to such 'novel ecosystems' and to understand the various interacting drivers which influence their formation. This study comparatively focused on 293 dike fields—rectangular units delimited by longitudinal and lateral submersible dikes constructed in the channel in the late 19th century to promote the navigability of the Rhône. They are distributed over four reaches by-passed in the 20th century for hydro-electric energy production. We investigated the spatio-temporal patterns of sediment deposition and the structure and composition of the forest stands using remote sensing and field data. We also propose a conceptual model of potential drivers and processes behind the observed patterns. Eighty percent of the dike fields have evolved from the aquatic to a terrestrial and forested stage, following variable historical trajectories both between and within reaches. The forest stands presented structural characteristics which differed from more natural reference stands and compositional characteristics closer to mature than to pioneer systems. They featured a high presence of non-native species, such as the invasive Box elder (*Acer negundo*). Our comparative approach constituted a first step to disentangle the cumulative effects of the drivers and define their individual roles: we discovered a prominent role of local factors, especially the connectivity to the main by-passed channel. The evolution of the environmental factors themselves added to the complexity of the patterns. This work provides a basis for future studies of novel ecosystems on rivers, and a new perspective to river managers on the Rhône due to its innovative spatial-scale.

Keywords: sedimentation patterns; woody riparian vegetation; Anthropocene; control factors; Rhône River; river training; river regulation; river rehabilitation